



UNIVERSITAT DE
BARCELONA

Study of the mTOR pathway in neurodegenerative diseases: from synapses to genes

Núria Martín Flores

ADVERTIMENT. La consulta d'aquesta tesi queda condicionada a l'acceptació de les següents condicions d'ús: La difusió d'aquesta tesi per mitjà del servei TDX (www.tdx.cat) i a través del Dipòsit Digital de la UB (diposit.ub.edu) ha estat autoritzada pels titulars dels drets de propietat intel·lectual únicament per a usos privats emmarcats en activitats d'investigació i docència. No s'autoritza la seva reproducció amb finalitats de lucre ni la seva difusió i posada a disposició des d'un lloc aliè al servei TDX ni al Dipòsit Digital de la UB. No s'autoritza la presentació del seu contingut en una finestra o marc aliè a TDX o al Dipòsit Digital de la UB (framing). Aquesta reserva de drets afecta tant al resum de presentació de la tesi com als seus continguts. En la utilització o cita de parts de la tesi és obligat indicar el nom de la persona autora.

ADVERTENCIA. La consulta de esta tesis queda condicionada a la aceptación de las siguientes condiciones de uso: La difusión de esta tesis por medio del servicio TDR (www.tdx.cat) y a través del Repositorio Digital de la UB (diposit.ub.edu) ha sido autorizada por los titulares de los derechos de propiedad intelectual únicamente para usos privados enmarcados en actividades de investigación y docencia. No se autoriza su reproducción con finalidades de lucro ni su difusión y puesta a disposición desde un sitio ajeno al servicio TDR o al Repositorio Digital de la UB. No se autoriza la presentación de su contenido en una ventana o marco ajeno a TDR o al Repositorio Digital de la UB (framing). Esta reserva de derechos afecta tanto al resumen de presentación de la tesis como a sus contenidos. En la utilización o cita de partes de la tesis es obligado indicar el nombre de la persona autora.

WARNING. On having consulted this thesis you're accepting the following use conditions: Spreading this thesis by the TDX (www.tdx.cat) service and by the UB Digital Repository (diposit.ub.edu) has been authorized by the titular of the intellectual property rights only for private uses placed in investigation and teaching activities. Reproduction with lucrative aims is not authorized nor its spreading and availability from a site foreign to the TDX service or to the UB Digital Repository. Introducing its content in a window or frame foreign to the TDX service or to the UB Digital Repository is not authorized (framing). Those rights affect to the presentation summary of the thesis as well as to its contents. In the using or citation of parts of the thesis it's obliged to indicate the name of the author.

Barcelona, 2018

Programa de Doctorat en Biomedicina



**UNIVERSITAT DE
BARCELONA**

STUDY OF THE mTOR PATHWAY IN NEURODEGENERATIVE DISEASES: FROM SYNAPSES TO GENES

Dissertation submitted by

NÚRIA MARTÍN FLORES

To opt for a doctoral degree in biomedicine for Universitat de Barcelona

This work was performed at the Department de Biomedicina de la Facultat de Medicina de la Universitat de Barcelona, under the supervision of Dr. Cristina Malagelada Grau

Doctoral student

Supervisor

Núria Martín Flores

Cristina Malagelada Grau

“Even the darkest night will end and the sun will rise”

Victor Hugo, *Les Misérables*

A totes les persones que han estat al meu costat

A Lucía y Sergio,
porque correr a vuestro lado es siempre liberador

AGRAÏMENTS

Sou molts els que m'heu acompanyat durant tots aquests anys i han fet d'aquesta tesi un camí molt més fàcil. Però tots aquells que heu compartit aquest camí ja sabreu que les línies que a continuació resulten han sigut probablement les més difícils d'escriure. Però com deia, vull agrair a tots els que m'heu acompanyat aquests anys, per la vostra ajuda, paraules i converses o simplement per escoltar i caminar al meu costat.

Com qualsevol llibre que al obrir-lo trobes a les seves pàgines l'inici d'una història, voldria senyalar el començament d'aquesta història. Però, on marcar l'inici quan arribar fins aquí ha sigut el resultat de tantes persones i esdeveniments que s'han creuat en el camí?

Si rebobino enrere aquesta història sembla tenir el seu inici entrant al despatx de la Cris, la que després d'anys de pràctiques de carrera, de màster i encara més pràctiques es va convertir en la meva directora de tesi. Recordo que ja des del primer moment vas encomanar-me la teva passió per la ciència, parlant encara amb més devoció sobre les funcions i propietats d'una fantàstica proteïna anomenada RTP801. Gràcies per obrir-me no només les portes al teu laboratori sinó també al món de la ciència, per ensenyar-me a afrontar cada moment que aquest món et presenta amb esperit de lluita però també sempre amb optimisme.

Però la història mai s'escriu sola, i al meu costat he tingut grans companys de laboratori amb els que he compartit tantes hores de feina i alguna també de festa. En primer lloc a en Joan i la Mercè, per ensenyar-m'ho tot quan vaig arribar, per les estones compartides al bar fent cerveses i, sobretot, per posar banda sonora a cadascun dels records que tinc al laboratori de Farmaco. I entre els records d'aquella primera etapa apareixen la Clara i la Cris, les nostres veïnes de laboratori sempre disposades a obrir la porta que ens comunicava per desconnectar un petit instant. Moltes gràcies a les dues per tots els consells quan vam endinsar-nos al món dels ratolins. Gràcies a tots per els dinars al claustre que ens permetien fugir de les quatre parets i respirar l'aire fresc del carrer.

I a meitat de la tesi va arribar el moment de mudar-se de laboratori, no gaire lluny, només un parell de plantes més amunt. La mudanza a la Unitat de Bioquímica estuvo acompañada de la llegada de Leti. Quiero agradecerle por ser la mejor compañera de laboratorio que podía haber tenido, porque después de pasar tantas horas entre poyata, estabulario y cultivos nos hemos convertido en grandes confidentes. Hemos compartido tantos y tantos dramas, unas veces al borde del llanto, otras al borde de la locura histérica y es que los ratones nos han provocado más de una noche de insomnio. Gracias por estar a mi lado en la poyata, pero también fuera de ella, porque los

AGRAÏMENTS

momentos de desesperación parecen desaparecer después de una buena charla y dos gintonics. Cuando este libro finalmente se cierre, echaré de menos tener la mesa siempre repleta de chocolates, que sean las siete de la tarde y cantemos los más cutre del pop nacional e internacional y, sobre todo, poder mirar al lado y encontrar con quien compartir todas las preocupaciones y cotilleos que acontecen entre los pasillos.

També vull agrair als estudiants de grau i màster que han passat pel laboratori. A la Clara, al Víctor que amb les seves ocurrencies era impossible no acabar rient de la sorpresa, i en especial a l'Arnau. Per estar sempre disposat a ajudar, excepte per fer alguna maxi..., i per compartir tantes estones de riures i confidències dins i fora del lab. Crec que la Leti i jo no podríem haver tingut un millor company de gintònics! També a la Júlia, que tot i que no hem tingut oportunitat de compartir gaires hores de feina, has aconseguit integrar-te a la perfecció a la vida del laboratori.

Amb cada canvi noves persones es creuen en el camí, i l'arribada al nou departament va ser el moment de conèixer nous companys. Moltes gràcies a l'Eva per estar sempre disposada a ajudar amb qualsevol problema experimental que es presentava, per ser la veu l'experiència i per tenir sempre preparat el millor consell quan ho necessitava. A l'Arnau, sempre transmetent tranquil·litat i calma, per totes les classes d'història que he après al teu costat a l'hora del tupper, i perquè em continua al·lucinant la teva capacitat d'abstracció davant d'una pantalla. A Esther, per ser ese soplo de aire fresco que anima el laboratorio, siempre dispuesta a hablar, cotillear y reír. També vull agrair a tots aquells que en un moment o altre hem compartit hores al lab. A la Cindy per totes les confidències que vam compartir, a l'Alexis i les seves interminables jornades laborals, a l'Aureli i l'Adriana, el seny i la bogeria, les dos cares del seu laboratori. También a Pedro, por todas las veces que has sido nuestro salvador ante los roedores.

A tota la resta de persones que fan molt més fàcil que treballar al laboratori. Al Mario, per salvar més d'un experiment amb algun aparell que ja ni sabíem que existia. A Carmen por toda la ayuda prestada en el criostato y por todos los consejos en nuestra lucha contra las inmunes. Y en especial a Rosario, siempre poniéndonos rectos pero siempre dispuesta a dar un abrazo. ¿¡Qué voy a hacer ahora sin tus conversaciones que tanto alegraban el día!? A la Marga, per la teva expertesa però a la vegada proximitat cada cop que xerràvem entre els ordinadors. Al Jou, per la serenitat que després i per tenir el millor criòstat que crec que hi ha a tota la facultat. Al Manolo, per ser un apassionat de la ciència i per tota l'ajuda i consells que m'has donat des de que vaig arribar a la unitat. A l'Eulàlia perquè la teva empenta es sempre motivadora i escoltar-te es sempre sinònim d'aprenentatge.

També vull donar les gràcies a tots els la cinquena planta, a tots els que encara hi sou i a aquells que ja heu marxat. A en Jordi Alberch per ajudar al laboratori en els pitjors moments i així, finalment, poder fer possible que dugués a terme la meva tesi en aquest grup. També vull agrair a l'Esther perquè l'inici d'aquesta tesi va començar com un projecte de col·laboració comú, i en cadascuna de les reunions que he tingut he pogut aprendre del teu esperit crític. A la Sílvia, per totes les aportacions que han ajudat a millorar aquesta tesi. A la Mercè, perquè sense ella hagués sigut impossible poder aprendre tot el comportament animal d'aquests últims anys. A Vero, por toda la ayuda y la paciencia explicándonos el mundo de las espinas dendríticas, y, sobre todo, por enseñarnos palabras tan extrañas como deconvolucionar y Smirnov-Kolmogórov. A Ana Saavedra, por las correcciones tan exhaustivas, por todos los consejos y discusiones de resultados que hemos tenido después de los seminarios del viernes. A Sara, por todas las ayuda que nos has dado con los cultivos primarios y por irradiar siempre alegría, aunque los resultados con nuestros fatídicos cultivos no acompañasen. Al Jordi, per totes les aportacions que m'has donat durant aquests anys de tesi, per les classes de dissecció en els meus inicis i d'operacions d'animals al final d'aquest trajecte, per estar sempre disposat a donar un cop de mà quan et demanava auxili amb els ratolins i per les converses tan interessants que poden acabar succeint a l'estabulari. A Rafa, porqué mientras estuviste en la quinta eras la persona a la que iba a preguntar por cualquier duda, protocolo o reactivo, y siempre estuviste dispuesto a ayudarme aunque te pillara en medio de un experimento. Al Marco, el Phil, la Raquel, l'Albert, l'Andrés, l'Andrea, la Laura, la Marta, la Mar, el Gerardo...moltes gràcies a tots pels vostres consells i ajuda que van ser claus perquè els experiments tiressin endavant.

També he d'agraciar al Mario i el Rubén per fer part d'aquesta tesi possible. Cada reunió amb vosaltres ha sigut molt enriquidora, fent-me la genètica una mica més entenedora. Gràcies a tots dos per resoldre cadascun dels dubtes que anaven succeint. També vull donar les gràcies a la Dra Fina Martí perquè les reunions amb ella també m'han ajudat a entendre la malaltia de Parkinson des de la clínica donat un sentit molt més ampli a tots els experiments que es desenvolupaven al laboratori. A la Francesca Antonelli, la Catalina Cerquerai la Verónica Moreno que van revisar tantes i tantes històries clíniques per fer possible després tots els anàlisis. Al David Soto i al David Gasull per apropar-me l'electrofisiologia una mica més i estar disposats a donar-nos sempre un cop de mà, bé sigui pujant corrents al laboratori per comentar un últim resultat o fent pancakes per començar amb energia un dia de congrés.

No voldria oblidar-me tampoc de totes aquelles persones que m'han ajudat tècnicament amb els experiments. A Josep Manel Rebled per tota l'ajuda alhora de plantejar i duur a

AGRAÏMENTS

terme els experiments de microscòpia electrònica. A la Maria Calvo, l'Anna Bosch i l'Elisenda per tota l'assistència tècnica durant les hores de confocal. Finalment, moltes gràcies al Gari i al Josep M^a Marimón per tots els consells que ens heu donat alhora d'afrontar el repte de mantenir una colònia de ratolins.

Determinar el moment exacte en què comença una història es una tasca complicada ja que moltes vegades la precedeix el pròleg que marcarà el propi inici. El pròleg d'aquesta tesi comença en els anys d'universitat, a la Facultat de Biologia, rodejada dels meus companys, compartint interminables hores de pràctiques, de tappers, de "breaks" a mitja tarda, de sol a la gespa, de nits de festa i d'alguna escapada. Gràcies a tots aquells amb qui aquest camí va començar, Carles, Uri, Guille, Carol, Maria, Xavi, Raquel per totes les vivències compartides que guardo en el record. Gràcies a la Tere, la Mireia i la Yaiza per tots els berenars i sopars periòdics, tan necessaris per posar-nos al dia i per fugir una estona del que ens preocupa. A les dos persones que em trobava entre classes i que la casualitat finalment va decidir que ens trobéssim després compartint vida a Barcelona. Moltes gràcies Carlos i Guillem perquè sou uns grans companys de pis, heu aconseguit que les nits d'avorriment siguin sempre molt més divertides al vostre costat.

Però en especial voldria agrair a dues persones amb qui he compartit les angoixes d'aquest camí, i que tant he trobat a faltar en aquesta última etapa del trajecte. La primera de ellas es Marc ya que sin ti la vida en el Clínic no hubiera sido tan fácil. Mil gracias por amenizar las tardes con un café, por todos los experimentos discutidos, pero sobre todo por estar a mi lado durante todos estos años. ¿Quién sabe?, quizás aún nos encontremos un buen día por las calles de New York. La segona d'aquestes persones es l'Angie. Recordo que als divuit anys ens vam trobar perdudes i innocents en el primer dia d'universitat, i des de llavors hem continuat caminant juntes. Ets la persona amb qui millor he pogut compartir les meves inquietuds, i et vull agrair cadascuna de les converses que hem tingut, des de la més absurda fins a aquelles converses filosòfiques a altes hores de la nit en que debatíem el que el futur ens depararia. I potser aquelles preguntes encara no tenen resposta, però continuarem compartint cada pas.

A les companyes de màster que juntament amb l'Angie vam superar les llargues i a vegades interminables jornades de classes. Moltes gràcies a l'Elena, La Laura, l'Inés i l'Aïda perquè hagués sigut impossible arribar fins aquí sense el vostre recolzament i sense l'ajuda que any rere any m'heu donat.

A Anna y Cris, porque no hay personas capaces de hacerme reír más que vosotras.

Finalmente, quiero dar las gracias a mi familia. A mis padres y a mi hermana Esther. Gracias por estar cerca y apoyar cada uno de los pasos que he dado. Gracias por

enseñarme a afrontar los retos sin rodeos ni quejas, con ese punto de vista crítico pero práctico que tantas veces salva de caer a un precipicio de desesperación. A mis abuelos, que nunca han acabado de entender muy bien a que dedicaba mis días, pero no por ello han dejado de interesarse.

A ti Jorge, que has estado a mi lado durante los últimos años de tesis. Gracias por aguantarme y por compartir conmigo las alegrías.

Por último, los dos pilares sobre los que se sustenta esta tesis. A Lucía y Sergio, que tantas tardes de verano me han acompañado escribiendo estas páginas mientras ellos se sumergían en su propia fantasía. A Lucía por ser la persona más desafiante que conozco, por conseguir que mi paciencia pierda la razón, y, aun así, por ser casi irremediable terminar cada discusión riéndonos la una de la otra. A Sergio, por retar mi imaginación y dotes artísticas con cada nuevo juego del tesoro, por cada una de las partidas de memory en que me has fulminado y por ser, sin ningún tipo de duda, quien mejor ha controlado el número de nuevas páginas escritas cada día. Aunque he llamado al orden más de una vez entre vosotros, no os engañéis, ese grito me permitía huir cuando las letras perdían ya su sentido entre las páginas y sólo quería unirme a vuestro mundo de fantasía.

El meu innumerable agraïment a tots vosaltres... Moltes gràcies.

ABBREVIATIONS

4E-BP1/2	Eukaryotic translation initiation factor 4E binding protein 1/2
6-OHDA	6-hydroxydopamine
AAO	Age-at-onset
AC	Adenylyl cyclase
AD	Alzheimer's disease
Akt	Serine/Threonine protein kinase B
Alix	ALG-2 interacting protein X
AMPA	Alpha-amino-3-hydroxy-5-methyl-isoxazole-4-propionic acid
ATF4	Activating transcription factor 4
Bad	Bcl-2-associated death promoter protein
Bax	Bcl-2-associated X protein
Bcl-2	B-cell lymphoma 2
BDNF	Brain-derived neurotrophic factor
Bim	Bcl-2-like protein 11
BSA	Bovine serum albumin
Ca²⁺	Calcium ion
CAG	Cytosine-Adenine-Guanine
CB1	Endocannabinoid receptor 1
CBP	CREB-binding protein
CD63	CD tetraspanin 63
CHX	Cycloheximide
CMV	Cytomegalovirus
COMT	Catechol-O-methyltransferase
CREB	Cyclic-adenosine monophosphate response element-binding protein
CSF	Cerebrospinal fluid
Cul4A	Culin-4a
CVC	Cross-validation consistency
DA	Dopamine
DDIT4	DNA-damage-inducible transcript 4
DEPTOR	DEP domain containing mTOR-interacting protein
Dig2	Dexamethasone-induced gene 2
DIV	Day-in-vitro
DJ-1	Protein deglycase DJ-1
DMEM	Dulbecco's Modified Eagle Medium
DNA	Deoxyribonucleic acid
DNAJC6	DNAJ subfamily C member 6

ABBREVIATIONS

DMSO	Dimethyl sulfoxide
eCB	Endogenous cannabinoid
EDS	Excessive daytime sleepiness
eGFP	Enhanced green fluorescent protein
EIF4G1	Eukaryotic translation initiation factor 4 gamma, 1
Elk-1	Ets-like gene 1
ENK	Enkephalin
ER	Endoplasmic reticulum
ERK 1/2	Extracellular-signal-regulated kinase 1/2
ESCRT	Endosomal sorting complexes required for transport
EV	Exosomal vesicle
FBS	Fetal bovine serum
FLZ	8-Methyl-6-Phenoxy-2-(Tetrahydro-2H-Pyran-4-Ylamino)pyrido[2,3-D]pyrimidin-7-One
GABA	Gamma-aminobutyric acid
GAP	GTPase activating protein
GAPDH	Glyceraldehyde 3-phosphate dehydrogenase
GBA	β -glucocerebrosidase
GDP	Guanosine diphosphate
GFP	Green fluorescent protein
GluA1	AMPA receptor subunit GluR1
GPe	External globus pallidus
GPI	Internal globus pallidus
GRB10	Growth factor receptor-bound protein 10
GSK3β	Glycogen synthase kinase 3 beta
GTP	Guanosine triphosphate
GWAS	Genome-wide association study
GβL	G protein beta subunit-like
HD	Huntington's disease
HIF-1	Hypoxia inducible factor 1
HRP	Horseradish peroxidase
Hsp70	Heat shock protein 70
Htt	Huntingtin
HWE	Hardy-Weinberg equilibrium
IGF1	Insulin-like growth factor
ILV	Intraluminal vesicle

IPSCs	Induced pluripotent stem cells
JNK	c-Jun N-terminal kinase
K	Amino acid lysine
KCl	Potassium chloride
KI	Knock-in
L1-CAM	L1 cell adhesion molecule
L2PD	LRRK2-associated PD
LB	Lewy body
L-DOPA	Levodopa
LID	L-DOPA-induced dyskinesia
LRRK2	Leucine-rich repeat kinase 2
LTD	Long term depression
LTP	Long term potentiation
mAF	Minor allele frequency
MAO	Monoamine oxidase enzyme
MAP2	Microtubule associated protein 2
MAPK	Mitogen activated protein kinase
MCI	Mild cognitive impairment
MDR	Multifactorial dimensionality reduction
MEM	Minimum essential media
mGluR	Metabotropic glutamate receptor
mhtt	Mutant huntingtin
miRNA	Micro RNA
mLST8	Mammalian lethal with sec-13 protein 8
MOI	Multiplicity of infection
MPTP	1-methyl-4-phenyl-1,2,3,6-tetrahydropyridine
mRNA	Messenger RNA
mSIN1	Mammalian stress-activated MAP kinase-interacting protein 1
MSNs	Medium spiny neurons
mTOR	Mechanistic target of rapamycin
mTORC	mTOR complex
MVB	Multivesicular body
NEDD4	Neural precursor cell-expressed developmentally down-regulated gene 4
NGF	Nerve growth factor
NMDA	N-methyl-D-aspartate
ORF	Open reading frame

ABBREVIATIONS

P	Phospho
p75^{NTR}	Pan-neurotrophin receptor
PARK	PD associated loci
PBS	Phosphate buffered saline
PD	Parkinson's disease
PDK1	Phosphoinositide-dependent protein kinase 1
PHLPP	PH domain leucine-rich repeat protein phosphatase 1
PI3K	Phosphoinositide 3-kinase
PINK	PTEN-induced kinase
PKA	Protein kinase A
PKC	Protein kinase C
PLCγ	Phospholipase C gamma
PolyQ	Polyglutamine
PP2A	Protein phosphatase 2
PPARγ	Peroxisome proliferator-activated receptor gamma
PPP1R1B	Protein phosphatase 1, regulatory (inhibitor) subunit 1B
PRAS40	Proline-rich Akt substrate 40 kDa
PRKN	Parkin E3 ubiquitin ligase
Protor	Protein observed with Rictor
PSD-95	Postsynaptic density 95
PTEN	Phosphatase and tensin homolog
Q	Amino acid glutamine
Raptor	Regulatory-associated protein of mTOR
RBD	REM sleep behaviour disorder
Redd1	Regulated in DNA damage response 1
Redd2	Regulated in DNA damage response 2
REM	Rapid eye movement
REST-NRSF	Repressor-element-1 transcription factor–neuron-restrictive silencer factor
Rheb	Ras homolog enriched in brain
Rhes	Ras homolog enriched in striatum
Rictor	Rapamycin-insensitive companion of mTOR
ROS	Reactive oxygen species
RT-qPCR	Reverse transcription quantitative polymerase chain reaction
S6	S6 ribosomal protein
S6K	S6 kinase

SAGE	Serial analysis of gene expression
SEM	Standard error of the mean
Ser	Amino acid serine
SGK1	Serum and glucocorticoid regulated protein kinase 1
shRNA	Short hairpin RNA
siRNA	Small interfering RNA
SNCA	α -synuclein gene
SNP	Single nucleotide polymorphism
SNpc	Substantia nigra pars compacta
SNpr	Substantia nigra pars reticulata
SOD1	Superoxide dismutase 1
SP1	Specificity protein 1
SREBP1	Sterol regulatory element-binding protein 1
STN	Subthalamic nucleus
Subs P	Substance P
SUMO	Small ubiquitin-like modifier
SV40	Simian Virus 40
SYNJ1	Synaptojanin-1
TafII130	TATA-binding protein-associated factor II130
TBS	Tris buffered saline
TEM	Transmission electron microscopy
Thr	Amino acid threonine
TLP	Time to LID peak
Trk B	Tropomyosin receptor kinase B
TSC 1/2	Tuberous sclerosis complex 1/2
TSG101	Tumor susceptibility gene 101
TTD	Time to dyskinesia
UCHL1	Ubiquitin C-terminal hydrolase L1
ULK-1	UNC-51-like autophagy activating
UPS	Ubiquitin-proteasome system
VPS35	Vacuolar protein sorting 35
VPS4	Sorting-associated protein 32
WB	Western blotting
WT	Wild-type
YAC	Yeast artificial chromosome

TABLE OF CONTENTS

AGRAÏMENTS.....	vii
ABBREVIATIONS.....	xv
TABLE OF CONTENTS.....	xxiii
LIST OF FIGURES AND TABLES	xxxii
1. List of figures.....	xxxiii
2. List of tables	xxxvii
INTRODUCTION	39
1. Huntington’s disease and Parkinson’s disease as neurodegenerative diseases...41	
1.1 Huntington’s disease	41
1.1.1 Etiology.....	42
1.1.2 Neuropathology	43
i. Basal ganglia pathophysiology in HD	44
1.1.3 Mechanisms underlying striatal neurodegeneration in HD.....	46
i. Protein misfolding and aggregation	47
ii. Impaired protein degradation.....	47
iii. Trans-synaptic spreading of mhtt.....	47
iv. Transcriptional dysregulation.....	48
v. Neurotrophic dysfunction	48
1.1.4 Treatment of HD	49
1.2 Parkinson’s disease.....	50
1.2.1 Etiology.....	51
1.2.2 Neuropathology	54
i. Basal ganglia pathophysiology in PD.....	56
1.2.3 Mechanisms underlying dopaminergic neurodegeneration in PD.....	57
i. Protein misfolding and aggregation	57
ii. Impaired protein degradation	57
iii. Trans-synaptic spreading of α -synuclein	58
iv. Mitochondrial dysfunction and oxidative stress.....	58
1.2.4 Treatment of PD	59
i. Levodopa-induced dyskinesia.....	60
2. The mTOR signaling pathway in Huntington’s and Parkinson’s diseases.....63	
2.1 Mechanistic target of rapamycin	63
2.2 mTOR signaling pathway.....	64
2.2.1 mTOR/Akt signaling alterations in HD	66
2.2.2 mTOR/Akt signaling alterations in PD.....	67
2.2.3 mTOR/Akt signaling in synaptopathies	68

TABLE OF CONTENTS

3. RTP801/Redd1 as a negative regulator of the mTOR/Akt pathway	70
3.1 DDIT4: a stress responsive gene.....	70
3.2 RTP801 protein.....	71
3.2.1 RTP801 protein sequence and structure	71
3.2.2 RTP801 function and regulation	73
3.3 RTP801 implication in neurodegenerative diseases	75
3.3.1 RTP801 in PD.....	75
4. Transneuronal communication via exosomes.....	78
4.1 Classification of extracellular vesicles.....	78
4.1.1 Exosomes	79
i. Exosome biogenesis, release and internalization	79
ii. Exosome composition.....	82
4.2 Neuronal-derived exosomes in physiology and pathology.....	83
AIMS	87
METHODOLOGY	91
1. Cell culture	93
1.2 HEK293T cells.....	93
1.2 PC12 cells	93
1.3 Striatal neuronal progenitor cell line.....	93
1.4 Cortical primary neurons.....	94
2. Cellular treatments	94
3. Molecular biology	95
3.1 DNA plasmid amplification and purification.....	95
3.1.1 Bacterial transformation	95
3.1.2 Plasmid DNA amplification and purification	95
3.1.3 Plasmid DNA sequencing	96
3.2 DNA subcloning.....	96
3.2.1 ShRNA sequence design.....	96
3.2.2 Vector linearization	96
3.2.3 DNA extraction from agarose gel	96
3.2.4 Ligation	97
3.3 Description of plasmids.....	97
4. Protein expression in cell cultures	99
4.1 Liposome-mediated transfection.....	99
4.1.1 Transfection of HEK293T, NGF-PC12 and STHdh cells.....	99
4.1.2 Transfection of rat cortical primary cultures	99
4.2 Lentiviral transduction.....	99
4.2.1 Lentiviral particles production	99

5. Gene expression analysis.....	100
6. Immunofluorescence	100
6.1 Immunocytofluorescence.....	100
6.2 Immunohistofluorescence of mouse brain sections	101
7. Western Blotting.....	102
8. Synaptosomal preparation	105
9. Isolation of exosomes from culture medium	106
9.1 Exosomes uptake study.....	107
9.2 Generation of red fluorescent labeled exosomes	107
9.3 Electron microscopy observation of exosomes.....	107
10. HD mouse models	108
11. Intrastratial injection of adeno-associated vectors	108
12. Accelerating rotarod	109
13. Statistics.....	109
14. Single Nucleotide Polymorphism analysis.....	109
14.1 Cohort of study and data collection.....	109
14.2 Single Nucleotide Polymorphism selection and genotyping.....	109
14.3 Statistical analyses	110
14.3.1 Hardy-Weinberg equilibrium	110
14.3.2 Allelic association analysis.....	110
14.3.3 Genotypic association analysis.....	110
14.3.4 Epistatic association analysis	111
RESULTS	113
1. Role of RTP801 protein in Huntington’s disease.....	115
1.1 Role of RTP801 in mhtt-induced cell death	115
1.1.1 Ectopic mhtt increases RTP801 protein levels in neural cells and induces cell death.....	116
i. Both RTP801 mRNA levels and protein degradation are altered in NGF-differentiated PC12 cells overexpressing mhtt.....	117
ii. RTP801 upregulation mediates mhtt-induced death of NGF-differentiated PC12 cells.	119
1.1.2 RTP801 is not altered in the striatum of HD murine models	120
1.1.3 RTP801 is increased in differentiated HD-iPSCs cells and in human postmortem HD brains.....	122
1.2 Role of RTP801 protein in dysfunctional neuronal plasticity associated to Huntington’s disease..	125

TABLE OF CONTENTS

1.2.1	Ectopic mhtt increases RTP801 at dendritic spines of rat cortical primary neurons.....	125
1.2.2	Study of synaptic RTP801 and components of the mTOR pathway in brain-affected areas of HD patients.....	126
i.	RTP801 is increased in striatal synapses from the putamen of Huntington's disease patients.....	127
ii.	RTP801 is not altered in synapses from the frontal cortex of Huntington's disease patients.....	130
1.2.3	Study of synaptic RTP801 and components of the mTOR pathway in HD mice models.....	132
i.	RTP801 is increased in striatal synapses of the Hdh ^{Q7/Q111} -knock-in mouse model.....	132
ii.	RTP801 is increased in striatal synapses of the R6/1 mouse model.....	135
1.2.4	Study of RTP801 striatal synaptic function in the HD murine model R6/1.....	137
i.	RTP801 knockdown improves motor learning in symptomatic R6/1 mice.....	138
ii.	RTP801 knockdown preserves phospho-Akt (Ser473) and enhances the expression of synaptic proteins in the R6/1 mice.....	139
2.	Study of exosomal RTP801 in toxic cellular models.....	145
2.1	RTP801 is present in exosomes released from HEK293 cells.....	146
2.2	Study of exosomal RTP801 in cortical neuronal cultures.....	147
2.2.1	RTP801 protein is not present in exosomes derived from control or depolarized neurons.....	147
2.2.2	Neurotoxin 6-OHDA induces exosomal release of RTP801 by neuronal cultures.....	149
2.2.3	6-OHDA-derived exosomes containing RTP801 are not able to activate the mTOR/Akt pro-survival signal in recipient neurons.....	152
i.	6-OHDA-induced exosomes do not mediate pro-survival signals in recipient cortical neurons.....	152
ii.	6-OHDA-induced RTP801 contributes to counteract EVs trophic effect in recipient neurons.....	154
2.3	Study of exosomal RTP801 in mhtt-expressing cells.....	157
2.3.1	Neither RTP801 nor mhtt are detected in the exosomal fraction derived from STHdh cells.....	157
2.3.2	Mutant htt-induced RTP801 upregulation contributes to the loss of exosomal trophic support by downregulating phospho-S6 ribosomal protein in recipient neurons.....	158
3.	Single Nucleotide Polymorphism-based mTOR pathway analysis in Parkinson's disease.....	161
3.1	SNCA and mTOR genetic variations interact to modulate risk and age at onset of Parkinson's disease.....	162

3.1.1	Single SNP analysis for the risk of idiopathic PD	162
3.1.2	Epistatic interactions of SNA and mTOR SNPs are associated with the risk of idiopathic PD.....	163
3.1.3	Single genotyping association with age-at-onset of idiopathic PD	165
3.1.4	Epistatic interactions of SNCA and mTOR SNPs are associated with AAO of idiopathic PD.....	165
3.1.5	Association of epistatic combinations of SNPs with the AAO of LRRK2-associated PD	167
3.2	Multilocus interactions in the mTOR pathway influence L-DOPA induced dyskinesia onset and severity in Parkinson's disease patients	169
3.2.1	Association of single SNPs with LID onset and LID peak	169
3.2.2	Epistatic association of SNPs with LID onset.....	170
3.2.3	Association of single SNPs with LID severity	172
3.2.4	Epistatic association of SNPs with LID severity	173
DISCUSSION		177
1.	RTP801 is a downstream effector of mutant htt-induced cell death.....	179
2.	Synaptic RTP801 is increased in HD models	183
3.	Synaptic mTOR signaling is altered in HD models	185
4.	Increase of striatal synaptic RTP801 contributes to dysfunctional motor learning plasticity in HD	187
5.	Cellular stress induces transneuronally propagation of RTP801 toxicity by exosomes	189
6.	RTP801 modulates exosomal trophic support through the mTOR pathway	192
7.	SNCA and mTOR pathway genetic variations interact to modulate risk and AAO of PD.....	194
8.	Associations of SNPs in the mTOR pathway influence LID onset and severity in PD patients.....	198
9.	RTP801 and modulation of the mTOR pathway as potential therapeutic targets and biomarkers in neurodegenerative diseases	201
CONCLUSIONS		205
BIBLIOGRAPHY		209
ANNEX I		263
ANNEX II		281

LIST OF FIGURES AND TABLES

1. LIST OF FIGURES

Figure 1. Representation of the <i>IT15</i> gene and the impact of CAG repeats on the onset of HD	42
Figure 2. HD brain pathology.....	44
Figure 3. Simplified basal ganglia circuit diagram.....	45
Figure 4. Basal ganglia circuitry in early and late stages of HD	46
Figure 5. Clinical symptoms and time course of PD progression.....	51
Figure 6. Risk factors for PD development	52
Figure 7. Coronal section through the midbrain of a control and a PD patient	54
Figure 8. Lewy pathology in PD	55
Figure 9. Basal ganglia circuitry in PD	56
Figure 10. Motor fluctuations and dyskinesia induced by levodopa treatment in PD patients	60
Figure 11. Major molecular mechanisms underlying LID	61
Figure 12. Composition and regulation of mTORC1 and mTORC2 complexes	64
Figure 13. mTOR signaling pathway	65
Figure 14. DDIT4 gene-induction by cellular stress.....	70
Figure 15. RTP801 sequence alignment from different species.....	72
Figure 16. RTP801 tridimensional structure show a unique topology.....	72
Figure 17. Proposed model for RTP801 mechanism of action.....	74
Figure 18. Schematic representation of the mTOR/Akt pathway regulation by RTP801 in neuronal cells.....	77
Figure 19. Categorization of extracellular vesicles	79
Figure 20. Biogenesis of exosomes	81
Figure 21. Canonical composition of exosomes	82
Figure 22. Role of exosomes in neurons	84
Figure 23. Scheme indicating the different aims developed in this thesis	90
Figure 24. Schematic representation of an isolated synaptosome.....	105
Figure 25. Schematic representation of exosome isolation protocol by differential ultracentrifugation from cell culture media	106
Figure 26. RTP801 protein levels are increased in NGF-differentiated PC12 cells overexpressing mhTt	116

LIST OF FIGURES AND TABLES

Figure 27. Overexpression of mhtt increases RTP801 protein in neural cells and induces cell apoptosis	117
Figure 28. Mutant htt upregulates RTP801 transcriptionally	118
Figure 29. Mutant htt alters RTP801 protein degradation rate	119
Figure 30. RTP801 mediates mhtt-induced cell death.....	120
Figure 31. RTP801 mRNA levels are not altered in the striatum of R6/1 mouse model	121
Figure 32. RTP801 protein levels are not altered in the striatum of HD mouse models	122
Figure 33. RTP801 protein levels are increased in HD-IPS cell line	123
Figure 34. RTP801 is highly expressed in affected-brain areas of HD patients	124
Figure 35. RTP801 protein is present in dendritic spines of cortical neurons and the overexpression of exon-1 mhtt increases its protein levels	126
Figure 36. Synaptosomal preparation from the putamen of HD patients	129
Figure 37. Synaptic enrichment of RTP801, P-Akt (Ser473) and P-S6 (235/236) in the putamen of HD patients.....	130
Figure 38. Synaptosomal preparation from the frontal cortex of HD patients	131
Figure 39. Synaptic enrichment of RTP801, P-Akt (Ser473) and P-S6 (235/236) in the frontal cortex of HD patients.....	132
Figure 40. Synaptosomal preparation from the striatum of Hdh ^{Q7/Q111} -KI mice.....	134
Figure 41. Synaptic enrichment of RTP801, P-Akt (Ser473) and P-S6 (235/236) in the striatum of HdhQ7/Q111-KI mice	135
Figure 42. Synaptosomal preparation from the striatum of R6/1 mice	136
Figure 43. Synaptic enrichment of RTP801, P-Akt (Ser473) and P-S6 (235/236) in the striatum of R6/1mice.....	137
Figure 44. Transduction efficiency of AAV-shCtr- and AAV-shRTP801-injected animals	138
Figure 45. Striatal RTP801 knockdown preserves motor learning in symptomatic R6/1 mice.....	139
Figure 46. Knockdown of RTP801 in the striatum of R6/1 mice does not alter P-mTOR (Ser2448) and P-S6 (Ser235/236)	140
Figure 47. Knockdown of RTP801 in the striatum of R6/1 mice prevents hyperphosphorylation of Akt at Ser473 by decreasing Rictor levels	141
Figure 48. Knockdown of RTP801 in the striatum of R6/1 mice enhances the expression of synaptic proteins.	143

Figure 49. RTP801 overexpression increases EVs release and produces EVs enriched in RTP801 in HEK293 cells. 147

Figure 50. RTP801 partially colocalizes with CD63-eGFP and is decreased in CD63-eGFP positive neurons 148

Figure 51. Depolarized cortical neurons release higher number of EVs but RTP801 is not present in the exosomal fraction 149

Figure 52. 6-OHDA treatment increases the release of exosomes from cortical neurons 150

Figure 53. RTP801 is present in the EV fraction of cortical primary cultures treated with 6-OHDA 151

Figure 54. Purified exosomes are internalized by recipient cortical neurons..... 152

Figure 55. Control-derived exosomes, but not 6-OHDA-derived, activate the mTOR/Akt survival signaling pathway in recipient neurons..... 153

Figure 56. 6-OHDA-induced RTP801 counteract EVs trophic effect in recipient neurons 155

Figure 57. Exosome treatment does not affect neuronal survival 156

Figure 58. RTP801 is increased in STHdh^{Q111/Q111} cells but is not enriched in exosomes 158

Figure 59. RTP801 upregulation in STHdh^{Q111/Q111} cells contributes to loss of exosomal trophic support. 160

Figure 60. Association of the SNPs rs356219 in *SNCA*, rs8111699 in *STK11*, rs456998 in *FCHSD1* and rs1732170 in *GSK3B* genes with PD risk..... 164

Figure 61. Association of the SNPs rs356219 in *SNCA*, rs11868112 in *RPTOR* and rs6456121 in *RPS6KA2* genes with PD AAO 167

Figure 62. Association of the SNPs rs1043098 in *EIF4EBP2*, rs2043112 in *RICTOR* and rs4790904 in *PRKCA* genes with LID onset..... 171

Figure 63. Association of the SNPs rs12628 in *HRAS*, rs5456121 in *RPS6KA2*, rs1292034 in *RPS6KB1* and rs456998 in *FCHSD1* genes with LID severity 174

Figure 64. RTP801 modulates mhtt-induced cell death..... 181

Figure 65. Proposed model of synaptic RTP801 increase in the putamen of HD patients 184

Figure 66. Proposed model of synaptic RTP801 increase in the striatum of HD murine 185

Figure 67. Comparison of RTP801 mechanistics over mTOR in PD and HD 187

Figure 68. RTP801 knockdown prevents corticostriatal learning deficits 189

Figure 69. RTP801 modulates trophic signals transneuronally through exosomes... 194

LIST OF FIGURES AND TABLES

Figure 70. Single SNP and SNP combinations modulate PD susceptibility and response to L-DOPA treatment.....	201
Figure A1. Distribution of high-risk and low-risk genotypes in the interaction of rs356219 in <i>SNCA</i> , rs8111699 in <i>STK11</i> , rs456998 in <i>FCHSD1</i> and rs1732170 in <i>GSK3B</i> with PD risk.....	269
Figure A2. Distribution of high-risk, early PD onset, and low-risk, late PD onset, genotypes in the interaction of rs11868112 in <i>RPTOR</i> , rs356219 in <i>SNCA</i> and rs6456121 in <i>RPS6KA2</i> with PD AAO	272
Figure A3. Association of the SNPs rs356219 in <i>SNCA</i> , rs11868112 in <i>RPTOR</i> and rs6456121 in <i>RPS6KA2</i> genes with PD age at onset (AAO) in LRKK2 PD patients	274
Figure A4. Distribution of high-risk, early LID onset, and low-risk, late LID onset, genotypes in the interaction of rs1043098 in <i>EIF4EBP2</i> , rs2043112 in <i>RICTOR</i> and rs4790904 in <i>PRKCA</i> with LID onset.....	275
Figure A5. Distribution of high-risk, moderate/severe LID, and low-risk, no/mild LID, genotypes in the interaction of rs1292034 in <i>RPS6KB1</i> , rs12628 in <i>HRAS</i> , rs6456121 in <i>RPS6KA2</i> and rs456998 in <i>FCHSD1</i> with LID severity.....	277

2. LIST OF TABLES

Table 1. Common familial PD-related genes and loci	53
Table 2. Compounds used for cellular treatments	95
Table 3. List of constructs used	98
Table 4. Primary antibodies used for immunofluorescence of cultured cells.....	101
Table 5. Primary antibodies used for WB analysis.....	104
Table 6. Human post-mortem HD brains.....	123
Table 7. Human post-mortem HD brains.....	127
Table 8. Allelic associations of SNPs rs356219 in <i>SNCA</i> and rs1800547 in <i>MAPT</i> with PD risk, adjusted by sex and age multiple testing by sex, age and multiple testing adjustments of <i>P</i> -values	163
Table 9. Genotypic association of SNPs with PD risk, adjusted by sex and age sex, age, and multiple testing adjustments of <i>P</i> -values	163
Table 10. MDR analysis of SNPs interactions with PD risk	164
Table 11. Genotypic association tests of <i>SNCA</i> rs356219 and <i>MAPT</i> rs1800547 SNPs with AAO of PD with gender, age and multiple testing adjustments of <i>P</i> -values	165
Table 12. MDR analysis of SNPs interactions with PD AAO	166
Table 13. Interaction of rs11868112 in <i>RPTOR</i> , rs356219 in <i>SNCA</i> and rs6456121 in <i>RPS6KA2</i> with PD AAO in mutant LRRK2 PD population.....	168
Table 14. Allelic association of SNPs with LID peak (TLP) and with LID onset (TTD)	170
Table 15. Genotypic association of rs1043098 genotypes in <i>EIF4EBP2</i> gene with LID Peak (TLP) and LID Onset (TTD).....	170
Table 16. MDR analysis of SNPs interactions with LID onset	171
Table 17. Allelic association of SNPs rs12628 in <i>HRAS</i> and rs1801582 in <i>PRKN</i> with LID	172
Table 18. MDR analysis of SNPs interactions with LID severity	173
Table 19. MDR forced analysis for the interaction between rs1292034 <i>RPS6KB1</i> , rs12628 <i>HRAS</i> , rs6456121 <i>RPS6KA2</i> and rs456998 <i>FCHSD1</i> with LID with severity as main variable	175
Table A1. Descriptive information of the SNPs in genes of the mTOR pathway selected for the analyses.....	265
Table A2. Genotypic association test of the SNPs in genes of the mTOR pathway selected for the analyses	267

LIST OF FIGURES AND TABLES

Table A3. Distribution of genotypes in the interaction of rs356219 in *SNCA*, rs8111699 in *STK11*, rs456998 in *FCHSD1* and rs1732170 in *GSK3B* with PD risk... 270

Table A4. Distribution of genotypes in the interaction of rs11868112 in *RPTOR*, rs356219 in *SNCA* and rs6456121 in *RPS6KA2* with PD AAO 273

Table A5. Distribution of genotypes in the interaction of rs1043098 in *EIF4EBP2*, rs2043112 in *RICTOR* and rs4790904 in *PRKCA* with LID onset 276

Table A6. Distribution of genotypes in the interaction of rs1292034 in *RPS6KB1*, rs12628 in *HRAS*, rs6456121 in *RPS6KA2* and rs456998 in *FCHSD1* with LID severity 278

INTRODUCTION

1. HUNTINGTON'S DISEASE AND PARKINSON'S DISEASE AS NEURODEGENERATIVE DISEASES

Neurodegenerative diseases are characterized by the progressive and selective loss of neuronal subpopulations and the appearance of aberrant synaptic transmission. Even though these disorders are diverse in their etiology and pathophysiology, all have in common that there are no treatments to completely prevent their progression. Neurodegeneration courses along with the clinical manifestations which can include motor and cognitive impairment and psychiatric symptoms. In this thesis we have focused on the study of common molecular mechanisms and targets altered in the basal ganglia disorders such as Huntington's disease and Parkinson's disease.

1.1 Huntington's disease

Huntington's disease (HD) was first described by George Huntington in 1872¹ and is the most common monogenic neurodegenerative disorder. HD has a variable prevalence between individuals of different geographical localizations and is more prevalent in Western populations. Of note, the prevalence in the Caucasian population is 10.6-13.7 cases per 100,000 individuals²⁻⁴.

HD clinical symptomatology is manifested with a triad of signs. Patients exhibit severe motor dysfunction, particularly characterized by involuntary movements (chorea), cognitive impairment and neuropsychiatric disorders. Onset generally occurs in the adulthood, between the fourth and the fifth decade, although approximately 5% of cases have a juvenile onset⁵. The fatal neurological deterioration progresses toward premature death 15-20 years after diagnosis⁶. At early stages of the disease, in addition to choreic movements in adult-onset HD patients, progressive gait instability and oculomotor disturbances emerge. During the progression, other somatomotor manifestations arise such as bradykinesia, ataxia, dystonia, dysarthria and dysphagia complicating the clinical course. Like motor impairment, cognitive and psychiatric symptomatology progress gradually. At late stages of the disease, patients become severely rigid and display irreversible dementing syndromes. Most frequently, HD patients finally die from complications of dysphagia, aspiration or pneumonia^{7,8}.

1.1.1 Etiology

HD is an autosomal dominant neurodegenerative disease characterized by a dynamic mutation on the chromosome 4p16.3^{9,10} of the *IT15* (*Interesting Transcript 15*) gene, which encodes for the huntingtin (htt) protein¹¹. The mutant gene contains an expansion of unstable trinucleotide repeat, cytosine-adenine-guanine (CAG), within the exon-1. Expanded CAG leads to a lengthening of the polyglutamine (polyQ) sequence located at the N-terminus of the htt protein and, as consequence, it exhibits toxic properties that eventually promote neuronal dysfunction and death (Figure 1). Mutant htt (mhtt) protein shows altered folding and higher propensity to aggregate and form fibrils and oligomers. Furthermore, htt protein can be subjected to several post-translation modifications including proteolytic cleavage, phosphorylation and myristylation. Proteolytic fragmentation through caspases, calpains and other endoproteases results in N-terminal fragments which contain the polyQ stretch¹²⁻¹⁶ and are prone to aggregate¹⁷⁻²⁰.

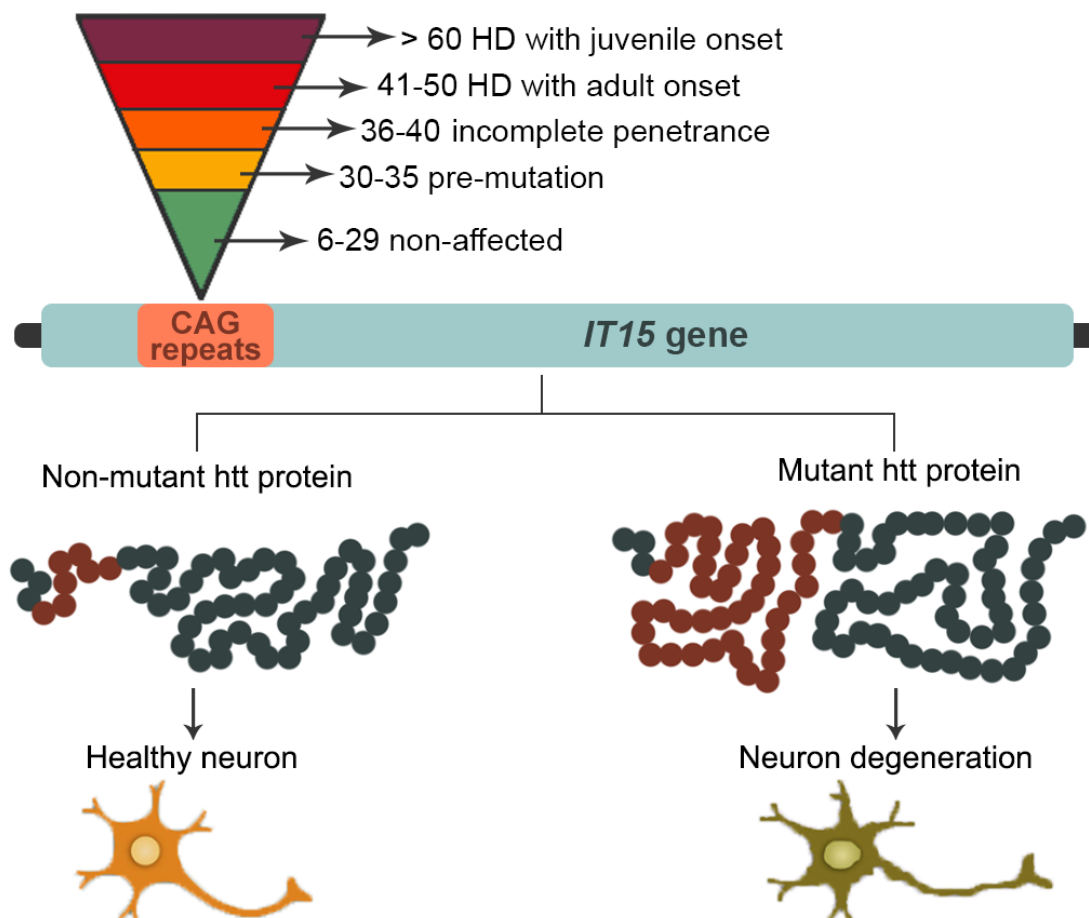


Figure 1. Representation of the *IT15* gene and the impact of CAG repeats on the onset of HD. Healthy individuals show between 6 to 35 CAG repeats, despite individuals with 29 to 35 CAG are at risk that descendants inherit the mutated form. Between 36 and 40 CAG repeats the penetrance of HD is incomplete. People with the adult-onset form of HD typically have 40 to 50 CAG repeats, and the juvenile onset is associated to those individuals with more than 60 repeats. The CAG repeat tract is translated into a polyglutamine stretch in the htt protein. Toxicity elicited by full-length mhtt or N-terminal fragments lead to neurodegeneration. Adapted from Rego A. & de Almeida L., et al. (2005)²¹.

Importantly, the number of CAG triplets has been related to the onset of the disease²²⁻²⁴. In the non-affected population, CAG repeats are in a range of 6 to 35 units, whereas HD patients display a number of repeats above 40. Moreover, CAG repeats between 36 and 39 units are considered of intermediate length and show incomplete penetrance, meaning that some of these individuals would manifest the disease while others would be unaffected. Indeed, there is an inverse correlation between the number of triplet repeats and the age at onset of the disease^{11,22,25}. Therefore, more units of CAG repeats cause earlier HD onset and higher severity of the symptomatology. Juvenile or early-onset HD is associated with more than 60 CAG repeat units, whereas adult-onset typically correlates with repeats of 40-50 units^{25,26}. Despite this inverse correlation, the number of CAG repeats only explains approximately the 56% of the variation in the age at onset of symptoms^{26,27}. Although the entire modifiers of age at onset are not well elucidated, genetic factors have been attributed to play a role in the interindividual variability. Accordingly, several candidate genes and single nucleotide polymorphisms (SNPs) of different pathways have been associated to the onset of symptoms but not with enough statistical strength (reviewed in ²⁷).

Interestingly, haplotypes in the *IT15* gene with different average of CAG repeats have been related to the prevalence variability between populations. For instance, the average of CAG repeats is higher in Europeans descendent population (18.4-18.7 repeats) than in Asian (17.5-17.7 repeats) or African (16.9-17.4 repeats) populations^{28,29}.

1.1.2 Neuropathology

Structural and functional brain alterations in HD occur before the onset of symptoms. Although *htt* is expressed ubiquitously in the body, some brain areas show enhanced susceptibility to the toxicity of the mutant form than other brain structures or even tissues. Striatal medium spiny neurons (MSNs) of the dorsal striatum, composed by caudate nucleus and putamen in humans, are the most vulnerable neuronal subpopulation^{30,31}. Even though *mhtt* toxicity severely affects striatal neurons, this is not the only neuronal subpopulation that undergoes neuronal degeneration during the disease. Atrophy and thinning of the cortex due to neuronal loss and shrinkage is another hallmark of the disease³². Other brain areas, including hippocampus, amygdala or cerebellum display neuronal atrophy and/or neuronal death depending on the disease stage^{33,34} (Figure 2A). The postmortem brain analysis reveals a different severity of striatal neurodegeneration which closely correlates with clinical and motor disability of the patients. In 1985 the neurologist Jean Paul Vonsattel developed a scale to grade the striatal neuropathology

in 5 grades from 0 (no anatomical abnormalities) to 4 (severe pathology) based on microscopic and macroscopic evidence (Figure 2B)³⁰.

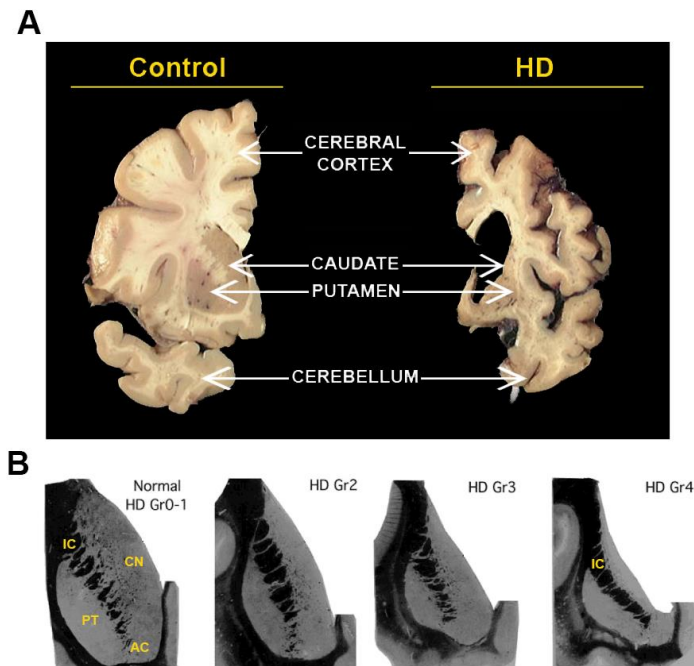


Figure 2. HD brain pathology. (A) Human brain coronal section showing a normal brain on the left and an advanced HD brain on the right. In the image representation the areas that undergo neurodegeneration are highlighted. Image obtained from Harvard Brain Tissue Resource Center (<https://hbtrc.mclean.harvard.edu/about/tour/slideview.php?page=41>). **(B)** Schematic illustrations representing progressive striatal neuropathology in the Vonsattel grade scale. Brain in grade 0 shows normal gross aspect, although 30-40% of neurons are already lost. The neuropathology progresses to grade 4 with progressive atrophy of first the caudate nucleus and then the putamen, along with astrogliosis and neuronal loss (95% in grade 4). Figure adapted from Rüb U., Vonsattel JP., Heinsen H. and Korft HW., et al. (2015)¹ and Reiner A., Dragatsis I., and Dietrich, P., et al. (2011)³⁵. Abbreviations: AC, nucleus accumbens; CN, caudate nucleus, IC, internal capsule; Gr; Vonsattel grade; HD, Huntington's disease; PT, putamen.

i. Basal ganglia pathophysiology in HD

The striatum is a key component of the basal ganglia circuitry. Basal ganglia consist of a variety of subcortical nuclei which control the motor function and learning, executive functions as well as behavior and emotions³⁶⁻³⁸. The main components of the circuitry that control the motor function are the dorsal striatum (caudate nucleus and putamen), the globus pallidus pars externa (GPe) and interna (GPi), the subthalamic nucleus (STN) and the substantia nigra pars compacta (SNpc) and pars reticulata (SNpr)³⁹. Additionally, the limbic functions are associated to other basal ganglia components that include the ventral striatum, specifically nucleus accumbens, ventral pallidum and ventral tegmental area. MSNs represent the 90-95% of total striatal neuronal population, and their excitability is modulated by interneurons which represent the remaining 5-10%^{40,41}. Striatum acts as a convergence point of activation by glutamatergic innervation from the cortex and dopaminergic projections from the SNpc. Regarding the intrinsic circuitry of the basal ganglia, two major striatal projections have been reported: a direct pathway

which project to GPi and SNpr and an indirect pathway which projects to SNpr through GPe and STN. The SNpc dopaminergic inputs are responsible for the balance maintenance between the direct and indirect pathway⁴² (Figure 3).

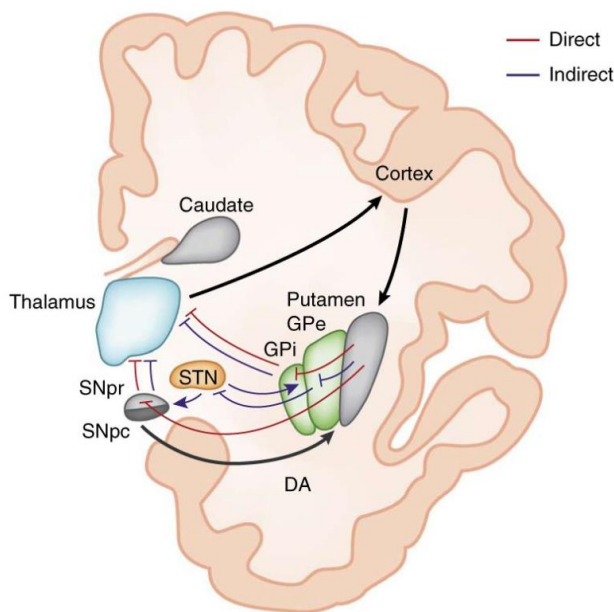


Figure 3. Simplified basal ganglia circuit diagram. The direct pathway is shown in red and the indirect path in blue. Abbreviations: DA, dopamine; GPe, globus pallidus pars externa; GPi, globus pallidus pars interna; STN, subthalamic nucleus; SNpr, substantia nigra pars reticulata, SNpc, substantia nigra pars compacta. Figure obtained from Calabresi P., et al. (2014)⁴³.

According to the canonical model, cortical activation induces the release of glutamate that activates MSNs projecting to the SNpr and GPi, which represents the direct pathway (Fig 3 in red). As GABAergic cells, MSNs exert an inhibitory action on their target neurons. The inactivation of SNpr lead to a disinhibition of the thalamic glutamatergic neurons which project and, thus, activate glutamatergic neurons in the cortex resulting in the facilitation of locomotor activity, gating of working memory and motor responses to specific stimuli. On the contrary, in the indirect pathway MSNs project to SNpr via the GPe and the STN (Figure 3 in blue). Through the activation of MSNs, GABAergic neurons of the GPe result inactivated which leads to a disinhibition of the glutamatergic neurons of the STN. Activation of STN, in turn, activates SNpr GABAergic neurons projecting to the thalamus. Finally, the activation of the indirect pathway results in the reduction of locomotor activity and thereby inhibition of specific motor programs based on associative learning (reviewed in ^{43,44}).

Furthermore, the two populations of MSNs that project to different target structures are characterized by differential expression of dopamine (DA) and acetylcholine receptors subtypes and peptide content⁴⁵. MSNs of the direct pathway express mainly dopamine D1 and muscarinic M4 receptors and colocalize with substance P, meanwhile MSNs of the indirect pathway express mainly dopamine D2 receptor and colocalize with enkephalin^{46–49}. The two dopamine receptors are associated with distinct G proteins that

INTRODUCTION

are linked to different intracellular signaling pathways and, therefore, different biochemical responses after DA activation. In fact, DA arising from the SNpc activates D1-expressing MSNs (direct pathway) and inhibits D2-expressing MSNs (indirect pathway)^{45,50,51}.

Importantly, MSNs of the indirect pathway are more vulnerable in early stages of HD pathogenesis and are the ones that degenerate earlier^{52,53}. Since in physiological conditions the indirect pathway inhibits the locomotor and voluntary motor activity, its degeneration leads to hyperkinetic and choreic movements. As the disease progresses, neurodegeneration affects MSNs of the direct pathway and motor symptoms evolve to hypokinetic movements and bradykinesia since this pathway is responsible for the activation of motor function^{50,54,55} (Figure 4). Other areas of this circuitry, specially GP and STN, also become atrophic during the progression of the HD pathogenesis³⁰.

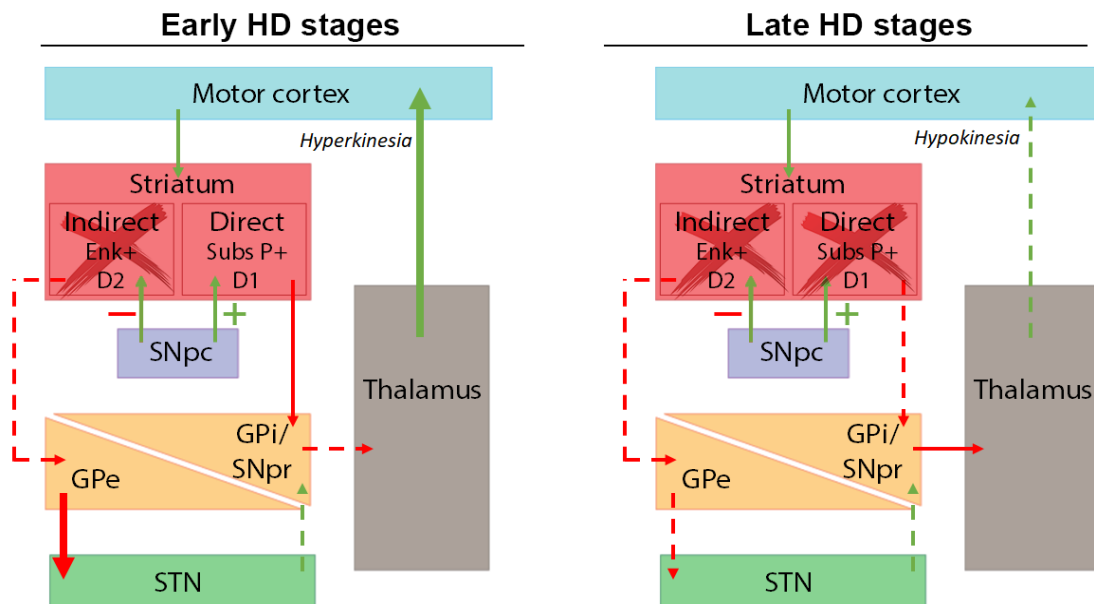


Figure 4. Basal ganglia circuitry in early and late stages of HD. Representation of basal ganglia activity at early (left panel) and late (right panel) of HD. At early stages of HD pathogenesis, MSNs of the indirect pathway that project to the GPe degenerate resulting in the inactivation of STN and the consequent disinhibition of the thalamus and finally increased stimulation of the motor cortex which results in chorea. Later in HD, MSN of the direct pathway that project to GPi also degenerate which enhances the inhibition of the thalamus and decreases the activation of the motor cortex, responsible for the hypokinetic phenotype. Dashed arrows indicate neurotransmitter signal loss, thick arrow enhance signal and thin arrow normal neurotransmitter signal. Abbreviations: GPe, globus pallidus pars externa; GPi, globus pallidus pars interna; STN, subthalamic nucleus; ENK, enkephalin; subs P, substance P. Figure adapted from Ramaswamy S., et al. (2007)⁵⁶.

1.1.3 Mechanisms underlying striatal neurodegeneration in HD

The presence of mhtt leads to multiple cellular dysfunctions which eventually triggers death of MSNs. These mechanisms include altered gene transcription, protein misfolding, impaired protein degradation, excitotoxicity, mitochondrial dysfunction and

neurotrophic and synaptic dysfunction. Recent studies suggest that neurodegeneration in HD results from combined effects of a gain of function in the mutated form of htt along with loss of function in the wild-type htt (reviewed in ^{57,58}).

i. Protein misfolding and aggregation

Inclusions of polyQ fragments are a key early step in the HD pathogenesis. Fragments can be detected in several HD mouse models as well as in human postmortem brains of affected individuals^{17,59–61}. Indeed, mhtt aggregates seem to precede the onset of symptoms in both transgenic mice and in human brain^{18,61}. Besides, mhtt is not only prone to aggregate by itself but also has the tendency to aggregate with other proteins^{62–64}, suggesting that mhtt additionally exerts its toxic properties by sequestering and impairing the function of others.

ii. Impaired protein degradation

Intracellular components have two main systems of degradation, the ubiquitin-proteasome system (UPS) and the lysosomal-autophagy system. The proteasome is responsible for rapid protein turnover, whereas autophagy typically degrades proteins with long half-life and other intracellular components such as organelles or lipid deposits^{65,66}. In HD, both systems are affected, triggering the accumulation and aggregation of proteins. Inclusions of mhtt colocalize with proteasome subunits^{67,68} as well as with components of the autophagy pathway^{69–72}. Importantly, autophagy is the main degradation pathway for aggregated proteins associated to neurodegenerative disorders^{72–74}. Pharmacological approaches that enhance autophagic activity have been shown to be protective in HD and to ameliorate symptoms in HD mouse models^{72,75}.

iii. Trans-synaptic spreading of mhtt

The aggregation of polyQ fragments through seeding suggest the possibility of mhtt cell-to-cell transmission^{76,77}. In fact, cells can efficiently take up small fibrils of polyQ proteins that can then recruit endogenous polyQ-containing proteins, such as htt exon-1, into aggregates and finally trigger cell death^{78,79}. Moreover, mhtt was found to be present in transplanted grafts of striatal tissue in different HD patients⁸⁰ which arises the hypothesis that mhtt can be spread between neurons. In fact, transneuronal spreading of mhtt has been demonstrated to occur in organotypic brain slices of an HD mouse model, in the corticostriatal pathway *in vivo*⁸¹, in the mouse brain⁸² and by exosomes in cell models^{82,83}.

iv. Transcriptional dysregulation

Transcription dysregulation is a central pathogenic mechanism in HD⁸⁴ which may occur before the onset of symptoms⁸⁵. On one hand, mhtt interacts abnormally with several nuclear proteins and transcription factors, recruiting them into polyQ aggregates and inhibiting their transcriptional activity^{57,58,84}. Some examples of this aberrant regulation are p53^{63,86}, TATA-binding protein⁶⁴, cyclic-adenosine monophosphate response element-binding protein (CREB)^{63,64}, specificity protein 1 (SP1)^{87,88} and TATA-binding protein-associated factor II130 (TafII130)⁸⁸. On the other hand, mhtt can fail to interact with other transcription factors such as repressor-element-1 transcription factor–neuron-restrictive silencer factor (REST-NRSF). REST-NRSF binds to DNA elements in neuronal genes promoters like in the *brain-derived neurotrophic factor (BDNF)* gene and represses their expression. Wild-type htt interacts with this transcription factor in the cytoplasm, thereby reducing its availability in the nucleus to repress transcription. Conversely, mhtt fails to interact with REST-NRSF, therefore the transcription factor is translocated into the nucleus and represses the expression of neuronal-specific genes including *BDNF*⁸⁹. Furthermore, mhtt also interferes in chromatin structure blocking the activity of histone acetyltransferase enzymes that open chromatin for transcription^{90,91}.

v. Neurotrophic dysfunction

Neurotrophins are growth factors that promote the development and survival of neurons and induce the activation of survival signaling pathways⁹². Among neurotrophins, BDNF has emerged as a major regulator of synaptic activity and neuronal survival^{93,94}. Indeed, deficiencies in BDNF-mediated signaling are sufficient to cause dendritic abnormalities and neuronal loss in the cortex and striatum^{95,96} and, particularly, striatal neurons are highly dependent on BDNF supply for their function and survival^{95,97,98}. In HD, BDNF downregulation is a widespread phenomenon in different brain regions of HD mouse models and in human HD patients^{99,100}. Moreover, BDNF levels regulate the onset and severity of cognitive and motor symptoms in HD mouse models^{101–103} and treatments focused on BDNF levels recovery improve cognitive and motor function as well as striatal neuronal survival^{101,104–108}.

The action of BDNF, among the other neurotrophins, is mediated by the Tropomyosin-receptor kinase (Trk) proteins. BDNF preferentially binds to TrkB receptor and to the p75 neurotrophin receptor (p75^{NTR}). To mediate its functions, BDNF firstly binds to the receptor causing the dimerization of homo- and/or heterodimers between TrkB and p75^{NTR} receptors and the autophosphorylation of their cytoplasmic domains^{109,110}. The homodimerization of TrkB activates different signaling cascades, including the PI3K-Akt,

Ras-MAPK and PLC γ -PKC, which results in neuroprotective signals^{111,112}. In contrast, the role of p75^{NTR} in the nervous system has been shown to be more complex depending on the receptor dimerization. p75^{NTR} homodimerization activates pro-apoptotic signals in the nervous system^{109,113–115}, whereas heterodimerization of p75^{NTR} can also act as a co-receptor along with Trk and signal for neuronal survival^{116–119}. Of note, reduced TrkB expression has been reported in HD cellular and mouse models as well as in HD patients^{100,120,121}. Moreover, p75^{NTR} mRNA and protein levels are diminished in different cellular and animal models of HD and in affected brain areas of HD patients^{100,122–124}. Consequently, p75^{NTR}/TrkB receptor imbalance along with decreased BDNF support increase the striatal vulnerability and both contribute to neurodegeneration.

1.1.4 Treatment of HD

Currently, there is no therapy that modifies the course of the disease or prevents its onset. In consequence, the management of HD is mainly focused on treating symptoms. The only drug specifically licensed by the US Food and Drug Administration (FDA) in HD patients is tetrabenazine, which is indicated to treat the chorea associated to the disease. Tetrabenazine reversely inhibits vesicular monoamine transporter 2, resulting in a reduced uptake of monoamines (dopamine, serotonin, norepinephrine and histamine) into synaptic vesicles¹²⁵. Neuropsychiatric symptoms of HD are treated with non-specific HD drugs, such as antidepressants or antipsychotics, which are also occasionally administered to manage involuntary movements (reviewed in¹²⁶). Physical and occupational therapies are also recommended to ameliorate the symptoms and help patients to cope.

Strategies to silence mhtt expression or block the protein product have been recently proposed as therapeutic treatment for HD¹²⁷. Currently, two ongoing clinical trials include the use of antisense oligonucleotide targeting the pre-mRNA transcript of hhtt, the first one being allele nonselective and the second, being allele specific, with the final goal of reducing the production of mhtt protein^{128,129}.

1.2 Parkinson's disease

Parkinson's disease (PD) was first described in 1817 by the neurologist James Parkinson^{130,131} who reported the main clinical features which later were redefined by Jean-Martin Charcot¹³¹. Worldwide prevalence of PD trends to increase with age, suggesting that age is the greatest risk factor for PD. Thus, PD prevalence is estimated in 41 per 100,000 in individuals of 40 to 49 years; 173 per 100,000 in individuals of 55 to 64 and 1,903 per 100,000 individuals over age 80¹³². These data reveal PD as the second most common neurodegenerative disorder after Alzheimer's disease (AD).

Most of PD cases are idiopathic since its cause is unknown. However, a percentage between 5 and 10% of PD cases are considered familial (or monogenic) because they are caused by mutations in specific genes which are inherited¹³³⁻¹³⁵. Whereas in idiopathic PD the onset is after 60 years, in monogenic PD the onset is normally before the fifth decade^{133,134}. For this reason, some forms of familial PD are also mentioned as young-onset PD.

The classical parkinsonian motor symptoms include bradykinesia, muscular rigidity, rest tremor, postural and gait impairment, flexed posture and freezing. The clinical diagnosis of PD is established by the presence of at least two of these motor symptoms, being one of them bradykinesia or tremor at rest, and the absence of absolute exclusion criteria^{135,136}. Although the diagnosis is made in base of motor alterations, non-motor symptoms are also common in PD and are associated with impaired quality of life^{137,138}. Non-motor signs include autonomic dysfunction, olfactory dysfunction, cognitive impairment, psychiatric symptoms, sleep disorders, pain and fatigue^{135,137,139,140}. These symptoms are also frequently exhibited before the onset of motor symptoms. This premotor or prodromal stage can be prolonged for 12-20 years before the final diagnosis of PD (Figure 5). Dementia and depression also occur in advanced stages of the disease since 75-80% and 40% of patients, respectively, experienced them during the neuropathological progression^{141,142}.

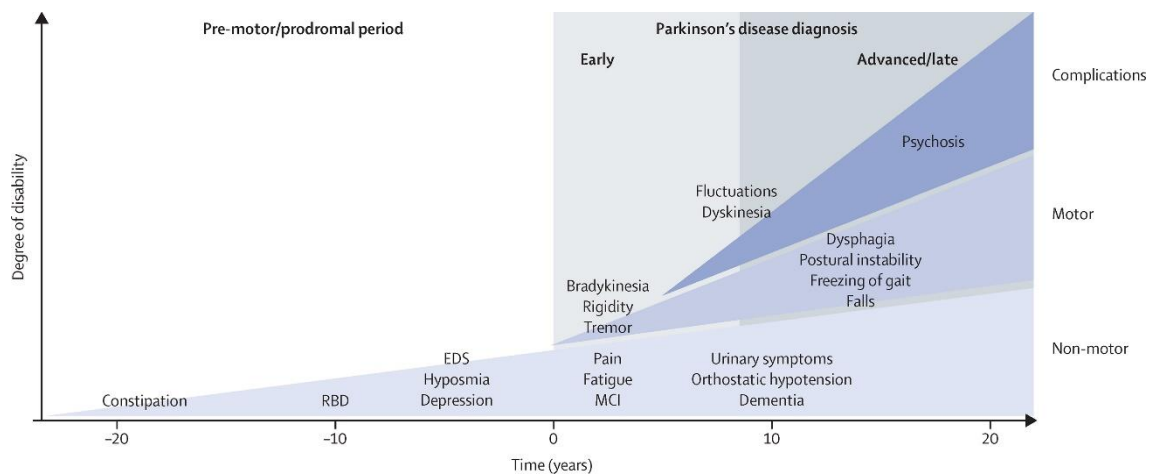


Figure 5. Clinical symptoms and time course of PD progression. Diagnosis of PD occurs with the onset of motor symptoms (time 0 years), but it is usually preceded by a premotor period characterized by non-motor symptoms. As the disease progress, non-motor and motor symptoms are developed causing clinically disability. Complications of long-term therapy dopamine replacement also contribute to disability. Abbreviations: EDS, excessive daytime sleepiness; MCI, mild cognitive impairment; RBD, REM sleep behavior disorder. Obtained from Kalia L.V. and Lang A.E., et al. (2015)¹³⁵.

1.2.1 Etiology

PD is idiopathic in a 90-95% of cases and the etiology in this high percentage of patients is unknown. Nowadays, it is widely accepted that PD is a multifactorial disease which combines environmental risk factors, genetics and aging (Figure 6). Actually, aging is the strongest risk factor for the development of PD and both prevalence and incidence increase nearly exponentially with age^{3,135}. Gender is another well-established risk factor, being males more often affected than females with a ratio of approximately 3:2¹⁴³⁻¹⁴⁵.

Other PD risk factors include environmental exposures. Factors that increase the risk of suffering PD are pesticide exposure, prior head injury, rural living, β -blocker use, agricultural occupation and well-water drinking. Otherwise, some environmental factors such as coffee drinking, non-steroidal anti-inflammatory drugs use, calcium channel blocker use or alcohol or tobacco consumption (decreased responsiveness to nicotine) are associated to reduced risk of PD^{135,146-148} (Figure 6 in blue).

Genetics also play an important role modulating the risk and the onset of PD, and several haplotypes, or in some cases mutations, of genes have been associated to increase or reduce the risk of PD. For instance, one of the greatest genetic risk factors identified are mutations in *GBA* gene which encodes the lysosomal enzyme β -glucocerebrosidase. *GBA* mutations increase the risk of developing PD¹⁴⁹⁻¹⁵³ and enhances the PD susceptibility approximately 5-fold^{149,150}. SNPs in *SNCA*¹⁵⁴⁻¹⁵⁸, *LRRK2*¹⁵⁹⁻¹⁶² and *MAPT*^{155,156,158,163-165} genes have also been linked to increase risk of PD or PD age at onset in the case of *SNCA* gene¹⁶⁶⁻¹⁶⁸ (Figure 6 in red).

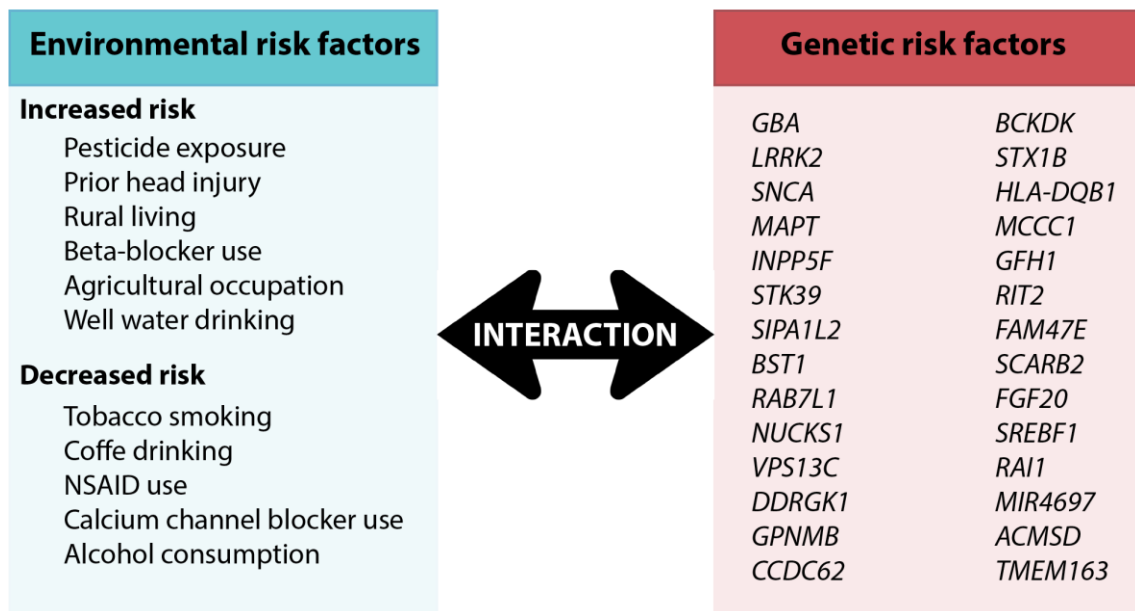


Figure 6. Risk factors for PD development. Epidemiological studies have revealed several environmental exposures that increase or decrease the risk of PD (in blue, left panel). Genome-wide association studies have also identified genetic variants which polymorphisms modulate the risk of PD (in red, right panel). Adapted from Kalia L.V. and Lang A.E., et al. (2015)¹³⁵.

The other 5-10% of PD cases are attributed to genetic mutations and are thereby monogenic forms of the disease^{134,135,169}. At least, 22 loci in different genes are associated to PD with classic mendelian inheritance and of these out six are unequivocally linked to PD inheritance (Table 1). Those mutations that trigger the onset of the disease between 20 and 50 years are considered early-PD onset. *SNCA* which encodes for alpha(α)-synuclein, was the first gene to be associated with familial PD. Mutations in *LRRK2* (*LRRK2* protein) and *PRKN* (*parkin* protein) are the most common causes of dominant and recessive monogenic PD, respectively^{134,135}. The functional characterization of the protein products of PD-related genes have raised the knowledge that mitochondrial dysfunction and impaired protein or organelle degradation play key roles in the neurodegeneration process associated to PD.

Loci	Gene	Protein	Inheritance	Age at onset
PARK1	<i>SNCA</i>	α -synuclein	AD Rarely sporadic	Early Rarely Late
PARK2	<i>PRKN</i>	Parkin E3 ubiquitin ligase	AR sporadic	Early
PARK3	Unknown	Unknown	AD	Late
PARK4	<i>SNCA</i>	α -synuclein	AD Rarely sporadic	Early Rarely Late
PARK5	<i>UCHL1</i>	Ubiquitin C-terminal hydrolase L1	AD	Late
PARK6	<i>PINK</i>	PTEN-induced kinase	AR	Early
PARK7	<i>DJ-1</i>	DJ-1	AR	Early
PARK8	<i>LRRK2</i>	Leucine-rich repeat kinase 2	AD sporadic	Late
PARK9	<i>ATP13A2</i>	Cation-transporting ATPase 13A2	AR	Early
PARK10	Unknown	Unknown	Unclear	Unclear
PARK11	<i>GIGYF2</i>	GRB10 interacting GYF protein 2	AD	Late
PARK12	Unknown	Unknown	Unclear	Unclear
PARK13	<i>Omi/HTRA2</i>	Serine peptidase 2	AD	Late
PARK14	<i>PLA2G6</i>	Phospholipase A2, group 6	AR	Early
PARK15	<i>FBXO7</i>	F-box protein 7	AR	Early
PARK17	<i>VPS35</i>	Vacuolar protein sorting 35	AD	Late
PARK18	<i>EIF4G1</i>	Eukaryotic translation initiation factor 4 gamma, 1	AD	Late
PARK19	<i>DNAJC6</i>	DNAJ subfamily C member 6	AR	Early
PARK20	<i>SYNJ1</i>	Synaptojanin-1	AR	Early
PARK21	<i>SNAJC13</i>	DNAJ subfamily C member 13	AD	Early
PARK22	<i>CHCHD2</i>	Coiled-coil-helix-coiled-coil- helix domain 2	AD	Late
PARK23	<i>VPS13C</i>	Vacuolar protein sorting 13C	AR	Early

Table 1. Common familial PD-related genes and loci. Early PD onset is considered between 20-50 years-old and late PD onset after 50 years. Abbreviations: AD, autosomal dominant; AR, autosomal recessive. Adapted from Karimi-Moghadam A., et al. (2018)¹³⁴.

1.2.2 Neuropathology

The crucial pathological hallmark of PD is the loss of dopaminergic neurons within the SNpc. As a remarkable feature, the vast majority of these neurons contain a cytoplasmic conspicuous dark pigment termed neuromelanin¹⁷⁰. Consequently, the loss of nigral neurons results in the SNpc depigmentation which is a classical neuropathological observation (Figure 7). Indeed, the degree of depigmentation correlates proportionally with the neuronal loss as well as with the PD severity¹⁷¹.

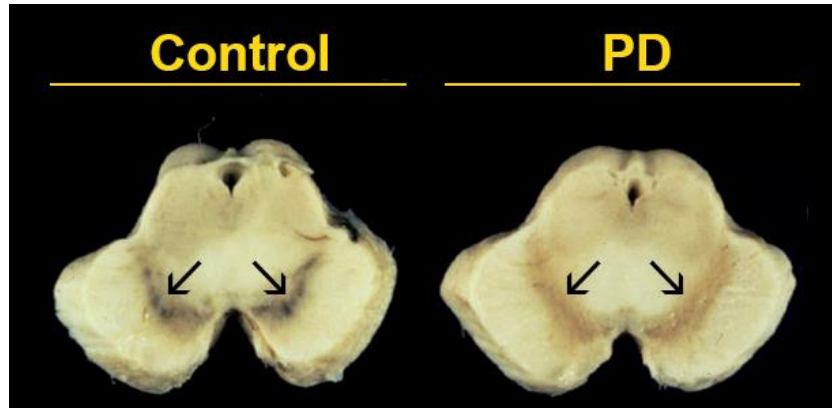


Figure 7. Coronal section through the midbrain of a control and a PD patient. Arrows indicate SNpc brain area. Loss of neuromelanin pigmentation in the PD specimen underlying nigral dopaminergic degeneration. Image adapted from <http://www.angelfire.com/art3/parkinsonsvoice/page3.html>

Dopaminergic neuronal bodies at the SNpc project to the dorsal putamen of the striatum assembling the nigrostriatal pathway responsible for movement control. Degeneration of dopaminergic neurons eventually leads to a considerable reduction of DA support to the putamen triggering the onset of parkinsonian motor symptoms¹⁷². Specifically, at early stages of the disease approximately 60% of DA neurons in the SNpc have been lost and 80% of DA has been depleted in the putamen^{173,174}. The mesolimbic dopaminergic neurons are much less affected in PD^{173,175} and, consequently, DA reduced supply in the caudate is less significant¹⁷³. Despite the critical degeneration in the SNpc, neuronal loss also occurs in other brain regions, including the locus coeruleus, nucleus basalis of Meynert, raphe nucleus, dorsal motor nucleus of the vagus, amygdala, and hypothalamus¹⁷⁶. Pathology is not restricted to the brain but can also be found in the spinal cord and peripheral nervous system, including the vagus nerve, sympathetic ganglia, cardiac plexus, enteric nervous system, salivary glands, adrenal medulla, cutaneous nerves and sciatic nerve, all leading to dysautonomia¹⁷⁷⁻¹⁸².

Another important hallmark of PD is Lewy pathology. Protein aggregation is a common feature in neurodegenerative disorders, and in PD the most abundant protein associated to these inclusions is α -synuclein^{183,184}. In a misfolded state, α -synuclein becomes insoluble and aggregates to form intracellular inclusions within the neuronal cytoplasm,

Lewy bodies (LBs) and processes, Lewy neurites¹⁸⁵ (Figure 8A). Lewy pathology can also be found in the spinal cord and different structures of the peripheral nervous system¹⁸⁵. LBs are found in 10% of pigmented neurons in the SNpc and more than 50% of those in the locus coeruleus¹⁸⁶.

Lewy pathology has been hypothesized to progress in a stereotyped pattern from the peripheral to the central nervous system in a caudal-to-rostral direction over PD pathogenesis. Braak et al. (2004) proposed six different progressive stages which temporally and spatially correlate with the clinical course of PD¹⁸⁷. Stages 1 and 2 would correspond with the pre-motor or prodromal phase, stage 3 with the onset of motor symptoms and stages 4-6 would correlate with the non-motor symptoms associated to advanced stages of the disease (Figure 8B). Recent hypotheses also suggest that α -synuclein plays a key role in transmitting the disease pathology transcellularly between susceptible neuronal populations in a prion-like process¹⁸⁸.

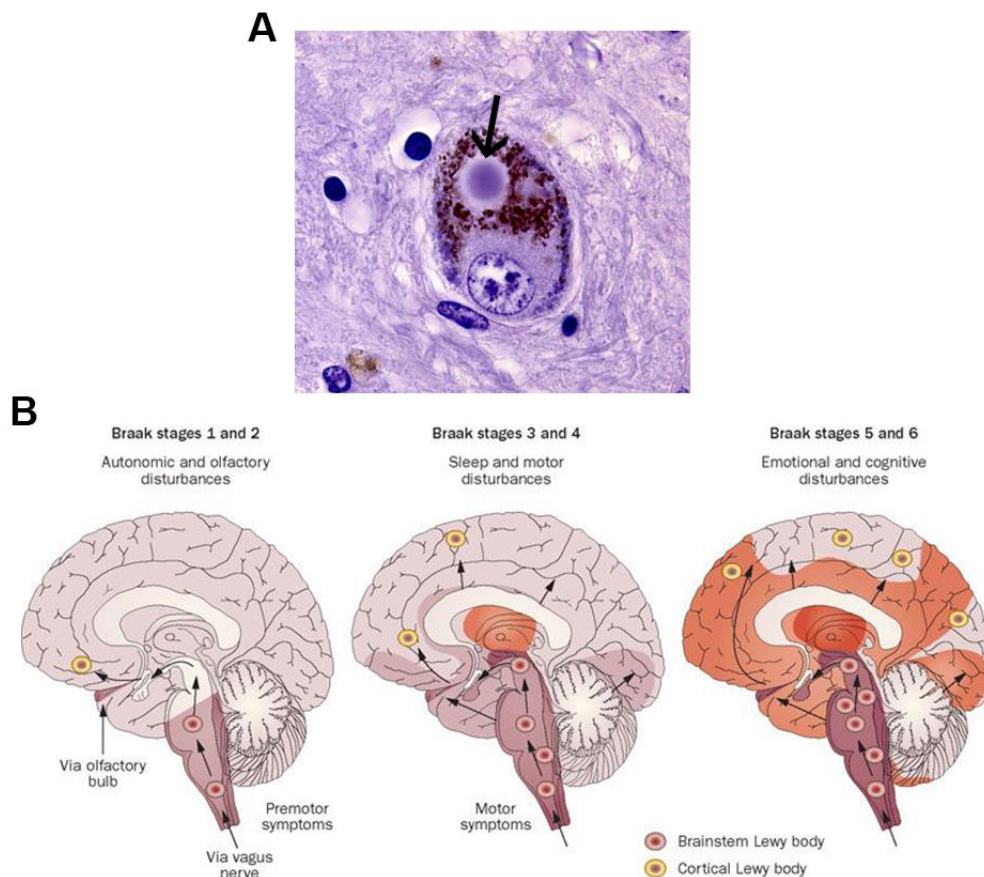


Figure 8. Lewy pathology in PD. (A) Lewy body presence in a dopaminergic neuron. Lewy bodies generally measure between 5-25 μ m in diameter and are characterized by a spherical dense hyaline core surrounded by a clear halo. Arrow indicates a Lewy body in a neuromelanin (brown dark pigmentation) positive dopaminergic neuron. Image adapted from <http://neuropathology-web.org/chapter9/chapter9dPD.html>. **(B) Illustration of Braak staging in PD.** According to his hypothesis, Lewy body pathology appears first in the olfactory bulb and brainstem regions. As the disease progresses, pathology spreads to the midbrain and basal forebrain before finally reaching the cortex. Image adapted from <https://media.nature.com/full/nature-assets/nrneurol/journal/v8/n6/images/nrneurol.2012.80-f1.jpg>.

i. Basal ganglia pathophysiology in PD

The basal ganglia circuitry receives signaling inputs from both glutamatergic neurons of cortex and dopaminergic neurons of SNpc. These dual glutamatergic and dopaminergic projections converge onto dendritic spines of the same striatal MSN to regulate movement execution (Figure 3).

In PD, degeneration of nigral neurons reduces DA receptor stimulation in the putamen which leads to an imbalance between the direct and indirect pathways. As stated before (section 1.1.2i) neurons from the direct and indirect pathway express different DA receptors subtypes. MSNs of the direct pathway express preferentially D1 receptor which enhances corticostriatal transmission, meanwhile activation of D2 receptor in MSNs of the indirect pathway prevents their cortical activation^{50,51}. Hence, DA deficiency in PD leads to a decreased activation of the direct pathway and to a hyperactivation of the indirect pathway. This imbalance inhibits the thalamocortical signaling activation leading to parkinsonian motor symptoms (Figure 9).

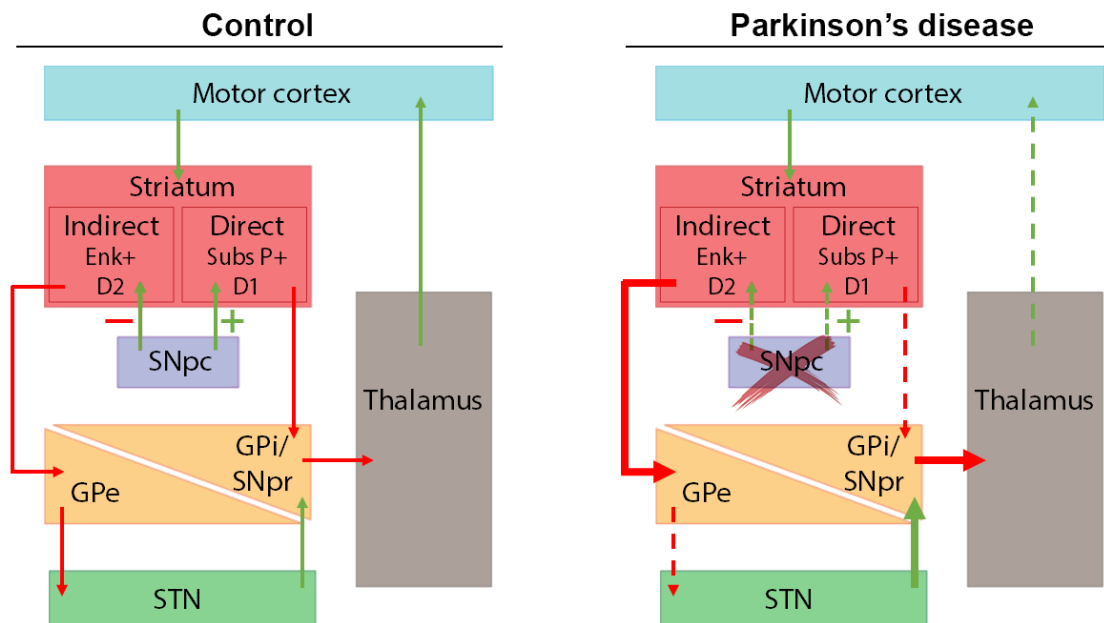


Figure 9. Basal ganglia circuitry in PD. Representation of basal ganglia circuitry in physiological conditions (left panel) and in PD due to SNpc neuronal loss (right panel). Neurodegeneration of DA neurons triggers enhance activation of the indirect pathway and, as consequence, STN inhibition is reduced. In parallel, DA support to MSN of the direct pathway decreases their activation which in turn enhances the inhibition of the thalamus and decreases the activation of the motor cortex. This reduced activation is responsible for parkinsonian motor symptoms. Dashed arrows indicate neurotransmitter signal loss, thick arrows enhance signal and thin arrows normal neurotransmitter signal. Abbreviations: GPe, globus pallidus pars externa; GPi, globus pallidus pars interna; STN, subthalamic nucleus; ENK, enkephalin; subs P, substance P. Figure adapted from Wichmann T., DeLong M.R., Guridi J. & Obeso J.A., et al. (2007)⁴².

1.2.3 Mechanisms underlying dopaminergic neurodegeneration in PD

Diverse potential mechanisms have been implicated in PD pathogenesis, even so, the cause underlying neuronal death remains poorly understood. To date, impairment in cellular processes involved in the regulation of protein homeostasis including protein misfolding and aggregation, protein degradation and intracellular and transcellular trafficking have been described. Moreover, aberrant synaptic structure along with mitochondrial dysfunction and oxidative stress are also involved in the nigral loss (reviewed in ^{135,173,189}).

i. Protein misfolding and aggregation

Aggregation of proteins has been associated to PD pathogenesis since LBs were found in affected brain regions^{183,187}. Besides α -synuclein as the main component of LBs, many other proteins belonging to up to ten different protein families have been shown to aggregate in PD¹⁸⁶. Protein aggregates that cannot be cleared out by the neuron can hamper its physiology eventually leading to degeneration^{190–192}.

ii. Impaired protein degradation

The presence of misfolded proteins points out a deficient protein degradation. As it has been shown in the pathology of HD (section 1.1.3ii), protein degradation is mediated by two pathways involving the UPS and autophagy-lysosomal system, and both are also affected in PD. Concerning the proteasome, many components of this complex have been found in LBs^{186,193,194}. Moreover, pharmacological inhibition of the system promotes the formation of α -synuclein inclusions and induces dopaminergic neuronal death^{195–198}. In PD patients, proteasome structure and activity is selectively altered in several brain areas, including the SNpc^{193,194}.

Regarding the autophagy-lysosomal pathway it is crucial to maintain synaptic function since neurotransmission requires a fine-tuned regulation of synaptic vesicles recycling and degradation¹⁹⁹ through the endosomal system. Interestingly, changes in the activity on endo-lysosomal enzymes are found in the cerebrospinal fluid (CSF) of idiopathic PD patients²⁰⁰. Additionally, autophagy clears out selective cellular structures and its impairment induces the gathering of abnormal proteins and damaged organelles^{201,202}. Of note, accumulation of autophagic vacuoles are observed in the SNpc of PD patients^{203,204}. Autophagy is important for α -synuclein degradation and, conversely, mutant forms of the protein can hamper the autophagy-lysosomal pathway. The

protective role of autophagy in PD is further supported by a delay in dopaminergic neurodegeneration when autophagy is enhanced in cell and animal models^{205–207}.

iii. Trans-synaptic spreading of α -synuclein

Evidences from four separate cases of PD patients who received transplants of embryonic mesencephalic neurons into their putamen showed LB inclusions within the grafted neurons, 15-20 years after the procedure^{208–210}. This finding suggests that spreading of PD pathology could be mediated by a prion-like transmission of α -synuclein between neurons. Moreover, injection of α -synuclein fibrils into various brain regions of mice leads to the formation of LB-like inclusions^{211–213}. Injection of LB-enriched homogenates from the SNpc of PD patients into SN or striatum of mice or macaque monkeys also causes the progressive nigrostriatal neurodegeneration²¹⁴. Furthermore, α -synuclein spreading may be mediated by different pathways, including perforation of the plasma membrane²¹⁵, tunneling nanotubes^{216,217} and exosomes^{218–220}.

iv. Mitochondrial dysfunction and oxidative stress

Abnormal function of the mitochondria has been proposed as a pathogenic mechanism in PD²²¹. Mitochondria dysfunction results in insufficient ATP production and reactive oxygen species (ROS) generation. Remarkably, findings revealed decreased activity of the mitochondrial complex I in the SNpc of PD patients²²². Mutations underlying monogenic PD confirm the importance of a proper mitochondria function. Parkin and PINK1 are implicated in mitophagy once the organelle is damaged^{223,224}, whereas DJ-1 protects mitochondria from oxidative stress^{225,226}. Furthermore, exposure to neurotoxins reported to affect mitochondria, such as 1-methyl-4-phenyl-1,2,3,6-tetrahydropyridine (MPTP) or 6-hydroxydopamine (6-OHDA), mimics several PD features^{227–229}.

Mitochondrial dysfunctions are not the only source of ROS generation. In addition, DA metabolism and autoxidation can also generate different ROS species, all leading to a state of oxidative stress that finally affects dopaminergic viability^{230,231}. To this end, many biological markers linked to oxidative stress are upregulated in the SNpc of PD patients, while the levels of antioxidants are reduced^{232,233}.

Besides the aforementioned pathological mechanisms, neuroinflammation, calcium deregulation and impaired kinase signaling mediate also toxicity, which finally leads to aberrant synaptic transmission and dopaminergic neuronal death in PD.

1.2.4 Treatment of PD

Up to now, no therapy has demonstrated to be effective in preventing neuronal loss, therefore PD treatment is focused on counteract motor and non-motor symptoms. Current therapies are classified in three groups: medication, surgery and physical therapy²³⁴.

Pharmacological treatment of PD does not slow or stop the underlying neurodegenerative process and is targeted at symptomatic relief. Treatment of motor signs is based on DA replacement therapy and drugs that enhance intracerebral DA concentrations or stimulate DA receptors are used. These drugs include levodopa (L-DOPA), which is the immediate precursor of DA, dopamine agonists, monoamine oxidase B (MAO-B) inhibitors and, less commonly, amantadine²³⁵. They can be administered alone or in combination to improve efficacy and reduce side effects^{235,236}. Currently, levodopa remains the most effective pharmacological treatment in PD, but long-term use is associated with motor complications (dyskinesia and motor fluctuations) which appear in almost half of PD patients after 5 years of L-DOPA treatment^{174,234}. To delay the onset of these side effects, DA agonists and MAO-B inhibitors are usually considered. However, DA receptor agonist can potentiate the development of hallucinations and impulsive control disorders^{235,236}.

The progression of L-DOPA treatment includes increasing frequency and dosages over the disease. The course of treatment is often characterized by “on” periods, where patients experience a good response to medication, and “off” periods, where symptoms re-emerge due to fluctuations in DA concentrations. Moreover, peak DA levels can lead to dyskinesia which is characterized by involuntary and choreic movements and it can be as disabling as parkinsonian classical symptoms (Figure 10). To reduce fluctuations in DA levels, levodopa is combined with DA agonists or inhibitors of MAO-B or catechol-O-methyltransferase (COMT) to enhance its half-life²³⁶.

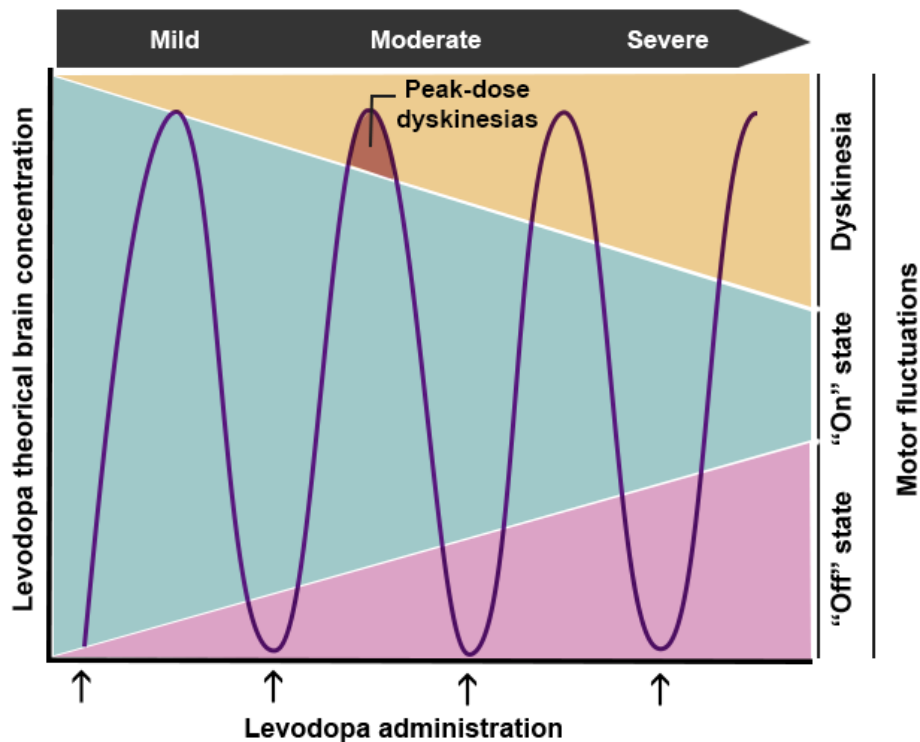


Figure 10. Motor fluctuations and dyskinesia induced by levodopa treatment in PD patients. Long-term levodopa intake induces motor fluctuations which are composed by an "on" state in which motor function is restored (blue, therapeutic window) and an "off" state in which parkinsonian symptoms reappear (pink). As PD progresses the therapeutic window for levodopa narrows and dyskinesia emerges as a side-effect of the drug treatment. Image adapted from <http://memobik.tk/behe/levodopa-parkinson-disease-jyx.php>.

In those patients whose parkinsonian motor symptoms respond to L-DOPA but whose motor fluctuations and dyskinesia become disabling, deep brain stimulation is an optional surgical treatment. Deep brain stimulation of either the STN or the GPi has been shown to be effective in moderate-to-severe PD²³⁷. Other non-motor features can also improve with deep brain stimulation, although further studies are needed²³⁸.

i. Levodopa-induced dyskinesia

Half of the patients that receive DA replacement therapy develop L-DOPA-induced dyskinesia (LID) after 3-5 years the onset of pharmacological treatment, and this percentage increases up to nearly 90% after 10 years²³⁹. The molecular mechanisms that trigger the onset of LID are still unclear. Emerging evidence suggests that the loss of nigral dopaminergic neurons induces synaptic plasticity abnormalities in the connectivity between the striatum and the motor cortex, establishing a disturbance in basal ganglia circuitry that can eventually lead to the onset of involuntary and choreic movements. Several molecular alterations affecting the presynaptic and postsynaptic neurons have been described (reviewed in ^{240–242}) but, nonetheless, the complete

knowledge of how neuronal striatal signals give rise to dyskinesia is far from being understood (Figure 11).

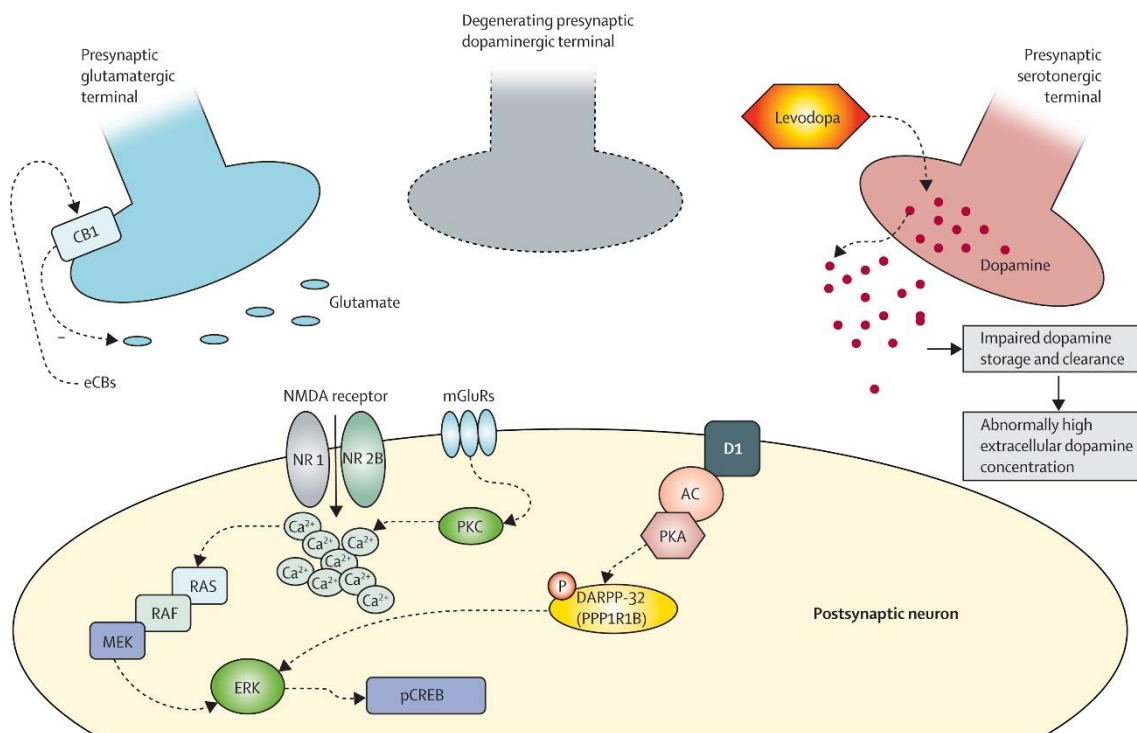


Figure 11. Major molecular mechanisms underlying LID. LID symptomatology may reflect maladaptive neuronal plasticity occurring both at presynaptic and postsynaptic compartments. At the presynaptic level, the degeneration of DA neurons (in grey) increases the role of serotonergic terminals (in red) which mediates levodopa conversion to DA. Besides, the storage and clearance of exogenously derived striatal DA are impaired, leading to fluctuations in extracellular DA. Two other potentially presynaptic mechanisms involve endocannabinoid CB1 receptor and metabotropic glutamate receptors expressed in glutamatergic terminals. Endocannabinoids reduce glutamate release from glutamatergic neurons into the striatum. At the postsynaptic level, different molecular alterations are involved, including downstream cascades triggered by NMDA receptor activation (by receptors expressing NR2B subunits), D1 receptors and metabotropic glutamate receptors (mGluRs). Downstream receptor signaling increases intracellular calcium concentrations that in turn modulate ERK pathway, whose activation results in several different physiological outcomes. Abbreviations: AC, adenylyl cyclase; Ca^{2+} , calcium ion; CB1, endocannabinoid receptor 1; pCREB, cAMP response element-binding protein; D1= D1 DA receptor; PPP1R1B, protein phosphatase 1, regulatory (inhibitor) subunit 1B; eCB, endogenous cannabinoid; ERK, extracellular signal-regulated kinase; Glu, glutamate; mGluR, metabotropic glutamate receptor; PKA, protein kinase A; PKC, protein kinase C. Figure obtained from Calabresi P., et al. (2010)²⁴³.

At a clinical level, different scales are used to assess LID severity but one of the most commonly applied is the unified Parkinson's disease rating scale section IV (UPDRS-IV)²⁴⁴. Accordingly, LID severity is categorized as "0" (no LID), "1" (slight or very mild LID; $\leq 25\%$ of on-time), "2" (mild LID; 26-50% of day-time), "3" (moderate LID; 51-75% day-time), and "4" (severe LID; $\leq 75\%$ of day-time). Nevertheless, the onset and severity of LID display a huge variability between PD patients.

INTRODUCTION

There are many epidemiological factors responsible for LID (reviewed in ²⁴⁵). Levodopa dosage and longer duration of treatment are key factors for developing dyskinesia. Moreover, PD age at onset and duration of the disease also arise as important risk factors. At a genetic level, polymorphisms of dopamine receptors, *DRD2*, dopamine transporter, *SL6CA3*, and *BDNF* genes have been identified as risk factors^{246–248}.

2. THE mTOR SIGNALING PATHWAY IN HUNTINGTON'S AND PARKINSON'S DISEASES

The impairment of cellular processes occurring in neurodegenerative diseases can trigger deregulation of important signaling cascades. In this thesis, we have focused on mechanistic target of rapamycin (mTOR) pathway and its implication in neuronal death and plasticity. This signaling cascade integrates both intra and extracellular cues to regulate major cellular functions, thus maintaining cellular homeostasis. As a regulator of these diverse cellular processes, mTOR plays important roles in brain physiology and pathology (reviewed in ^{249,250}).

2.1 Mechanistic target of rapamycin

Rapamycin is a macrolide produced by *Streptomyces Hygroscopicus* bacteria that was first isolated from a soil sample of the Easter Island, or Rapa Nui as is called by the aboriginal Polynesian inhabitants^{251,252}. This molecule was found to be a specific inhibitor of a novel kinase that was named mechanistic target of rapamycin (mTOR). mTOR is an atypical serine/threonine protein kinase that belongs to the phosphoinositide 3-kinase (PI3K)-related kinase family. It is an extremely large protein of 289 kDa, highly conserved throughout evolution and ubiquitously expressed in all tissues and cell types²⁵³.

mTOR kinase interacts with different proteins to form two distinct complexes named mTOR complex 1 (mTORC1) and mTOR complex 2 (mTORC 2). The differential protein composition defines the variable sensitivities to upstream inputs and downstream outputs of each mTOR complex and therefore their function (Figure 12). Both complexes share the catalytic mTOR subunit, and also assemble mammalian lethal with sec-13 protein 8 (mLST8 or GβL), likewise termed G protein beta subunit-like (GβL), DEP domain containing mTOR-interacting protein (DEPTOR), and the Tt1/Tel2 complexes. In contrast, regulatory-associated protein of mammalian target of rapamycin (Raptor) and proline-rich Akt substrate 40 kDa (PRAS40) are specific of mTORC1, whereas rapamycin-insensitive companion mTOR (Rictor), mammalian stress-activated MAP kinase-interacting protein 1 (mSin1) and protein observed with Rictor 1 and 2 (protor1/2) are only part of mTORC2^{249,250,253}.

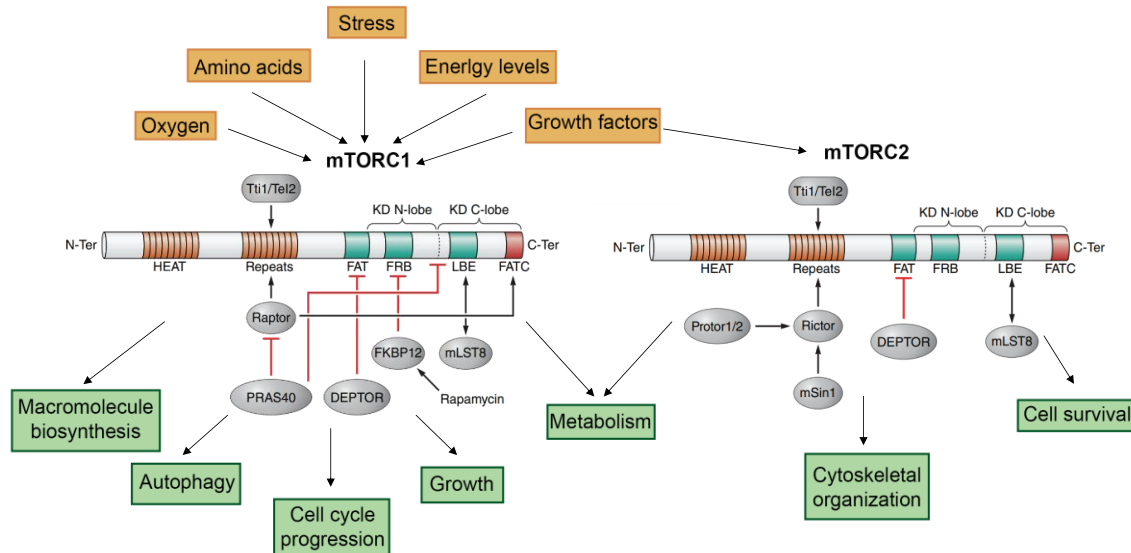


Figure 12. Composition and regulation of mTORC1 and mTORC2 complexes. The mTOR kinase is the key component of two distinct complexes named mTORC1 and mTORC2. The protein components of each complex and their interaction sites are depicted. Brown boxes indicate the stimulus that trigger mTORC1/2 activation and green boxes their functions. Figure adapted from Laplante M. and Sabatini D.M., et al. (2012)²⁴⁹ and Bockaert J. and Marin P., et al. (2015)²⁵⁰.

Regulatory components of mTORC1 and mTORC2 not only determine specific regulation of their functions but also dictate substrate specificity. mTORC1 senses oxygen, amino acids, stress, energy and growth factors to modulate macromolecular biosynthesis, cell cycle progression, growth, metabolism and autophagy. In contrast, mTORC2 responds to growth factors to regulate metabolism, cytoskeletal organization and cell survival^{249,250,253}.

Furthermore, mTORC1 and mTORC2 show different sensitivities to the inhibitory compound rapamycin. Rapamycin interacts with the intracellular 12-kDa FK506-binding protein (FKBP12) which only binds to raptor-bound mTOR, inhibiting mTORC1 kinase activity by probably compromising its structural integrity and reducing its kinase activity. Although mTORC2 was initially known as rapamycin insensitive, prolonged rapamycin exposure also inhibits this complex in eukaryotic cells by disrupting its assembly²⁵⁴.

2.2 mTOR signaling pathway

Several growth factors, such as insulin and insulin-like growth factor 1 (IGF1) can stimulate the PI3K and Ras pathways through its effector kinases protein kinase B (PKB or also known as Akt), extracellular-signal-regulated kinase 1/2 (Erk1/2) and ribosomal S6 kinase (S6K). Both pathways converge into TSC2 phosphorylation which inactivates the heterodimer TSC1/2 (tuberous sclerosis 1 and 2) complex and thus activate mTORC1^{255–258}. Recently Tre2-Bub2-Cdc16 (TBC) 1 domain family, member 7 (TBC1D7) was identified as a third subunit of this complex, although its function within

the TSC1/2 is not well established²⁵⁹. TSC1/2 is a key upstream regulator of mTORC1 and functions as a GTPase activating protein (GAP) towards Rheb (Ras homolog enriched in brain), promoting its conversion into the inactive state (Rheb-GDP)^{257,260}. Hence, inactivation of TSC1/2 complex triggered by growth factors stimulates the formation of the active Rheb-GTP form. Rheb-GTP directly interacts with mTORC1 and strongly stimulates its kinase activity^{260–262}. Even though mTORC2 is less characterized than mTORC1, Rheb-GTP also seems to induce mTORC2 activity^{263–265} (Figure 13).

Like growth factors, many cellular stresses also regulate mTOR activity through TSC1/2 complex. For instance, hypoxia induces the expression of transcriptional regulation of DNA damage response 1 (Redd1 or RTP801) which enhances TSC2 function, leading to mTOR signaling repression^{266,267}.

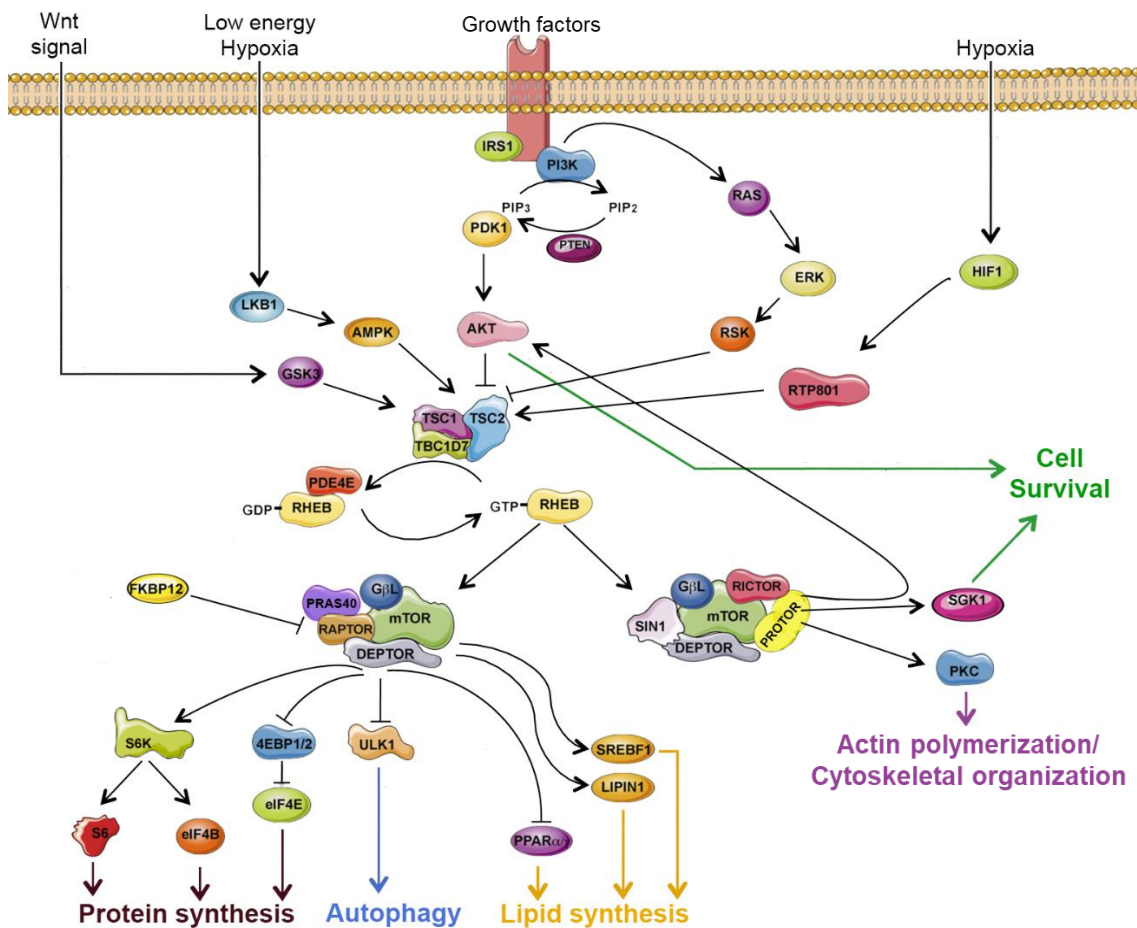


Figure 13. mTOR signaling pathway. Schematic representation of the key upstream regulators and downstream effectors of mTORC1 and mTORC2 and their signaling interrelation. mTORC1 controls CAP-dependent protein translation via 4E-BP1/2 (eukaryotic translation initiation factor 4E binding protein 1 and 2) and S6 kinase phosphorylation, autophagy via ULK1 (Unc-51 like autophagy activating kinase) complex inhibition and lipogenesis by phosphorylating Lipin-1, SREBP1 (sterol regulatory element-binding protein 1) and PPAR γ (peroxisome proliferator-activated receptor gamma). Besides, mTORC1 also regulates cellular metabolism and ribosome biogenesis. mTORC2 phosphorylates PKC (protein kinase C) to control actin polymerization, and altogether with phosphorylation of Akt and SGK1 (serum and glucocorticoid regulated protein kinase 1) promotes cell survival. Figure adapted from Laplante M. and Sabatini D.M., et al. (2012)²⁴⁹.

Akt protein is a crucial component of the mTOR pathway due to the regulation of numerous cellular processes, including cell survival, proliferation and metabolism^{268,269}. Akt is phosphorylated by phosphoinositide-dependent kinase 1 (PDK1) at threonine residue 308 (Thr308) and by mTORC2 at serine residue 473 (Ser473), requiring phosphorylation at both sites to be fully active. Furthermore, Akt is upstream mTORC1 and activates it by phosphorylating and inhibiting TSC1/2^{255,270,271}. Akt also signals to mTORC1 independently from TSC1/2 by phosphorylating PRAS40, an mTORC1 component inhibitor, and inducing its dissociation from raptor²⁷²⁻²⁷⁵.

In the central nervous system, mTOR pathway has emerged as a critical hub by integrating signals that controls autophagy, survival and protein translation. Accordingly, the mTOR/Akt pathway is essential for survival maintenance in several neuronal contexts^{264,276-280} since Akt kinase inactivates several pro-apoptotic downstream targets, such as Bad, Bax, Bim and JNK^{278,281}. Moreover, protein synthesis is critical for the formation and consolidation of synaptic contacts and neuronal plasticity²⁸²⁻²⁸⁴.

Because both Akt and mTOR are associated to neuronal survival and maintenance of synaptic contacts, mTOR/Akt pathway has been extensively studied in neurodegenerative diseases. Remarkably, impairment of the mTOR pathway is a hallmark of many neurodegenerative disorders including HD and PD. Indeed, rapamycin has been described as pharmacological treatment to reverse or ameliorate the symptoms of these diseases in animal models^{203,206,285,286}.

2.2.1 mTOR/Akt signaling alterations in HD

As the central kinase of mTORC1 and 2 complexes, phosphorylation at Ser2481 and at Ser2448 are considered as markers of intrinsic mTOR catalytic activity. In this regard, phospho(P)-mTOR Ser2448 is increased in the striatum of HD mouse models but not in human striatal samples²⁸⁷. In HD models, the inactivation of mTOR by rapamycin^{72,75} or other rapalogs^{288,289} has been suggested to be beneficial by the activation of autophagy, and therefore clearance of mhtt. In fact, it has been proposed that combined inhibition of both mTORC1 and mTORC2 is necessary for increasing autophagy and degrading mhtt aggregates²⁸⁹. Nevertheless, overexpression of Rhes, which, like Rheb, increases mTORC1 activity and decreases autophagy promoting neuroprotection in HD models²⁹⁰, is able to enhance autophagy in neurons by interacting with Beclin-1 and promoting neuroprotective effects in an mTOR-independent manner²⁹¹. Rhes is the Rheb variant specifically expressed in the striatum and displays an additional function of SUMO (small ubiquitin-like modifier) E3 ligase. By this alternative function, Rhes is able to stimulate the sumoylation of mhtt, which leads to cytotoxicity by enhancing its aggregation²⁹².

Relative to this function, the deletion of Rhes protein delays the striatal damage in a pharmacological model of HD²⁹³ and is also able to delay motor symptoms^{293,294}.

Concerning Akt function, increased phosphorylation levels of striatal P-Akt Ser473 are detected in different HD murine models^{295,296} and in HD patient's brain²⁹⁶. In correlation with these results, PHLPP1 (PH domain leucine-rich repeat protein phosphatase 1) shows decreased levels in the striatum of these animals due to reduced gene expression²⁹⁶. PHLPP1 is a key regulator of Akt activity since it mediates the dephosphorylation of the Ser473 residue in Akt and thus partially inactivates it^{297,298}. Moreover, mTORC2-regulator protein Rictor, but not mTORC1-regulator protein Raptor, is elevated in the striatum of HD mouse models and in the putamen of HD patients²⁸⁷, which would reinforce the increasing phosphorylation of Akt at Ser473 residue. These results arise the hypothesis that increased Rictor and decreased PHLPP1 levels allow to maintain Akt hyperactivation counteracting mhtt toxicity and delaying neuronal death. Interestingly, in an acute rat model of HD showing massive cell death, decreased P-Akt Ser473 levels were observed during cell dysfunction, just before neurodegeneration occurs²⁹⁹.

Despite these conflicting results, evidences show that mTOR pathway displays an aberrant signaling over the HD pathogenesis, although it is not clearly defined whether these alterations could be toxic or neuroprotective. To clarify the role of mTOR/Akt pathway in HD more studies should be performed.

2.2.2 mTOR/Akt signaling alterations in PD

As we have seen in HD, studies regarding PD pathology indicate that inactivating mTORC1 and promoting autophagy would preserve DA neurons viability, by probably enhancing α -synuclein aggregation removal^{300,301}. Actually, α -synuclein degradation is in part mediated by the autophagy-lysosomal pathway system^{73,302}. Thus, compounds which enhance autophagy by the inhibition of mTORC1, such as rapamycin, are able to delay neurodegeneration *in vitro* and *in vivo*²⁰⁵⁻²⁰⁷ and to prevent memory deficits in a mouse model of PD³⁰³.

In contrast, activation of mTORC1 is protective in *in vitro* and neurotoxin-induced murine models of PD. Neurotoxins such as 1-methyl-4-phenyl-1,2,3,6-tetrahydropyridine (MPTP), 6-hydroxydopamine (6-OHDA) or rotenone induce oxidative stress and subsequent degeneration specifically in DA neurons (reviewed in ³⁰⁴). Besides, PD mimetic treatments induce mitochondrial dysfunction which leads to impaired calcium homeostasis, and, finally, inhibit mTOR activity^{228,305,306}. In these pharmacological

models, increasing mTORC2 activity by constitutively active forms of Akt^{307,308}, Rheb³⁰⁹ or deletion of PTEN³¹⁰ prevented, or at least, delayed DA neuronal death. Moreover, in cells exposed to PD toxins, inhibition of downstream mTORC1 effectors S6K and 4E-BP1 contribute to neuronal death^{311,312}.

On the other hand, alterations in Akt kinase activity have also been reported in PD. Indeed, phosphorylation levels of Akt at both residues Ser473 and Thr308 are significantly reduced in the 6-OHDA *in vitro* model and, importantly, in nigral neurons from postmortem PD brains²⁶⁴. Supporting this evidence, overexpression of mTOR or constitutively active Akt are able to rescue cell death in front of 6-OHDA toxicity²⁶⁴. In the same cellular model, rapamycin also results neuroprotective by blocking mTORC1-dependent protein translation³⁰⁶. In this context, neuroprotective properties of rapamycin arise from its capacity to block S6K activation, responsible for CAP-dependent protein synthesis, and preventing the loss of Akt phosphorylation at the residue Thr308. Rapamycin reduces the translation of RTP801, a protein inhibitor of mTOR pathway^{267,313} which promotes neuronal loss by suppressing the activation of mTOR complexes and therefore Akt pro-survival kinase²⁶³.

2.2.3 mTOR/Akt signaling in synaptopathies

The mTOR pathway regulates key functions in the formation and maintenance of synapsis (reviewed in ³¹⁴). mTORC1 controls the initiation of translation which is crucial for protein synthesis-dependent synaptic plasticity^{283,284,315}. For instance, during development, mTORC1 activation is necessary to promote the growth of neuronal processes and the arborization of dendrites but, an hyperactivation of the complex can lead to the onset of neurological diseases such as autism^{316,317}. In the synaptic transmission of the adult brain, mTORC1 regulates long-term potentiation (LTP) and depression (LTD) in response to NMDA ionotropic glutamate receptor and to metabotropic glutamate receptor activation^{318–321}. Furthermore, mTORC1 promotes the synthesis of the AMPA receptor subunits GluA1 and GluA2 and their localization at the cell surface^{322,323}, upregulating synaptic activity³²³. Neurotrophic factors as BDNF activate the PI3K/PDK1/Akt pathway through TrkB receptor. Stimulation of TrkB receptor in turn activates mTORC1³²⁴ enhancing AMPA receptor synthesis³²⁵ and decreasing internalization rate of this surface receptors, by inhibiting GSK3^{326–328}.

Moreover, regulation of actin cytoskeleton by mTORC2 allows the dynamic remodulation that underlie morphological changes at neuronal synapses^{329,330}. Regulation of actin polymerization by mTORC2 is, in fact, required for long-term memory consolidation, and

the knockdown of Rictor, essential component of mTORC2, impairs synapse formation³³⁰.

HD and PD are considered synaptopathies since synaptic dysfunction is a common hallmark for both diseases. Neurons affected in these neurodegenerative disorders display alterations in neurotransmitter release, synaptic vesicle endocytosis and dynamics, and synaptic transmission alterations which contribute to clinical symptoms (reviewed in ³³¹).

Dissecting PD pathology, LID onset is elicited by aberrant forms of plasticity in the striatum of PD patients (previously mentioned in section 1.2.4i). Administration of L-DOPA to 6-OHDA-lesioned mice activates mTORC1 pathway in the striatum, probably by the activation of those MSN that express D1 receptor^{332,333}. Moreover, LID severity shows a significant correlation with the magnitude of mTORC1 increase activity, based on phosphorylation levels of S6K and S6³³². Strikingly, rapamycin or other mTOR inhibitors prevent the development of LID without affecting the therapeutic efficacy of L-DOPA^{332,334}.

3. RTP801/REDD1 AS A NEGATIVE REGULATOR OF THE mTOR/AKT PATHWAY

RTP801, also known as Redd1 (regulated in development and DNA damage responses 1) or Dig2 (dexamethasone-induced gene 2) is a stress responsive protein encoded by the gene *DNA-damage-inducible transcript 4 (DDIT4)*. This gene was initially identified by two groups simultaneously in 2002, under hypoxia²⁶⁶ or DNA damage³³⁵.

3.1 DDIT4: a stress responsive gene

DDIT4 is rapidly induced in response to cellular stressors under the control of different transcription factors (Figure 14). For instance, *DDIT4* is upregulated by hypoxia through hypoxia inducible factor 1 (HIF-1) and Sp1 transcription factor^{266,336}, by DNA damage in a p53-manner³³⁵ and by oxidative and endoplasmic reticulum (ER) stress under the control of activating transcriptional factor 4 (ATF4)^{337,338}. Other cell stresses like energy depletion³³⁹, glucocorticoid treatment^{340,341} and overexpression of toxic proteins such as β -amyloid peptide³⁴² also induce *DDIT4* expression.

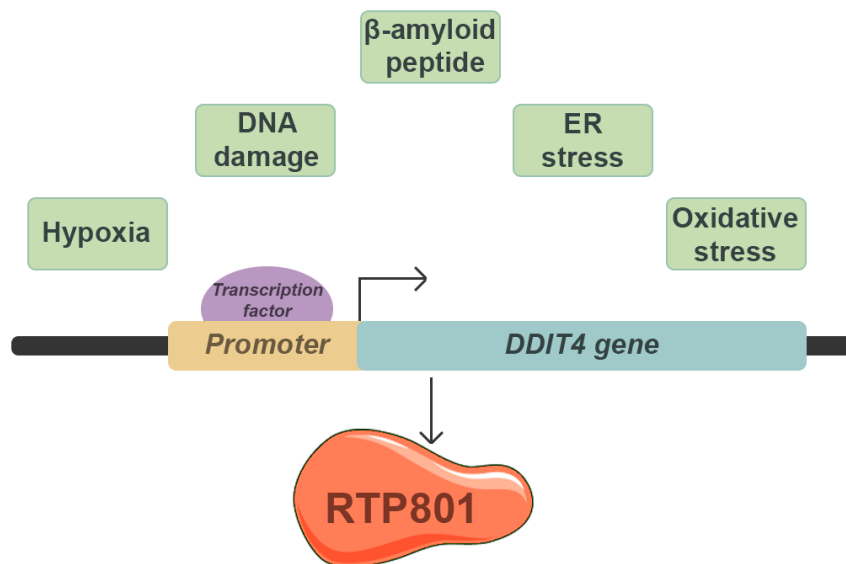


Figure 14. DDIT4 gene-induction by cellular stress. Distinct types of stressors induce the expression of *DDIT4* gene, which is translated to an increase of RTP801 protein. Abbreviations: ER, endoplasmic reticulum; DNA, deoxyribonucleic acid.

3.2 RTP801 protein

RTP801 protein is ubiquitously expressed in several human tissues at low levels, and it only increases in response to cell stresses that rapidly and sharply induce its transcription²⁶⁶. Within the cell, this protein can be localized at the cytoplasm^{335,343,344}, the nucleus^{343,344}, the plasma membrane^{313,344} and also associated to mitochondria^{345,346}. In neurons, results from our laboratory show that RTP801 is localized at both the soma and the dendrites and that it is highly enriched at the synaptic compartment of human and rat brain (unpublished data).

3.2.1 RTP801 protein sequence and structure

RTP801 open reading frame (ORF) encodes for 232 amino acid (aa) in humans, with orthologs in rat, mouse, *Xenopus* and *Drosophila* displaying evolutionary sequence conservation at the carboxyl terminus (C-terminus)³³⁵. Rat and mouse RTP801 ORF encodes for a 229 aa protein which sequence is highly homologous to human RTP801^{266,347} (Figure 15). Interestingly, there is a related transcript termed RTP801-like or Redd2 of 193 aa in human and mouse, that displays 50% of sequence homology and similar functions compared to RTP801^{335,348}.

Regardless a predicted molecular weight of 25 kDa, RTP801 usually migrates at 34 kDa by western immunoblot. This altered migration is probably caused by the presence of multiple lysine residues (K) positively charged at the C-terminus of the sequence³³⁵.

The analysis of RTP801 aa sequence did not revealed any functional motif or structural domain. RTP801 exhibits a poorly preserved NH₂ terminus (N-terminus) and highly conserved C-terminus. In consequence, N-terminus seems not to be necessary for RTP801 to exert its function. The 84 aa at the N-terminus of human RTP801 are neither necessary to maintain its inhibitory action towards mTOR, whereas only few residues could be omitted from the C-terminus without disturbing the function. Studies with different RTP801 truncated forms finally concluded that there are two RTP801 segments required for its function: from residues 85 to 193 and from 207 to 225³⁴⁷.

INTRODUCTION

HOMO SAPIENS	1	MPSLWDRFSSSSSTSSSPSLPRTPTTPDRPPRS	AWGSATREEGFDRSTSLESSDCESLDSS	60	
RATTUS NORVEGICUS	1	MPSLWDRFSSSSSSSSSSSS ···	RTPAADRPPRS	AWGSAAREEGLDRCASLESSDCESLDSS	57
MUS MUSCULUS	1	MPSLWDRFSSSSSSSSSSSS ···	RTPAADRPPRS	AWGSAAREEGLDRCASLESSDCESLDSS	57
α1					
HOMO SAPIENS	61	NSGFGPEEDTAYLDGVSLPDFELLSDP	DEHLCANLMQLLQESLAQARLGSRRPARLLMP	120	
RATTUS NORVEGICUS	58	NSGFGPEEDSSYLDGVSLPDFELLSDP	DEHLCANLMQLLQESLSQARLGSRRPARLLMP	117	
MUS MUSCULUS	58	NSGFGPEEDSSYLDGVSLPDFELLSDP	DEHLCANLMQLLQESLSQARLGSRRPARLLMP	117	
XENOPUS L.	78		GEQLCPSLLKLINRCLTRKARINSLRCSRLLIP	110	
DROSOPHILA M.	165		SASAVRELSQQLOAQLRDAKRRLACTEVTLP	197	
α2 β1 β2 β3					
HOMO SAPIENS	121	SQLVSVQV KK ELLRLAYSEPCGLRGALLDVCVE ·	Q KK SCHSVGQALALDPSLVPTFQLTLVLR	180	
RATTUS NORVEGICUS	118	SQLLSQV KK ELLRLAYSEPCGLRGALLDVCVE ·	Q KK SCHSVAQALALDPSLVPTFQLTLVLR	177	
MUS MUSCULUS	118	SQLVSVQV KK ELLRLAYSEPCGLRGALLDVCVE ·	Q KK SCHSVAQALALDPSLVPTFQLTLVLR	177	
XENOPUS L.	111	DELLCNLQ EL LHLAYSEPCGLRGALIDLCVE ·	NGKDCHSVAQITVDQAVPTFQLTVLLR	170	
DROSOPHILA M.	198	NDLTQRIAAEII RM SE FE PCGERACTL FE FE	SEPNKVKRIAYFKVDPDTVSIFELYTLR	259	
β4					
HOMO SAPIENS	181	LDSRLW PK IQGLFSSANSFPFLPGFSQSLT	TLSTGFRVI KKK LYSSEQLLIEEC	232	
RATTUS NORVEGICUS	178	LDSRLW PK IQGLLSSANS SLV PGYSQSLT	TLSTGFRVI KKK LYSSEQLLIEEC	229	
MUS MUSCULUS	178	LDSRLW PK IQGLLSSANS SLV PGYSQSLT	TLSTGFRVI KKK LYSSEQLLIEEC	229	
XENOPUS L.	171	LDSRLW PRI QGLFSTKP ···	VPGSGQSLKLSPGFKVI KKK LYSSELIIEEC	219	
DROSOPHILA M.	260	QDKSGWSSSLVPQFIK NLT ··· ·	RSNTINISPDFTL KKK LYSSE ··· ·	299	

Figure 15. RTP801 sequence alignment from different species. Amino acid sequence alignment of RTP801 protein from human (*Homo sapiens*), rat (*Rattus norvegicus*), mouse (*Mus musculus*), frog (*Xenopus laevis*) and fly (*Drosophila melanogaster*). The non-well conserved N-terminus sequence of *Xenopus l.* and *Drosophila m.* are not included. Lysine residues are highlighted in bold. The degree of conservation is represented in orange color as higher darkness indicate higher homology. The partial sequences that are necessary for its inhibitory function over mTOR are indicated in discontinuous red boxes. Figure adapted from Vega-Rubin-de-Celis S., et al. (2010)³⁴⁷.

Furthermore, a segment of human RTP801 protein containing from the 89 to the 226 residues with a deletion of the hydrophobic region ²⁰⁰FLPGF²⁰⁴ was crystallized (RTP801^{89-226ΔΦ}) (Figure 16A). This RTP801 mutant form maintained its function and was more soluble. The resulting structure displayed a novel topology characterized by a two-layered α-helix/β-sheet sandwich with a psi-loop motif where the beta(β)-sheet is composed of four strands ordered β2-β1-β3-β ⁴347 (Figure 16B).

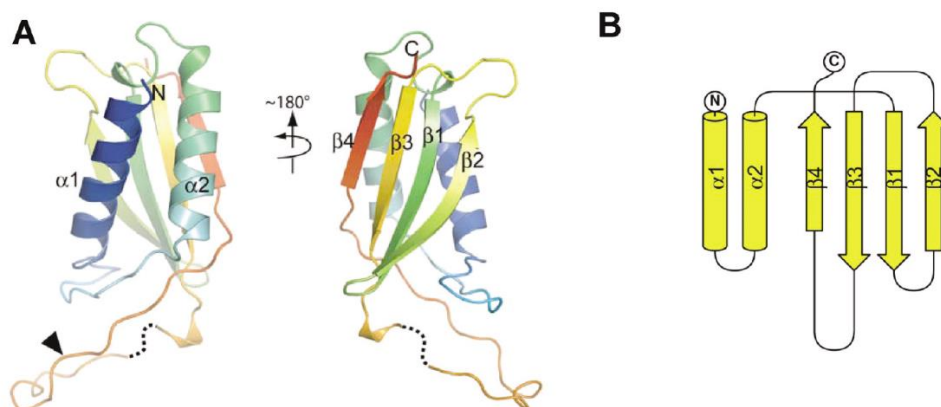


Figure 16. RTP801 tridimensional structure show a unique topology. (A) Representation of the RTP801^{189-226ΔΦ} structure colored in rainbow mode from the N- to the C-terminus. The discontinuous dotted line represents a disordered region and the black arrowhead indicates the location of the hydrophobic ²⁰⁰FLPGF²⁰⁴ deletion. (B) Diagram of RTP801 topology. Images obtained from Vega-Rubin-de-Celis S., et al. (2010)³⁴⁷.

Importantly, two separated segments, ¹³⁸EPCG¹⁴¹ and ²¹⁸KKKLYSSE²²⁵, adjacent in the three-dimensional structure were suggested to be critical for RTP801 function. Moreover, the sequence ²¹⁸KKK²²⁰ has been reported necessary for targeting RTP801 to mitochondria³⁴⁵ and plasma membrane³⁴⁴. Nevertheless, the mutation of this stretch did not impair RTP801 function although ²¹⁸KKK²²⁰ stretch is necessary for RTP801 ubiquitination and degradation³⁴⁹.

3.2.2 RTP801 function and regulation

The only known function of RTP801 is its ability to repress mTOR activity^{267,348}. Under stress conditions, downregulation of mTOR activity requires the quick expression of RTP801 which may be crucial for coping stress and maintaining cellular homeostasis and viability^{263,350}.

Up to now, the RTP801 inhibitory mechanism towards mTOR pathway has not been completely elucidated. It has been proposed that RTP801 suppresses mTOR activity through the activation of TSC1/2 complex^{263,267,339}, although RTP801 does not interact physically with either TSC1 or TSC2³⁴⁷. In fact, evidences seem to indicate that RTP801 binds and sequesters 14-3-3 protein³⁵¹⁻³⁵³ and therefore disrupts the inhibitory function of this protein against TSC2 promoting the inactivation of mTOR³¹³. Nevertheless, this direct interaction of RTP801 and 14-3-3 has been questioned, since the supposed 14-3-3 binding motif (¹³³RLAYSEP¹³⁹) is not conserved within species and the crystallized RTP801 structure analysis does not reveal any established domain for 14-3-3 binding³⁴⁷. In parallel, RTP801 promotes protein phosphatase 2 (PP2A) dependent dephosphorylation of Akt at Thr308 residue, preventing TSC2 phosphorylation, attenuating Rheb-GTP loading and leading to the subsequent mTOR signaling repression³⁵⁴ (Figure 17).

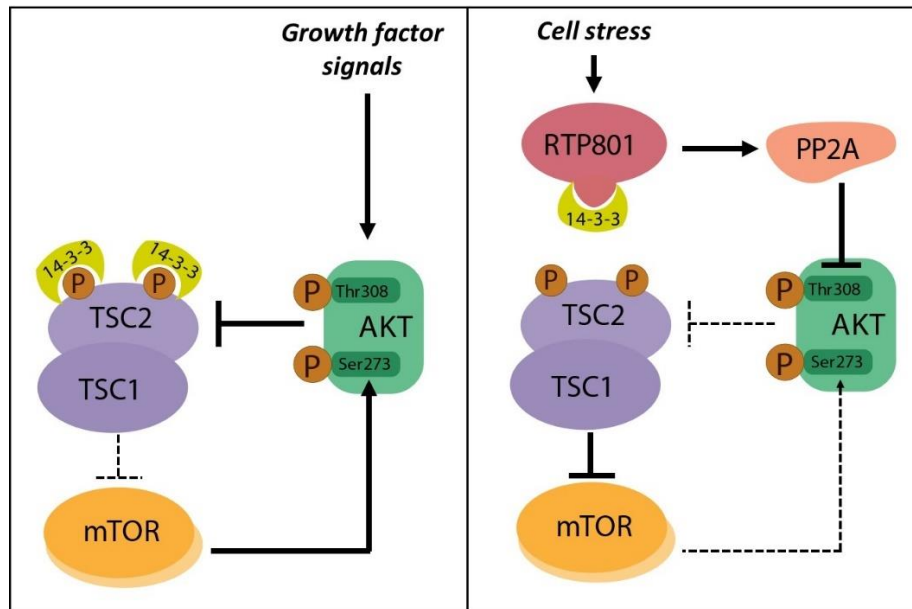


Figure 17. Proposed model for RTP801 mechanism of action. Insulin and other growth factors can activate mTOR signaling through Akt-mediated phosphorylation of TSC2, which promotes TSC2/14-3-3 interaction and inhibits TSC1/2 function. In response to cell stresses, RTP801 is upregulated and binds 14-3-3 protein, resulting in TSC2/14-3-3 dissociation, TSC1/2 activation and mTOR inhibition. Akt pro-survival kinase is dephosphorylated at both residues, at Ser473 due to mTORC1 blockade and at Ther308 due to PP2A overactivation which is also induced by RTP801. Dashed arrows indicate signal loss, thick arrow enhance signal. Figure adapted from DeYoung M.P., et al. (2008)³¹³.

Strikingly, RTP801 has a dual role depending on the cellular context. In proliferating cells, RTP801 exerts a protective role and results anti-apoptotic in front of several toxic environmental stimuli, like H₂O₂-induced oxidative stress²⁶⁶, dexamethasone treatment^{340,341}, serum deprivation³⁵⁵ or DNA damage³³⁵. In contrast, in non-proliferating and differentiated cells, such as NGF-differentiated PC12 cells and sympathetic and cortical primary neurons, RTP801 has a pro-apoptotic function increasing their sensitivity to oxidative stress and promoting degeneration^{263,266,349}. In accordance with its dual function, RTP801 has been identified as regulator of cortical neuronal differentiation and migration. In embryonic cortical neuroprogenitors, RTP801 is increased without being toxic, whereas in newborn and mature neurons RTP801 gradually decreases contributing to the progression of neuronal migration and maturation. Indeed, sustained accumulation of RTP801 in differentiating neurons becomes pro-apoptotic³⁵⁶.

Besides RTP801 rapid gene induction under cell stress, RTP801 proteostasis also determines its stability and thereby its regulatory function towards mTOR. Both RTP801 mRNA³⁴⁰ and RTP801 protein^{306,357,358} display extremely short half-lives between 2 and 7 minutes. Hence, RTP801 is a highly unstable protein with a fine-tuned post-translational regulation.

Ubiquitylation of lysine residues tags proteins mostly to be degraded. In fact, RTP801 protein when ubiquitylated with K48 Ubiquitins at its lysine residues is rapidly degraded by the proteasomal system^{349,359}. To date, only three E3 ligases have been described to poly-ubiquitinate RTP801. The first one described was CUL4A-DDB1-ROC1- β -TRCP E3 ligase complex which mediates RTP801 proteasomal degradation in a GSK3 β -phosphorylation dependent manner³⁵⁸. Additionally, our group described that parkin, a RING E3 ligase, also poly-ubiquitinates RTP801 mediating its proteasomal degradation³⁵⁹. Interestingly, our group also identified the existence of a pool of RTP801 that, when ubiquitinated with K63 Ubiquitins at its lysine residues, is degraded through the lysosomal pathway and this degradation is, at least in part, mediated by the E3 ligase NEDD4³⁴⁹.

3.3 RTP801 implication in neurodegenerative diseases

RTP801 behaves like many other stress-induced genes, where a slight increase may be beneficial but a chronic and sustained elevation is detrimental for neuronal survival. Interestingly, since RTP801 represses protein translation, through mTORC1 inhibition, and survival, via mTORC2 and the neuronal survival kinase Akt, its pro-apoptotic role may be relevant to neurodegenerative diseases. Indeed, RTP801 has been involved in the pathogenesis of neurodegenerative disorders such as PD or Alzheimer's disease (AD). RTP801 has been identified as an amyloid- β -peptide responsive gene. Besides, silencing RTP801 expression protects neuronal cells from amyloid- β -induced toxicity, whereas RTP801 overexpression increases cell sensitivity towards amyloid- β toxicity³⁴². Further studies confirmed its association to AD neurodegeneration. Lymphocytes of AD patients show increased levels of both RTP801 mRNA and protein when compared to age-matched controls³⁶⁰. Nevertheless, no implications of RTP801 in HD were yet described.

3.3.1 RTP801 in PD

RTP801 protein has been related to PD since in 2005 was described as the most induced transcript in a Serial Analysis of Gene Expression (SAGE) performed in a cellular model of the disease³⁶¹. RTP801 transcript resulted in a 98-fold increase in those NGF-differentiated PC12 cells treated with the PD mimetic 6-OHDA. This finding identified RTP801 as a candidate to be considered to trigger neuronal death in PD.

RTP801 transcriptional elevation was further confirmed and extended to protein level in other cell and animal PD models. RTP801 protein is also increased in NGF-differentiated

PC12 exposed to PD toxins 6-OHDA, MPTP and rotenone, and at SNpc DA neurons of the MPTP mouse model. Interestingly, RTP801 elevation is not only observed at *in vivo* and *in vitro* PD models but also at nigral neurons from both idiopathic and mutant parkin PD patients brains^{263,349,359}. Moreover, RTP801 upregulation mediates 6-OHDA-induced cell death in models of PD since silencing its expression is protective in NGF-differentiated PC12 cells and in sympathetic neurons. On the other hand, overexpression of RTP801 is sufficient to induce neuronal death²⁶³. Based on these results, RTP801 upregulation may be toxic for nigral neurons in PD patients.

RTP801 increase triggers cell death through mTOR repression since mTOR phosphorylation at Ser2448 is reduced²⁶³. Indeed, RTP801 also suppresses the phosphorylation of Akt at Ser473 and Thr308 residues^{264,281}. RTP801-induced neuronal loss under 6-OHDA exposure can be rescued by TSC2 knockdown, mTOR overexpression or constitutively active Akt^{263,264,306}. Remarkably, the loss of mTOR and Akt phosphorylation is also observed in DA neurons of postmortem PD brains^{264,306}. As previously described (section 2.2.2), rapamycin is protective in PD animal and cellular models by blocking RTP801 translation and by preserving Akt phosphorylation at Thr308 residue³⁰⁶.

Importantly, RTP801 gene induction and impairment of its degradation lead to RTP801 increase in PD. In the context of PD, two different E3 ubiquitin-protein ligases, Parkin and NEDD4, have been described to mediate RTP801 protein degradation. Parkin dysfunction due to mutations, since *PRKN* gene contains a PD causative loci (Table 1), or oxidative/nitrosative stress has been linked to PD³⁶²⁻³⁶⁴. Thus, increased RTP801 is observed at parkin knockout mice brains, postmortem brains and fibroblasts of parkin mutant PD patients. Additionally, ectopic wild-type parkin, but not its mutant forms, protects neuronal cells from 6-OHDA-induced death by mediating proteasomal degradation of RTP801³⁵⁹. Furthermore, NEDD4 E3 ligase is impaired in PD contributing to RTP801 elevation. NEDD4 protein levels are decreased at DA neurons from human postmortem idiopathic and parkin mutant PD brains and, interestingly, 6-OHDA diminishes its levels in neuronal models. Moreover, NEDD4 protects NGF-differentiated PC12 cells from both 6-OHDA and RTP801-induced toxicity by promoting RTP801 lysosomal degradation³⁴⁹. These findings suggest that both parkin and NEDD4 loss of function in PD may contribute to toxic accumulation of RTP801 and subsequent neurodegeneration in PD.

Based on these data, a working model has been suggested³⁵⁰. It is proposed that at early stages of neurodegenerative diseases, RTP801 induction by cellular stresses may

contribute to mTOR suppression in an attempt to preserve neuronal function and viability. However, at more advanced stages, mTOR sustained inhibition by RTP801 can eventually promote neuronal death through Akt inactivation (Figure 18).

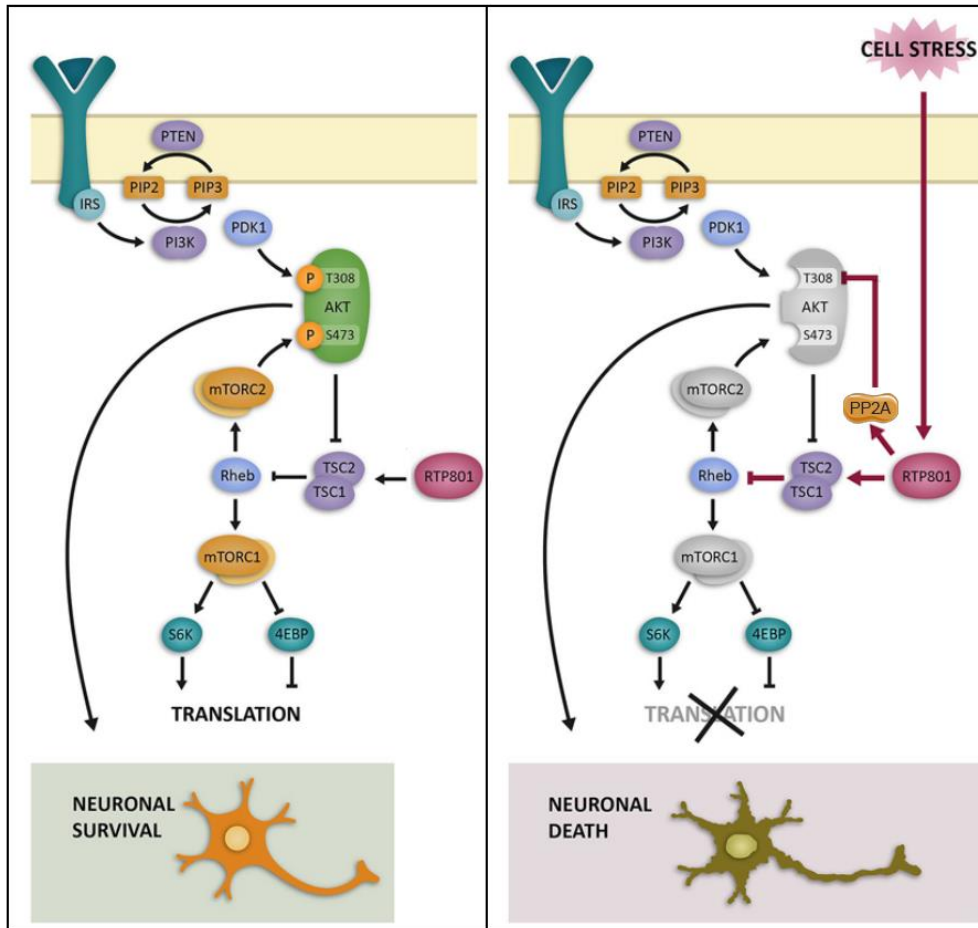


Figure 18. Schematic representation of the mTOR/Akt pathway regulation by RTP801 in neuronal cells. In physiological conditions RTP801 levels are low contributing to maintain mTOR/Akt activity and thereby protein translation and neuronal survival (left panel). However, when neurons are exposed to cell stress RTP801 is increased promoting mTORC1 and mTORC2 inhibition and subsequently Akt repression. This sequential mTOR/Akt suppression contributes to abrogate protein synthesis and survival signaling. If this situation is sustained over time neuronal death occurs (right panel). Image adapted from Canal M., et al (2014)³⁵⁰.

4. TRANSNEURONAL COMMUNICATION VIA EXOSOMES

The secretion of extracellular vesicles was initially described in 1987 as a mechanism to remove unneeded compounds from the cell³⁶⁵. Nevertheless, novel evidences show that extracellular vesicles are more than just waste carriers and have the capacity to exchange components between cells and to act as signaling vehicles to maintain cell homeostasis or as consequence of pathological alterations^{366–369}.

4.1 Classification of extracellular vesicles

Extracellular vesicles are produced by virtually any cell type and represent a highly heterogeneous population which can change dynamically in number and content in response to physiologic and environmental conditions^{370,371}. In the brain, extracellular vesicles are released from neuronal progenitor cells^{372,373}, neurons^{374,375}, astrocytes^{376,377}, oligodendrocytes^{378–382} and microglia^{383,384} as well as Schwann cells in the peripheral nervous system^{385,386}. Importantly, healthy neurons secrete extracellular vesicles that activate microglia phagocytosis for the clearance of inactive synapses and toxic proteins^{387,388}. Nevertheless, neuronal vesicles can also accumulate toxic proteins such as tau, β -amyloid, α -synuclein and prion protein which are associated with neuronal degeneration^{219,220,389,390}.

The different types of extracellular vesicles differ in their mechanism of biogenesis and distinct cargoes, which can vary from nucleic acids to lipids and proteins. Based on the current knowledge of their biogenesis, extracellular vesicles can be broadly classified into two main categories: exosomes (50 to 150nm in diameter), which are formed from multivesicular bodies, and microvesicles and ectosomes (50nm to 1 μ m in diameter), which bud from the cell surface (reviewed in ³⁹¹) (Figure 19). In addition, during apoptosis, dying cells can release apoptotic blebs (500nm to 2 μ m in diameter)^{367,368,392}.

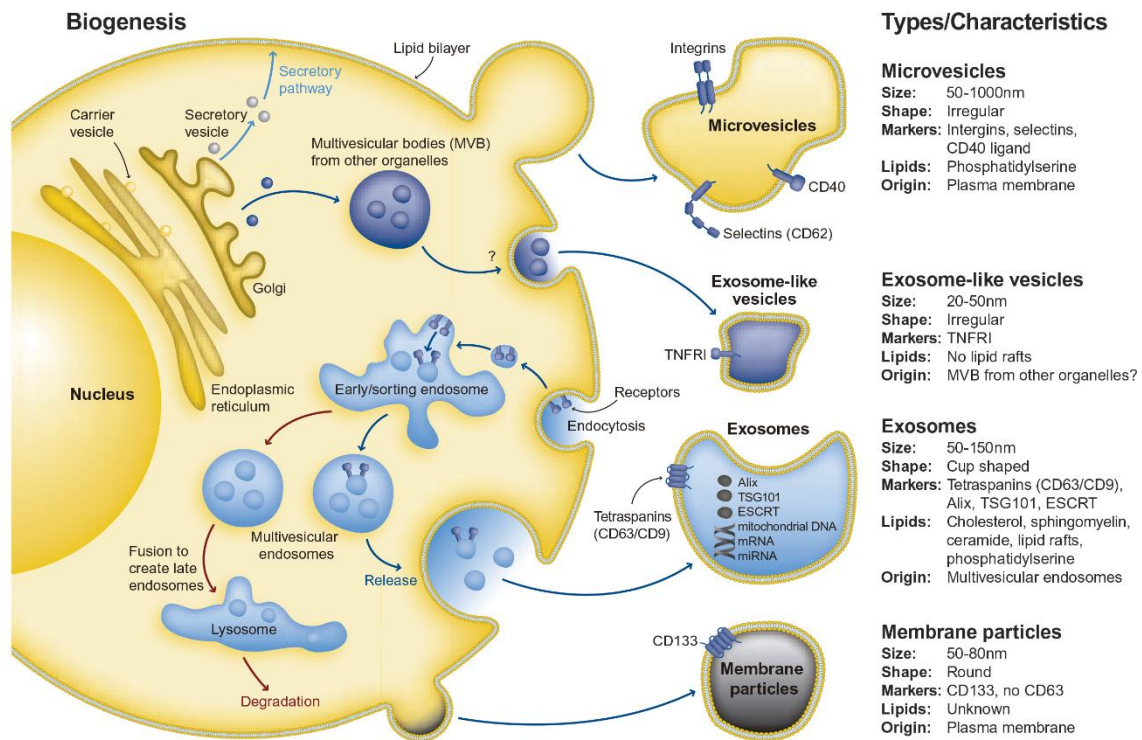


Figure 19. Categorization of extracellular vesicles. Extracellular vesicles are formed either by seeding of the plasma membrane, in which case they are referred to as microvesicles, or within the lumen of multivesicular endosomes and then fuse with the plasma membrane to release vesicles that are then named exosomes. Additionally to the main types, the pool of extracellular vesicles also include apoptotic bodies, membrane particles which directly bud from the plasma membrane resembling the budding of viruses, and, finally, exosome-like vesicles which are basically composed from ESCRT-related proteins³⁹³. Their cargo composition is cell-type specific and is mainly determined by the origin of the biogenesis^{394,395}. Abbreviations: ESCRT, endosomal sorting complex required for transport; mRNA, messenger RNA; miRNA, microRNA; MVB, multivesicular body, TSG101, tumor susceptibility gene 101; nm, nanometers. Image adapted from the website http://docs.abcam.com/pdf/general/secreted_extracellular_vesicles_web.pdf.

4.1.1 Exosomes

In the central nervous system, exosomes are the most extensively studied subtype of extracellular vesicles. Exosomes show the singularity that their cargo composition is influenced by the physiological or pathological status of the donor cell as well as the stimuli that modulate their production and release^{394,395}. Consequently, exosomes have emerged as possible biomarkers for the clinical use in neurodegenerative diseases. Moreover, exosomes can be used as cargo vehicles for the targeted delivery of compounds to modulate neuronal behaviors³⁹¹.

i. Exosome biogenesis, release and internalization

Exosomes are generated as intraluminal vesicles (ILVs) within the lumen of endosomes during their maturation into multivesicular bodies (MVBs), in a process that involves the endosomal sorting complex required for transport (ESCRT) machinery.

ESCRT consists of four different protein complexes, ESCRT-0, -I, -II -III, that work in a stepwise manner^{391,396} (Figure 20). ESCRT-related proteins are associated with other accessory proteins, such as ALG-2 interacting protein X (Alix) or sorting-associated protein 32 (VPS4)^{396,397}. The inactivation of ESCRT or associated proteins affects either efficiency and composition of secreted exosomes³⁹⁸. Remarkably, exosomes can also be originated in an ESCRT-independent manner revealed by the formation of ILVs upon the depletion of ESCRT complexes³⁹⁹. The most studied ESCRT-independent mechanism of exosome biogenesis requires the production of ceramide by neutral type II sphingomyelinase (nSMase2), which hydrolyses sphingomyelin to ceramide⁴⁰⁰. Ceramide may then allow the generation of membrane subdomains which impose a spontaneous negative curvature on the membrane that triggers the formation of ILVs^{391,401}.

Once released into the extracellular space, exosomes can reach recipient cells and deliver their contents to induce functional responses and promote signaling changes that will affect the cell homeostasis^{391,402,403}. Exosome-induced intercellular communication can be mediated by different mechanisms, including docking at the plasma membrane, activation of surface receptors and intracellular signaling, vesicle endocytosis or fusion with the target cell. However, the complete mechanism that underlies exosome intercellular communication is not fully uncovered since it appears to be dependent on exosome origin and target cell type³⁹¹. Moreover, the signaling pathways that are stimulated or the trophic support that is provided is determinant by the mode of interaction and the fate of exosomes in case of being internalized^{391,404}.

Of note, exosomes are taken up by microglia nonspecifically by macropinocytosis³⁷⁹, whereas neurons mainly mediate their internalization by clathrin- and dynamin-dependent endocytosis^{381,405}. The ultimate, and probably the most frequent fate of exosomes, is targeting to lysosomes, leading to the degradation of exosomal proteins and lipids. This degradative pathway would offer a relevant source of metabolites to the target cells providing trophic support⁴⁰⁶.

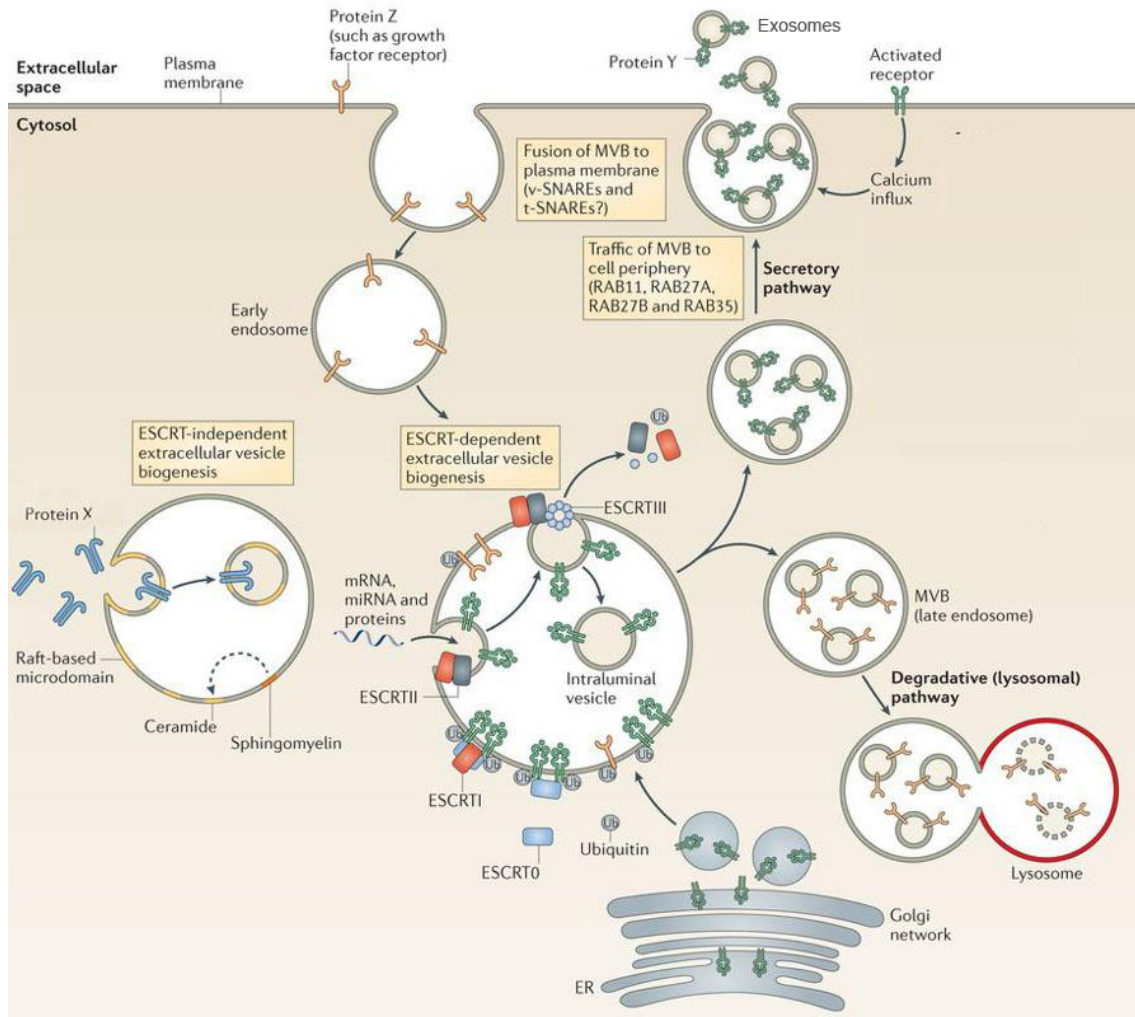


Figure 20. Biogenesis of exosomes. Exosomes are generated as ILVs in MVBs by mechanisms that are ESCRT dependent or independent. Proteins that are transported from the Golgi or that are internalized from the cell surface are ubiquitinated on their cytosolic domains. The ESCRT-O complex recognizes ubiquitinated proteins on the cytosolic side of endosomes or MVBs and binds the ESCRT-I complex, which in turn recruits ESCRT-II subunits initiating the budding of ILVs within MVBs. Following, cytosolic RNAs and proteins have direct access into the inner part of forming vesicles. Next, the ESCRT-II recruits the ESCRT-III subunits for cleaving into free ILVs. Other mechanism of sorting into ILVs is independent of the ESCRT machinery through raft-based microdomains that are enriched in sphingolipids which is transformed into ceramide by sphingomyelinases. Ceramide then induces ILVs formation by the invagination of microdomains. The MVBs follow either the secretory or the degradative pathway. In the degradative pathway, MVBs release ILVs into lysosomes to digest and clear their components. In the secretory route, MVBs traffic to the cell periphery and fuse with the plasma membrane releasing ILVs, now termed exosomes. The release of exosomes can be constitutively or mediated by surface receptors that trigger calcium influx. RABs, actin and SNARE protein are involved in final steps of exosomal release. Abbreviations: ER, endoplasmic reticulum; miRNA, microRNA; RABs, Ras-related proteins in brain; t-SNARE, target SNAP receptor, v-SNARE, vesicle SNARE. Figure adapted from Robbins P.D. and Morelli A.E., et al. (2014)⁴⁰².

ii. Exosome composition

One of the decisive factors in exosomal composition is their biogenesis pathway, so both ESCRT-dependent and -independent routes contribute to the cargo variability between different subpopulation of exosomes^{391,398}. Yet, a canonical exosome model has been proposed as a lipid-enclosed vesicle containing various types of cytosolic and membrane proteins (Figure 21).

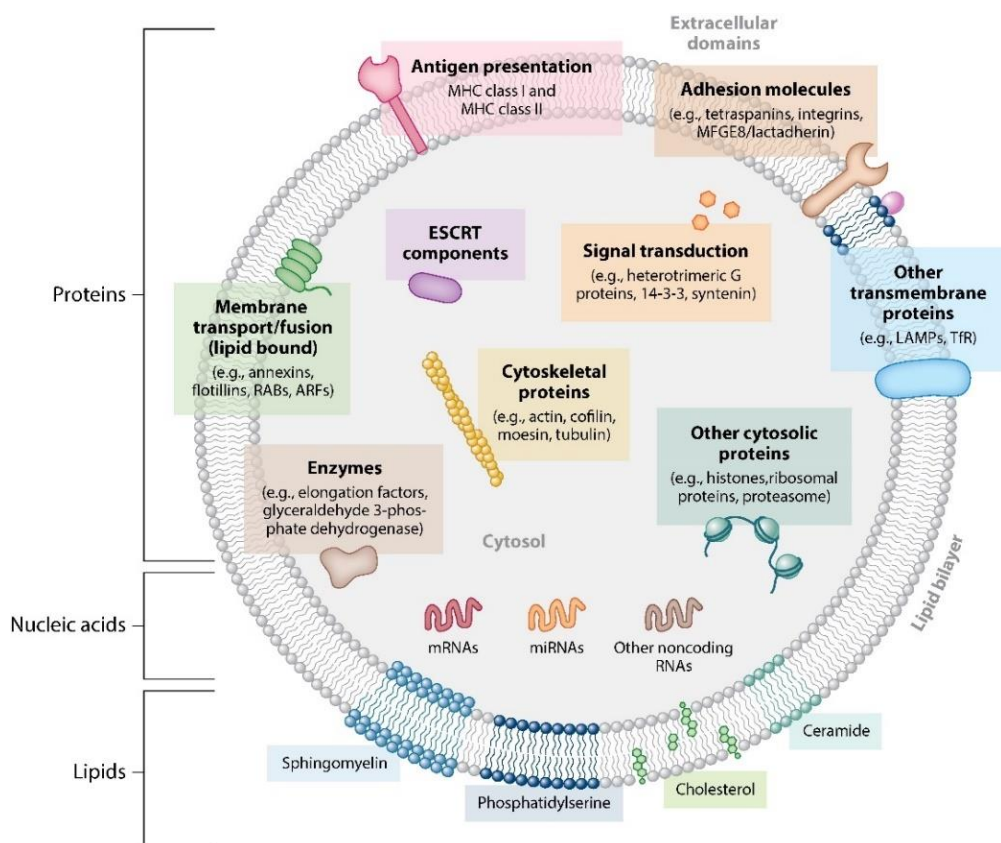


Figure 21. Canonical composition of exosomes. Schematic representation of the molecular composition (proteins, lipids and nucleic acids) of exosomes. Examples of each subtype of proteins are listed. Abbreviations: ARF, ADP ribosylation factor; ESCRT, endosomal sorting complex required for transport; LAMP, lysosome-associated membrane protein; MHC, major histocompatibility complex; MFGE8, milk fat globule–epidermal growth factor-factor VIII; RABs, Ras-related proteins in brain; TFR, transferrin receptor. Figure obtained from Colombo M., Raposo G. and Théry C., et al. (2014)³⁶⁶.

Exosomes are composed by a lipid bilayer which protects their cargo from plasma and immune components and helps to deliver it to recipient cells without compromising its intrinsic function^{404,407,408}. The composition of the exosomal bilayer differs from the lipid composition of the plasma membrane of the donor cell. Exosomal membrane is enriched in sphingomyelin, cholesterol and saturated fatty acids^{409–411}. Moreover, ceramide and its derivatives are enriched in exosomes^{400,410,412}. Proteins associated to lipid rafts, such as flotillins or glycosylphosphatidylinositol-anchored proteins, are also highly expressed in exosomes⁴¹¹.

The protein content of exosomes is heterogeneous but specific. The heterogeneity is based on a non-homogeneous exosomal population whose protein composition can differ depending on the exosomal origin and the status of the recipient cell^{366,403,413}. However, several exosomal protein markers have been described to be widely present. Specific transmembrane or membrane associated proteins, like flotillins, tetraspanins or integrins, components of the ESCRT machinery, such as alix, tumor susceptibility gene 101 (TSG101), or cytosolic proteins as heat shock protein 70 kDa (Hsp70) are common exosomal markers. They also carry a variety of cytoskeletal proteins including actin and tubulin and some metabolic enzymes as pyruvate kinase or glyceraldehyde-3-phosphate dehydrogenase (GAPDH). Most of exosomes do not contain proteins associated to mitochondria, nucleus, ER or Golgi (reviewed in ^{391,398}). Moreover, it has been proposed that some cytosolic proteins modified by ubiquitylation are segregated in ILVs and then secreted within exosomes⁴¹⁴. Proteins highly enriched in neurons such as L1 cell adhesion molecule (L1-CAM)^{375,415}, AMPA, but not NMDA, receptors³⁷⁴, and NEDD4⁴¹⁶ have also arise as specific markers for neuronal exosomes.

Apart from proteins and lipids, exosomes also carry nucleic acids, including RNAs (mRNAs, microRNAs and long-non-coding RNAs)^{417,418} and DNA sequences only under tumorigenesis^{419,420}.

4.2 Neuronal-derived exosomes in physiology and pathology

Exosomes are released from the soma and the dendrites of mature neurons³⁷⁵. Their release can be enhanced by depolarization mediated by glutamate excitatory neurotransmitter through the activation of AMPA and NMDA receptors. Indeed, calcium influx is determinant for boosting exosomal secretion in neurons^{374,375}. Further studies confirmed that release of exosomes by neurons is dependent on synaptic activity^{416,421} and participates in the neuron-to-neuron communication (reviewed in ⁴²²) (Figure 22).

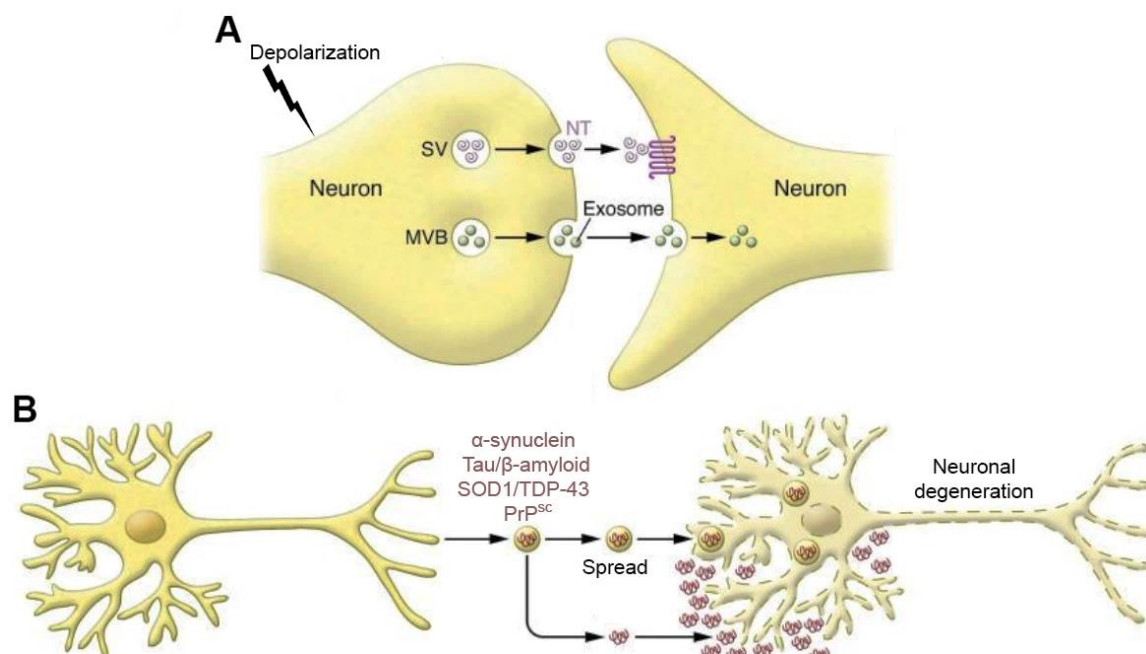


Figure 22. Role of exosomes in neurons. (A) Depolarization of neurons results in the release of neurotransmitters from synaptic vesicles and of exosomes. Exosomes released from the presynaptic neuron are taken up by postsynaptic neurons modulating synaptic strength and retrograde signaling. Exosomes can also stimulate other neural cells as microglia to activate phagocytosis for the clearance of inactive synapses. **(B)** In neurodegenerative diseases, exosomes act as vehicle carriers for the extracellular release of toxic proteins, cell-to-cell spreading and finally the accumulation of those toxic proteins in the recipient cell eventually promoting neurodegeneration. Abbreviations: MVB, multivesicular body; NT, neurotransmitter; PrP^{Sc}, prion protein scrapie; SOD1, superoxide dismutase 1; SV, synaptic vesicle, TDP-43, TAR DNA-binding protein 43. Figure adapted from Zappulli V., et al. (2016)⁴⁰³.

Exosomes play crucial roles in neuronal physiologic processes but also contribute to the development of disease states. Neurodegenerative disorders, including HD, PD, AD and prion diseases, are characterized by the aggregation of misfolded proteins that become toxic for the neuron. However, exosomes appear to act at cross-purposes in neurodegeneration, particularly in their clearance function. On the one hand, exosomes are used as vehicles to transneuronally spread the toxic proteins across different regions of the brain^{219,220,389,423,424}. On the other hand, exosomes play a crucial role for disassembling and clearing toxic proteins by microglial cells^{379,387,425–427}. Even though exosomes have been extensively studied regarding the propagation of prion protein and amyloid and Tau proteins in AD^{387,389,424,427,428}, they have also been involved in other neurodegenerative disorders describing the spreading of PD-associated proteins and mhtt in HD.

Recently, the propagation of mhtt by exosomes has been uncovered. Indeed, both expanded repeat RNA and polyQ-mhtt protein are found in exosomes derived from HD cell models. Nevertheless, no toxicity emerged after exposing primary neurons to those exosomes⁸³. Another study also revealed that propagation of full-length mhtt occurs *in*

vivo suggesting that, at least in part, its spreading is mediated by exosomes. Additionally, injection of exosomes carrying mhtt to wild-type mice triggers the development of pathological and behavioral HD phenotype⁸².

The accumulation and cell-to-cell transmission of α -synuclein has been also demonstrated to occur in part via exosomes and, additionally, its spreading affects the viability of neighboring neurons^{218–220}. Furthermore, exosomal release is enhanced by lysosomal impairment associated to PD pathogenesis and the inhibition of lysosomal function leads to an increase in the secretion of exosomal α -synuclein and its spreading to recipient cells⁴²⁹. In agreement with this data, exosomal α -synuclein is also found in the cerebrospinal fluid (CSF) of PD patients and its levels correlate with the severity of cognitive impairment in those individuals²¹⁹. However, the levels of exosomal α -synuclein in the plasma are lower in PD patients compared to controls⁴³⁰ and there is an inverse significant correlation between plasma exosomal α -synuclein and PD severity⁴³¹. All these findings support the hypothesis that α -synuclein aggregates can be spread from neuron to neuron promoting the gradual progression of the disease. Besides α -synuclein, other PD-related proteins including deglycase DJ-1 and leucine-rich repeat kinase 2 (LRRK2) have been found in blood-, CSF- or urine-derived exosomes in patients with PD^{432–435}.

AIMS

Both HD and PD are devastating neurodegenerative diseases characterized by the death of selective neuronal subpopulations. As a modulator of numerous cellular processes, the mTOR pathway is fine-tuned regulated to maintain neuronal survival and synaptic plasticity. One of the proteins that modulates this signaling cascade is RTP801. RTP801 is induced in response to cellular stressors and its increase triggers neuronal death by negatively regulating the mTOR/Akt pathway. RTP801 upregulation in PD has been extensively studied, nonetheless RTP801 function in HD pathogenesis has never been explored. Thus, identifying RTP801 as a new target in HD would be valuable to design new therapies to block neurodegeneration.

Interestingly, exosomes have recently emerged as a key mechanism to maintain trophic support between neural cells and as vehicle for the clearance of toxic proteins from neurons. Since RTP801 is upregulated under stressful conditions, its propagation by exosomes may allow the neuron-to-neuron spreading of RTP801 toxicity through the modulation of mTOR/Akt pathway.

Importantly, impaired protein functions of the mTOR pathway are a common hallmark in many neurodegenerative diseases, including HD and PD. However, little is known about the contribution of genetic variants of the genes belonging to the mTOR pathway to the risk of PD and how they influence the interindividual variability response to pharmacological treatment with L-DOPA.

Hence, the specific aims of this thesis are (Figure 23):

AIM 1. To characterize whether RTP801 is upregulated in Huntington’s disease and whether it is a downstream effector of mutant huntingtin-induced toxicity.

1.1 To study the contribution of RTP801 to mutant huntingtin-induced cell death.

1.2 To analyze the participation of RTP801 in motor learning deficits in Huntington’s disease.

AIM 2. To investigate whether RTP801 is propagated by exosomes and whether it is able to modulate transneuronally the mTOR/Akt pathway in cellular models of Parkinson’s disease and Huntington’s disease.

AIM 3. To assess whether genetic variations in the mTOR pathway contribute to Parkinson’s disease pathogenesis and response to pharmacological therapy.

3.1 To explore whether interaction of SNPs in the mTOR pathway influences risk and age at onset of PD.

3.2 To study whether interaction of SNPs in the mTOR pathway modulates levodopa-induced dyskinesia onset and severity in PD patients.

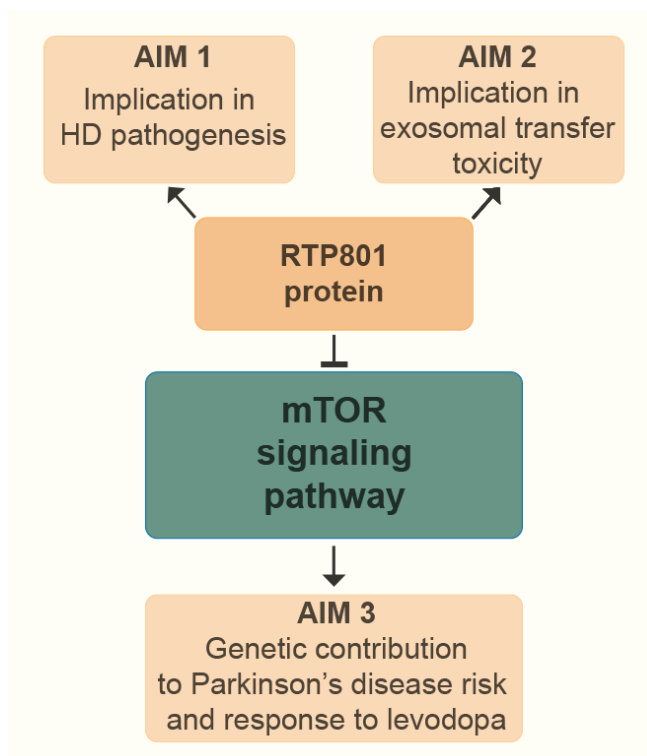


Figure 23. Scheme indicating the different aims developed in this thesis. In this work we have studied the contribution of the mTOR pathway to HD and PD neurodegenerative diseases, from a protein and genetic approximation. On one hand, we have explored the implication of RTP801 as a negative regulator of mTOR in the pathogenesis of HD (aim 1) and its propagation by exosomes spreading its toxicity to other neurons in models of the aforementioned diseases (aim 2). On the other hand, we have analyzed the contribution of genetic variants in mTOR-related genes to the onset of PD and the response to the pharmacological treatment with L-DOPA (aim 3).

METHODOLOGY

1. CELL CULTURE

1.2 HEK293T cells

Human Embryonic Kidney 293T cell (HEK293T) is a human cell line originally derived from human embryonic kidney cells which are commonly used for the production of lentiviruses⁴³⁶. HEK293T cells were cultured in Dulbecco's modified Eagle's medium (DMEM) medium supplemented with 10% Fetal Bovine Serum and 1% Penicillin/Streptomycin (all from Thermo Fisher Scientific) in a 5% CO₂ atmosphere at 37°C. Medium was replenished every other day and before transfection. Cells were reseeded when confluent.

1.2 PC12 cells

PC12 cells is a cell line originally derived from a pheochromocytoma of the rat adrenal medulla⁴³⁷. They are characterized by the presence of catecholaminergic vesicles which can be stored and released. Upon the exposure to nerve growth factor (NGF), PC12 cells respond exiting the cell cycle and differentiating into a neuron-like phenotype. NGF-differentiated PC12 cells are characterized by the presence of branched neurites and the expression of several neuronal markers. Moreover, they are electrically excitable and release neurotransmitters, mostly dopamine^{438–441}. Thus, NGF-differentiated PC12 cells have widely been used in neurobiological and neurochemical studies.

Proliferating naïve PC12 cells were maintained in RPMI 1640 medium (Thermo Fisher Scientific) supplemented with 10% heat-inactivated horse serum (Sigma-Aldrich), 1% FBS and 1% Penicillin/Streptomycin in a 7.5% CO₂ atmosphere at 37°C. Cells were reseeded when confluence was reached on plates treated with collagen type I rat tail (Corning). To obtain neuronal-like NGF-differentiated PC12 cells, standard medium was replaced for differentiation medium containing RPMI 1640 supplemented with 1% heat-inactivated horse serum, 1% penicillin/streptomycin and 50 ng/ml recombinant human β -NGF (Alomone Labs). Cells were differentiated for 6-7 days prior performing experiments. Medium was changed every other day and before transfection.

1.3 Striatal neuronal progenitor cell line

Conditionally immortalized wild-type STHdh^{Q7/Q7} and mutant STHdh^{Q111/Q111} striatal neuronal progenitor cell line expressing endogenous levels of normal and mutant htt with 7 and 111 glutamines, respectively, were used. These cells were originally derived from

striatal precursors isolated from HdhQ7 and HdhQ111 mice at embryonic day 14, and after were immortalized with the SV40 Large T antigen containing the tsA58/u19 temperature-sensitive mutations and the neomycin resistance gene⁴⁴².

Cultures were grown in DMEM medium supplemented with 10% FBS, 1% penicillin/streptomycin and 400 µg/ml neomycin analogue G418 (Geneticin; Gibco, Thermo Fisher Scientific) in a 5% CO₂ atmosphere at 33°C. Medium was replenished every other day and before transfection. Cells were reseeded when confluent.

1.4 Cortical primary neurons

Primary cultures of cortical neurons were performed from rat or mice depending on the experiment. Experiments were performed at day-in-vitro (DIV) 14 or 21.

Rat primary cortical cultures were performed from Sprague-Dawley rats at embryonic day 18 (E18). Cortices were dissected out, dissociated in 0.05% trypsin (Sigma-Aldrich) and maintained in Neurobasal medium supplemented with B27 and 2mM GlutaMAX™ (all from Thermo Fisher Scientific) in a 5% CO₂ humidified atmosphere at 37°C. For imaging experiments, neurons were plated at a density of 300 cells/mm² on poly-L-lysine-coated (Sigma-Aldrich) in seeding medium containing MEM medium supplemented with 100 mM pyruvic acid (all from Thermo Fisher Scientific), 10% heat-inactivated serum and 20% glucose (all from Sigma-Aldrich). After 60 minutes, medium was replaced for supplemented Neurobasal. For biochemistry experiments, neurons were plated at a density of 750 cells/mm² on poly-L-lysine-coated plates in supplemented Neurobasal. Medium was replenished one third every 7 days.

Mouse primary cortical cultures were obtained from E16.5 B6;129 embryos, dissociated in 0.05% trypsin and plated at a density of 500 cells/mm² on poly-D-lysine-coated plates for biochemical analysis. Neurons were maintained in Neurobasal medium supplemented with B27 and 2mM GlutaMAX™ in a 5% CO₂ atmosphere at 37°C. One third of the medium was replenished every 3 days.

2. CELLULAR TREATMENTS

All treatments were performed in NGF-differentiated PC12 cells at day 6-7 after differentiation or in rat cortical primary neurons DIV13-14. Before treatment, medium was totally replaced for NGF-differentiated PC12 cells and half-replaced for neuronal cultures. Cell cultures were exposed to the following compounds as indicated (Table 2):

Compound (Source)	Function	Cell type	Concentration	Exposure time
Cycloheximide (Calbiochem)	Protein synthesis inhibitor	NGF-differentiated PC12 cells	10µg/ml	10' or 60'
Actinomycin (Gibco)	RNA synthesis inhibitor	NGF-differentiated PC12 cells	3µg/ml	10' or 60'
6-OHDA (Tocris Bioscience)	PD neurotoxin	Rat cortical neurons	50µM	16h

Table 2. Compounds used for cellular treatments.

3. MOLECULAR BIOLOGY

3.1 DNA plasmid amplification and purification

All DNA plasmids used in this thesis were amplified by bacterial transformation and then purified following the next steps:

3.1.1 Bacterial transformation

Escherichia coli DH5α competent cells (Thermo Fisher Scientific) were used to transform and amplify the DNA content of plasmids and ligation products. Vector DNA was added to bacterial competent cells, mixed and incubated for 15 minutes at 4°C. To induce transformation by heat shock, the mixture was placed at 42°C for 2 minutes and placed back at 4°C for 5 minutes. Next, S.O.C. medium (Thermo Fisher Scientific) was added and incubated at 37°C for 60 minutes to grow transformed bacterial. Finally, bacteria were seeded on lysogeny-broth agar (Panreac) plates supplemented with 100µg/ml of ampicillin (Thermo Fisher Scientific) or 50µg/ml of kanamycin (Sigma Aldrich), depending on the antibiotic resistance gene of the plasmid. LB-agar plates were incubated overnight at 37°C.

3.1.2 Plasmid DNA amplification and purification

A single copy colony was selected from the lysogeny-broth agar plate and inoculated in Terrific Broth medium (Thermo Fisher Scientific) containing 100µg/ml of ampicillin or 50µg/ml of kanamycin. The bacterial culture was grown overnight at 37°C and 300 rpm.

The commercial kit HiPure plasmid Maxiprep kit (Thermo Fisher Scientific) was used to isolate plasmid DNA. Final DNA concentration was measured using a Nanodrop™ One Spectrophotometer (Thermo Fisher Scientific).

3.1.3 Plasmid DNA sequencing

All new and ceded plasmid constructions were analyzed by DNA sequencing. DNA sequencing was performed at the Servei de Genòmica from the Universitat Autònoma de Barcelona.

3.2 DNA subcloning

In this thesis, a short hairpin RNA (shRNA) sequence against RTP801 and a scrambled shRNA were subcloned into the lentiviral vector pLL3.7 (Addgene). For this purpose, the following steps were performed:

3.2.1 ShRNA sequence design

Validated shRNA targeting human, rat and mouse RTP801 sequence^{263,356} and a scrambled control sequence were used to design new oligonucleotides which were flanked by HpaI and XhoI restriction sites. Prior ligation, oligonucleotides were 5' phosphorylated and annealed. The scrambled (shCtr) and shRTP801 sequence were:

shCtr: 5'-GTGCGTTGCTAGTACCAAC-3'

shRTP801: 5'-AAGACTCCTCATACTGGATG-3'

3.2.2 Vector linearization

The pLL3.7 vector was linearized with the restriction enzymes HpaI and XhoI (New England Biolabs) at 37°C for 2 hours. To dephosphorylate the linearized vector and avoid its recircularization, calf-intestinal alkaline phosphatase (New England Biolabs) was added to the digestion products and incubated at 37°C for 60 minutes.

3.2.3 DNA extraction from agarose gel

Digested pLL3.7 vector was separated by electrophoresis in a 1% agarose gel containing 0,5 µg/ml of ethidium bromide to visualize DNA. DNA samples were mixed with DNA loading dye (Thermo Fisher Scientific) and gels were run in TAE buffer (Thermo Fisher Scientific). DNA bands were visualized under ultraviolet light and bands corresponding to

linearized vector were cut from the gel. DNA bands were purified using QIAquick Gel Extraction Kit (QIAGEN) following manufacturer's instructions.

3.2.4 Ligation

The linearized pLL3.7 vector purified from agarose gel and the annealed oligonucleotides were ligated using a molar ratio of 1:2. Vector and insert DNA were mixed with T4 DNA Ligase and T4 DNA Ligase Buffer (all from New England Biolabs). The reaction was incubated overnight (18 hours approximately) at 16°C and after inactivated at 65°C for 20 minutes. *Escherichia coli DH5α* were transformed with the ligation products and the resulting colonies were grown in Terrific Broth medium (all from Thermo Fisher Scientific) and the sequence was verified by sequencing the vector (see section 3.1.3).

3.3 Description of plasmids

All constructs used in this thesis and their specifications are listed below (Table 3):

METHODOLOGY

Backbone/Empty vector	Construct	Source
<p>pcDNA3.1-eGFP</p> <p>Obtained from Addgene</p> <ul style="list-style-type: none"> • Ampicillin resistance • Expresses eGFP under the control of CMV promoter⁴⁴³ 	pCDNA3.1-Q25-eGFP	<p>Provided by Dr. G.M. Lawless (Cure HD Initiative, Reagent Resource Bank of the Hereditary Disease Foundation)</p>
	pCDNA3.1-Q72-eGFP	
	pCDNA3.1-Q72-eGFP	
<p>pEGFP-C1bos</p> <p>Provided by Dr. Giovanna Bossi</p> <ul style="list-style-type: none"> • Kanamycin resistance • Expresses eGFP under the control of Bos promoter 	pEGFP-C1bos-CD63	<p>Provided by Dr. Giovanni Bossi (University of Oxford)</p>
<p>pEGFP-C3</p> <p>Provided by Dr. Clarissa Waites (Columbia University)</p> <ul style="list-style-type: none"> • Kanamycin resistance • Expresses eGFP or the insert fused to eGFP under the control of CMV promoter 	pEGFP-C3-RTP801	<p>Subcloned by Dr. Joan Romaní</p>
<p>pCMS-EGFP</p> <p>Provided by Dr. Lloyd Greene (Columbia University)</p> <ul style="list-style-type: none"> • Ampicillin resistance • Expresses eGFP under the control of SV40 promoter 	pCMS-eGFP-shG	<p>Provided by Dr. Cristina Malagelada^{263,356}</p>
	pCMS-eGFP-shRTP801 1	
	pCMS-eGFP-shRTP801 4	
<p>pLL3.7</p> <p>Obtained from Addgene</p> <ul style="list-style-type: none"> • Lentiviral vector. Ampicillin resistance • Expresses eGFP under the control of CMV promoter and the insert under the control of U6 promoter 	pLL3.7-shCtr	<p>Subcloning (section 3.2)</p>
	pLL3.7-shRTP801	
<p>rAAV2/8</p> <p>Provided by the Viral Vector Production Unit (Universitat Autònoma de Barcelona)</p> <ul style="list-style-type: none"> • Adenoassociated virus serotype 2/8 • Expresses eGFP under the control of CMV promoter 	rAAV2/8-shCtr	<p>Provided by the Viral Vector Production Unit (Universitat Autònoma de Barcelona) (section 11)</p>
	rAAV2/8-shRTP801	

Table 3. List of constructs used. SV40=Simian Virus 40; CMV=Cytomegalovirus, Bos= EF-Bos Taurus promoter.

4. PROTEIN EXPRESSION IN CELL CULTURES

4.1 Liposome-mediated transfection

Transient transfections were carried in different cell cultures using the lipid reagent Lipofectamine 2000® (Thermo Fisher Scientific).

4.1.1 Transfection of HEK293T, NGF-PC12 and STHdh cells

Briefly, cell culture was grown up to 70-90% of confluence, and 30 minutes before transfection medium was replaced for transfection medium (medium without serum and antibiotics). Plasmidic DNA and Lipofectamine 2000® were mixed and added to cells following manufacturer's instructions. Four hours later, medium was replaced by fresh complete medium (supplemented with serum and antibiotics).

4.1.2 Transfection of rat cortical primary cultures

Coverslip-plated cortical neurons were transfected for 24- or 48-hours prior paraformaldehyde fixation (section 6.1) for imaging experiment at DIV14 or DIV21, respectively. Coverslip were first transferred into a new plate with conditioned and fresh neurobasal medium in a 1:2 ratio. Plasmidic DNA and Lipofectamine 2000® mixtures were prepared and added to cultures as indicated by the manufacturer. Four hour later, coverslips were transferred back to the plate containing conditioned medium. We referred to conditioned medium, neurobasal supplemented medium which have been previously cultivated within cell.

4.2 Lentiviral transduction

Rat cortical primary neurons were transduced with lentiviral particles packaging a shRNA construct against RTP801 (pLL3.7-shRTP801) or a scrambled control sequence (pLL3.7-shCtr). Lentiviral transductions were performed with a MOI (Multiplicity Of Infection) of 2 at DIV 6-7 and six days later (DIV 13-14) cultures were harvested.

4.2.1 Lentiviral particles production

To produce lentiviral particles, 10 cm plates containing HEK293T at 70-80% of confluency were transfected with Lipofectamine 2000® as described in section 4.1.1. Cultures were transfected with 5 µg of pMDL/pRRE, 5 µg of pRSV-REV, 5 µg of pMD2.G (all from Addgene) and 10 µg of the target vector (pLL3.7-shCtr or pLL3.7-shRTP801).

Lentiviruses were purified using polyethylene glycol (PEG) precipitation. Seventy-two hours post-transfection, cell medium was collected and centrifuged 5 minutes at 5,000g to remove cell debris. Then, supernatant was mixed with 8,5% PEG 6000 and 0.5 M NaCl and incubated 90 minutes at 4°C with occasional mixing every 20-30 minutes. Finally, the resulting mix was centrifuged at 7,500g for 15 minutes in a SS-34 fixed angle rotor in a Sorvall R5-5C Superspeed Centrifuge. The pellet-containing lentiviruses was resuspended with PBS-Ca²⁺/Mg²⁺ and stored at -80°C. Viral titer was assessed by transduction of several viral dilutions.

5. GENE EXPRESSION ANALYSIS

The gene expression of RTP801 was quantified by reverse transcription quantitative polymerase chain reaction (RT-qPCR). Total RNA was isolated from NGF-PC12 cells or extracted from 12-week old wild type and R6/1 mice striatal samples using the High Pure RNA Isolation Kit (Roche Diagnostics Corporation) following manufacturer's instructions. Transcriptor Strand cDNA Synthesis Kit (Roche Diagnostics Corporation) was used to reverse transcribe cDNA from 1 µg of total RNA. Specific primers for quantitative PCR (qPCR) were used as follows: rat RTP801 forward primer, 5'-GCTCTGGACCCCAGTCTAGT-3'; rat RTP801 reverse primer, 5'-GGGACAGTCCTTCAGTCCTT-3'; mouse RTP801 forward primer, 5'-ACCTGTGTGCCAACCTGAT-3'; mouse RTP801 reverse primer, 5'-TAACAGCCCCTGGATCTTG-3'; rat/mouse actin forward primer, 5'-GGGTATGGGTCAGAAGGACT-3'; rat/mouse actin reverse primer, 5'-GAGGCATACAGGGACAACAC-3'.

Quantitative PCR was performed with SYBR® master mix (Thermo Fisher Scientific) in a 7500 Real Time PCR System (Applied Biosystems) using equal amounts of cDNA templates. RTP801 expression results were normalized by actin and analyzed using the comparative quantification.

6. IMMUNOFLUORESCENCE

6.1 Immunocytofluorescence

NGF-differentiated PC12 cells and cortical neurons were both fixed with 4% paraformaldehyde (Electron Microscopy Sciences) in PBS for 15 minutes at room temperature. Next, NGF-differentiated PC12 cells were blocked and permeabilized with SuperBlock™ (PBS) Blocking Buffer (SuperBlock-PBS; Thermo Fisher Scientific)

containing 0.3% Triton X-100 (Sigma Aldrich) for 60 minutes at room temperature. In contrast, primary cultures were firstly permeabilized with PBS containing 0.25% Triton X-100 for 5 minutes and then blocked with SuperBlock-PBS for 30 minutes at room temperature. Primary antibodies were diluted in Superblock-PBS and incubated overnight at 4°C (Table 4):

Antibody	Host specie	Dilution	Source
eGFP	Mouse monoclonal	1:1000	Santa Cruz Biotech
MAP2	Mouse monoclonal	1:500	Abcam
RTP801	Rabbit monoclonal	1:150	Proteintech

Table 4. Primary antibodies used for immunofluorescence of cultured cells.

After primary antibody incubation, cells were incubated with the corresponding secondary antibody diluted 1:500-1:1000 in SuperBlock-PBS for 2 hours at room temperature. The secondary antibodies used were goat anti-Mouse IgG (H+L) conjugated to AlexaFluor™ 488 or goat anti-Rabbit IgG (H+L) conjugated with Alexa Fluor® 568 or AlexaFluor™ 647 (all from Thermo Fisher Scientific). For nuclear staining, nuclei were revealed with Hoescht 3342 (Thermo Fisher Scientific) diluted 1:5000 along with the secondary antibody incubation. In the case of actin filamentous labelling, AlexaFluor™ 568 Phalloidin diluted 1:10000 was incubated along with the secondary antibody and Hoescht 3342. Cells were washed in PBS between different steps, after secondary antibody incubation and a final wash with MiliQ water was performed prior coverslip mounting. Finally, coverslips were mounted onto a slide with the mountant liquid ProLong™ Gold Antifade Mountant (Thermo Fisher Scientific).

Coverslips were observed with by epifluorescent microscopy (Leica AF6000) or by confocal microscopy (Leica TCS SP5) at Centres Científics i Tecnològics de la Universitat de Barcelona, Campus Clínic-Casanova.

6.2 Immunohistofluorescence of mouse brain sections

Animals were deeply anesthetized with dolethal (Vétoquinol) (60 mg/kg) and intracardially perfused with 4% paraformaldehyde in PBS buffer (pH=7.2-7.4). Brains were removed and post-fixed for 18-24h. Then, brains were cryoprotected through sucrose gradient: 10%, 20% and 30% sucrose solutions in PBS 0.02% sodium azide for 18-24 hours each step. Finally, brains were frozen in chilled 2-methyl butane (Sigma Aldrich) at -20°C and stored at -80°C. Serial cryostat 25 µm-thick sections were collected

in PBS 0.2% sodium azide as free-floating sections and processed for immunohistofluorescence.

Sections were washed with PBS and incubated with 50 mM NH₄Cl for 30 minutes to block aldehyde free-induced fluorescence. Tissue was blocked with SuperBlock-PBS containing 0.3% Triton X-100 for 2 hours at room temperature. After, slices were incubated overnight at 4°C with the primary antibodies anti-GFP chicken polyclonal (Synaptic Systems) diluted 1:500 in SuperBlock-PBS 0,3% Triton X-100.

After primary antibody incubation, sections were washed in PBS and incubated for 2 hours at room temperature with the secondary antibody goat anti-Chicken IgY (H+L) conjugated to AlexaFluor™ 488 diluted 1:500 in SuperBlock-PBS 0.3% Triton X-100. For nuclear staining, nuclei were revealed with Hoescht 3342 diluted 1:5000 along with the secondary antibody incubation. Slices were washed with PBS before being mounted with ProLong™ Gold Antifade Mountant on SuperFrost™ Plus Adhesion Slides (Thermo Fisher Scientific).

Stained mouse brain sections were observed by epifluorescent microscopy.

7. WESTERN BLOTTING

Western blotting or western immunoblot (WB) was used to quantify the protein content of cellular extracts or tissue homogenates.

Whole cell extracts were collected in Cell Lysis Buffer (Cell Signaling Technology; 20 mM Tris-HCl (pH 7.5), 150 mM NaCl, 1 mM Na₂EDTA, 1 mM EGTA, 1% Triton, 2.5 mM sodium pyrophosphate, 1 mM β-glycerophosphate, 1 mM Na₃VO₄, 1 μg/ml leupeptin) supplemented with 1mM phenylmethanesulfonyl fluoride (Sigma Aldrich; PMSF) as protease inhibitor. Samples were next sonicated and centrifuged at 14,000g for 10 minutes to separate the insoluble fraction. For the protein content analysis of the insoluble fraction, the resulting pellet was washed in PBS, resuspended in Pierce™ Lane Marker Reducing Sample Buffer (Thermo Fisher Scientific) and finally sonicated and heated at 97°C for 5 minutes. The supernatant containing the soluble fraction was kept for protein quantification.

R6/1 and Hdh^{Q7/Q111} animals and their respective wild-type littermates were killed by decapitation at different ages. Brains were removed, and the striatum was dissected out and homogenized in Cell Lysis Buffer with PMSF. Postmortem human brain areas (frontal cortex, hippocampus, caudate nucleus, putamen and cerebellum) of HD patients and control individuals were obtained from the Neurological Tissue Bank (Biobank-HC-

IDIBAPS) thanks to Dr. Ellen Gelpi collaboration. Human brain areas were homogenized in Cell lysis buffer with PMSF. Murine and human tissue homogenates were cleared by centrifugation at 1,000g for 10 minutes at 4°C to remove debris. Next, supernatant was sonicated and centrifuged at 14,000g for 10 minutes and the protein content was determined.

Protein concentration of cellular extracts and homogenized samples was established using Bradford reagent (Bio-Rad). Before loading, samples were prepared with Pierce™ Lane Marker Reducing Sample Buffer and heated 5 minutes at 97°C. Samples were finally resolved in different polyacrylamide gels depending on the molecular weight of the analyzed proteins. For high molecular weight protein analysis was used 3-8% polyacrylamide gels (NuPAGE™ Novex™ 3-8% Tris-Acetate Protein Gels) with running buffer NuPAGE® Tris-Acetate SDS Running Buffer. For small or intermediate weight protein analysis, samples were resolved in a 4-12% polyacrylamide gels (NuPAGE™ Novex™ 4-12% Bis-Tris Protein Gels) with NuPAGE® MOPS SDS Running Buffer (all from Thermo Fisher Scientific). The molecular weight marker used was the PageRuler™ Prestained Protein Ladder (Thermo Fisher Scientific). Gels were run in the XCell SureLock™ Mini-Cell system (Thermo Fisher Scientific).

Proteins were transferred to nitrocellulose membranes with the iBLOT® 2 Dry Blotting System using iBLOT® Transfer Stack supports (all from Thermo Scientific). Membranes were washed with TBS-T (Tris-buffered Saline (Thermo Fisher Scientific) containing 0.1% Tween® 20 (Sigma Aldrich)) and blocked with TBS-T 5% milk (Bio-Rad) for 60 minutes at room temperature. Next, membranes were incubated with the corresponding primary antibody (Table 5) diluted in TBS-T 5% BSA (Bovine Serum Albumin, Sigma Aldrich) overnight at 4°C, except anti-actin-Peroxidase antibody with which was incubated 30 minutes at room temperature.

METHODOLOGY

Antibody	Host specie	Dilution	Source
Actin-HRP conjugated	Mouse monoclonal	1:100000	Sigma Aldrich
Akt	Rabbit polyclonal	1:1000	Cell Signaling
Akt-phospho Ser473	Rabbit polyclonal	1:1000	Cell Signaling
Alix	Rabbit Polyclonal	1:1000	Merck Millipore
eGFP	Mouse monoclonal	1:1000	Clontech
EM48	Mouse monoclonal	1:500	Merck Millipore
Flotillin-1	Mouse monoclonal	1:1000	BD Biosciences
GAPDH	Mouse monoclonal	1:1000	Merck Millipore
GFP	Rabbit polyclonal	1:1000	Santa Cruz Biotech
GluA1	Rabbit polyclonal	1:1000	Merck Millipore
mTOR	Rabbit polyclonal	1:1000	Cell Signaling
mTOR-phospho Ser2448	Rabbit polyclonal	1:1000	Cell Signaling
NEDD4	Rabbit polyclonal	1:1000	Santa Cruz Biotech
NR1	Mouse monoclonal	1:1000	Chemicon
p75 ^{NTR}	Rabbit polyclonal	1:1000	Promega
PHLPP1	Rabbit polyclonal	1:500	Cayman Chemical
PSD-95	Mouse monoclonal	1:1000	Thermo Fisher
Rictor	Rabbit polyclonal	1:1000	Cell Signaling
RTP801	Rabbit polyclonal	1:500	Proteintech
S6	Mouse monoclonal	1:500	Cell Signaling
S6-phospho Ser235/236	Rabbit polyclonal	1:1000	Cell Signaling
SV2A	Mouse monoclonal	1:1000	Santa Cruz Biotech
TrkB	Mouse monoclonal	1:1000	BD Bioscience
TSG101	Mouse monoclonal	1:1000	Abcam

Table 5. Primary antibodies used for WB analysis.

After primary antibody incubation, membranes were washed with TBS-T three times for 10 minutes. Then, membranes were incubated with the corresponding secondary antibody diluted 1:10000 in TBS-T 5% milk during 60 minutes at room temperature. The secondary antibodies used were goat anti-Mouse IgG (H+L) and goat anti-Rabbit IgG (H+L) conjugated to horseradish peroxidase (HRP) (all from Thermo Fisher Scientific). Anti-actin-Peroxidase antibody is already conjugated with HRP, in consequence it was not necessary to incubate it with the secondary antibody.

Membranes were next washed with TBS-T three times for 10 minutes to remove the excess of secondary antibody and finally washed in TBS for 5 minutes. Proteins were detected with Supersignal™ West Pico Plus Chemiluminescent Substrate (Thermo Fisher Scientific). Chemiluminescent images were acquired using LAS-3000 (Fujifilm) or ChemiDoc (Bio-Rad) imaging systems and quantified by densitometric analysis using ImageJ software (NIH). In case of reincubation with another primary antibody, membranes were washed with Restore™ PLUS Western Blot Stripping Buffer (Thermo Fisher Scientific) for 5-20 minutes to remove previous signal and blocked again with TBST-T 5% milk.

8. SYNAPTOSOMAL PREPARATION

Synaptosomes are referred to the synaptic terminals isolated from the presynaptic compartment and postsynaptic neuron. They are composed by the entire presynaptic terminal attached to the postsynaptic membrane (Figure 24).

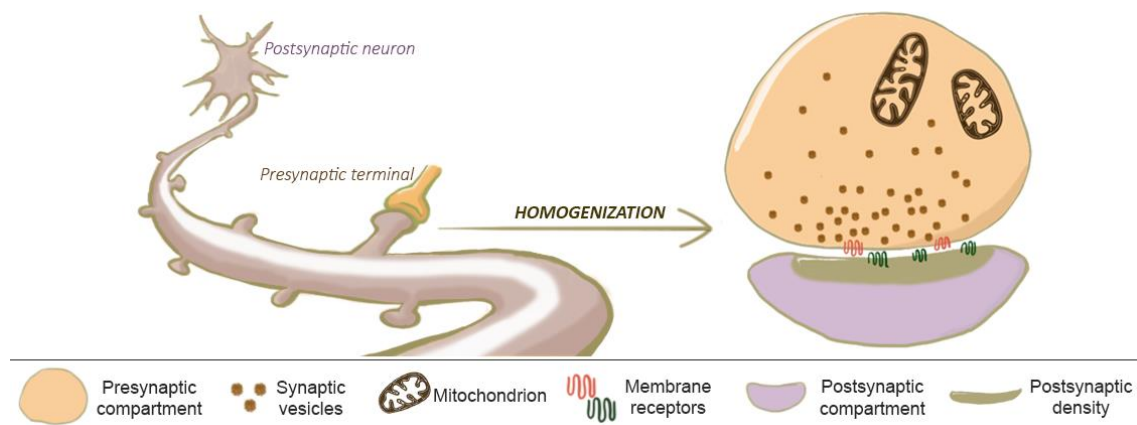


Figure 24. Schematic representation of an isolated synaptosome. When brain tissue is homogenized, the synaptic terminals detach from neuronal processes and reseal into vesicular objects. Synaptosomes consist of isolated functional synaptic terminals composed by the resealed presynaptic compartment associated with the also resealed postsynaptic membrane containing the postsynaptic density.

Postmortem striatal and frontal cortical brain tissues from control and HD patients were obtained from the Neurological Tissue Bank (Biobank-HC-IDIBAPS) thanks to Dr. Ellen Gelpi collaboration. Striatum of R6/1 and Hdh^{Q7/Q111} and WT mice was also dissected out.

Mice striata, putamen and frontal cortex were homogenized in Krebs-Ringer (KR) buffer (125 mM NaCl, 1.2 mM KCl, 22 mM NaHCO₃, 1 mM H₂PO₄, 1.2 mM MgSO₄, 1.2 mM CaCl₂, 10 mM glucose (pH=7.4)) supplemented with 0.32 M Sucrose. Then, samples were subjected to a first centrifugation at 1,000g for 10 minutes (4°C) to discard debris.

A sample of the supernatant was kept as the homogenate fraction. After, the supernatant was subjected to a second centrifugation at 16,000g for 15 minutes (4°C) to obtain the synaptosomal fraction. The pellet was finally resuspended in KR 0.32M Sucrose buffer and subjected to WB to analyze the protein content (section 7).

9. ISOLATION OF EXOSOMES FROM CULTURE MEDIUM

Exosomal vesicles (EVs) were isolated from depleted-DMEM culture media of HEK293 or STDHdh cells. FBS is highly enriched in exosomes and other microvesicles. To eliminate function extracellular vesicles, FBS was mixed with DMEM in 1:1 proportion and subjected to ultracentrifugation at 100,000g for 18 hours. The resulting supernatant was used to supplement DMEM culture medium. Exosomes were also purified from Neurobasal culture media from rat cortical cultures DIV13 or DIV14 depending on the experiment.

To isolate exosomes cell culture was subjected to sequential centrifugations and ultracentrifugations (Figure 25). First, cell media was collected and centrifuged at 300g for 5 minutes at room temperature to remove cell debris and centrifuged again for 20 minutes at 2,500g and 4°C. After, cell media was centrifuged for 30 minutes at 10,000g (4°C) to remove other microvesicles of bigger diameter. Finally, supernatant was ultracentrifuged for 2 hours at 100,000g (4°C) in the 70.1 Ti fix angled rotor using thickwall polycarbonate tubes (Beckman Coulter) in a Beckman Coulter Optima L-100 XP ultracentrifuge. Final supernatant was discarded, and the resulting pellet was washed with PBS and ultracentrifuged again for 1 hour at 100,000g (4°C) in the S140-AT fix angled rotor using polycarbonate tubes (Thermo Fisher Scientific) in a Sorvall MX Plus 150 microultracentrifuge. The resulting pellet contained the exosomal fraction.

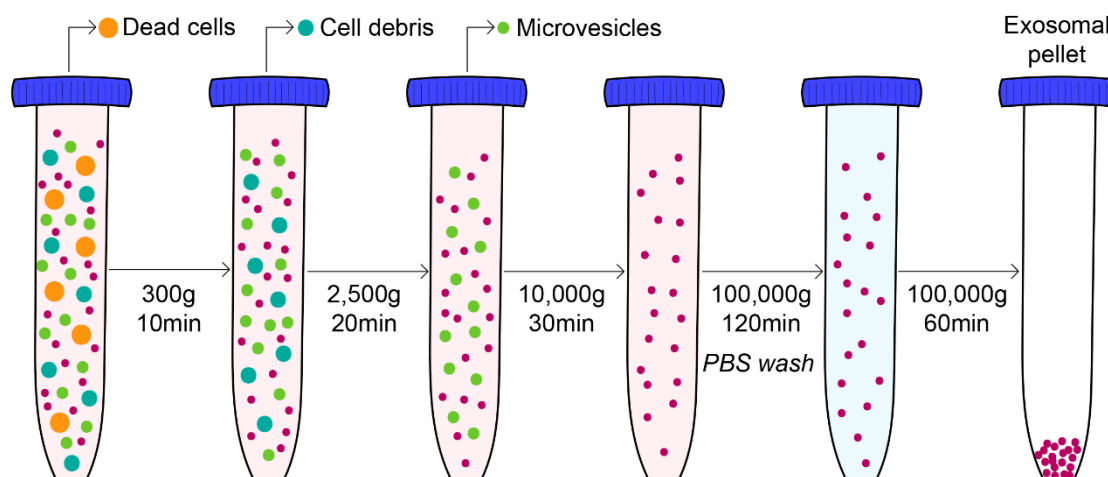


Figure 25. Schematic representation of exosome isolation protocol by differential ultracentrifugation from cell culture media. All centrifugations were performed at 4°C.

For protein content analysis the pellet was resuspended in Pierce™ Lane Marker Reducing Sample Buffer (Thermo Fisher Scientific), heated at 97°C 5 minutes and loaded into WB gel. For exosome quantification, the pellet was resuspended in PBS and vesicles size and concentration were determined using the NanoSight nanoparticle tracking LM10 system (Malvern) thanks to Dr. Hernando del Portillo and his technician Joan Seguí (Institut d'Investigació Germans Trias i Pujol, IGTP).

9.1 Exosomes uptake study

Concentration of isolated exosomal vesicles was determined by NanoSight LM10. The volume corresponding to a concentration of 800,000 particles/ml was immediately added to rat/mouse cortical primary neurons and incubated for 4-24 hours. After the incubation period, cultures were lysed to analyze protein composition (section 7) or fixed to visualize exosomal uptake by confocal microscopy (section 6.1).

9.2 Generation of red fluorescent labeled exosomes

Exosomal fluorescent labelling was performed after the quantification of particles by NanoSight LM10. To generate red fluorescent exosomes, the resulting pellet of the final ultracentrifugation was labelled with PKH26 (Sigma Aldrich) following manufacturer's instructions. PKH26 suspension was incubated for 4 minutes at room temperature and the reaction was stopped adding PBS 1% BSA. Then, suspension was ultracentrifuged at 100,000 for 60 minutes at 4°C (rotor S140-AT), washed in PBS and ultracentrifuged at 100,000g for 60 minutes at 4°C (rotor S140-AT). Finally, the pellet was resuspended in PBS for the study of exosomal uptake.

9.3 Electron microscopy observation of exosomes

For transmission electron microscopy (TEM) observation, the resulting pellet of the last ultracentrifugation was resuspended in PBS-2% paraformaldehyde and then subjected to negative staining. Suspension was adsorbed on 400-mesh copper grids supported with formvar/carbon membrane for 25 minutes. Grids were washed and contrasted with 2% saturated aqueous uranyl acetate for 2 minutes and finally washed in water.

Exosomal samples were observed with JEOL J1010 80kV microscope (Centres Científics i Tecnològics de la Universitat de Barcelona, Campus Diagonal) at 20,000x or 50,000x magnification.

10. HD MOUSE MODELS

R6/1 mice expressing exon-1 of mhtt were obtained from Jackson Laboratory and maintained in B6CBA background. Two different lines of R6/1 mice with 145 or 115 CAG repeats were used depending on the experiment. WT littermate animals were used as the control group. Hdh^{Q7} WT mice with 7 CAG repeats and Hdh^{Q111} knock-in mice, with targeted insertion of 109 CAG repeats that extends the glutamine segment in murine htt to 111 residues, were maintained on a C54Bl/6 genetic background. Male and female Hdh^{Q7/Q111} heterozygous were intercrossed to generate age-matched Hdh^{Q7/Q7} WT and Hdh^{Q7/Q111} knock-in littermates. All mice used were males and were housed together in numerical birth order in groups of mixed genotypes. Data were recorded for analysis by microchip mouse number. Animals were housed with access to food and water ad libitum in a colony room kept at 19-22 °C and 40-60% humidity, under a 12:12 hours light/dark cycle.

11. INTRASTRIATAL INJECTION OF ADENO-ASSOCIATED VECTORS

To knockdown RTP801 expression, shRNA verified scrambled sequence and the one against RTP801 (sequences are mentioned in section 3.2.1) were cloned into a rAAV2/8-GFP adenoviral vector at restriction sites BamHI at 5' and AgeI at the 3' (section 3.3). The rAAV2/8 plasmids and infectious AAV viral particles containing GFP expression cassette with shCtr or shRTP801 were generated by the Unitat de Producció de Vectors from the Center of Animal Biotechnology and Gene Therapy at the Universitat Autònoma de Barcelona.

8-week-old WT and R6/1 mice were subjected to bilateral intrastriatal injections of rAAV2/8 expressing shRTP801 or control shRNA. Animals were deeply anesthetized with a mixture of oxygen and isoflurane (4-5 for induction and 1-2 for maintaining anesthesia) and placed in a stereotaxic apparatus for bilateral intrastriatal injections (2 µl; 15 × 10⁹ genomic copies). Two injections were performed in the striatum at the following coordinates relative to bregma: (1) anteroposterior (AP), + 0.8; mediolateral (ML), +/- 1.8; and profundity, -2.6 mm and (2) AP, + 0.3; ML, +/- 2; and profundity, - 2.6 mm, below the dural surface. Viral vectors were injected using a 10 µl-Hamilton microliter syringe at an infusion rate of 200 nl/min. The needle was left in place for 5 min to ensure complete diffusion of the viruses and then slowly retracted from the brain. Both hemispheres were injected with the same shRNA. Five weeks after injection, motor learning was evaluated at the accelerating rotarod.

12. ACCELERATING ROTAROD

Five weeks after intrastriatal injection of rAAV2/8-shRNAs, animals were subjected to the accelerating rotarod test. Mice were placed on a 3 cm rod (Panlab) with an increasing speed from 4 to 40 rpm over 5 minutes. Latency to fall was recorded as the time mice spent in the rod before falling. Accelerating rotarod test was performed for 4 days, 3 trials per day. Trials in the same day were separated by 1 hour.

13. STATISTICS

All experiments were performed at least in triplicate, and results are reported as mean \pm SEM. Student's T-test was performed as unpaired, two-tailed sets of arrays and presented as probability *P* values. One-way ANOVA with Bonferroni's multiple comparison test and Two-way ANOVA followed by Bonferroni's *post-hoc* tests were performed for the comparison of multiple groups. Values of *P* < 0.05 were considered as statistically significant.

14. SINGLE NUCLEOTIDE POLYMORPHISM ANALYSIS

14.1 Cohort of study and data collection

1,819 subjects with 898 PD cases and 921 unrelated healthy controls were recruited at the Movement Disorders Unit from the Hospital Clínic de Barcelona. All participants were from European origin from the northeastern regions of Iberian Peninsula. Patients had a clinical diagnosis of definite PD according to UKPDS criteria⁴⁴⁴ except that family history was not used as exclusion criterion, or a neuropathological diagnosis of definite PD according to proposed criteria⁴⁴⁵. At recruitment, an informed written consent was obtained and whole blood samples were obtained from each subject. Genomic DNA was isolated from peripheral blood lymphocytes as previously described⁴⁴⁶ and stored at -80°C until use. The study was approved by the Ethics Committee of the Hospital Clínic de Barcelona.

14.2 Single Nucleotide Polymorphism selection and genotyping

64 Single Nucleotide Polymorphisms (SNPs) from 57 genes in the mTOR pathway and from genes involved in PD were selected based on the following criteria: (i) a minor allele frequency (MAF) > 0,1 according to data from the HapMap project and (ii) an already published (Pubmed) association of the SNP with a neurological disorder, a psychiatric

disorder, or other diseases. All these 64 selected SNPs were genotyped using TaqMan® OpenArray® Genotyping Plates, Custom Format 64 QuantStudio™ 12K Flex, in the Genomics Core facility (Universitat Pompeu Fabra, Parc de Recerca Biomèdica de Barcelona).

Next, SNPs were filtered out and removed from the study those which were not in Hardy-Weinberg equilibrium (HWE) or that did not surpass a genotyping call-rate above 95% of all studied samples. This quality control reduced the list to 54 SNPs.

14.3 Statistical analyses

14.3.1 Hardy-Weinberg equilibrium

Hardy-Weinberg equilibrium (HWE) assumes that allele and genotype frequencies in a population will remain constant from generation to generation in the absence of evolutionary influences. If frequencies deviate significantly from HWE it could indicate systematic errors in genotyping. For each SNP, HWE was analyzed separately in cases and controls using an exact test in the SNPstats software (<http://bioinfo.iconcologia.net/SNPstats>).

14.3.2 Allelic association analysis

Differences of SNPs allelic frequencies between cases and controls were calculated using the Expectation-Maximization algorithm as implemented in the software UNPHASED 3.1.7 (<http://www.mrcbsu.cam.ac.uk/personal/frank/software/unphased/>)⁴⁴⁷ and adjusting by potential confounders including gender and age. We used a *P* level of statistical significance of 0.05. We corrected all *P*-values for multiple testing by using the false discovery rate (FDR) adjustment⁴⁴⁸ ($n=54$ tests).

14.3.3 Genotypic association analysis

Statistically significant SNPs detected in the allelic analysis were further analyzed at the genotypic level under the different possible models of inheritance as computed in the SNPstats software (<http://bioinfo.iconcologia.net/SNPstats>)⁴⁴⁹, and also considering as covariates gender and age, and adjusting *P*-values by the Benjamini & Hochberg FDR multiple testing adjustment⁴⁴⁸. As implemented in SNPstats, among all possible inheritance models for each SNP, the model best fitting the data was automatically defined as the model with the lowest Akaike information (AIC) value and therefore minimized expected entropy.

14.3.4 Epistatic association analysis

The multifactorial dimensionality reduction (MDR) software (version 3.04; <http://www.multifactorialdimensionalityreduction.org>) was used to identify possible high-order interaction associated with the phenotype in study. The MDR method provides a data mining strategy for detecting and characterizing nonlinear interactions among discrete attributes such as SNPs, or their multiple combinations, that are predictive of a discrete outcome such as case-control status⁴⁵⁰. In this study, the best model was considered if it had a minimal prediction error and maximal cross-validation consistency (CVC). MDR analyses were performed using 10-fold cross-validation, therefore the training set comprises 90% of the data, whereas the testing set comprises the remaining 10% to test the predictive power of the interaction. Statistical significance was evaluated using 1000-time permutation test.

The cross-validation consistency is the measure of the number of times a particular SNP interaction is identified in each possible 90% of the subjects⁴⁵¹. All *P*-values were two-sided and considered statistically significant with less than 0.05.

RESULTS

1. ROLE OF RTP801 PROTEIN IN HUNTINGTON'S DISEASE

The activity of mTOR pathway has been extensively studied in cellular and animal models of neurodegenerative diseases as it regulates important neuronal functions such as neuronal survival, protein translation and autophagy²⁴⁹. Interestingly, impairment of the mTOR pathway is a hallmark of many neurodegenerative disorders including HD^{285,290,452}. Furthermore, the inactivation of mTOR pathway in HD has been suggested to be beneficial, since its inhibition with rapamycin or rapalogs activates autophagy and therefore the clearance of mhtt^{72,285}. Interestingly, mTOR is fine-tuned regulated by several proteins and one of these relevant regulators is RTP801²⁶⁷.

RTP801 is as a stress-related protein whose expression is induced in response to stressful environmental conditions in an attempt to maintain cellular viability and function²⁶⁶. However, a sustained and chronic RTP801 increase can be detrimental and lead to neuronal death by a sequential inhibition of first mTOR and subsequently Akt kinase^{263,266,267}. Inactivated Akt would be unable to enhance pro-survival signals thereby triggering neuronal death²⁶⁴.

In the central nervous system, RTP801 expression is upregulated in response to toxic stimuli such as chronic unpredictable stress⁴⁵³, ischemia^{266,454,455}, β -amyloid peptide^{342,456} and 6-OHDA^{263,361} and MPTP PD mimetics²⁶³. Importantly, RTP801 not only accumulates in cellular and animal toxic models, but also in samples from patients suffering from neurodegenerative diseases. RTP801 protein levels were found increased in dopaminergic neurons from the SNpc in idiopathic and mutant parkin PD patients^{263,349,359} and in lymphocytes from AD patients³⁶⁰. Nevertheless, involvement of RTP801 in mhtt toxicity was never investigated.

1.1 Role of RTP801 in mhtt-induced cell death

Neuronal death is the main pathological hallmark of HD. Despite the ubiquitous expression pattern of htt in the brain, the most vulnerable regions are the putamen and caudate nucleus³⁰ and the motor cortex³² which undergo severe neurodegeneration. However, mhtt toxicity also extends to other brain structures such as the hippocampus³³ and the cerebellum³⁴ showing neuronal dysfunction or slight neuronal death, respectively. Currently, the exact mechanisms underlying mhtt-induced toxicity are not clearly defined, although the mTOR pathway is one of the signaling cascades affected in the disease^{285,290,452}. This prompted us to investigate whether RTP801 could be involved in mhtt-induced toxicity.

RESULTS

1.1.1 Ectopic mhtt increases RTP801 protein levels in neural cells and induces cell death

RTP801 is upregulated in neuronal cells as response to different types of toxic stimuli^{263,342,423,455,456}. Thus, we asked whether mhtt could also upregulate RTP801 levels. For that purpose, NGF-differentiated PC12 cells were transfected with eGFP alone (empty vector) or with exon-1-encoded N-terminal htt with 25 (Q25, non-toxic form), 72 or 103 (Q72 and Q103, toxic forms) CAG repeats fused to eGFP. Twenty-four hours after transfection, RTP801 and ectopic htt protein levels were analyzed by WB. First, we detected the protein product of all three forms of htt by WB and, as expected, the mutant products of Q72 and Q103 were found in both the soluble and insoluble fraction. Moreover, we also observed insoluble Q72 and Q103 retained in the stacking gel (Figure 26A). Interestingly, we observed that RTP801 protein levels were increased about 70% in cells overexpressing Q72 or Q103 in comparison to those cells transfected with control eGFP or Q25 expressing plasmids (Figure 26A).

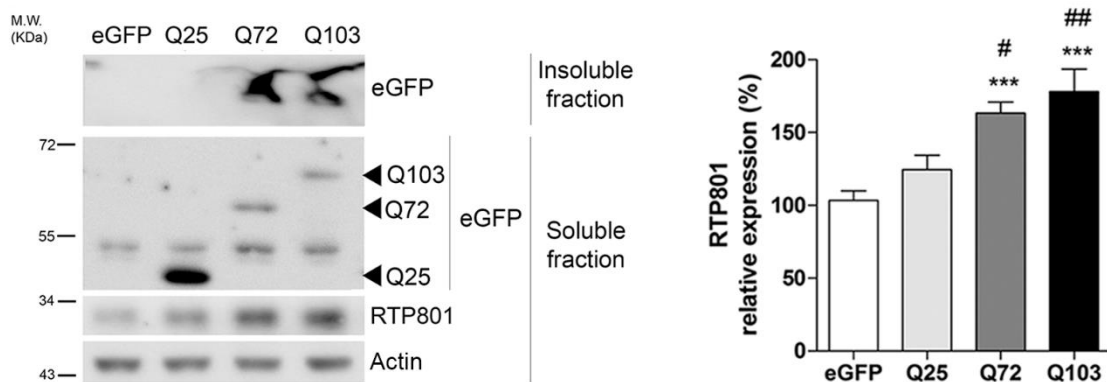


Figure 26. RTP801 protein levels are increased in NGF-differentiated PC12 cells overexpressing mhtt. Extracts from transfected NGF-differentiated PC12 cells with eGFP, Q25, Q72 or Q103 constructs for 24 hours were subjected to WB. Membranes of the soluble and insoluble fractions were probed with antibodies against eGFP and RTP801, and then re-probed with an anti-actin antibody as a loading control. Representative immunoblots are shown along with densitometry analysis for RTP801 signal from at least 3 independent experiments and expressed as the mean \pm SEM. Data were analyzed by One-way ANOVA with Dunnett's multiple comparison test test (*** P <0.001 vs. eGFP; # P <0.05, ## P <0.01 vs. Q25).

Furthermore, by immunofluorescence we confirmed that Q72 and Q103 overexpressing cells showed higher levels of RTP801 (Figure 27A1 & 27A2). Interestingly, around 35% of mhtt-transfected cells that were highly stained for RTP801 also displayed pyknotic nuclei (Fig. 27A3). To corroborate our results in another cell model, rat primary cortical neurons were transfected with the same constructs and the increase of RTP801 levels and cell death were assessed by immunofluorescence. Similarly to NGF-differentiated PC12 cells, primary neurons DIV21 overexpressing mhtt displayed increased levels of

RTP801 (Figure 27B1 & 27B2) and, of those almost the 50% showed pyknotic nuclei (Fig. 27B3). Remarkably, in both neuronal models RTP801 formed aggregates that often co-localized with mhtt aggregates.

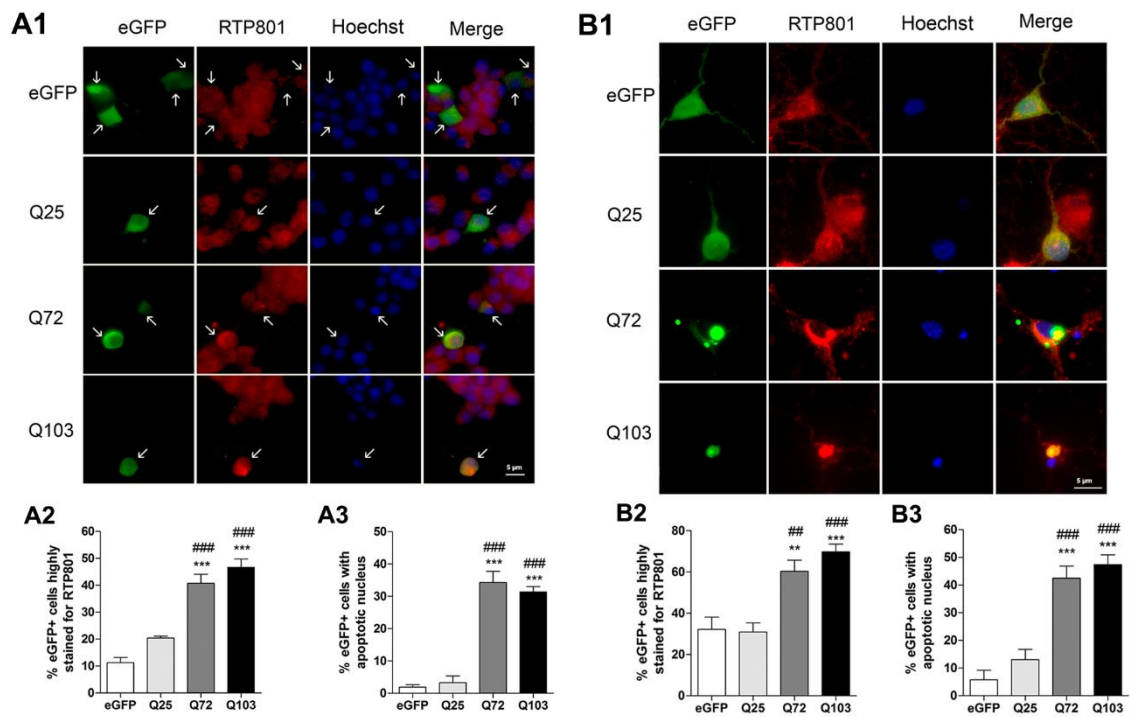


Figure 27. Overexpression of mhtt increases RTP801 protein in neural cells and induces cell apoptosis. (A1) NGF-differentiated PC12 cells or (B1) rat cortical neurons DIV19 were transfected with eGFP, Q25, Q72 or Q103 constructs. After 24h (in NGF-differentiated PC12 cells) or 48h (in cortical neurons) of transfection, cultures were fixed and immunostained against eGFP (in green) and RTP801 (in red). Nuclei were revealed with Hoechst 33342 (in blue). Transfected cells are indicated with white arrows. Graph represents values of at least three independent experiments. Scale bar, 5 μ m. (A2 & B2) Surviving eGFP+ cells highly positive stain for RTP801 were scored and represented as a percentage of total transfected cells. (A3 & B3) The number of eGFP+ cells with increased RTP801 staining and containing pyknotic nuclei were scored and represented as a percentage of total transfected cells. Values represent mean \pm SEM for at least three independent experiments performed in triplicate. Data were analyzed by One-way ANOVA with Dunnett's multiple comparison test (** P <0.01 and *** P <0.001 vs. eGFP; ## P <0.01 and ### P <0.001 vs. Q25).

i. Both RTP801 mRNA levels and protein degradation are altered in NGF-differentiated PC12 cells overexpressing mhtt

Next, we investigated the mechanisms by which mhtt induces RTP801 protein accumulation. A sustained RTP801 increase could be the end point of several processes, including gene expression and impaired protein degradation.

We first analyzed RTP801 mRNA levels in NGF-differentiated PC12 cells transfected with eGFP, Q25, Q72 or Q103 mhtt constructs to assess whether mhtt induces RTP801 expression at the transcriptional level. By RT-qPCR we found that pathogenic Q72 or

RESULTS

Q103-overexpressing cells displayed a 3-fold increase in RTP801 mRNA levels compared to cells transfected with eGFP or Q25-expressing plasmids (Figure 28A).

In order to investigate whether the increase in RTP801 mRNA levels could result from an upregulation of gene expression or a reduction of the mRNA degradation rate, we analyzed mRNA half-life in NGF-differentiated PC12 cells transfected with eGFP, Q25, Q72 or Q103 constructs. Twenty-four hours after transfection, actinomycin D as an inhibitor of RNA synthesis was added to the culture medium for 10 or 60 minutes. The cells were subsequently harvested and the RNA isolated. RTP801 transcripts were analyzed by RT-qPCR. As shown in Figure 28B, mhtt did not alter the half-life of RTP801 mRNA. This result points out that increased RTP801 mRNA levels are due to stress-induced gene expression.

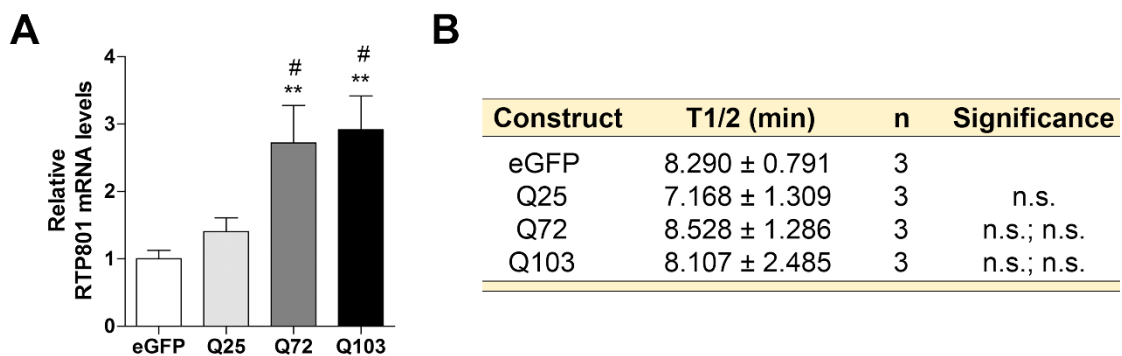


Figure 28. Mutant htt upregulates RTP801 transcriptionally. (A) NGF-differentiated PC12 cells were transfected with eGFP, Q25, Q72 or Q103 constructs. RNA was extracted 24 hours post-transfection and samples were analyzed by RT-qPCR to quantify RTP801 mRNA under the indicated conditions. Values represent mean \pm SEM of at least three independent experiments. Data were analyzed using One-way ANOVA with Dunnett's Multiple comparison test. (** $P < 0.01$ vs eGFP; # $p < 0.05$ vs. Q25). **(B)** Mutant htt does not alter RTP801 mRNA half-life. NGF-differentiated PC12 cells were transfected with eGFP, Q25, Q72 or Q103 constructs. Actinomycin D was added to the media 24 h post-transfection for 10 or 60 minutes. RNA was extracted, and RT-qPCR was performed to quantify RTP801 mRNA under the indicated conditions. RTP801 mRNA half-life (min) was calculated and expressed as the mean \pm SEM of three independent experiments performed in triplicate. Data were analyzed by One-way ANOVA with Dunnett's Multiple comparison test (n.s., not significant).

Next, we assessed whether mhtt, apart from inducing RTP801 gene expression, could impair RTP801 protein degradation. RTP801 show an extremely short half-life between 2 and 7 minutes^{306,357,358} and is mainly degraded by the proteasomal system^{349,359}. To this end, NGF-differentiated PC12 cells were transfected with eGFP, Q25-, Q72- or Q103-expressing plasmids. Twenty-four hours later, cultures were treated with cycloheximide (CHX), a protein synthesis inhibitor, for 10 or 60 minutes. Relative RTP801 protein levels were resolved in a WB to calculate the protein degradation rate. Interestingly, we found that ectopic mutant Q72 and Q103 increased the RTP801 protein half-life by 4 and 10 minutes, respectively (Figure 29).

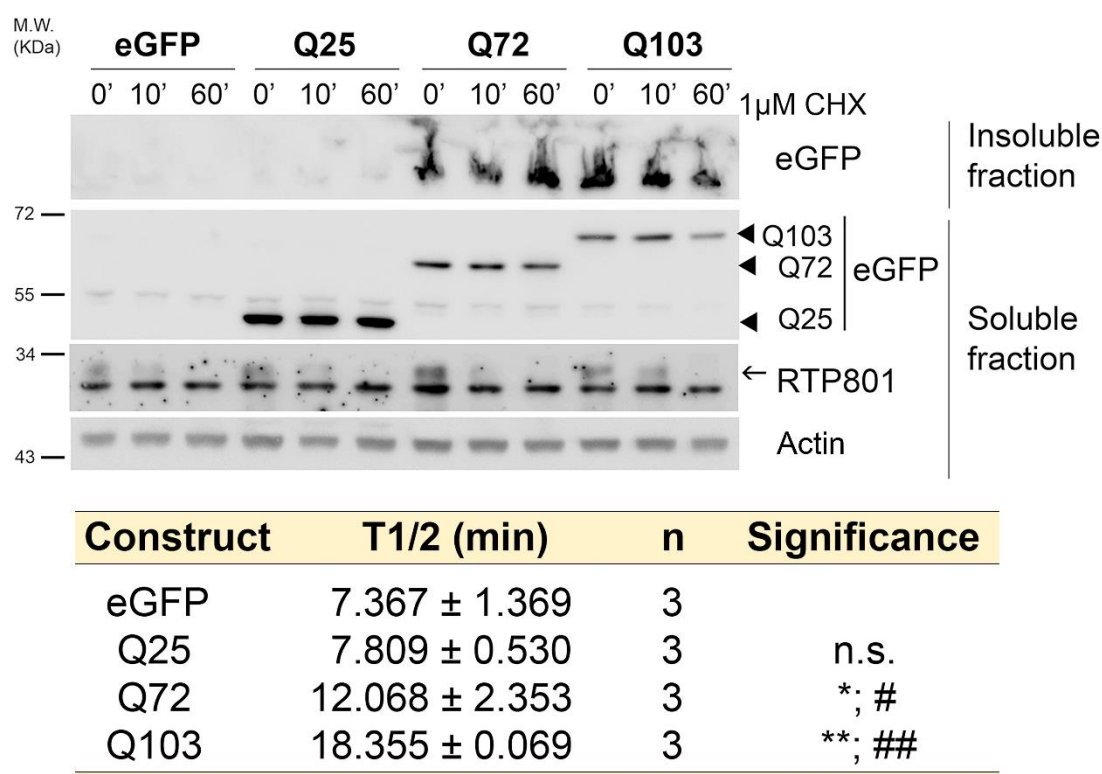


Figure 29. Mutant htt alters RTP801 protein degradation rate. NGF-differentiated PC12 cells were transfected with eGFP, Q25, Q72 or Q103 constructs for 24 hours and then treated with cycloheximide (CHX) for 10- or 60-min. Cell extracts were harvested, and insoluble and soluble protein fractions were subjected to WB. Membranes were probed with antibodies against eGFP and RTP801, and with anti-actin antibody as a loading control. Representative immunoblots are shown. Note that the RTP801 specific band in the WB is denoted with an arrow. RTP801 half-life (min) was calculated and expressed as the mean ± SEM of 3 independent experiments performed in triplicate. Data were analyzed by One-way ANOVA with Dunnett's Multiple comparison test (* P <0.05, ** P <0.01 vs. eGFP; # P <0.05, ## P <0.01 vs. Q25).

Taken together, our results show that mhtt elevates RTP801 protein levels by both increasing RTP801 expression and impairing RTP801 proteasomal degradation.

ii. RTP801 upregulation mediates mhtt-induced death of NGF-differentiated PC12 cells

In cellular models of PD, evidence demonstrated that RTP801 is sufficient and necessary to induce cell death^{263,266}. Besides, we have shown in two different cellular models, NGF-differentiated PC12 cells and primary cortical neurons, that at least half of the mhtt-overexpressing cells displayed apoptotic nuclei.

To explore whether RTP801 elevation mediates mhtt-induced toxicity, we co-transfected NGF-differentiated PC12 cells with control Q25 htt or pathogenic Q72 mhtt and shRNAs to knockdown RTP801 expression. To discard off-target effects, we tested two different nucleotide sequences (shRTP801 1 and shRTP801 4). Forty-eight hours after transfection RTP801 protein levels were analyzed by WB. We confirmed that RTP801

RESULTS

knockdown was about 20-30% in cells transfected with RTP801 shRNAs compared to those transfected with the scrambled shRNA (Figure 30A). Remarkably, when mhtt-induced RTP801 accumulation was abrogated with shRNAs, mhtt-induced cell death was significantly prevented (Figure 30B). Thus, these results highlight RTP801 important contribution to mhtt-induced toxicity.

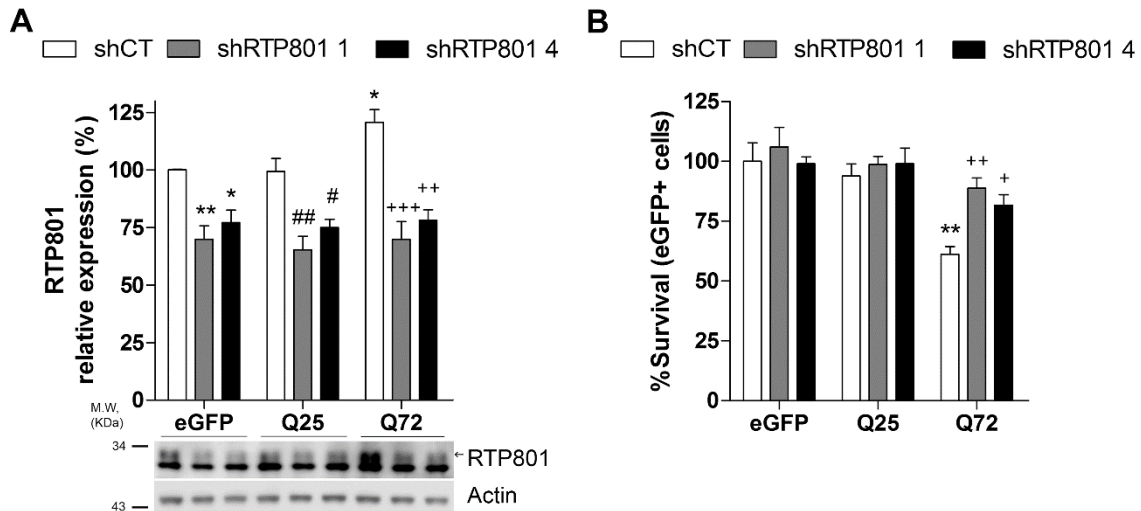


Figure 30. RTP801 mediates mhtt-induced cell death. (A) Specific shRNAs against RTP801 abrogated mhtt-induced RTP801 expression. NGF-differentiated PC12 cells were co-transfected with eGFP, Q25 or Q72, and either pCMS-eGFP-shG (scrambled shRNA as a control), pCMS-eGFP-shRTP801-1 or pCMS-eGFP-shRTP801-4. Two days later RTP801 protein levels were analyzed by WB. Representative immunoblots for RTP801 and actin as loading control are shown along with densitometry analysis. Values represent the mean \pm SEM of at least three independent experiments. Note that the RTP801 specific band in the WB is denoted with an arrow. **(B)** Under the same transfection conditions, cell survival (eGFP+ cells) was scored using fluorescence microscopy. The graph shows the number of surviving cells in each condition. Values represent the mean \pm SEM of three independent experiments. Data were analyzed using One-way ANOVA with Dunnett's multiple comparison test (* P <0.05, ** P <0.01 vs eGFP shG; # P <0.05, ## P <0.01 vs Q25 shG; + P <0.05, ++ P <0.01 and +++ P <0.001 vs. Q72 shG).

1.1.2 RTP801 is not altered in the striatum of HD murine models

To further extend our results to HD mouse models, we investigated whether RTP801 protein was also altered in the striatum of HD murine models: the R6/1 mice that express the human exon-1 of mhtt, and the knock-in mice model Hdh^{Q7/Q111} (KI) which express the endogenous full-length mhtt. Both mouse models are characterized by almost no neuronal death, although medium spiny neurons have a smaller morphology and the striatal volume is reduced^{103,457–460}. Remarkably, these two mouse models display motor and cognitive impairment but differ at the onset and the progression of HD pathology. R6/1 mice show earlier onset and faster disease progression than Hdh^{Q7/Q111} KI mice^{461,462}. Of note, motor deficits begin to appear in R6/1 mice at 12-weeks of age and are evident at 3-months, whereas in Hdh^{Q7/Q111} KI mice does at 8-months⁴⁶¹.

As shown in Figure 28, mhtt upregulates the gene expression of RTP801 in cellular models. Therefore, we first studied whether RTP801 gene expression was induced in an HD mouse model at early stages of the disease. For that purpose, we first analyzed RTP801 mRNA levels in the 12-weeks old R6/1 mice. We found that RTP801 mRNA levels did not vary in comparison with the wild-type (WT) littermates (Fig 31).

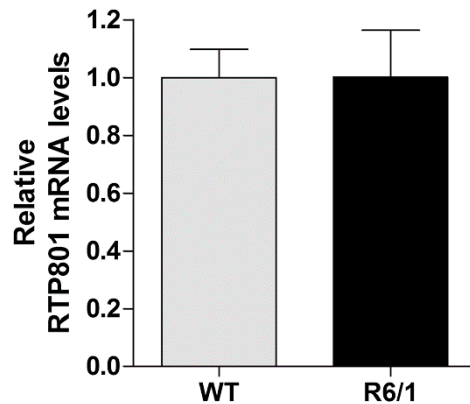


Figure 31. RTP801 mRNA levels are not altered in the striatum of R6/1 mouse model. RTP801 mRNA levels from the striatum of 12-week-old WT and R6/1 mice were analyzed by RT-qPCR. Results are expressed as fold increase respect RTP801 mRNA levels in WT mice and represented as mean \pm SEM of seven animals per condition. Data were analyzed by Student's T-test.

Next, we analyzed RTP801 protein at different stages of the disease ranging from asymptomatic stages to the appearance of cognitive and motor deficits. Thus, RTP801 protein levels were analyzed by WB in the striatum of R6/1 and Hdh^{Q7/Q111} KI HD animal models. Interestingly, we did not detect changes at RTP801 protein levels in the striatum of either R6/1 or Hdh^{Q7/Q111} KI mice at any stage when compared with the corresponding WT littermates (Figure 32A & 32B).

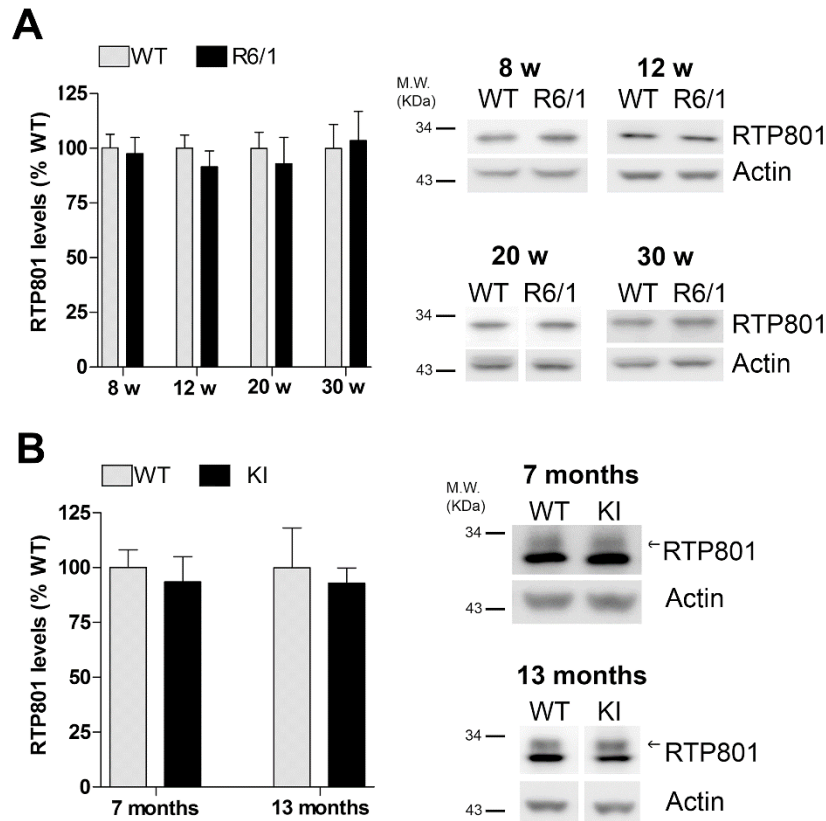


Figure 32. RTP801 protein levels are not altered in the striatum of HD mouse models. (A) Striata from WT and R6/1 mice at different stages of disease progression (from 8 to 30 weeks (w) of age) were subjected to WB. Membranes were probed with antibodies against RTP801 and actin as a loading control. The left panel shows densitometric analysis with the values represented as the mean \pm SEM of 6 animals per condition. **(B)** Striata from 7 and 13 months old Hdh^{Q7/Q7} (WT) and Hdh^{Q7/Q111} knock-in (KI) mice were subjected to WB. Membranes were probed with antibodies against RTP801 and actin as a loading control. The left panel shows densitometric analysis with the values represented as the mean \pm SEM of 5 animals per condition. The specific RTP801 band is denoted with an arrow. Data were analyzed using Student's T-test.

1.1.3 RTP801 is increased in differentiated HD-iPSCs cells and in human postmortem HD brains

We next tested our hypothesis in human HD-iPSCs and human brain tissue. To achieve this, we analyzed RTP801 levels in iPSCs derived from a non-affected individual (expressing htt containing 33 CAG repeats, referred as controls; Ctr33) and from an HD patient (expressing mhtt containing 60 CAG repeats, referred as HD60) that were differentiated according to a neuronal differentiation protocol that generates striatal medium-sized spiny neurons⁴⁶³. Cells were harvested 12 days after starting the differentiation process, when they display a medial telencephalic identity. As shown in Figure 33A, mhtt-expressing cells displayed a 37% increase in RTP801 protein levels compared to control patient-derived cells. Hence, this result show that RTP801 is elevated in response to mhtt in human HD-iPSCs.

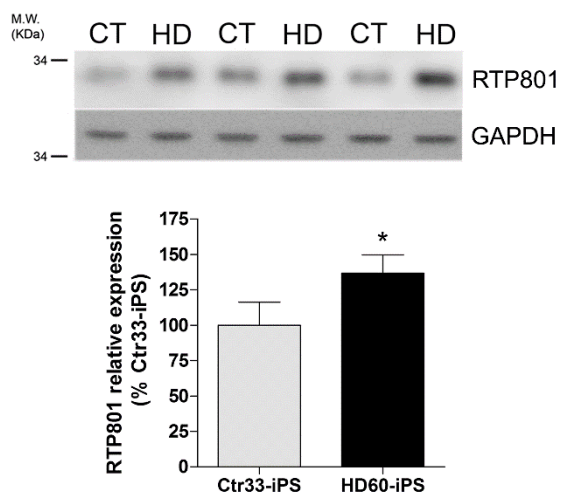


Figure 33. RTP801 protein levels are increased in HD-iPS cell line. iPSCs expressing control (Ctr33) or mutant (HD60) htt were subjected to WB after 12 days of differentiation towards medium spiny neurons. Membranes were probed with antibodies against RTP801 and GAPDH, as a loading control. The graph displays values obtained by densitometric analysis, shown as the mean \pm SEM of 3 independent iPSC differentiations. Data were analyzed using Student's T-test ($*P < 0.05$ vs. Ctr33).

Next, we explored whether RTP801 expression is also altered in brain structures of HD patients. Atrophy of the striatum (caudate nucleus and putamen) and thinning of the cortex are the most significant neuropathological abnormalities in HD, although other brain areas such as hippocampus, cerebellum or amygdala show neuronal dysfunction³⁰.

Thus, in order to study whether increase of RTP801 also occurs in HD patients, we analyzed RTP801 protein levels by WB in tissue lysates from the putamen, caudate nucleus, frontal cortex, hippocampus and cerebellum of seven control and six HD donors (Table 6), and in the caudate nucleus of 3 HD patients.

Patient	Pathological diagnosis	Gender	Age (years)	CAG repetitions
1	Normal	Female	60	-
2	Normal	Female	68	-
3	Normal	Female	71	-
4	Normal	Female	81	-
5	Normal	Male	39	-
6	Normal	Male	56	-
7	Normal	Male	64	-
8	HD, Vonsattel grade 4	Female	28	62
9	HD, Vonsattel grade 3	Female	72	42
10	HD, Vonsattel grade 3	Male	53	45
11	HD, Vonsattel grade 3-4	Male	55	-
12	HD, Vonsattel grade 4	Male	59	44
13	HD, Vonsattel grade 4	Male	60	43

Table 6. Human post-mortem HD brains.

RESULTS

We observed increased levels of RTP801 in the putamen, caudate nucleus and cerebellum (Figure 34A, 34B and 34C) whereas no changes were detected in frontal cortex and hippocampus (Figure 34D and 34E) when compared with control cases. Hence, our results show for the first time that RTP801 protein levels are specifically increased in the striatum and cerebellum of HD patients.

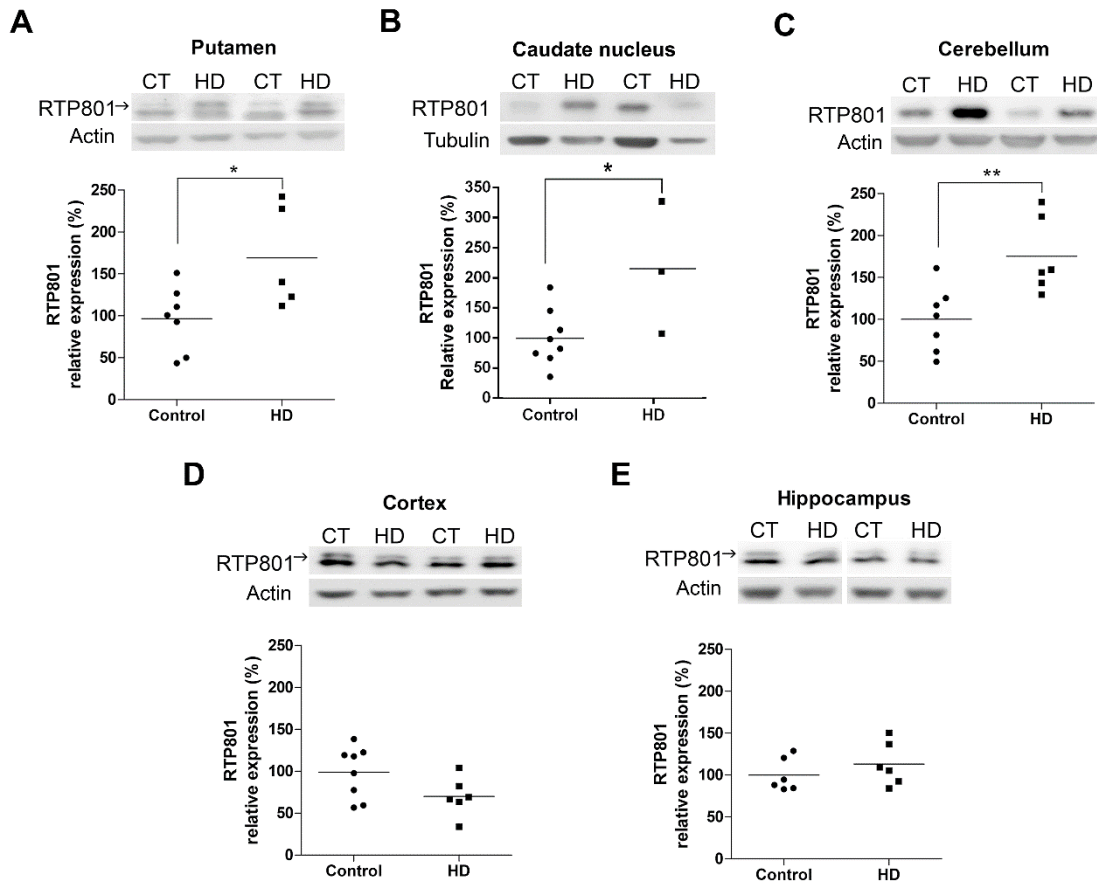


Figure 34. RTP801 is highly expressed in affected-brain areas of HD patients. RTP801 levels were analyzed by WB in protein extracts obtained from (A) putamen, (B) caudate nucleus, (C) cerebellum, (D) frontal cortex and (E) hippocampus of control individuals and HD post-mortem brains. Representative immunoblots of RTP801 and actin or tubulin, as loading controls, are shown. The graphs display values obtained by densitometric analysis of western blot data. Note that the specific RTP801 band is indicated with an arrow. Results are shown as the mean \pm SEM. Student's T-test. Data was analyzed using Student's T-test (* P <0.05 and ** P <0.01 vs. control).

Taken together, our results indicate that RTP801 can be considered a novel downstream effector of mhtt toxicity.

1.2 Role of RTP801 protein in dysfunctional neuronal plasticity associated to Huntington's disease

Several works indicate that cell death does not occur until late stages of HD pathogenesis, suggesting that neuronal dysfunction and abnormal synaptic plasticity are likely the main early pathogenic events that finally result in neurodegeneration^{464–466}. Moreover, the aberrant synaptic function display in the disease^{17,467–471} led to consider HD as a synaptopathy⁴⁷². In fact, *de novo* protein translation is one of the critical functions to maintain synaptic plasticity^{282,284,316,473}. In this regard, mTOR acts as the main regulator of the protein synthesis, and consequently its role in neuronal plasticity is crucial³¹⁷. Besides, mTOR regulates the actin cytoskeleton which is essential to maintain the structural plasticity in mature synapses and to regulate LTP and LTD processes^{474–478}. As a regulator of the mTOR pathway, the upregulation of RTP801 by mhtt could impair synaptic function and affect plasticity. Hence, in this section we will study whether mhtt disrupts neuronal plasticity by increasing synaptic RTP801 levels and impairing the mTOR pathway.

1.2.1 Ectopic mhtt increases RTP801 at dendritic spines of rat cortical primary neurons

Previous data have demonstrated that the overexpression of the pathogenic exon-1 of mhtt induces RTP801 accumulation in neural cell models. To extend this result, we next wondered whether mhtt increases RTP801 protein levels at the synapse. For this reason, rat cortical primary neurons DIV13 were transfected with eGFP, Q25, Q72- or Q103-expressing plasmids. Twenty-four hours after transfection, cultures were fixed, and dendritic F-actin puncta were labelled (Figure 35A1). As indicated with an arrow RTP801 was found within the dendritic spines. The overexpression of exon-1-mhtt induced a reduction in the number of dendritic spines (Figure 35A2) along with an increase in somatic RTP801 (Figure 35A3), as previously reported (Figure 27B). Importantly, mhtt overexpression increased RTP801 levels at dendritic spines almost a 50% (Figure 35A4).

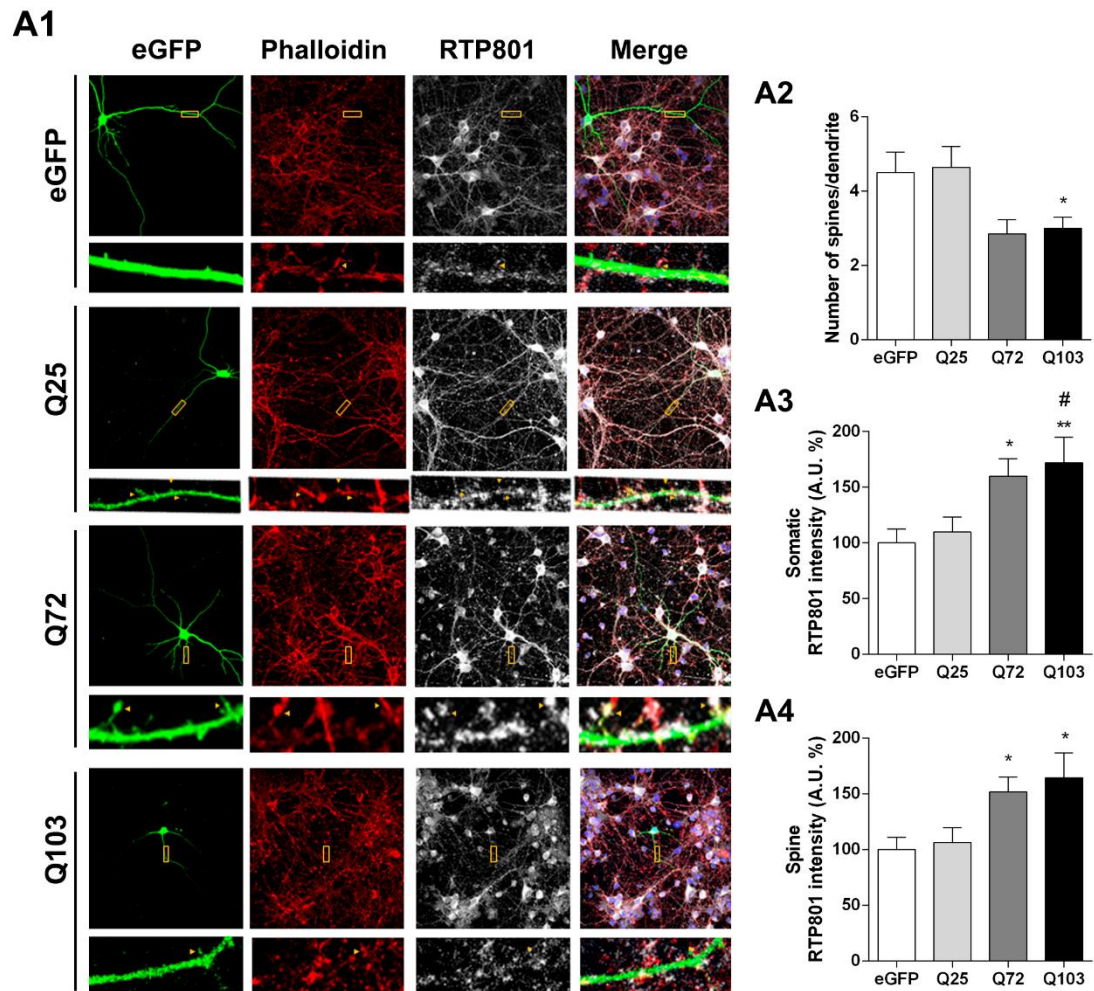


Figure 35. RTP801 protein is present in dendritic spines of cortical neurons and the overexpression of exon-1 mhtt increases its protein levels. (A1) Rat cortical cultures at DIV13 were transfected with eGFP, Q25, Q72 or Q103 plasmids. Twenty-four hours after transfection cultures were fixed and stained against GFP (in green), RTP801 (in grey) and phalloidin (in red) to visualize the actin cytoskeleton. Images were acquired by confocal microscopy. Yellow rectangles show digital zoom of dendrites with spines and yellow arrows show RTP801 staining at the puncta. (A2) Graphs display the number of spines scored for each 15 μ m dendrite-length and RTP801 staining intensity quantification at (A3) the neuronal soma and at (A4) the spines. Data are shown as percentage of RTP801 intensity (mean \pm SEM) and were analyzed with One-way ANOVA followed by Dunnett's multiple comparisons test (* P <0.05 and ** P <0.01 vs. eGFP and # P <0.05 vs. Q72).

1.2.2 Study of synaptic RTP801 and components of the mTOR pathway in brain-affected areas of HD patients

The caudate nucleus and the putamen of HD patients is one of the most affected areas in the disease although cortex also undergoes a severe atrophy³⁰. We have already shown that RTP801 is particularly increased in striatum nucleus but not at frontal cortex of HD patients (Figure 33A, 33B & 33D). To further investigate whether the increase of RTP801 in human affected regions also occurs at the synaptic level, we isolated synaptosomes of the putamen and frontal cortex of control and HD individuals (Table 7).

Patient	Pathological diagnosis	Gender	Age (years)	CAG repetitions	Area analyzed
1	Normal	Male	83	-	Str & Ctx
2	Normal	Male	73	-	Ctx
3	Normal	Male	76	-	Str & Ctx
4	Normal	Male	64	-	Str & Ctx
5	Normal	Male	86	-	Str & Ctx
6	Normal	Male	58	-	Str & Ctx
7	HD, Vonsattel grade 3-4	Male	55	-	Str & Ctx
8	HD, Vonsattel grade 3	Male	53	45	Str
9	HD, Vonsattel grade 1	Male	73	40	Ctx
10	HD, Vonsattel grade 3	Male	85	40	Str & Ctx
11	HD, Vonsattel grade 2	Male	76	41	Str & Ctx
12	HD, Vonsattel grade 2	Male	72	-	Str & Ctx
13	HD, Vonsattel grade 2-3	Male	68	42	Str & Ctx

Table 7. Human post-mortem HD brains. Str = Striatum (Putamen); Ctx = Frontal Cortex.

Synaptosomes have emerged as an useful tool to dissect the protein composition of the synapse since they are composed by the entire presynaptic terminal, including mitochondria, synaptic vesicles and the active zone, attached to the postsynaptic membrane and the postsynaptic density (PSD)^{479–484}. Besides, synaptosomes contain all the molecular machinery necessary for the uptake, storage and release of neurotransmitters as well as presynaptic and postsynaptic receptors. For this reason, synaptosomes are susceptible to pharmacological manipulations and are also helpful for functional synaptic assays^{485–490}.

i. RTP801 is increased in striatal synapses from the putamen of Huntington's disease patients

First, we investigated whether RTP801 protein levels were increased in the striatal synaptic terminals of HD patients. Additionally, the status of the mTOR pathway in the synaptic compartment was also studied. We tested the S6 ribosomal protein phosphorylation at Ser235/236 as readout of mTORC1 complex activity⁴⁹¹ and Akt phosphorylation at Ser473 as readout of mTORC2 complex activity^{298,492}.

We isolated synaptosomes from the putamen of 5 controls (CT) and 5 HD donors and analyzed its protein content by WB (Figure 36A). We first analyzed the synaptosomal

RESULTS

enrichment of each of our proteins of interest. Then, homogenates and synaptosomes were analyzed separately to compare the protein levels in each cellular compartment between CT and HD donors.

Interestingly, RTP801 was found to be highly enriched in the synaptic fraction of the human putamen. We observed increased levels of RTP801 in the putamen of HD patients at both homogenates and synaptosomes in comparison to the control group (Figure 36B).

To confirm proper purification of synaptosomes, we checked the enrichment of synaptic markers that are highly expressed in this compartment. Postsynaptic density protein 95 (PSD-95) was used as a postsynaptic marker since it is localized at the postsynaptic density of excitatory synapses^{169,493}. Synaptic vesicle glycoprotein 2A (SV2A) is a membrane glycoprotein associated with synaptic vesicles and, therefore it was used as a presynaptic marker^{494,495}. Effectively, both PSD-95 and SV2A were enriched in the synaptosomal fraction of the control group but not in the HD group (Figure 36C & 36C). Moreover, PSD-95 was significantly reduced in the synaptosomal fraction of HD patients in comparison to controls (Figure 36C). Meanwhile, synaptosomal SV2A did not display differences between groups (Figure 36D).

Regarding the mTOR pathway, we analyzed the levels of phospho(P)-Akt (Ser473) and phospho(P)-S6 (Ser235/236) as readouts of the mTOR activity (Figure 36E & 36F). Both proteins showed higher levels in the synaptosomal fraction of the putamen, although the enrichment of neither of them reached significance. At total (homogenate) level, both P-Akt (Ser473) and P-S6 (Ser235/236) were increase in HD patients when compared to controls, but no differences were found in the synaptosomal compartment.

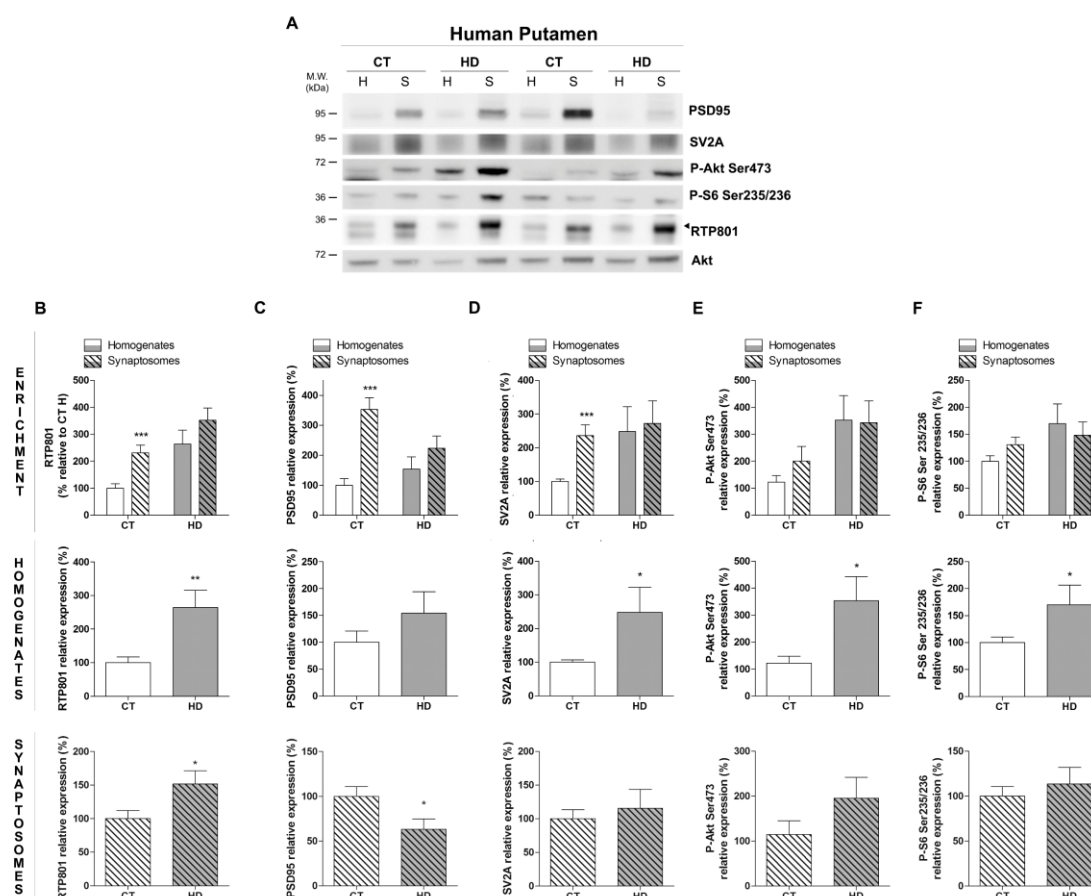


Figure 36. Synaptosomal preparation from the putamen of HD patients. Putamen of 5 HD patients and 5 control individuals were dissected and homogenized in Krebs-Ringer buffer. Later, synaptosomes were isolated and samples were subjected to WB. Membranes were probed against RTP801, P-Akt (Ser473), P-S6 (Ser235/236), PSD-95, SV2A and total Akt as a loading control. Graphs show the densitometric quantification. Data is shown as a mean \pm SEM. Data were analyzed with Two-way ANOVA followed by Bonferroni's multiple comparisons test for post-hoc analyses ($***P < 0.001$ vs. CT homogenate) and data of homogenates and synaptosomes were analyzed by Student's T-test ($*P < 0.05$).

Based on the reduction of the synaptic markers in synaptosomes, we analyzed the levels of RTP801 and the two readouts of mTOR in the synaptic fraction. In order to correct the synaptic loss, the synaptosomal levels of each protein were expressed *versus* the levels of synaptic markers PSD-95, as PSD-95-postsynaptic fraction, (Fig 37A) and SV2A, as SV2A-presynaptic fraction (Fig 37B).

The results showed that RTP801 was increased in the PSD-95- and SV2A-synaptic fractions in the HD group in comparison to the control. Furthermore, both P-Akt (Ser473) and P-S6 (Ser235/236) were elevated in the PSD-95-synaptic fraction of HD patients respect to unaffected individuals, and showed the same tendency in the SV2A-synaptic fraction. These data support the impairment of the mTOR pathway in HD^{72,285,290,452}.

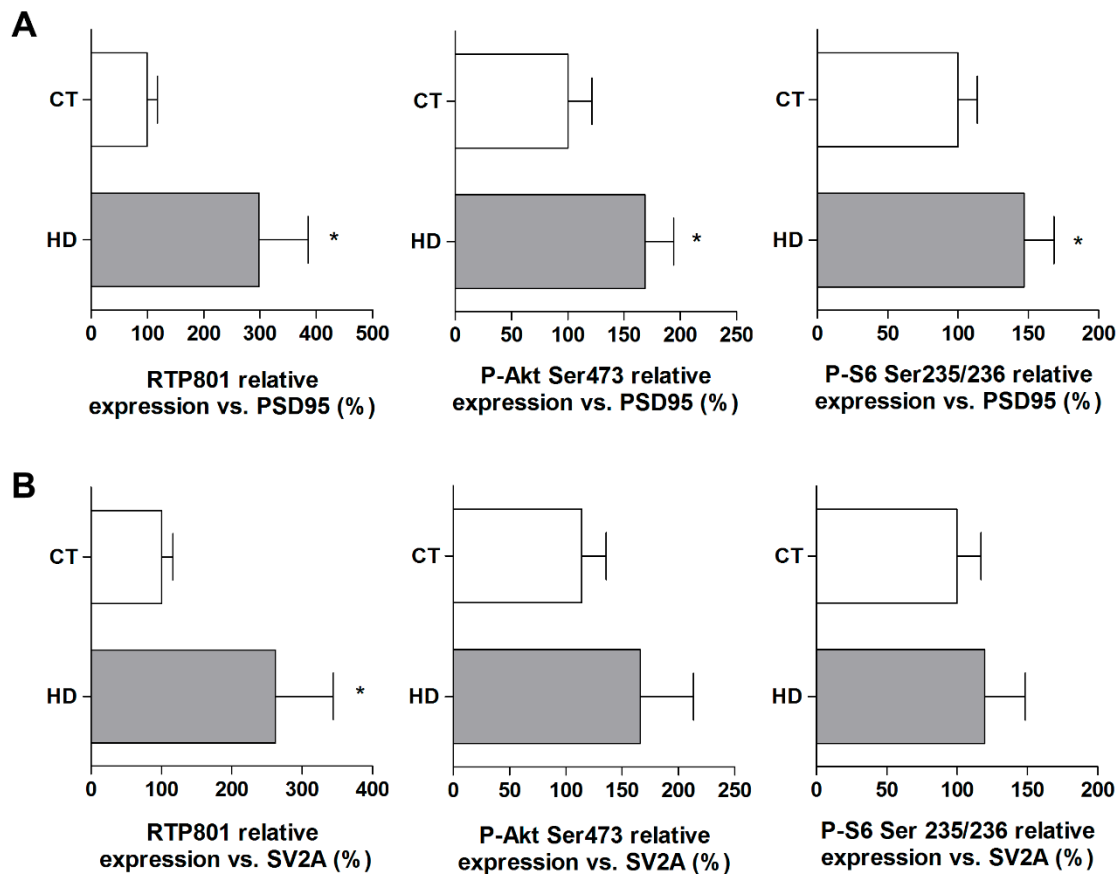


Figure 37. Synaptic enrichment of RTP801, P-Akt (Ser473) and P-S6 (235/236) in the putamen of HD patients. Graphs indicate the levels of RTP801, P-Akt (Ser473) and P-S6 (235/236) corrected by the levels of the synaptic markers **(A)** PSD-95 and **(B)** SV2A in the synaptosomes derived from the putamen of CT and HD donor analyzed in the previous experiment. The results are shown as mean \pm SEM . Data were analyzed by Student's T-test (* $P < 0.05$).

Taken together, these results show that RTP801 is increased in synaptic terminals of the putamen of HD patients, along with the mTOR signaling effectors.

ii. RTP801 is not altered in synapses from the frontal cortex of Huntington's disease patients

To further analyze synaptic RTP801 enrichment, we performed synaptosomal preparations derived from the frontal cortex of 6 CT and 6 HD individuals. The protein content was investigated by WB, and the results were expressed firstly as the protein synaptic enrichment and secondly, as protein levels in homogenates and synaptosomes to compare between disease status (Figure 38A).

In correlation with putamen data, RTP801 was highly enriched in the synaptosomal compartment (Figure 38B). Unfortunately, we did not detect variations in the levels of RTP801 neither in homogenates nor in synaptosomes. We corroborated the proper

isolation of synaptosomes by the enrichment of PSD-95 and SV2A (Figure 38C & 38D), which also did not show differences in their protein levels between HD and CT group.

Moreover, the two mTOR downstream effectors, P-Akt (Ser473) and P-S6 (Ser235/236), were studied in the synaptosomes (Figure 38E & 38F). In contrast to putamen, only P-S6 (Ser235/26) showed a significant decrease in synaptosomes of HD in contrast to control cases.

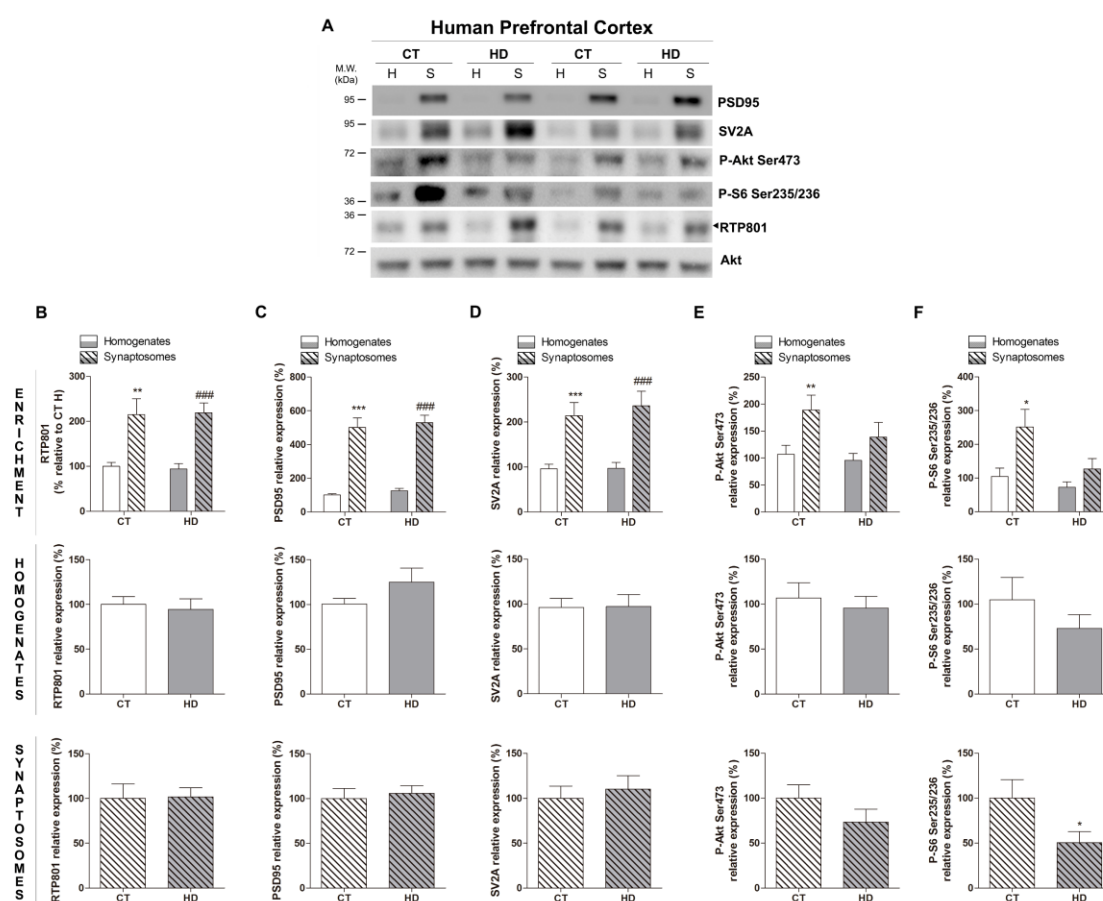


Figure 38. Synaptosomal preparation from the frontal cortex of HD patients. Prefrontal cortex of 6 HD patients and 6 control individuals were dissected and homogenized in Krebs-Ringer buffer. Later, synaptosomes were isolated and samples were subjected to WB. Membranes were probed against RTP801, P-Akt (Ser473), P-S6 (Ser235/236), PSD-95, SV2A and total Akt as a loading control. Graphs show the densitometric quantification. Data is shown as a mean ± SEM. Data were analyzed with Two-way ANOVA followed by Bonferroni's multiple comparisons test for post-hoc analyses (* $P < 0.05$, ** $P < 0.01$, *** $P < 0.001$ vs. CT homogenate; ### $P < 0.001$ vs. HD homogenate) and data of homogenates and synaptosomes were analyzed by Student's T-test (* $P < 0.05$).

Even though the absence of alterations in the synaptic markers, we expressed the synaptosomal levels of the proteins relative to PSD-95 or to SV2A to obtain the PSD-95- (Figure 39A) and SV2A-synaptic fraction (Figure 39B). No alterations were found at RTP801 or P-Akt (Ser273) synaptic levels. However synaptic P-S6 (Ser235/236) was significantly diminished in the HD prefrontal cortex compared to controls.

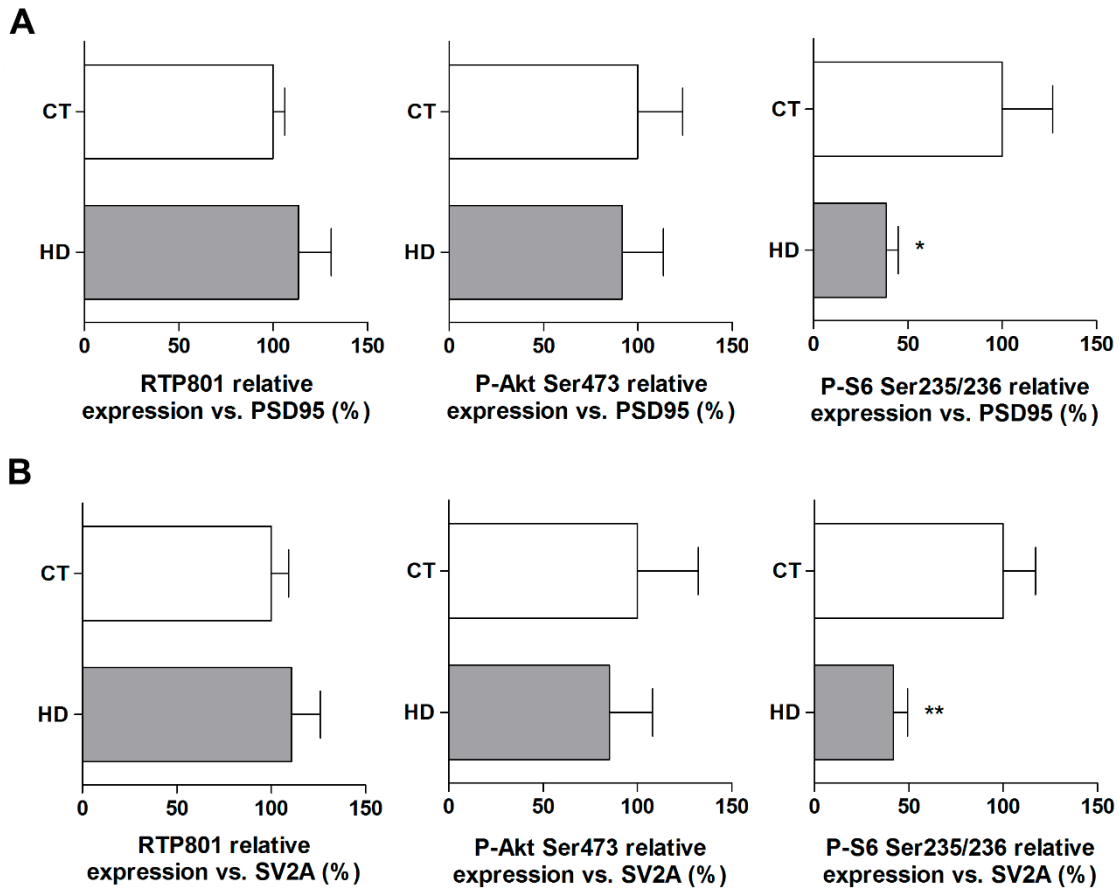


Figure 39. Synaptic enrichment of RTP801, P-Akt (Ser473) and P-S6 (235/236) in the frontal cortex of HD patients. Graphs indicate the levels of RTP801, P-Akt (Ser473) and P-S6 (235/236) corrected by the levels of synaptic markers **(A)** PSD-95 and **(B)** SV2A in the synaptosomes derived from the prefrontal cortex of the CT and HD donor analyzed in the previous experiment. The results are shown as mean \pm SEM of all samples. Data were analyzed by Student's T-test (* $P < 0.05$, ** $P < 0.01$).

1.2.3 Study of synaptic RTP801 and components of the mTOR pathway in HD mice models

HD mouse models are reported to exhibit cognitive deficits before the appearance of motor symptoms indicating that abnormal synaptic plasticity occurs at early stages of the disease^{103,457,459,461,496–498}. To further study the synaptic machinery we isolated synaptosomes from the striatum of *Hdh*^{Q7/Q111}-KI mice and R6/1 mice.

*i. RTP801 is increased in striatal synapses of the *Hdh*^{Q7/Q111}-knock-in mouse model*

To assess whether the enrichment of RTP801 in the striatal synapses of HD patients also occurs in HD mouse models, we investigated the synaptic levels of RTP801 in the striatum of *Hdh*^{Q7/Q111} knock-in (KI) mice at 10-months of age. At this age KI mice already display abnormal neuronal plasticity⁴⁶¹.

We purified synaptosomes from 6 Hdh^{Q7/Q7} (WT) and 6 Hdh^{Q7/Q111} (KI) mice and analyzed the protein content by WB (Figure 40A). RTP801 quantification revealed its enrichment in the synaptosomal fraction derived from the striatum of WT and KI mice (Figure 40B). However, RTP801 protein levels did not differ between genotypes in either homogenates or synaptosomes.

We also corroborated that synaptosomal isolation was properly performed by the enrichment of PSD-95 (Figure 40C) and SV2A (Figure 40D) in the synaptosomal fraction of both WT and KI groups. At the synaptosomal fraction of KI mice, only PSD-95 displayed decreased protein levels in comparison to the WT group.

Concerning the mTOR pathway, P-Akt (Ser473) and P-S6 (Ser235/236) levels were also investigated. P-S6 (Ser235/236) was enriched in synaptosomes but, on the contrary to human HD samples, P-Akt (Ser473) was not. Neither of the two mTOR readouts showed differences between animal genotypes in homogenates or synaptosomes (Figure 40E & 40F).

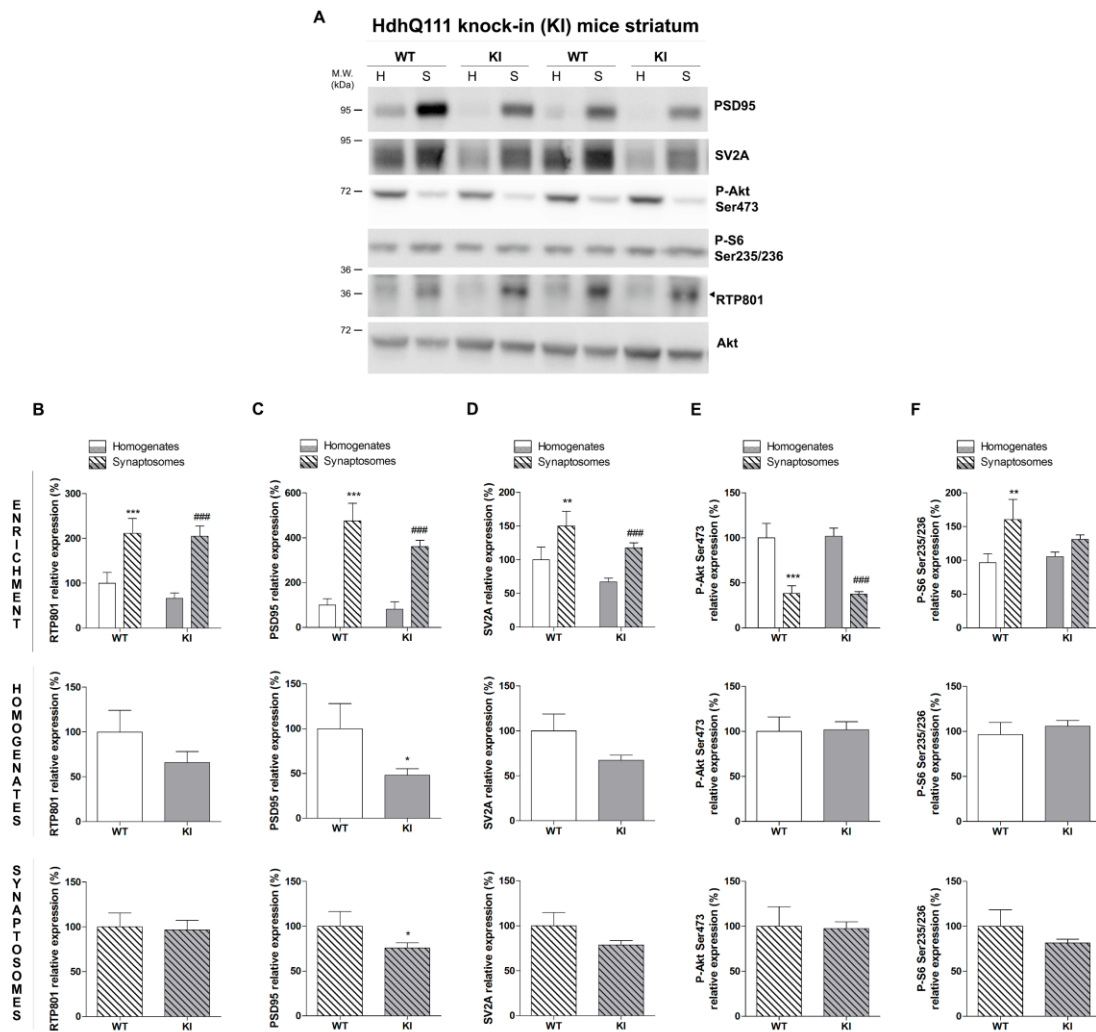


Figure 40. Synaptosomal preparation from the striatum of Hdh^{Q7/Q111}-KI mice. Striata of 6 KI and 6 WT animals at 10-months of age were dissected out and homogenized in Krebs-Ringer buffer. Later, synaptosomes were isolated and samples were subjected to WB. Membranes were probed against RTP801, P-Akt (Ser473), P-S6 (Ser235/236), PSD-95, SV2A and total Akt as a loading control. Graph show the densitometric quantification. Data in shown as a mean \pm SEM. Data were analyzed with Two-way ANOVA followed by Bonferroni's multiple comparisons test for post-hoc analyses (** $P < 0.01$, *** $P < 0.001$ vs. WT homogenate, ## $P < 0.01$, ### $P < 0.001$ vs. R6/1 homogenate) and data of homogenates and synaptosomes were analyzed by Student's T-test (* $P < 0.05$).

Furthermore, we analyzed the synaptic levels of RTP801, P-Akt (Ser473) and P-S6 (Ser235/236) at PSD-95- (Figure 41A) and SV2A-synaptic fractions (Figure 41B). We observed a higher enrichment of RTP801 in the PSD-95- and SV2A-synaptic fractions in KI animals compared to the WT mice. P-Akt (Ser473) was also increased at the synaptic fraction of KI mice, but P-S6 (Ser235/236) did not show differences between animals, suggesting an impairment of mTORC2 but not mTORC1.

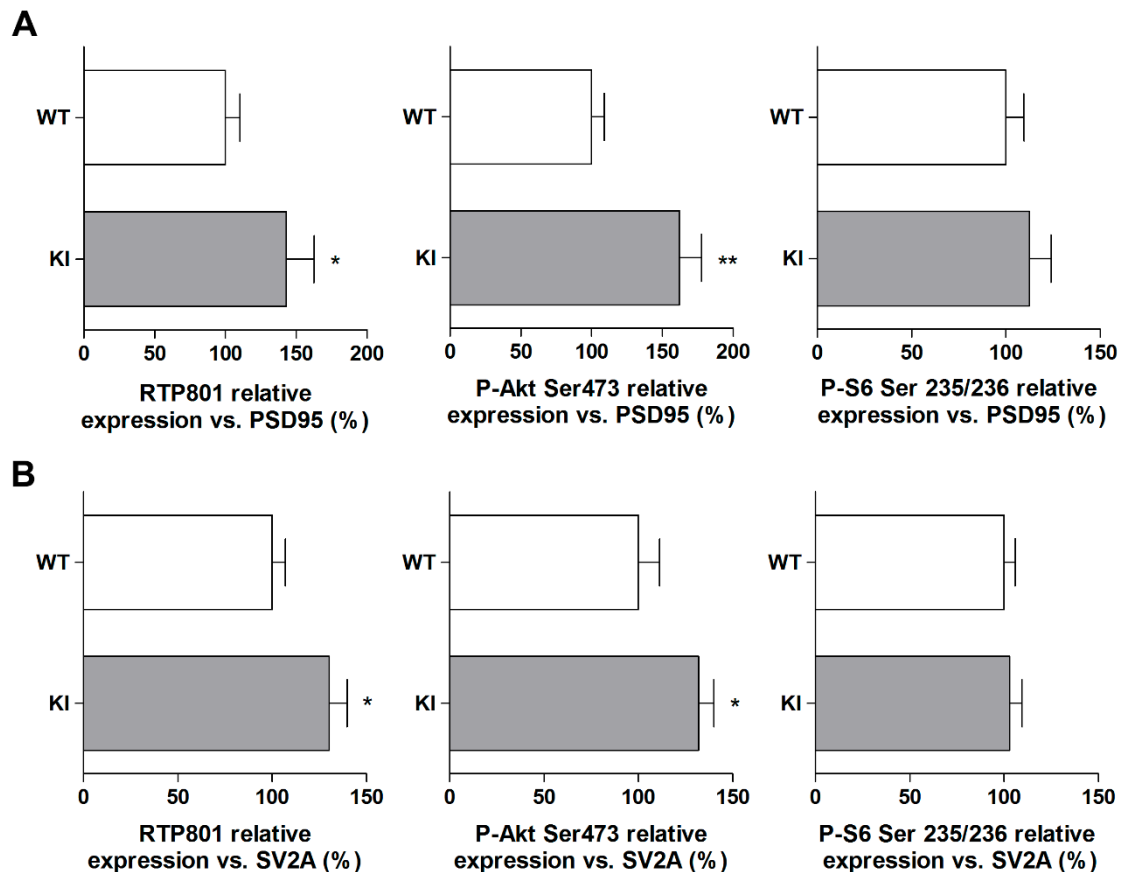


Figure 41. Synaptic enrichment of RTP801, P-Akt (Ser473) and P-S6 (235/236) in the striatum of HdhQ7/Q111-KI mice. Graphs indicate the levels of RTP801, P-Akt (Ser473) and P-S6 (235/236) corrected by the levels of synaptic markers (A) PSD-95 and (B) SV2A in striatal synaptosomes of the KI and WT mice analyzed in the previous experiment. The results are shown as mean \pm SEM. Data were analyzed by Student's T-test (* $P < 0.05$).

ii. RTP801 is increased in striatal synapses of the R6/1 mouse model

In order to confirm the previous results in another HD mouse model, we investigated the synaptic levels of RTP801 in the striatum of R6/1 mice at 16-weeks of age. At 16-weeks age the R6/1 already present cognitive and motor alterations^{457,461,496-498}.

Synaptosomal preparations were obtained from the striatum of 7 R6/1 mice and 6 WT littermates (Figure 42A). As we detected in Hdh^{Q7/Q7} and Hdh^{Q7/Q111} animals, RTP801 was also enriched in the synaptosomal fraction of the WT animal and the same tendency was exhibit in the R6/1 model although it did not reach significance (Figure 42B). Moreover, we confirmed that RTP801 was not increased in either striatal homogenates or synaptosomes of the R6/1 mice in comparison to WT animals.

Proper synaptosomal purification was confirmed by the enrichment of PSD-95 and SV2A synaptic markers (Figure 42C & 42D). At synaptosomal level, R6/1 mice showed decrease PSD-95 in comparison to WT littermates. This result was in accordance with

RESULTS

the Hdh^{Q7/Q111}-KI model, in which we also observed a reduction of PSD-95 in the synaptic fraction (Figure 42C).

Furthermore, we analyzed the striatal levels of P-Akt (473) and P-S6 (Ser235/236) in the R6/1 mice model. R6/1 striatal samples displayed increased levels of P-Akt (Ser473) respect to WT animals, both at homogenates and synaptosomes (Figure 42E). P-S6 (Ser235/236) showed no differences between genotypes (Figure 42F).

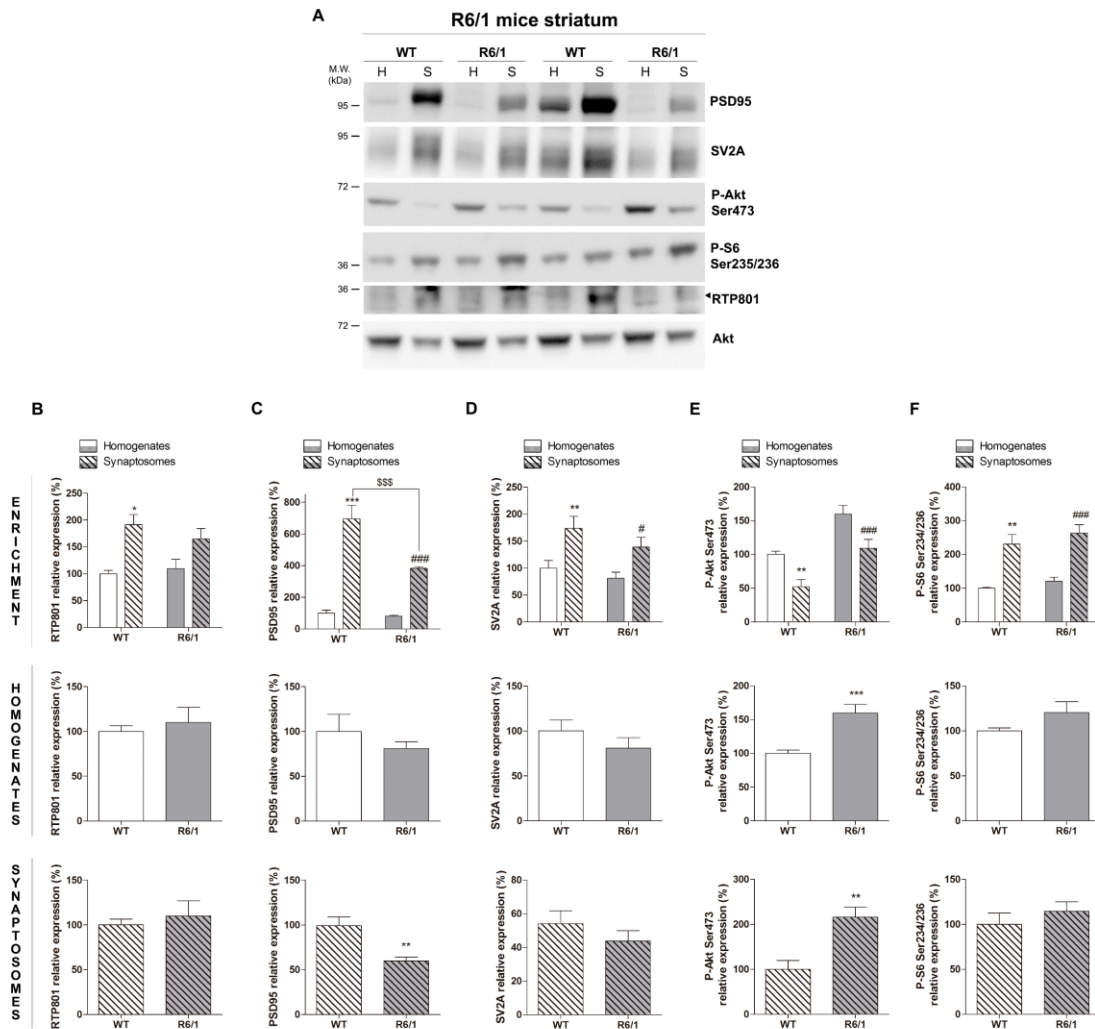


Figure 42. Synaptosomal preparation from the striatum of R6/1 mice. Striata of 7 R6/1 and 6 WT animals at 16-weeks of age were dissected out and homogenized in Krebs-Ringer buffer. Later, synaptosomes were isolated and samples were subjected to WB. Membranes were probed against RTP801, P-Akt (Ser473), P-S6 (Ser235/236), PSD-95, SV2A and total Akt as a loading control. Graph show the densitometric quantification. Data in shown as a mean \pm SEM. Data were analyzed with Two-way ANOVA followed by Bonferroni's multiple comparisons test for post-hoc analyses ($*P < 0.05$, $**P < 0.01$, $***P < 0.001$ vs. WT homogenate, $\#P < 0.05$, $###P < 0.001$ vs. R6/1 homogenate) and data of homogenates and synaptosomes were analyzed by Student's T-test ($**P < 0.01$, $***P < 0.001$).

To correct for the synaptic loss, synaptosomal levels of RTP801, P-Akt (Ser473) and P-S6 (Ser235/236) were normalized to PSD-95 and SV2A (Figure 43A & 43B). We detected a significant increase of RTP801 at the synaptic compartment when adjusting

for PSD-95 and a trend for SV2A ($P=0.0641$) in the R6/1 mice in comparison to their WT littermates.

We also found differences in the mTOR readouts. P-Akt (Ser473) was increased in the PSD-95- and SV2A-synaptic fractions of R6/1 mice when compared to WT littermates. P-S6 Ser235/236 also displayed increased protein levels in the PSD-95-synaptic fraction but not in the SV2A-synaptic fraction.

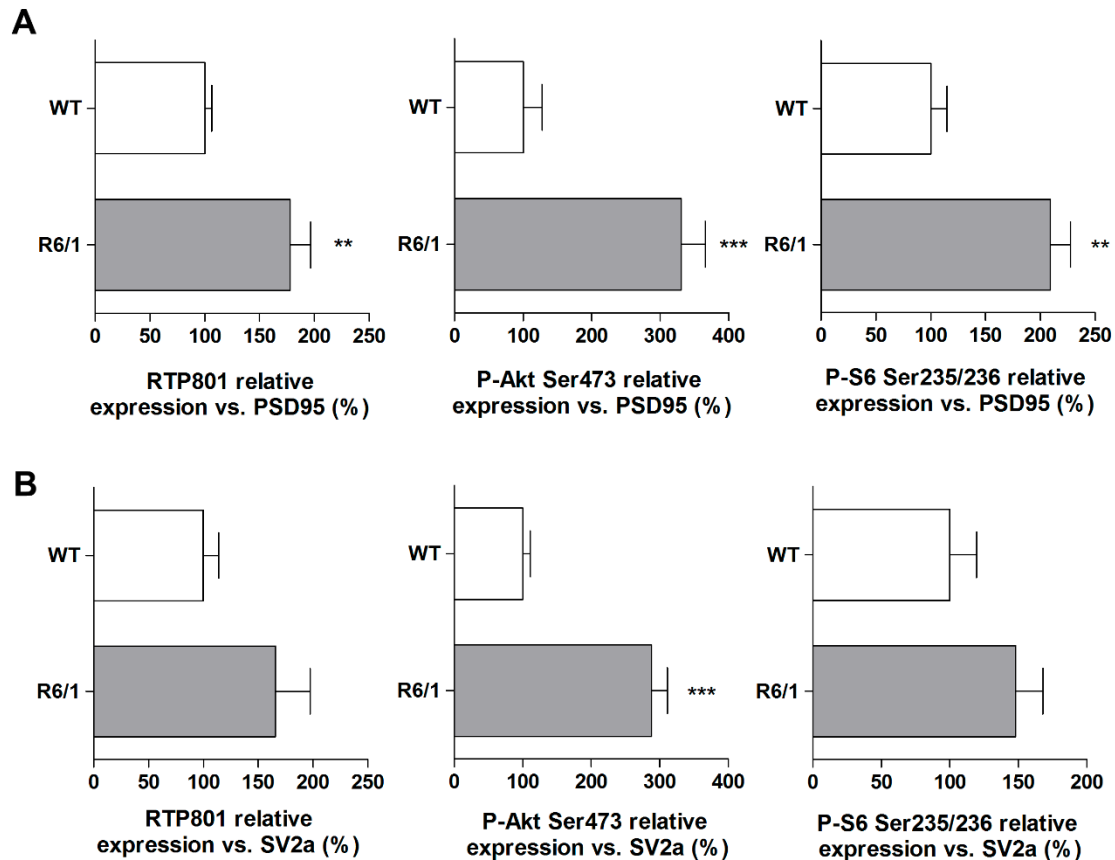


Figure 43. Synaptic enrichment of RTP801, P-Akt (Ser473) and P-S6 (235/236) in the striatum of R6/1 mice. Graph indicate the levels of RTP801, P-Akt (Ser473) and P-S6 (235/236) corrected by the synaptic markers **(A)** PSD-95 and **(B)** SV2A in striatal synaptosomes of the R6/1 and WT mice analyzed in the previous experiment. The results are shown as mean \pm SEM of all samples. Data were analyzed by Student's T-test (** $P<0.01$, *** $P<0.001$).

Results obtained so far show that RTP801 is increased in the striatal synaptic fraction of two different HD mouse models, and in the putamen of HD patients.

1.2.4 Study of RTP801 striatal synaptic function in the HD murine model R6/1

Synaptic increase of RTP801 suggests that RTP801 could mediate plasticity dysfunction in HD. Thus, we investigated whether striatal RTP801 knockdown may prevent or delay motor learning impairment in the R6/1 mice.

RESULTS

i. RTP801 knockdown improves motor learning in symptomatic R6/1 mice

In order to evaluate the putative implication of synaptic RTP801 in motor learning impairment, 9-week-old WT and R6/1 mice were bilaterally injected with AAV-shCtr or AAV-shRTP801 into the striatum. After five weeks, behavioral test was performed and a week later, mice striata were dissected and processed for immunohistochemistry or biochemical analysis. By immunofluorescence, we detected comparable GFP signal in the striatum of WT and R6/1 that confirmed the transduction of AAV-shCtr and AAV-shRTP801 (Figure 44A). Moreover, striatal injections of AAV-shRTP801 reduced RTP801 protein expression between 25-30%, both in WT and R6/1 animals (Figure 44B).

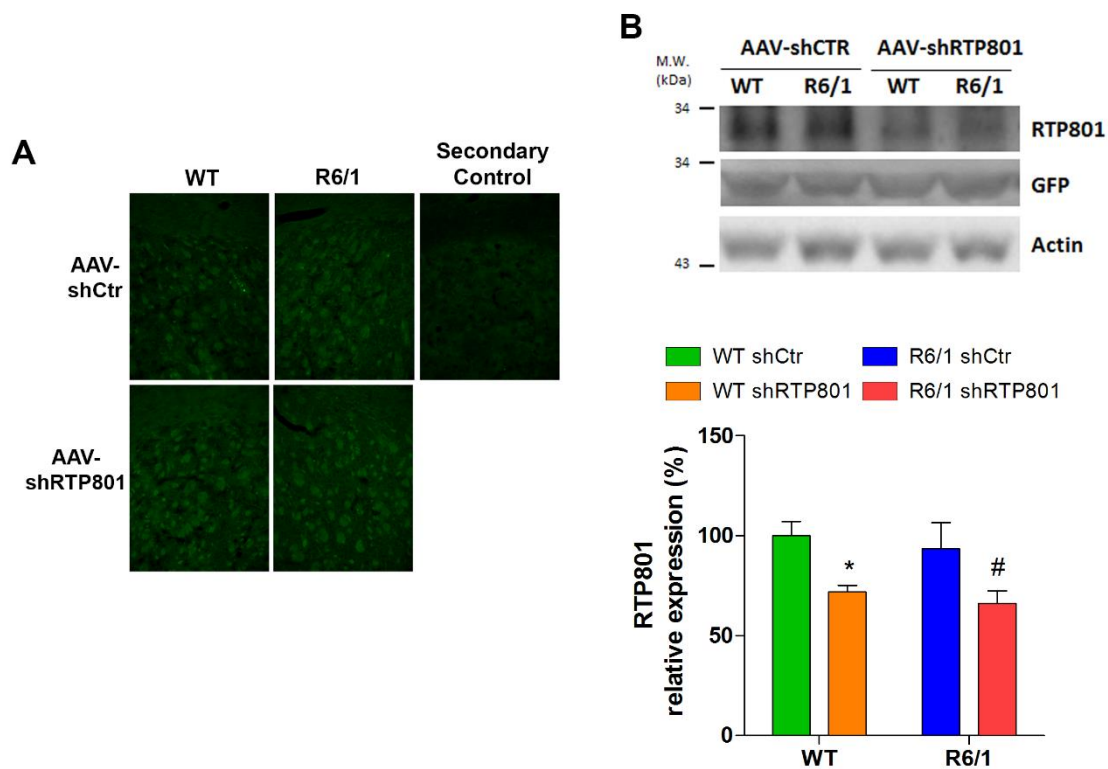


Figure 44. Transduction efficiency of AAV-shCtr- and AAV-shRTP801-injected animals. (A) GFP immunofluorescence confirmed the transduction of AAV-shCtr and AAV-shRTP801 in striatal cells of WT and R6/1 mice. A secondary control was performed without the incubation of primary antibody (anti-GFP). **(B)** Striata of WT and R6/1 injected with AAV-shCtr (n=6 WT and n=6 R6/1) or AAV-shRTP801 (n=6 WT and n=7 R6/1) were dissected, homogenized in Krebs-Ringer buffer and subjected to WB. Membranes were probed against RTP801, GFP and actin as a loading control. Graph show the densitometric quantification of RTP801 signal. Data are shown as a mean \pm SEM and were analyzed with Two-way ANOVA followed by Bonferroni's multiple comparisons test for *post-hoc* analyses (* P <0.05 vs. WT AAV-shCtr # P <0.05 vs. R6/1 AAV-shCtr).

In our investigation, to study corticostriatal function, motor learning was evaluated by the accelerating rotarod. R6/1-shCtr-injected animals performed poorly in this motor task in comparison to WT-shCtr-injected animals. Surprisingly, RTP801 silencing in the R6/1 mice preserved their motor learning by increasing the latency to fall. Indeed, AAV-shCtr or AAV-shRTP801-injected WT mice showed no differences in motor learning capabilities (Figure 45).

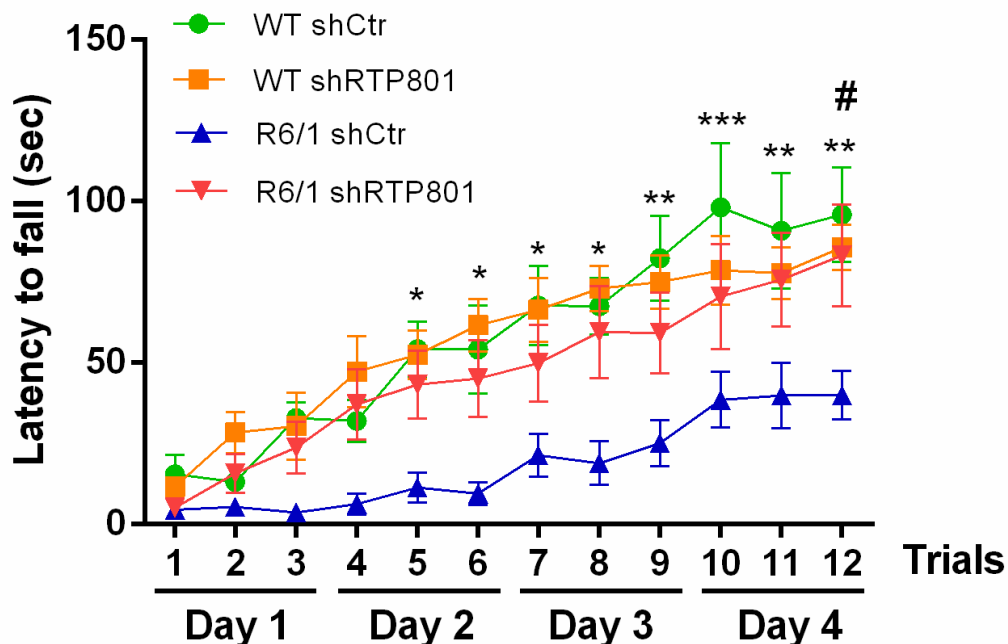


Fig 45. Striatal RTP801 knockdown preserves motor learning in symptomatic R6/1 mice. 9-weeks-old WT and R6/1 mice were injected bilaterally with AAV-shCtr (n=8 WT and n=9 R6/1) or AAV-shRTP801 (n=8 WT and n=9 R6/1) in the striatum. Five weeks after, motor learning was assessed by the accelerating rotarod. The graph shows the latency to fall as the mean of three trials tested each day. Values are expressed as mean \pm SEM and were analyzed with Two-way ANOVA followed by Bonferroni's multiple comparisons test for post-hoc analyses (* P <0.05, ** P <0.01 and *** P <0.001 R6/1 AAV-shCtr vs. WT AAV-shCtr and # P <0.05 R6/1 AAV-shRTP801 vs. R6/1 AAV-shCtr).

ii. RTP801 knockdown preserves phospho-Akt (Ser473) and enhances the expression of synaptic proteins in the R6/1 mice

In order to understand the biochemical consequences of RTP801 knockdown that leads to a better motor learning performance, we analyzed different components of the mTOR pathway in the synaptic compartment. For that purpose, we isolated synaptosomes from WT and R6/1 mice transduced with AAV-shCtr or AAV-shRTP801 and analyzed protein content by WB.

Knocking down RTP801 did not affect either the levels of P-mTOR (Ser2448) or the levels of P-S6 (Ser235/236), as mTORC1 readout (Figure 46A & 46B).

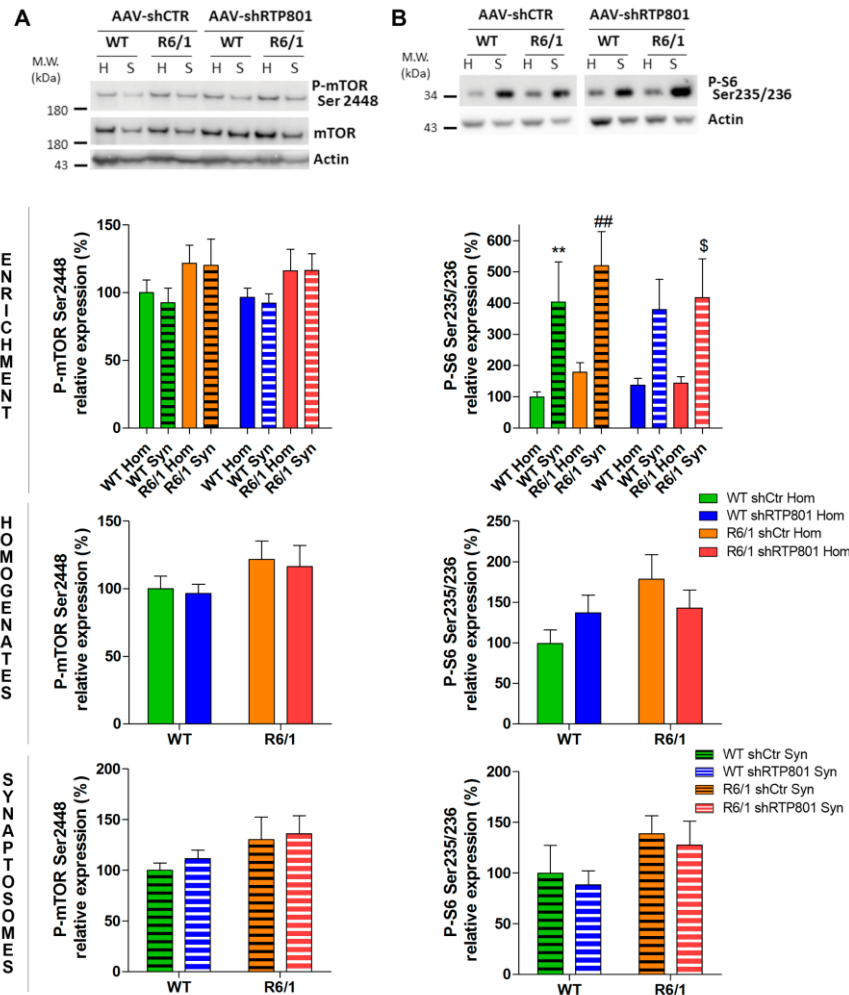


Figure 46. Knockdown of RTP801 in the striatum of R6/1 mice does not alter P-mTOR (Ser2448) and P-S6 (Ser235/236). Striata of WT and R6/1 injected with AAV-shCtr (n=6 WT and n=6 R6/1) or AAV-shRTP801 (n=6 WT and n=7 R6/1) were dissected and homogenized in Krebs-Ringer buffer. Later, synaptosomes were isolated and samples were subjected to WB. Membranes were probed against P-mTOR (Ser2448), P-S6 (Ser235/236) and total mTOR and actin as a loading control. Graphs show the densitometric quantification. Values are shown as a mean \pm SEM. Enrichment data were analyzed with Two-way ANOVA followed by Bonferroni's multiple comparisons test for *post-hoc* analyses (** $P < 0.01$ vs. WT AAV-shCtr Hom; ## $P < 0.01$ vs. R6/1 AAV-shCtr Hom; \$ $P < 0.05$ vs. R6/1 AAV-shRTP801 Hom). Homogenates and synaptosomes data were analyzed with Two-way ANOVA followed by Bonferroni's multiple comparisons test for *post-hoc* analyses.

Then, we analyzed the mTORC2 readout P-Akt (Ser473) which we have already shown that is overactivated in the R6/1 model, not only at total levels but also at the synaptic fraction (Figure 42E & 43). Surprisingly, the knockdown of RTP801 in the striatum of R6/1 restored P-Akt (Ser473) levels and had no significant effect in WT animals (Figure 47A), indicating a specific regulation of RTP801 upon Akt activity on this pathological context.

Akt phosphorylation on the residue Ser473 depends on mTORC2 kinase activity when complexed with Rictor protein^{499,500}. On the other hand, Ser473 residue of Akt is dephosphorylated by the specific phosphatase PHLPP1^{297,298}. In fact, increased levels

of Rictor and reduced levels of PHLPP1 phosphatase are responsible for Akt hyperactivation in the R6/1 mouse model^{287,296}.

Hence, we investigated whether RTP801 knockdown in R6/1 mice could affect these two Akt modulators. Interestingly, we found that Rictor levels were decreased in R6/1-shRTP801-injected animals in comparison to the R6/1-shCtr-injected mice (Figure 47B). On the other hand, RTP801 silencing did not alter PHLPP1 (Figure 47C). All these results suggest that RTP801 knockdown prevents Akt hyperactivation by decreasing Rictor protein levels.

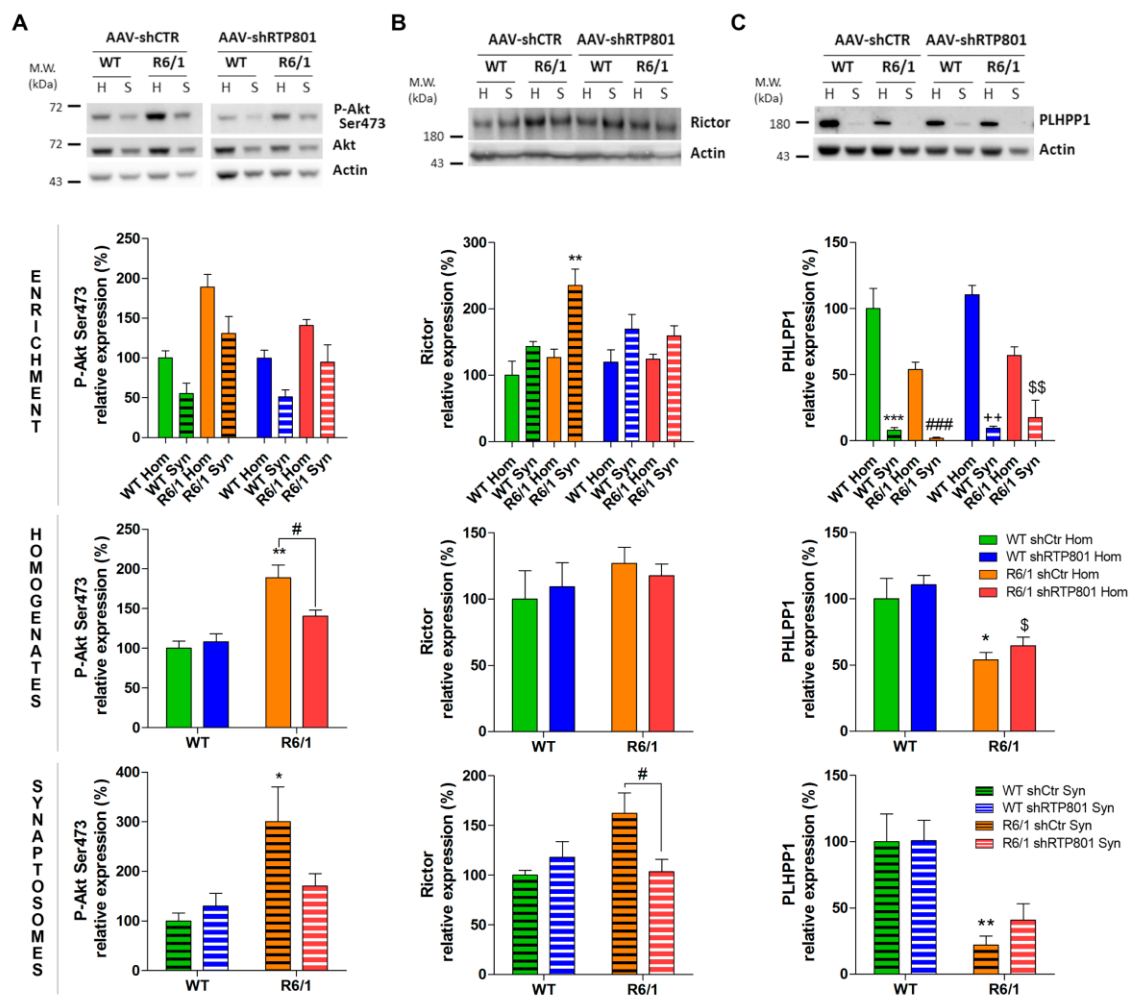


Figure 47. Knockdown of RTP801 in the striatum of R6/1 mice prevents hyperphosphorylation of Akt at Ser473 by decreasing Rictor levels. Striata of WT and R6/1 injected with AAV-shCtr (n=6 WT and n=6 R6/1) or AAV-shRTP801 (n=6 WT and n=7 R6/1) were dissected and homogenized in Krebs-Ringer buffer. Later, synaptosomes were isolated and samples were subjected to WB. Membranes were probed against P-Akt (Ser273), Rictor, PHLPP1 and total Akt and actin as a loading control. Graphs show the densitometric quantification. Values are shown as a mean ± SEM. Enrichment data were analyzed with Two-way ANOVA followed by Bonferroni's multiple comparisons test for *post-hoc* analyses (****P*<0.001 vs. WT AAV-shCtr Hom; ##*P*<0.01, ###*P*<0.001 vs. R6/1 AAV-shCtr Hom; ++*P*<0.01 vs. WT AAV-shRTP801 Hom, \$\$*P*<0.01 vs. R6/1 AAV-shRTP801 Hom). Homogenates and synaptosomes data were analyzed with Two-way ANOVA followed by Bonferroni's multiple comparisons test for *post-hoc* analyses ANOVA (**P*<0.05, ***P*<0.01 vs. WT AAV-shCtr; \$<0.05 vs. WT AAV-shRTP801; #*P*<0.05 vs. R6/1 AAV-shCtr).

RESULTS

We next asked whether RTP801 downregulation could be translated to synaptic transmission modulation. Hence, we assessed the protein levels of different glutamatergic receptor subunits.

As expected, all synaptic proteins studied were enriched in the synaptosomal fraction. In fact, PSD-95 (Figure 48A) and the NMDA receptor subunit NR1 (Figure 48B) were not detectable in the homogenate fraction. Nevertheless, the knockdown of RTP801 did not alter the synaptosomal protein levels of either PSD-95 or NR1.

We also analyzed the subunit AMPA receptor GluA1. Interestingly, striatal RTP801 silencing induced an increase of GluA1 at the homogenate fraction of R6/1 mice in comparison to WT animals (Fig 48C). Similar non-significant tendencies were observed at the synaptic compartment.

Furthermore, one of the mechanisms which contributes to synaptic impairment in HD models is the imbalance between BDNF receptor TrkB and BDNF low affinity receptor p75^{NTR} 122,124. Thus, we explored whether the knockdown of RTP801 could restore this TrkB and p75^{NTR} imbalance. As well as GluA1, TrkB increased after knocking down RTP801 expression in the homogenates of R6/1 mice in comparison to their WT littermates (Figure 48D). Again, only similar non-significant tendencies were observed at the synaptic fraction. Regarding p75^{NTR}, no differences were observed in this low affinity BDNF receptor (Figure 48E).

These results suggest that the knockdown of RTP801 enhances the expression of synaptic proteins, which could explain the better performance of R6/1 mice in the accelerating rotarod.

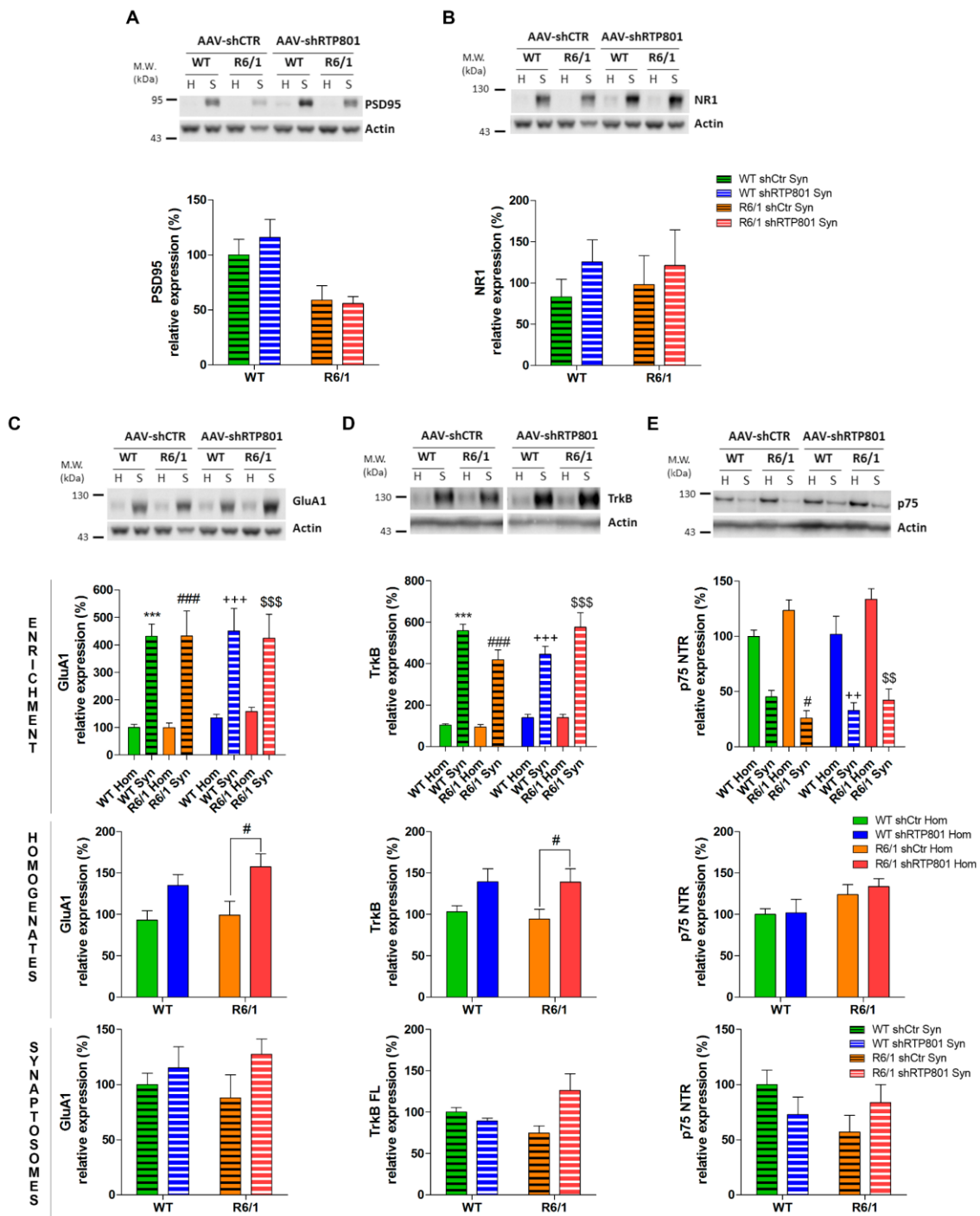


Figure 48. Knockdown of RTP801 in the striatum of R6/1 mice enhances the expression of synaptic proteins. Striata of WT and R6/1 injected with AAV-shCtr (n=6 WT and n=6 R6/1) or AAV-shRTP801 (n=6 WT and n=7 R6/1) were dissected and homogenized in Krebs-Ringer buffer. Later, synaptosomes were isolated and samples were subjected to WB. Membranes were probed against GluA1, full-length TrkB and p75^{NTR} actin as a loading controls. Graphs show the densitometric quantification. Values are shown as a mean ± SEM. Enrichment data were analyzed with Two-way ANOVA followed by Bonferroni's multiple comparisons test for *post-hoc* analyses (****P*<0.001 vs. WT AAV-shCtr Hom; # *P*<0.05, ### *P*<0.001 vs. R6/1 AAV-shCtr Hom; ++ *P*<0.01, +++ *P*<0.001 vs. WT AAV-shRTP801 Hom, \$\$ *P*<0.01, \$\$\$ *P*<0.001 vs. R6/1 AAV-shRTP801 Hom). Homogenates and synaptosomes data were analyzed with Two-way ANOVA followed by Bonferroni's multiple comparisons test for *post-hoc* analyses (# *P*<0.05 vs. R6/1 AAV-shCtr).

RESULTS

These evidences show that striatal RTP801 knockdown recues R6/1 motor performance by restoring P-Akt (Ser473) levels through the reduction of Rictor and by enhancing postsynaptic signaling. These findings indeed support that hyperphosphorylation of Akt on Ser473 contributes to modulate motor learning impairment in R6/1 mice.

Altogether, the results indicate that RTP801 is increased at the synapses of HD affected areas in both humans and HD mouse models and its upregulation contributes to impair motor learning plasticity.

2. STUDY OF EXOSOMAL RTP801 IN TOXIC CELLULAR MODELS

Cell-to-cell transmission is a common mechanism for the progression of several neurodegenerative disorders including PD and HD. Recently, evidence indicate that prion-like transmission of protein aggregates such as α -synuclein^{218–220} or mhtt^{81–83} can contribute to neurodegenerative diseases^{501,502}. For instance, in PD was observed that neural grafts derived from fetal midbrain healthy tissue transplanted into the striatum of patients with PD showed Lewy pathology after 10-16 years in addition to the expected inclusions observed in the host tissue²⁰⁹. This reinforces the hypothesis that α -synuclein could be transferred transneuronally. In HD models, mhtt seems to be propagated transneuronally in neuronal cultures and also in the corticostriatal pathway *in vivo*, in a synaptic activity-dependent manner⁸¹. Therefore, neuron-to-neuron propagation of toxic proteins must be considered to investigate the pathophysiology of neurodegenerative disorders.

One of the important key players in cell-to-cell communication are exosomal vesicles since they act as vehicles for intercellular transfer of bioactive molecules⁵⁰³. Besides, exosomes have been suggested as an unconventional pathway for removing toxic proteins from the neuron⁵⁰⁴, playing an essential role in the propagation of pathogenic proteins involved in neurodegenerative diseases^{505–507}. Exosome composition is highly influenced by environmental challenges and its sorting out can be modulated by intracellular stress³⁷⁰. In consequence, the exosomal content is modified, and thus the biological response of recipient cells^{371,381}.

Based on this background, here we investigated whether stress-induced RTP801 is present in exosomes derived from cellular models and whether exosomal RTP801 mediate a specific effect in recipient cells through the modulation of mTOR/Akt pathway.

2.1 RTP801 is present in exosomes released from HEK293 cells

To explore our hypothesis, we first investigated whether RTP801 could be found in exosomes secreted by cellular cultures. For this reason, we transfected HEK293 cells with ectopic eGFP-tagged RTP801. Forty-eight hour after transfection, cell lysates and exosomes released into the culture media were obtained and analyzed by WB. Due to the eGFP tag, we monitored both ectopic RTP801 (with a higher molecular weight around 55 kDa) and endogenous RTP801 (molecular weight around 34 kDa). We observed that ectopic RTP801 was found in exosomes as well as the ectopic control protein eGFP. Interestingly, endogenous RTP801 was also present in exosomes (Figure 49A and 49B).

To corroborate a proper exosome isolation, we analyzed the enrichment of exosomal markers in the extracellular exosomal vesicles fraction (EVs). We used two protein markers that differ in their exosomal localization to ensure to include the whole population of exosomes⁴¹³. Tumor susceptibility gene 101 (TSG101) protein is part of the endosomal sorting complex required for transport (ESCRT) and mediates the cargo sorting into intraluminal vesicles³⁹⁶. Flotillin-1 is found in the lipid-rafts at the exosomal surface⁵⁰⁸, participates in the formation of non-caveolar membrane microdomains^{509,510} and in membrane trafficking processes⁵¹¹.

Both target proteins were found enriched in the exosomal fraction. In fact, ectopic RTP801 expression induced a higher exosomal secretion as detected by the increase of TSG101 and Flotillin-1 markers (Fig 49A, 49C & 49D). This observation was confirmed by quantification of particles density by the NanoSight software ($1.11 \times 10^{11} \pm 2.46 \times 10^{10}$ particles/ml in eGFP-overexpressing cultures vs. $2.36 \times 10^{11} \pm 1.69 \times 10^{10}$ particles/ml in eGFP-RTP801-overexpressing cultures; P -valor < 0.05 Student's T-test).

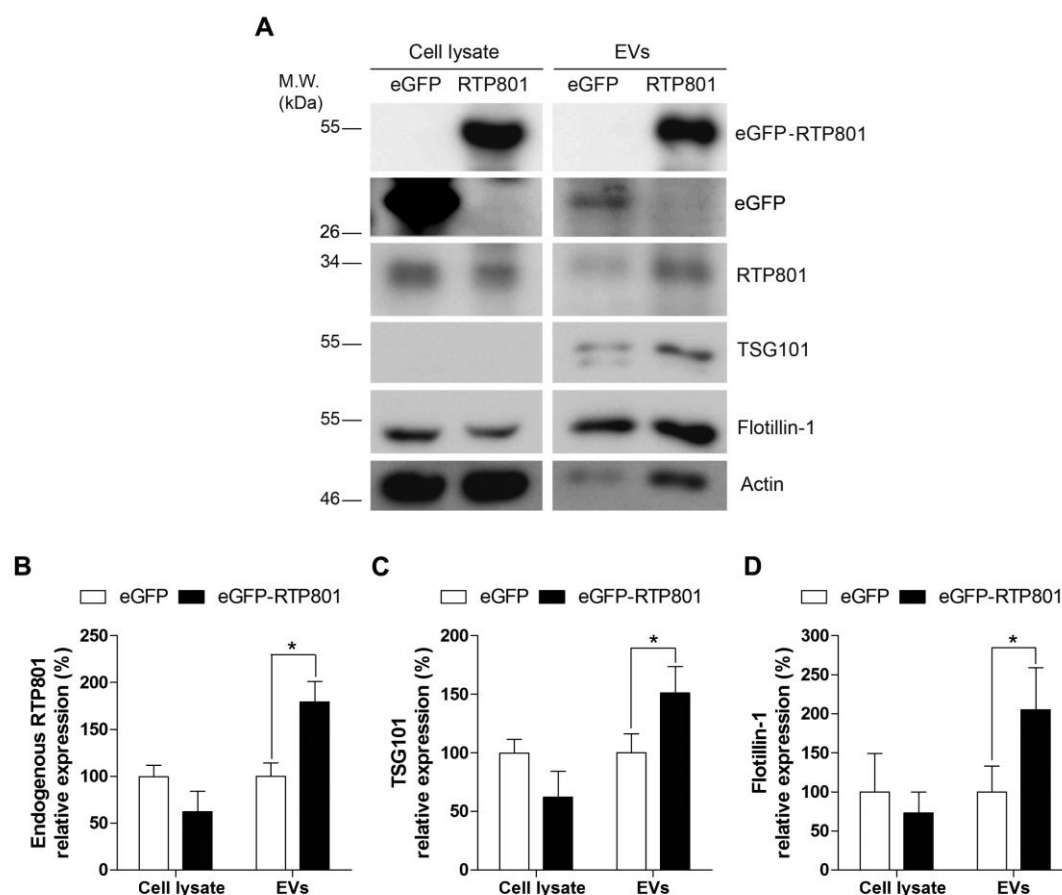


Figure 49. RTP801 overexpression increases EVs release and produces EVs enriched in RTP801 in HEK293 cells. (A) HEK293 cells were transfected with pEGFP-C3 empty vector (as control) or pEGFP-C3-RTP801 tagged vector and incubated in DMEM depleted of exosomes. Forty-eight hours after, exosomes were isolated by sequential centrifugation of cell media and total protein content was analyzed by WB. Membranes were probed against RTP801, TSG101 and flotillin-1 as exosomal markers and actin as a loading control. Graphs show values obtained by densitometric analysis of exosomal (B) endogenous RTP801, (C) TSG101 and (D) Flotillin-1 WB data relative to the total protein content of the cell lysate. Values are represented as mean \pm SEM (n = 3). Representative immunoblots are shown. Data were analyzed by Student's T-test in the cell lysate and in the EVs fraction (*P<0.05).

2.2 Study of exosomal RTP801 in cortical neuronal cultures

We have showed that both ectopic and endogenous RTP801 are found in the exosomal fraction derived from HEK293 cells, and that RTP801 overexpression alters exosomal release. We next wondered whether RTP801 was also present in exosomes secreted by cortical neurons and whether its content is modified by cellular stressors.

2.2.1 RTP801 protein is not present in exosomes derived from control or depolarized neurons

Here, we studied whether endogenous RTP801 colocalizes with MVBs in neuronal culture. The loading of ILVs is sorted inside MVBs and once fused with the plasma membrane ILVs are released into the extracellular media as exosomes (reviewed in ⁵¹²). With this purpose, cortical neurons at DIV12 were transfected with CD63-tagged eGFP

RESULTS

or eGFP alone as control. CD63 is typically incorporated into ILVs and after their release is a well-described exosomal marker⁵¹³. Forty-eight hours after transfection, cultures were fixed and immunostained against eGFP and RTP801. Under confocal imaging we confirmed that RTP801 and CD63 colocalized in the somatodendritic compartment (Figure 50A). Interestingly, CD63 overexpression decreased intracellular levels of RTP801 (Figure 50B).

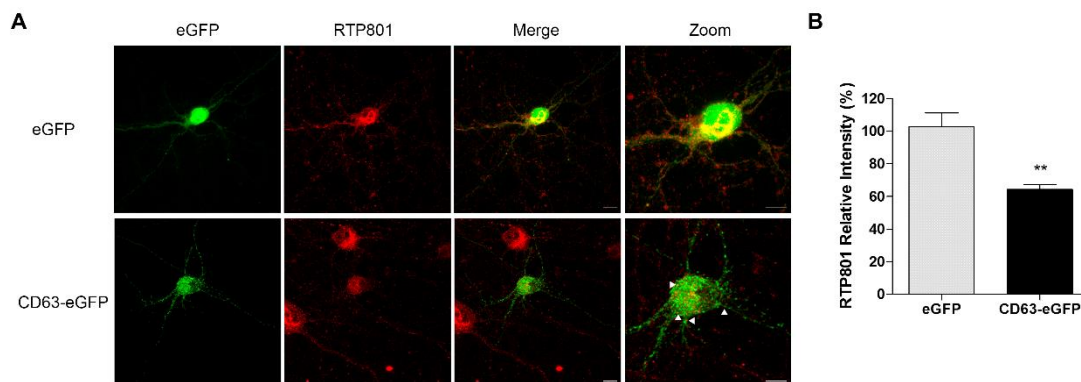


Figure 50. RTP801 partially colocalizes with CD63-eGFP and is decreased in CD63-eGFP positive neurons. (A) Cortical primary neurons DIV12 were transfected with pEGFP-C1bos-CD63 or pEGFP-C1bos as a control. Forty-eight hours later, cultures were fixed and stained against eGFP (in green) and RTP801 (in red). Images were acquired by confocal microscopy and endogenous RTP801. Scale bar, 5 μ m. **(B)** RTP801 staining was measured by Integral density with ImageJ. Values are represented as mean \pm SEM (n=3). Data were analyzed using Student's T-test (**P<0.01 vs eGFP).

Exosomal release is an active mechanism that is calcium dependent^{374,375}. To investigate whether RTP801 could be loaded into exosomes, we induced the depolarization of neurons with 30mM Potassium Chloride (KCl) for 3 hours which induces a nontoxic influx of calcium³⁷⁵. Sixteen hours later, released exosomes were isolated from the culture media. By nanoparticle tracking analysis (NTA) measurements we confirmed that 30mM KCl depolarization increased the number of vesicles released ($5.38 \times 10^{10} \pm 1.74 \times 10^{10}$ particles/ml in 5mM KCl vs. $2.89 \times 10^{11} \pm 2.46 \times 10^{10}$ particles/ml in 30mM KCl; *P*-value < 0.05 Student's T-test). Moreover, 30mM KCl treatment did not affect vesicles' mode size (139.33 \pm 7.30 nm in 5mM KCl vs. 145.06 \pm 8.23 nm in 30mM KCl).

In parallel, cell lysates and exosomal protein content were analyzed by WB (Figure 51). In addition to the aforementioned exosomal proteins, we used NEDD4 as an exosomal marker highly enriched in neurons⁴¹⁶. Interestingly from our previous work, we described that NEDD4 is involved in RTP801 lysosomal degradation³⁴⁹. As expected, we found increased levels of TSG101, Flotillin-1 and NEDD4 in the exosomal fraction of 30mM KCl depolarized cultures in comparison to 5mM KCl control, corroborating higher release of vesicles after a calcium influx. However, depolarization did not increase RTP801 protein levels either in cell lysates or in exosomes.

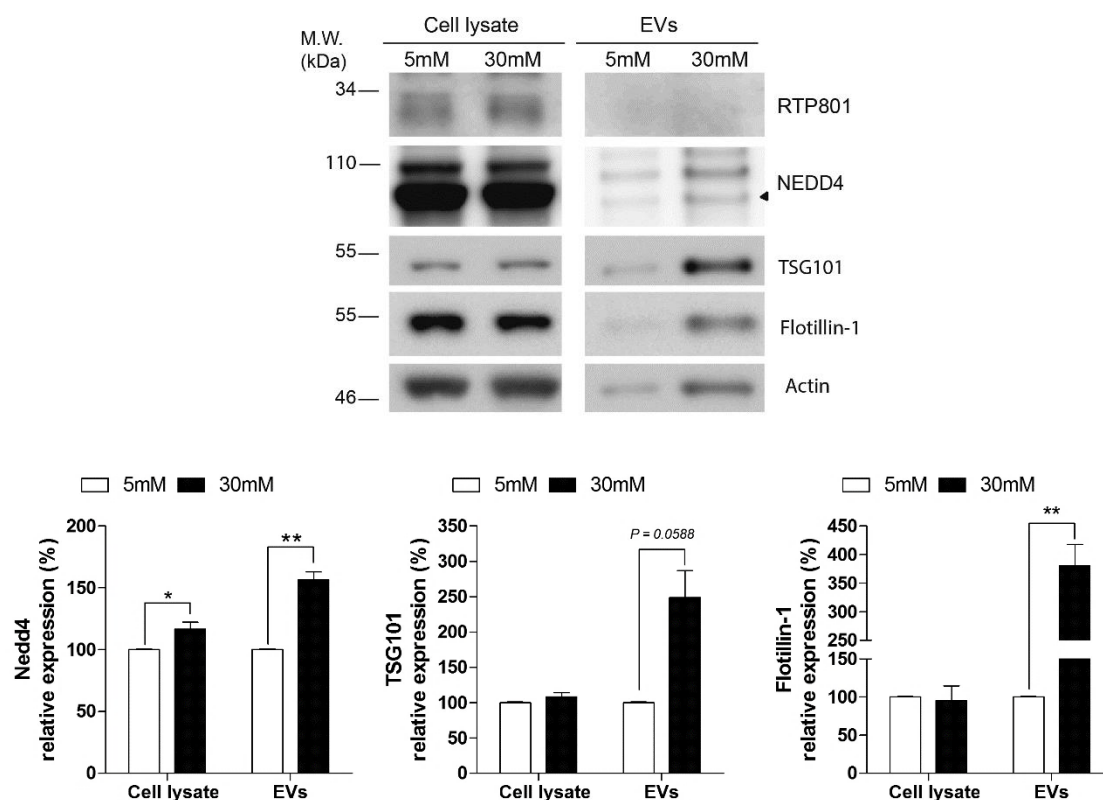


Figure 51. Depolarized cortical neurons release higher number of EVs but RTP801 is not present in the exosomal fraction. Rat cortical neurons at DIV14 were depolarized with 30mM KCl or 5mM KCl as control for 3h. Sixteen hours later, exosomes were isolated by sequential centrifugations. Total lysate and exosomal total protein content were analyzed by immunoblotting and membranes were incubated with RTP801 and NEDD4, TSG101 and flotillin-1 as exosomal markers and actin as a loading control. Graphs show values obtained by densitometric analysis of WB data relative to the total protein content of the cell lysate. Values are represented as mean \pm SEM (n = 3). Representative immunoblots are shown. Data were analyzed by Student's T-test in the cell lysate and in the EVs fraction (**P<0.01).

2.2.2 Neurotoxin 6-OHDA induces exosomal release of RTP801 by neuronal cultures

We next investigated whether a toxic cellular stress was necessary for the loading of RTP801 in exosomes. With this purpose, we treated neuronal cultures with the PD mimetic 6-hydroxidopamine (6-OHDA). In cortical neurons, this neurotoxin is known to autoxidize itself generating ROS and promoting the release of calcium from intracellular reservoirs such as the ER and the mitochondria⁵¹⁴⁻⁵¹⁶.

Thus, cortical neurons DIV14 were exposed to 6-OHDA for 16 hours. Then, exosomes and neuronal lysates were collected for analysis. The NanoSight quantification revealed that 6-OHDA treatment promoted the release of vesicles ($3.60 \times 10^{10} \pm 9.00 \times 10^9$ particles/ml in untreated cultures vs. $1.52 \times 10^{11} \pm 3.88 \times 10^9$ particles/ml in 6-OHDA-treated cultures; P -value<0.01 Student's T-test) and no variation in vesicle's mode size was found (145.05 ± 10.11 nm in untreated cultures vs. 134.54 ± 7.31 nm in 6-OHDA exposed cultures). This result was further confirmed by transmission electron microscopy (TEM).

RESULTS

As shown in Figure 52, TEM micrographs confirmed that vesicles released by cortical neurons have the size and shape of exosomes. Furthermore, we also confirmed that 6-OHDA neurotoxin increased the release of exosomes in comparison to untreated cultures.

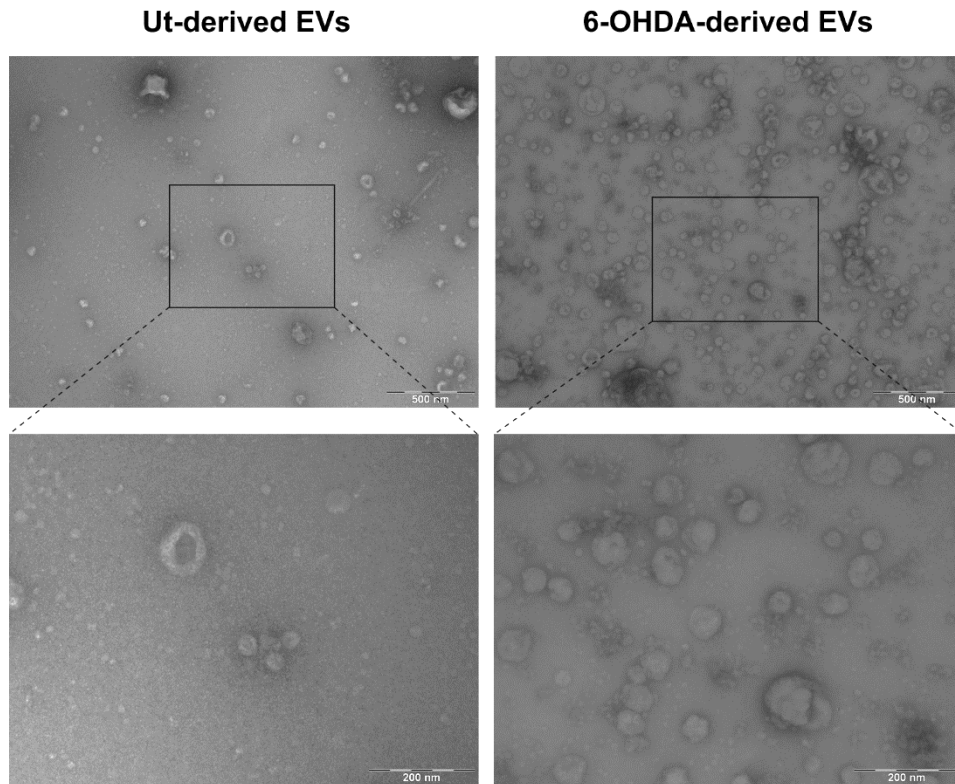


Figure 52. 6-OHDA treatment increases the release of exosomes from cortical neurons. Rat cortical neurons at DIV14 were exposed to the toxin 6-OHDA 50 μ M for 16h or untreated (ut) as control. Afterwards, cell media was collected, and exosomes were isolated by sequential centrifugations. Exosomal suspension was negative stain and observed by TEM. Electron micrographs show the presence of vesicles between 30 and 110nm. Scale bars are 500nm and 200nm in magnification micrographs.

In addition, the study of protein content by WB revealed that 6-OHDA exposure not only increased RTP801 at neuronal lysates but also induced the loading of RTP801 in exosomes (Figure 53A & 53B). Results regarding the induction of exosomal release by 6-OHDA were corroborated by WB. Exosomal markers NEDD4, TSG101 and Flotillin-1 displayed a decrease in cell lysates and were increased in the exosomal fraction, as readout for exosomal loading and release (Figure 53C, 53D & 53E).

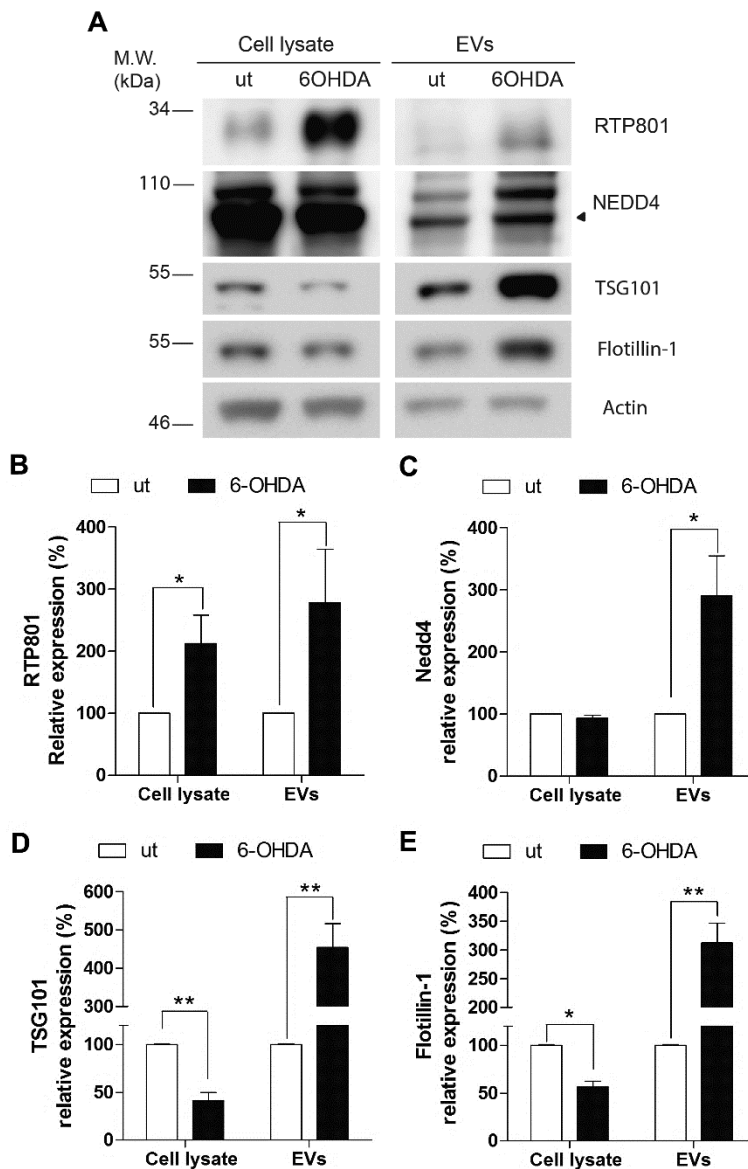


Figure 53. RTP801 is present in the EV fraction derived from cortical primary cultures treated with 6-OHDA. (A) Rat cortical neurons at DIV14 were exposed to the toxin 6-OHDA 50µM or untreated (ut) as control. Sixteen hours later, cell media was collected, and exosomes were isolated by sequential centrifugations. Total protein content was analyzed by WB. Membranes were probed against RTP801 and NEDD4, TSG101 and flotillin-1 as exosomal markers and actin as a loading control. Graphs show values obtained by densitometric analysis of **(B)** RTP801, **(C)** Nedd4, **(D)** TSG101 and **(E)** Flotillin-1 western blot data relative to the total protein content of the cell lysate. Values are represented as mean ± SEM (n = 3). Representative immunoblots are shown. Data were analyzed by Student's T-test in the cell lysate and in the EVs fraction (* $P < 0.05$, ** $P < 0.01$).

Up to now, results show that both ectopic and endogenous RTP801 are found in the exosomal fraction derived from HEK293 cells. In contrast, in cortical primary neurons RTP801 is not present in the exosomal fraction isolated from control or depolarized neurons. Nevertheless, neuronal exposure to 6-OHDA increases both intracellular and exosomal RTP801 protein suggesting that RTP801 is specifically released by exosomes under this stressful stimulus.

2.2.3 6-OHDA-derived exosomes containing RTP801 are not able to activate the mTOR/Akt pro-survival signal in recipient neurons

Exosomes can either have a pro-apoptotic or a pro-survival role in recipient cells. In order to elucidate the biological role of exosomes in our cellular model, we investigated whether exosomes derived from 6-OHDA-exposed neurons are internalized by recipient neurons and translate signal transduction.

i. 6-OHDA-induced exosomes do not mediate pro-survival signals in recipient cortical neurons

First, to demonstrate that exosomes were taken up by recipient cells, we isolated exosomes from donor rat neuronal cultures exposed or not to 6-OHDA and labeled them with the lipophilic dye PKH26. Sister cultures of recipient cortical neurons were treated with labeled exosomes and twenty-four hours later cultures were observed under confocal microscopy. Confocal images confirmed that recipient neurons, stained with microtubule associated protein 2 (MAP2) in green, were able to internalize PKH26-positive exosomes, in red, as revealed in their somatodendritic compartment (Figure 54).

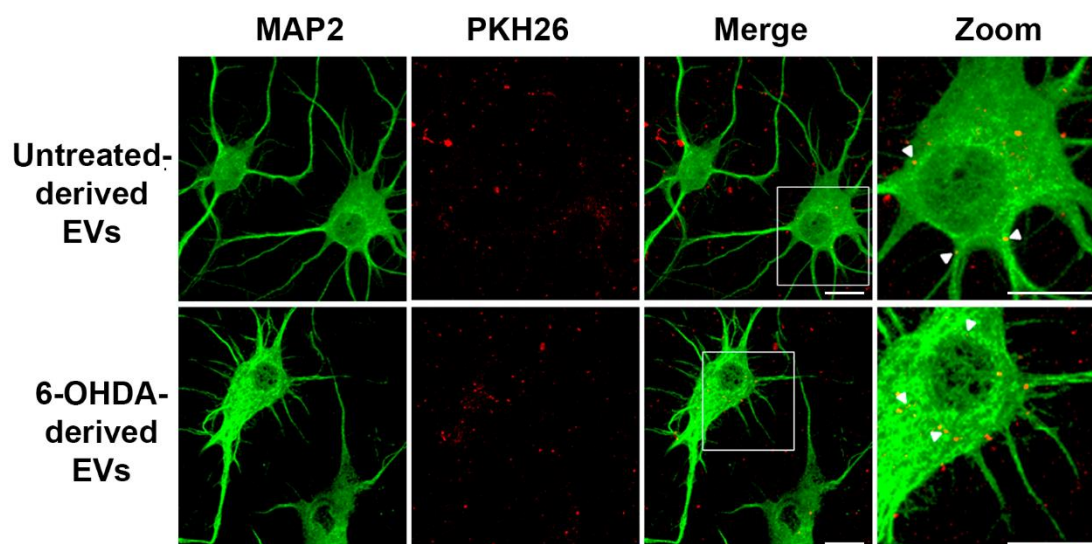


Figure 54. Purified exosomes are internalized by recipient cortical neurons. Rat cortical neurons DIV14 were untreated (ut) or exposed to 6-OHDA 50 μ M and 16h later exosomes were isolated from the culture media. Exosomes were then labeled with PKH26 dye (in red) according to manufacturer's protocol and 800,000 particles were administered to cortical cultures. Twenty-four hours later, neurons were fixed and stained against the neuronal marker MAP2 (in green). Images were acquired by confocal microscopy. Arrowheads indicate representative PKH26 dots internalized by neurons. Scale bar 5 μ m.

We next explored whether exosomes derived from untreated cultures or from cultures exposed to 6-OHDA were able to affect signaling pathways in recipient naïve neurons. Since RTP801 is a negative regulator of the mTOR pathway²⁶⁷, we focused on studying the effect of exosomes towards the mTOR/Akt pathway in recipient cells.

Exosomes were isolated from untreated or 6-OHDA-treated cortical cultures and sixteen hours later exosomes were purified from the culture media. Then, exosomes were added to recipient rat cortical neurons and the protein content of cultures was analyzed over a time course. Interestingly, we observed that 24 hours after exosomal administration, exosomes derived from untreated neuronal cultures were able to stimulate the mTOR/Akt pathway, judged by the increased phosphorylation of the Ser235/236 residues in S6 ribosomal protein and Ser473 residue of Akt, as readouts of mTORC 1 and 2 activity respectively (Figure 55).

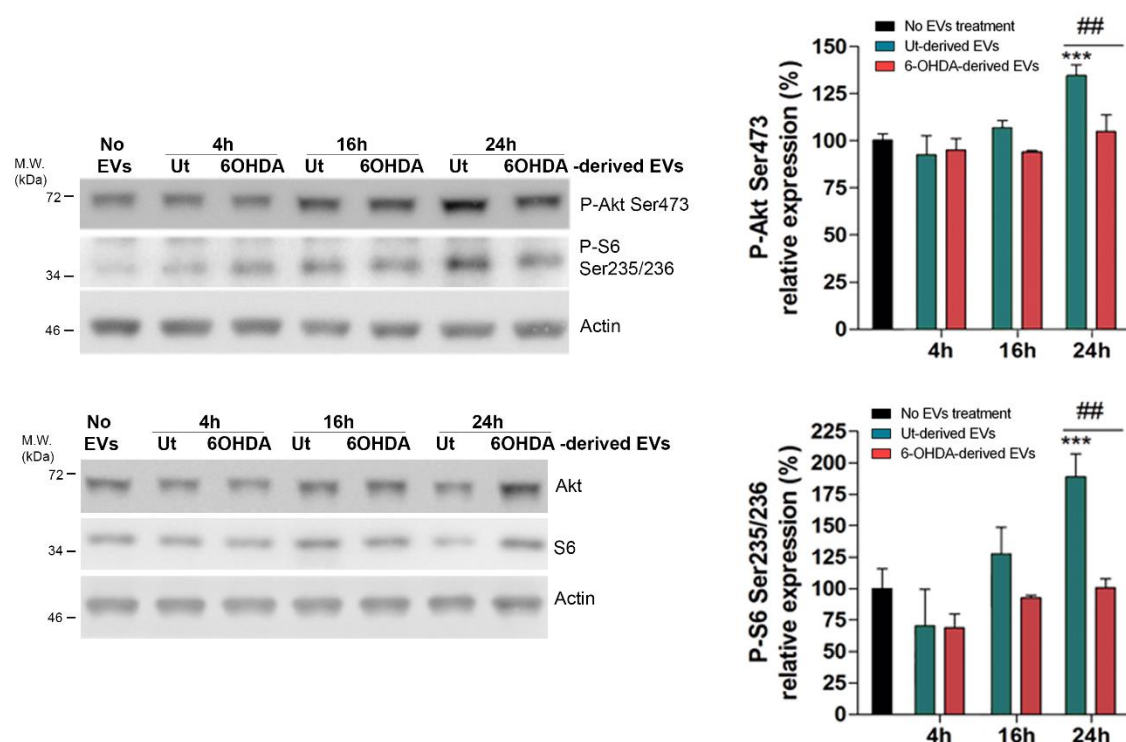


Figure 55. Control-derived exosomes, but not 6-OHDA-derived, activate the mTOR/Akt survival signaling pathway in recipient neurons. Rat cortical neurons DIV14 were untreated (ut) or exposed to 6-OHDA 50 μ M, and 16h later exosomes were obtained from the culture media. 800,000 particles were administered to target rat cortical primary neurons and a control condition without exosome treatment was performed as negative control. After 4, 16 or 24h of treatment, cell extracts were collected and subjected to WB. Representative immunoblots show P-Akt Ser473, P-S6 Ser235/236, total Akt, total S6 and actin as a loading control. Values are represented as mean \pm SEM (n = 3). Data were analyzed by One-way ANOVA with Bonferroni's multiple comparison test (***) $P < 0.001$ vs. No EVs treatment and (##) $P < 0.01$ vs. Ut-derived EVs).

ii. 6-OHDA-induced RTP801 contributes to counteract EVs trophic effect in recipient neurons

Based on these results, we next asked whether RTP801 levels modulate the trophic effect of exosomes. To test this hypothesis, we exposed to 6-OHDA untransduced neuronal cultures or cultures transduced with lentiviral particles packed with scrambled shRNA or an shRNA against RTP801. After 3 days, exosomes from all conditions were isolated from the culture media and were used to treat naïve rat cortical cultures. Twenty-four hours after the administration, recipient neurons were analyzed by WB or immunofluorescence (Figure 56A). As before, exosomes derived from untreated control neurons increased the phosphorylation levels of P-Akt (Ser473) and P-S6 (Ser235/236), independently of the transduced construct. However, exosomes derived from untransduced neurons or transduced with the scrambled shRNA and exposed to 6-OHDA did not exert this activation. Strikingly, exosomes derived from neurons where RTP801 was knocked down and exposed to 6-OHDA, could partially prevent the loss of pro-survival signaling activation (Figure 56B).

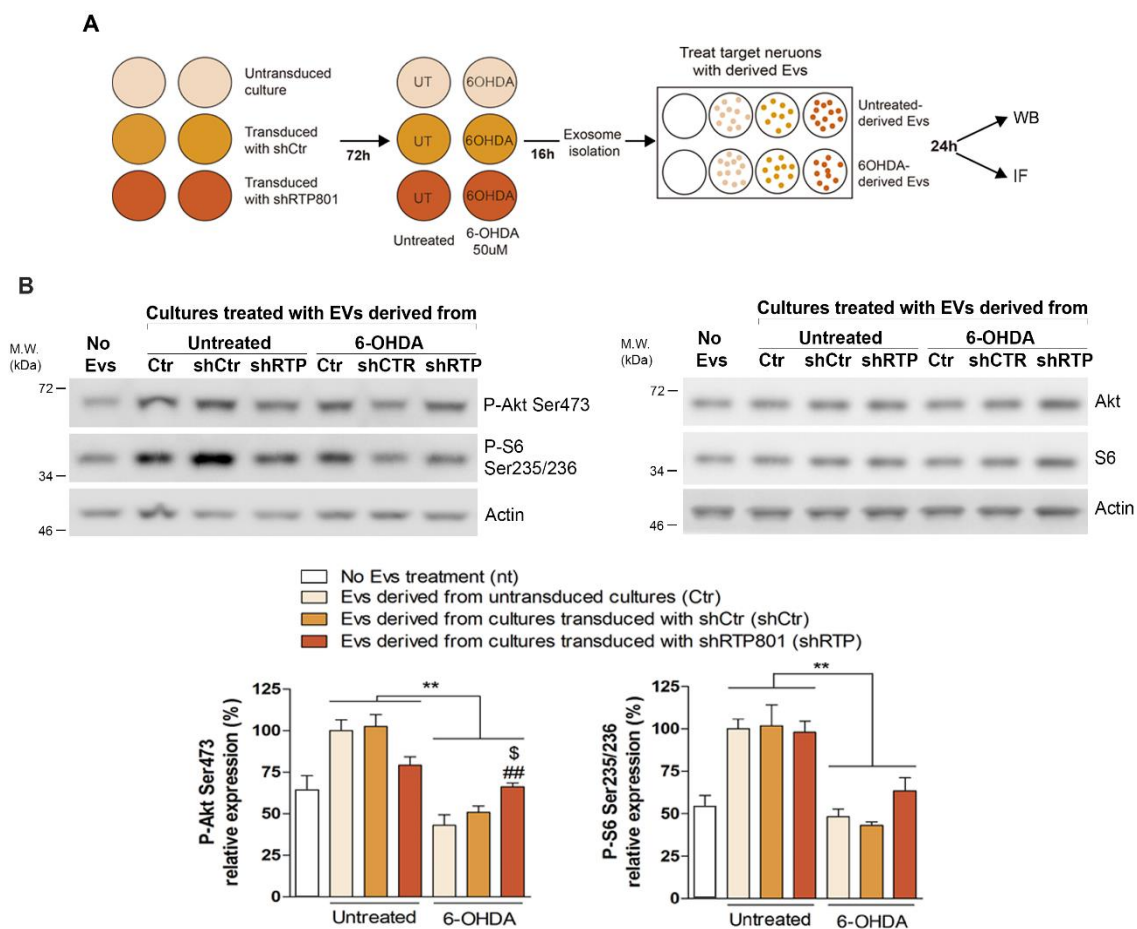


Figure 56. 6-OHDA-induced RTP801 counteract EVs trophic effect in recipient neurons. (A) Scheme of the protocol followed. **(B)** Rat cortical neurons DIV10 were untransduced (Ctr) or transduced with pLL3.7-shCtr or pLL3.7-shRTP801. Seventy-hours later, cells were untreated or exposed to 6-OHDA 50µM for 16h. After that, exosomes were isolated from the culture media by sequential centrifugations and 800,000 particles were administered to rat cortical cultures. As negative control, a condition without exosome treatment was performed. Twenty-four hours later, cells were harvested, and protein extracts were subjected to WB. Membranes were probed against P-Akt (Ser473), P-S6 (Ser235/236), total Akt, total S6 and actin as a loading control. Representative immunoblots are shown. Values are represented as mean ± SEM (n=3). Data were analyzed by Two-way ANOVA followed by Bonferroni's post-hoc test. (** $P < 0.01$, ## $P < 0.01$ vs. Ctr 6-OHDA and \$ $P < 0.05$ vs. shCtr 6-OHDA).

RESULTS

In parallel we assessed whether exosomes could affect neuronal survival. Exosomal vesicles were isolated from the abovementioned conditions and administered to recipient naïve cortical cultures. None of the exosomal treatments affected neuronal viability 24 hours after the administration (Figure 57).

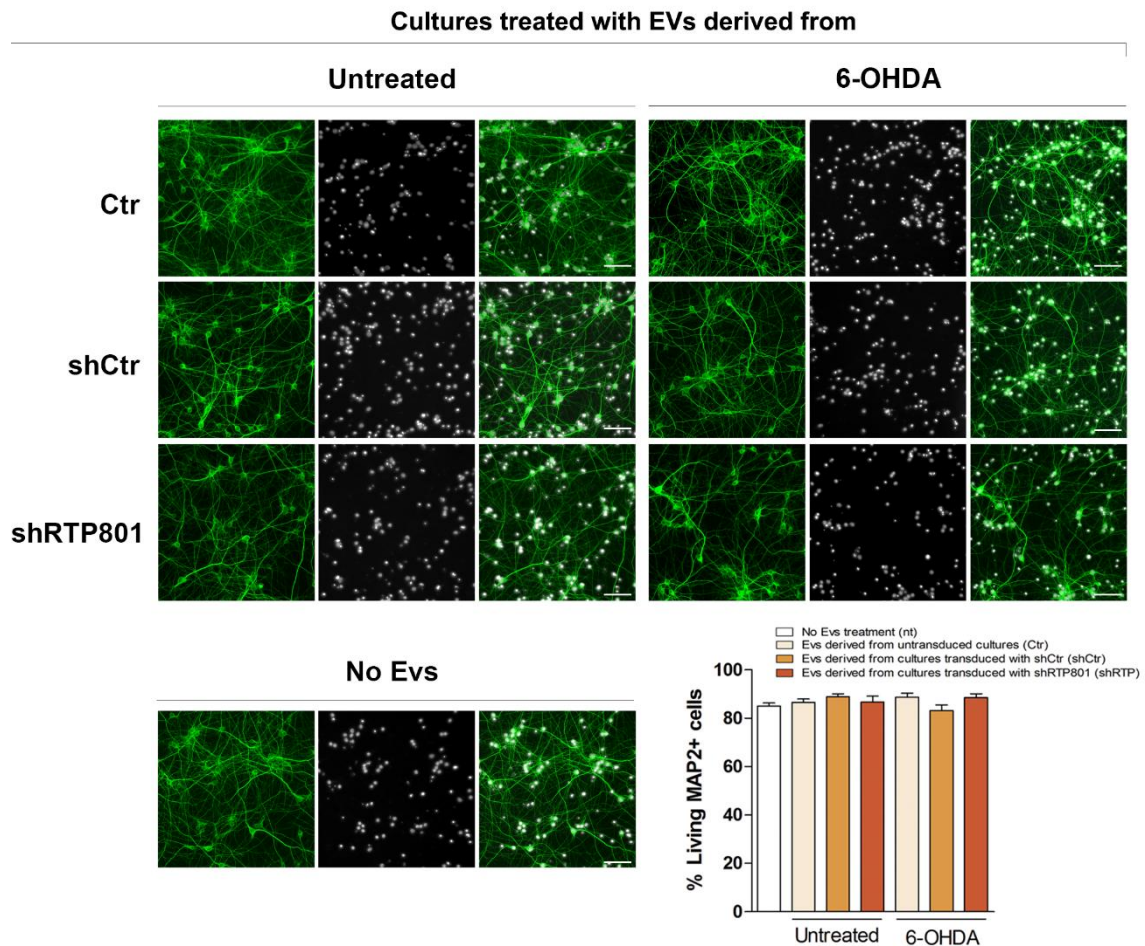


Figure 57. Exosome treatment does not affect neuronal survival. Rat cortical neurons DIV10 were untransduced (Ctr) or transduced with pLL3.7-shCtr or pLL3.7-shRTP801. Seventy-hours later, cells were untreated or exposed to 6-OHDA 50 μ M for 16h. Afterwards, exosomes were isolated from the culture media by sequential centrifugations and 800,000 particles were administered to rat cortical cultures. As negative control, a condition without exosome treatment was performed. After 24h cultures were fixed, and cells were immunostained against MAP2 (in green) and co-stained with Hoechst 33342 (in blue) to reveal the nuclei. Surviving MAP2+ cells were scored and represented as a percentage of total MAP2+ cells. Data were analyzed by Two-way ANOVA followed by Bonferroni's post-hoc test. Data showed no differences in the percentage of survival.

Taken together, our data indicate that 6-OHDA-induced RTP801 is loaded into exosomes and contributes to counteract the trophic properties of exosomal vesicles in cortical neurons.

2.3 Study of exosomal RTP801 in mhtt-expressing cells

In the previous section of this thesis we described that mhtt increases RTP801 protein levels and, importantly, RTP801 upregulation contributes to mhtt toxicity in cellular models and impairs motor plasticity in animal models. In our next aim we studied whether mhtt-induced stress increases also exosomal RTP801 and interferes the exosomal trophic support.

2.3.1 Neither RTP801 nor mhtt are detected in the exosomal fraction derived from STHdh cells

To address this issue, we used the immortalized mouse striatal cell lines that express WT (STHdh^{Q7/Q7}; WT) or mutant (STHdh^{Q111/Q111}; KI) htt. As we have previously shown in HD cell models, we confirmed that RTP801 levels were increased in the KI cell line in comparison to the WT (Figure 58A).

Even though mhtt increases RTP801 in KI cells, we could not detect enriched RTP801 in the exosomal fraction (Figure 58B), unlike 6-OHDA neuronal model. Proper exosomal isolation was corroborated by the presence of the markers TSG101, Flotillin-1 and alix. Alix was used as an additional exosomal marker since it is also associated to the ESCRT machinery and is contained inside exosomes^{397,517}. We could not observe full-length or N-terminal fragments of mhtt in the exosomes derived from the culture media of the cell lines (Figure 58C).

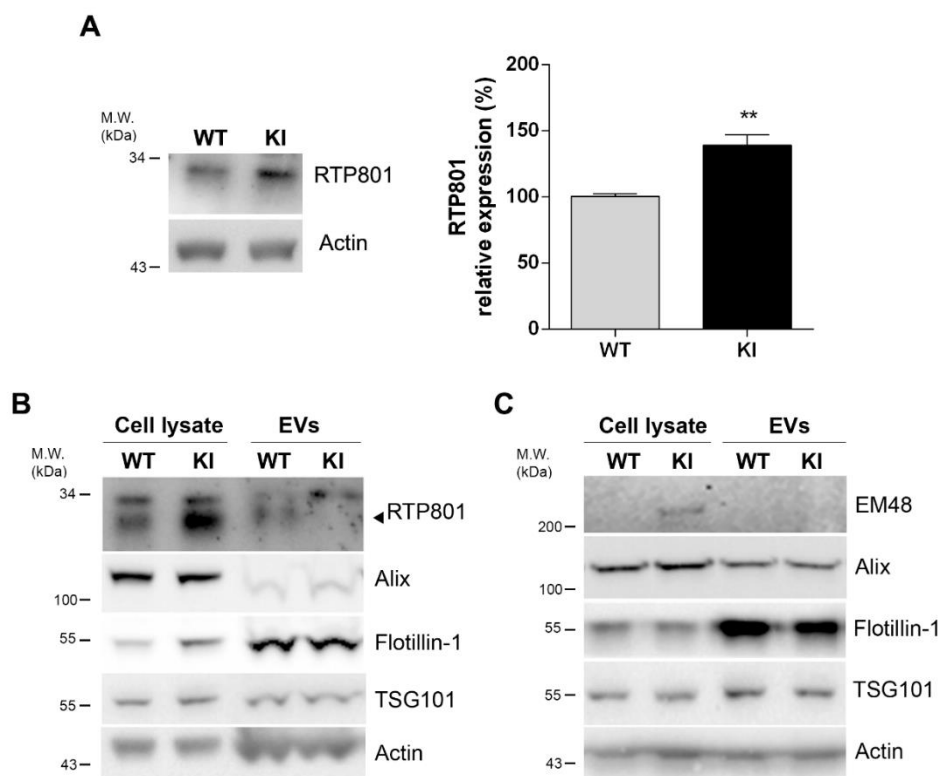


Figure 58. RTP801 is increased in STHdh^{Q111/Q111} cells but is not enriched in exosomes. (A) RTP801 protein content was analyzed in STHdh^{Q7/Q7} (WT) and STHdh^{Q111/Q111} (KI) cell extracts by WB. Membranes were probed with antibodies against RTP801 and actin as a loading control. Representative immunoblots are shown along with densitometry analysis for RTP801 signal from at least 3 independent experiments. Data was analyzed with Student's T-test (**P<0.01 vs. WT). **(B, C)** Exosomes derived from WT and KI cells were isolated from the cell media by sequential centrifugations. Membranes were probed against RTP801, EM48 to detect htt forms and Alix, Flotillin-1 and TSG101 as exosomal markers, and actin as loading control.

2.3.2 Mutant htt-induced RTP801 upregulation contributes to the loss of exosomal trophic support by downregulating phospho-S6 ribosomal protein in recipient neurons

Nevertheless, we sought to investigate whether exosomes derived from STHdh cell lines could also affect the mTOR signaling pathway in recipient cells and whether RTP801, although not being present within exosomes, could somehow modulate intercellular communication. Both WT and KI cell lines were transfected with a scrambled shRNA or with a specific shRNA against RTP801, which knockdown efficiency was proved by WB (Figure 59A). Forty-eight hours later, exosomes were isolated from the culture media and used to treat naïve mouse cortical neurons for another 24 hours (Figure 59B). WB analysis of neuronal lysates showed that exosomes induced a different effect on mTORC 1 and 2. Exosomes derived from KI cells did not lose the trophic effect over P-Akt (Ser473), as mTORC2 readout. However, RTP801 silencing in both WT and KI exosome-producing cells tended to increase the levels of P-Akt (Ser473) in recipient

naïve neurons. Moreover, this effect was independent to the cells expressing WT htt or mhtt.

On the other hand, exosomes derived from KI cells were not able to increase P-S6 (Ser235/236), and thus activate mTORC1, in comparison to WT cells. Remarkably, when RTP801 was knocked down in KI cells, exosome effect upon S6 phosphorylation was recapitulated (Figure 59C). These results confirmed that somatic RTP801 increase induced by mhtt interferes with the trophic effect that exosomes exert in recipient neurons.

Summarizing, we have shown that both ectopic and endogenous RTP801 are found in the exosomal fraction derived from HEK293 cells. In cortical primary neurons, the increase of RTP801 in exosomes is sensitive to 6-OHDA neurotoxin but not to potassium depolarization. Moreover, exosomes derived from 6-OHDA exposed neurons or mhtt-overexpressing cells loses the trophic ability to activate mTOR/Akt pathway. Interestingly, the downregulation of RTP801 in exosome-producing cells under stress partially rescued trophic effect in recipient neurons.

RESULTS

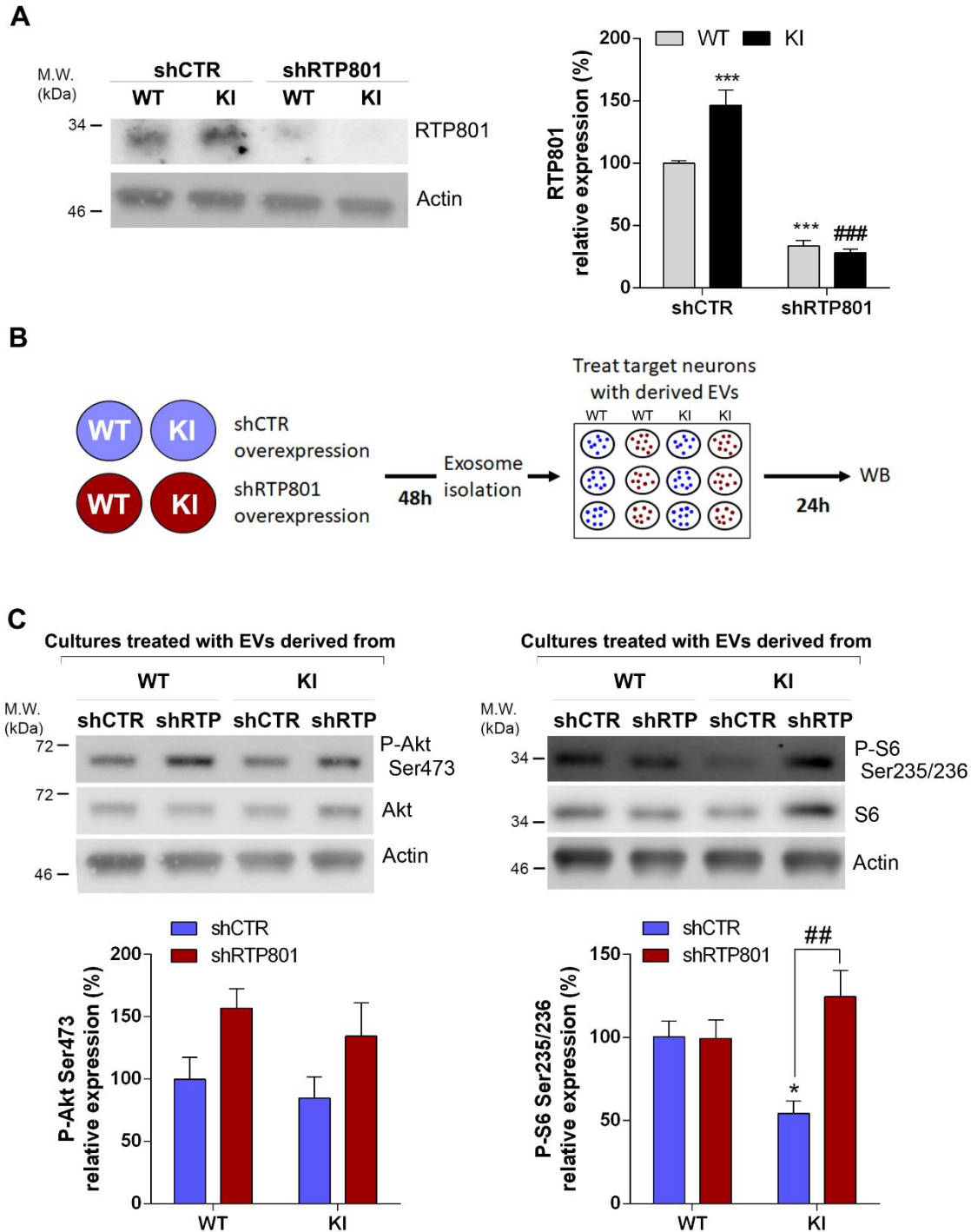


Figure 59. RTP801 upregulation in *STHdh*^{Q111/Q111} cells contributes to loss of exosomal trophic support. (A) *STHdh*^{Q7/Q7} (WT) and *STHdh*^{Q111/Q111} (KI) cell were transfected with pCMS-shCTR or pCMS-shRTP801 and 48h later cell extracts were subjected to WB. Membranes were probed with antibodies against RTP801 and actin as a loading control. Representative immunoblots are shown along with densitometry analysis for RTP801 signal from at least 3 independent experiments. Data was analyzed with Two-way ANOVA followed by Bonferroni's post-hoc test (** $P < 0.01$, *** $P < 0.001$ vs. WT shCTR; #### $P < 0.001$ vs. KI shCTR). (B) Scheme of the protocol followed. (C) Sister *STHdh*^{Q7/Q7} (WT) and *STHdh*^{Q111/Q111} (KI) cell cultures were transfected with pCMS-shCTR or pCMS-shRTP801. Forty-four hours later exosomes were isolated from the culture media by sequential centrifugations and 800,000 particles were administered to mouse cortical cultures. Twenty-four hours later, cells were harvested and protein extracts were subjected to WB. Membranes were probed against P-Akt (Ser473), P-S6 (Ser235/236), total Akt and total S6 and actin as loading control. Representative immunoblots are shown. Values are represented as mean \pm SEM ($n=3$). Data were analyzed by Two-way ANOVA followed by Bonferroni's post-hoc test (* $P < 0.05$ vs. WT shCTR and ## $P < 0.01$ vs. KI shCTR).

3. SINGLE NUCLEOTIDE POLYMORPHISM-BASED mTOR PATHWAY ANALYSIS IN PARKINSON'S DISEASE

The mTOR pathway is one of the several pathways that have been proposed to be involved in PD, a neurodegenerative disease mainly characterized by the loss of dopaminergic neurons in the SNpc¹⁷³. Deregulation of both mTORC 1 and 2 occurs in PD (reviewed in ^{249,518}). For instance, mTOR activity is impaired in neurons of the SNpc from idiopathic PD patients. Moreover, the restitution of the mTOR or Akt activity prevents neuronal cell death in cellular and animal models of PD^{263,264,286}. Besides neuronal death, around 40% of PD patients undergo dementia or alterations in working memory¹³⁷ which points out that PD brain also displays aberrant plasticity⁵¹⁹. Interestingly, it has been described that the development of L-DOPA induced dyskinesia (LID) involves an aberrant form of plasticity at the corticostriatal synapse^{240–243}.

Dopamine replacement therapy by oral administration of L-DOPA (or levodopa) is the standard treatment used to counteract motor symptoms in PD patients^{520,521}. However, chronic treatment with L-DOPA triggers other motor complications including LID. Recent studies indicate that LID is associated with a loss of homeostatic synaptic mechanisms in the basal ganglia and in the cortical transmission^{240–243}. Although the molecular basis of LID has not been yet elucidated, mTOR pathway has been also involved in LID development. Indeed, in PD animal models pharmacological inactivation of mTOR with rapamycin or rapalogs prevented LID appearance^{332,334}.

Genetic approaches have been very useful for identifying the genetic mutations in PD causative genes, but they only represent a 5-10% of the total cases¹⁷³. Importantly, genetic variations in the *SNCA* and *MAPT* genes have been top associated with increased risk of PD^{154,156,157}. Although other genetic risk factors for PD have been identified^{149–151,522,523}, the genetic contribution to PD as complex multifactorial disorder remains yet unclear and far from being uncovered.

Based on the biochemical evidences, we performed an mTOR candidate pathway approach and explored whether common genetic variability in selected genes from the mTOR signaling cascade may modulate PD and LID.

To this purpose, we genotyped 64 SNPs in mTOR-related genes and PD-related genes in a Spanish cohort of 898 PD patients and 921 healthy controls (ANNEX I Table A1 for descriptive information and Table A2 for genotypic analysis data). We filtered out SNPs which were not in Hardy-Weinberg equilibrium and SNPs which did not surpass a genotyping quality threshold of unambiguous genotypes in above 90% in all studied

samples, resulting in a total of 54 SNPs which were further analyzed. We explored the association of SNPs or their complex epistatic interactions with PD and LID risk.

This project has been developed in collaboration with Dr. Mario Ezquerra and Dr. Rubén Fernández-Santiago from IDIBAPS and from the Neurology Service of Hospital Clínic de Barcelona and with Dr. María Josep Martí from the Neurology Service of Hospital Clínic de Barcelona.

3.1 SNCA and mTOR genetic variations interact to modulate risk and age at onset of Parkinson's disease

Among the different genetic variations in the *SNCA* gene that have a positive outcome for PD risk, the SNP rs356219 is one of the most studied. This SNP is located at the 3' untranslated region (UTR) of the gene and has been related to increase *SNCA* expression^{524,525}. Furthermore, *SNCA* rs356219 has also been described to modulate PD age-at-onset (AAO) in both idiopathic PD and LRRK2-associated PD (L2PD)^{166,167}.

By classical allelic and genotypic association analyses, we investigated whether individual SNPs in the mTOR pathway are associated with differential PD susceptibility and PD AAO. Since gene-gene interaction or epistasis can be relevant in genetically complex disorders like PD, we also assessed the existence of potential multi-locus interactions among mTOR SNPs to modulate PD by themselves and/or interactions with PD-related SNPs in *SNCA* and *MAPT*, to modulate the risk and the AAO of PD.

3.1.1 Single SNP analysis for the risk of idiopathic PD

We first performed an allelic association analysis of single markers with the susceptibility to PD. After adjusting by gender, age and multiple testing (n=54 tests), we found a statistically significant association of the SNP rs356219 in the *SNCA* gene with a differential risk for PD in which the G risk allele had a frequency of 0.41 in PD cases and 0.33 in controls [O.R. (95% C.I.) = 1.39 (1.16-1.57), adj. *P*-value = 0.0346]. Regarding the other SNPs, we could only confirm a significant association of SNP rs1800547 in *MAPT* gene with PD risk (Table 8).

Gene	SNP	Alleles (M/m)	mAF PD	mAF Controls	O.R. (95% C.I.)	<i>P</i> -value	FDR <i>P</i> -value
<i>SNCA</i>	rs356219	A(1)/G(2)	0.41	0.33	1.39(1.16-1.57)	0.0006	0.0346
<i>MAPT</i>	rs1800547	A(1)/G(2)	0.25	0.31	0.75(0.64-0.88)	0.0013	0.0349

Table 8. Allelic associations of SNPs rs356219 in *SNCA* and rs1800547 in *MAPT* with PD risk, adjusted by sex, age and multiple testing adjustments of *P*-values. Allelic test calculated in Unphased 6.0 with sex- and age-adjustment of *P*-values. *P*-values were adjusted for 54 multiple testing by using FDR correction. N=898 PD cases; 921 controls (N=1,819). M=major allele; m=minor allele; mAF= minor allele frequency, O.R., Odds Ratio. Statistically significant *P*-values are highlighted in bold.

At a genotypic level, we also detected significant association of *SNCA* rs356219 [O.R. (95% C.I.) = 0.73 (0.64-0.84), *P*-value < 0,0027] and *MAPT* rs1800547 [O.R. (95% C.I.) = 1.33 (1.15-1.54, *P*-value = 0.0027], both under a log-additive model (Table 9). These data are in agreement with previous findings^{156,157,156–158,164,166}. On the contrary, we did not find significant association with PD risk for any of the other 54 mTOR genetic markers but top signals included *DDIT4L* rs1053227 (not corrected *P*-value = 0.01) and *EIF4EBP1* rs6605631 (not corrected *P*-value = 0.01).

Gene	SNP	Alleles (M/m)	PD			Control			O.R. (95% C.I.)	Model	Genotypic <i>P</i> -value	Adj. Gen. <i>P</i> -value
			Freq. 11	Freq. 12	Freq. 22	Freq. 11	Freq. 12	Freq. 22				
<i>SNCA</i>	rs356219	A(1)/G(2)	0.36	0.47	0.17	0.45	0.44	0.11	0.73 (0.64-0.84)	Log-additive	<0.0001	<0.0027
<i>MAPT</i>	rs1800547	A(1)/G(2)	0.56	0.38	0.06	0.49	0.41	0.11	1.33 (1.15-1.54)	Log-additive	0.0001	0.0027
<i>DDIT4L</i>	rs1053227	G(1)/A(2)	0.33	0.49	0.18	0.37	0.49	0.14	0.84 (0.73-0.96)	Log-additive	0.0100	0.1350
<i>EIF4EBP1</i>	rs6605631	T(1)/C(2)	0.69	0.29	0.26	0.66	0.29	0.46	1.98 (1.16-3.38)	Recessive	0.0100	0.1350
<i>LPIN1</i>	rs7595221	A(1)/G(2)	0.29	0.48	0.23	0.25	0.53	0.22	1.23 (1.02-1.49)	Overdominant	0.0270	0.2916
<i>PRKCA</i>	rs887797	G(1)/A(2)	0.48	0.40	0.12	0.43	0.45	0.12	1.22 (1.01-1.48)	Overdominant	0.0360	0.2922

Table 9. Genotypic association of SNPs with PD risk, adjusted by sex and age sex, age, and multiple testing adjustments of *P*-values. Genotypic test calculated in SNPstats software with sex- and age-adjustment of *P*-values. *P*-values were adjusted for 54 multiple testing by using FDR correction. The genotypic test was chosen as the genetic test model with lower AIC/lower *P*-value. N= 897 PD cases; 921 controls (N=1,819). M=major allele; m=minor allele; Freq.= frequency; O.R.= Odds Ratio. Statistically significant *P*-values are highlighted in bold.

3.1.2 Epistatic interactions of *SNA* and mTOR SNPs are associated with the risk of idiopathic PD

Subsequently, we explored possible interactions involving more than two loci by performing a multifactor dimensionality reduction (MDR) analysis. Using this analysis, we found that the SNP rs356219 in *SNCA* interacts with other markers including the polymorphisms rs8111699 in *STK11*, rs456998 in *FCHSD1*, and rs1732170 in *GSK3B* to modulate a differential risk for PD. We identified multiple specific combinations of these markers which were associated with differential risk of PD [O.R. (95% C.I.) = 2.59 (2.14-3.13), *P*-value < 0.001], which showed the maximum 10/10 score for cross-validation consistency (Table 10 & Figure 60).

RESULTS

Gene	SNP	Bal. Acc. CV Training	Bal. Acc. CV Testing	CVC	Odds-ratio (95% CI)	P-value *	P-value#
<i>SNCA</i>	rs356219	0.5378	0.5245	7/10	1.37 (1.13 – 1.66)	0.306 - 0.307	0.925 - 0.926
<i>STK11</i>	rs8111699	0.5529	0.5283	5/10	1.52 (1.26 – 1.83)	0.214 - 0.215	0.874 - 0.875
<i>SNCA</i>	rs356219	0.5729	0.5247	5/10	1.79 (1.48 – 2.16)	0.300 - 0.301	0.924 - 0.925
<i>SNCA</i>	rs356219	0.6181	0.5875	10/10	2.59 (2.14 – 3.13)	< 0.001	< 0.001
<i>STK11</i>	rs8111699						
<i>FCHSD1</i>	rs456998						
<i>GSK3B</i>	rs1732170						

Table 10. MDR analysis of SNPs interactions with PD risk. N = 897 PD cases and N=920 unrelated controls. Random Seed = 10; CVC = Cross-Validation Count = 10; *Normal P-Value and #P-value of Explicit test of interaction obtained with 1.000 permutations. Statistically significant P-values are highlighted in bold.

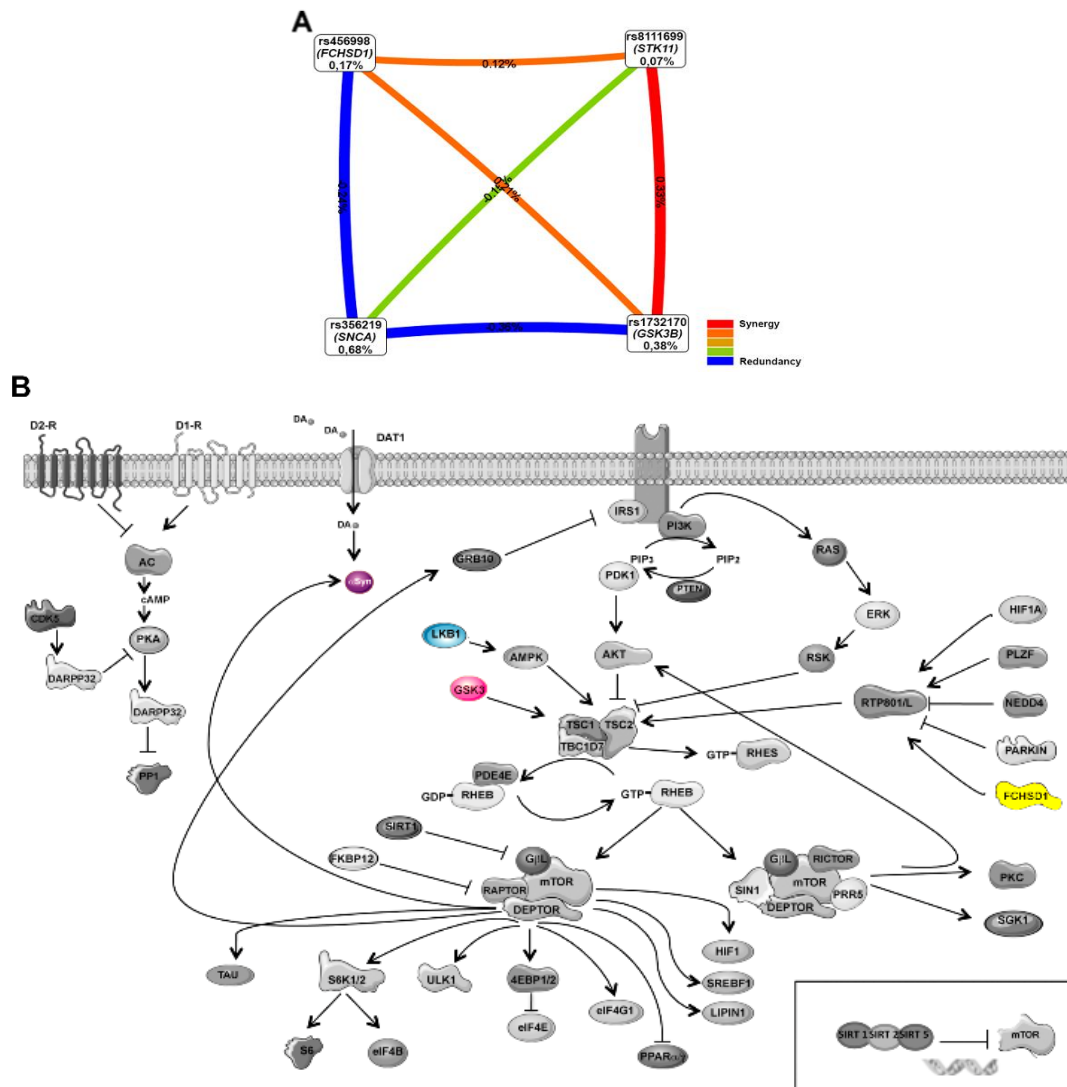


Figure 60. Association of the SNPs rs356219 in *SNCA*, rs8111699 in *STK11*, rs456998 in *FCHSD1* and rs1732170 in *GSK3B* genes with PD risk. (A) SNP interaction map with PD risk. The nodes were obtained in the epistatic analyses with the MDR software and represent the polymorphisms, including the genes that contain the SNP, while the numeric values inside represent the main information gain. The links show the interaction between SNPs. The color of the lines indicates the type of interaction explaining synergy or redundancy (yellow=independency, blue=correlation and orange=synergistic relationship). (B) Localization in the mTOR pathway of the proteins translated from the genes with SNPs significantly associated with PD risk. In color are highlighted the proteins alpha-synuclein (violet), LKB1 (blue), GSK3-beta (pink) and FCHSD1 (yellow) that are the product of the genes *SNCA*, *STK11*, *FCHSD1* and *GSK3B* respectively.

The percentage for precision, specificity and sensitivity of the abovementioned association however, was only around 60% (Sensitivity 63.28%; Specificity 60.06%; Precision 60.71%; Accuracy 61.67%). As an example, among others, the specific combination AG/CC/GT/CT had a 2.04% frequency in PD patients and the ratio PD/Control was 1.7 which predicts a PD outcome (ANNEX I Figure A1 & Table A3).

Collectively these results indicate that SNPs in the *SNCA* or in the *MAPT* genes alone modulate the risk of PD, as expected. However, in the case of the SNP in *SNCA* other polymorphisms in loci from the mTOR pathway genes contribute epistatically to PD risk modulation.

3.1.3 Single genotyping association with age-at-onset of idiopathic PD

Apart from the risk to suffer from PD, other parameter crucial for disease progression studies and therapeutic approaches is the age at onset (AAO) of PD. In our study, in the single marker genotypic analysis of 54 SNPs, adjusting by gender, age and multiple testing, we found that the SNP rs356219 in *SNCA* was the only SNP associated with differential AAO of PD. More specifically we found a mean of 55.6 ± 0.8 year for GG carriers, 55.8 ± 0.5 years for AG, and 58.0 ± 0.5 years for AA with an adjusted *P*-value of 0.0034 under a log-additive model. In contrast, we did not find association of *MAPT* rs1800547 with the AAO of PD (Table 11). These data are in line with previously described results in idiopathic PD^{166,526} and in LRRK2-associated PD^{156,167}.

Gene	SNP	Alleles (M/m)	Freq. 11	Freq. 12	Freq. 22	AAO 11 (y)	AAO 12 (y)	AAO 22 (y)	O.R. (95% C.I.)	Model	<i>P</i> -value	FDR-adj. <i>P</i> -value
<i>SNCA</i>	rs356219	A(1)/G(2)	0.36	0.47	0.17	58.03 ±0.5	55.84 ±0.48	55.64 ±0.85	-1.35 (-2.19 - -0.51)	log-additive	0.0017	0.0034
<i>MAPT</i>	rs1800547	A(1)/G(2)	0.56	0.38	0.06	56.46 ±0.61	56.15 ±0.75	58.36 ±1.73	0.30 (-0.66 - 1.26)	log-additive	0.54	0.54

Table 11. Genotypic association tests of *SNCA* rs356219 and *MAPT* rs1800547 SNPs with AAO of PD with gender, age and multiple testing adjustments of *P*-values. Genotypic test calculated in the SNPstats software with sex- and age-adjustment of *P*-values. The model of inheritance best fitting the data was automatically selected as the model with the lowest Akaike information (AIC) value. Three SNPs considered for *P*-value multiple test adjustment. N= 748 PD cases with AAO available. M=major allele; m=minor allele; mAF= minor allele frequency; Freq.=frequency; O.R.= Odds Ratio; y=years. Statistically significant *P*-values are highlighted in bold.

3.1.4 Epistatic interactions of *SNCA* and mTOR SNPs are associated with AAO of idiopathic PD

We then explored whether epistatic combinations of mTOR SNPs were also involved in the AAO of idiopathic PD. By MDR analysis, we found that the abovementioned *SNCA* SNP rs356219 interacts in epistatic combination with two other loci at the mTOR pathway including rs11868112 in *RPTOR* and rs6456121 in *RPS6KA2*. We found a significant

RESULTS

association of this three-loci-interaction with AAO with the maximum cross-validation consistency of 10/10 (P -value < 0.001) (Table 12 & Figure 61). The odds-ratio for the association of this interaction with AAO of idiopathic PD was O.R. (95%C.I.) = 2.89 (2.90-4.00). Interestingly, the specific genotypic combination AG/CC/CC in rs356219 *SNCA*, rs11868112 *RPTOR* and rs6456121 *RPS6KA2* respectively, was associated with a 4-years earlier AAO of PD (ANNEX I Figure A2 & Table A4).

Gene	SNP	T-statistic CV Training	T-statistic CV Testing	CVC	Odds-ratio (95% CI)	P -value *	P -value#
<i>SNCA</i>	rs356219	2.6757	1.0612	5/10	1.31 (0.96-1.79)	0.477 - 0.478	0.640 - 0.641
<i>RPTOR</i> <i>RPS6KA2</i>	rs11868112 rs6456121	4.1806	3.1885	8/10	1.63 (1.20-2.21)	0.0260 - 0.0270	0.0460 - 0.0470
<i>RPTOR</i> <i>SNCA</i> <i>RPS6KA2</i>	rs11868112 rs356219 rs6456121	7.6501	6.0162	10/10	2.89 (2.90-4.00)	< 0.001	< 0.001

Table 12. MDR analysis of SNPs interactions with PD AAO. N = 748 PD cases; Random Seed = 10; CVC = Cross-Validation Count = 10; *Normal P -Value and # P -value of Explicit test of interaction obtained with 1.000 permutations. Statistically significant P -values are highlighted in bold. Odds-ratio was obtained generating a dichotomous dataset comparing early PD AAO (before 57 years) and late PD AAO (after 58 years) based on the average of AAO found with the MDR (56.66 years).

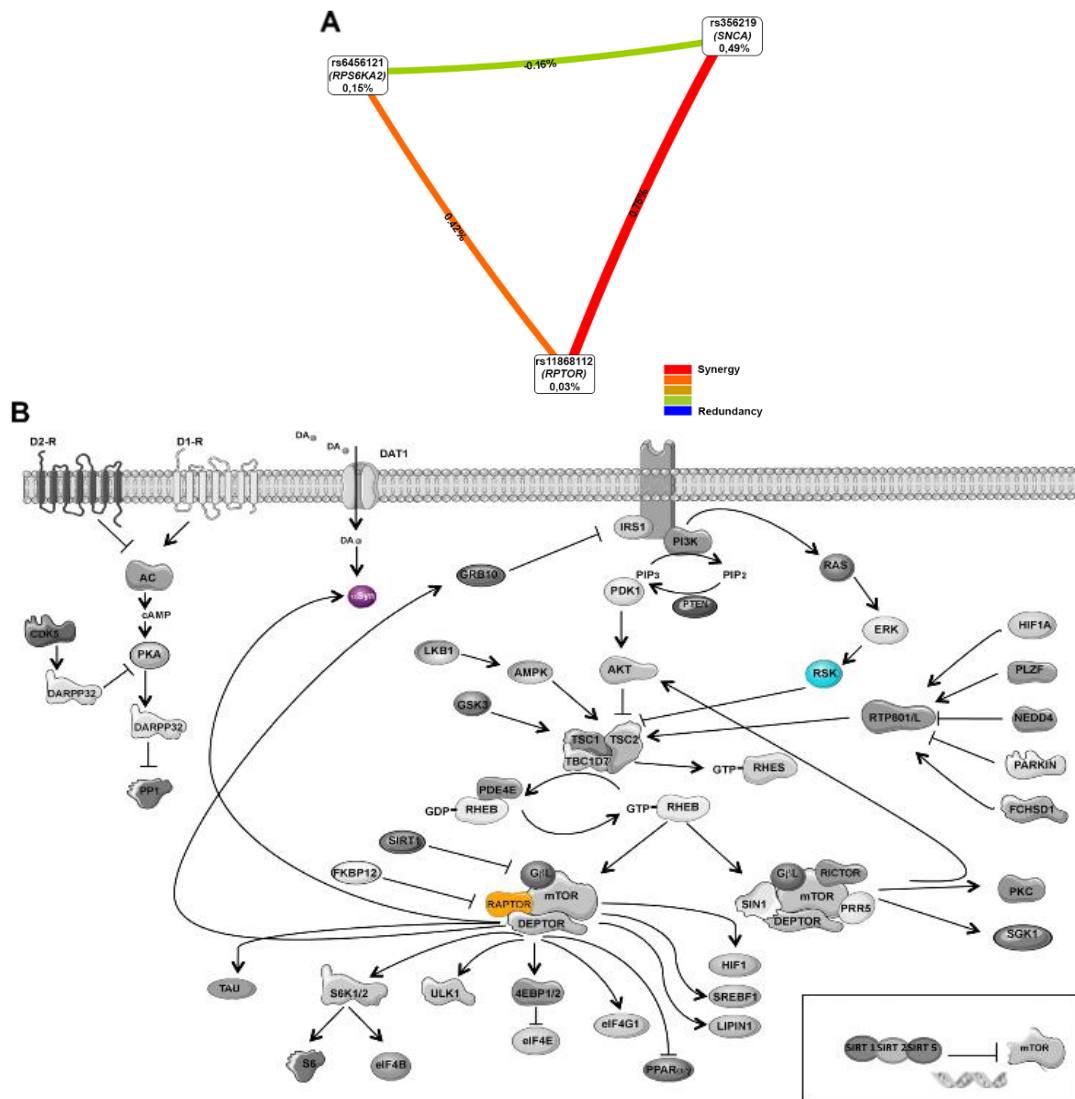


Figure 61. Association of the SNPs rs356219 in *SNCA*, rs11868112 in *RPTOR* and rs6456121 in *RPS6KA2* genes with PD AAO. (A) SNP interaction map with PD AAO. The nodes were obtained in the epistatic analyses with the MDR software and represent the polymorphisms, including the gene that contain the SNP, while the numeric values inside represent the main information gain. The links show the interaction between SNPs. The color of the lines indicates the type of interaction explaining synergy or redundancy (yellow=independency, blue=correlation and orange=synergistic relationship). (B) Localization in the mTOR pathway of the proteins translated from the genes with SNPs significantly associated with PD AAO. In color are highlighted the proteins alpha-synuclein (violet), Raptor (orange), ribosomal protein s6 kinase alpha-2 (blue) that are encoded by the genes *SNCA*, *RPTOR*, *RPS6KA2* respectively.

3.1.5 Association of epistatic combinations of SNPs with the AAO of LRRK2-associated PD

We next investigated whether the epistatic interaction described above, ie. *SNCA* rs356219, *RPTOR* rs11868112, and *RPS6KA2* rs6456121, could also modulate the AAO of PD patients with monogenic L2PD carrying the p.G2019S mutation. To this end we performed a multi-dimension reduction analysis in 127 patients with L2PD. The mean of AAO of this cohort was of 56.74 years and was the same as the mean of AAO of 56.66 years observed in idiopathic PD. We observed a similar trend in the epistatic interaction

RESULTS

with the idiopathic PD, but it was not statistically significant. The odds-ratio for this association was O.R. (95% C.I.) = 3.99 (1.89-8.40) (Table 13). Statistical significance was achieved only when we over sampled the cohort (N=127) to reach the same number of individuals as in the idiopathic cohort (N=748). Similarly, as we found in the idiopathic PD population, the combination AG/CC/CC in rs356219 *SNCA*, rs11868112 *RPTOR* and rs6456121 *RPS6KA2* was associated with 3.4 years- earlier PD AAO in L2PD patients (ANNEX I Figure A3).

Gene	SNP	T-statistic CV Training	T-statistic CV Testing	CVC	Odds-ratio (95% CI)	P-value *	P-value#
<i>RPTOR</i>	rs11868112						
<i>SNCA</i>	rs356219	3.9948	0.8422	10/10	3.99 (1.89-8.40)	0.2860 - 0.2870	0.1170 - 0.1180
<i>RPS6KA2</i>	rs6456121						

Table 13. Interaction of rs11868112 in *RPTOR*, rs356219 in *SNCA* and rs6456121 in *RPS6KA2* with PD AAO in mutant LRRK2 PD population. Interaction of SNPs with PD age at onset (AAO). N=127 LRRK2 mutant PD cases; MDR forced analysis of rs11868112, rs356219 and rs6456121; Random Seed = 10; CVC = Cross-Validation Count = 10; *Normal P-Value and #P-value of Explicit test of interaction obtained with 1,000 permutations. Odds-ratio was obtained generating a dichotomous dataset comparing early PD AAO (before 57 years) and late PD AAO (after 58 years) based on the average of AAO found with the MDR (56.74 years).

In summary, SNPs in the mTOR pathway genes contribute to both the risk and the AAO by interacting with *SNCA* rs356219.

3.2 Multilocus interactions in the mTOR pathway influence L-DOPA induced dyskinesia onset and severity in Parkinson's disease patients

L-DOPA induced dyskinesia (LID) is a common side effect of the treatment of PD to restore dopamine transmission in patients. It is estimated that about 80-90% of L-DOPA-treated PD patients develop LID within 5-10 years after initiation of DA replacement therapy^{239,242}. Imbalances in L-DOPA metabolism induce LID in a dose-dependent manner⁵²⁷. Among the risk factors for LID appearance are early PD onset, nigrostriatal severe denervation, length of L-DOPA treatment or excessive doses of L-DOPA (reviewed in ⁵²⁸). Yet, there is a large clinical heterogeneity regarding LID onset and LID severity that suggest the existence of additional and unknown factors modulating LID susceptibility⁵²⁹. Recent studies have reported genetic associations with LID predisposition, however most of them have used a single-gene candidate approach²⁴⁶⁻²⁴⁸.

Since impairment of mTOR pathway is a hallmark in PD pathogenesis^{249,263,264,306} and, moreover, the pharmacological inhibition of mTOR prevents LID appearance^{332,334}, we performed a genetic pathway analysis by screening SNPs at genes belonging to the mTOR pathway (ANNEX I Table A1 & Table A2). We explored the association of single SNPs or complex epistatic interactions in the mTOR pathway with the development of LID in PD patients by analyzing their potential modulatory role in LID risk and LID severity.

3.2.1 Association of single SNPs with LID onset and LID peak

We first performed the allelic association analysis of individual SNPs with time to dyskinesia (TTD), the time period from initiation of L-DOPA treatment to the development LID, and with time to LID Peak (TLP), the corresponding time to highest LID, or LID peak. We found a statistically significant association between the SNP rs1043098 in *EIF4EBP2* with TLP (FDR-adjusted P -value = 0.0179). In addition, we found a trend of association of this SNP with TTD (P -value = 0.015) which did not reach statistical significance after FDR multiple testing correction (Table 14).

RESULTS

LID Peak					LID Onset				
Gene	SNP	P-value	FDR P-value	Addval	Gene	SNP	P-value	FDR P-value	Addval
<i>EIF4EBP2</i>	rs1043098	0.0003	0.0179	0.2204	<i>EIF4EBP2</i>	rs1043098	0.0152	0.5481	0.1572
<i>CDK5</i>	rs2069442	0.0043	0.3520	0.2167	<i>PIK3CB</i>	rs361072	0.0238	0.5481	0.1407
<i>RPS6KB1</i>	rs1292034	0.0236	0.3520	0.1347	<i>HRAS</i>	rs12628	0.0486	0.5481	0.1207

Table 14. Allelic association of SNPs with LID peak (TLP) and with LID onset (TTD). Allelic test calculated in Unphased 6.0 software using the quantitative trait model. Sex was used as a cofounder and L-DOPA dosage and time from PD onset to L-DOPA onset as modifiers. P-values were adjusted for 54 multiple testing by using FDR correction. Addval: for quantitative traits, Unphased shows the estimated additive genetic value between different alleles. (N=216 for LID Peak and N=230 for LID Onset). Statistically significant P-values are highlighted in bold.

Nevertheless, the genotypic association revealed that *EIF4EBP2* rs1043098 was statically significant associated with both TTD and TLP (Table 15). More specifically, CC homozygous for *EIF4EBP2* had 2.84 years delay of LID onset and 3.84 years of delay in the appearance of LID peak than TT carriers (P -value = 0.0004 for LID onset and P -value < 0.001 for peak LID). Both P -values passed the Bonferroni correction.

LID Peak					LID Onset				
	n	Years (mean±SE)	Difference (95% CI)	P-value		n	Years (mean±SE)	Difference (95% CI)	P-value
CC	61	10.52±0.65	0	<0.0001	CC	61	8.34±0.62	0	0.0004
CT	68	9.28±0.54	-1.54 (-3.06 – -0.01)		CT	74	7.89±0.49	-0.96 (-2.26 – 0.35)	
TT	41	7.2±0.67	-3.89 (-5.63 – -2.15)		TT	42	6.05±0.56	-2.84 (-4.35 – -1.33)	

Table 15. Genotypic association of rs1043098 genotypes in *EIF4EBP2* gene with LID Peak (TLP) and LID Onset (TTD). P-value under the Log additive model are calculated by SNPstats software, and adjusted for gender, L-DOPA dosage and time from PD onset to L-DOPA treatment as implemented in SNPstats software.

3.2.2 Epistatic association of SNPs with LID onset

To investigate whether combinations of SNPs could be associated with TTD, we performed an epistatic association analysis using the data mining MDR software assuming TTD trait as a quantitative and continuous variable. We found an association of SNPs *EIF4EBP2* rs1043098 and *RICTOR* rs2043112 (P -value = 0.05) with LID onset (TTD), which was confirmed using the classical interaction analysis of SNPstats (P -value = 0.0140). Importantly, the combined association of these two loci with LID onset was statistically significant in combination with the third SNP rs4790904 located in the *PRKCA* gene, which yielded the maximum cross-validation consistency score of 10/10 (P -value < 0.001) (Table 16 & Figure 62).

Gene	SNP	T-statistic CV Training	T-statistic CV Testing	CVC	Odds-ratio (95% CI)	P-value *	P-value#
<i>PRKCA</i>	rs4790904	2.7069	-9.1020	4/10	1.98 (1.11-3.50)	0.9340 - 0.9350	0.9730 - 0.9740
<i>EIF4EBP2</i>	rs1043098	3.9678	2.9091	7/10	2.48 (1.42-4.31)	0.0490 - 0.0500	0.0910 - 0.0920
<i>RICTOR</i>	rs2043112	6.1882	4.7244	10/10	6.85 (3.57-13.16)	< 0.001	< 0.001
<i>EIF4EBP2</i>	rs1043098						
<i>RICTOR</i>	rs2043112						
<i>PRKCA</i>	rs4790904						

Table 16. MDR analysis of SNPs interactions with LID onset. N = 218; Random Seed = 10; CVC = Cross-Validation Count = 10; *Normal P-Value and #P-value of Explicit test of interaction obtained with 1,000 permutations. Statistically significant P-values are highlighted in bold. Odds-ratio was obtained generating a dichotomous dataset comparing early LID population (before 7 years) and late LID population (after 8 years) based on the average LID onset found with the MDR (7.64 years).

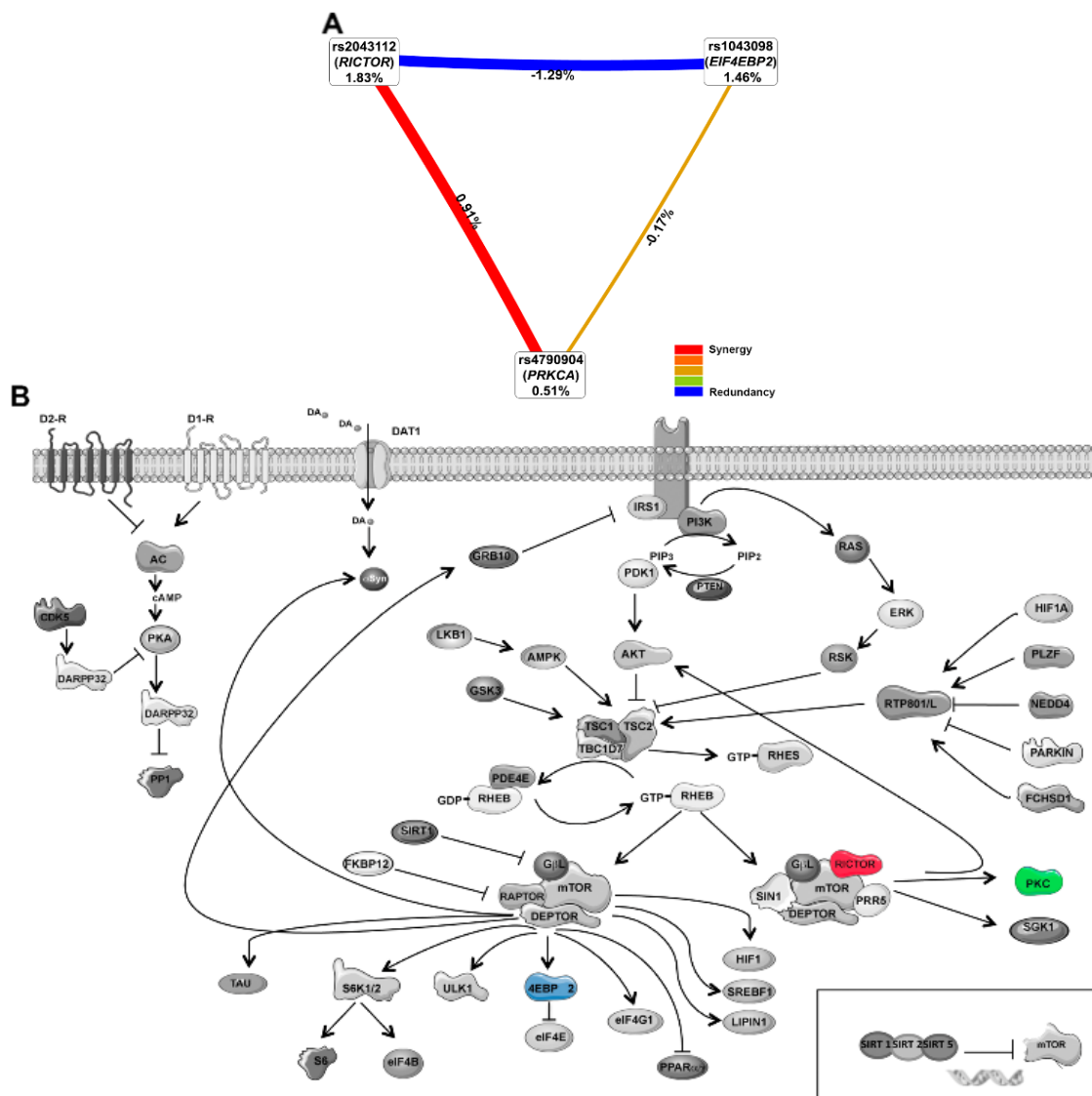


Figure 62. Association of the SNPs rs1043098 in *EIF4EBP2*, rs2043112 in *RICTOR* and rs4790904 in *PRKCA* genes with LID onset. (A) SNP interaction map with LID onset. The nodes were obtained in the epistatic analyses with the MDR software and represent the polymorphisms, including the genes that contain the SNP, while the numeric values inside represent the main information gain. The links show the interaction between SNPs. The color of the lines indicates the type of interaction explaining synergy or redundancy (yellow=independency, blue=correlation and orange=synergistic relationship). (B) Localization in the mTOR pathway of the proteins translated from the genes with SNPs significantly associated with LID onset. In color are highlighted the proteins 4EBP2 (blue), Rictor (pink) and PKC (green) that are the product of the genes *EIF4EBP2*, *RICTOR* and *PRKCA*, respectively.

RESULTS

As a continuous trait, TTD average was found at 7.62 years and from this data was established the distribution of high risk (LID before 7.6 years; early) and low-risk (after 7.6 years; late) genotypes (ANNEX I Figure A4 & Table A5). Among all distributions, two protective combinations of *EIF4EBP2* rs1043098/*RICTOR* rs2043112/rs4790904 *PRKCA* highlighted with high frequency and high impact on the LID onset. The combination CC/AG/TT with a frequency of 11.01% in the total PD population that delayed the appearance of LID in 5.2511 years, and the combination CT/AA/TT with a frequency of 5.50% that delayed the appearance of LID in 3.87761 years.

Collectively, these results indicate that the mentioned SNP in *EIF4EBP2* alone or in combination with other SNPs from the mTOR pathway are associated with the time to develop LID after initiation of L-DOPA treatment in PD patients.

3.2.3 Association of single SNPs with LID severity

Next, we studied whether SNPs in the mTOR pathway were associated with LID severity. According to the patient clinical data, LID severity was grades following the unified Parkinson's disease rating scale section IV (UPDRS-IV) that assesses disability due to LID⁵³⁰. Hence, LID severity was categorized as "0" (no LID), "1" (very mild LID), "2" (mild LID), "3" (moderate LID) and "4" (severe LID). Due to methodological approaches, samples were then stratified to compare two groups: (i) no/very mild/ mild LID (severity 0-2) (N=331 cases) and (ii) moderate/severe LID (severity 3-4) (N=70 cases).

First, we performed a crude association analysis of mTOR SNPs with LID severity and we found that the SNPs rs12628 in *HRAS* and rs1801582 in *PRKN* were individually associated with LID severity (FDR-adjusted *P*-values = 0.01080, respectively) (Table 17).

Gene	SNP	Alleles (M/m)	mAF LID severity 3-4	mAF LID severity 0-2	<i>P</i> -value	FDR <i>P</i> -value
<i>HRAS</i>	rs12628	A/G	0.49	0.33	0.0006	0.0180
<i>PRKN</i>	rs1801582	C/G	0.1	0.21	0.0007	0.0180
<i>RPTOR</i>	rs7211818	A/G	0.16	0.24	0.0007	0.0590
<i>RPS6KB1</i>	rs1292034	G/A	0.51	0.4	0.0293	0.3961
<i>RPTOR</i>	rs11868112	C/T	0.54	0.41	0.0452	0.4087
<i>STK11</i>	rs8111699	C/G	0.59	0.48	0.0454	0.4087

Table 17. Allelic association of SNPs rs12628 in *HRAS* and rs1801582 in *PRKN* with LID severity. Allelic test calculated in Unphased 6.0 software using the dichotomous analysis. Age, sex, L-DOPA dosage and TTD were used as cofounders. *P*-values were adjusted for 54 multiple testing by using FDR correction. N=401 PD cases; 70 severe LID, 331 with no/mild LID. M=major allele; m=minor allele; mAF= minor allele frequency. Statistically significant *P*-values are highlighted in bold.

3.2.4 Epistatic association of SNPs with LID severity

Following the same strategy that in LID risk, we next performed the epistatic association analysis of SNPs with LID severity using the MDR software. One of the main premises of MDR software is that the subjects in the groups to compare must be balanced in number. To balance the no/ very mil/ mild LID group (n=331) with the moderate/ severe LID group (n=70), different datasets were created randomly to under-sample the no/ very mild/mild severity group or, on the other way around, to over-sample the moderate/ severe severity group, as specified by the MDR developers. Each data set from one group was compared to the others independently. Using this dual approach, we detected a significant interaction of four-loci including rs1292034 *RPS6KB1*, rs12628 *HRAS*, rs6456121 *RPS6KA2* and rs456998 *FCHSD1* which was associated with LID severity (10/10 of cross-validation score. *P*-value < 0.001) (Table 18& Figure 63).

Gene	SNP	Bal. Acc. CV Training	Bal. Acc. CV Testing	CVC	Odds-ratio (95% CI)	P-value *	P-value#
<i>HRAS</i>	rs12628	0.6082	0.5924	9/10	2.56 (1.65 - 3.33)	0.0310 - 0.0300	> 0.5000
<i>HRAS</i> <i>RPTOR</i>	rs12628 rs7211818	0.6603	0.6382	9/10	3.79 (2.66 - 5.35)	0.0020 - 0.0030	> 0.5000
<i>ULK1</i> <i>PPARG</i> <i>EIF4EBP2</i>	rs12303764 rs2959272 rs1043098	0.7226	0.6206	4/10	7.01 (4.37 - 9.09)	0.0050 - 0.0060	> 0.5000
<i>RPS6KB1</i> <i>HRAS</i> <i>RPS6KA2</i> <i>FCHSD1</i>	rs1292034 rs12628 rs6456121 rs456998	0.8297	0.8173	10/10	31.56 (19.57 - 50.91)	< 0.0010	< 0.0010

Table 18. MDR analysis of SNPs interactions with LID severity. N = 328 with no to mild LID (0-1-2 in LID severity scale); N=301 with moderate to severe LID (3-4 in LID severity scale) in an oversampling dataset. Random Seed = 10; CVC = Cross-Validation Count = 10; *Normal *P*-Value and #*P*-value of Explicit test of interaction obtained with 1,000 permutations. Statistically significant *P*-values are highlighted in bold.

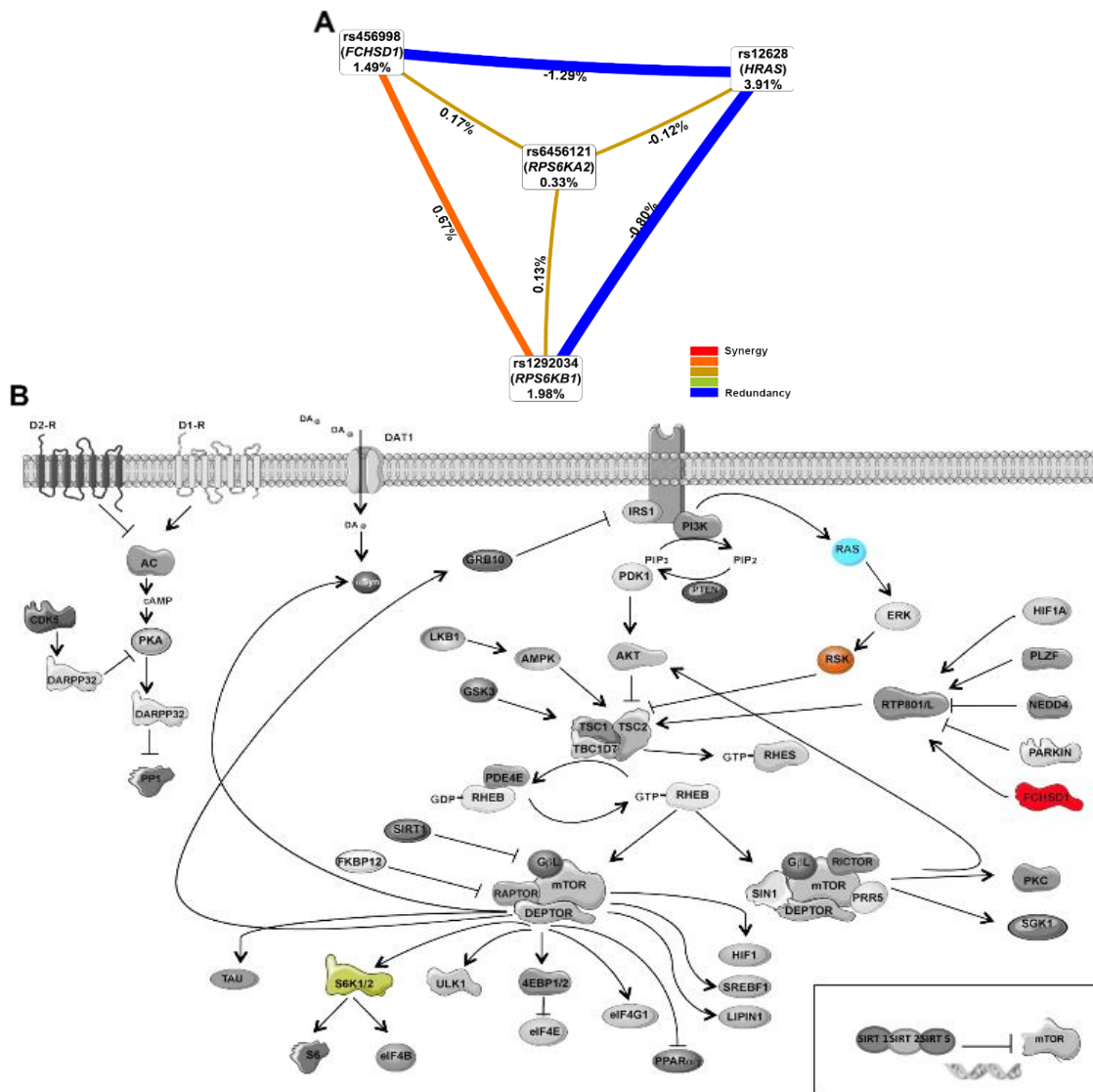


Figure 63. Association of the SNPs rs12628 in *HRAS*, rs5456121 in *RPS6KA2*, rs1292034 in *RPS6KB1* and rs456998 in *FCHSD1* genes with LID severity. (A) SNP interaction map with LID onset. The nodes were obtained in the epistatic analyses with the MDR software and represent the polymorphisms, including the gene that contain the SNP, while the numeric values inside represent the main information gain. The links show the interaction between SNPs. The color of the lines indicates the type of interaction explaining synergy or redundancy (yellow=independency, blue=correlation and orange=synergistic relationship). (B) Localization in the mTOR pathway of the proteins translated from the genes with SNPs significantly associated with LID severity. In color are highlighted the proteins H-Ras (violet), ribosomal protein S6 kinase beta-1, S6K-beta-1, and ribosomal protein S6 kinase alpha-2, S6K-alpha-2, (green and orange, respectively) and FCHSD1 (pink) that are encoded by the genes *HRAS*, *RPS6KB1*, *RPS6KA2* and *FCHSD1*, respectively.

From this analysis many different genotypic combinations were found to predict the status of LID severity with similar frequencies in the PD population (ANNEX I Figure A5 & Table A6). As an illustrative example for *RPS6KB1* rs1292034, *HRAS* rs12628, *RPS6KA2* rs6456121 and *FCHSD1* rs456998 interaction, we found that the combination AG/AG/CT/GT was present in a frequency of 5.56% of the total population in the group of moderate/severe LID and 1.59% in the control group of no/mild LID. The resulting ratio (3.5) indicated that this specific genotype combinations would predict moderate/severe

LID. All ratios above 1 were considered as risk combinations to develop moderate/severe LID status.

The four-loci interaction was confirmed *in-silico* using the forced analysis MDR option, which allows to evaluate only this particular combination for all generated datasets. Importantly, the average of the sensitivity and the precision of the method, as measures to correctly predict and discriminate LID severity was 83% and 86% respectively (Table 19).

Dataset type	Undersampling 1	Undersampling 2	Undersampling 3	Undersampling 4	Undersampling 5	Oversampling
Ratio case/control	1.06	1.05	1.04	1.00	1.21	0.89
Sensitivity	0.90	0.75	0.80	0.80	0.81	0.92
Specificity	0.80	0.92	0.97	0.85	0.87	0.74
Precision	0.81	0.91	0.96	0.84	0.88	0.77
NPV	0.93	0.76	0.82	0.87	0.80	0.82
Accuracy	0.85	0.83	0.88	0.83	0.84	0.83
Odds-ratio (95% CI)	36.60 (12.97-103.63)	33.59 (11.46-98.51)	115.73 (24.93-537.23)	23.59 (9.14-60.90)	28.39 (11.05-72.97)	31.56 (19.57-50.91)
<i>P</i> -Value*	0.0040 - 0.0050	0.0030 - 0.0040	< 0.001	0.0010 - 0.0020	< 0.001	< 0.001
<i>P</i> -Value#	0.0010 - 0.0020	0.0020 - 0.0030	< 0.0010	0.1020 - 0.1090	0.0050 - 0.0060	< 0.0010

Table 19. MDR forced analysis for the interaction between rs1292034 *RPS6KB1*, rs12628 *HRAS*, rs6456121 *RPS6KA2* and rs456998 *FCHSD1* with LID with severity as main variable. Random Seed=10; Cross-Validation Count=10; Number of Permutations=1,000. *Normal *P*-Value and #*P*-value of Explicit test of interaction obtained with 1,000 permutations.

In summary, we found associations of individual SNPs or combinations of SNPs in the mTOR pathway with both LID onset and LID severity, suggesting a role of this genetic pathway in the development of LID. These results may help to identify subjects who are more susceptible to develop earlier LID and those who are more susceptible to develop severe LID, with the ultimate goal to redesign the pharmacological therapeutic.

DISCUSSION

Research in neurodegenerative diseases is a major issue since there is currently no treatment available to prevent or delay their progression. Neuronal dysfunction and death are consequence of multiple pathogenic processes which alter signaling cascades. The identification of such molecular pathways is crucial to understand the cellular processes that triggers the symptomatology of diseases as well as for designing proper pharmacological treatments. One of the common affected pathways in neurodegeneration is the mTOR pathway. It regulates multiple cellular processes to preserve cellular viability and function^{249,250,253}. Consequently, to maintain a proper function mTOR activity needs to be fine-tuned. RTP801 is an mTOR negative regulator whose action over this pathway plays a significant role in neurodegeneration^{263,264,306,342,349,350,359,456}. RTP801 protein is induced in an attempt to cope cellular stress^{266,335,337-339,342}. However a sustained RTP801 increase leads to neuronal death by sequentially inactivating first mTOR and then Akt pro-survival kinase^{263,267,348}. RTP801 pathological increase has been involved in neurodegenerative diseases such as PD.

Specifically, our results have identified RTP801 as a mediator of mhtt-toxicity. Moreover, we show that RTP801 toxicity can be propagated to other neurons through exosomes contributing to the spreading of pathological features. Finally, we demonstrate that genetic variations in mTOR protein components modulate the susceptibility to PD and the response to L-DOPA treatment. Taken together, our findings indicate that mTOR deregulation plays an important role in the pathogenesis associated to PD and HD and its regulation is crucial to maintain a proper neuronal function and viability.

1. RTP801 IS A DOWNSTREAM EFFECTOR OF MUTANT HTT-INDUCED CELL DEATH

Here, we demonstrate that overexpression of pathogenic N-terminal htt increases RTP801 levels by both lengthening the protein half-life and up-regulating its gene expression. Blockade of RTP801 expression also prevents mhtt-induced cell death in HD cellular models. However, striatal levels of RTP801 at the Hdh^{Q7/Q111} and R6/1 mice models are not altered. Importantly, RTP801 is elevated in HD-iPSC and putamen, caudate nucleus and cerebellum of human HD postmortem brains.

First, we show that mhtt increases both RTP801 mRNA and protein, in cultured cells. RTP801 induction occurs in response to several stressful cellular conditions^{266,335-338,340,341}. Specifically in the nervous system, RTP801 expression is upregulated by oxidative stress induced by PD toxins^{263,264}, ischemia^{266,454,455}, chronic unpredictable stress⁴⁵³ and β -amyloid peptide^{342,456}. We observe similar RTP801 increase at different

DISCUSSION

cell types such as NGF-differentiated PC12 cells and rat primary cortical neurons overexpressing exon-1 mhtt with 72 or 103 CAG repeats in comparison to eGFP empty vector or exon-1 with 25 CAG repeats. Furthermore, our results indicate that changes in RTP801 protein and mRNA levels seem independent of the number of CAG repeats, as similar results were obtained by ectopically expressing exon-1 with 72 or 103 CAG repeats.

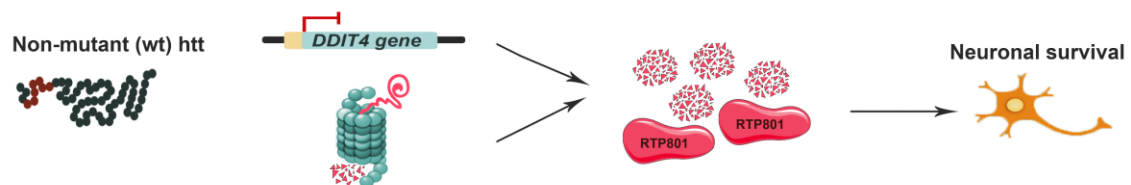
Regarding *DDIT4* gene upregulation, many transcription factors are described to induce its expression depending on the stimulus. For instance, hypoxia upregulates it through HIF-1 and Sp1 transcription factors^{266,336}, p53 in response to DNA damage³³⁵ and ATF4 under oxidative and ER stress^{337,338}. Indeed, another group pointed out that p53 may act in cooperation of Elk-1 transcription factor to upregulate RTP801 expression³⁴³. HD courses along with multiple and codominant cellular stress such as oxidative stress and excitotoxicity^{531,532}, DNA damage response⁵³³ or ER stress^{534,535}. Interestingly, p53 and Sp1 levels are elevated in HD cellular models^{442,463,536-538} and, importantly, p53 has been proposed to mediate neuronal dysfunction and behavioral abnormalities in the disease⁸⁶. Moreover, increased Elk1 levels are reported to occur in HD cellular and animal models and the lack of interaction with mhtt aggregates suggested higher transcriptional activity⁵³⁹, which could also explain the induction of RTP801 gene expression that we observed.

In addition, our results show that mhtt increases RTP801 protein levels by impairing its proteasomal degradation. In agreement with previous evidences, RTP801 displays a very short half-life between 2 and 7 minutes^{306,357,358} that is lengthened up to 12 and 18 minutes in the presence of mhtt with 72 or 103 CAG repeats, respectively. Proteins which exhibit extremely short half-life are considered more prone to be degraded by the proteasome^{74,190}. This is the case of RTP801 protein which is mainly degraded by the proteasome^{349,359}, yet a small pool of it is degraded through the lysosomal system³⁴⁹. Only three E3 ligases have been reported to ubiquitinate and mediate RTP801 protein degradation. Parkin and CUL4A-DDB1-ROC1- β -TRCP regulate its degradation through the proteasome^{358,359} and NEDD4, through the lysosomes³⁴⁹. Interestingly, parkin has been shown to colocalize with mhtt aggregates in HD animal models and in HD-affected brain areas of patients⁵⁴⁰ suggesting that parkin is sequestered, impairing its degradative function. Importantly, dysfunction of proteasome and autophagy-lysosome systems have been described in HD^{67-72,74}. Hence, both pathways may be contributing to increase RTP801 protein in HD.

According to previous data, our findings indicate that ectopic expression of exon-1 mhtt results in htt aggregate formation and induces cell death at both NGF-differentiated PC12 cells and in rat cortical neurons^{541–544}. One unexpected observation was that mhtt also induces the RTP801 aggregation in both cellular models. Remarkably, RTP801 aggregates do not always colocalize with mhtt inclusions. Sequestration of RTP801 into mhtt aggregates could also interfere with RTP801 degradation thereby contributing to RTP801 increase. To verify this issue, it may be interesting to assess whether RTP801 aggregation and sequestration into mhtt inclusions affect its function towards the mTOR pathway.

Besides, we identified RTP801 as a new player in mediating mhtt toxicity. Several mechanisms have been proposed to mediate mhtt toxicity including protein misfolding and aggregation, excitotoxicity, mitochondria dysfunction, transcriptional dysregulation or lack of trophic support^{57,58}. RTP801 emerges as a downstream effector of mhtt toxicity since silencing its expression prevents mhtt-induced cell death in NGF-differentiated PC12 cells (Figure 64). Considering that RTP801 functions as a repressor of the mTOR/Akt pathway, a logic rationale would be that RTP801 upregulation inactivates pro-survival Akt signaling leading to neuronal death. Similarly, knockdown of RTP801 confers neuroprotection in cellular models of AD³⁴² or PD^{263,545} and its inhibition results protective in front of ischemic injury⁴⁵⁴ and depressive behavior⁴⁵³. Overall, RTP801 arise as an important mediator of cellular damage which is induced in attempt to maintain cellular viability, but its sustained upregulation results detrimental for neurons.

Control



Huntington's disease

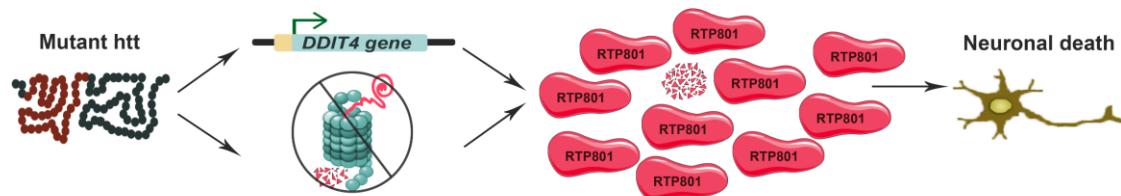


Figure 64. RTP801 modulates mhtt-induced cell death. In control conditions WT htt does not alter RTP801 expression or RTP801 proteostasis and thus maintaining RTP801 protein at basal levels triggering neuronal survival. In contrast, the presence of mhtt induces RTP801 gene upregulation and impairs its protein degradation elevating RTP801 protein levels. RTP801 increase eventually leads to neuronal death. Abbreviations: htt, huntingtin; wt, WT.

DISCUSSION

We extended our results to telencephalic progenitors differentiated from HD-iPSCs as another cellular model. HD-iPSCs display many of the biological properties found in the human HD brain, although the lack of the brain architecture and the lack of interaction with other non-neuronal cells limits the model⁵⁴⁶. Interestingly, increased levels of RTP801 are detected in the mhtt cell line respect to the control line. This fact supports the hypothesis that mhtt elevates RTP801 levels. However, since progenitors are still proliferative RTP801 does not induce cell death as it occurs in non-dividing and differentiated mature neurons³⁵⁶.

Furthermore, we studied brain regions affected in HD. RTP801 protein levels are increased in the caudate nucleus, putamen and cerebellum of HD patients. Consistent with a role of RTP801 in mhtt-induced cell death, putamen and caudate nucleus exhibit massive neuronal death in HD patients^{30,31}. The cerebellum also displays considerable atrophy as well as loss of Purkinje neurons along with the four deep cerebellar nuclei (fastigial, globose, emboliform and dentate nuclei)³⁴. Nevertheless, RTP801 levels are not affected in the cortex of HD patients which also undergoes severe neurodegeneration³². This may suggest that GABAergic neurons are more prone to increase RTP801 levels in the presence of mhtt or that cerebral cortex displays compensatory mechanisms to overcome RTP801 toxicity.

The levels of RTP801 were also investigated in two HD mouse models, the R6/1 and the Hdh^{Q7/Q111} mice. At any of the ages analyzed the striatal levels of RTP801 are affected in comparison to the control mice. These results reinforce the role of RTP801 as a mediator of mhtt-induced cell death since these animals show almost no neuronal death in the striatum^{103,457–460}. Supporting this observation, has been reported that R6/1 mice display less neuronal damage following intrastriatal injection of 6-OHDA⁵⁴⁷, a PD toxin that induces RTP801 increase and neuronal death^{263,361}. It is not known whether these mice could have mechanisms to counteract oxidative stress involving the blockade of stress-induced RTP801. To highlight the role of RTP801 also in animal models would be valuable to analyze RTP801 protein levels in an HD model undergoing neuronal death. Several HD murine models show neuronal death including those that mhtt viral vectors are stereotaxically transduced into the striatum^{548–550} or the chemical model which consists in intrastrially infused quinolinic acid⁵⁵¹. Interestingly, quinolinic acid induces excitotoxic lesions specifically in MSN and has been reported to upregulate RTP801 in cellular models⁵⁵².

Altogether, our results show that mhtt increases RTP801 by inducing its gene expression and impairing its degradation in HD cellular models. Downregulation of RTP801

expression prevents mhtt-induced cell death pointing out that RTP801 mediates mhtt toxicity in cellular models. Moreover, vulnerable brain regions that degenerate in HD pathogenesis display increased RTP801 levels. Hence, RTP801 is identified as a novel downstream effector of mhtt which mediates its toxicity.

2. SYNAPTIC RTP801 IS INCREASED IN HD MODELS

mTOR pathway is critical for neuronal plasticity²⁸². Beyond neuronal death, HD also undergoes aberrant synaptic plasticity^{17,467–471}. Thus, we investigated whether mhtt-induced RTP801 modulates synaptic plasticity in HD. Our results show that synaptic RTP801 is elevated in cortical neurons overexpressing exon-1 of mhtt. Moreover, RTP801 is highly enriched in the striatal synaptic compartment of Hdh^{Q7/Q111} and R6/1 mice when compared to control animals. Importantly, putamen, but not cortex, of HD patients also display increased levels of synaptic RTP801 respect to unaffected individuals. Importantly, the knockdown of RTP801 expression in the striatum of R6/1 mice rescues the performance in the accelerating rotarod indicating a preservation of motor learning plasticity.

Here, we demonstrate that mhtt induces RTP801 at a somatic but also at a synaptic level. We corroborate that the overexpression of exon-1 mhtt with 72 or 103 CAG repeats increases RTP801 levels at the neuronal soma, similarly to previous experiments. Consistent with this, RTP801 is also elevated at dendritic spines of mhtt-overexpressing neurons. These results indicate, first, that RTP801 is present in dendritic spines of cortical primary neurons and, second, that synaptic RTP801 is also modulated by mhtt. Interestingly, RTP801 increase course along with a reduction of dendritic spines in those neurons expressing ectopic mhtt. Loss of dendritic spines in neurons overexpressing mhtt have been exhaustive reported in the literature^{553,554}. Still whether increased RTP801 may contribute to dendritic spine loss remains unexplored.

Furthermore, RTP801 protein is enriched in synaptosomes derived from human brain and mice brain striatum. We proved that levels of synaptic RTP801 are increased in the putamen of HD patients in comparison to unaffected individuals. Corroborating our previous results, homogenate levels of RTP801 are already increased in HD putamen and, strikingly, this observation is extended to the synaptosomal fraction. Interestingly, the postsynaptic excitatory marker PSD-95 shows reduced levels in HD. In fact, structural and morphological synaptic alterations in striatal spiny neurons^{555,556} and prefrontal cortical pyramidal neurons⁵⁵⁷ from HD post-mortem brain have been reported. In accordance with our findings, PSD-95 is described to be decreased in the striatum,

DISCUSSION

both putamen and caudate nucleus, of HD patients⁵⁵⁸. Therefore, synaptic RTP801, namely levels of RTP801 respect to synaptic markers, are even more increased since reduction of PSD-95 levels enhances RTP801 rise (Figure 65).

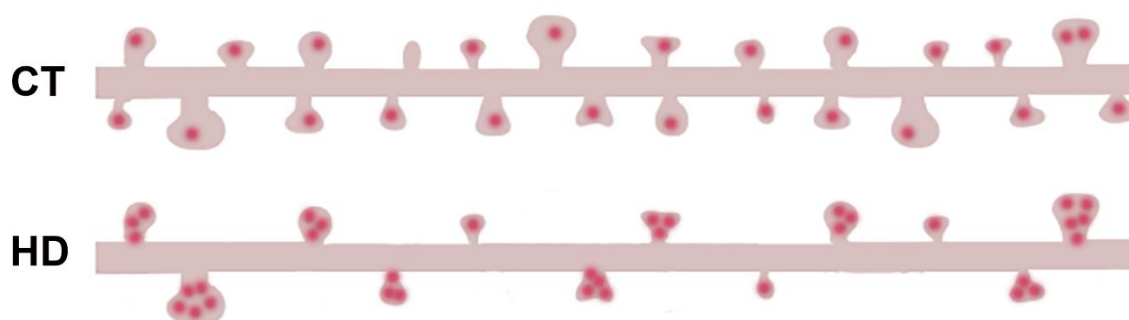


Figure 65. Proposed model of synaptic RTP801 increase in the putamen of HD patients. Our results show that RTP801 is increased in the synaptosomal fraction derived from the putamen of HD patients. Moreover, evidence indicate morphological alterations and loss of dendritic spines in this area^{555,556,558}. Hence, we hypothesize that remaining dendritic spines in the putamen of HD patients exhibit increased RTP801 respect to CT putamen. RTP801 protein is represented as magenta dots. Abbreviations: CT, control cases; HD, Huntington's disease patients.

Supporting previous experiments, synaptosomal preparations of frontal cortex of HD patients revealed no differences of RTP801 levels at homogenate or synaptosomal fractions. Neither the postsynaptic marker PSD-95 nor the presynaptic marker SV2A exhibit altered levels. Even though morphological alterations in prefrontal cortical pyramidal neurons have been described⁵⁵⁷, RTP801 elevation seems to be striatal-specific and does not contribute to cortical degeneration or cortical altered plasticity.

Evidences have suggested that synaptic alterations precedes motor symptoms in HD pathogenesis^{464–466}. At early and mild disease stages R6/1 and Hdh^{Q7/Q11} HD murine models show motor learning deficits without motor coordination alterations while at more advanced stages motor cognitive deficits occur along with motor impairment^{461,462}. In fact, motor learning deficits on the accelerating rotarod are evident at 2-months age at both models whereas motor impairment on the fixed-speed rotarod appears at 3-months in the R6/1 and at 8-months in the Hdh^{Q7/Q11} model⁴⁶¹. This highlights that dysfunction of the corticostriatal pathway, rather than striatal or cortical degeneration, drive cognitive impairment^{465,559}.

Findings from our previous work have shown that total striatal levels of RTP801 levels are not altered in R6/1 and Hdh^{Q7/Q11} HD murine models, which is in accordance with the lack of neuronal death in these animals^{103,457–460}. Despite RTP801 is not altered at protein levels, we could not discard that mhtt leads to an aberrant RTP801 distribution or compartmentalization within neurons which may contribute to synaptic impairment. For that purpose, we isolated synaptosomes from the striatum of R6/1 and Hdh^{Q7/Q11}

mice at 3-months or 10-months of age and analyzed RTP801 levels at the homogenate and the synaptosomal fraction.

In line with our previous results, homogenate levels of RTP801 are not altered in the striatum of R6/1 and Hdh^{Q7/Q111} mice in comparison to their control animals at an age that already display motor learning and motor performance disturbances. Remarkably, synaptosomal RTP801 levels shows differences between animals neither. However, PSD-95 synaptic marker is decreased in the synaptosomal fraction of both murine models. Moreover, structural alterations at the morphology and/or spine number in the R6/1⁵⁶⁰ and the Hdh^{Q7/Q111}⁴⁶¹ striatum, being mushroom-consolidated spines the most affected type, have been reported. Other HD murine models such as N-terminal fragment R6/2 models^{561–563} and transgenic htt full-length YAC128 mice¹⁰⁷ also exhibit decreased spine density. As well, PSD-95 levels are described to be reduced in the two murine models that were analyzed^{461,564–566} corroborating our results. Hence, due to reduced synaptic spine density and PSD-95 levels in HD murine models, we propose a model in which remaining dendritic spines of HD mice display higher levels of RTP801 (Figure 66). To further explore these issues quantification of RTP801 density and intensity puncta in striatal sections of both HD murine models could be studied.

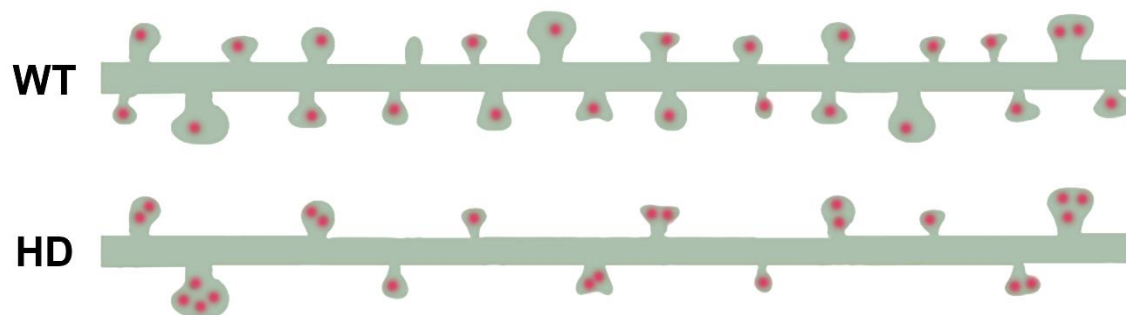


Figure 66. Proposed model of synaptic RTP801 increase in the striatum of HD murine models. Our results show that synaptosomal levels of RTP801 are not altered in the striatum of R6/1 and Hdh^{Q7/Q111} mice *versus* the corresponding WT animals. However, striatal levels of PSD-95 are reduced and evidences indicate alterations in spine density and morphology^{461,560}. Thus, we suggest that HD mice models display fewer number of spines and RTP801 levels in those are increased in comparison to the levels in WT dendritic spines. RTP801 protein is represented as magenta dots. Abbreviations: HD, Huntington's disease mice model, WT, wild-type mice.

3. SYNAPTIC mTOR SIGNALING IS ALTERED IN HD MODELS

mTOR signaling alterations are a common hallmark in several neurodegenerative diseases (reviewed in ³³¹). In HD, alterations in the activity of both complexes mTORC1^{72,290,452} and mTORC2²⁸⁷ have been described, although conflicting results have been shown regarding the activity of mTORC1 complex. Here, we confirm that both mTOR complexes

DISCUSSION

display aberrant activity and, moreover, alterations found at total cell level are extended to the synaptic compartment.

Results from the synaptosomal fractionation in the human HD putamen and in the striatum of R6/1 animals validates previous findings regarding the hyperphosphorylation of Akt Ser473 residue in HD models^{287,295,296}, indicating a hyperactivation of mTORC2 complex²⁸⁷. Furthermore, we extend this observation from total neuronal level to synaptic level since P-Akt Ser473 increase is exhibited similarly at the synaptosomal fraction of both models. Even though no differences are detected at total levels, the Hdh^{Q7/Q111} mice also displays higher levels of P-Akt Ser473 at the synaptic fraction relative to synaptic markers. Overactivation of Akt has been proposed to be a pro-survival response to counteract mhtt toxicity in the disease. Thus, hyperphosphorylation of Akt Ser473 could explain the absence of neurodegeneration in HD murine models whereas in the human striatum would not be sufficient or would take place too late to compensate mhtt toxicity. It is important to highlight that Akt is enriched in the synaptosomal fraction of human brain tissue whereas in mice striatal tissue, it is present but not enriched, indicating a different compartmentalization depending on the species which could also lead to a differential regulation.

Regarding P-S6 Ser235/236, it is increased at the homogenate fractions of human HD putamen and at the synaptic fraction relative to PSD-95 protein, since in mice brain is mostly enriched in the postsynaptic compartment^{567,568}. In contrast, P-S6 Ser235/236 is not altered at homogenates or synaptosomes derived from R6/1 and Hdh^{Q7/Q111} striatum and it is only increased at the synaptic fraction relative to PSD-95 in the R6/1 mice. Since S6 ribosomal protein regulates protein synthesis, an overactivation and an excessive protein translation may lead to altered synaptic plasticity^{316,317,569}. Indeed, cellular models of HD have shown P-S6 elevated levels⁴⁵² whereas other authors described decreased levels of the protein in cellular models⁷², in striatal tissue from HD patients and in N-terminal fragment N71-82Q mice model⁵⁷⁰. Therefore, our results suggest that may be intrinsic neuronal properties that modulate the effect of mhtt depending on the cellular type or depending on the HD murine model (exon-1 or full-length htt expressing mice, with different number of CAG repeats).

So far, evidence suggest that the classical model of RTP801 function in the nervous system differs in the context of HD pathogenesis. Based in PD studies, RTP801 upregulation upon cell stress represses mTOR and finally inhibits Akt pro-survival signals triggering neuronal death. In PD cellular models and nigral neurons of PD brains, RTP801 increases along with decrease phosphorylation of Akt and S6^{263,306,349,359}. Here,

on the contrary, we show that mhtt increases RTP801 at total and synaptic levels despite the hyperphosphorylation of Akt at Ser473 residue. Interestingly, P-S6 Ser235/236 displays the same trend (Figure 67). Thus, we wonder whether RTP801 could have another function that may explain its toxicity in HD since the presence of mhtt seems to inactivate, or at least mask, its repressor function towards mTOR pathway. In addition, increased RTP801 levels observed in HD models may be consequence of mTOR pathway hyperactivity since RTP801 protein synthesis is mTORC1-dependent³⁰⁶. Future experiments to uncover a novel mechanism for RTP801 would be necessary to completely understand these observations.

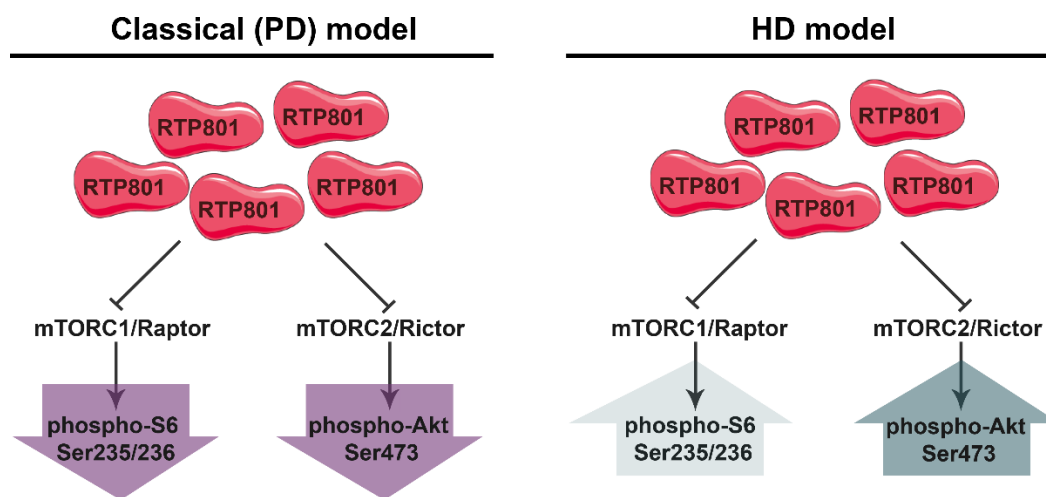


Figure 67. Comparison of RTP801 mechanistic models over mTOR in PD and HD. Several studies in the context of PD indicate that RTP801 increase leads to the inhibition of mTOR triggering the repression of its downstream substrates S6 ribosomal protein and Akt reducing their phosphorylated levels (violet arrows). However, in striatal tissue of HD putamen and HD mice we observe increased levels of RTP801 at the synapse but also consistent elevated levels of P-Akt Ser473 (dark aquamarine arrow) and phospho-S6 Ser235/236 in some models (light aquamarine arrow) which would not fit with the known function of RTP801 as mTOR repressor.

4. INCREASE OF STRIATAL SYNAPTIC RTP801 CONTRIBUTES TO DYSFUNCTIONAL MOTOR LEARNING PLASTICITY IN HD

Our results suggest that increase of synaptic RTP801 in the striatum of HD mice contributes to abnormal motor learning plasticity. To evaluate the corticostriatal function, responsible for motor learning⁵⁷¹, mice were subjected to the accelerating rotarod test. Interestingly, silencing RTP801 in the striatum of R6/1 preserves their performance in the accelerating rotarod, comparable to WT mice, indicating that RTP801 knockdown rescues the ability to learn new motor skills in the HD mice. The fact that silencing RTP801 in WT animals does not affect their performance at this procedure could suggest remaining basal levels of the protein are sufficient to maintain proper motor learning plasticity and, therefore, corticostriatal functionality. Besides, RTP801 downregulation

DISCUSSION

has also been shown to restore motor learning skills in a PD mice model subjected to chronic stress⁵⁴⁵.

Supporting the synaptic role of RTP801, RTP801 silencing also alters the levels of mTOR pathway associated protein components and enhances the expression of postsynaptic proteins.

Striatal RTP801 downregulation increases AMPA subunit receptor GluA1 and TrkB levels at the R6/1 homogenate and the same trend at the synaptosomal fraction. However, p75^{NTR} levels are not altered by RTP801 knockdown. Both TrkB and p75^{NTR} are BDNF receptors, although each receptor activates different signaling pathways. BDNF mediates neuronal survival by the activation of TrkB receptor^{111,112} whereas p75^{NTR} can activate apoptotic signals leading to neuronal death^{109,113–115,122}. In fact, imbalance of TrkB and p75^{NTR} has been proposed to mediate impaired plasticity in HD^{122,572}. Hence, increased TrkB and GluA1 levels could promote neuroprotective signaling activation and plasticity signals^{111,112,122,572}. Unfortunately, we have no data revealing BDNF levels in the striatum to evaluate whether the enhancement of postsynaptic receptors is due to increased BDNF trophic support or to the alteration of postsynaptic receptor trafficking.

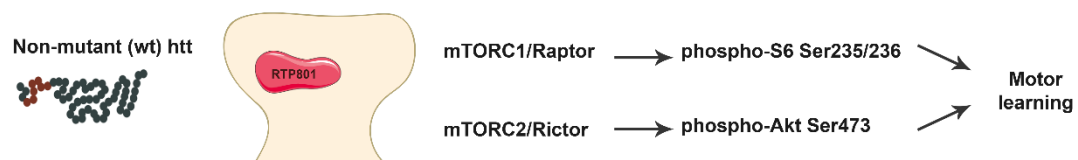
Furthermore, we analyzed the levels of mTOR pathway related proteins since the only known function of RTP801 is as a mTOR signaling repressor. Our data indicate that RTP801 downregulation in the R6/1 mice prevents hyperphosphorylation of Akt at Ser473 residue, both at homogenates and synaptosome. Some evidences point out that synaptic plasticity alterations occur along with hyperphosphorylation of Akt. For instance, impaired synaptic plasticity and memory in the hippocampus are associated to alterations in the phosphorylation status of mTOR signaling components, including Akt⁵⁷³. Besides, continuous activation of Akt could be detrimental for cell survival since elevated P-Akt Ser473 levels induces progressive Purkinje neuronal loss⁵⁷⁴. Thus, our data suggest that even though Akt Ser473 hyperphosphorylation prevents neuronal death it impairs motor learning, and this is modulated by RTP801 in the R6/1 mice.

Moreover, we show that Rictor is responsible for the restoration of Akt levels upon RTP801 downregulation in the striatum of R6/1 mice. The complex composed by mTOR and Rictor mediates Akt phosphorylation at Ser473 residue⁴⁹² while its dephosphorylation and, thus, inactivation depends on PHLPP^{297,298}. Hence, regulation of P-Akt Ser473 depends on a proper activity of the mTOR kinase complexed with Rictor and the phosphatase PHLPP. In fact, increased Rictor and decreased PHLPP levels are both responsible for Akt overactivation in HD^{287,296}. Significantly, RTP801 knockdown

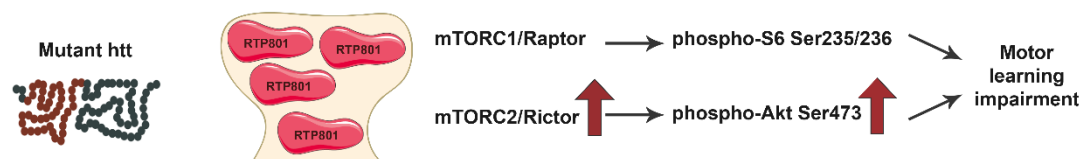
specifically reduces synaptosomal Rictor levels without affecting PHLPP, indicating that RTP801 modulates Akt levels through Rictor. Still the regulation of RTP801 towards Rictor or whether any feedback mechanisms exists over Akt phosphorylation remain uncertain.

Altogether, our results indicate that downregulation of striatal RTP801 rescues motor learning skills in R6/1 mice by restoring P-Akt Ser473 levels though downregulating Rictor levels and increasing postsynaptic GluA1 and TrkB receptors (Figure 68).

WT mice



R6/1 mice



R6/1 mice + RTP801 knockdown

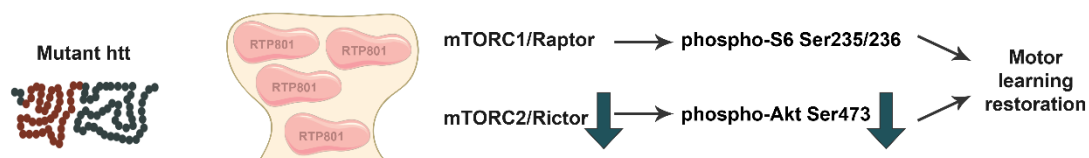


Figure 68. RTP801 knockdown prevents corticostriatal learning deficits. In comparison to WT mice, R6/1 mice display increased RTP801 at the striatal synapse along with increased Rictor²⁸⁷ and P-Akt Ser473^{295,296} and motor learning deficits. RTP801 silencing preserves corticostriatal motor learning function by decreasing the levels of Rictor and P-Akt Ser473 and enhancing postsynaptic signaling by increasing GluA1 and TrkB receptors.

5. CELLULAR STRESS INDUCES TRANSNEURONALLY PROPAGATION OF RTP801 TOXICITY BY EXOSOMES

From this part of our studies, we have elucidated a novel function of RTP801 as an exosomal protein. We demonstrate that both ectopic and endogenous RTP801 can be found in exosomes derived from HEK293 cells. In cortical neurons, exosomal RTP801 elevation is sensitive to PD mimetic 6-OHDA but not to potassium depolarization. Consequently, 6-OHDA exposure induces the loading of RTP801 into exosomes released from cortical neurons. Intriguingly, mhtt does not elevate RTP801 in exosomes obtained from a cellular model.

DISCUSSION

The role of exosomes as vehicles for intercellular transfer of bioactive molecules has been widely investigated in the nervous system. Neuronal-derived exosomes have a dual role in a pathogenic process. On one hand, exosomes exert as conveyors of toxic proteins, therefore, once released to the extracellular space, they can be phagocytosed by microglia and their content cleared out^{379,387,425–427}. However, this initially beneficial function can turn out into a pathogenic process. Neuronal exosomes loaded with toxic molecules are released upon depolarization^{374,375} and can also be internalized by other “healthy” neurons^{219,220,389,424}. Exosomes then can alter several signaling pathways in the recipient neurons, propagating their toxicity^{391,404}. Thus, exosomes have been suggested to play a role in the propagation of aggregate-prone proteins which result lethal for neurons^{391,422}. Several pathogenic proteins involved in neurodegenerative diseases have been described to be released through this pathway. For instance, exosomes can contain β -amyloid peptide^{387,389,427,575}, Tau^{424,507,576}, SOD1⁵⁰⁶, mHtt^{82,83} and several PD related proteins such as α -synuclein^{218–220,429,430}, DJ-1⁴³² and LRRK2^{433,434,577}.

Our initial data revealed that not only ectopic but also endogenous RTP801 were present in exosomes. Indeed, ectopic RTP801 increases exosomal release in these cells. The mechanism by which RTP801 could potentiate exosomal release is not yet known. In proliferating cells such as HEK293, RTP801 upregulation downregulates mTOR inducing autophagy without being toxic^{341,570}. Since autophagy and exosome biogenesis share molecular machinery and organelles^{369,402}, they are two cellular events highly intertwined^{578,579} and an increase of RTP801 could be affecting both processes. Another explanation could be that RTP801 induces an elevation of cytoplasmic calcium levels from mitochondrial reservoirs, as it is associated to mitochondria membrane and regulate mitochondria metabolism and ROS production^{266,345,580}. Since exosomal release is a calcium-dependent mechanism^{374,375,581}, overexpression of RTP801 could alter ROS mitochondrial production triggering calcium-dependent exosomal release.

Previous work have showed that RTP801 is involved in PD pathogenesis and its upregulation triggers neuronal death by inactivating mTOR and suppressing Akt pro-survival signals^{263,264,306}. Here, we show that RTP801 is found in exosomes derived from primary neurons treated with the neurotoxin 6-OHDA, as a PD cellular model. The presence of RTP801 in neuronal exosomes would be consistent with the suggested role of exosomes as an unconventional pathway for removing toxic proteins from the cell^{391,422}.

Supporting this role, we demonstrate that RTP801 colocalizes with CD63 protein. CD63 protein is involved in the formation of ILVs in MVBs and sorting during exosome

biogenesis⁵¹³. Therefore, CD63 colocalization with RTP801 suggests that RTP801 is part of the exosome production path. Strikingly, the overexpression of CD63 decreases the levels of RTP801 protein. Ectopic expression of CD63 has been described to enhance exosomal release^{582,583} but also to accelerate the lysosomal degradation of specific proteins⁵⁸⁴. Since RTP801 is also degraded by the lysosomal pathway through the ubiquitination of NEDD4 E3 ligase³⁴⁹, RTP801 reduction could be the consequence of a higher rate of lysosomal degradation and/or increase RTP801-exosomal release.

Indeed, our data also indicate that RTP801 loading into exosomes is stress-specific, since we could only detect it after 6-OHDA exposure but not in physiological conditions, under nontoxic depolarization or even in mhtt-overexpressing cells. As previously reported, exosomal release is an active mechanism calcium dependent and, in neuronal models, synaptic activity triggers their secretion^{374,375,416,421,422}. Our results confirmed that neuronal depolarization by potassium stimulation enhances exosomal release, nonetheless neither the levels of intracellular RTP801 nor the presence of RTP801 in exosomes are altered, probably because depolarization is a physiological process and is not toxic³⁷⁵.

As previously mentioned, we only detected RTP801 presence in neuronal-derived exosomes under 6-OHDA exposure. Exosome molecular composition is highly influenced by environmental challenges and intracellular stress can modulate its sorting^{370,402,403}. Exposure of cortical neurons to 6-OHDA induces oxidative stress by its autoxidation and ROS generation which causes a high cytoplasmic influx of calcium and, in the end, apoptosis^{514,516}. In fact, calcium influx triggered by oxidative stress enhances exosomal secretion in several cell types^{375,581,585,586}. Hence, our results showing increased exosomal release after 6-OHDA exposure provide additional evidence supporting the potentiation of exosomal secretion by oxidative stress. Moreover, under pathological conditions, exosomal release is enhanced to alleviate the proteotoxic stress and thus supporting autophagic mechanisms which may be hampered or insufficient to degrade harmful proteins^{578,579}.

In HD, transneuronal spreading of mhtt has been described to occur in cultured neurons and *in vivo*^{81,82} by a process which seems to be synaptic activity-dependent⁸¹. In our experiments, we used the non-differentiated proliferating STHdh cell line as an *in vitro* HD model and, confirming our previous results, mhtt-cell line displays increased levels of RTP801. Intriguingly, we did not detect an enrichment of RTP801 at the exosomal fraction, neither at the WT nor the mutant cell line, in contradiction with recent studies^{82,83}. It is possible that such discrepancies may be explained from use of different cell models

in each work. In fact, in these studies, authors over expressed mutant forms of htt in HEK293⁸³ or SH-SY5Y⁸² cells, in comparison to our strategy to use a cell line that expresses htt or mhtt endogenously. This fact may force the cells to remove the ectopic protein by different degradative pathways, including exosomes. This could lead to exosomal non-specific passive loading of the ectopic protein⁵⁸⁷. To further verify this issue, it would be interesting to test the presence of exosomal RTP801 and mhtt in cells that express htt and mhtt at a physiological level such as iPSC or primary neurons derived from HD mouse models.

6. RTP801 MODULATES EXOSOMAL TROPHIC SUPPORT THROUGH THE mTOR PATHWAY

Our results suggest that neuronal exosomes play a protective role by promoting the phosphorylation of S6 ribosomal protein at residues Ser235/236 and Akt at residue Ser473, as downstream effectors of the mTORC1 and mTORC2 kinase activities, respectively.

As aforementioned, exosomes play a crucial role in pathogenic conditions spreading pathological alterations through the brain. Nevertheless, exosomes not only act as vehicle to transfer toxic proteins during pathogenesis but also can be neuroprotective counteracting stressful situations^{426,588–590}. In basal conditions, they regulate synaptic strength, neuronal plasticity and axonal regeneration^{403,422}. Moreover, the enhancement of the mTOR pathway by exosomes in different recipient cell types has been previously pointed out^{591–593}. Specifically in the central nervous system, oligodendroglia-derived exosomes exhibit neuroprotective functions upon neurons by inducing the phosphorylation of Akt and ERK under oxidative stress or starvation³⁸². Therefore, our results indicate that neuronal exosomes provide trophic support to recipient neurons enhancing the mTOR pathway, which may help to maintain a proper neuronal network functionality.

Interestingly, we observed that 6-OHDA-induced exosomes abrogate trophic signals in recipient neurons, but when RTP801 expression was suppressed, exosomes could partially preserve the phosphorylation of both Akt and S6. Hence, these data suggest that increase RTP801 negatively modulate pro-survival signals transneuronally. Even though 6-OHDA-derived exosomes do not induce neuronal death in cultures, the abolishment of survival and trophic signals may sensitize neurons to environmental insults. To clarify this question, neuronal cultures could be treated with exosomes derived from non-treated or 6-OHDA treated neurons and, then exposed to stressors. We

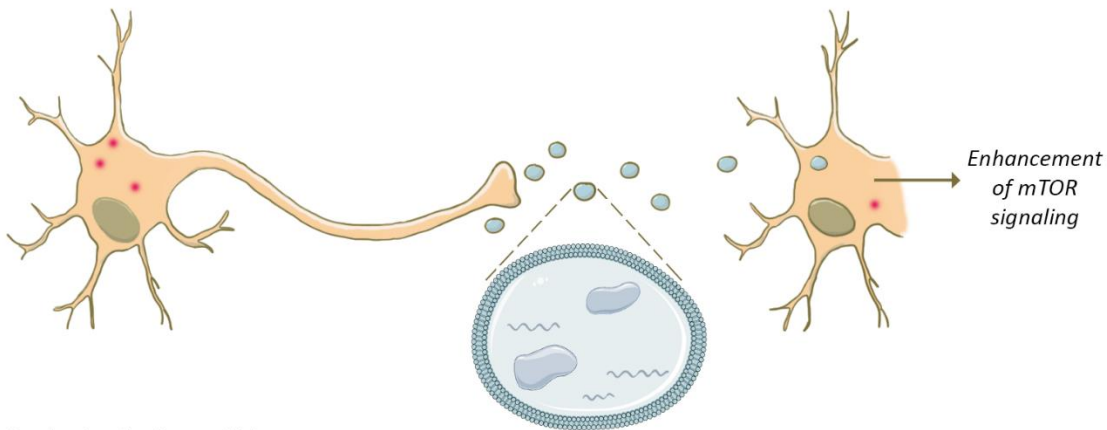
speculate that cultures pretreated with trophic exosomes would cope with posterior cellular stress.

On the other hand, in the HD cellular model we confirmed that RTP801 was able to transcellularly modulate Akt, independently of the presence of mhtt in derived exosomes, in neuronal cultures. Yet, the phosphorylation of S6 ribosomal protein was more sensitive to exosomes from mhtt-overexpressing cells in an RTP801-dependent manner. Although we corroborated that exosomes enhance the mTOR pathway in recipient neurons and that RTP801 modulates this function, these results seem to indicate that the cellular type and/or the specific cell stressor is crucial to determine the exosome composition and, in consequence, the effect in recipient cells. In fact, the profile of exosome content highly differs between cells^{366,403,413} and, importantly, both the amount and the kind of cellular stress also influences exosomal biogenesis and composition^{370,402,403}.

Nonetheless, exosomes can carry variable cargoes and thereby exosome trophic/toxic effect could be additionally achieved by alterations in molecules other than proteins. For instance, exosomes contain multiple species of RNAs which are selectively loaded depending the physiological or pathological status of the cells^{417,418,591} and they can also mediate different responses in recipient neurons. In addition, lipids are essential for the biogenesis of exosomes^{391,400,401} and are also involved in signal transduction^{380,409,594,595}. Importantly, RTP801 upregulates the sphingolipid ceramide, triggering cell death^{596,597}. Ceramide, which is induced under stress and apoptosis, is responsible for exosome budding and formation in a ESCRT-independent manner^{400,401} and the inhibition or downregulation of nSMase2, responsible for ceramide generation, decreases exosomal release^{413,598}. Hence, ceramide may represent a necessary link between RTP801 and exosome biogenesis and release.

Summarizing, our results indicate exosomes provide a source of trophic support and RTP801, via exosomes, modulate the mTOR pathway in recipient cells (Figure 69).

Physiological conditions



Pathological conditions

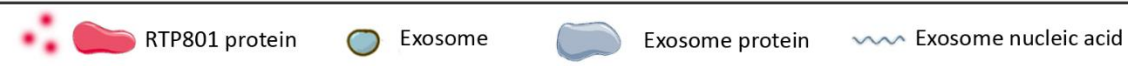
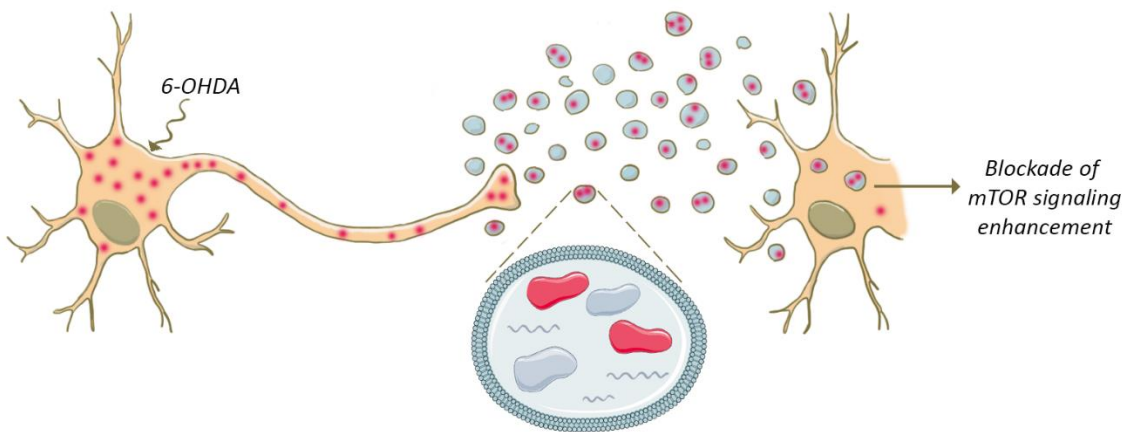


Figure 69. RTP801 modulates trophic signals transneuronally through exosomes. In physiological conditions, RTP801 is maintained at basal levels and it is not present at released exosomes from neurons. Once those are internalized by recipient neurons, exosomes upregulate the phosphorylation at Akt Ser473 and S6 ribosomal protein Ser2356/236 inducing an enhancement of the mTOR pathway. In pathological conditions, under a cellular stress such as 6-OHDA exposure, RTP801 levels increase and it is loaded into exosomes. Once exosomes are released, stress-induced exosomes are internalized by target neurons and counteract the trophic support by blocking the enhancement of mTOR signaling. In magenta, RTP801 protein units are represented, and, in blue, exosome vesicles.

7. SNCA AND mTOR PATHWAY GENETIC VARIATIONS INTERACT TO MODULATE RISK AND AAO OF PD

The genetic component of any pathology is crucial for its development of diseases. In the case of HD, it is caused by mutations in the single gene *IT15* that codifies for htt protein. Nevertheless, other common disorders are much more complex and do not have a single genetic cause. In these diseases, multiple gene variants along with environmental factors contribute to the pathogenic process. So far, we know that the deregulation of mTOR pathway is evident for both HD and PD^{249,250,331,518}. To go one step further, we wanted to uncover the genetic contribution of the mTOR pathway to PD.

Hence, we explored the association of SNPs in mTOR-associated genes with PD pathogenesis. Genetic analysis corroborated a significant individual association of *SNCA* SNP rs356219 and *MAPT* SNP rs1800547 with PD risk. Moreover, four-loci interaction including *SNCA* rs356219 along with the SNPs in the mTOR genes *STK11* rs8111699, *FCHSD1* rs456998 and *GSK3B* rs1732170 were found to contribute to PD risk. Importantly, the interaction of *SNCA* rs356219 with PD AAO was also confirmed. Besides, we detected a three-loci epistatic combination of *SNCA* rs356219 with SNPs *RPTOR* rs11868112 and *RPS6KA2* rs6456121 from the mTOR pathway which was associated with differential AAO in idiopathic PD and with a similar trend in *LRRK2*-associated PD. In summary, our findings indicate that genetic variability in the mTOR pathway contributes to differential disease susceptibility and age-at-onset in both idiopathic and in a monogenic form of PD through modulating the effect of *SNCA* rs356219.

Epistasis is referred to the combinatorial effect of more than one genetic variant, in this case SNPs, in which one SNP masks the phenotypic effects of another SNP. At biochemical level, epistatic interaction arise from different loci which encode for proteins that participate in a specific signaling pathway^{599,600}. In contrast, additive interaction occurs when genes that codify for proteins act through different pathways⁶⁰¹ but they have a very small effect in the phenotype. In fact, complex disorders such as PD, are poorly explained by additive models and is expected epistatic gene interactions to substantially contribute to the genetics of the disease⁵⁹⁹. Only recent, studies have started deciphering the complex effects of high order genetic interactions and, following this approach, several multilocus interactions have been identified to be associated with several disease risk^{602–607} including PD^{608–610} and with patients' differential response to drug treatments^{611–614}.

The association of SNPs rs356219 in *SNCA* and rs1800547 in *MAPT* genes with PD susceptibility have been previously reported in different populations^{156,158,164} and in wide association studies (GWAS)^{154,155}. In accordance with previous evidences, the GG homozygous for the SNP in *SNCA* (O.R. = 0.73; 95%C.I.= 0.64-0.84; *P*-value<0,0027) and AA for the SNP in *MAPT* (O.R. = 1.33, 95%C.I.=1.15-1,54, *P*-value=0.0027) emerged as risk factors for suffering PD. Furthermore, the *MAPT* H1/H2 haplotypes, which are in complete linkage disequilibrium with the rs1800547 A/G alleles respectively, have been associated with increased risk for tauopathies such as frontotemporal dementia, progressive supranuclear palsy or corticobasal degeneration^{615–617} and also to synucleinopathies such as PD and multiple system atrophy^{618–620}. Importantly, the

DISCUSSION

association of *SNCA* rs356219 and *MAPT* rs1800547 with PD risk validated our PD cohort for the study and established ground to perform further analysis.

The implication of both *SNCA* and *MAPT*, encoding for α -synuclein and tau proteins respectively, has been extensively described in PD at genetic but also at protein level. The SNP rs356219 is located in the 3' untranslated region (UTR) of *SNCA* and has been related to increased *SNCA* expression^{621,622}. In the same way, the H1 haplotype of *MAPT*, risk factor for PD and in linkage disequilibrium with rs1800547, has been associated with increased tau expression in human brain¹⁵⁵. Regarding α -synuclein, the first link of PD to α -synuclein was the discovery of genetic mutations in the *SNCA* gene leading to PD and, in fact, the first loci genetically associated with the disease was found in the *SNCA* gene and later other loci in the same gene were identified (*PARK2*)^{134,135,623}. At protein level, α -synuclein is the primary structural component of LBs^{183,184} which is the major histopathological hallmark in PD. Accordingly, have been demonstrated that α -synuclein species which are contained in PD-derived LBs or synthetic and preformed mouse α -synuclein fibrils are potentially pathogenic and have the capacity to initiate PD-like processes in murine models triggering the nigrostriatal axis degeneration due to dopaminergic neuronal death^{211,212,214,624}. Moreover, hyperphosphorylated tau protein colocalize with α -synuclein⁶²⁵ and is a component of LBs⁶²⁶. Increased tau phosphorylation has also been detected in the synapse-enriched fraction from PD brains along with phosphorylated α -synuclein⁶²⁷. In fact, α -synuclein has been shown to bind tau and promote its phosphorylation leading to impaired stabilization of microtubules and failure in axonal transport and eventually accumulation of both α -synuclein and Tau⁶²⁸. This hyperphosphorylation of Tau by α -synuclein is mediated by the kinase GSK3- β complex⁶²⁹. Interestingly, we found a four loci interaction including the aforementioned SNP rs356219 in *SNCA* along with *GSK3B* rs1732170 and *STK11* rs8111699, *FCHSD1* rs456998 (CVC=10/10, O.R.=2.59, 95%C.I.=2.14-3.13, *P*-value < 0,001) with PD risk, although any of the mTOR genetic markers was individually associated with the PD status.

As mentioned, GSK3- β complex mediates the phosphorylation of Tau by α -synuclein but its implication in PD goes far beyond. For instance, GSK3- β is a component of LBs and is described to be upregulated in *in vitro* and *in vivo* models of PD and in postmortem brain areas of idiopathic PD (reviewed in ⁶³⁰). *STK11* which encodes for LKB1 protein, has not been related to PD pathogenesis. Nevertheless, it participates in axon branching and myelination through mitochondria^{631,632}, promotes axon initiation⁶³³ and regulates dendrite formation^{634,635}. Finally, *FCHSD1* encodes for a protein that regulates actin polymerization⁶³⁶, F-actin assembly and synaptic growth⁶³⁷. Interestingly, rs456998 in

FCHSD1 gene is significant associated with the expression of *DDIT4*⁶³⁸, gene encoding for RTP801 protein which triggers neuronal death in PD^{263,264}.

Regarding PD AAO, we found a significant association of *SNCA* rs356219 with a 2.4 mean AAO difference of idiopathic PD with 55,6 years for carriers of the GG risk genotype and 58 years for AA carriers. Previously, the SNP rs356219 was shown to modulate AAO of idiopathic PD in the German population¹⁶⁶. Another report from Northern Spain showed that *SNCA* rs356219 is in linkage disequilibrium with the neighboring marker rs356165¹⁵⁸, which is associated with AAO of idiopathic PD in this population⁵²⁶. More recently, has been described that *SNCA* rs356219 also influences the AAO of L2PD¹⁶⁷. Overall, we used the finding of the association of *SNCA* rs356219 with PD AAO as starting point to further explore the potential interaction of mTOR SNPs on AAO. Indeed, we found a higher-order epistatic interaction involving *SNCA* rs356219, *RPTOR* rs11868112, and *RPS6KA2* rs6456121 (CVC=10/10; O.R.=2.89, 95%C.I.=2.90-4.00; *P*-value<0.0010) which was associated with differential AAO in idiopathic PD. *RPTOR* gene codifies for Raptor protein that is the main component of mTORC1 complex. This complex regulates important cellular functions such as protein synthesis and autophagy^{249,250,253} and, importantly, the induction of autophagy in PD models results beneficial since it preserves dopaminergic neuronal viability²⁰⁵⁻²⁰⁷.

The 3-loci epistatic interaction was also tested in L2PD cohort. Unfortunately, the association did not reach significance, mostly because the number of L2PD cases was not balanced with the number of idiopathic PD cases (N=748 idiopathic PD cases vs. N=127 L2PD cases). Nevertheless, the comparison of the genotype combinations that predict the PD status showed the same tendency suggesting that *SNCA* rs356219, *RPTOR* rs11868112, and *RPS6KA2* rs6456121 epistatic combination (CVC=10/10, O.R.=3.99, 95%C.I.=1.89-8.40, *P*-value=0.1180) also predicts PD AAO in L2PD. For instance, the combination AG/CC/CC of the aforementioned interaction was associated with 4 years earlier PD in idiopathic PD and to 3.4 years in monogenic L2PD.

Altogether, our results indicate that genetic variability in the mTOR pathway contributes to differential disease susceptibility and AAO in both idiopathic and monogenic form of L2PD through modulating the effect of *SNCA* rs356219.

8. ASSOCIATIONS OF SNPS IN THE mTOR PATHWAY INFLUENCE LID ONSET AND SEVERITY IN PD PATIENTS

The deregulation of the mTOR pathway is a biochemical hallmark in PD^{249,250,518}. Besides the implication of mTOR in the pathogenic process of the disease, the pathway is also involved in the development of LID^{332–334}. For this reason, we explored whether genetic variations in the mTOR pathway could contribute to the differential sensitivity to L-DOPA in PD patients. Regarding LID development, we found a significant genotypic association of SNP rs1043098 in the *EIF4EBP2* gene with LID onset and LID peak. Moreover, at an epistatic level we also identified *EIF4EBP2* rs1043098 in a 3-locus interaction along with *RICTOR* rs2043112 and *PRKCA* rs4790904 to be associated with LID onset. Concerning LID severity, polymorphisms rs12628 in *HRAS* and rs1801582 in *PRKN* genes were associated with the severity of LID manifestation. Further analysis demonstrated that LID severity was also associated with a higher order multilocus interaction involving *HRAS* rs12628 in combination with rs5456121 in *RPS6KA2*, rs1292034 in *RPS6KB1* and rs456998 in *FCHSD1*. Collectively, these results indicate that common genetic variability in the mTOR pathway modulates the development and the severity of LID in L-DOPA-treated PD patients.

As we have previously reported, high order epistatic interactions are not only associated to the development of diseases but also determine the response of patients to specific drug treatments^{611–614}, such as the extrapyramidal symptoms developed by antipsychotic drugs in schizophrenia patients⁶¹². In fact, authors described a four-loci interaction of mTOR related genes involving rs1130214 in *AKT1*, rs456998 in *FCHSD1*, rs7211818 in *RPTOR* and rs1053639 in *DDIT4* genes which suggest an important role for mTOR signaling cascade in the modulation of pharmacological response in treated patients.

Focusing on LID development, degeneration of nigral neuron and nigrostriatal denervation along with continuous DA support to the brain lead to maladaptive neuronal plasticity in the striatum of PD patients^{240,242,243,639}. Interestingly, mTOR signaling is involved in those processes since pharmacological inactivation of mTOR with rapamycin or rapalogs abrogate not only dopaminergic neuronal death^{286,306} but also LID^{332,334} in PD animal models. Our findings regarding SNPs association support the idea that mTOR pathway modulate the response to L-DOPA.

In our study, we found an allelic association of the SNP rs1043098 in *EIF4EBP2* gene with LID onset and LID peak. More specifically, we found that TT risk genotype was associated with nearly 4 years (3.89 years) earlier time to peak LID as compared to the reference genotype CC. Accordingly, also TT carriers displayed almost 3 years (2.84

years) earlier onset of LID compared to CC protective genotype. At a protein level, EIF4EBP2 is a translational repressor with a pivotal role in synaptic plasticity and memory formation⁶⁴⁰. In PD, *EIF4EBP2* mRNA levels are increased in PD postmortem brain tissue⁶⁴¹ and in peripheral blood⁶⁴². Moreover, *EIF4EBP2* expression has been shown to be diminished in the 6-OHDA-denervated striatum of mice after acute L-DOPA administration⁶⁴³. Since aberrant plasticity of the corticostriatal pathway following L-DOPA treatment is crucial for LID onset, genetic variations in the *EIF4EBP2* gene could modulate differential susceptibility to L-DOPA by affecting protein synthesis and thus plasticity. Although *EIF4EBP2* has been previously associated with PD risk⁶⁴¹, to the best of our knowledge, this is the first time that the gene and the SNP rs1043098 have been linked to LID onset.

Furthermore, we show that *EIF4EBP2* rs1043098 is not only associated to LID onset as a single marker, but also as part of a multilocus association concerning *RICTOR* rs2043112 and *PRKCA* rs4790904 (CVC=10/10, O.R.=6.85, 95%C.I.=3.57-73.16, *P*-value<0.0010). Among multiple genotype combinations, the protective one CC/AG/TT was associated with 5.25 years delayed LID onset after the initiation of DA replacement therapy. Importantly, this combination was frequent in our cohort affecting to 11.01% of the sample. Rictor protein is a component of the mTORC2 complex which regulates Akt phosphorylation and, thereby, neuronal survival and actin polymerization^{249,250,253}. PKC α , encode by *PRKCA*, is a substrate of the mTORC2 complex and is responsible for the reorganization of the actin cytoskeleton^{499,500}. Both neuronal survival and actin polymerization are essential processes for maintaining synaptic plasticity in neurons. Hence, these genetic variations could deregulate in the end mTORC1/2 activities affecting plasticity and modulating the timing of LID onset.

In parallel, we also investigated whether genetic variations in the mTOR pathway were associated to LID severity. First, we found that the polymorphisms rs12628 in *HRAS* and rs1801582 in *PRKN* genes (both FDR-corrected *P*-value=0.0180) were individually associated with LID severity. Nevertheless, when adjusting for L-DOPA dosage and dosage of DA agonists we found no association for any studied SNP. This finding suggests that the contribution of the dose of L-DOPA and DA agonists to LID is higher than that of susceptibility SNPs in the mTOR pathway. However, this finding is somehow expected since DA replacement therapy is the responsible for LID appearance and, indeed, non-treated patients do not develop dyskinesia^{242,243,639}. *PRKN* encodes for parkin protein and mutations in this gene are known to cause autosomal young-onset PD^{134,135,364,644}. Parkin is an E3 ubiquitin ligase that targets specific substrates to proteasomal degradation and it is involved in neuroplasticity, controlling neurotransmitter

DISCUSSION

trafficking at the presynaptic terminal^{359,645}. Parkin activity is compromised in both genetic and sporadic PD^{362–364}. Interestingly, one of its substrates is the stress-responsive protein RTP801 and Parkin functional alteration in PD contribute to RTP801 increase by impairing its proteasomal degradation³⁵⁹. In addition to rs1801582 in *PRKN*, the SNP rs12628 in *HRAS* was also associated with LID severity. *HRAS* encodes for the GTPase protein H-Ras, which activates PI3K and finally results in the activation of Akt and mTOR pathway playing a key role in the translation of extracellular signals into cell^{646,647}.

In this direction, we found a four-locus interaction involving the aforementioned polymorphism rs12628 SNP in *HRAS* along with rs5456121 in *RPS6KA2*, rs1292034 in *RPS6KB1* and rs456998 in *FCHSD1* with LID severity (CVC=10/10; O.R.=31.56; 95%C.I.=19.57-50.91; *P*-value<0.0010). Specifically, among multiple combinations, the risk genotype AG/AG/CT/GT genotype was associated with more severe LID and was present in 5.56% patients with severe LID vs. 1.59% in those with no or mild LID. Remarkably, the precision and sensitivity to correctly predict and discriminate LID severity was up to 80% which validated the interaction as method to predict LID severity in PD patients.

The proteins encoded by the genes with polymorphisms associated with LID severity are also related, directly or indirectly, with PD pathogenesis. H-Ras, as previously stated, modulates Akt and mTOR activities^{646,647}. S6K-alpha-2 and S6K-beta-1 are downstream ERK and mTORC1, respectively^{648,649}. Such pathways modulate a crucial process in plasticity that is protein synthesis initiation via the phosphorylation of the eukaryotic translation initiation factor B (eIF4B)¹⁵³. Finally, as previously have been described in the previous section of the discussion, *FCHSD1* protein controls the actin cytoskeleton⁶³⁷. Striking, the gene expression of *FCHSD1* is affected after acute L-DOPA administration in the striatum of 6-OHDA-lesioned mice⁶⁴³.

Overall, the results shown here suggest that the correct regulation of synaptic plasticity involving processes such as protein synthesis and cytoskeleton reorganization which are regulated by downstream effectors of the mTOR pathway, are crucial for the appearance of LID. Taking into account that about 90% of the L-DOPA-treated PD patients develop LID within 10 years after initiation of the DA replacement therapy²³⁹, our findings may have relevant implications for the clinical practice in PD. They may help to identify subjects who are more susceptible to develop earlier LID, with up to 5 years differences, and those who are more susceptible to develop severe LID, with the ultimate goal to redesign the therapeutic approach, accordingly. These findings may also help to stratify

PD patients in clinical trials for disease modifying drugs or possible anti-dyskinetic, when available.

Summarizing, the data found indicate that polymorphisms in genetic markers of the mTOR pathway contribute to the susceptibility to PD and the response to L-DOPA treatment in these patients. We show that these SNPs influence the outcome individually or interacting epistatically with other genetic markers (Figure 70). Altogether, the results support the important role of the mTOR signaling in neurodegenerative diseases.

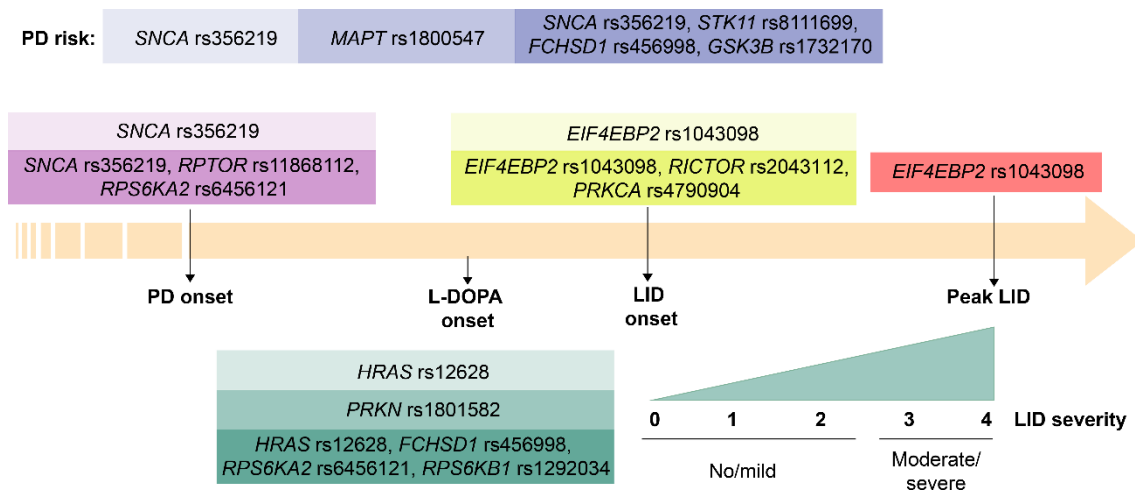


Figure 70. Single SNP and SNP combinations modulate PD susceptibility and response to L-DOPA treatment. SNPs associations found in the different analysis are indicated over the timeline of PD pathogenic process (association with PD risk in blue boxes, with PD AAO in violet boxes, with LID onset in green boxes, with Peak LID in red box and with LID severity in aquamarine boxes. PD onset is considered at the age when motor symptoms appear.

9. RTP801 AND MODULATION OF THE mTOR PATHWAY AS POTENTIAL THERAPEUTIC TARGETS AND BIOMARKERS IN NEURODEGENERATIVE DISEASES

HD and PD are characterized by the loss of selective neuronal populations^{30,31,170,172}. Unfortunately, current treatments at both neurodegenerative disorders ameliorate motor and non-motor symptoms but do not prevent neuronal death. Hence, it is crucial to study the molecular mechanisms underlying neurodegeneration to identify proteins involved in the pathogenesis and design new therapeutic approaches able to halt or at least delay neuronal death and dysfunctional plasticity.

RTP801 emerged as an important protein in PD pathogenesis since its upregulation promotes neuronal death by repressing mTOR/Akt signaling^{263,264}. Importantly, we have identified RTP801 as a mediator of mhtt-induced cell death and impaired plasticity. Moreover, we have shown that RTP801 levels are increased in the putamen and caudate

nucleus of HD patients. Therefore, RTP801 has also arisen as an important protein in HD pathogenesis and strategies to block RTP801 toxic accumulation or modulate mTOR/Akt pathway can become potential therapeutic targets for both diseases.

In fact, some protective molecules that modulate RTP801/mTOR axis have been already reported. 8-methyl-6-phenoxy-2-(tetrahydro-2H-pyran-4-ylamino)pyrido[2,3-D]pyrimidin-7-one (FLZ) is a synthetic compound derived from a Chinese herb which confers protection in cellular and animal models of PD by inhibiting RTP801 expression and, thus maintaining Akt pro-survival kinase activity^{650–653}. On the other hand, rapamycin functions as an mTOR allosteric inhibitor and is also protective in cellular and animal models of PD and HD. It represses the translation of a subset of transcripts, including RTP801, and leading to the maintenance of Akt survival kinase activity by preserving phosphorylation at threonine 308 residue³⁰⁶. In addition, rapamycin enhances autophagy attenuating pathogenic protein aggregation^{72,75,206,285,654}.

Another valuable strategy would be to block RTP801 expression with microRNAs (miRNAs) or small interfering RNAs (siRNAs). To date, several miRNAs including miR-495, miR-221, miR-22, miR-30c have been described to negatively regulate RTP801 gene expression in a context of tumorigenesis^{655–659}. In the brain, mir-7 has been suggested to regulate RTP801 expression during chronic stress in a PD mice model⁵⁴⁵ and miR-181a downregulates RTP801 to facilitate hippocampal fear memory consolidation⁶⁶⁰. Moreover, a siRNA against RTP801 is being evaluated in clinical trials for retinopathy treatment^{661–664}. Therefore, miRNAs and siRNAs may have a relevant impact in the regulation of RTP801 levels and function as therapeutic agents for PD and HD treatment to prevent neuronal death and synaptic dysfunction. Importantly, RTP801 downregulation at basal levels does not affect neuronal survival or plasticity and motor learning.

Interestingly, we have described that 6-OHDA toxin induces the loading of RTP801 into exosomes. Nevertheless, it is still necessary to study whether RTP801 is present in purified exosomes from fluids such as blood, CSF, saliva or urine and whether its levels correlate with PD stage to be use as biomarker. Furthermore, 6-OHDA PD mimetic and mhtt abrogate the trophic effects of exosomes on the pro-survival mTOR/Akt pathway in recipient neurons. Monitoring trophic effect of exosomes by the quantification of mTOR protein components levels could be also used to monitor disease progression.

Recently, exosomes are being used as vehicles for therapeutic cargo delivery. Due to low immunogenicity, a long half-life and the ability to cross the blood brain barrier, exosomes have been used efficiently for delivering drugs, siRNAs or miRNAs to neuronal

cells^{407,417,665}. In order to enhance the activity of drugs and as a delivery vehicle, exosomes may be loaded with the prior mentioned compounds, siRNAs and miRNAs to target RTP801 protein or modulate mTOR/Akt signaling pathway.

In this thesis we have also uncovered SNPs in genes encoding protein components of the mTOR pathway which interact epistatically to determine the susceptibility to PD pathogenesis and, importantly, the response to L-DOPA treatment. Our findings may help to design personalized DA replacement therapy determine previously the risk of patients to develop early and/or severe LID.

CONCLUSIONS

1. Exon-1 of mutant huntingtin increases RTP801 protein levels by upregulating its gene expression and impairing its protein degradation in HD cellular models.
2. Somatic and synaptic RTP801 protein are increased in HD cellular models and in the putamen of HD patients. R6/1 and Hdh^{Q7/Q111} mouse models display accumulation of striatal RTP801 only at the synaptic compartment.
3. Upregulation of RTP801 mediates mutant huntingtin-induced cell death and contributes to impair motor learning plasticity in R6/1 mouse model. Normalization of striatal RTP801 in R6/1 mice preserves the corticostriatal function, by enhancing GluA1 and TrkB expression and restoring basal levels of phosphorylated Akt at Ser473 residue through decreasing Rictor.
4. Exosomes secreted by neurons enhance the pro-survival mTOR/Akt pathway in recipient cells and this function is regulated by RTP801. Neuronal exposure to 6-OHDA toxin increases the release of exosomes containing RTP801 protein which counteract the exosomal activation of the mTOR/Akt pro-survival pathway in target neurons.
5. Exosomes derived from mhtt-expressing cells abrogate the enhancement of mTOR/Akt pathway in recipient neurons, however RTP801 protein is not present in these exosomes.
6. SNPs in genes encoding mTOR pathway protein components interact epistatically with *SNCA* rs356219 to modulate risk and age at onset of PD. Particularly, *SNCA* rs356219 along with *STK11* rs8111699, *FCHSD1* rs456998 and *GSK3B* rs1732170 contribute PD susceptibility, whereas *SNCA* rs356219 interacts with *RPTOR* rs11868112 and *RPS6KA2* rs6456121 to modulate age at onset of idiopathic and LRRK2 PD patients.
7. Single SNPs and associations of SNPs in the mTOR pathway modulate the response to levodopa treatment in PD patients. Specifically, *EIF4EBP2* rs1043098 alone or in combination with *RICTOR* rs2043112 and *PRKCA* rs4790904 contribute to the onset of LID. Single SNPs *PRKN* rs1801582 and *HRAS* rs12628 are associated to LID severity and *HRAS* rs12628 in combination with *RPS6KA2* rs5456121, *RPS6KB1* rs1292034 and *FCHSD1* rs456998 predict the severity of them.

BIBLIOGRAPHY

1. Rüb U, Vonsattel JP V, Heinsen H, Korf H-W (2015) The Neuropathology of Huntington's disease: classical findings, recent developments and correlation to functional neuroanatomy. *Adv Anat Embryol Cell Biol* 217:1–146
2. Rawlins MD, Wexler NS, Wexler AR, Tabrizi SJ, Douglas I, Evans SJW, Smeeth L (2016) The Prevalence of Huntington's Disease. *Neuroepidemiology* 46:144–153 . doi: 10.1159/000443738
3. Pringsheim T, Wiltshire K, Day L, Dykeman J, Steeves T, Jette N (2012) The incidence and prevalence of Huntington's disease: A systematic review and meta-analysis. *Mov Disord* 27:1083–1091 . doi: 10.1002/mds.25075
4. Fisher ER, Hayden MR (2014) Multisource ascertainment of Huntington disease in Canada: Prevalence and population at risk. *Mov Disord* 29:105–114 . doi: 10.1002/mds.25717
5. Aziz NA, Jurgens CK, Landwehrmeyer GB, van Roon-Mom WMC, van Ommen GJB, Stijnen T, Roos RAC (2009) Normal and mutant HTT interact to affect clinical severity and progression in Huntington disease. *Neurology* 73:1280–1285 . doi: 10.1212/WNL.0b013e3181bd1121
6. Martin JB, Gusella JF (1986) Huntington's disease. Pathogenesis and management. *N Engl J Med* 315:1267–1276
7. Folstein SE, Leigh RJ, Parhad IM, Folstein MF (1986) The diagnosis of Huntington's disease. *Neurology* 36:1279–83
8. Sturrock A, Leavitt BR (2010) The Clinical and Genetic Features of Huntington Disease. *J Geriatr Psychiatry Neurol* 23:243–259 . doi: 10.1177/0891988710383573
9. Gilliam TC, Bucan M, MacDonald ME, Zimmer M, Haines JL, Cheng S V, Pohl TM, Meyers RH, Whaley WL, Allitto BA (1987) A DNA segment encoding two genes very tightly linked to Huntington's disease. *Science* 238:950–2
10. Wexler NS, Young AB, Tanzi RE, Travers H, Starosta-Rubinstein S, Penney JB, Snodgrass SR, Shoulson I, Gomez F, Arroyo MAR, Penchaszadeh GK, Moreno H, Gibbons K, Faryniarz A, Hobbs W, Anderson MA, Bonilla E, Conneally PM, Gusella JF (1987) Homozygotes for Huntington's disease. *Nature* 326:194–197 . doi: 10.1038/326194a0
11. MacDonald ME, Ambrose CM, Duyao MP, Myers RH, Lin C, Srinidhi L, Barnes G, Taylor SA, James M, Groot N, MacFarlane H, Jenkins B, Anderson MA, Wexler NS, Gusella JF, Bates GP, Baxendale S, Hummerich H, Kirby S, North M, Youngman S, Mott R, Zehetner G, Sedlacek Z, Poustka A, Frischauf A-M, Lehrach H, Buckler AJ, Church D, Doucette-Stamm L, O'Donovan MC, Riba-Ramirez L, Shah M, Stanton VP, Strobel SA, Draths KM, Wales JL, Dervan P, Housman DE, Altherr M, Shiang R, Thompson L, Fielder T, Wasmuth JJ, Tagle D, Valdes J, Elmer L, Allard M, Castilla L, Swaroop M, Blanchard K, Collins FS, Snell R, Holloway T, Gillespie K, Datson N, Shaw D, Harper PS (1993) A novel gene containing a trinucleotide repeat that is expanded and unstable on Huntington's disease chromosomes. *Cell* 72:971–983 . doi: 10.1016/0092-8674(93)90585-E
12. Gafni J, Hermel E, Young JE, Wellington CL, Hayden MR, Ellerby LM (2004) Inhibition of Calpain Cleavage of Huntingtin Reduces Toxicity. *J Biol Chem* 279:20211–20220 . doi: 10.1074/jbc.M401267200
13. Goldberg YP, Nicholson DW, Rasper DM, Kalchman MA, Koide HB, Graham RK, Bromm M, Kazemi-Esfarjani P, Thornberry NA, Vaillancourt JP, Hayden MR

BIBLIOGRAPHY

- (1996) Cleavage of huntingtin by apopain, a proapoptotic cysteine protease, is modulated by the polyglutamine tract. *Nat Genet* 13:442–449 . doi: 10.1038/ng0896-442
14. Kim YJ, Yi Y, Sapp E, Wang Y, Cuiffo B, Kegel KB, Qin ZH, Aronin N, DiFiglia M (2001) Caspase 3-cleaved N-terminal fragments of wild-type and mutant huntingtin are present in normal and Huntington's disease brains, associate with membranes, and undergo calpain-dependent proteolysis. *Proc Natl Acad Sci U S A* 98:12784–9 . doi: 10.1073/pnas.221451398
 15. Miller JP, Holcomb J, Al-Ramahi I, de Haro M, Gafni J, Zhang N, Kim E, Sanhueza M, Torcassi C, Kwak S, Botas J, Hughes RE, Ellerby LM (2010) Matrix Metalloproteinases Are Modifiers of Huntingtin Proteolysis and Toxicity in Huntington's Disease. *Neuron* 67:199–212 . doi: 10.1016/j.neuron.2010.06.021
 16. Wellington CL, Singaraja R, Ellerby L, Savill J, Roy S, Leavitt B, Cattaneo E, Hackam A, Sharp A, Thornberry N, Nicholson DW, Bredesen DE, Hayden MR (2000) Inhibiting caspase cleavage of huntingtin reduces toxicity and aggregate formation in neuronal and nonneuronal cells. *J Biol Chem* 275:19831–8 . doi: 10.1074/jbc.M001475200
 17. DiFiglia M, Sapp E, Chase KO, Davies SW, Bates GP, Vonsattel JP, Aronin N (1997) Aggregation of huntingtin in neuronal intranuclear inclusions and dystrophic neurites in brain. *Science* 277:1990–3
 18. Gutekunst CA, Li SH, Yi H, Mulroy JS, Kuemmerle S, Jones R, Rye D, Ferrante RJ, Hersch SM, Li XJ (1999) Nuclear and neuropil aggregates in Huntington's disease: relationship to neuropathology. *J Neurosci* 19:2522–34
 19. Martindale D, Hackam A, Wieczorek A, Ellerby L, Wellington C, McCutcheon K, Singaraja R, Kazemi-Esfarjani P, Devon R, Kim SU, Bredesen DE, Tufaro F, Hayden MR (1998) Length of huntingtin and its polyglutamine tract influences localization and frequency of intracellular aggregates. *Nat Genet* 18:150–4 . doi: 10.1038/ng0298-150
 20. Sieradzan KA, Mehan AO, Jones L, Wanker EE, Nukina N, Mann DM (1999) Huntington's disease intranuclear inclusions contain truncated, ubiquitinated huntingtin protein. *Exp Neurol* 156:92–9 . doi: 10.1006/exnr.1998.7005
 21. Rego A, de Almeida L (2005) Molecular Targets and Therapeutic Strategies in Huntingtons Disease. *Curr Drug Target -CNS Neurol Disord* 4:361–381 . doi: 10.2174/1568007054546081
 22. Duyao M, Ambrose C, Myers R, Novellettoa, Persichetti F, Frontali M, Folstein S, Ross C, Franz M, Abbott M (1993) Trinucleotide repeat length instability and age of onset in Huntington's disease. *Nat Genet* 4:387–392 . doi: 10.1038/ng0893-387
 23. Lee J-M, Ramos EM, Lee J-H, Gillis T, Mysore JS, Hayden MR, Warby SC, Morrison P, Nance M, Ross CA, Margolis RL, Squitieri F, Orobello S, Di Donato S, Gomez-Tortosa E, Ayuso C, Suchowersky O, Trent RJA, McCusker E, Novelletto A, Frontali M, Jones R, Ashizawa T, Frank S, Saint-Hilaire MH, Hersch SM, Rosas HD, Lucente D, Harrison MB, Zanko A, Abramson RK, Marder K, Sequeiros J, Paulsen JS, Landwehrmeyer GB, Myers RH, MacDonald ME, Gusella JF, HD-MAPS Study Group, MacDonald ME, Gusella JF, COHORT study of the HSG (2012) CAG repeat expansion in Huntington disease determines age at onset in a fully dominant fashion. *Neurology* 78:690–695 . doi: 10.1212/WNL.0b013e318249f683
 24. Kremer B, Goldberg P, Andrew SE, Theilmann J, Telenius H, Zeisler J, Squitieri

- F, Lin B, Bassett A, Almqvist E, Bird TD, Hayden MR (1994) A Worldwide Study of the Huntington's Disease Mutation: The Sensitivity and Specificity of Measuring CAG Repeats. *N Engl J Med* 330:1401–1406 . doi: 10.1056/NEJM199405193302001
25. Rubinsztein DC, Leggo J, Coles R, Almqvist E, Biancalana V, Cassiman JJ, Chotai K, Connarty M, Crauford D, Curtis A, Curtis D, Davidson MJ, Differ AM, Dode C, Dodge A, Frontali M, Ranen NG, Stine OC, Sherr M, Abbott MH, Franz ML, Graham CA, Harper PS, Hedreen JC, Hayden MR (1996) Phenotypic characterization of individuals with 30-40 CAG repeats in the Huntington disease (HD) gene reveals HD cases with 36 repeats and apparently normal elderly individuals with 36-39 repeats. *Am J Hum Genet* 59:16–22
 26. Andresen JM, Gayán J, Djoussé L, Roberts S, Brocklebank D, Cherny SS, Cardon LR, Gusella JF, MacDonald ME, Myers RH, Housman DE, Wexler NS, Housman DE, Wexler NS (2007) The Relationship Between CAG Repeat Length and Age of Onset Differs for Huntington's Disease Patients with Juvenile Onset or Adult Onset. *Ann Hum Genet* 71:295–301 . doi: 10.1111/j.1469-1809.2006.00335.x
 27. Gusella JF, MacDonald ME, Lee J-M (2014) Genetic modifiers of Huntington's disease. *Mov Disord* 29:1359–1365 . doi: 10.1002/mds.26001
 28. Baine FK, Kay C, Ketelaar ME, Collins JA, Semaka A, Doty CN, Krause A, Jacquie Greenberg L, Hayden MR (2013) Huntington disease in the South African population occurs on diverse and ethnically distinct genetic haplotypes. *Eur J Hum Genet* 21:1120–1127 . doi: 10.1038/ejhg.2013.2
 29. Warby SC, Visscher H, Collins JA, Doty CN, Carter C, Butland SL, Hayden AR, Kanazawa I, Ross CJ, Hayden MR (2011) HTT haplotypes contribute to differences in Huntington disease prevalence between Europe and East Asia. *Eur J Hum Genet* 19:561–566 . doi: 10.1038/ejhg.2010.229
 30. Vonsattel JP, Myers RH, Stevens TJ, Ferrante RJ, Bird ED, Richardson Jr. EP (1985) Neuropathological classification of Huntington's disease. *J Neuropathol Exp Neurol* 44:559–577 . doi: 10.1097/00005072-198511000-00003
 31. Halliday GM, McRitchie DA, Macdonald V, Double KL, Trent RJ, McCusker E (1998) Regional Specificity of Brain Atrophy in Huntington's Disease. *Exp Neurol* 154:663–672 . doi: 10.1006/exnr.1998.6919
 32. Mann DM, Oliver R, Snowden JS (1993) The topographic distribution of brain atrophy in Huntington's disease and progressive supranuclear palsy. *Acta Neuropathol* 85:553–9 . doi: 10.1007/BF00230496
 33. Rosas HD, Koroshetz WJ, Chen YI, Skeuse C, Vangel M, Cudkovicz ME, Caplan K, Marek K, Seidman LJ, Makris N, Jenkins BG, Goldstein JM (2003) Evidence for more widespread cerebral pathology in early HD: an MRI-based morphometric analysis. *Neurology* 60:1615–1620 . doi: 10.1212/WNL.62.3.523-a
 34. Rüb U, Hoche F, Brunt ER, Heinsen H, Seidel K, Del Turco D, Paulson HL, Bohl J, von Gall C, Vonsattel JP, Korf HW, den Dunnen WF (2013) Degeneration of the cerebellum and brainstem in Huntington's disease (HD). *J Neurol Sci* 333:e141–e142 . doi: 10.1016/j.jns.2013.07.471
 35. Reiner A, Dragatsis I, Dietrich P (2011) Genetics and neuropathology of Huntington's disease. *Int Rev Neurobiol* 98:325–72 . doi: 10.1016/B978-0-12-381328-2.00014-6
 36. Balleine BW, Liljeholm M, Ostlund SB (2009) The integrative function of the basal

BIBLIOGRAPHY

- ganglia in instrumental conditioning. *Behav Brain Res* 199:43–52 . doi: 10.1016/j.bbr.2008.10.034
37. Brown LL, Schneider JS, Lidsky TI (1997) Sensory and cognitive functions of the basal ganglia. *Curr Opin Neurobiol* 7:157–63
38. Lanciego JL, Luquin N, Obeso JA (2012) Functional Neuroanatomy of the Basal Ganglia. *Cold Spring Harb Perspect Med* 2:a009621–a009621 . doi: 10.1101/cshperspect.a009621
39. Bolam JP, Hanley JJ, Booth PA, Bevan MD (2000) Synaptic organisation of the basal ganglia. *J Anat* 196 (Pt 4):527–42
40. Kreitzer AC (2009) Physiology and pharmacology of striatal neurons. *Annu Rev Neurosci* 32:127–47 . doi: 10.1146/annurev.neuro.051508.135422
41. Kita H, Kitai ST (1988) Glutamate decarboxylase immunoreactive neurons in rat neostriatum: their morphological types and populations. *Brain Res* 447:346–52
42. Wichmann T, DeLong MR, Guridi J, Obeso JA (2011) Milestones in research on the pathophysiology of Parkinson's disease. *Mov Disord* 26:1032–1041 . doi: 10.1002/mds.23695
43. Calabresi P, Picconi B, Tozzi A, Ghiglieri V, Di Filippo M (2014) Direct and indirect pathways of basal ganglia: a critical reappraisal. *Nat Neurosci* 17:1022–1030 . doi: 10.1038/nn.3743
44. Schroll H, Hamker FH (2013) Computational models of basal-ganglia pathway functions: focus on functional neuroanatomy. *Front Syst Neurosci* 7:122 . doi: 10.3389/fnsys.2013.00122
45. Gerfen CR (1992) The neostriatal mosaic: multiple levels of compartmental organization. *Trends Neurosci* 15:133–9
46. Aizman O, Brismar H, Uhlén P, Zettergren E, Levey AI, Forssberg H, Greengard P, Aperia A (2000) Anatomical and physiological evidence for D1 and D2 dopamine receptor colocalization in neostriatal neurons. *Nat Neurosci* 3:226–230 . doi: 10.1038/72929
47. Smith Y, Bevan MD, Shink E, Bolam JP (1998) Microcircuitry of the direct and indirect pathways of the basal ganglia. *Neuroscience* 86:353–87
48. Surmeier DJ, Song WJ, Yan Z (1996) Coordinated expression of dopamine receptors in neostriatal medium spiny neurons. *J Neurosci* 16:6579–91
49. Obeso JA, Rodríguez-Oroz MC, Benitez-Temino B, Blesa FJ, Guridi J, Marin C, Rodriguez M (2008) Functional organization of the basal ganglia: Therapeutic implications for Parkinson's disease. *Mov Disord* 23:S548–S559 . doi: 10.1002/mds.22062
50. Gerfen CR, Engber TM, Mahan LC, Susel Z, Chase TN, Monsma FJ, Sibley DR (1990) D1 and D2 dopamine receptor-regulated gene expression of striatonigral and striatopallidal neurons. *Science* 250:1429–32
51. Gerfen CR, Surmeier DJ (2011) Modulation of Striatal Projection Systems by Dopamine. *Annu Rev Neurosci* 34:441–466 . doi: 10.1146/annurev-neuro-061010-113641
52. Richfield EK, Maguire-Zeiss KA, Vonkeman HE, Voorn P (1995) Preferential loss of preproenkephalin versus preprotachykinin neurons from the striatum of Huntington's disease patients. *Ann Neurol* 38:852–861 . doi:

- 10.1002/ana.410380605
53. Sapp E, Ge P, Aizawa H, Bird E, Penney J, Young AB, Vonsattel JP, DiFiglia M (1995) Evidence for a preferential loss of enkephalin immunoreactivity in the external globus pallidus in low grade Huntington's disease using high resolution image analysis. *Neuroscience* 64:397–404
 54. Albin RL, Young AB, Penney JB (1989) The functional anatomy of basal ganglia disorders. *Trends Neurosci* 12:366–75
 55. Alexander GE, Crutcher MD (1990) Functional architecture of basal ganglia circuits: neural substrates of parallel processing. *Trends Neurosci* 13:266–71
 56. Ramaswamy S, McBride JL, Kordower JH (2007) Animal models of Huntington's disease. *ILAR J* 48:356–73
 57. Landles C, Bates GP (2004) Huntingtin and the molecular pathogenesis of Huntington's disease. Fourth in molecular medicine review series. *EMBO Rep* 5:958–63 . doi: 10.1038/sj.embor.7400250
 58. Bates GP, Dorsey R, Gusella JF, Hayden MR, Kay C, Leavitt BR, Nance M, Ross CA, Scahill RI, Wetzel R, Wild EJ, Tabrizi SJ (2015) Huntington disease. *Nat Rev Dis Prim* 1:15005 . doi: 10.1038/nrdp.2015.5
 59. Landles C, Sathasivam K, Weiss A, Woodman B, Moffitt H, Finkbeiner S, Sun B, Gafni J, Ellerby LM, Trottier Y, Richards WG, Osmand A, Paganetti P, Bates GP (2010) Proteolysis of mutant huntingtin produces an exon 1 fragment that accumulates as an aggregated protein in neuronal nuclei in Huntington disease. *J Biol Chem* 285: . doi: 10.1074/jbc.M109.075028
 60. Lunkes A, Lindenberg KS, Ben-Haïem L, Weber C, Devys D, Landwehrmeyer GB, Mandel J-L, Trottier Y (2002) Proteases acting on mutant huntingtin generate cleaved products that differentially build up cytoplasmic and nuclear inclusions. *Mol Cell* 10:259–69 . doi: 10.1016/S1097-2765(02)00602-0
 61. Davies SW, Turmaine M, Cozens BA, DiFiglia M, Sharp AH, Ross CA, Scherzinger E, Wanker EE, Mangiarini L, Bates GP (1997) Formation of neuronal intranuclear inclusions underlies the neurological dysfunction in mice transgenic for the HD mutation. *Cell* 90:537–48
 62. Busch A, Engemann S, Lurz R, Okazawa H, Lehrach H, Wanker EE (2003) Mutant huntingtin promotes the fibrillogenesis of wild-type huntingtin: a potential mechanism for loss of huntingtin function in Huntington's disease. *J Biol Chem* 278:41452–61 . doi: 10.1074/jbc.M303354200
 63. Steffan JS, Kazantsev A, Spasic-Boskovic O, Greenwald M, Zhu YZ, Gohler H, Wanker EE, Bates GP, Housman DE, Thompson LM (2000) The Huntington's disease protein interacts with p53 and CREB-binding protein and represses transcription. *Proc Natl Acad Sci U S A* 97:6763–8 . doi: 10.1073/pnas.100110097
 64. Schaffar G, Breuer P, Boteva R, Behrends C, Tzvetkov N, Strippel N, Sakahira H, Siegers K, Hayer-Hartl M, Hartl FU (2004) Cellular toxicity of polyglutamine expansion proteins: mechanism of transcription factor deactivation. *Mol Cell* 15:95–105 . doi: 10.1016/j.molcel.2004.06.029
 65. Dikic I (2017) Proteasomal and Autophagic Degradation Systems. *Annu Rev Biochem* 86:193–224 . doi: 10.1146/annurev-biochem-061516-044908
 66. Schreiber A, Peter M (2014) Substrate recognition in selective autophagy and the ubiquitin–proteasome system. *Biochim Biophys Acta - Mol Cell Res* 1843:163–

- 181 . doi: 10.1016/j.bbamcr.2013.03.019
67. Warrick JM, Chan HY, Gray-Board GL, Chai Y, Paulson HL, Bonini NM (1999) Suppression of polyglutamine-mediated neurodegeneration in *Drosophila* by the molecular chaperone HSP70. *Nat Genet* 23:425–8 . doi: 10.1038/70532
68. Wyttenbach A, Carmichael J, Swartz J, Furlong RA, Narain Y, Rankin J, Rubinsztein DC (2000) Effects of heat shock, heat shock protein 40 (HDJ-2), and proteasome inhibition on protein aggregation in cellular models of Huntington's disease. *Proc Natl Acad Sci U S A* 97:2898–903
69. Martinez-Vicente M, Talloczy Z, Wong E, Tang G, Koga H, Kaushik S, de Vries R, Arias E, Harris S, Sulzer D, Cuervo AM (2010) Cargo recognition failure is responsible for inefficient autophagy in Huntington's disease. *Nat Neurosci* 13:567–76 . doi: 10.1038/nn.2528
70. Nagaoka U, Kim K, Jana NR, Doi H, Maruyama M, Mitsui K, Oyama F, Nukina N (2004) Increased expression of p62 in expanded polyglutamine-expressing cells and its association with polyglutamine inclusions. *J Neurochem* 91:57–68 . doi: 10.1111/j.1471-4159.2004.02692.x
71. Rué L, López-Soop G, Gelpi E, Martínez-Vicente M, Alberch J, Pérez-Navarro E (2013) Brain region- and age-dependent dysregulation of p62 and NBR1 in a mouse model of Huntington's disease. *Neurobiol Dis* 52:219–228 . doi: 10.1016/j.nbd.2012.12.008
72. Ravikumar B, Vacher C, Berger Z, Davies JE, Luo S, Oroz LG, Scaravilli F, Easton DF, Duden R, O'Kane CJ, Rubinsztein DC (2004) Inhibition of mTOR induces autophagy and reduces toxicity of polyglutamine expansions in fly and mouse models of Huntington disease. *Nat Genet* 36:585–95 . doi: 10.1038/ng1362
73. Webb JL, Ravikumar B, Atkins J, Skepper JN, Rubinsztein DC (2003) Alpha-Synuclein is degraded by both autophagy and the proteasome. *J Biol Chem* 278:25009–13 . doi: 10.1074/jbc.M300227200
74. Li X-JJ, Li S (2011) Proteasomal dysfunction in aging and Huntington disease
75. Sarkar S, Perlstein EO, Imarisio S, Pineau S, Cordenier A, Maglathlin RL, Webster JA, Lewis TA, O'Kane CJ, Schreiber SL, Rubinsztein DC (2007) Small molecules enhance autophagy and reduce toxicity in Huntington's disease models. *Nat Chem Biol* 3:331–338 . doi: 10.1038/nchembio883
76. Kim D-K, Cho K-W, Ahn WJ, Perez-Acuña D, Jeong H, Lee H-J, Lee S-J (2017) Cell-to-cell Transmission of Polyglutamine Aggregates in *C. elegans*. *Exp Neurol* 26:321–328 . doi: 10.5607/en.2017.26.6.321
77. Frost B, Diamond MI (2010) Prion-like mechanisms in neurodegenerative diseases. *Nat Rev Neurosci* 11:155–159 . doi: 10.1038/nrn2786
78. Yang W, Dunlap JR, Andrews RB, Wetzell R (2002) Aggregated polyglutamine peptides delivered to nuclei are toxic to mammalian cells. *Hum Mol Genet* 11:2905–17
79. Ren P-H, Lauckner JE, Kachirskaia I, Heuser JE, Melki R, Kopito RR (2009) Cytoplasmic penetration and persistent infection of mammalian cells by polyglutamine aggregates. *Nat Cell Biol* 11:219–225 . doi: 10.1038/ncb1830
80. Cicchetti F, Lacroix S, Cisbani G, Vallières N, Saint-Pierre M, St-Amour I, Tolouei R, Skepper JN, Hauser RA, Mantovani D, Barker RA, Freeman TB (2014) Mutant huntingtin is present in neuronal grafts in huntington disease patients. *Ann Neurol*

- 76:31–42 . doi: 10.1002/ana.24174
81. Pecho-Vrieseling E, Rieker C, Fuchs S, Bleckmann D, Esposito MS, Botta P, Goldstein C, Bernhard M, Galimberti I, Müller M, Lüthi A, Arber S, Bouwmeester T, van der Putten H, Di Giorgio FP (2014) Transneuronal propagation of mutant huntingtin contributes to non-cell autonomous pathology in neurons. *Nat Neurosci* 17:1064–72 . doi: 10.1038/nn.3761
 82. Jeon I, Cicchetti F, Cisbani G, Lee S, Li E, Bae J, Lee N, Li L, Im W, Kim M, Kim HS, Oh S-H, Kim T-A, Ko JJ, Aubé B, Oueslati A, Kim YJ, Song J (2016) Human-to-mouse prion-like propagation of mutant huntingtin protein. *Acta Neuropathol* 132:577–92 . doi: 10.1007/s00401-016-1582-9
 83. Zhang X, Abels ER, Redzic JS, Margulis J, Finkbeiner S, Breakefield XO (2016) Potential Transfer of Polyglutamine and CAG-Repeat RNA in Extracellular Vesicles in Huntington's Disease: Background and Evaluation in Cell Culture. *Cell Mol Neurobiol* 36:459–70 . doi: 10.1007/s10571-016-0350-7
 84. Cha JH (2000) Transcriptional dysregulation in Huntington's disease. *Trends Neurosci* 23:387–92
 85. Cha J-HJ (2007) Transcriptional signatures in Huntington's disease. *Prog Neurobiol* 83:228–248 . doi: 10.1016/j.pneurobio.2007.03.004
 86. Bae B-I, Xu H, Igarashi S, Fujimuro M, Agrawal N, Taya Y, Hayward SD, Moran TH, Montell C, Ross CA, Snyder SH, Sawa A (2005) p53 Mediates Cellular Dysfunction and Behavioral Abnormalities in Huntington's Disease. *Neuron* 47:29–41 . doi: 10.1016/j.neuron.2005.06.005
 87. Li S-H, Cheng AL, Zhou H, Lam S, Rao M, Li H, Li X-J (2002) Interaction of Huntington disease protein with transcriptional activator Sp1. *Mol Cell Biol* 22:1277–87
 88. Dunah AW, Jeong H, Griffin A, Kim Y-M, Standaert DG, Hersch SM, Mouradian MM, Young AB, Tanese N, Krainc D (2002) Sp1 and TAFII130 transcriptional activity disrupted in early Huntington's disease. *Science* 296:2238–43 . doi: 10.1126/science.1072613
 89. Zuccato C, Tartari M, Crotti A, Goffredo D, Valenza M, Conti L, Cataudella T, Leavitt BR, Hayden MR, Timmusk T, Rigamonti D, Cattaneo E (2003) Huntingtin interacts with REST/NRSF to modulate the transcription of NRSE-controlled neuronal genes. *Nat Genet* 35:76–83 . doi: 10.1038/ng1219
 90. Cong S-Y, Pepers BA, Evert BO, Rubinsztein DC, Roos RAC, van Ommen G-JB, Dorsman JC (2005) Mutant huntingtin represses CBP, but not p300, by binding and protein degradation. *Mol Cell Neurosci* 30:560–71
 91. Steffan JS, Bodai L, Pallos J, Poelman M, McCampbell A, Apostol BL, Kazantsev A, Schmidt E, Zhu YZ, Greenwald M, Kurokawa R, Housman DE, Jackson GR, Marsh JL, Thompson LM (2001) Histone deacetylase inhibitors arrest polyglutamine-dependent neurodegeneration in *Drosophila*. *Nature* 413:739–43 . doi: 10.1038/35099568
 92. Kaplan DR, Miller FD (2000) Neurotrophin signal transduction in the nervous system. *Curr Opin Neurobiol* 10:381–91
 93. Arancio O, Chao M V (2007) Neurotrophins, synaptic plasticity and dementia. *Curr Opin Neurobiol* 17:325–30 . doi: 10.1016/j.conb.2007.03.013
 94. Liu Y-F, Chen H, Yu L, Kuo Y-M, Wu F-S, Chuang J-I, Liao P-C, Jen CJ (2008)

- Upregulation of hippocampal TrkB and synaptotagmin is involved in treadmill exercise-enhanced aversive memory in mice. *Neurobiol Learn Mem* 90:81–89 . doi: 10.1016/j.nlm.2008.02.005
95. Baquet ZC, Gorski JA, Jones KR (2004) Early striatal dendrite deficits followed by neuron loss with advanced age in the absence of anterograde cortical brain-derived neurotrophic factor. *J Neurosci* 24:4250–8 . doi: 10.1523/JNEUROSCI.3920-03.2004
96. Gorski JA, Zeiler SR, Tamowski S, Jones KR (2003) Brain-derived neurotrophic factor is required for the maintenance of cortical dendrites. *J Neurosci* 23:6856–65
97. Pérez-Navarro E, Canudas AM, Akerund P, Alberch J, Arenas E (2000) Brain-derived neurotrophic factor, neurotrophin-3, and neurotrophin-4/5 prevent the death of striatal projection neurons in a rodent model of Huntington's disease. *J Neurochem* 75:2190–9
98. Altar CA, Wiegand SJ, Cai N, Bliven T, Juhasz M, Conner JM, Acheson AL, Lindsay RM (1997) Anterograde transport of brain-derived neurotrophic factor and its role in the brain. *Nature* 389:856–860 . doi: 10.1038/39885
99. Zuccato C, Cattaneo E (2007) Role of brain-derived neurotrophic factor in Huntington's disease. *Prog. Neurobiol.* 81:294–330
100. Zuccato C, Marullo M, Conforti P, MacDonald ME, Tartari M, Cattaneo E (2008) Systematic assessment of BDNF and its receptor levels in human cortices affected by Huntington's disease. *Brain Pathol* 18:225–238 . doi: 10.1111/j.1750-3639.2007.00111.x
101. Giralt A, Rodrigo T, Martín ED, Gonzalez JR, Milà M, Ceña V, Dierssen M, Canals JM, Alberch J (2009) Brain-derived neurotrophic factor modulates the severity of cognitive alterations induced by mutant huntingtin: Involvement of phospholipaseC γ activity and glutamate receptor expression. *Neuroscience* 158:1234–1250 . doi: 10.1016/j.neuroscience.2008.11.024
102. Lynch G, Kramar EA, Rex CS, Jia Y, Chappas D, Gall CM, Simmons DA (2007) Brain-Derived Neurotrophic Factor Restores Synaptic Plasticity in a Knock-In Mouse Model of Huntington's Disease. *J Neurosci* 27:4424–4434 . doi: 10.1523/JNEUROSCI.5113-06.2007
103. Canals JM, Pineda JR, Torres-Peraza JF, Bosch M, Martín-Ibañez R, Muñoz MT, Mengod G, Ernfors P, Alberch J (2004) Brain-derived neurotrophic factor regulates the onset and severity of motor dysfunction associated with enkephalinergic neuronal degeneration in Huntington's disease. *J Neurosci* 24:7727–7739 . doi: 10.1523/JNEUROSCI.1197-04.2004
104. Gharami K, Xie Y, An JJ, Tonegawa S, Xu B (2008) Brain-derived neurotrophic factor over-expression in the forebrain ameliorates Huntington's disease phenotypes in mice. *J Neurochem* 105:369–379 . doi: 10.1111/j.1471-4159.2007.05137.x
105. Simmons DA, Rex CS, Palmer L, Pandeyarajan V, Fedulov V, Gall CM, Lynch G (2009) Up-regulating BDNF with an ampakine rescues synaptic plasticity and memory in Huntington's disease knockin mice. *Proc Natl Acad Sci* 106:4906–4911 . doi: 10.1073/pnas.0811228106
106. Simmons DA, Mehta RA, Lauterborn JC, Gall CM, Lynch G (2011) Brief ampakine treatments slow the progression of Huntington's disease phenotypes in R6/2 mice.

- Neurobiol Dis* 41:436–444 . doi: 10.1016/j.nbd.2010.10.015
107. Xie Y, Hayden MR, Xu B (2010) BDNF Overexpression in the Forebrain Rescues Huntington's Disease Phenotypes in YAC128 Mice. *J Neurosci* 30:14708–14718 . doi: 10.1523/JNEUROSCI.1637-10.2010
 108. Gratacòs E, Checa N, Pérez-Navarro E, Alberch J (2001) Brain-derived neurotrophic factor (BDNF) mediates bone morphogenetic protein-2 (BMP-2) effects on cultured striatal neurones. *J Neurochem* 79:747–55
 109. Chao M V. (2003) Neurotrophins and their receptors: A convergence point for many signalling pathways. *Nat Rev Neurosci* 4:299–309 . doi: 10.1038/nrn1078
 110. Lu B, Pang PT, Woo NH (2005) The yin and yang of neurotrophin action. *Nat Rev Neurosci* 6:603–614 . doi: 10.1038/nrn1726
 111. Arévalo JC, Wu SH (2006) Neurotrophin signaling: many exciting surprises! *Cell Mol Life Sci* 63:1523–1537 . doi: 10.1007/s00018-006-6010-1
 112. Reichardt LF (2006) Neurotrophin-regulated signalling pathways. *Philos Trans R Soc B Biol Sci* 361:1545–1564 . doi: 10.1098/rstb.2006.1894
 113. Kalb R (2005) The protean actions of neurotrophins and their receptors on the life and death of neurons. *Trends Neurosci* 28:5–11 . doi: 10.1016/j.tins.2004.11.003
 114. María Frade J, Rodríguez-Tébar A, Barde Y-A (1996) Induction of cell death by endogenous nerve growth factor through its p75 receptor. *Nature* 383:166–168 . doi: 10.1038/383166a0
 115. Friedman WJ (2000) Neurotrophins induce death of hippocampal neurons via the p75 receptor. *J Neurosci* 20:6340–6
 116. Culmsee C, Gerling N, Lehmann M, Nikolova-Karakashian M, Prehn JHM, Mattson MP, Kriegstein J (2002) Nerve growth factor survival signaling in cultured hippocampal neurons is mediated through TrkA and requires the common neurotrophin receptor P75. *Neuroscience* 115:1089–108
 117. He X-L, Garcia KC (2004) Structure of nerve growth factor complexed with the shared neurotrophin receptor p75. *Science* 304:870–5 . doi: 10.1126/science.1095190
 118. Zaccaro MC, Ivanisevic L, Perez P, Meakin SO, Saragovi HU (2001) p75 Co-receptors regulate ligand-dependent and ligand-independent Trk receptor activation, in part by altering Trk docking subdomains. *J Biol Chem* 276:31023–9 . doi: 10.1074/jbc.M104630200
 119. Nykjaer A, Willnow TE, Petersen CM (2005) p75NTR--live or let die. *Curr Opin Neurobiol* 15:49–57 . doi: 10.1016/j.conb.2005.01.004
 120. Ginés S, Bosch M, Marco S, Gavaldà N, Díaz-Hernández M, Lucas JJ, Canals JM, Alberch J (2006) Reduced expression of the TrkB receptor in Huntington's disease mouse models and in human brain. *Eur J Neurosci* 23:649–658 . doi: 10.1111/j.1460-9568.2006.04590.x
 121. Ginés S, Paoletti P, Alberch J (2010) Impaired TrkB-mediated ERK1/2 activation in huntington disease knock-in striatal cells involves reduced p52/p46 Shc expression. *J Biol Chem* 285:21537–48 . doi: 10.1074/jbc.M109.084202
 122. Brito V, Puigdel·l·ivol M, Giralt a, del Toro D, Alberch J, Ginés S (2013) Imbalance of p75(NTR)/TrkB protein expression in Huntington's disease: implication for neuroprotective therapies. *Cell Death Dis* 4:e595 . doi: 10.1038/cddis.2013.116

BIBLIOGRAPHY

123. Brito V, Ginés S (2016) p75^{&sup>}NTR^{&sup>} in Huntington's disease: beyond the basal ganglia. *Oncotarget* 7:1–2 . doi: 10.18632/oncotarget.6646
124. Suelves N, Miguez A, López-Benito S, Barriga GG-D, Giralt A, Alvarez-Periel E, Arévalo JC, Alberch J, Ginés S, Brito V (2018) Early Downregulation of p75NTR by Genetic and Pharmacological Approaches Delays the Onset of Motor Deficits and Striatal Dysfunction in Huntington's Disease Mice. *Mol Neurobiol*. doi: 10.1007/s12035-018-1126-5
125. Paleacu D (2007) Tetrabenazine in the treatment of Huntington's disease. *Neuropsychiatr Dis Treat* 3:545–51
126. Frank S (2014) Treatment of Huntington's disease. *Neurotherapeutics* 11:153–60 . doi: 10.1007/s13311-013-0244-z
127. Kim SD, Fung VSC (2014) An update on Huntington's disease. *Curr Opin Neurol* 27:477–483 . doi: 10.1097/WCO.000000000000116
128. Rodrigues FB, Wild EJ (2017) Clinical Trials Corner: September 2017. *J Huntingtons Dis* 6:255–263 . doi: 10.3233/JHD-170262
129. Rodrigues FB, Wild EJ (2018) Huntington's Disease Clinical Trials Corner: August 2018. *J Huntingtons Dis* 7:279–286 . doi: 10.3233/JHD-189003
130. Parkinson J (2002) An essay on the shaking palsy. 1817. *J Neuropsychiatry Clin Neurosci* 14:223–36; discussion 222 . doi: 10.1176/jnp.14.2.223
131. Goetz CG (2011) The history of Parkinson's disease: early clinical descriptions and neurological therapies. *Cold Spring Harb Perspect Med* 1:a008862 . doi: 10.1101/cshperspect.a008862
132. Pringsheim T, Jette N, Frolkis A, Steeves TDL (2014) The prevalence of Parkinson's disease: A systematic review and meta-analysis. *Mov Disord* 29:1583–1590 . doi: 10.1002/mds.25945
133. Lesage S, Brice A (2009) Parkinson's disease: from monogenic forms to genetic susceptibility factors. *Hum Mol Genet* 18:R48–R59 . doi: 10.1093/hmg/ddp012
134. Karimi-moghadam A, Charsouei S, Bell B, Mohammad , Jabalameli R, Karimi-Moghadam A, Charsouei S, Bell B, Jabalameli MR Parkinson Disease from Mendelian Forms to Genetic Susceptibility: New Molecular Insights into the Neurodegeneration Process. *Cell Mol Neurobiol* 0:1–26 . doi: 10.1007/s10571-018-0587-4
135. Kalia L V, Lang AE (2015) Parkinson's disease. *Lancet* 386:896–912 . doi: 10.1016/S0140-6736(14)61393-3
136. Postuma RB, Berg D, Stern M, Poewe W, Olanow CW, Oertel W, Obeso J, Marek K, Litvan I, Lang AE, Halliday G, Goetz CG, Gasser T, Dubois B, Chan P, Bloem BR, Adler CH, Deuschl G (2015) MDS clinical diagnostic criteria for Parkinson's disease. *Mov Disord* 30:1591–1601 . doi: 10.1002/mds.26424
137. Yarnall AJ, Breen DP, Duncan GW, Khoo TK, Coleman SY, Firbank MJ, Nombela C, Winder-Rhodes S, Evans JR, Rowe JB, Mollenhauer B, Kruse N, Hudson G, Chinnery PF, O'Brien JT, Robbins TW, Wesnes K, Brooks DJ, Barker RA, Burn DJ, ICICLE-PD Study Group (2014) Characterizing mild cognitive impairment in incident Parkinson disease: The ICICLE-PD Study. *Neurology* 82:308–316 . doi: 10.1212/WNL.0000000000000066

138. Duncan GW, Khoo TK, Yarnall AJ, O'Brien JT, Coleman SY, Brooks DJ, Barker RA, Burn DJ (2014) Health-related quality of life in early Parkinson's disease: The impact of nonmotor symptoms. *Mov Disord* 29:195–202 . doi: 10.1002/mds.25664
139. Solla P, Cannas A, Mulas CS, Perra S, Corona A, Bassareo PP, Marrosu F (2014) Association between fatigue and other motor and non-motor symptoms in Parkinson's disease patients. *J Neurol* 261:382–391 . doi: 10.1007/s00415-013-7207-5
140. Dujardin K, Langlois C, Plomhause L, Carette A-S, Delliaux M, Duhamel A, Defebvre L (2014) Apathy in untreated early-stage Parkinson disease: Relationship with other non-motor symptoms. *Mov Disord* 29:1796–1801 . doi: 10.1002/mds.26058
141. Marsh L (2013) Depression and Parkinson's disease: current knowledge. *Curr Neurol Neurosci Rep* 13:409 . doi: 10.1007/s11910-013-0409-5
142. Emre M, Ford PJ, Bilgiç B, Uç EY (2014) Cognitive impairment and dementia in Parkinson's disease: Practical issues and management. *Mov Disord* 29:663–672 . doi: 10.1002/mds.25870
143. de Lau LM, Breteler MM (2006) Epidemiology of Parkinson's disease. *Lancet Neurol* 5:525–535 . doi: 10.1016/S1474-4422(06)70471-9
144. Miller IN, Cronin-Golomb A (2010) Gender differences in Parkinson's disease: Clinical characteristics and cognition. *Mov Disord* 25:2695–2703 . doi: 10.1002/mds.23388
145. Goetz CG, Liu Y, Stebbins GT, Wang L, Tilley BC, Teresi JA, Merkitch D, Luo S (2016) Gender-, age-, and race/ethnicity-based differential item functioning analysis of the movement disorder society-sponsored revision of the Unified Parkinson's disease rating scale. *Mov Disord* 31:1865–1873 . doi: 10.1002/mds.26847
146. Warner TT, Schapira AH V. (2003) Genetic and environmental factors in the cause of Parkinson's disease. *Ann Neurol* 53:S16–S25 . doi: 10.1002/ana.10487
147. Klingelhoefer L, Reichmann H (2015) Pathogenesis of Parkinson disease—the gut–brain axis and environmental factors. *Nat Rev Neurol* 11:625–636 . doi: 10.1038/nrneurol.2015.197
148. Kiebertz K, Wunderle KB (2013) Parkinson's disease: Evidence for environmental risk factors. *Mov Disord* 28:8–13 . doi: 10.1002/mds.25150
149. Sidransky E (2005) Gaucher disease and parkinsonism. *Mol Genet Metab* 84:302–304 . doi: 10.1016/J.YMGME.2004.11.007
150. Eblan MJ, Scholz S, Stubblefield B, Gutti U, Goker-Alpan O, Hruska KS, Singleton AB, Sidransky E (2006) Glucocerebrosidase mutations are not found in association with LRRK2 G2019S in subjects with parkinsonism. *Neurosci Lett* 404:163–165 . doi: 10.1016/j.neulet.2006.05.032
151. Aharon-Peretz J, Rosenbaum H, Gershoni-Baruch R (2004) Mutations in the Glucocerebrosidase Gene and Parkinson's Disease in Ashkenazi Jews. *N Engl J Med* 351:1972–1977 . doi: 10.1056/NEJMoa033277
152. Neudorfer O, Elstein D, Abrahamov A, Turezkite T, Aghai E, Reches A, Bembi B, Zimran A (1996) Occurrence of Parkinson's syndrome in type I Gaucher disease

BIBLIOGRAPHY

153. Shahbazian D, Roux PP, Mieulet V, Cohen MS, Raught B, Taunton J, Hershey JWB, Blenis J, Pende M, Sonenberg N (2006) The mTOR/PI3K and MAPK pathways converge on eIF4B to control its phosphorylation and activity. *EMBO J* 25:2781–91 . doi: 10.1038/sj.emboj.7601166
154. Nalls MA, Pankratz N, Lill CM, Do CB, Hernandez DG, Saad M, Destefano AL, Kara E, Bras J, Sharma M, Schulte C, Keller MF, Arepalli S, Letson C, Edsall C, Stefansson H, Liu X, Pliner H, Lee JH, Cheng R, Ikram MA, Ioannidis JPA, Hadjigeorgiou GM, Bis JC, Martinez M, Perlmutter JS, Goate A, Marder K, Fiske B, Sutherland M, Xiromerisiou G, Myers RH, Clark LN, Stefansson K, Hardy JA, Heutink P, Chen H, Wood NW, Houlden H, Payami H, Brice A, Scott WK, Gasser T, Bertram L, Eriksson N, Foroud T, Singleton AB (2014) Large-scale meta-analysis of genome-wide association data identifies six new risk loci for Parkinson's disease. *Nat Genet* 46:989–993 . doi: 10.1038/ng.3043
155. Simón-Sánchez J, Schulte C, Bras JM, Sharma M, Gibbs JR, Berg D, Paisan-Ruiz C, Lichtner P, Scholz SW, Hernandez DG, Krüger R, Federoff M, Klein C, Goate A, Perlmutter J, Bonin M, Nalls MA, Illig T, Gieger C, Houlden H, Steffens M, Okun MS, Racette BA, Cookson MR, Foote KD, Fernandez HH, Traynor BJ, Schreiber S, Arepalli S, Zonozi R, Gwinn K, Van Der Brug M, Lopez G, Chanock SJ, Schatzkin A, Park Y, Hollenbeck A, Gao J, Huang X, Wood NW, Lorenz D, Deuschl G, Chen H, Riess O, Hardy JA, Singleton AB, Gasser T (2009) Genome-wide association study reveals genetic risk underlying Parkinson's disease. *Nat Genet* 41:1308–1312 . doi: 10.1038/ng.487
156. Botta-Orfila T, Ezquerra M, Ríos J, Fernández-Santiago R, Cervantes S, Samaranch L, Pastor P, Martí MJ, Muñoz E, Valdeoriola F, Aguilar M, Calopa M, Hernández-Vara J, Tolosa E (2011) Lack of interaction of SNCA and MAPT genotypes in Parkinson's disease. *Eur. J. Neurol.* 18
157. Marti M, Ezquerra Y, Compta MJ (2011) Identifying the genetic components underlying the pathophysiology of movement disorders. *Appl Clin Genet* 4:81 . doi: 10.2147/TACG.S7333
158. Mata IF, Yearout D, Alvarez V, Coto E, de Mena L, Ribacoba R, Lorenzo-Betancor O, Samaranch L, Pastor P, Cervantes S, Infante J, Garcia-Gorostiaga I, Sierra M, Combarros O, Snapinn KW, Edwards KL, Zabetian CP (2011) Replication of MAPT and SNCA, but not PARK16-18, as susceptibility genes for Parkinson's disease. *Mov Disord* 26:819–23 . doi: 10.1002/mds.23642
159. Tan EK, Zhao Y, Skipper L, Tan MG, Di Fonzo A, Sun L, Fook-Chong S, Tang S, Chua E, Yuen Y, Tan L, Pavanni R, Wong MC, Kolatkar P, Lu CS, Bonifati V, Liu JJ (2007) The LRRK2 Gly2385Arg variant is associated with Parkinson's disease: genetic and functional evidence. *Hum Genet* 120:857–863 . doi: 10.1007/s00439-006-0268-0
160. Di Fonzo A, Wu-Chou Y-H, Lu C-S, van Doeselaar M, Simons EJ, Rohé CF, Chang H-C, Chen R-S, Weng Y-H, Vanacore N, Breedveld GJ, Oostra BA, Bonifati V (2006) A common missense variant in the LRRK2 gene, Gly2385Arg, associated with Parkinson's disease risk in Taiwan. *Neurogenetics* 7:133–138 . doi: 10.1007/s10048-006-0041-5
161. Farrer MJ, Stone JT, Lin C-H, Dächsel JC, Hulihan MM, Haugarvoll K, Ross OA, Wu R-M (2007) Lrrk2 G2385R is an ancestral risk factor for Parkinson's disease in Asia. *Parkinsonism Relat Disord* 13:89–92 . doi: 10.1016/j.parkreldis.2006.12.001
162. Tan EK, Schapira AH (2008) Uniting Chinese across Asia: the LRRK2 Gly2385Arg

- risk variant. *Eur J Neurol* 15:203–204 . doi: 10.1111/j.1468-1331.2007.02053.x
163. Skipper L, Wilkes K, Toft M, Baker M, Lincoln S, Hulihan M, Ross OA, Hutton M, Aasly J, Farrer M (2004) Linkage disequilibrium and association of MAPT H1 in Parkinson disease. *Am J Hum Genet* 75:669–77 . doi: 10.1086/424492
164. Elbaz A, Ross OA, Ioannidis JPA, Soto-Ortolaza AI, Moisan F, Aasly J, Annesi G, Bozi M, Brighina L, Chartier-Harlin M-C, Destée A, Ferrarese C, Ferraris A, Gibson JM, Gispert S, Hadjigeorgiou GM, Jasinska-Myga B, Klein C, Krüger R, Lambert J-C, Lohmann K, van de Loo S, Lorient M-A, Lynch T, Mellick GD, Mutez E, Nilsson C, Opala G, Puschmann A, Quattrone A, Sharma M, Silburn PA, Stefanis L, Uitti RJ, Valente EM, Vilariño-Güell C, Wirdefeldt K, Wszolek ZK, Xiromerisiou G, Maraganore DM, Farrer MJ (2011) Independent and joint effects of the MAPT and SNCA genes in Parkinson disease. *Ann Neurol* 69:778–92 . doi: 10.1002/ana.22321
165. Wider C, Vilariño-Güell C, Heckman MG, Jasinska-Myga B, Ortolaza-Soto AI, Diehl NN, Crook JE, Cobb SA, Bacon JA, Aasly JO, Gibson JM, Lynch T, Uitti RJ, Wszolek ZK, Farrer MJ, Ross OA (2011) SNCA, MAPT, and GSK3B in Parkinson disease: a gene-gene interaction study. *Eur J Neurol* 18:876–881 . doi: 10.1111/j.1468-1331.2010.03297.x
166. Brockmann K, Schulte C, Hauser AK, Lichtner P, Huber H, Maetzler W, Berg D, Gasser T (2013) SNCA: Major genetic modifier of age at onset of Parkinson's disease. *Mov Disord* 28:1217–1221 . doi: 10.1002/mds.25469
167. Fernández-Santiago R, Garrido A, Infante J, González-Aramburu I, Sierra M, Fernández M, Valldeoriola F, Muñoz E, Compta Y, Martí MJ, Ríos J, Tolosa E, Ezquerro M (2018) α -synuclein (SNCA) but not dynamin 3 (DNM3) influences age at onset of leucine-rich repeat kinase 2 (LRRK2) Parkinson's disease in Spain. *Mov Disord* 33:637–641 . doi: 10.1002/mds.27295
168. Botta-Orfila T, Ezquerro M, Pastor P, Fernández-Santiago R, Pont-Sunyer C, Compta Y, Lorenzo-Betancor O, Samaranch L, Martí MJ, Valldeoriola F, Calopa M, Fernández M, Aguilar M, de Fabregas O, Hernández-Vara J, Tolosa E (2012) Age at onset in LRRK2-associated PD is modified by SNCA variants. *J Mol Neurosci* 48:245–7 . doi: 10.1007/s12031-012-9820-7
169. Garner CC, Kindler S (1996) Synaptic proteins and the assembly of synaptic junctions. *Trends Cell Biol* 6:429–433 . doi: 10.1016/S0962-8924(96)10036-2
170. Marsden CD (1983) Neuromelanin and Parkinson's disease. *J Neural Transm Suppl* 19:121–41
171. Halliday GM, Ophof A, Broe M, Jensen PH, Kettle E, Fedorow H, Cartwright MI, Griffiths FM, Shepherd CE, Double KL (2005) α -Synuclein redistributes to neuromelanin lipid in the substantia nigra early in Parkinson's disease. *Brain* 128:2654–2664 . doi: 10.1093/brain/awh584
172. Bernheimer H, Birkmayer W, Hornykiewicz O, Jellinger K, Seitelberger F (1973) Brain dopamine and the syndromes of Parkinson and Huntington. Clinical, morphological and neurochemical correlations. *J Neurol Sci* 20:415–55 . doi: 10.1016/0022-510X(73)90175-5
173. Dauer W, Przedborski S (2003) Parkinson's disease: mechanisms and models. *Neuron* 39:889–909 . doi: S0896627303005683 [pii]
174. Fahn S (2003) Description of Parkinson's disease as a clinical syndrome. *Ann N Y Acad Sci* 991:1–14

BIBLIOGRAPHY

175. Uhl GR, Hedreen JC, Price DL (1985) Parkinson's disease: loss of neurons from the ventral tegmental area contralateral to therapeutic surgical lesions. *Neurology* 35:1215–8 . doi: 10.1212/WNL.35.8.1215
176. Dickson DW (2012) Parkinson's disease and parkinsonism: neuropathology. *Cold Spring Harb Perspect Med* 2: . doi: 10.1101/cshperspect.a009258
177. Iwanaga K, Wakabayashi K, Yoshimoto M, Tomita I, Satoh H, Takashima H, Satoh A, Seto M, Tsujihata M, Takahashi H (1999) Lewy body-type degeneration in cardiac plexus in Parkinson's and incidental Lewy body diseases. *Neurology* 52:1269–71
178. Fumimura Y, Ikemura M, Saito Y, Sengoku R, Kanemaru K, Sawabe M, Arai T, Ito G, Iwatsubo T, Fukayama M, Mizusawa H, Murayama S (2007) Analysis of the Adrenal Gland Is Useful for Evaluating Pathology of the Peripheral Autonomic Nervous System in Lewy Body Disease. *J Neuropathol Exp Neurol* 66:354–362 . doi: 10.1097/nen.0b013e3180517454
179. Beach TG, Adler CH, Sue LI, Vedders L, Lue L, White III CL, Akiyama H, Caviness JN, Shill HA, Sabbagh MN, Walker DG, Consortium APD (2010) Multi-organ distribution of phosphorylated α -synuclein histopathology in subjects with Lewy body disorders. *Acta Neuropathol* 119:689–702 . doi: 10.1007/s00401-010-0664-3
180. Del Tredici K, Hawkes CH, Ghebremedhin E, Braak H (2010) Lewy pathology in the submandibular gland of individuals with incidental Lewy body disease and sporadic Parkinson's disease. *Acta Neuropathol* 119:703–713 . doi: 10.1007/s00401-010-0665-2
181. Goldstein DS (2003) Dysautonomia in Parkinson's disease: neurocardiological abnormalities. *Lancet Neurol* 2:669–676 . doi: 10.1016/S1474-4422(03)00555-6
182. Micieli G, Tosi P, Marcheselli S, Cavallini A (2003) Autonomic dysfunction in Parkinson's disease. *Neurol Sci* 24:s32–s34 . doi: 10.1007/s100720300035
183. Shults CW (2006) Lewy bodies. *Proc Natl Acad Sci* 103:1661–1668 . doi: 10.1073/pnas.0509567103
184. Spillantini MG, Schmidt ML, Lee VM-Y, Trojanowski JQ, Jakes R, Goedert M (1997) α -Synuclein in Lewy bodies. *Nature* 388:839–840 . doi: 10.1038/42166
185. Goedert M, Spillantini MG, Del Tredici K, Braak H (2013) 100 years of Lewy pathology. *Nat Rev Neurol* 9:13–24 . doi: 10.1038/nrneurol.2012.242
186. Wakabayashi K, Tanji K, Mori F, Takahashi H (2007) The Lewy body in Parkinson's disease: molecules implicated in the formation and degradation of alpha-synuclein aggregates. *Neuropathology* 27:494–506 . doi: 10.1111/j.1440-1789.2007.00803.x
187. Braak H, Ghebremedhin E, Rub U, Bratzke H, Del Tredici K (2004) Stages in the development of Parkinson's disease-related pathology. *Cell Tissue Res* 318:121–134 . doi: 10.1007/s00441-004-0956-9
188. Visanji NP, Brooks PL, Hazrati L-N, Lang AE (2013) The prion hypothesis in Parkinson's disease: Braak to the future. *Acta Neuropathol Commun* 1:2 . doi: 10.1186/2051-5960-1-2
189. Surmeier DJ (2018) Determinants of dopaminergic neuron loss in Parkinson's disease. *FEBS J*. doi: 10.1111/febs.14607

190. Cook C, Stetler C, Petrucelli L (2012) Disruption of Protein Quality Control in Parkinson's Disease. *Cold Spring Harb Perspect Med* 2:a009423–a009423 . doi: 10.1101/cshperspect.a009423
191. Smith WW, Jiang H, Pei Z, Tanaka Y, Morita H, Sawa A, Dawson VL, Dawson TM, Ross CA (2005) Endoplasmic reticulum stress and mitochondrial cell death pathways mediate A53T mutant alpha-synuclein-induced toxicity. *Hum Mol Genet* 14:3801–3811 . doi: 10.1093/hmg/ddi396
192. Tanaka Y, Engelender S, Igarashi S, Rao RK, Wanner T, Tanzi RE, Sawa A, Dawson V, Dawson TM, Ross CA (2001) Inducible expression of mutant alpha-synuclein decreases proteasome activity and increases sensitivity to mitochondria-dependent apoptosis. *Hum Mol Genet* 10:919–26
193. McNaught KS., Jenner P (2001) Proteasomal function is impaired in substantia nigra in Parkinson's disease. *Neurosci Lett* 297:191–194 . doi: 10.1016/S0304-3940(00)01701-8
194. McNaught KSP, Belizaire R, Isacson O, Jenner P, Olanow CW (2003) Altered proteasomal function in sporadic Parkinson's disease. *Exp Neurol* 179:38–46
195. McNaught KSP, Mytilineou C, JnoBaptiste R, Yabut J, Shashidharan P, Jenner P, Olanow CW (2002) Impairment of the ubiquitin-proteasome system causes dopaminergic cell death and inclusion body formation in ventral mesencephalic cultures. *J Neurochem* 81:301–306 . doi: 10.1046/j.1471-4159.2002.00821.x
196. McNaught KSP, Björklund LM, Belizaire R, Isacson O, Jenner P, Olanow CW (2002) Proteasome inhibition causes nigral degeneration with inclusion bodies in rats. *Neuroreport* 13:1437–41
197. Rideout HJ, Lang-Rollin ICJ, Savalle M, Stefanis L (2005) Dopaminergic neurons in rat ventral midbrain cultures undergo selective apoptosis and form inclusions, but do not up-regulate iHSP70, following proteasomal inhibition. *J Neurochem* 93:1304–1313 . doi: 10.1111/j.1471-4159.2005.03124.x
198. Rideout HJ, Larsen KE, Sulzer D, Stefanis L (2001) Proteasomal inhibition leads to formation of ubiquitin/alpha-synuclein-immunoreactive inclusions in PC12 cells. *J Neurochem* 78:899–908
199. Perrett RM, Alexopoulou Z, Tofaris GK (2015) The endosomal pathway in Parkinson's disease. *Mol Cell Neurosci* 66:21–8 . doi: 10.1016/j.mcn.2015.02.009
200. van Dijk KD, Persichetti E, Chiasserini D, Eusebi P, Beccari T, Calabresi P, Berendse HW, Parnetti L, van de Berg WDJ (2013) Changes in endolysosomal enzyme activities in cerebrospinal fluid of patients with Parkinson's disease. *Mov Disord* 28:747–754 . doi: 10.1002/mds.25495
201. Alvarez-Erviti L, Rodriguez-Oroz MC, Cooper JM, Caballero C, Ferrer I, Obeso JA, Schapira AH V. (2010) Chaperone-Mediated Autophagy Markers in Parkinson Disease Brains. *Arch Neurol* 67:1464–72 . doi: 10.1001/archneurol.2010.198
202. Banerjee R, Beal MF, Thomas B (2010) Autophagy in neurodegenerative disorders: pathogenic roles and therapeutic implications. *Trends Neurosci* 33:541–549 . doi: 10.1016/j.tins.2010.09.001
203. Spencer B, Potkar R, Trejo M, Rockenstein E, Patrick C, Gindi R, Adame A, Wyss-Coray T, Masliah E (2009) Beclin 1 gene transfer activates autophagy and ameliorates the neurodegenerative pathology in alpha-synuclein models of Parkinson's and Lewy body diseases. *J Neurosci* 29:13578–88 . doi: 10.1523/JNEUROSCI.4390-09.2009

BIBLIOGRAPHY

204. Xilouri M, Stefanis L (2011) Autophagic pathways in Parkinson disease and related disorders. *Expert Rev Mol Med* 13:e8 . doi: 10.1017/S1462399411001803
205. Decressac M, Mattsson B, Weikop P, Lundblad M, Jakobsson J, Bjorklund A (2013) TFEB-mediated autophagy rescues midbrain dopamine neurons from -synuclein toxicity. *Proc Natl Acad Sci* 110:E1817–E1826 . doi: 10.1073/pnas.1305623110
206. Dehay B, Bové J, Rodríguez-Muela N, Perier C, Recasens A, Boya P, Vila M (2010) Pathogenic lysosomal depletion in Parkinson's disease. *J Neurosci* 30:12535–44 . doi: 10.1523/JNEUROSCI.1920-10.2010
207. Xiong N, Jia M, Chen C, Xiong J, Zhang Z, Huang J, Hou L, Yang H, Cao X, Liang Z, Sun S, Lin Z, Wang T (2011) Potential autophagy enhancers attenuate rotenone-induced toxicity in SH-SY5Y. *Neuroscience* 199:292–302 . doi: 10.1016/j.neuroscience.2011.10.031
208. Kordower JH, Chu Y, Hauser RA, Olanow CW, Freeman TB (2008) Transplanted dopaminergic neurons develop PD pathologic changes: A second case report. *Mov Disord* 23:2303–2306 . doi: 10.1002/mds.22369
209. Kordower JH, Chu Y, Hauser RA, Freeman TB, Olanow CW (2008) Lewy body–like pathology in long-term embryonic nigral transplants in Parkinson's disease. *Nat Med* 14:504–506 . doi: 10.1038/nm1747
210. Li J-Y, Englund E, Holton JL, Soulet D, Hagell P, Lees AJ, Lashley T, Quinn NP, Rehn Crona S, Björklund A, Widner H, Revesz T, Lindvall O, Brundin P (2008) Lewy bodies in grafted neurons in subjects with Parkinson's disease suggest host-to-graft disease propagation. *Nat Med* 14:501–503 . doi: 10.1038/nm1746
211. Luk KC, Kehm V, Carroll J, Zhang B, O'Brien P, Trojanowski JQ, Lee VM-Y (2012) Pathological -Synuclein Transmission Initiates Parkinson-like Neurodegeneration in Nontransgenic Mice. *Science* (80-) 338:949–953 . doi: 10.1126/science.1227157
212. Luk KC, Kehm VM, Zhang B, O'Brien P, Trojanowski JQ, Lee VMY (2012) Intracerebral inoculation of pathological α -synuclein initiates a rapidly progressive neurodegenerative α -synucleinopathy in mice. *J Exp Med* 209:975–986 . doi: 10.1084/jem.20112457
213. Masuda-Suzukake M, Nonaka T, Hosokawa M, Oikawa T, Arai T, Akiyama H, Mann DMA, Hasegawa M (2013) Prion-like spreading of pathological α -synuclein in brain. *Brain* 136:1128–1138 . doi: 10.1093/brain/awt037
214. Recasens A, Dehay B, Bové J, Carballo-Carbajal I, Dovero S, Pérez-Villalba A, Fernagut P-O, Blesa J, Parent A, Perier C, Fariñas I, Obeso JA, Bezard E, Vila M (2014) Lewy body extracts from Parkinson disease brains trigger α -synuclein pathology and neurodegeneration in mice and monkeys. *Ann Neurol* 75:351–362 . doi: 10.1002/ana.24066
215. Danzer KM, Haasen D, Karow AR, Moussaud S, Habeck M, Giese A, Kretschmar H, Hengerer B, Kostka M (2007) Different Species of -Synuclein Oligomers Induce Calcium Influx and Seeding. *J Neurosci* 27:9220–9232 . doi: 10.1523/JNEUROSCI.2617-07.2007
216. Fontaine SN, Zheng D, Sabbagh JJ, Martin MD, Chaput D, Darling A, Trotter JH, Stothert AR, Nordhues BA, Lussier A, Baker J, Shelton L, Kahn M, Blair LJ, Stevens SM, Dickey CA (2016) DnaJ/Hsc70 chaperone complexes control the extracellular release of neurodegenerative-associated proteins. *EMBO J*

- 35:1537–49 . doi: 10.15252/embj.201593489
217. Abounit S, Bousset L, Loria F, Zhu S, de Chaumont F, Pieri L, Olivo-Marin J-C, Melki R, Zurzolo C (2016) Tunneling nanotubes spread fibrillar α -synuclein by intercellular trafficking of lysosomes. *EMBO J* 35:2120–2138 . doi: 10.15252/embj.201593411
 218. Emmanouilidou E, Melachroinou K, Roumeliotis T, Garbis SD, Ntzouni M, Margaritis LH, Stefanis L, Vekrellis K (2010) Cell-produced alpha-synuclein is secreted in a calcium-dependent manner by exosomes and impacts neuronal survival. *J Neurosci* 30:6838–51 . doi: 10.1523/JNEUROSCI.5699-09.2010
 219. Stuendl A, Kunadt M, Kruse N, Bartels C, Moebius W, Danzer KM, Mollenhauer B, Schneider A (2016) Induction of α -synuclein aggregate formation by CSF exosomes from patients with Parkinson's disease and dementia with Lewy bodies. *Brain* 139:481–494 . doi: 10.1093/brain/awv346
 220. Danzer KM, Kranich LR, Ruf WP, Cagsal-Getkin O, Winslow AR, Zhu L, Vanderburg CR, McLean PJ (2012) Exosomal cell-to-cell transmission of alpha synuclein oligomers. *Mol Neurodegener* 7:42 . doi: 10.1186/1750-1326-7-42
 221. Winklhofer KF, Haass C (2010) Mitochondrial dysfunction in Parkinson's disease. *Biochim Biophys Acta - Mol Basis Dis* 1802:29–44 . doi: 10.1016/j.bbadis.2009.08.013
 222. Mann VM, Cooper JM, Daniel SE, Srai K, Jenner P, Marsden CD, Schapira AH V. (1994) Complex I, Iron, and ferritin in Parkinson's disease substantia nigra. *Ann Neurol* 36:876–881 . doi: 10.1002/ana.410360612
 223. Pickrell AM, Youle RJ (2015) The Roles of PINK1, Parkin, and Mitochondrial Fidelity in Parkinson's Disease. *Neuron* 85:257–273 . doi: 10.1016/j.neuron.2014.12.007
 224. McLelland G-L, Soubannier V, Chen CX, McBride HM, Fon EA (2014) Parkin and PINK1 function in a vesicular trafficking pathway regulating mitochondrial quality control. *EMBO J* 33:n/a-n/a . doi: 10.1002/embj.201385902
 225. Tanti GK, Goswami SK (2014) SG2NA recruits DJ-1 and Akt into the mitochondria and membrane to protect cells from oxidative damage. *Free Radic Biol Med* 75:1–13 . doi: 10.1016/j.freeradbiomed.2014.07.009
 226. van der Merwe C, Jalali Sefid Dashti Z, Christoffels A, Loos B, Bardien S (2015) Evidence for a common biological pathway linking three Parkinson's disease-causing genes: *parkin*, *PINK1* and *DJ-1*. *Eur J Neurosci* 41:1113–1125 . doi: 10.1111/ejn.12872
 227. Langston JW, Ballard P, Tetrud JW, Irwin I (1983) Chronic Parkinsonism in humans due to a product of meperidine-analog synthesis. *Science* 219:979–80
 228. Blum D, Torch S, Lambeng N, Nissou M, Benabid AL, Sadoul R, Verna JM (2001) Molecular pathways involved in the neurotoxicity of 6-OHDA, dopamine and MPTP: contribution to the apoptotic theory in Parkinson's disease. *Prog Neurobiol* 65:135–72
 229. Martinez TN, Greenamyre JT (2012) Toxin Models of Mitochondrial Dysfunction in Parkinson's Disease. *Antioxid Redox Signal* 16:920–934 . doi: 10.1089/ars.2011.4033
 230. Jenner P (1998) Oxidative mechanisms in nigral cell death in Parkinson's disease. *Mov Disord* 13 Suppl 1:24–34

BIBLIOGRAPHY

231. Muñoz P, Huenchuguala S, Paris I, Segura-Aguilar J (2012) Dopamine Oxidation and Autophagy. *Parkinsons Dis* 2012:1–13 . doi: 10.1155/2012/920953
232. Sian J, Dexter DT, Lees AJ, Daniel S, Agid Y, Javoy-Agid F, Jenner P, Marsden CD (1994) Alterations in glutathione levels in Parkinson's disease and other neurodegenerative disorders affecting basal ganglia. *Ann Neurol* 36:348–355 . doi: 10.1002/ana.410360305
233. Przedborski S, Jackson-Lewis V, Vila M, Wu DC, Teismann P, Tieu K, Choi D-K, Cohen O (2003) Free radical and nitric oxide toxicity in Parkinson's disease. *Adv Neurol* 91:83–94
234. Fahn S (2011) Classification of movement disorders. *Mov Disord* 26:947–57 . doi: 10.1002/mds.23759
235. Connolly BS, Lang AE (2014) Pharmacological Treatment of Parkinson Disease. *JAMA* 311:1670 . doi: 10.1001/jama.2014.3654
236. Fox SH, Katzenschlager R, Lim S-Y, Ravina B, Seppi K, Coelho M, Poewe W, Rascol O, Goetz CG, Sampaio C (2011) The Movement Disorder Society Evidence-Based Medicine Review Update: Treatments for the motor symptoms of Parkinson's disease. *Mov Disord* 26:S2–S41 . doi: 10.1002/mds.23829
237. Kalia SK, Sankar T, Lozano AM (2013) Deep brain stimulation for Parkinson's disease and other movement disorders. *Curr Opin Neurol* 26:374–380 . doi: 10.1097/WCO.0b013e3283632d08
238. Fasano A, Daniele A, Albanese A (2012) Treatment of motor and non-motor features of Parkinson's disease with deep brain stimulation. *Lancet Neurol* 11:429–442 . doi: 10.1016/S1474-4422(12)70049-2
239. Ahlskog JE (2001) Parkinson's disease: medical and surgical treatment. *Neurol Clin* 19:579–605, vi
240. Jenner P (2008) Molecular mechanisms of L-DOPA-induced dyskinesia. *Nat Rev Neurosci* 9:665–677 . doi: 10.1038/nrn2471
241. Picconi B, Hernández LF, Obeso JA, Calabresi P (2018) Motor complications in Parkinson's disease: Striatal molecular and electrophysiological mechanisms of dyskinesias. *Mov Disord* 33:867–876 . doi: 10.1002/mds.27261
242. Bastide MF, Meissner WG, Picconi B, Fasano S, Fernagut P-OO, Feyder M, Francardo V, Alcacer C, Ding Y, Brambilla R, Fisone G, Jon Stoessl A, Bourdenx M, Engeln M, Navailles S, De Deurwaerdère P, Ko WKD, Simola N, Morelli M, Groc L, Rodriguez M-CC, Gurevich E V., Quik M, Morari M, Mellone M, Gardoni F, Tronci E, Guehl D, Tison FF, Crossman AR, Kang UJ, Steece-Collier K, Fox S, Carta M, Angela Cenci M, Bézard E (2015) Pathophysiology of L-dopa-induced motor and non-motor complications in Parkinson's disease 132:96-168. doi: 10.1016/j.pneurobio.2015.07.002
243. Calabresi P, Filippo M Di, Ghiglieri V, Tambasco N, Picconi B (2010) Levodopa-induced dyskinesias in patients with Parkinson's disease: filling the bench-to bedside gap. *Lancet Neurol* 9:1106–1117 . doi: 10.1016/S1474-4422(10)70218-0
244. Goetz CG, Stebbins GT, Tilley BC (2012) Calibration of unified Parkinson's disease rating scale scores to Movement Disorder Society-unified Parkinson's disease rating scale scores. *Mov Disord* 27:1239–1242 . doi: 10.1002/mds.25122
245. Manson A, Stirpe P, Schrag A (2012) Levodopa-induced-dyskinesias clinical features, incidence, risk factors, management and impact on quality of life. *J*

- Parkinsons Dis* 2:189–98 . doi: 10.3233/JPD-2012-120103
246. Kaplan N, Vituri A, Korczyn AD, Cohen OS, Inzelberg R, Yahalom G, Kozlova E, Milgrom R, Laitman Y, Friedman E, Rosset S, Hassin-Baer S (2014) Sequence variants in SLC6A3, DRD2, and BDNF genes and time to levodopa-induced dyskinesias in Parkinson's disease. *J Mol Neurosci* 53:183-8 . doi: 10.1007/s12031-014-0276-9
247. Foltynie T, Cheeran B, Williams-Gray CH, Edwards MJ, Schneider SA, Weinberger D, Rothwell JC, Barker RA, Bhatia KP (2009) BDNF val66met influences time to onset of levodopa induced dyskinesia in Parkinson's disease. *J Neurol Neurosurg Psychiatry* 80:141–4 . doi: 10.1136/jnnp.2008.154294
248. Zappia M, Annesi G, Nicoletti G, Arabia G, Annesi F, Messina D, Pugliese P, Spadafora P, Tarantino P, Carrideo S, Civitelli D, De Marco E V., Cirò-Candiano IC, Gambardella A, Quattrone A (2005) Sex Differences in Clinical and Genetic Determinants of Levodopa Peak-Dose Dyskinesias in Parkinson Disease. *Arch Neurol* 62:601 . doi: 10.1001/archneur.62.4.601
249. Laplante M, Sabatini DM (2012) mTOR Signaling in Growth Control and Disease. *Cell* 149:274–293 . doi: 10.1016/j.cell.2012.03.017
250. Bockaert J, Marin P (2015) mTOR in Brain Physiology and Pathologies. *Physiol Rev* 95:1157–1187 . doi: 10.1152/physrev.00038.2014
251. Vézina C, Kudelski A, Sehgal SN (1975) Rapamycin (AY-22,989), a new antifungal antibiotic. I. Taxonomy of the producing streptomycete and isolation of the active principle. *J Antibiot (Tokyo)* 28:721–6
252. Martel RR, Klicius J, Galet S (1977) Inhibition of the immune response by rapamycin, a new antifungal antibiotic. *Can J Physiol Pharmacol* 55:48–51
253. Laplante M, Sabatini DM (2009) mTOR signaling at a glance. *J Cell Sci* 122:3589–94 . doi: 10.1242/jcs.051011
254. Sarbassov DD, Ali SM, Sengupta S, Sheen J-H, Hsu PP, Bagley AF, Markhard AL, Sabatini DM (2006) Prolonged rapamycin treatment inhibits mTORC2 assembly and Akt/PKB. *Mol Cell* 22:159–68 . doi: 10.1016/j.molcel.2006.03.029
255. Inoki K, Li Y, Zhu T, Wu J, Guan K-L (2002) TSC2 is phosphorylated and inhibited by Akt and suppresses mTOR signalling. *Nat Cell Biol* 4:648–57 . doi: 10.1038/ncb839
256. Ma L, Chen Z, Erdjument-Bromage H, Tempst P, Pandolfi PP (2005) Phosphorylation and Functional Inactivation of TSC2 by Erk. *Cell* 121:179–193 . doi: 10.1016/j.cell.2005.02.031
257. Tee AR, Fingar DC, Manning BD, Kwiatkowski DJ, Cantley LC, Blenis J (2002) Tuberous sclerosis complex-1 and -2 gene products function together to inhibit mammalian target of rapamycin (mTOR)-mediated downstream signaling. *Proc Natl Acad Sci U S A* 99:13571–6 . doi: 10.1073/pnas.202476899
258. Roux PP, Ballif BA, Anjum R, Gygi SP, Blenis J (2004) Tumor-promoting phorbol esters and activated Ras inactivate the tuberous sclerosis tumor suppressor complex via p90 ribosomal S6 kinase. *Proc Natl Acad Sci U S A* 101:13489–94 . doi: 10.1073/pnas.0405659101
259. Dibble CC, Elis W, Menon S, Qin W, Klekota J, Asara JM, Finan PM, Kwiatkowski DJ, Murphy LO, Manning BD (2012) TBC1D7 Is a Third Subunit of the TSC1-TSC2 Complex Upstream of mTORC1. *Mol Cell* 47:535–546 . doi:

- 10.1016/j.molcel.2012.06.009
260. Inoki K, Li Y, Xu T, Guan K-L (2003) Rheb GTPase is a direct target of TSC2 GAP activity and regulates mTOR signaling. *Genes Dev* 17:1829–1834 . doi: 10.1101/gad.1110003
261. Tee AR, Manning BD, Roux PP, Cantley LC, Blenis J (2003) Tuberous sclerosis complex gene products, Tuberin and Hamartin, control mTOR signaling by acting as a GTPase-activating protein complex toward Rheb. *Curr Biol* 13:1259–68
262. Garami A, Zwartkruis FJT, Nobukuni T, Joaquin M, Rocco M, Stocker H, Kozma SC, Hafen E, Bos JL, Thomas G (2003) Insulin activation of Rheb, a mediator of mTOR/S6K/4E-BP signaling, is inhibited by TSC1 and 2. *Mol Cell* 11:1457–66
263. Malagelada C, Ryu EJ, Biswas SC, Jackson-Lewis V, Greene LA (2006) RTP801 is elevated in Parkinson brain substantia nigral neurons and mediates death in cellular models of Parkinson's disease by a mechanism involving mammalian target of rapamycin inactivation. *J Neurosci* 26:9996–10005 . doi: 10.1523/JNEUROSCI.3292-06.2006
264. Malagelada C, Zong HJ, Greene LALA, Jin ZH, Greene LALA (2008) RTP801 is induced in Parkinson's disease and mediates neuron death by inhibiting Akt phosphorylation/activation. *J Neurosci* 28:14363–71 . doi: 10.1523/JNEUROSCI.3928-08.2008
265. Wullschleger S, Loewith R, Hall MN (2006) TOR Signaling in Growth and Metabolism. *Cell* 124:471–484 . doi: 10.1016/j.cell.2006.01.016
266. Shoshani T, Faerman A, Mett I, Zelin E, Tenne T, Gorodin S, Moshel Y, Elbaz S, Budanov A, Chajut A, Kalinski H, Kamer I, Rozen A, Mor O, Keshet E, Leshkowitz D, Einat P, Skaliter R, Feinstein E (2002) Identification of a novel hypoxia-inducible factor 1-responsive gene, RTP801, involved in apoptosis. *Mol Cell Biol* 22:2283–93 . doi: 10.1128/MCB.22.7.2283
267. Brugarolas J, Lei K, Hurley RL, Manning BD, Reiling JH, Hafen E, Witters LA, Ellisen LW, Kaelin Jr. WG, Kaelin WG (2004) Regulation of mTOR function in response to hypoxia by REDD1 and the TSC1/TSC2 tumor suppressor complex. *Genes Dev* 18:2893–2904 . doi: 10.1101/gad.1256804
268. Manning BD, Cantley LC (2007) AKT/PKB Signaling: Navigating Downstream. *Cell* 129:1261–1274 . doi: 10.1016/j.cell.2007.06.009
269. Franke TF (2008) PI3K/Akt: getting it right matters. *Oncogene* 27:6473–6488 . doi: 10.1038/onc.2008.313
270. Manning BD, Tee AR, Logsdon MN, Blenis J, Cantley LC (2002) Identification of the tuberous sclerosis complex-2 tumor suppressor gene product tuberin as a target of the phosphoinositide 3-kinase/akt pathway. *Mol Cell* 10:151–62
271. Potter CJ, Pedraza LG, Xu T (2002) Akt regulates growth by directly phosphorylating Tsc2. *Nat Cell Biol* 4:658–665 . doi: 10.1038/ncb840
272. Sancak Y, Thoreen CC, Peterson TR, Lindquist RA, Kang SA, Spooner E, Carr SA, Sabatini DM (2007) PRAS40 is an insulin-regulated inhibitor of the mTORC1 protein kinase. *Mol Cell* 25:903–15 . doi: 10.1016/j.molcel.2007.03.003
273. Thedieck K, Polak P, Kim ML, Molle KD, Cohen A, Jenö P, Arriemerlou C, Hall MN (2007) PRAS40 and PRR5-like protein are new mTOR interactors that regulate apoptosis. *PLoS One* 2:e1217 . doi: 10.1371/journal.pone.0001217

274. Vander Haar E, Lee S-I, Bandhakavi S, Griffin TJ, Kim D-H (2007) Insulin signalling to mTOR mediated by the Akt/PKB substrate PRAS40. *Nat Cell Biol* 9:316–23 . doi: 10.1038/ncb1547
275. Wang L, Harris TE, Roth RA, Lawrence JC (2007) PRAS40 regulates mTORC1 kinase activity by functioning as a direct inhibitor of substrate binding. *J Biol Chem* 282:20036–44 . doi: 10.1074/jbc.M702376200
276. Dudek H, Datta SR, Franke TF, Birnbaum MJ, Yao R, Cooper GM, Segal RA, Kaplan DR, Greenberg ME (1997) Regulation of neuronal survival by the serine-threonine protein kinase Akt. *Science* 275:661–5
277. Crowder RJ, Freeman RS (1998) Phosphatidylinositol 3-kinase and Akt protein kinase are necessary and sufficient for the survival of nerve growth factor-dependent sympathetic neurons. *J Neurosci* 18:2933–43
278. Brunet A, Datta SR, Greenberg ME (2001) Transcription-dependent and -independent control of neuronal survival by the PI3K-Akt signaling pathway. *Curr Opin Neurobiol* 11:297–305
279. Orike N, Middleton G, Borthwick E, Buchman V, Cowen T, Davies AM (2001) Role of PI 3-kinase, Akt and Bcl-2-related proteins in sustaining the survival of neurotrophic factor-independent adult sympathetic neurons. *J Cell Biol* 154:995–1005 . doi: 10.1083/jcb.200101068
280. Duronio V (2008) The life of a cell: apoptosis regulation by the PI3K/PKB pathway. *Biochem J* 415:333–344 . doi: 10.1042/BJ20081056
281. Greene LA, Levy O, Malagelada C (2011) Akt as a Victim, Villain and Potential Hero in Parkinson's Disease Pathophysiology and Treatment. *Cell Mol Neurobiol* 31:969–978 . doi: 10.1007/s10571-011-9671-8
282. Costa-Mattioli M, Sossin WS, Klann E, Sonenberg N (2009) Translational Control of Long-Lasting Synaptic Plasticity and Memory. *Neuron* 61:10–26 . doi: 10.1016/j.neuron.2008.10.055
283. Buffington SA, Huang W, Costa-Mattioli M (2014) Translational Control in Synaptic Plasticity and Cognitive Dysfunction. *Annu Rev Neurosci* 37:17–38 . doi: 10.1146/annurev-neuro-071013-014100
284. Richter JD, Klann E (2009) Making synaptic plasticity and memory last: mechanisms of translational regulation. *Genes Dev* 23:1–11 . doi: 10.1101/gad.1735809
285. Sarkar S, Ravikumar B, Floto R a, Rubinsztein DC (2009) Rapamycin and mTOR-independent autophagy inducers ameliorate toxicity of polyglutamine-expanded huntingtin and related proteinopathies. *Cell Death Differ* 16:46–56 . doi: 10.1038/cdd.2008.110
286. Tain LS, Mortiboys H, Tao RN, Ziviani E, Bandmann O, Whitworth AJ (2009) Rapamycin activation of 4E-BP prevents parkinsonian dopaminergic neuron loss. *Nat Neurosci* 12:1129–1135 . doi: nn.2372 [pii]10.1038/nn.2372
287. Creus-Muncunill J, Rué L, Alcalá-Vida R, Badillos-Rodríguez R, Romani-Aumedes J, Marco S, Alberch J, Perez-Otaño I, Malagelada C, Pérez-Navarro E (2018) Increased Levels of Rictor Prevent Mutant Huntingtin-Induced Neuronal Degeneration. *Mol Neurobiol*. doi: 10.1007/s12035-018-0956-5
288. Floto RA, Sarkar S, Perlstein EO, Kampmann B, Schreiber SL, Rubinsztein DC Small molecule enhancers of rapamycin-induced TOR inhibition promote

- autophagy, reduce toxicity in Huntington's disease models and enhance killing of mycobacteria by macrophages. *Autophagy* 3:620–2
289. Roscic A, Baldo B, Crochemore C, Marcellin D, Paganetti P (2011) Induction of autophagy with catalytic mTOR inhibitors reduces huntingtin aggregates in a neuronal cell model. *J Neurochem* 119:398–407 . doi: 10.1111/j.1471-4159.2011.07435.x
290. Lee JH, Tecedor L, Chen YH, Monteys AM, Sowada MJ, Thompson LM, Davidson BL (2015) Reinstating Aberrant mTORC1 Activity in Huntington's Disease Mice Improves Disease Phenotypes. *Neuron* 85:303–315 . doi: 10.1016/j.neuron.2014.12.019
291. Mealer RG, Murray AJ, Shahani N, Subramaniam S, Snyder SH (2014) Rhes, a striatal-selective protein implicated in Huntington disease, binds beclin-1 and activates autophagy. *J Biol Chem* 289:3547–54 . doi: 10.1074/jbc.M113.536912
292. Subramaniam S, Sixt KM, Barrow R, Snyder SH (2009) Rhes, a striatal specific protein, mediates mutant-huntingtin cytotoxicity. *Science* 324:1327–30 . doi: 10.1126/science.1172871
293. Mealer RG, Subramaniam S, Snyder SH (2013) Rhes Deletion Is Neuroprotective in the 3-Nitropropionic Acid Model of Huntington's Disease. *J Neurosci* 33:4206–4210 . doi: 10.1523/JNEUROSCI.3730-12.2013
294. Baiamonte BA, Lee FA, Brewer ST, Spano D, LaHoste GJ (2013) Attenuation of Rhes Activity Significantly Delays the Appearance of Behavioral Symptoms in a Mouse Model of Huntington's Disease. *PLoS One* 8:e53606 . doi: 10.1371/journal.pone.0053606
295. Gines S, Ivanova E, Seong I-S, Saura CA, MacDonald ME (2003) Enhanced Akt signaling is an early pro-survival response that reflects N-methyl-D-aspartate receptor activation in Huntington's disease knock-in striatal cells. *J Biol Chem* 278:50514–22 . doi: 10.1074/jbc.M309348200
296. Saavedra A, García-Martínez JM, Xifró X, Giralt A, Torres-Peraza JF, Canals JM, Díaz-Hernández M, Lucas JJ, Alberch J, Pérez-Navarro E (2010) PH domain leucine-rich repeat protein phosphatase 1 contributes to maintain the activation of the PI3K/Akt pro-survival pathway in Huntington's disease striatum. *Cell Death Differ* 17:324–335 . doi: 10.1038/cdd.2009.127
297. Gao T, Furnari F, Newton AC (2005) PHLPP: A Phosphatase that Directly Dephosphorylates Akt, Promotes Apoptosis, and Suppresses Tumor Growth. *Mol Cell* 18:13–24 . doi: 10.1016/j.molcel.2005.03.008
298. Bayascas JR, Alessi DR (2005) Regulation of Akt/PKB Ser473 Phosphorylation. *Mol Cell* 18:143–145 . doi: 10.1016/j.molcel.2005.03.020
299. Colin E, Régulier E, Perrin V, Dürr A, Brice A, Aebischer P, Déglon N, Humbert S, Saudou F (2005) Akt is altered in an animal model of Huntington's disease and in patients. *Eur J Neurosci* 21:1478–1488 . doi: 10.1111/j.1460-9568.2005.03985.x
300. Spencer B, Potkar R, Trejo M, Rockenstein E, Patrick C, Gindi R, Adame A, Wyss-Coray T, Masliah E (2009) Beclin 1 Gene Transfer Activates Autophagy and Ameliorates the Neurodegenerative Pathology in α -Synuclein Models of Parkinson's and Lewy Body Diseases. *J Neurosci* 29:13578–13588 . doi: 10.1523/JNEUROSCI.4390-09.2009
301. Crews L, Spencer B, Desplats P, Patrick C, Paulino A, Rockenstein E, Hansen L, Adame A, Galasko D, Masliah E (2010) elective molecular alterations in the

- autophagy pathway in patients with Lewy body diseases and in models of alpha-synucleinopathy. *PLoS One* 5:e9313 . doi: 10.1371/journal.pone.0009313
302. Cuervo AM, Stefanis L, Fredenburg R, Lansbury PT, Sulzer D (2004) Impaired degradation of mutant alpha-synuclein by chaperone-mediated autophagy. *Science* 305:1292–5 . doi: 10.1126/science.1101738
303. Masini D, Bonito-Oliva A, Bertho M, Fisone G (2018) Inhibition of mTORC1 Signaling Reverts Cognitive and Affective Deficits in a Mouse Model of Parkinson's Disease. *Front Neurol* 9:208 . doi: 10.3389/fneur.2018.00208
304. Bové J, Prou D, Perier C, Przedborski S (2005) Toxin-induced models of Parkinson's disease. *NeuroRx* 2:484–94 . doi: 10.1602/neurorx.2.3.484
305. Rieker C, Engblom D, Kreiner G, Domanskyi A, Schober A, Stotz S, Neumann M, Yuan X, Grummt I, Schütz G, Parlato R (2011) Nucleolar disruption in dopaminergic neurons leads to oxidative damage and parkinsonism through repression of mammalian target of rapamycin signaling. *J Neurosci* 31:453–60 . doi: 10.1523/JNEUROSCI.0590-10.2011
306. Malagelada C, Jin ZH, Jackson-Lewis V, Przedborski S, Greene LA (2010) Rapamycin protects against neuron death in in vitro and in vivo models of Parkinson's disease. *J Neurosci* 30:1166–1175 . doi: 10.1523/JNEUROSCI.3944-09.2010
307. Cheng H-C, Kim SR, Oo TF, Kareva T, Yarygina O, Rzhetskaya M, Wang C, Doring M, Talloczy Z, Tanaka K, Komatsu M, Kobayashi K, Okano H, Kholodilov N, Burke RE (2011) Akt Suppresses Retrograde Degeneration of Dopaminergic Axons by Inhibition of Macroautophagy. *J Neurosci* 31:2125–2135 . doi: 10.1523/JNEUROSCI.5519-10.2011
308. Ries V, Henchcliffe C, Kareva T, Rzhetskaya M, Bland R, Doring MJ, Kholodilov N, Burke RE (2006) Oncoprotein Akt/PKB induces trophic effects in murine models of Parkinson's disease. *Proc Natl Acad Sci U S A* 103:18757–62 . doi: 10.1073/pnas.0606401103
309. Kim SR, Kareva T, Yarygina O, Kholodilov N, Burke RE (2012) AAV transduction of dopamine neurons with constitutively active Rheb protects from neurodegeneration and mediates axon regrowth. *Mol Ther* 20:275–86 . doi: 10.1038/mt.2011.213
310. Domanskyi A, Geißler C, Vinnikov IA, Alter H, Schober A, Vogt MA, Gass P, Parlato R, Schütz G (2011) *Pten* ablation in adult dopaminergic neurons is neuroprotective in Parkinson's disease models. *FASEB J* 25:2898–2910 . doi: 10.1096/fj.11-181958
311. Xu Y, Liu C, Chen S, Ye Y, Guo M, Ren Q, Liu L, Zhang H, Xu C, Zhou Q, Huang S, Chen L (2014) Activation of AMPK and inactivation of Akt result in suppression of mTOR-mediated S6K1 and 4E-BP1 pathways leading to neuronal cell death in in vitro models of Parkinson's disease. *Cell Signal* 26:1680–1689 . doi: 10.1016/j.cellsig.2014.04.009
312. Zhou Q, Liu C, Liu W, Zhang H, Zhang R, Liu J, Zhang J, Xu C, Liu L, Huang S, Chen L (2015) Rotenone Induction of Hydrogen Peroxide Inhibits mTOR-mediated S6K1 and 4E-BP1/eIF4E Pathways, Leading to Neuronal Apoptosis. *Toxicol Sci* 143:81–96 . doi: 10.1093/toxsci/kfu211
313. DeYoung MP, Horak P, Sofer A, Sgroi D, Ellisen LW (2008) Hypoxia regulates TSC1/2-mTOR signaling and tumor suppression through REDD1-mediated 14-3-

- 3 shuttling. *Genes Dev* 22:239–51 . doi: 10.1101/gad.1617608
314. Costa-Mattioli M, Monteggia LM (2013) mTOR complexes in neurodevelopmental and neuropsychiatric disorders. *Nat Neurosci* 16:1537–1543 . doi: 10.1038/nn.3546
315. LiCausi F, Hartman NW (2018) Role of mTOR Complexes in Neurogenesis. *Int J Mol Sci* 19:1544 . doi: 10.3390/ijms19051544
316. Santini E, Huynh TN, Klann E (2014) Mechanisms of Translation Control Underlying Long-Lasting Synaptic Plasticity and the Consolidation of Long-Term Memory. In: *Progress in molecular biology and translational science*. pp 131–167
317. Lipton JO, Sahin M (2014) The Neurology of mTOR. *Neuron* 84:275–291 . doi: 10.1016/j.neuron.2014.09.034
318. Stoica L, Zhu PJ, Huang W, Zhou H, Kozma SC, Costa-Mattioli M (2011) Selective pharmacogenetic inhibition of mammalian target of Rapamycin complex I (mTORC1) blocks long-term synaptic plasticity and memory storage. *Proc Natl Acad Sci* 108:3791–3796 . doi: 10.1073/pnas.1014715108
319. Hoeffler CA, Tang W, Wong H, Santillan A, Patterson RJ, Martinez LA, Tejada-Simon M V., Paylor R, Hamilton SL, Klann E (2008) Removal of FKBP12 Enhances mTOR-Raptor Interactions, LTP, Memory, and Perseverative/Repetitive Behavior. *Neuron* 60:832–845 . doi: 10.1016/j.neuron.2008.09.037
320. Hou L, Klann E (2004) Activation of the Phosphoinositide 3-Kinase-Akt-Mammalian Target of Rapamycin Signaling Pathway Is Required for Metabotropic Glutamate Receptor-Dependent Long-Term Depression. *J Neurosci* 24:6352–6361 . doi: 10.1523/JNEUROSCI.0995-04.2004
321. Huber KM, Kayser MS, Bear MF (2000) Role for rapid dendritic protein synthesis in hippocampal mGluR-dependent long-term depression. *Science* 288:1254–7
322. Wang Y, Barbaro MF, Baraban SC (2006) A role for the mTOR pathway in surface expression of AMPA receptors. *Neurosci Lett* 401:35–39 . doi: 10.1016/j.neulet.2006.03.011
323. Ran I, Gkogkas CG, Vasuta C, Tartas M, Khoutorsky A, Laplante I, Parsyan A, Nevarko T, Sonenberg N, Lacaille J-C (2013) Selective regulation of GluA subunit synthesis and AMPA receptor-mediated synaptic function and plasticity by the translation repressor 4E-BP2 in hippocampal pyramidal cells. *J Neurosci* 33:1872–86 . doi: 10.1523/JNEUROSCI.3264-12.2013
324. Fortin DA, Srivastava T, Dwarakanath D, Pierre P, Nygaard S, Derkach VA, Soderling TR (2012) Brain-Derived Neurotrophic Factor Activation of CaM-Kinase Kinase via Transient Receptor Potential Canonical Channels Induces the Translation and Synaptic Incorporation of GluA1-Containing Calcium-Permeable AMPA Receptors. *J Neurosci* 32:8127–8137 . doi: 10.1523/JNEUROSCI.6034-11.2012
325. Li X, Wolf ME (2011) Brain-derived neurotrophic factor rapidly increases AMPA receptor surface expression in rat nucleus accumbens. *Eur J Neurosci* 34:190–8 . doi: 10.1111/j.1460-9568.2011.07754.x
326. Wei J, Liu W, Yan Z (2010) Regulation of AMPA Receptor Trafficking and Function by Glycogen Synthase Kinase 3. *J Biol Chem* 285:26369–26376 . doi: 10.1074/jbc.M110.121376

327. Yagishita S, Murayama M, Ebihara T, Maruyama K, Takashima A (2015) Glycogen Synthase Kinase 3 β -mediated Phosphorylation in the Most C-terminal Region of Protein Interacting with C Kinase 1 (PICK1) Regulates the Binding of PICK1 to Glutamate Receptor Subunit GluA2. *J Biol Chem* 290:29438–48 . doi: 10.1074/jbc.M114.619668
328. Beurel E, Grieco SF, Amadei C, Downey K, Jope RS (2016) Ketamine-induced inhibition of glycogen synthase kinase-3 contributes to the augmentation of α -amino-3-hydroxy-5-methylisoxazole-4-propionic acid (AMPA) receptor signaling. *Bipolar Disord* 18:473–480 . doi: 10.1111/bdi.12436
329. Dillon C, Goda Y (2005) The actin cytoskeleton: integrating form and function at the synapse. *Annu Rev Neurosci* 28:25–55 . doi: 10.1146/annurev.neuro.28.061604.135757
330. Huang W, Zhu PJ, Zhang S, Zhou H, Stoica L, Galiano M, Krnjević K, Roman G, Costa-Mattoli M (2013) mTORC2 controls actin polymerization required for consolidation of long-term memory. *Nat Neurosci* 16:441–8 . doi: 10.1038/nn.3351
331. Lepeta K, Lourenco M V., Schweitzer BC, Martino Adami P V., Banerjee P, Catuara-Solarz S, de La Fuente Revenga M, Guillem AM, Haidar M, Ijomone OM, Nadorp B, Qi L, Perera ND, Refsgaard LK, Reid KM, Sabbar M, Sahoo A, Schaefer N, Sheean RK, Suska A, Verma R, Vicidomini C, Wright D, Zhang X-D, Seidenbecher C (2016) Synaptopathies: synaptic dysfunction in neurological disorders - A review from students to students. *J Neurochem* 138:785–805 . doi: 10.1111/jnc.13713
332. Santini E, Heiman M, Greengard P, Valjent E, Fisone G (2009) Inhibition of mTOR Signaling in Parkinson's Disease Prevents L-DOPA-Induced Dyskinesia. *Sci Signal* 2:ra36-ra36 . doi: 10.1126/scisignal.2000308
333. Santini E, Valjent E, Fisone G (2010) mTORC1 signaling in Parkinson disease and L-DOPA-induced dyskinesia: A sensitized matter. *Cell Cycle* 9:2785–2790 . doi: 10.4161/cc.9.14.12180
334. Decressac M, Björklund A (2013) mTOR inhibition alleviates L-DOPA-induced dyskinesia in parkinsonian rats. *J Parkinsons Dis* 3:13–7 . doi: 10.3233/JPD-120155
335. Ellisen LW, Ramsayer KD, Johannessen CM, Yang A, Beppu H, Minda K, Oliner JD, McKeon F, Haber DA (2002) REDD1, a developmentally regulated transcriptional target of p63 and p53, links p63 to regulation of reactive oxygen species. *Mol Cell* 10:995–1005 . doi: 10.1016/S1097-2765(02)00706-2
336. Jin HO, An S, Lee HC, Woo SH, Seo SK, Choe TB, Yoo DH, Lee SB, Um HD, Lee SJ, Park MJ, Kim J II, Hong S II, Rhee CH, Park IC (2007) Hypoxic condition- and high cell density-induced expression of Redd1 is regulated by activation of hypoxia-inducible factor-1 α and Sp1 through the phosphatidylinositol 3-kinase/Akt signaling pathway. *Cell Signal* 19:1393–1403 . doi: 10.1016/j.cellsig.2006.12.014
337. Jin H-O, Seo S-K, Woo S-H, Kim E-S, Lee H-C, Yoo D-H, An S, Choe T-B, Lee S-J, Hong S-I, Rhee C-H, Kim J-I, Park I-C (2009) Activating transcription factor 4 and CCAAT/enhancer-binding protein- β negatively regulate the mammalian target of rapamycin via Redd1 expression in response to oxidative and endoplasmic reticulum stress. *Free Radic Biol Med* 46:1158–1167 . doi: 10.1016/j.freeradbiomed.2009.01.015
338. Whitney ML, Jefferson LS, Kimball SR (2009) ATF4 is necessary and sufficient

- for ER stress-induced upregulation of REDD1 expression. *Biochem Biophys Res Commun* 379:451–5 . doi: 10.1016/j.bbrc.2008.12.079
339. Sofer A, Lei K, Johannessen CM, Ellisen LW (2005) Regulation of mTOR and cell growth in response to energy stress by REDD1. *Mol Cell Biol* 25:5834–5845 . doi: 10.1128/MCB.25.14.5834-5845.2005
340. Wang Z, Malone MH, Thomenius MJ, Zhong F, Xu F, Distelhorst CW (2003) Dexamethasone-induced gene 2 (dig2) is a novel pro-survival stress gene induced rapidly by diverse apoptotic signals. *J Biol Chem* 278:27053–27058 . doi: 10.1074/jbc.M303723200
341. Molitoris JK, McColl KS, Swerdlow S, Matsuyama M, Lam M, Finkel TH, Matsuyama S, Distelhorst CW (2011) Glucocorticoid Elevation of Dexamethasone-induced Gene 2 (Dig2/RTP801/REDD1) Protein Mediates Autophagy in Lymphocytes. *J Biol Chem* 286:30181–30189 . doi: 10.1074/jbc.M111.245423
342. Kim J-R, Lee S-R, Chung HJ, Kim S, Baek S-H, Kim JH, Kim Y-S (2003) Identification of amyloid beta-peptide responsive genes by cDNA microarray technology: involvement of RTP801 in amyloid beta-peptide toxicity. *Exp Mol Med* 35:403–11 . doi: 10.1038/emm.2003.53
343. Lin L, Stringfield TM, Shi X, Chen Y (2005) Arsenite induces a cell stress-response gene, RTP801, through reactive oxygen species and transcription factors Elk-1 and CCAAT/enhancer-binding protein. *Biochem J* 392:93–102 . doi: 10.1042/BJ20050553
344. Michel G, Matthes HWD, Hachet-Haas M, El Baghdadi K, de Mey J, Pepperkok R, Simpson JC, Galzi J-L, Lecat S (2014) Plasma membrane translocation of REDD1 governed by GPCRs contributes to mTORC1 activation. *J Cell Sci* 127:773–87 . doi: 10.1242/jcs.136432
345. Horak P, Crawford AR, Vadysirisack DD, Nash ZM, DeYoung MP, Sgroi D, Ellisen LW (2010) Negative feedback control of HIF-1 through REDD1-regulated ROS suppresses tumorigenesis. *Proc Natl Acad Sci U S A* 107:4675–80 . doi: 10.1073/pnas.0907705107
346. del Olmo-Aguado S, Núñez-Álvarez C, Ji D, Manso AG, Osborne NN (2013) RTP801 immunoreactivity in retinal ganglion cells and its down-regulation in cultured cells protect them from light and cobalt chloride. *Brain Res Bull* 98:132–44 . doi: 10.1016/j.brainresbull.2013.08.002
347. Vega-Rubin-de-Celis S, Abdallah Z, Kinch L, Grishin N V., Brugarolas J, Zhang X (2010) Structural Analysis and Functional Implications of the Negative mTORC1 Regulator REDD1 . *Biochemistry* 49:2491–2501 . doi: 10.1021/bi902135e
348. Corradetti MN, Inoki K, Guan K-L (2005) The stress-induced proteins RTP801 and RTP801L are negative regulators of the mammalian target of rapamycin pathway. *J Biol Chem* 280:9769–72 . doi: 10.1074/jbc.C400557200
349. Canal M, Martín-Flores N, Pérez-Sisqués L, Romani-Aumedes J, Altas B, Man H-Y, Kawabe H, Alberch J, Malagelada C (2016) Loss of NEDD4 contributes to RTP801 elevation and neuron toxicity: implications for Parkinson's disease. *Oncotarget* 7:58813–58831 . doi: 10.18632/oncotarget.11020
350. Canal M, Romani-Aumedes J, Martín-Flores N, Pérez-Fernández V, Malagelada C (2014) RTP801/REDD1: a stress coping regulator that turns into a troublemaker in neurodegenerative disorders. *Front Cell Neurosci* 8:313 . doi:

- 10.3389/fncel.2014.00313
351. Favier FB, Costes F, Defour A, Bonnefoy R, Lefai E, Baugé S, Peinnequin A, Benoit H, Freyssenet D (2010) Downregulation of Akt/mammalian target of rapamycin pathway in skeletal muscle is associated with increased REDD1 expression in response to chronic hypoxia. *Am J Physiol Regul Integr Comp Physiol* 298:R1659-66 . doi: 10.1152/ajpregu.00550.2009
 352. Hernández G, Lal H, Fidalgo M, Guerrero A, Zalvide J, Force T, Pombo CM (2011) A novel cardioprotective p38-MAPK/mTOR pathway. *Exp Cell Res* 317:2938-49 . doi: 10.1016/j.yexcr.2011.09.011
 353. Pieri BLS, Souza DR, Luciano TF, Marques SO, Pauli JR, Silva ASR, Ropelle ER, Pinho RA, Lira FS, De Souza CT (2014) Effects of physical exercise on the P38MAPK/REDD1/14-3-3 pathways in the myocardium of diet-induced obesity rats. *Horm Metab Res* 46:621-7 . doi: 10.1055/s-0034-1371824
 354. Dennis MD, Coleman CS, Berg A, Jefferson LS, Kimball SR (2014) REDD1 enhances protein phosphatase 2A-mediated dephosphorylation of Akt to repress mTORC1 signaling. *Sci Signal* 7:ra68-ra68 . doi: 10.1126/scisignal.2005103
 355. Dennis MD, McGhee NK, Jefferson LS, Kimball SR (2013) Regulated in DNA damage and development 1 (REDD1) promotes cell survival during serum deprivation by sustaining repression of signaling through the mechanistic target of rapamycin in complex 1 (mTORC1). *Cell Signal* 25:2709-16 . doi: 10.1016/j.cellsig.2013.08.038
 356. Malagelada C, López-Toledano MA, Willett RT, Jin ZH, Shelanski ML, Greene L a (2011) RTP801/REDD1 regulates the timing of cortical neurogenesis and neuron migration. *J Neurosci* 31:3186-3196 . doi: 10.1523/JNEUROSCI.4011-10.2011
 357. Kimball SR, Do AND, Kutzler L, Cavener DR, Jefferson LS (2008) Rapid turnover of the mTOR complex 1 (mTORC1) repressor REDD1 and activation of mTORC1 signaling following inhibition of protein synthesis. *J Biol Chem* 283:3465-3475 . doi: 10.1074/jbc.M706643200
 358. Katiyar S, Liu E, Knutzen CA, Lang ES, Lombardo CR, Sankar S, Toth JI, Petroski MD, Ronai Z, Chiang GG (2009) REDD1, an inhibitor of mTOR signalling, is regulated by the CUL4A-DDB1 ubiquitin ligase. *EMBO Rep* 10:866-72 . doi: 10.1038/embor.2009.93
 359. Romani-Aumedes J, Canal M, Martín-Flores N, Sun X, Pérez-Fernández V, Wewering S, Fernández-Santiago R, Ezquerro M, Pont-Sunyer C, Lafuente A, Alberch J, Luebbert H, Tolosa E, Levy OA, Greene L a, Malagelada C (2014) Parkin loss of function contributes to RTP801 elevation and neurodegeneration in Parkinson's disease. *Cell Death Dis* 5:e1364 . doi: 10.1038/cddis.2014.333
 360. Damjanac M, Page G, Ragot S, Laborie G, Gil R, Hugon J, Paccalin M (2009) PKR, a cognitive decline biomarker, can regulate translation via two consecutive molecular targets p53 and Redd1 in lymphocytes of AD patients. *J Cell Mol Med* 13:1823-1832 . doi: 10.1111/j.1582-4934.2009.00688.x
 361. Ryu EJ, Angelastro JM, Greene LA (2005) Analysis of gene expression changes in a cellular model of Parkinson disease. *Neurobiol Dis* 18:54-74 . doi: 10.1016/j.nbd.2004.08.016
 362. Winklhofer KF, Henn IH, Kay-Jackson PC, Heller U, Tatzelt J (2003) Inactivation of Parkin by Oxidative Stress and C-terminal Truncations. *J Biol Chem*

- 278:47199–47208 . doi: 10.1074/jbc.M306769200
363. LaVoie MJ, Ostaszewski BL, Weihofen A, Schlossmacher MG, Selkoe DJ (2005) Dopamine covalently modifies and functionally inactivates parkin. *Nat Med* 11:1214–21 . doi: 10.1038/nm1314
364. Kitada T, Asakawa S, Hattori N, Matsumine H, Yamamura Y, Minoshima S, Yokochi M, Mizuno Y, Shimizu N (1998) Mutations in the parkin gene cause autosomal recessive juvenile parkinsonism. *Nature* 392:605–608 . doi: 10.1038/33416
365. Johnstone RM, Adam M, Hammond JR, Orr L, Turbide C (1987) Vesicle formation during reticulocyte maturation. Association of plasma membrane activities with released vesicles (exosomes). *J Biol Chem* 262:9412–20
366. Colombo M, Raposo G, Théry C (2014) Biogenesis, Secretion, and Intercellular Interactions of Exosomes and Other Extracellular Vesicles. *Annu Rev Cell Dev Biol* 30:255–289 . doi: 10.1146/annurev-cellbio-101512-122326
367. Yáñez-Mó M, Siljander PR-M, Andreu Z, Zavec AB, Borràs FE, Buzas EI, Buzas K, Casal E, Cappello F, Carvalho J, Colás E, Cordeiro-da Silva A, Fais S, Falcon-Perez JM, Ghobrial IM, Giebel B, Gimona M, Graner M, Gursel I, Gursel M, Heegaard NHH, Hendrix A, Kierulf P, Kokubun K, Kosanovic M, Kralj-Iglic V, Krämer-Albers E-M, Laitinen S, Lässer C, Lener T, Ligeti E, Linē A, Lipps G, Llorente A, Lötvall J, Manček-Keber M, Marcilla A, Mittelbrunn M, Nazarenko I, Nolte-’t Hoen ENM, Nyman TA, O’Driscoll L, Olivan M, Oliveira C, Pállinger É, Del Portillo HA, Reventós J, Rigau M, Rohde E, Sammar M, Sánchez-Madrid F, Santarém N, Schallmoser K, Ostendorf MS, Stoorvogel W, Stukelj R, Van der Grein SG, Vasconcelos MH, Wauben MHM, De Wever O (2015) Biological properties of extracellular vesicles and their physiological functions. *J Extracell vesicles* 4:27066
368. Raposo G, Stoorvogel W (2013) Extracellular vesicles: Exosomes, microvesicles, and friends. *J Cell Biol* 200:373–383 . doi: 10.1083/jcb.201211138
369. Cicero A Lo, Delevoye C, Gilles-Marsens F, Loew D, Dingli F, Guéré C, André N, Vié K, van Niel G, Raposo G (2015) Exosomes released by keratinocytes modulate melanocyte pigmentation. *Nat Commun* 6:7506 . doi: 10.1038/ncomms8506
370. Villarroya-Beltri C, Baixauli F, Gutiérrez-Vázquez C, Sánchez-Madrid F, Mittelbrunn M (2014) Sorting it out: Regulation of exosome loading. *Semin Cancer Biol* 28:3–13 . doi: 10.1016/j.semcan.2014.04.009
371. Eldh M, Ekström K, Valadi H, Sjöstrand M, Olsson B, Jernås M, Lötvall J (2010) Exosomes Communicate Protective Messages during Oxidative Stress; Possible Role of Exosomal Shuttle RNA. *PLoS One* 5:e15353 . doi: 10.1371/journal.pone.0015353
372. Marzesco A-MM, Janich P, Wilsch-Brauninger M, Dubreuil V, Langenfeld K, Corbeil D, Huttner WB, Wilsch-Brauninger M, Dubreuil V, Langenfeld K, Corbeil D, Huttner WB, Wilsch-Brauninger M, Dubreuil V, Langenfeld K, Corbeil D, Huttner WB (2005) Release of extracellular membrane particles carrying the stem cell marker prominin-1 (CD133) from neural progenitors and other epithelial cells. *J Cell Sci* 118:2849–2858 . doi: 10.1242/jcs.02439
373. Yuan A, Farber EL, Rapoport AL, Tejada D, Deniskin R, Akhmedov NB, Farber DB (2009) Transfer of MicroRNAs by Embryonic Stem Cell Microvesicles. *PLoS One* 4:e4722 . doi: 10.1371/journal.pone.0004722

374. Fauré J, Lachenal G, Court M, Hirrlinger J, Chatellard-Causse C, Blot B, Grange J, Schoehn G, Goldberg Y, Boyer V, Kirchhoff F, Raposo G, Garin J, Sadoul R (2006) Exosomes are released by cultured cortical neurones. *Mol Cell Neurosci* 31:642–648 . doi: 10.1016/j.mcn.2005.12.003
375. Lachenal G, Pernet-Gallay K, Chivet M, Hemming FJ, Belly A, Bodon G, Blot B, Haase G, Goldberg Y, Sadoul R (2011) Release of exosomes from differentiated neurons and its regulation by synaptic glutamatergic activity. *Mol Cell Neurosci* 46:409–418 . doi: 10.1016/j.mcn.2010.11.004
376. Taylor AR, Robinson MB, Gifondorwa DJ, Tytell M, Milligan CE (2007) Regulation of heat shock protein 70 release in astrocytes: Role of signaling kinases. *Dev Neurobiol* 67:1815–1829 . doi: 10.1002/dneu.20559
377. Bianco F, Perrotta C, Novellino L, Francolini M, Riganti L, Menna E, Saglietti L, Schuchman EH, Furlan R, Clementi E, Matteoli M, Verderio C (2009) Acid sphingomyelinase activity triggers microparticle release from glial cells. *EMBO J* 28:1043–1054 . doi: 10.1038/emboj.2009.45
378. Bakhti M, Winter C, Simons M (2011) Inhibition of Myelin Membrane Sheath Formation by Oligodendrocyte-derived Exosome-like Vesicles. *J Biol Chem* 286:787–796 . doi: 10.1074/jbc.M110.190009
379. Fitzner D, Schnaars M, van Rossum D, Krishnamoorthy G, Dibaj P, Bakhti M, Regen T, Hanisch U-K, Simons M (2011) Selective transfer of exosomes from oligodendrocytes to microglia by macropinocytosis. *J Cell Sci* 124:447–458 . doi: 10.1242/jcs.074088
380. Krämer-Albers E-M, Bretz N, Tenzer S, Winterstein C, Möbius W, Berger H, Nave K-A, Schild H, Trotter J (2007) Oligodendrocytes secrete exosomes containing major myelin and stress-protective proteins: Trophic support for axons? *PROTEOMICS – Clin Appl* 1:1446–1461 . doi: 10.1002/prca.200700522
381. Frühbeis C, Fröhlich D, Kuo WP, Amphornrat J, Thilemann S, Saab AS, Kirchhoff F, Möbius W, Goebbels S, Nave K-A, Schneider A, Simons M, Klugmann M, Trotter J, Krämer-Albers E-M (2013) Neurotransmitter-triggered transfer of exosomes mediates oligodendrocyte-neuron communication. *PLoS Biol* 11:e1001604 . doi: 10.1371/journal.pbio.1001604
382. Fröhlich D, Kuo WP, Frühbeis C, Sun J-J, Zehendner CM, Luhmann HJ, Pinto S, Toedling J, Trotter J, Kramer-Albers E-M (2014) Multifaceted effects of oligodendroglial exosomes on neurons: impact on neuronal firing rate, signal transduction and gene regulation. *Philos Trans R Soc B Biol Sci* 369:20130510–20130510 . doi: 10.1098/rstb.2013.0510
383. Potalicchio I, Carven GJ, Xu X, Stipp C, Riese RJ, Stern LJ, Santambrogio L (2005) Proteomic analysis of microglia-derived exosomes: metabolic role of the aminopeptidase CD13 in neuropeptide catabolism. *J Immunol* 175:2237–43
384. Bianco F, Pravettoni E, Colombo A, Schenk U, Möller T, Matteoli M, Verderio C (2005) Astrocyte-derived ATP induces vesicle shedding and IL-1 beta release from microglia. *J Immunol* 174:7268–77
385. Lopez-Verrilli MA, Picou F, Court FA (2013) Schwann cell-derived exosomes enhance axonal regeneration in the peripheral nervous system. *Glia* 61:1795–1806 . doi: 10.1002/glia.22558
386. Lopez-Verrilli MA, Court FA (2012) Transfer of Vesicles From Schwann Cells to Axons: a Novel Mechanism of Communication in the Peripheral Nervous System.

- Front Physiol* 3:205 . doi: 10.3389/fphys.2012.00205
387. Yuyama K, Sun H, Mitsutake S, Igarashi Y (2012) Sphingolipid-modulated Exosome Secretion Promotes Clearance of Amyloid- β by Microglia. *J Biol Chem* 287:10977–10989 . doi: 10.1074/jbc.M111.324616
388. Bahrini I, Song J, Diez D, Hanayama R (2015) Neuronal exosomes facilitate synaptic pruning by up-regulating complement factors in microglia. *Sci Rep* 5:7989 . doi: 10.1038/srep07989
389. Joshi P, Turola E, Ruiz A, Bergami A, Libera DD, Benussi L, Giussani P, Magnani G, Comi G, Legname G, Ghidoni R, Furlan R, Matteoli M, Verderio C (2014) Microglia convert aggregated amyloid- β into neurotoxic forms through the shedding of microvesicles. *Cell Death Differ* 21:582–593 . doi: 10.1038/cdd.2013.180
390. Guo BB, Bellingham SA, Hill AF (2015) The Neutral Sphingomyelinase Pathway Regulates Packaging of the Prion Protein into Exosomes. *J Biol Chem* 290:3455–3467 . doi: 10.1074/jbc.M114.605253
391. van Niel G, D'Angelo G, Raposo G (2018) Shedding light on the cell biology of extracellular vesicles. *Nat Rev Mol Cell Biol* 19:213–228 . doi: 10.1038/nrm.2017.125
392. Caruso S, Poon IKH (2018) Apoptotic Cell-Derived Extracellular Vesicles: More Than Just Debris. *Front Immunol* 9:1486 . doi: 10.3389/fimmu.2018.01486
393. Gould SJ, Raposo G (2013) As we wait: coping with an imperfect nomenclature for extracellular vesicles. *J Extracell vesicles* 2:20389 . doi: 10.3402/jev.v2i0.20389
394. Minciacchi VR, Freeman MR, Di Vizio D (2015) Extracellular Vesicles in Cancer: Exosomes, Microvesicles and the Emerging Role of Large Oncosomes. *Semin Cell Dev Biol* 40:41–51 . doi: 10.1016/j.semcdb.2015.02.010
395. Kowal J, Arras G, Colombo M, Jouve M, Morath JP, Primdal-Bengtson B, Dingli F, Loew D, Tkach M, Théry C (2016) Proteomic comparison defines novel markers to characterize heterogeneous populations of extracellular vesicle subtypes. *Proc Natl Acad Sci U S A* 113:E968–77 . doi: 10.1073/pnas.1521230113
396. Raiborg C, Stenmark H (2009) The ESCRT machinery in endosomal sorting of ubiquitylated membrane proteins. *Nature* 458:445–452 . doi: 10.1038/nature07961
397. Hurley JH, Odorizzi G (2012) Get on the exosome bus with ALIX. *Nat Cell Biol* 14:654–655 . doi: 10.1038/ncb2530
398. Colombo M, Moita C, van Niel G, Kowal J, Vigneron J, Benaroch P, Manel N, Moita LF, Théry C, Raposo G (2013) Analysis of ESCRT functions in exosome biogenesis, composition and secretion highlights the heterogeneity of extracellular vesicles. *J Cell Sci* 126:5553–5565 . doi: 10.1242/jcs.128868
399. Stuffers S, Sem Wegner C, Stenmark H, Brech A (2009) Multivesicular Endosome Biogenesis in the Absence of ESCRTs. *Traffic* 10:925–937 . doi: 10.1111/j.1600-0854.2009.00920.x
400. Trajkovic K, Hsu C, Chiantia S, Rajendran L, Wenzel D, Wieland F, Schwille P, Brugger B, Simons M (2008) Ceramide Triggers Budding of Exosome Vesicles into Multivesicular Endosomes. *Science* (80-) 319:1244–1247 . doi: 10.1126/science.1153124

401. Goñi FM, Alonso A (2009) Effects of ceramide and other simple sphingolipids on membrane lateral structure. *Biochim Biophys Acta - Biomembr* 1788:169–177 . doi: 10.1016/j.bbamem.2008.09.002
402. Robbins PD, Morelli AE (2014) Regulation of immune responses by extracellular vesicles. *Nat Rev Immunol* 14:195–208 . doi: 10.1038/nri3622
403. Zappulli V, Friis KP, Fitzpatrick Z, Maguire CA, Breakefield XO (2016) Extracellular vesicles and intercellular communication within the nervous system. *J Clin Invest* 126:1198–207 . doi: 10.1172/JCI81134
404. Mulcahy LA, Pink RC, Carter DRF (2014) Routes and mechanisms of extracellular vesicle uptake. *J Extracell Vesicles* 3:24641 . doi: 10.3402/jev.v3.24641
405. Tian T, Zhu Y-L, Zhou Y-Y, Liang G-F, Wang Y-Y, Hu F-H, Xiao Z-D (2014) Exosome Uptake through Clathrin-mediated Endocytosis and Macropinocytosis and Mediating miR-21 Delivery. *J Biol Chem* 289:22258–22267 . doi: 10.1074/jbc.M114.588046
406. Zhao H, Yang L, Baddour J, Achreja A, Bernard V, Moss T, Marini JC, Tudawe T, Seviour EG, San Lucas FA, Alvarez H, Gupta S, Maiti SN, Cooper L, Peehl D, Ram PT, Maitra A, Nagrath D (2016) Tumor microenvironment derived exosomes pleiotropically modulate cancer cell metabolism. *Elife* 5:e10250 . doi: 10.7554/eLife.10250
407. Alvarez-Erviti L, Seow Y, Yin H, Betts C, Lakhai S, Wood MJA (2011) Delivery of siRNA to the mouse brain by systemic injection of targeted exosomes. *Nat Biotechnol* 29:341–345 . doi: 10.1038/nbt.1807
408. Parolini I, Federici C, Raggi C, Lugini L, Palleschi S, De Milito A, Coscia C, Iessi E, Logozzi M, Molinari A, Colone M, Tatti M, Sargiacomo M, Fais S (2009) Microenvironmental pH Is a Key Factor for Exosome Traffic in Tumor Cells. *J Biol Chem* 284:34211–34222 . doi: 10.1074/jbc.M109.041152
409. Laulagnier K, Motta C, Hamdi S, Roy S, Fauvelle F, Pageaux J-F, Kobayashi T, Salles J-P, Perret B, Bonnerot C, Record M (2004) Mast cell- and dendritic cell-derived exosomes display a specific lipid composition and an unusual membrane organization. *Biochem J* 380:161–71 . doi: 10.1042/BJ20031594
410. Llorente A, Skotland T, Sylvänne T, Kauhanen D, Róg T, Orłowski A, Vattulainen I, Ekroos K, Sandvig K (2013) Molecular lipidomics of exosomes released by PC-3 prostate cancer cells. *Biochim Biophys Acta* 1831:1302–9
411. Wubbolts R, Leckie RS, Veenhuizen PTM, Schwarzmann G, Möbius W, Hoernschemeyer J, Slot J-W, Geuze HJ, Stoorvogel W (2003) Proteomic and biochemical analyses of human B cell-derived exosomes. Potential implications for their function and multivesicular body formation. *J Biol Chem* 278:10963–72 . doi: 10.1074/jbc.M207550200
412. Laulagnier K, Vincent-Schneider H, Hamdi S, Subra C, Lankar D, Record M (2005) Characterization of exosome subpopulations from RBL-2H3 cells using fluorescent lipids. *Blood Cells Mol Dis* 35:116–21 . doi: 10.1016/j.bcmd.2005.05.010
413. Willms E, Johansson HJ, Mäger I, Lee Y, Blomberg KEM, Sadik M, Alaarg A, Smith CIE, Lehtiö J, EL Andaloussi S, Wood MJA, Vader P (2016) Cells release subpopulations of exosomes with distinct molecular and biological properties. *Sci Rep* 6:22519 . doi: 10.1038/srep22519
414. Buschow SI, Liefhebber JMP, Wubbolts R, Stoorvogel W (2005) Exosomes

- contain ubiquitinated proteins. *Blood Cells, Mol Dis* 35:398–403 . doi: 10.1016/j.bcmed.2005.08.005
415. Maness PF, Schachner M (2007) Neural recognition molecules of the immunoglobulin superfamily: signaling transducers of axon guidance and neuronal migration. *Nat Neurosci* 10:19–26 . doi: 10.1038/nn1827
416. Putz U, Howitt J, Lackovic J, Foot N, Kumar S, Silke J, Tan S-S (2008) Nedd4 Family-interacting Protein 1 (Ndfip1) Is Required for the Exosomal Secretion of Nedd4 Family Proteins. *J Biol Chem* 283:32621–32627 . doi: 10.1074/jbc.M804120200
417. Valadi H, Ekstrom K, Bossios A, Sjostrand M, Lee JJ, Lotvall JO, Ekström K, Bossios A, Sjöstrand M, Lee JJ, Lötvalld JO, Ekstrom K, Bossios A, Sjostrand M, Lee JJ, Lotvall JO (2007) Exosome-mediated transfer of mRNAs and microRNAs is a novel mechanism of genetic exchange between cells. *Nat Cell Biol* 9:654–659 . doi: 10.1038/ncb1596
418. Nolte-'t Hoen ENM, Buermans HPJ, Waasdorp M, Stoorvogel W, Wauben MHM, 't Hoen PAC (2012) Deep sequencing of RNA from immune cell-derived vesicles uncovers the selective incorporation of small non-coding RNA biotypes with potential regulatory functions. *Nucleic Acids Res* 40:9272–9285 . doi: 10.1093/nar/gks658
419. Thakur BK, Zhang H, Becker A, Matei I, Huang Y, Costa-Silva B, Zheng Y, Hoshino A, Brazier H, Xiang J, Williams C, Rodriguez-Barrueco R, Silva JM, Zhang W, Hearn S, Elemento O, Paknejad N, Manova-Todorova K, Welte K, Bromberg J, Peinado H, Lyden D (2014) Double-stranded DNA in exosomes: a novel biomarker in cancer detection. *Cell Res* 24:766–769 . doi: 10.1038/cr.2014.44
420. Kahlert C, Melo SA, Protopopov A, Tang J, Seth S, Koch M, Zhang J, Weitz J, Chin L, Futreal A, Kalluri R (2014) Identification of Double-stranded Genomic DNA Spanning All Chromosomes with Mutated *KRAS* and *p53* DNA in the Serum Exosomes of Patients with Pancreatic Cancer. *J Biol Chem* 289:3869–3875 . doi: 10.1074/jbc.C113.532267
421. Ghidoni R, Paterlini A, Albertini V, Glionna M, Monti E, Schiaffonati L, Benussi L, Levy E, Binetti G (2011) Cystatin C is released in association with exosomes: A new tool of neuronal communication which is unbalanced in Alzheimer's disease. *Neurobiol Aging* 32:1435–1442 . doi: 10.1016/j.neurobiolaging.2009.08.013
422. Chivet M, Javalet C, Hemming F, Pernet-Gallay K, Laulagnier K, Fraboulet S, Sadoul R (2013) Exosomes as a novel way of interneuronal communication. *Biochem Soc Trans* 41:241–4 . doi: 10.1042/BST20120266
423. Wang L, Zhang B, Zheng W, Kang M, Chen Q, Qin W, Li C, Zhang Y, Shao Y, Wu Y (2017) Exosomes derived from pancreatic cancer cells induce insulin resistance in C2C12 myotube cells through the PI3K/Akt/FoxO1 pathway. *Sci Rep* 7:5384 . doi: 10.1038/s41598-017-05541-4
424. Polanco JC, Scicluna BJ, Hill AF, Götz J (2016) Extracellular Vesicles Isolated from the Brains of rTg4510 Mice Seed Tau Protein Aggregation in a Threshold-dependent Manner. *J Biol Chem* 291:12445–66 . doi: 10.1074/jbc.M115.709485
425. Yuyama K, Sun H, Usuki S, Sakai S, Hanamatsu H, Mioka T, Kimura N, Okada M, Tahara H, Furukawa J, Fujitani N, Shinohara Y, Igarashi Y (2015) A potential function for neuronal exosomes: sequestering intracerebral amyloid- β peptide. *FEBS Lett* 589:84–8 . doi: 10.1016/j.febslet.2014.11.027

426. Yuyama K, Sun H, Sakai S, Mitsutake S, Okada M, Tahara H, Furukawa JI, Fujitani N, Shinohara Y, Igarashi Y (2014) Decreased amyloid- β pathologies by intracerebral loading of glycosphingolipid-enriched exosomes in Alzheimer model mice. *J Biol Chem* 289:24488–24498 . doi: 10.1074/jbc.M114.577213
427. Tamboli IY, Barth E, Christian L, Siepmann M, Kumar S, Singh S, Tolksdorf K, Heneka MT, Lütjohann D, Wunderlich P, Walter J (2010) Statins promote the degradation of extracellular amyloid {beta}-peptide by microglia via stimulation of exosome-associated insulin-degrading enzyme (IDE) secretion. *J Biol Chem* 285:37405–14 . doi: 10.1074/jbc.M110.149468
428. Fevrier B, Vilette D, Archer F, Loew D, Faigle W, Vidal M, Laude H, Raposo G (2004) Cells release prions in association with exosomes. *Proc Natl Acad Sci* 101:9683–9688 . doi: 10.1073/pnas.0308413101
429. Alvarez-Erviti L, Seow Y, Schapira AH, Gardiner C, Sargent IL, Wood MJA, Cooper JM (2011) Lysosomal dysfunction increases exosome-mediated alpha-synuclein release and transmission. *Neurobiol Dis* 42:360–367 . doi: 10.1016/j.nbd.2011.01.029
430. Shi M, Liu C, Cook TJ, Bullock KM, Zhao Y, Ghingina C, Li Y, Aro P, Dator R, He C, Hipp MJ, Zabetian CP, Peskind ER, Hu S-C, Quinn JF, Galasko DR, Banks WA, Zhang J (2014) Plasma exosomal α -synuclein is likely CNS-derived and increased in Parkinson's disease. *Acta Neuropathol* 128:639–650 . doi: 10.1007/s00401-014-1314-y
431. Cerri S, Ghezzi C, Sampieri M, Siani F, Avenali M, Dornini G, Zangaglia R, Minafra B, Blandini F (2018) The Exosomal/Total α -Synuclein Ratio in Plasma Is Associated With Glucocerebrosidase Activity and Correlates With Measures of Disease Severity in PD Patients. *Front Cell Neurosci* 12:125 . doi: 10.3389/fncel.2018.00125
432. Ho DH, Yi S, Seo H, Son I, Seol W (2014) Increased DJ-1 in Urine Exosome of Korean Males with Parkinson's Disease. *Biomed Res Int* 2014:1–8 . doi: 10.1155/2014/704678
433. Vella L, Hill A, Cheng L (2016) Focus on Extracellular Vesicles: Exosomes and Their Role in Protein Trafficking and Biomarker Potential in Alzheimer's and Parkinson's Disease. *Int J Mol Sci* 17:173 . doi: 10.3390/ijms17020173
434. Fraser KB, Moehle MS, Alcalay RN, West AB, LRRK2 Cohort Consortium (2016) Urinary LRRK2 phosphorylation predicts parkinsonian phenotypes in G2019S *LRRK2* carriers. *Neurology* 86:994–999 . doi: 10.1212/WNL.0000000000002436
435. Fraser KB, Moehle MS, Daher JPL, Webber PJ, Williams JY, Stewart CA, Yacoubian TA, Cowell RM, Dokland T, Ye T, Chen D, Siegal GP, Galemno RA, Tsika E, Moore DJ, Standaert DG, Kojima K, Mobley JA, West AB (2013) LRRK2 secretion in exosomes is regulated by 14-3-3. *Hum Mol Genet* 22:4988–5000 . doi: 10.1093/hmg/ddt346
436. Merten O-W, Hebben M, Bovolenta C (2016) Production of lentiviral vectors. *Mol Ther Methods Clin Dev* 3:16017 . doi: 10.1038/mtm.2016.17
437. Greene LA, Tischler AS (1976) Establishment of a noradrenergic clonal line of rat adrenal pheochromocytoma cells which respond to nerve growth factor. *Proc Natl Acad Sci U S A* 73:2424–8
438. Greene LA (1978) Nerve growth factor prevents the death and stimulates the neuronal differentiation of clonal PC12 pheochromocytoma cells in serum-free

BIBLIOGRAPHY

- medium. *J Cell Biol* 78:747–55
439. Greene LA, Rein G (1977) Release of (3H)norepinephrine from a clonal line of pheochromocytoma cells (PC12) by nicotinic cholinergic stimulation. *Brain Res* 138:521–8
440. Grau CM, Greene LA (2012) Use of PC12 Cells and Rat Superior Cervical Ganglion Sympathetic Neurons as Models for Neuroprotective Assays Relevant to Parkinson's Disease. In: *Methods in molecular biology* (Clifton, N.J.). pp 201–211
441. Malagelada C, Greene LA (2008) PC12 Cells as a model for parkinson's disease research. In: *Parkinson's Disease*. Elsevier, pp 375–387
442. Trettel F, Rigamonti D, Hilditch-Maguire P, Wheeler VC, Sharp AH, Persichetti F, Cattaneo E, MacDonald ME (2000) Dominant phenotypes produced by the HD mutation in STHdh(Q111) striatal cells. *Hum Mol Genet* 9:2799–809 . doi: citeulike-article-id:11622336\rdoi: 10.1093/hmg/9.19.2799
443. Kazantsev A, Preisinger E, Dranovsky A, Goldgaber D, Housman D (1999) Insoluble detergent-resistant aggregates form between pathological and nonpathological lengths of polyglutamine in mammalian cells. *Proc Natl Acad Sci U S A* 96:11404–9
444. Hughes AJ, Daniel SE, Blankson S, Lees AJ (1993) A clinicopathologic study of 100 cases of Parkinson's disease. *Arch Neurol* 50:140–148
445. Dickson DW, Braak H, Duda JE, Duyckaerts C, Gasser T, Halliday GM, Hardy J, Leverenz JB, Del Tredici K, Wszolek ZK, Litvan I (2009) Neuropathological assessment of Parkinson's disease: refining the diagnostic criteria. *Lancet Neurol*. 8:1150–1157
446. Fernández-Santiago R, Iranzo A, Gaig C, Serradell M, Fernández M, Tolosa E, Santamaría J, Ezquerra M (2016) Absence of *LRRK2* mutations in a cohort of patients with idiopathic REM sleep behavior disorder. *Neurology* 86:1072–1073 . doi: 10.1212/WNL.0000000000002304
447. Dudbridge F (2003) Pedigree disequilibrium tests for multilocus haplotypes. *Genet Epidemiol* 25:115–121 . doi: 10.1002/gepi.10252
448. Benjamini Y, Hochberg Y (1995) Benjamini Y, Hochberg Y. Controlling the false discovery rate: a practical and powerful approach to multiple testing. *J R Stat Soc B* 57:289–300 . doi: 10.2307/2346101
449. Sole X, Guino E, Valls J, Iniesta R, Moreno V (2006) SNPStats: a web tool for the analysis of association studies. *Bioinformatics* 22:1928–1929 . doi: 10.1093/bioinformatics/btl268
450. Ritchie M, Hahn L, Roodi N, Bailey L, Dupont W, Parl F, Moore J (2001) Multifactor-dimensionality reduction reveals high-order interactions among estrogen-metabolism genes in sporadic breast cancer. *Am J Hum Genet* 69:138–47 . doi: 10.1086/321276
451. Motsinger AA, Ritchie MD (2006) The effect of reduction in cross-validation intervals on the performance of multifactor dimensionality reduction. *Genet Epidemiol* 30:546–555 . doi: 10.1002/gepi.20166
452. Pryor WM, Biagioli M, Shahani N, Swarnkar S, Huang W-C, Page DT, MacDonald ME, Subramaniam S (2014) Huntingtin promotes mTORC1 signaling in the pathogenesis of Huntington's disease. *Sci Signal* 7:ra103-ra103 . doi:

- 10.1126/scisignal.2005633
453. Ota KT, Liu R-J, Voleti B, Maldonado-Aviles JG, Duric V, Iwata M, Dutheil S, Duman C, Boikess S, Lewis DA, Stockmeier CA, DiLeone RJ, Rex C, Aghajanian GK, Duman RS (2014) REDD1 is essential for stress-induced synaptic loss and depressive behavior. *Nat Med* 20:531–535 . doi: 10.1038/nm.3513
454. Wu X, Su J, Chen L, Ma B, Gu X, Zhu L (2015) Ginkgolide B Protects Neurons from Ischemic Injury by Inhibiting the Expression of RTP801. *Cell Mol Neurobiol* 35:943–952 . doi: 10.1007/s10571-015-0189-3
455. Lee M, Bikram M, Oh S, Bull DA, Kim SW (2004) Sp1-Dependent Regulation of the RTP801 Promoter and Its Application to Hypoxia-Inducible VEGF Plasmid for Ischemic Disease. *Pharm Res* 21:736–741 . doi: 10.1023/B:PHAM.0000026421.09367.b3
456. Morel M, Couturier J, Pontcharraud R, Gil R, Fauconneau B, Paccalin M, Page G (2009) Evidence of molecular links between PKR and mTOR signalling pathways in A β neurotoxicity: Role of p53, Redd1 and TSC2. *Neurobiol Dis* 36:151–161 . doi: 10.1016/j.nbd.2009.07.004
457. Mangiarini L, Sathasivam K, Seller M, Cozens B, Harper A, Hetherington C, Lawton M, Trotter Y, Lehrach H, Davies SW, Bates GP (1996) Exon I of the HD gene with an expanded CAG repeat is sufficient to cause a progressive neurological phenotype in transgenic mice. *Cell* 87:493–506 . doi: 10.1016/S0092-8674(00)81369-0
458. Martín-Aparicio E, Yamamoto A, Hernández F, Hen R, Avila J, Lucas JJ (2001) Proteasomal-dependent aggregate reversal and absence of cell death in a conditional mouse model of Huntington's disease. *J Neurosci* 21:8772–8781 . doi: 10.1523/JNEUROSCI.3183-05.2005
459. Wheeler VC, Gutekunst C-A, Vrbancic V, Lebel L-A, Schilling G, Hersch S, Friedlander RM, Gusella JF, Vonsattel J-P, Borchelt DR, MacDonald ME (2002) Early phenotypes that presage late-onset neurodegenerative disease allow testing of modifiers in Hdh CAG knock-in mice. *Hum Mol Genet* 11:633–40
460. Díaz-Hernández M, Torres-Peraza J, Salvatori-Abarca A, Morán M a, Gómez-Ramos P, Alberch J, Lucas JJ (2005) Full motor recovery despite striatal neuron loss and formation of irreversible amyloid-like inclusions in a conditional mouse model of Huntington's disease. *J Neurosci* 25:9773–9781 . doi: 10.1523/JNEUROSCI.3183-05.2005
461. Puigdel·l·ivol M, Cherubini M, Brito V, Giralt A, Suelves N, Ballesteros J, Zamora-Moratalla A, Martín ED, Eipper BA, Alberch J, Ginés S (2015) A role for Kalirin-7 in corticostriatal synaptic dysfunction in Huntington's disease. *Hum Mol Genet* 24:7265–7285 . doi: 10.1093/hmg/ddv426
462. Kim J, Bordiuk OL, Ferrante RJ (2011) Experimental Models of HD and Reflection on Therapeutic Strategies. In: International review of neurobiology. pp 419–481
463. The HD iPSC Consortium, The HD iPSC Consortium (2012) Induced pluripotent stem cells from patients with huntington's disease show cag-repeat-expansion-associated phenotypes. *Cell Stem Cell* 11:264–278 . doi: 10.1016/j.stem.2012.04.027
464. Caramins M, Halliday G, McCusker E, Trent RJ (2003) Genetically confirmed clinical Huntington's disease with no observable cell loss. *J Neurol Neurosurg Psychiatry* 74:968–70

BIBLIOGRAPHY

465. Levine MS, Cepeda C, Hickey MA, Fleming SM, Chesselet M-F (2004) Genetic mouse models of Huntington's and Parkinson's diseases: illuminating but imperfect. *Trends Neurosci* 27:691–697 . doi: 10.1016/j.tins.2004.08.008
466. Turmaine M, Raza A, Mahal A, Mangiarini L, Bates GP, Davies SW (2000) Nonapoptotic neurodegeneration in a transgenic mouse model of Huntington's disease. *Proc Natl Acad Sci* 97:8093–8097 . doi: 10.1073/pnas.110078997
467. Murphy KP, Carter RJ, Lione LA, Mangiarini L, Mahal A, Bates GP, Dunnett SB, Morton AJ (2000) Abnormal synaptic plasticity and impaired spatial cognition in mice transgenic for exon 1 of the human Huntington's disease mutation. *J Neurosci* 20:5115–23
468. Usdin MT, Shelbourne PF, Myers RM, Madison D V (1999) Impaired synaptic plasticity in mice carrying the Huntington's disease mutation. *Hum Mol Genet* 8:839–46
469. Cepeda C, Ariano MA, Calvert CR, Flores-Hernández J, Chandler SH, Leavitt BR, Hayden MR, Levine MS (2001) NMDA receptor function in mouse models of Huntington disease. *J Neurosci Res* 66:525–539 . doi: 10.1002/jnr.1244
470. Cepeda C, Galvan L, Holley SM, Rao SP, Andre VM, Botelho EP, Chen JY, Watson JB, Deisseroth K, Levine MS (2013) Multiple Sources of Striatal Inhibition Are Differentially Affected in Huntington's Disease Mouse Models. *J Neurosci* 33:7393–7406 . doi: 10.1523/JNEUROSCI.2137-12.2013
471. Cepeda C, Hurst RS, Calvert CR, Hernández-Echeagaray E, Nguyen OK, Jocoy E, Christian LJ, Ariano MA, Levine MS (2003) Transient and progressive electrophysiological alterations in the corticostriatal pathway in a mouse model of Huntington's disease. *J Neurosci* 23:961–9
472. Li J-Y, Plomann M, Brundin P (2003) Huntington's disease: a synaptopathy? *Trends Mol Med* 9:414–20
473. Santini E, Muller RU, Quirk GJ (2001) Consolidation of extinction learning involves transfer from NMDA-independent to NMDA-dependent memory. *J Neurosci* 21:9009–17
474. Matus A (2000) Actin-based plasticity in dendritic spines. *Science* 290:754–8
475. Meng Y, Zhang Y, Tregoubov V, Janus C, Cruz L, Jackson M, Lu WY, MacDonald JF, Wang JY, Falls DL, Jia Z (2002) Abnormal spine morphology and enhanced LTP in LIMK-1 knockout mice. *Neuron* 35:121–33
476. Fukazawa Y, Saitoh Y, Ozawa F, Ohta Y, Mizuno K, Inokuchi K (2003) Hippocampal LTP is accompanied by enhanced F-actin content within the dendritic spine that is essential for late LTP maintenance in vivo. *Neuron* 38:447–60
477. Szabó EC, Manguinhas R, Fonseca R (2016) The interplay between neuronal activity and actin dynamics mimic the setting of an LTD synaptic tag. *Sci Rep* 6:33685 . doi: 10.1038/srep33685
478. Cingolani LA, Goda Y (2008) Actin in action: the interplay between the actin cytoskeleton and synaptic efficacy. *Nat Rev Neurosci* 9:344–356 . doi: 10.1038/nrn2373
479. HEBB CO, WHITTAKER VP (1958) Intracellular distributions of acetylcholine and choline acetylase. *J Physiol* 142:187–96

480. GRAY EG, WHITTAKER VP (1962) The isolation of nerve endings from brain: an electron-microscopic study of cell fragments derived by homogenization and centrifugation. *J Anat* 96:79–88
481. Hell JW, Maycox PR, Stadler H, Jahn R (1988) Uptake of GABA by rat brain synaptic vesicles isolated by a new procedure. *EMBO J* 7:3023–9
482. Wilhelm BG, Mandad S, Truckenbrodt S, Krohnert K, Schafer C, Rammner B, Koo SJ, Classen GA, Krauss M, Haucke V, Urlaub H, Rizzoli SO (2014) Composition of isolated synaptic boutons reveals the amounts of vesicle trafficking proteins. *Science (80-)* 344:1023–1028 . doi: 10.1126/science.1252884
483. Tao C-L, Liu Y-T, Sun R, Zhang B, Qi L, Shivakoti S, Tian C-L, Zhang P, Lau P-M, Zhou ZH, Bi G-Q (2018) Differentiation and Characterization of Excitatory and Inhibitory Synapses by Cryo-electron Tomography and Correlative Microscopy. *J Neurosci* 38:1493–1510 . doi: 10.1523/JNEUROSCI.1548-17.2017
484. Phillips GR, Huang JK, Wang Y, Tanaka H, Shapiro L, Zhang W, Shan WS, Arndt K, Frank M, Gordon RE, Gawinowicz MA, Zhao Y, Colman DR (2001) The presynaptic particle web: ultrastructure, composition, dissolution, and reconstitution. *Neuron* 32:63–77
485. Südhof TC (2013) Neurotransmitter release: the last millisecond in the life of a synaptic vesicle. *Neuron* 80:675–90 . doi: 10.1016/j.neuron.2013.10.022
486. Lonart G, Simsek-Duran F (2006) Deletion of synapsins I and II genes alters the size of vesicular pools and rabphilin phosphorylation. *Brain Res* 1107:42–51 . doi: 10.1016/j.brainres.2006.05.092
487. Lonart G, Janz R, Johnson KM, Südhof TC (1998) Mechanism of action of rab3A in mossy fiber LTP. *Neuron* 21:1141–50 . doi: 10.1016/S0896-6273(00)80631-5
488. Pozzo-Miller LD, Gottschalk W, Zhang L, McDermott K, Du J, Gopalakrishnan R, Oho C, Sheng ZH, Lu B (1999) Impairments in high-frequency transmission, synaptic vesicle docking, and synaptic protein distribution in the hippocampus of BDNF knockout mice. *J Neurosci* 19:4972–83 . doi: 10.1523/JNEUROSCI.19-12-04972.1999
489. Sumioka A, Brown TE, Kato AS, Brecht DS, Kauer JA, Tomita S (2011) PDZ binding of TARPy-8 controls synaptic transmission but not synaptic plasticity. *Nat Neurosci* 14:1410–1412 . doi: 10.1038/nn.2952
490. Prieto GA, Trieu BH, Dang CT, Bilousova T, Gylys KH, Berchtold NC, Lynch G, Cotman CW (2017) Pharmacological Rescue of Long-Term Potentiation in Alzheimer Diseased Synapses. *J Neurosci* 37:1197–1212 . doi: 10.1523/JNEUROSCI.2774-16.2016
491. Ruvinsky I, Meyuhas O (2006) Ribosomal protein S6 phosphorylation: from protein synthesis to cell size. *Trends Biochem Sci* 31:342–348 . doi: 10.1016/j.tibs.2006.04.003
492. Sarbassov DD, Guertin DA, Ali SM, Sabatini DM (2005) Phosphorylation and Regulation of Akt/PKB by the Rictor-mTOR Complex. *Science (80-)* 307:1098–1101 . doi: 10.1126/science.1106148
493. Elias GM, Funke L, Stein V, Grant SG, Brecht DS, Nicoll RA (2006) Synapse-Specific and Developmentally Regulated Targeting of AMPA Receptors by a Family of MAGUK Scaffolding Proteins. *Neuron* 52:307–320 . doi: 10.1016/j.neuron.2006.09.012

BIBLIOGRAPHY

494. Bajjalieh SM, Peterson K, Linial M, Scheller RH (1993) Brain contains two forms of synaptic vesicle protein 2. *Proc Natl Acad Sci U S A* 90:2150–4
495. Bajjalieh SM, Frantz GD, Weimann JM, McConnell SK, Scheller RH (1994) Differential expression of synaptic vesicle protein 2 (SV2) isoforms. *J Neurosci* 14:5223–35
496. Naver B, Stub C, Møller M, Fenger K, Hansen AK, Hasholt L, Sørensen SA (2003) Molecular and behavioral analysis of the R6/1 Huntington's disease transgenic mouse. *Neuroscience* 122:1049–57
497. Giralt A, Saavedra A, Carretón O, Xifró X, Alberch J, Pérez-Navarro E (2011) Increased PKA signaling disrupts recognition memory and spatial memory: role in Huntington's disease. *Hum Mol Genet* 20:4232–4247 . doi: 10.1093/hmg/ddr351
498. Giralt A, Puigdellivol M, Carreton O, Paoletti P, Valero J, Parra-Damas A, Saura CA, Alberch J, Gines S (2012) Long-term memory deficits in Huntington's disease are associated with reduced CBP histone acetylase activity. *Hum Mol Genet* 21:1203–1216 . doi: 10.1093/hmg/ddr552
499. Jacinto E, Loewith R, Schmidt A, Lin S, Ruegg MA, Hall A, Hall MN, Rüeegg MA, Hall A, Hall MN, Ruegg MA, Hall A, Hall MN (2004) Mammalian TOR complex 2 controls the actin cytoskeleton and is rapamycin insensitive. *Nat Cell Biol* 6:1122–1128 . doi: ncb1183 [pii]10.1038/ncb1183
500. Sarbassov DD, Ali SM, Kim D-HH, Guertin DA, Latek RR, Erdjument-Bromage H, Tempst P, Sabatini DM, Dos D. Sarbassov DD, Ali SM, Kim D-HH, Guertin DA, Latek RR, Erdjument-Bromage H, Tempst P, Sabatini DM (2004) Rictor, a Novel Binding Partner of mTOR, Defines a Rapamycin-Insensitive and Raptor-Independent Pathway that Regulates the Cytoskeleton. *Curr Biol* 14:1296–1302 . doi: 10.1016/j.cub.2004.06.054S0960982204004713 [pii]
501. Guo JL, Lee VMY (2014) Cell-to-cell transmission of pathogenic proteins in neurodegenerative diseases. *Nat Med* 20:130–8 . doi: 10.1038/nm.3457
502. Lee S-J, Desplats P, Sigurdson C, Tsigelny I, Masliah E (2010) Cell-to-cell transmission of non-prion protein aggregates. *Nat Rev Neurol* 6:702–6 . doi: 10.1038/nrneurol.2010.145
503. Simons M, Raposo G (2009) Exosomes – vesicular carriers for intercellular communication. *Curr Opin Cell Biol* 21:575–581 . doi: 10.1016/j.ceb.2009.03.007
504. Bellingham SA, Guo BB, Coleman BM, Hill AF (2012) Exosomes: Vehicles for the Transfer of Toxic Proteins Associated with Neurodegenerative Diseases? *Front Physiol* 3:124 . doi: 10.3389/fphys.2012.00124
505. Rajendran L, Honscho M, Zahn TR, Keller P, Geiger KD, Verkade P, Simons K (2006) Alzheimer's disease beta-amyloid peptides are released in association with exosomes. *Proc Natl Acad Sci* 103:11172–11177 . doi: 10.1073/pnas.0603838103
506. Basso M, Pozzi S, Tortarolo M, Fiordaliso F, Bisighini C, Pasetto L, Spaltro G, Lidonnici D, Gensano F, Battaglia E, Bendotti C, Bonetto V (2013) Mutant Copper-Zinc Superoxide Dismutase (SOD1) Induces Protein Secretion Pathway Alterations and Exosome Release in Astrocytes. *J Biol Chem* 288:15699–15711 . doi: 10.1074/jbc.M112.425066
507. Saman S, Kim W, Raya M, Visnick Y, Miro S, Saman S, Jackson B, McKee AC, Alvarez VE, Lee NCY, Hall GF (2012) Exosome-associated Tau Is Secreted in Tauopathy Models and Is Selectively Phosphorylated in Cerebrospinal Fluid in

- Early Alzheimer Disease. *J Biol Chem* 287:3842–3849 . doi: 10.1074/jbc.M111.277061
508. de Gassart A, Geminard C, Fevrier B, Raposo G, Vidal M (2003) Lipid raft-associated protein sorting in exosomes. *Blood* 102:4336–4344 . doi: 10.1182/blood-2003-03-0871
509. Glebov OO, Bright NA, Nichols BJ (2006) Flotillin-1 defines a clathrin-independent endocytic pathway in mammalian cells. *Nat Cell Biol* 8:46–54 . doi: 10.1038/ncb1342
510. Fernow I, Icking A, Tikkanen R (2007) Reggie-1 and reggie-2 localize in non-caveolar rafts in epithelial cells: Cellular localization is not dependent on the expression of caveolin proteins. *Eur J Cell Biol* 86:345–352 . doi: 10.1016/j.ejcb.2007.03.004
511. Bickel PE, Scherer PE, Schnitzer JE, Oh P, Lisanti MP, Lodish HF (1997) Flotillin and epidermal surface antigen define a new family of caveolae-associated integral membrane proteins. *J Biol Chem* 272:13793–802
512. Piper RC, Katzmann DJ (2007) Biogenesis and function of multivesicular bodies. *Annu Rev Cell Dev Biol* 23:519–47 . doi: 10.1146/annurev.cellbio.23.090506.123319
513. Edgar JR, Eden ER, Futter CE (2014) Hrs- and CD63-Dependent Competing Mechanisms Make Different Sized Endosomal Intraluminal Vesicles. *Traffic* 15:197–211 . doi: 10.1111/tra.12139
514. Blum D, Torch S, Nissou MF, Benabid AL, Verna JM (2000) Extracellular toxicity of 6-hydroxydopamine on PC12 cells. *Neurosci Lett* 283:193–6
515. Hanrott K, Gudmunsen L, O'Neill MJ, Wonnacott S (2006) 6-Hydroxydopamine-induced Apoptosis Is Mediated via Extracellular Auto-oxidation and Caspase 3-dependent Activation of Protein Kinase C δ . *J Biol Chem* 281:5373–5382 . doi: 10.1074/jbc.M511560200
516. Clement M-V, Long LH, Ramalingam J, Halliwell B (2002) The cytotoxicity of dopamine may be an artefact of cell culture. *J Neurochem* 81:414–21
517. Bissig C, Gruenberg J (2014) ALIX and the multivesicular endosome: ALIX in Wonderland. *Trends Cell Biol* 24:19–25 . doi: 10.1016/j.tcb.2013.10.009
518. Garelick MG, Kennedy BK (2011) TOR on the brain. *Exp Gerontol* 46:155–163 . doi: 10.1016/j.exger.2010.08.030
519. Calabresi P, Galletti F, Saggese E, Ghiglieri V, Picconi B (2007) Neuronal networks and synaptic plasticity in Parkinson's disease: beyond motor deficits. *Park Relat Disord* 13 Suppl 3:S259-62 . doi: 10.1016/S1353-8020(08)70013-0
520. Cotzias GC, Papavasiliou PS, Gellene R (1969) Modification of Parkinsonism — Chronic Treatment with L-Dopa. *N Engl J Med* 280:337–345 . doi: 10.1056/NEJM196902132800701
521. Cotzias GC (1968) L-Dopa for Parkinsonism. *N Engl J Med* 278:630 . doi: 10.1056/NEJM196803142781127
522. Kyrtzi E, Pavlaki M, Stefanis L (2008) The S18Y polymorphic variant of UCH-L1 confers an antioxidant function to neuronal cells. *Hum Mol Genet* 17:2160–71 . doi: 10.1093/hmg/ddn115
523. Golab-Janowska M, Honczarenko K, Gawronska-Szklarz B, Potemkowski A

- (2007) CYP2D6 gene polymorphism as a probable risk factor for Alzheimer's disease and Parkinson's disease with dementia. *Neurol Neurochir Pol* 41:113–121
524. Fuchs J, Nilsson C, Kachergus J, Munz M, Larsson E-M, Schüle B, Langston JW, Middleton FA, Ross OA, Hulihan M, Gasser T, Farrer MJ (2007) Phenotypic variation in a large Swedish pedigree due to *SNCA* duplication and triplication. *Neurology* 68:916–922 . doi: 10.1212/01.wnl.0000254458.17630.c5
525. Emelyanov AK, Andoskin PA, Miliukhina I V, Timofeeva AA, Yakimovskii AF, Senkevich KA, Nikolaev MA, Pchelina SN (2016) *SNCA* rs356219 AND rs356165 variants are associated with Parkinson's disease and increased alpha-synuclein gene expression in the CD45(+)-blood cells. *Tsitologija* 58:99–104
526. Cardo LF, Coto E, de Mena L, Ribacoba R, Lorenzo-Betancor O, Pastor P, Samaranch LI, Mata IF, Díaz M, Moris G, Menéndez M, Corao AI, Alvarez V (2012) A Search for *SNCA* 3' UTR Variants Identified SNP rs356165 as a Determinant of Disease Risk and Onset Age in Parkinson's Disease. *J Mol Neurosci* 47:425–430 . doi: 10.1007/s12031-011-9669-1
527. Chondrogiorgi M, Tatsioni A, Reichmann H, Konitsiotis S (2014) Dopamine agonist monotherapy in Parkinson's disease and potential risk factors for dyskinesia: a meta-analysis of levodopa-controlled trials. *Eur J Neurol* 21:433–440 . doi: 10.1111/ene.12318
528. Jankovic J (2005) Motor fluctuations and dyskinesias in Parkinson's disease: Clinical manifestations. *Mov Disord* 20:S11–S16 . doi: 10.1002/mds.20458
529. Nadjar A, Gerfen CR, Bezard E (2009) Priming for l-dopa-induced dyskinesia in Parkinson's disease: A feature inherent to the treatment or the disease? *Prog Neurobiol* 87:1–9 . doi: 10.1016/j.pneurobio.2008.09.013
530. Fahn S, Elton R (1987) Unified Parkinson's Disease Rating Scale. In: Recent developments in Parkinson's disease. pp 153–63
531. Bano D, Zanetti F, Mende Y, Nicotera P (2011) Neurodegenerative processes in Huntington's disease. *Cell Death Dis* 2:e228–e228 . doi: 10.1038/cddis.2011.112
532. Kumar A, Ratan RR (2016) Oxidative Stress and Huntington's Disease: The Good, The Bad, and The Ugly. *J Huntingtons Dis* 5:217–237 . doi: 10.3233/JHD-160205
533. Askeland G, Dosoudilova Z, Rodinova M, Klempir J, Liskova I, Kuśnierczyk A, Bjørås M, Nesse G, Klungland A, Hansikova H, Eide L (2018) Increased nuclear DNA damage precedes mitochondrial dysfunction in peripheral blood mononuclear cells from Huntington's disease patients. *Sci Rep* 8:9817 . doi: 10.1038/s41598-018-27985-y
534. Duennwald ML, Lindquist S (2008) Impaired ERAD and ER stress are early and specific events in polyglutamine toxicity. *Genes Dev* 22:3308–3319 . doi: 10.1101/gad.1673408
535. Reijonen S, Putkonen N, Norremolle A, Lindholm D, Korhonen L (2008) Inhibition of endoplasmic reticulum stress counteracts neuronal cell death and protein aggregation caused by N-terminal mutant huntingtin proteins. *Exp Cell Res* 314:950–960 . doi: 10.1016/j.yexcr.2007.12.025
536. Qiu Z, Norflus F, Singh B, Swindell MK, Buzescu R, Bejarano M, Chopra R, Zucker B, Benn CL, DiRocco DP, Cha J-HJHJ, Ferrante RJ, Hersch SM (2006) Sp1 is up-regulated in cellular and transgenic models of huntington disease, and its

- reduction is neuroprotective. *J Biol Chem* 281:16672–16680 . doi: 10.1074/jbc.M511648200
537. Illuzzi J, Yerkes S, Parekh-Olmedo H, Kmiec EB (2009) DNA breakage and induction of DNA damage response proteins precede the appearance of visible mutant huntingtin aggregates. *J Neurosci Res* 87:733–47 . doi: 10.1002/jnr.21881
538. Chae J-I, Kim D-W, Lee N, Jeon Y-J, Jeon I, Kwon J, Kim J, Soh Y, Lee D-S, Seo KS, Choi N-J, Park BC, Kang SH, Ryu J, Oh S-H, Shin DA, Lee DR, Do JT, Park I-H, Daley GQ, Song J (2012) Quantitative proteomic analysis of induced pluripotent stem cells derived from a human Huntington's disease patient. *Biochem J* 446:359–71 . doi: 10.1042/BJ20111495
539. Anglada-Huguet M, Giralt A, Perez-Navarro E, Alberch J, Xifró X (2012) Activation of Elk-1 participates as a neuroprotective compensatory mechanism in models of Huntington's disease. *J Neurochem* 121:639–648 . doi: 10.1111/j.1471-4159.2012.07711.x
540. Tsai YC, Fishman PS, Thakor N V, Oyler GA (2003) Parkin facilitates the elimination of expanded polyglutamine proteins and leads to preservation of proteasome function. *J Biol Chem* 278:22044–55 . doi: 10.1074/jbc.M212235200
541. Igarashi S, Morita H, Bennett KM, Tanaka Y, Engelender S, Peters MF, Cooper JK, Wood JD, Sawa A, Ross CA (2003) Inducible PC12 cell model of Huntington's disease shows toxicity and decreased histone acetylation. *Neuroreport* 14:565–8 . doi: 10.1097/01.wnr.0000062604.01019.e1
542. Poirier MA, Jiang H, Ross CA (2005) A structure-based analysis of huntingtin mutant polyglutamine aggregation and toxicity: evidence for a compact beta-sheet structure. *Hum Mol Genet* 14:765–774 . doi: 10.1093/hmg/ddi071
543. Tagawa K, Marubuchi S, Qi M-L, Enokido Y, Tamura T, Inagaki R, Murata M, Kanazawa I, Wanker EE, Okazawa H (2007) The induction levels of heat shock protein 70 differentiate the vulnerabilities to mutant huntingtin among neuronal subtypes. *J Neurosci* 27:868–80 . doi: 10.1523/JNEUROSCI.4522-06.2007
544. Bertoni A, Giuliano P, Galgani M, Rotoli D, Ulianich L, Adornetto A, Santillo MR, Porcellini A, Avvedimento VE (2011) Early and late events induced by polyQ-expanded proteins: identification of a common pathogenic property of polyQ-expanded proteins. *J Biol Chem* 286:4727–41 . doi: 10.1074/jbc.M110.156521
545. Zhang Z, Chu S-F, Wang S-S, Jiang Y-N, Gao Y, Yang P-F, Ai Q-D, Chen N-H (2018) RTP801 is a critical factor in the neurodegeneration process of A53T α -synuclein in a mouse model of Parkinson's disease under chronic restraint stress. *Br J Pharmacol* 175:590–605 . doi: 10.1111/bph.14091
546. Dolmetsch R, Geschwind DH (2011) The human brain in a dish: the promise of iPSC-derived neurons. *Cell* 145:831–4 . doi: 10.1016/j.cell.2011.05.034
547. Petersén Å, Hansson O, Puschban Z, Sapp E, Romero N, Castilho RF, Sulzer D, Rice M, DiFiglia M, Przedborski S, Brundin P (2001) Mice transgenic for exon 1 of the Huntington's disease gene display reduced striatal sensitivity to neurotoxicity induced by dopamine and 6-hydroxydopamine. *Eur J Neurosci* 14:1425–1435 . doi: 10.1046/j.0953-816X.2001.01765.x
548. de Almeida LP, Ross CA, Zala D, Aebischer P, Déglon N (2002) Lentiviral-mediated delivery of mutant huntingtin in the striatum of rats induces a selective neuropathology modulated by polyglutamine repeat size, huntingtin expression levels, and protein length. *J Neurosci* 22:3473–83 . doi: 20026337

BIBLIOGRAPHY

549. Franich NR, Fitzsimons HL, Fong DM, Klugmann M, During MJ, Young D (2008) AAV Vector-mediated RNAi of Mutant Huntingtin Expression Is Neuroprotective in a Novel Genetic Rat Model of Huntington's Disease. *Mol Ther* 16:947–956 . doi: 10.1038/mt.2008.50
550. DiFiglia M, Sena-Esteves M, Chase K, Sapp E, Pfister E, Sass M, Yoder J, Reeves P, Pandey RK, Rajeev KG, Manoharan M, Sah DWY, Zamore PD, Aronin N (2007) Therapeutic silencing of mutant huntingtin with siRNA attenuates striatal and cortical neuropathology and behavioral deficits. *Proc Natl Acad Sci* 104:17204–17209 . doi: 10.1073/pnas.0708285104
551. Beal MF, Ferrante RJ, Swartz KJ, Kowall NW (1991) Chronic quinolinic acid lesions in rats closely resemble Huntington's disease. *J Neurosci* 11:1649–59
552. Huang X, Yang K, Zhang Y, Wang Q, Li Y (2016) Quinolinic acid induces cell apoptosis in PC12 cells through HIF-1-dependent RTP801 activation. *Metab Brain Dis* 31:435–444 . doi: 10.1007/s11011-015-9782-x
553. Richards P, Didszun C, Campesan S, Simpson A, Horley B, Young KW, Glynn P, Cain K, Kyriacou CP, Giorgini F, Nicotera P (2011) Dendritic spine loss and neurodegeneration is rescued by Rab11 in models of Huntington's disease. *Cell Death Differ* 18:191–200 . doi: 10.1038/cdd.2010.127
554. Murmu RP, Li W, Holtmaat A, Li J-Y (2013) Dendritic spine instability leads to progressive neocortical spine loss in a mouse model of Huntington's disease. *J Neurosci* 33:12997–3009 . doi: 10.1523/JNEUROSCI.5284-12.2013
555. Ferrante RJ, Kowall NW, Richardson EP (1991) Proliferative and degenerative changes in striatal spiny neurons in Huntington's disease: a combined study using the section-Golgi method and calbindin D28k immunocytochemistry. *J Neurosci* 11:3877–87
556. Graveland GA, Williams RS, DiFiglia M (1985) Evidence for degenerative and regenerative changes in neostriatal spiny neurons in Huntington's disease. *Science* 227:770–3
557. Sotrel A, Williams RS, Kaufmann WE, Myers RH (1993) Evidence for neuronal degeneration and dendritic plasticity in cortical pyramidal neurons of Huntington's disease: a quantitative Golgi study. *Neurology* 43:2088–96
558. Fourie C, Kim E, Waldvogel H, Wong JM, McGregor A, Faull RLM, Montgomery JM (2014) Differential Changes in Postsynaptic Density Proteins in Postmortem Huntington's Disease and Parkinson's Disease Human Brains. *J Neurodegener Dis* 2014:1–14 . doi: 10.1155/2014/938530
559. Cepeda C, Starling AJ, Wu N, Nguyen OK, Uzgil B, Soda T, André VM, Ariano MA, Levine MS (2004) Increased GABAergic function in mouse models of Huntington's disease: Reversal by BDNF. *J Neurosci Res* 78:855–867 . doi: 10.1002/jnr.20344
560. Spires TL, Grote HE, Garry S, Cordery PM, Van Dellen A, Blakemore C, Hannan AJ (2004) Dendritic spine pathology and deficits in experience-dependent dendritic plasticity in R6/1 Huntington's disease transgenic mice. *Eur J Neurosci* 19:2799–2807 . doi: 10.1111/j.0953-816X.2004.03374.x
561. Heck N, Betuing S, Vanhoutte P, Caboche J (2012) A deconvolution method to improve automated 3D-analysis of dendritic spines: application to a mouse model of Huntington's disease. *Brain Struct Funct* 217:421–434 . doi: 10.1007/s00429-011-0340-y

562. Klapstein GJ, Fisher RS, Zanjani H, Cepeda C, Jokel ES, Chesselet M-F, Levine MS (2001) Electrophysiological and Morphological Changes in Striatal Spiny Neurons in R6/2 Huntington's Disease Transgenic Mice. *J Neurophysiol* 86:2667–2677 . doi: 10.1152/jn.2001.86.6.2667
563. Simmons DA, Belichenko NP, Ford EC, Semaan S, Monbureau M, Aiyaswamy S, Holman CM, Condon C, Shamloo M, Massa SM, Longo FM (2016) A small molecule p75NTR ligand normalizes signalling and reduces Huntington's disease phenotypes in R6/2 and BACHD mice. *Hum Mol Genet* 25:4920–4938 . doi: 10.1093/hmg/ddw316
564. Torres-Peraza JF, Giralt A, García-Martínez JM, Pedrosa E, Canals JM, Alberch J (2008) Disruption of striatal glutamatergic transmission induced by mutant huntingtin involves remodeling of both postsynaptic density and NMDA receptor signaling. *Neurobiol Dis* 29:409–421 . doi: 10.1016/j.nbd.2007.10.003
565. Valencia A, Sapp E, Kimm JS, McClory H, Ansong KA, Yohrling G, Kwak S, Kegel KB, Green KM, Shaffer SA, Aronin N, DiFiglia M (2013) Striatal synaptosomes from Hdh140Q/140Q knock-in mice have altered protein levels, novel sites of methionine oxidation, and excess glutamate release after stimulation. *J Huntingtons Dis* 2:459–75 . doi: 10.3233/JHD-130080
566. Anglada-Huguet M, Vidal-Sancho L, Giralt A, García-Díaz Barriga G, Xifró X, Alberch J (2016) Prostaglandin E2 EP2 activation reduces memory decline in R6/1 mouse model of Huntington's disease by the induction of BDNF-dependent synaptic plasticity. *Neurobiol Dis* 95:22–34 . doi: 10.1016/j.nbd.2015.09.001
567. Pirbhoy PS, Farris S, Steward O (2017) Synaptically driven phosphorylation of ribosomal protein S6 is differentially regulated at active synapses versus dendrites and cell bodies by MAPK and PI3K/mTOR signaling pathways. *Learn Mem* 24:341–357 . doi: 10.1101/lm.044974.117
568. Pirbhoy PS, Farris S, Steward O (2016) Synaptic activation of ribosomal protein S6 phosphorylation occurs locally in activated dendritic domains. *Learn Mem* 23:255–69 . doi: 10.1101/lm.041947.116
569. Kapur M, Monaghan CE, Ackerman SL (2017) Review Regulation of mRNA Translation in Neurons-A Matter of Life and Death. doi: 10.1016/j.neuron.2017.09.057
570. Qiao S, Dennis M, Song X, Vadysirisack DD, Salunke D, Nash Z, Yang Z, Liesa M, Yoshioka J, Matsuzawa S-I, Shirihaï OS, Lee RT, Reed JC, Ellisen LW (2015) A REDD1/TXNIP pro-oxidant complex regulates ATG4B activity to control stress-induced autophagy and sustain exercise capacity. *Nat Commun* 6:7014 . doi: 10.1038/ncomms8014
571. Marco S, Giralt A, Petrovic MM, Pouladi MA, Martínez-Turrillas R, Martínez-Hernández J, Kaltenbach LS, Torres-Peraza J, Graham RK, Watanabe M, Luján R, Nakanishi N, Lipton SA, Lo DC, Hayden MR, Alberch J, Wesseling JF, Pérez-Otaño I (2013) Suppressing aberrant GluN3A expression rescues synaptic and behavioral impairments in Huntington's disease models. *Nat Med* 19:1030–1038 . doi: 10.1038/nm.3246
572. Brito V, Giralt A, Enriquez-Barreto L, Puigdel·lívol M, Suelves N, Zamora-Moratalla A, Ballesteros JJ, Martín ED, Dominguez-Iturza N, Morales M, Alberch J, Ginés S (2014) Neurotrophin receptor p75NTR mediates Huntington's disease-associated synaptic and memory dysfunction. *J Clin Invest* 124:4411–4428 . doi: 10.1172/JCI74809

BIBLIOGRAPHY

573. Spinelli M, Fusco S, Mainardi M, Scala F, Natale F, Lapenta R, Mattera A, Rinaudo M, Li Puma DD, Ripoli C, Grassi A, D'Ascenzo M, Grassi C (2017) Brain insulin resistance impairs hippocampal synaptic plasticity and memory by increasing GluA1 palmitoylation through FoxO3a. *Nat Commun* 8:2009 . doi: 10.1038/s41467-017-02221-9
574. Marino S, Krimpenfort P, Leung C, van der Korput HAGM, Trapman J, Camenisch I, Berns A, Brandner S (2002) PTEN is essential for cell migration but not for fate determination and tumourigenesis in the cerebellum. *Development* 129:3513–22
575. Perez-Gonzalez R, Gauthier SA, Kumar A, Levy E (2012) The Exosome Secretory Pathway Transports Amyloid Precursor Protein Carboxyl-terminal Fragments from the Cell into the Brain Extracellular Space. *J Biol Chem* 287:43108–43115 . doi: 10.1074/jbc.M112.404467
576. Tang Z, Ioja E, Berezcki E, Hultenby K, Li C, Guan Z, Winblad B, Pei J-J (2015) mTor mediates tau localization and secretion: Implication for Alzheimer's disease. *Biochim Biophys Acta - Mol Cell Res* 1853:1646–1657 . doi: 10.1016/j.bbamcr.2015.03.003
577. Fraser KB, Moehle MS, Daher JPL, Webber PJ, Williams JY, Stewart CA, Yacoubian TA, Cowell RM, Dokland T, Ye T, Chen D, Siegal GP, Galemno RA, Tsika E, Moore DJ, Standaert DG, Kojima K, Mobley JA, West AB (2013) LRRK2 secretion in exosomes is regulated by 14-3-3. *Hum Mol Genet* 22:4988–5000 . doi: 10.1093/hmg/ddt346
578. Xu J, Camfield R, Gorski SM (2018) The interplay between exosomes and autophagy – partners in crime. *J Cell Sci* 131:jcs215210 . doi: 10.1242/jcs.215210
579. Baixauli F, López-Otín C, Mittelbrunn M (2014) Exosomes and autophagy: coordinated mechanisms for the maintenance of cellular fitness. *Front Immunol* 5:403 . doi: 10.3389/fimmu.2014.00403
580. Hernández-Saavedra D, Sanders L, Perez MJ, Kosmider B, Smith LP, Mitchell JD, Yoshida T, Tudor RM (2017) RTP801 Amplifies Nicotinamide Adenine Dinucleotide Phosphate Oxidase-4–Dependent Oxidative Stress Induced by Cigarette Smoke. *Am J Respir Cell Mol Biol* 56:62–73 . doi: 10.1165/rcmb.2016-0144OC
581. Savina A, Furlán M, Vidal M, Colombo MI (2003) Exosome release is regulated by a calcium-dependent mechanism in K562 cells. *J Biol Chem* 278:20083–20090 . doi: 10.1074/jbc.M301642200
582. Nakamura K, Jinnin M, Harada M, Kudo H, Nakayama W, Inoue K, Ogata A, Kajihara I, Fukushima S, Ihn H (2016) Altered expression of CD63 and exosomes in scleroderma dermal fibroblasts. *J Dermatol Sci* 84:30–39 . doi: 10.1016/j.jdermsci.2016.06.013
583. Gauthier SA, Pérez-González R, Sharma A, Huang F-K, Alldred MJ, Pawlik M, Kaur G, Ginsberg SD, Neubert TA, Levy E Enhanced exosome secretion in Down syndrome brain—a protective mechanism to alleviate neuronal endosomal abnormalities. doi: 10.1186/s40478-017-0466-0
584. Takino T, Miyamori H, Kawaguchi N, Uekita T, Seiki M, Sato H (2003) Tetraspanin CD63 promotes targeting and lysosomal proteolysis of membrane-type 1 matrix metalloproteinase. *Biochem Biophys Res Commun* 304:160–6
585. Atienzar-Aroca S, Flores-Bellver M, Serrano-Heras G, Martinez-Gil N, Barcia JM, Aparicio S, Perez-Cremades D, Garcia-Verdugo JM, Diaz-Llopis M, Romero FJ,

- Sancho-Pelluz J (2016) Oxidative stress in retinal pigment epithelium cells increases exosome secretion and promotes angiogenesis in endothelial cells. *J Cell Mol Med* 20:1457–1466 . doi: 10.1111/jcmm.12834
586. Li X-B, Zhang Z-R, Schluesener HJ, Xu S-Q Role of exosomes in immune regulation. *J Cell Mol Med* 10:364–75
587. Yim N, Choi C (2016) Extracellular vesicles as novel carriers for therapeutic molecules. *BMB Rep* 49:585–586 . doi: 10.5483/BMBREP.2016.49.11.174
588. Harrison EB, Hochfelder CG, Lamberty BG, Meays BM, Morsey BM, Kelso ML, Fox HS, Yelamanchili S V. (2016) Traumatic brain injury increases levels of miR-21 in extracellular vesicles: implications for neuroinflammation. *FEBS Open Bio* 6:835–846 . doi: 10.1002/2211-5463.12092
589. An K, Klyubin I, Kim Y, Jung J, Mably AJ, O'Dowd ST, Lynch T, Kanmert D, Lemere CA, Finan GM, Park J, Kim T-W, Walsh DM, Rowan MJ, Kim J-H (2013) Exosomes neutralize synaptic-plasticity-disrupting activity of A β assemblies in vivo. *Mol Brain* 6:47 . doi: 10.1186/1756-6606-6-47
590. Jarmalavičiūtė A, Tunaitis V, Pivoraitė U, Venalis A, Pivoriūnas A (2015) Exosomes from dental pulp stem cells rescue human dopaminergic neurons from 6-hydroxy-dopamine-induced apoptosis. *Cytotherapy* 17:932–939 . doi: 10.1016/j.jcyt.2014.07.013
591. Arslan F, Lai RC, Smeets MB, Akeroyd L, Choo A, Agnor ENE, Timmers L, van Rijen H V., Doevendans PA, Pasterkamp G, Lim SK, de Kleijn DP (2013) Mesenchymal stem cell-derived exosomes increase ATP levels, decrease oxidative stress and activate PI3K/Akt pathway to enhance myocardial viability and prevent adverse remodeling after myocardial ischemia/reperfusion injury. *Stem Cell Res* 10:301–312 . doi: 10.1016/j.scr.2013.01.002
592. Wang K, Jiang Z, Webster KA, Chen J, Hu H, Zhou Y, Zhao J, Wang L, Wang Y, Zhong Z, Ni C, Li Q, Xiang C, Zhang L, Wu R, Zhu W, Yu H, Hu X, Wang J (2017) Enhanced Cardioprotection by Human Endometrium Mesenchymal Stem Cells Driven by Exosomal MicroRNA-21. *Stem Cells Transl Med* 6:209–222 . doi: 10.5966/sctm.2015-0386
593. Mutschelknaus L, Azimzadeh O, Heider T, Winkler K, Vetter M, Kell R, Tapio S, Merl-Pham J, Huber SM, Edalat L, Radulović V, Anastasov N, Atkinson MJ, Moertl S (2017) Radiation alters the cargo of exosomes released from squamous head and neck cancer cells to promote migration of recipient cells. *Sci Rep* 7:12423 . doi: 10.1038/s41598-017-12403-6
594. Subra C, Grand D, Laulagnier K, Stella A, Lambeau G, Paillasse M, De Medina P, Monsarrat B, Perret B, Silvente-Poirot S, Poirot M, Record M (2010) Exosomes account for vesicle-mediated transcellular transport of activatable phospholipases and prostaglandins. *J Lipid Res* 51:2105–2120 . doi: 10.1194/jlr.M003657
595. Phuyal S, Hessvik NP, Skotland T, Sandvig K, Llorente A (2014) Regulation of exosome release by glycosphingolipids and flotillins. *FEBS J* 281:2214–2227 . doi: 10.1111/febs.12775
596. Dai W, Miller WP, Toro AL, Black AJ, Dierschke SK, Feehan RP, Kimball SR, Dennis MD (2018) Deletion of the stress-response protein REDD1 promotes ceramide-induced retinal cell death and JNK activation. *FASEB J* 32:1313–1324 . doi: 10.1096/fj.201800413RR
597. Kamocki K, Van Demark M, Fisher A, Rush NI, Presson RG, Hubbard W,

- Berdyshev E V., Adamsky S, Feinstein E, Gandjeva A, Tudor RM, Petrache I (2013) RTP801 Is Required for Ceramide-Induced Cell-Specific Death in the Murine Lung. *Am J Respir Cell Mol Biol* 48:87–93 . doi: 10.1165/rcmb.2012-0254OC
598. Menck K, Sönmezer C, Stefan Worst T, Schulz M, Helene Dihazi G, Streit F, Erdmann G, Kling S, Boutros M, Binder C, Christina Gross J (2017) Neutral sphingomyelinases control extracellular vesicles budding from the plasma membrane. doi: 10.1080/20013078.2017.1378056
599. Niel C, Sinoquet C, Dina C, Rocheleau G (2015) A survey about methods dedicated to epistasis detection. *Front Genet* 6:285 . doi: 10.3389/fgene.2015.00285
600. Cordell HJ (2002) Epistasis: what it means, what it doesn't mean, and statistical methods to detect it in humans. *Hum Mol Genet* 11:2463–8
601. Bornscheuer UT, Huisman GW, Kazlauskas RJ, Lutz S, Moore JC, Robins K (2012) Engineering the third wave of biocatalysis. *Nature* 485:185–194 . doi: 10.1038/nature11117
602. Elbers CC, van Eijk KR, Franke L, Mulder F, van der Schouw YT, Wijmenga C, Onland-Moret NC (2009) Using genome-wide pathway analysis to unravel the etiology of complex diseases. *Genet Epidemiol* 33:419–431 . doi: 10.1002/gepi.20395
603. Su M-W, Tung K-Y, Liang P-H, Tsai C-H, Kuo N-W, Lee YL (2012) Gene-Gene and Gene-Environmental Interactions of Childhood Asthma: A Multifactor Dimension Reduction Approach. *PLoS One* 7:e30694 . doi: 10.1371/journal.pone.0030694
604. Licastro F, Chiappelli M, Porcellini E, Campo G, Buscema M, Grossi E, Garoia F, Ferrari R (2010) Gene-gene and gene - clinical factors interaction in acute myocardial infarction: a new detailed risk chart. *Curr Pharm Des* 16:783–8
605. Lanktree MB, Hegele RA (2009) Gene-gene and gene-environment interactions: new insights into the prevention, detection and management of coronary artery disease. *Genome Med* 1:28 . doi: 10.1186/gm28
606. Ellis JA, Scurrah KJ, Li YR, Ponsonby A-L, Chavez RA, Pezic A, Dwyer T, Akikusa JD, Allen RC, Becker ML, Thompson SD, Lie BA, Flatø B, Førre Ø, Punaro M, Wise C, Finkel TH, Hakonarson H, Munro JE (2015) Epistasis amongst PTPN2 and genes of the vitamin D pathway contributes to risk of juvenile idiopathic arthritis. *J Steroid Biochem Mol Biol* 145:113–120 . doi: 10.1016/j.jsbmb.2014.10.012
607. Zhou J-B, Liu C, Niu W-Y, Xin Z, Yu M, Feng J-P, Yang J-K (2012) Contributions of Renin-Angiotensin System-Related Gene Interactions to Obesity in a Chinese Population. *PLoS One* 7:e42881 . doi: 10.1371/journal.pone.0042881
608. Holmans P, Moskvina V, Jones L, Sharma M, Vedernikov A, Buchel F, Sadd M, Bras JM, Bettella F, Nicolaou N, Simón-Sánchez J, Mittag F, Gibbs JR, Schulte C, Durr A, Guerreiro R, Hernandez D, Brice A, Stefánsson H, Majamaa K, Gasser T, Heutink P, Wood NW, Martinez M, Singleton AB, Nalls MA, Hardy J, Morris HR, Williams NM, Arepalli S, Barker R, Barrett J, Ben-Shlomo Y, Berendse HW, Berg D, Bhatia K, de Bie RMA, Biffi A, Bloem B, Brice A, Bochdanovits Z, Bonin M, Bras JM, Brockmann K, Brooks J, Burn DJ, Charlesworth G, Chen H, Chinnery PF, Chong S, Clarke CE, Cookson MR, Cooper JM, Corvol J-C, Counsell C, Damier P, Dartigues JF, Deloukas P, Deuschl G, Dexter DT, van Dijk KD, Dillman A, Durif

- F, Durr A, Edkins S, Evans JR, Foltynie T, Gao J, Gardner M, Gasser T, Gibbs JR, Goate A, Gray E, Guerreiro R, Gústafsson Ó, Hardy J, Harris C, Hernandez DG, Heutink P, van Hilten JJ, Hofman A, Hollenbeck A, Holmans P, Holton J, Hu M, Huber H, Hudson G, Hunt SE, Huttenlocher J, Illig T, Langford C, Lees A, Lesage S, Lichtner P, Limousin P, Lopez G, Lorenz D, Martinez M, McNeill A, Moorby C, Moore M, Morris H, Morrison KE, Moskvina V, Mudanohwo E, Nalls MA, Pearson J, Perlmutter JS, Pétursson H, Plagnol V, Pollak P, Post B, Potter S, Ravina B, Revesz T, Riess O, Rivadeneira F, Rizzu P, Ryten M, Saad M, Sawcer S, Schapira A, Scheffer H, Sharma M, Shaw K, Sheerin U-M, Shoulson I, Schulte C, Sidransky E, Simón-Sánchez J, Singleton AB, Smith C, Stefánsson H, Stefánsson K, Steinberg S, Stockton JD, Sveinbjornsdottir S, Talbot K, Tanner CM, Tashakkori-Ghanbaria A, Tison F, Trabzuni D, Traynor BJ, Uitterlinden AG, Velseboer D, Vidailhet M, Walker R, van de Warrenburg B, Wickremaratchi M, Williams N, Williams-Gray CH, Winder-Rhodes S, Wood N (2013) A pathway-based analysis provides additional support for an immune-related genetic susceptibility to Parkinson's disease. *Hum Mol Genet* 22:1039–1049 . doi: 10.1093/hmg/dd5492
609. Lesnick TG, Papapetropoulos S, Mash DC, Ffrench-Mullen J, Shehadeh L, de Andrade M, Henley JR, Rocca WA, Ahlskog JE, Maraganore DM (2007) A Genomic Pathway Approach to a Complex Disease: Axon Guidance and Parkinson Disease. *PLoS Genet* 3:e98 . doi: 10.1371/journal.pgen.0030098
610. Singh NK, Banerjee BD, Bala K, Chhillar M, Chhillar N (2014) Gene-gene and gene-environment interaction on the risk of Parkinson's disease. *Curr Aging Sci* 7:101–9
611. Cui J-J, Wang L-Y, Zhu T, Gong W-J, Zhou H-H, Liu Z-Q, Yin J-Y (2017) Gene-gene and gene-environment interactions influence platinum-based chemotherapy response and toxicity in non-small cell lung cancer patients. *Sci Rep* 7:5082 . doi: 10.1038/s41598-017-05246-8
612. Mas S, Gassó P, Ritter MAA, Malagelada C, Bernardo M, Lafuente A (2015) Pharmacogenetic predictor of extrapyramidal symptoms induced by antipsychotics: multilocus interaction in the mTOR pathway. *Eur Neuropsychopharmacol* 25:51–9 . doi: 10.1016/j.euroneuro.2014.11.011
613. Moore PE (2011) Influence of gene–gene interactions on response to albuterol therapy. *Pharmacogenomics* 12:1–3 . doi: 10.2217/pgs.10.192
614. Rajagopal VM, Rajkumar AP, Jacob KS, Jacob M (2018) Gene–gene interaction between DRD4 and COMT modulates clinical response to clozapine in treatment-resistant schizophrenia. *Pharmacogenet Genomics* 28:31–35 . doi: 10.1097/FPC.0000000000000314
615. Cruchaga C, Vidal-Taboada JM, Ezquerra M, Lorenzo E, Martinez-Lage P, Blazquez M, Tolosa E, Pastor P, Pastor P (2009) 5'-upstream variants of CRHR1 and MAPT genes associated with age at onset in progressive supranuclear palsy and cortical basal degeneration. *Neurobiol Dis* 33:164–170 . doi: 10.1016/j.nbd.2008.09.027
616. Baker M, Litvan I, Houlden H, Adamson J, Dickson D, Perez-Tur J, Hardy J, Lynch T, Bigio E, Hutton M (1999) Association of an extended haplotype in the tau gene with progressive supranuclear palsy. *Hum Mol Genet* 8:711–5
617. Pastor P, Ezquerra M, Tolosa E, Muñoz E, José Martí M, Valdeoriola F, Molinuevo JL, Calopa M, Oliva R (2002) Further extension of the H1 haplotype associated with progressive supranuclear palsy. *Mov Disord* 17:550–556 . doi:

- 10.1002/mds.10076
618. Ezquerra M, Compta Y, Martí MJ, Ezquerra Y, Compta MJ (2011) Identifying the genetic components underlying the pathophysiology of movement disorders. *App Clin Genet* 4:81-92 . doi: 10.2147/TACG.S7333
619. Pastor P, Ezquerra M, Muñoz E, Martí MJ, Blesa R, Tolosa E, Oliva R (2000) Significant association between the tau gene A0/A0 genotype and Parkinson's disease. *Ann Neurol* 47:242-5
620. Fung HC, Xiromerisiou G, Gibbs JR, Wu YR, Eerola J, Gourbali V, Hellström O, Chen CM, Duckworth J, Papadimitriou A, Tienari PJ, Hadjigeorgiou GM, Hardy J, Singleton AB (2006) Association of Tau Haplotype-Tagging Polymorphisms with Parkinson's Disease in Diverse Ethnic Parkinson's Disease Cohorts. *Neurodegener Dis* 3:327-333 . doi: 10.1159/000097301
621. Fuchs J, Tichopad A, Golub Y, Munz M, Schweitzer KJ, Wolf B, Berg D, Mueller JC, Gasser T (2008) Genetic variability in the SNCA gene influences α -synuclein levels in the blood and brain. *FASEB J* 22:1327-1334 . doi: 10.1096/fj.07-9348com
622. Mata IF, Shi M, Agarwal P, Chung KA, Edwards KL, Factor SA, Galasko DR, Ghingina C, Griffith A, Higgins DS, Kay DM, Kim H, Leverenz JB, Quinn JF, Roberts JW, Samii A, Snapinn KW, Tsuang DW, Yearout D, Zhang J, Payami H, Zabetian CP (2010) SNCA Variant Associated With Parkinson Disease and Plasma α -Synuclein Level. *Arch Neurol* 67:1350-6 . doi: 10.1001/archneurol.2010.279
623. Polymeropoulos MH, Lavedan C, Leroy E, Ide SE, Dehejia A, Dutra A, Pike B, Root H, Rubenstein J, Boyer R, Stenroos ES, Chandrasekharappa S, Athanassiadou A, Papapetropoulos T, Johnson WG, Lazzarini AM, Duvoisin RC, Di Iorio G, Golbe LI, Nussbaum RL (1997) Mutation in the alpha-synuclein gene identified in families with Parkinson's disease. *Science* 276:2045-7
624. Paumier KL, Luk KC, Manfredsson FP, Kanaan NM, Lipton JW, Collier TJ, Steece-Collier K, Kemp CJ, Celano S, Schulz E, Sandoval IM, Fleming S, Dirr E, Polinski NK, Trojanowski JQ, Lee VM, Sortwell CE (2015) Intrastratial injection of pre-formed mouse α -synuclein fibrils into rats triggers α -synuclein pathology and bilateral nigrostriatal degeneration. *Neurobiol Dis* 82:185-199 . doi: 10.1016/j.nbd.2015.06.003
625. Ishizawa T, Mattila P, Davies P, Wang D, Dickson DW (2003) Colocalization of Tau and Alpha-Synuclein Epitopes in Lewy Bodies. *J Neuropathol Exp Neurol* 62:389-397 . doi: 10.1093/jnen/62.4.389
626. Arima K, Hirai S, Sunohara N, Aoto K, Izumiyama Y, Uéda K, Ikeda K, Kawai M (1999) Cellular co-localization of phosphorylated tau- and NACP/ α -synuclein-epitopes in Lewy bodies in sporadic Parkinson's disease and in dementia with Lewy bodies. *Brain Res* 843:53-61 . doi: 10.1016/S0006-8993(99)01848-X
627. Muntané G, Dalfó E, Martínez A, Ferrer I (2008) Phosphorylation of tau and α -synuclein in synaptic-enriched fractions of the frontal cortex in Alzheimer's disease, and in Parkinson's disease and related α -synucleinopathies. *Neuroscience* 152:913-923 . doi: 10.1016/J.NEUROSCIENCE.2008.01.030
628. Jensen PH, Hager H, Nielsen MS, Hojrup P, Gliemann J, Jakes R (1999) alpha-synuclein binds to Tau and stimulates the protein kinase A-catalyzed tau phosphorylation of serine residues 262 and 356. *J Biol Chem* 274:25481-9

629. Duka T, Duka V, Joyce JN, Sidhu A (2009) α -Synuclein contributes to GSK-3 β -catalyzed Tau phosphorylation in Parkinson's disease models. *FASEB J* 23:2820–2830 . doi: 10.1096/fj.08-120410
630. Golpich M, Amini E, Hemmati F, Ibrahim NM, Rahmani B, Mohamed Z, Raymond AA, Dargahi L, Ghasemi R, Ahmadiani A (2015) Glycogen synthase kinase-3 beta (GSK-3 β) signaling: Implications for Parkinson's disease. *Pharmacol Res* 97:16–26
631. Pooya S, Liu X, Kumar VBS, Anderson J, Imai F, Zhang W, Ciralo G, Ratner N, Setchell KDR, Yoshida Y, Jankowski MP, Dasgupta B, Dasgupta B (2014) The tumour suppressor LKB1 regulates myelination through mitochondrial metabolism. *Nat Commun* 5:4993 . doi: 10.1038/ncomms5993
632. Courchet J, Lewis TL, Lee S, Courchet V, Liou D-Y, Aizawa S, Polleux F (2013) Terminal Axon Branching Is Regulated by the LKB1-NUAK1 Kinase Pathway via Presynaptic Mitochondrial Capture. *Cell* 153:1510–1525 . doi: 10.1016/j.cell.2013.05.021
633. Shelly M, Cancedda L, Heilshorn S, Sumbre G, Poo M (2007) LKB1/STRAD Promotes Axon Initiation During Neuronal Polarization. *Cell* 129:565–577
634. Huang W, She L, Chang X -y. X, Yang R -r. R, Wang L, Ji HH -b., Jiao J -w. J, Poo M (2014) Protein kinase LKB1 regulates polarized dendrite formation of adult hippocampal newborn neurons. *Proc Natl Acad Sci U S A* 111:469–74 . doi: 10.1073/pnas.1321454111
635. Shelly M, Poo M-M (2011) Role of LKB1-SAD/MARK pathway in neuronal polarization. *Dev Neurobiol* 71:508–527 . doi: 10.1002/dneu.20884
636. Cao H, Yin X, Cao Y, Jin Y, Wang S, Kong Y, Chen Y, Gao J, Heller S, Xu Z (2013) FCHSD1 and FCHSD2 Are Expressed in Hair Cell Stereocilia and Cuticular Plate and Regulate Actin Polymerization In Vitro. *PLoS One* 8: . doi: 10.1371/journal.pone.0056516
637. Coyle IP, Koh YH, Lee WCM, Slind J, Fergestad T, Littleton JT, Ganetzky B (2004) Nervous Wreck, an SH3 Adaptor Protein that Interacts with Wsp, Regulates Synaptic Growth in *Drosophila*. *Neuron* 41:521–534 . doi: 10.1016/S0896-6273(04)00016-9
638. Huang RS, Duan S, Shukla SJ, Kistner EO, Clark TA, Chen TX, Schweitzer AC, Blume JE, Dolan ME (2007) Identification of genetic variants contributing to cisplatin-induced cytotoxicity by use of a genomewide approach. *Am J Hum Genet* 81:427–437 . doi: 10.1086/519850
639. Picconi B, Centonze D, Håkansson K, Bernardi G, Greengard P, Fisone G, Cenci MA, Calabresi P (2003) Loss of bidirectional striatal synaptic plasticity in L-DOPA-induced dyskinesia. *Nat Neurosci* 6:501–506 . doi: 10.1038/nn1040
640. Banko JL (2005) The Translation Repressor 4E-BP2 Is Critical for eIF4F Complex Formation, Synaptic Plasticity, and Memory in the Hippocampus. *J Neurosci* 25:9581–9590 . doi: 10.1523/JNEUROSCI.2423-05.2005
641. Grünblatt E, Mandel S, Jacob-Hirsch J, Zeligson S, Amariglio N, Rechavi G, Li J, Ravid R, Roggendorf W, Riederer P, Youdim MBH (2004) Gene expression profiling of parkinsonian substantia nigra pars compacta; alterations in ubiquitin-proteasome, heat shock protein, iron and oxidative stress regulated proteins, cell adhesion/cellular matrix and vesicle trafficking genes. *J Neural Transm* 111:1543–1573 . doi: 10.1007/s00702-004-0212-1

BIBLIOGRAPHY

642. Mandel SA, Youdim MBH, Riederer P, Grunblatt E, Rabey JM, Molochnikov L (2013) Peripheral blood gene markers for early diagnosis of parkinson's disease. Google Patents
643. Charbonnier-Beaupel F, Malerbi M, Alcacer C, Tahiri K, Carpentier W, Wang C, Doring M, Xu D, Worley PF, Girault J-A, Herve D, Corvol J-C (2015) Gene Expression Analyses Identify Narp Contribution in the Development of L-DOPA-Induced Dyskinesia. *J Neurosci* 35:96–111 . doi: 10.1523/JNEUROSCI.5231-13.2015
644. van Duijn CM, Dekker MCJ, Bonifati V, Galjaard RJ, Houwing-Duistermaat JJ, Snijders PJLM, Testers L, Breedveld GJ, Horstink M, Sandkuijl LA, van Swieten JC, Oostra BA, Heutink P (2001) PARK7, a Novel Locus for Autosomal Recessive Early-Onset Parkinsonism, on Chromosome 1p36. *Am J Hum Genet* 69:629–634 . doi: 10.1086/322996
645. Helton TD, Otsuka T, Lee MC, Mu Y, Ehlers MD (2008) Pruning and loss of excitatory synapses by the parkin ubiquitin ligase. *Proc Natl Acad Sci U S A* 105:19492–19497 . doi: 0802280105 [pii]10.1073/pnas.0802280105
646. Rodriguez-Viciana P, Warne PH, Dhand R, Vanhaesebroeck B, Gout I, Fry MJ, Waterfield MD, Downward J (1994) Phosphatidylinositol-3-OH kinase direct target of Ras. *Nature* 370:527–532 . doi: 10.1038/370527a0
647. Pacold ME, Suire S, Perisic O, Lara-Gonzalez S, Davis CT, Walker EH, Hawkins PT, Stephens L, Eccleston JF, Williams RL (2000) Crystal structure and functional analysis of Ras binding to its effector phosphoinositide 3-kinase gamma. *Cell* 103:931–43
648. Wang L, Gout I, Proud CG (2001) Cross-talk between the ERK and p70 S6 Kinase (S6K) Signaling Pathways: MEK-dependent activation of S6K2 in cardiomyocytes. *J Biol Chem* 276:32670–32677 . doi: 10.1074/jbc.M102776200
649. Pardo OE, Seckl MJ (2013) S6K2: The Neglected S6 Kinase Family Member. *Front Oncol* 3:191 . doi: 10.3389/fonc.2013.00191
650. Zhang D, Zhang J-J, Liu G-T (2007) The novel squamosamide derivative (compound FLZ) attenuated 1-methyl, 4-phenyl-pyridinium ion (MPP+)-induced apoptosis and alternations of related signal transduction in SH-SY5Y cells. *Neuropharmacology* 52:423–429 . doi: 10.1016/j.neuropharm.2006.08.020
651. Bao X-Q, Wu L-Y, Wang X-L, Sun H, Zhang D (2015) Squamosamide derivative FLZ protected tyrosine hydroxylase function in a chronic MPTP/probenecid mouse model of Parkinson's disease. *Naunyn Schmiedebergs Arch Pharmacol* 388:549–556 . doi: 10.1007/s00210-015-1094-5
652. Bao X-Q, Kong X-C, Kong L-B, Wu L-Y, Sun H, Zhang D (2014) Squamosamide derivative FLZ protected dopaminergic neuron by activating Akt signaling pathway in 6-OHDA-induced in vivo and in vitro Parkinson's disease models. *Brain Res* 1547:49–57 . doi: 10.1016/j.brainres.2013.12.026
653. Bao X-Q, Kong X-C, Qian C, Zhang D (2012) FLZ protects dopaminergic neuron through activating protein kinase B/mammalian target of rapamycin pathway and inhibiting RTP801 expression in Parkinson's disease models. *Neuroscience* 202:396–404 . doi: 10.1016/j.neuroscience.2011.11.036
654. Sarkar S, Krishna G, Imarisio S, Saiki S, O'Kane CJ, Rubinsztein DC (2008) A rational mechanism for combination treatment of Huntington's disease using lithium and rapamycin. *Hum Mol Genet* 17:170–178 . doi: 10.1093/hmg/ddm294

655. Hwang-Verslues WW, Chang P-H, Wei P-C, Yang C-Y, Huang C-K, Kuo W-H, Shew J-Y, Chang K-J, Lee EY-HP, Lee W-H (2011) miR-495 is upregulated by E12/E47 in breast cancer stem cells and promotes oncogenesis and hypoxia resistance via downregulation of E-cadherin and REDD1. *Oncogene* 30:2463–2474 . doi: 10.1038/onc.2010.618
656. Pineau P, Volinia S, McJunkin K, Marchio A, Battiston C, Terris B, Mazzaferro V, Lowe SW, Croce CM, Dejean A (2010) miR-221 overexpression contributes to liver tumorigenesis. *Proc Natl Acad Sci U S A* 107:264–9 . doi: 10.1073/pnas.0907904107
657. Li XH, Ha CT, Fu D, Xiao M (2012) Micro-RNA30c negatively regulates REDD1 expression in human hematopoietic and osteoblast cells after gamma-irradiation. *PLoS One* 7:e48700 . doi: 10.1371/journal.pone.0048700
658. Baida G, Bhalla P, Kirsanov K, Lesovaya E, Yakubovskaya M, Yuen K, Guo S, Lavker RM, Readhead B, Dudley JT, Budunova I (2015) REDD1 functions at the crossroads between the therapeutic and adverse effects of topical glucocorticoids. *EMBO Mol Med* 7:42–58 . doi: 10.15252/emmm.201404601
659. Zeng Q, Liu J, Cao P, Li J, Liu X, Fan X, Liu L, Cheng Y, Xiong W, Li J, Bo H, Zhu Y, Yang F, Hu J, Zhou M, Zhou Y, Zou Q, Zhou J, Cao K (2018) Inhibition of REDD1 Sensitizes Bladder Urothelial Carcinoma to Paclitaxel by Inhibiting Autophagy. *Clin Cancer Res* 24:445–459 . doi: 10.1158/1078-0432.CCR-17-0419
660. Xu X-F, Jing X, Ma H-X, Yuan R-R, Dong Q, Dong J-L, Han X-F, Chen Z-Y, Li X-Z, Wang Y (2018) miR-181a Participates in Contextual Fear Memory Formation Via Activating mTOR Signaling Pathway. *Cereb Cortex* 28:3309–3321 . doi: 10.1093/cercor/bhx201
661. Nguyen QD, Schachar RA, Nduaka CI, Sperling M, Basile AS, Klamerus KJ, Chi-Burris K, Yan E, Paggiarino DA, Rosenblatt I, Khan A, Aitchison R, Erlich SS, PF-04523655 Study Group (2012) Phase 1 dose-escalation study of a siRNA targeting the RTP801 gene in age-related macular degeneration patients. *Eye* 26:1099–1105 . doi: 10.1038/eye.2012.106
662. Nguyen QD, Schachar RA, Nduaka CI, Sperling M, Basile AS, Klamerus KJ, Chi-Burris K, Yan E, Paggiarino DA, Rosenblatt I, Aitchison R, Erlich SS, DEGAS Clinical Study Group (2012) Dose-Ranging Evaluation of Intravitreal siRNA PF-04523655 for Diabetic Macular Edema (the DEGAS Study). *Investig Ophthalmology Vis Sci* 53:7666 . doi: 10.1167/iovs.12-9961
663. Rittenhouse KD, Johnson TR, Vicini P, Hirakawa B, Kalabat D, Yang AH, Huang W, Basile AS (2014) RTP801 Gene Expression Is Differentially Upregulated in Retinopathy and Is Silenced by PF-04523655, a 19-Mer siRNA Directed Against RTP801. *Investig Ophthalmology Vis Sci* 55:1232 . doi: 10.1167/iovs.13-13449
664. Lee DU, Huang W, Rittenhouse KD, Jessen B (2012) Retina Expression and Cross-Species Validation of Gene Silencing by PF-655, a Small Interfering RNA Against RTP801 for the Treatment of Ocular Disease. *J Ocul Pharmacol Ther* 28:222–230 . doi: 10.1089/jop.2011.0116
665. Sun D, Zhuang X, Xiang X, Liu Y, Zhang S, Liu C, Barnes S, Grizzle W, Miller D, Zhang H-G (2010) A novel nanoparticle drug delivery system: the anti-inflammatory activity of curcumin is enhanced when encapsulated in exosomes. *Mol Ther* 18:1606–14 . doi: 10.1038/mt.2010.105
666. Martín-Flores N, Romaní-Aumedes J, Rué L, Canal MM, Sanders P, Straccia M, Allen ND, Alberch J, Canals JM, Pérez-Navarro E, Malagelada C (2015) RTP801

BIBLIOGRAPHY

- Is Involved in Mutant Huntingtin-Induced Cell Death. *Mol. Neurobiol.* 53:2857–2868 . doi: 10.1007/s12035-015-9166-6.
667. Martín-Flores N, Fernández-Santiago R, Antonelli F, Cerquera C, Moreno V, Martí MJ, Ezquerra M, Malagelada C (2018) MTOR Pathway-Based Discovery of Genetic Susceptibility to L-DOPA-Induced Dyskinesia in Parkinson's Disease Patients. *Mol Neurobiol.* doi: 10.1007/s12035-018-1219-1

ANNEX I

SNP	Gene	Alleles	Functionality related to	PMID number
rs1042009	<i>ADCY1</i>	A/G	Neurotransmission and bipolar disorder	18444252
rs1130214	<i>AKT1</i>	G/T	Schizophrenia	20132317
rs2069442	<i>CDK5</i>	C/G	Alzheimer's disease	18350355
rs1053639	<i>DDIT4</i>	A/T	Utr variant 3 prime	na
rs1053227	<i>DDIT4L</i>	C/T	Utr variant 3 prime	na
rs9297608	<i>DEPTOR</i>	C/G	Bone size	18776929
rs12498533	<i>EIF4E</i>	A/C	Autism	24818597
rs6605631	<i>EIF4EBP1</i>	A/G	Obesity	20532202
rs1043098	<i>EIF4EBP2</i>	C/T	Alzheimer's disease	16385451
rs2178403	<i>EIF4G1</i>	C/T	Parkinson's disease	21907011
rs456998	<i>FCHSD1</i>	G/T	Cisplatin-induced toxicity	17701890
rs2237457	<i>GRB10</i>	C/T	Treatment resistance in Schizophrenia	25223841
rs334558	<i>GSK3B</i>	A/G	Bipolar disorder, MS, Parkinson's disease	15351432; 23628795
rs1732170	<i>GSK3B</i>	A/G	Impulsivity in bipolar disorder	24486183
rs12628	<i>HRAS</i>	C/T	Risk of melanoma	22618666
rs2943641	<i>IRS1</i>	C/T	Diabetes 2	22046406
rs1934534	<i>LATS1</i>	A/G	Progressive supranuclear palsy	17357082
rs7595221	<i>LPIN1</i>	A/G	Insulin resistance, body weight, and lipodystrophy	18591397
rs66737902	<i>LRRK2</i>	C/T	Parkinson's disease	24758914
rs536861	<i>MAPKAP1</i>	A/C	Autism/Longevity	20824210
rs1800547	<i>MAPT</i>	A/G	Parkinson's disease/Progressive supranuclear palsy	19879020
rs2024627	<i>MTOR</i>	C/T	Colon cancer risk	20622004
rs1912403	<i>NEDD4</i>	C/T	Parkinson's disease	18853455
rs292449	<i>NEDD4L</i>	C/G	Hypertension and response to treatments	23353631
rs4149601	<i>NEDD4L</i>	A/G	Hypertension and orthostatic hypotension	23353631
rs966221	<i>PDE4D</i>	C/T	Cognitive dysfunction, ischemic stroke	23863764
rs2677760	<i>PIK3CA</i>	C/T	Obesity and breast cancer	25108739
rs361072	<i>PIK3CB</i>	A/G	GH replacement, insulin resistance	24114431
rs2959272	<i>PPARG</i>	A/C	Schizophrenia	24843374
rs907094	<i>PPP1R1B</i>	C/T	Regulation of dopamine signaling in the frontal cortex	24144248
rs887797	<i>PRKCA</i>	C/T	Multiple Sclerosis	16596167
rs4790904	<i>PRKCA</i>	A/G	Memory capacity and risk for post-traumatic stress disorder	22586106
rs1801582	<i>PRKN</i>	C/G	Sporadic Parkinson's disease	10319889
rs132404	<i>PRR5</i>	A/G	Regulation of gene expression	18466591
rs2735343	<i>PTEN</i>	C/G	Smoking initiation and nicotine dependence	16331670
rs736212	<i>RASD2</i>	C/G	Schizophrenia	18571626
rs875588	<i>RHEB</i>	C/T	Non-BRCA1/2 breast cancer	17760956
rs2043112	<i>RICTOR</i>	A/G	Childhood obesity	23251661
rs2229714	<i>RPS6KA1</i>	A/G	Role in growth hormone signaling	24805830
rs6456121	<i>RPS6KA2</i>	C/T	Psychotic bipolar disorder and schizophrenia	24778245
rs1292034	<i>RPS6KB1</i>	C/T	Associated with STK11 expression	24959314
rs11868112	<i>RPTOR</i>	C/T	Expression functional effects	21060808

ANNEX I

rs7211818	<i>RPTOR</i>	A/G	Bladder cancer risk	19875696
rs9493857	<i>SGK1</i>	A/G	Gene expression response to stress and GH	19461886
rs3758391	<i>SIRT1</i>	C/T	p53 binding site/nutrient sensitive/longevity/cognitive function	20693263
rs12778366	<i>SIRT1</i>	C/T	Long-term survival and glucose tolerance	19652658
rs10410544	<i>SIRT2</i>	C/T	Alzheimer's disease	23712749
rs9382222	<i>SIRT5</i>	C/T	Brain Health	30143810
rs356219	<i>SNCA</i>	A/G	Parkinson's disease	20070850; 22425546
rs11868035	<i>SREBF1</i>	A/G	Parkinson's disease	24514572
rs8111699	<i>STK11</i>	C/G	Insulin sensitivity and metformin efficacy	20357370
rs2496143	<i>TBC1D7</i>	C/T	Cognitive abilities	21302343
rs7874234	<i>TSC1</i>	C/T	Increased transcription	20658316
rs12303764	<i>ULK1</i>	G/T	Crohn's disease	21560199
rs495248	<i>ZBTB16</i>	C/T	Psychotic bipolar disorder and schizophrenia	24778245
rs17116334	<i>ZBTB16</i>	C/T	ADHD	18846501
rs242557	<i>MAPT</i>	A/G	Parkinson's disease/Progressive supranuclear palsy	19912324; 19879020
rs2301113	<i>HIF1A</i>	A/C	Death and recurrence risks in non-small-cell lung cancer patients	24567056
rs4402960	<i>IGF2BP2</i>	G/T	Diabetes type II, obesity and hypertension	24636221
rs4804833	<i>MAP2K7</i>	A/G	Schizophrenia	22899651
rs135549	<i>PPARA</i>	A/G	Cardiovascular risk	22547144
rs879606	<i>PPP1R1B</i>	A/G	Schizophrenia, bipolar and associative emotional learning	23295814
rs393795	<i>SLC6A3</i>	A/C	Extend the time to LID onset	24633632
rs13335638	<i>TSC2</i>	C/T	High conservative region	20658316

Table A1. Descriptive information of the SNPs in genes of the mTOR pathway selected for the analyses. SNPs in grey were excluded from the analysis.

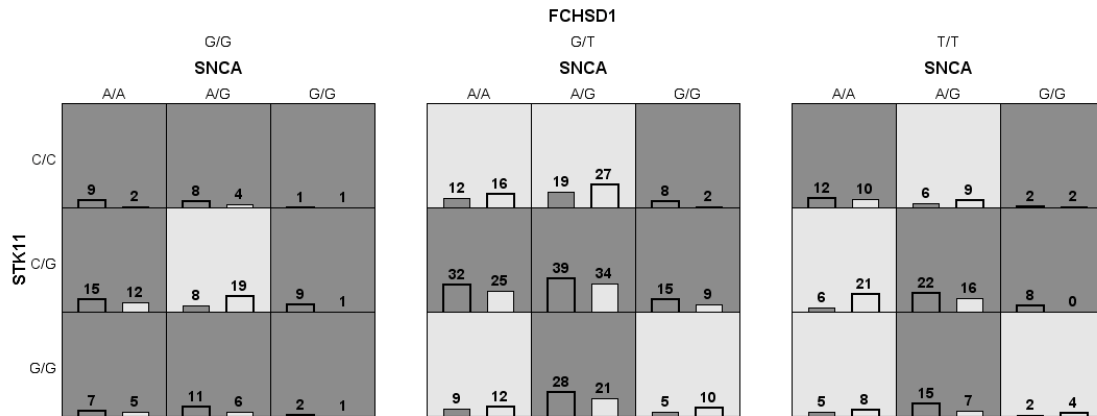
SNP	Alleles (M/m)	mAF PD	mAF Ctr	HWE P-value PD	HWE P-value Ctr	Freq 11 PD	Freq 12 PD	Freq 22 PD	Freq 11 Ctr	Freq 12 Ctr	Freq 22 Ctr
rs1042009	A(1)/G(2)	0.34	0.33	0.12	0.65	0.45	0.43	0.13	0.45	0.44	0.11
rs1130214	C(1)/A(2)	0.3	0.31	0.20	0.94	0.48	0.44	0.08	0.48	0.42	0.1
rs2069442	G(1)/C(2)	0.22	0.24	1.00	0.85	0.60	0.35	0.05	0.58	0.36	0.06
rs1053639	T(1)/A(2)	0.37	0.38	1.00	0.18	0.40	0.47	0.13	0.39	0.47	0.14
rs1053227	G(1)/A(2)	0.43	0.38	0.89	0.58	0.33	0.49	0.18	0.37	0.48	0.14
rs9297608	G(1)/C(2)	0.25	0.24	0.24	0.58	0.57	0.36	0.07	0.58	0.37	0.05
rs12498533	A(1)/C(2)	0.46	0.44	0.25	0.68	0.28	0.52	0.20	0.31	0.49	0.20
rs6605631	T(1)/C(2)	0.17	0.19	0.63	0.089	0.69	0.29	0.03	0.66	0.29	0.05
rs1043098	C(1)/T(2)	0.46	0.45	0.46	0.25	0.3	0.48	0.22	0.31	0.48	0.22
rs2178403	G(1)/A(2)	0.23	0.24	0.10	0.24	0.61	0.33	0.06	0.58	0.35	0.07
rs456998	T(1)/G(2)	0.45	0.48	0.78	0.63	0.30	0.50	0.20	0.26	0.51	0.23
rs2237457	C(1)/T(2)	0.35	0.34	0.24	0.55	0.41	0.48	0.12	0.43	0.46	0.11
rs334558	A(1)/G(2)	0.05	0.04	0.69	0.15	0.90	0.10	0.00	0.92	0.08	0.00
rs1732170	C(1)/T(2)	0.41	0.41	0.33	0.15	0.36	0.47	0.17	0.34	0.51	0.15
rs12628	A(1)/G(2)	0.34	0.34	0.085	0.085	0.45	0.42	0.13	0.45	0.42	0.13
rs2943641	C(1)/T(2)	0.35	0.34	0.16	0.45	0.43	0.43	0.13	0.44	0.44	0.12
rs1934534	T(1)/C(2)	0.37	0.38	0.72	0.83	0.4	0.46	0.14	0.39	0.47	0.14
rs7595221	A(1)/G(2)	0.47	0.49	0.25	0.071	0.29	0.48	0.23	0.25	0.53	0.22
rs66737902	T(1)/C(2)	0.14	0.11	0.63	0.30	0.75	0.23	0.02	0.79	0.19	0.02
rs536861	C(1)/A(2)	0.44	0.44	0.41	0.42	0.32	0.48	0.2	0.31	0.51	0.18
rs1800547	A(1)/G(2)	0.25	0.31	0.93	0.16	0.56	0.37	0.06	0.49	0.41	0.11
rs2024627	C(1)/T(2)	0.26	0.26	0.37	0.16	0.56	0.37	0.07	0.55	0.37	0.08
rs1912403	T(1)/C(1)	0.08	0.09	0.015	0.05	0.85	0.14	0.01	0.84	0.15	0.10
rs292449	G(1)/C(2)	0.34	0.35	0.41	1.00	0.44	0.44	0.12	0.42	0.46	0.12
rs4149601	G(1)/A(2)	0.37	0.37	0.21	0.82	0.39	0.49	0.12	0.40	0.47	0.13
rs1801582	C(1)/G(2)	0.2	0.22	1.00	0.77	0.64	0.32	0.04	0.61	0.34	0.05
rs966221	G(1)/A(2)	0.39	0.41	0.94	0.53	0.37	0.47	0.15	0.34	0.49	0.16
rs2677760	T(1)/C(2)	0.42	0.41	0.54	0.89	0.33	0.50	0.17	0.35	0.49	0.17
rs361072	A(1)/G(2)	0.47	0.5	0.40	0.58	0.27	0.51	0.21	0.26	0.49	0.25
rs2959272	T(1)/G(2)	0.44	0.46	0.34	0.84	0.32	0.48	0.20	0.29	0.49	0.21
rs907094	A(1)/G(2)	0.27	0.26	0.93	1.00	0.54	0.39	0.07	0.55	0.38	0.07
rs887797	G(1)/A(2)	0.32	0.34	0.016	0.77	0.48	0.40	0.12	0.44	0.45	0.12
rs4790904	T(1)/C(2)	0.22	0.25	0.92	0.72	0.61	0.34	0.05	0.57	0.37	0.06
rs132404	G(1)/A(2)	0.29	0.31	0.12	0.70	0.51	0.39	0.10	0.47	0.43	0.09
rs2735343	G(1)/C(2)	0.34	0.35	0.15	0.48	0.42	0.47	0.11	0.42	0.47	0.11
rs736212	G(1)/C(2)	0.30	0.31	0.63	0.25	0.49	0.42	0.08	0.48	0.41	0.11
rs875588	T(1)/C(2)	0.46	0.46	0.42	0.23	0.29	0.51	0.20	0.30	0.47	0.22
rs2043112	G(1)/A(2)	0.39	0.39	1.00	0.44	0.38	0.48	0.18	0.37	0.49	0.14
rs2229714	G(1)/A(2)	0.12	0.13	0.27	0.88	0.77	0.21	0.02	0.175	0.023	0.02
rs6456121	C(1)/T(2)	0.31	0.28	0.58	0.87	0.48	0.42	0.1	0.51	0.41	0.08
rs1292034	G(1)/A(2)	0.44	0.45	0.17	1.00	0.33	0.47	0.20	0.30	0.50	0.30
rs11868112	C(1)/T(2)	0.43	0.43	1.00	0.45	0.33	0.49	0.18	0.33	0.48	0.20
rs7211818	A(1)/G(2)	0.23	0.24	0.70	0.064	0.58	0.37	0.05	0.59	0.34	0.07

ANNEX I

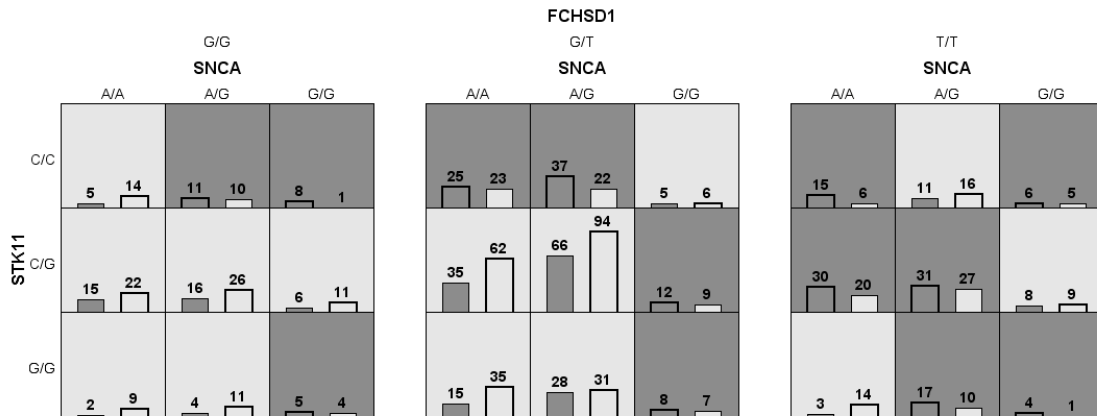
rs9493857	G(1)/A(2)	0.21	0.21	0.84	0.92	0.63	0.33	0.04	0.62	0.33	0.05
rs3758391	C(1)/T(2)	0.34	0.31	0.37	0.94	0.43	0.46	0.11	0.48	0.43	0.09
rs12778366	T(1)/C(2)	0.13	0.12	0.77	1.00	0.75	0.23	0.02	0.78	0.21	0.01
rs10410544	C(1)/T(2)	0.4	0.39	0.48	0.47	0.37	0.47	0.17	0.37	0.49	0.15
rs9382222	C(1)/T(2)	0.36	0.35	0.25	0.66	0.40	0.48	0.12	0.42	0.45	0.13
rs356219	A(1)/G(2)	0.41	0.33	0.43	0.76	0.36	0.47	0.17	0.45	0.44	0.11
rs11868035	G(1)/A(2)	0.29	0.28	0.023	0.32	0.51	0.38	0.10	0.53	0.39	0.08
rs8111699	C(1)/G(2)	0.49	0.51	0.69	0.38	0.27	0.49	0.24	0.25	0.48	0.27
rs2496143	C(1)/T(2)	0.34	0.33	0.71	1.00	0.43	0.45	0.12	0.45	0.44	0.11
rs7874234	C(1)/T(2)	0.24	0.24	0.71	0.78	0.57	0.37	0.06	0.58	0.37	0.05
rs12303764	T(1)/G(2)	0.36	0.39	0.38	0.44	0.40	0.48	0.13	0.36	0.49	0.15
rs495248	G(1)/A(2)	0.24	0.23	0.23	0.92	0.58	0.35	0.07	0.59	0.36	0.06
rs17116334	C(1)/T(2)	0.19	0.18	0.66	0.64	0.65	0.31	0.03	0.67	0.30	0.03
rs242557	G(1)/A(2)	0.36	0.31	0.032	0.0021	0.43	0.42	0.14	0.49	0.38	0.12
rs2301113	A(1)/C(2)	0.33	0.31	0.0001	0.0001	0.38	0.58	0.03	0.42	0.55	0.04
rs4402960	G(1)/T(2)	0.4	0.39	0.0001	0.0001	0.27	0.66	0.07	0.3	0.61	0.08
rs4804833	G(1)/A(2)	0.45	0.46	0.0001	0.0001	0.17	0.76	0.07	0.19	0.7	0.11
rs135549	T(1)/C(2)	0.42	0.43	0.067	0.0001	0.34	0.49	0.17	0.3	0.56	0.15
rs879606	G(1)/A(2)	0.21	0.21	0.54	0.015	0.62	0.034	0.04	0.61	0.36	0.03
rs393795	G(1)/T(2)	0.05	0.03	0.31	0.065	0.9	0.1	0.00	0.93	0.06	0.00
rs13335638	C(1)/T(2)	0.37	0.33	0.00069	0.0001	0.37	0.52	0.11	0.40	0.55	0.05

Table A2. Genotypic association test of the SNPs in genes of the mTOR pathway selected for the analyses. Genotypic test was calculated in the SNPstats software. SNPs in grey were excluded from the analysis. M= major allele; m=minor allele; mAF= minor allele frequency; HWE=Hardy-Weinberg equilibrium; Freq.=frequency; PD=Parkinson's disease group; Ctr=Control group. SNPs in grey were excluded from the analysis.

GSK3B(2) = C/C



GSK3B(2) = C/T



GSK3B(2) = T/T

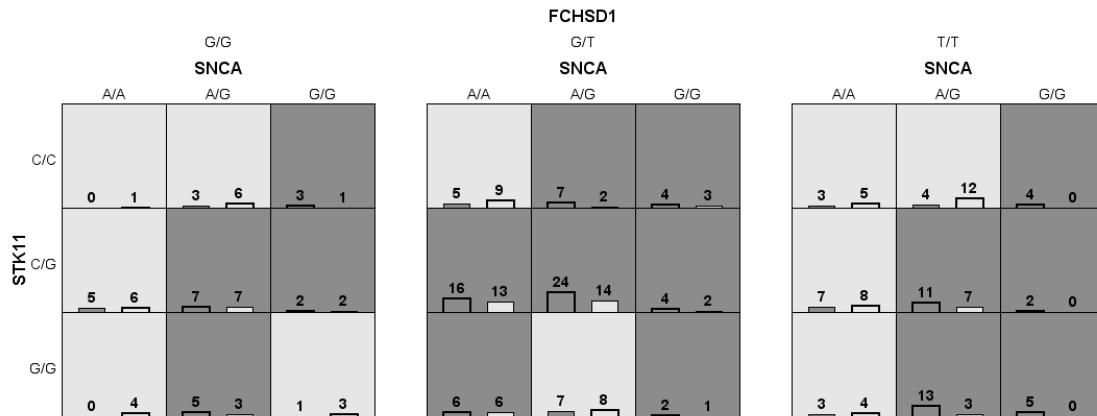


Figure A1. Distribution of high-risk and low-risk genotypes in the interaction of rs356219 in *SNCA*, rs8111699 in *STK11*, rs456998 in *FCHSD1* and rs1732170 in *GSK3B* with PD risk. Dark gray boxes present the high-risk factor combinations (PD) and light gray boxes present the low-risk factor combinations (non-affected). Each cell shows the number of PD patients with that specific genotype on the left bar and control group on the right bar.

Genotypes				Predicted PD status	Freq. PD (%)	Freq. Ctr (%)	Ratio PD/Control
SNCA rs356219	STK11 rs8111699	FCHSD1 rs456998	GSK3B rs1732170				
A/A	C/G	G/T	C/C	PD	1.76	1.38	1.28
A/A	C/G	G/T	T/T	PD	0.88	0.72	1.23
A/A	C/G	G/G	C/C	PD	0.83	0.66	1.25
A/A	C/G	T/T	C/T	PD	1.65	1.10	1.50
A/A	G/G	G/T	T/T	PD	0.33	0.33	1.00
A/A	G/G	G/G	C/C	PD	0.39	0.28	1.40
A/A	C/C	G/T	C/T	PD	1.38	1.27	1.09
A/A	C/C	G/G	C/C	PD	0.50	0.11	4.50
A/A	C/C	T/T	C/C	PD	0.66	0.55	1.20
A/A	C/C	T/T	C/T	PD	0.83	0.33	2.50
A/G	C/G	G/T	C/C	PD	2.15	1.87	1.15
A/G	C/G	G/T	T/T	PD	1.32	0.77	1.71
A/G	C/G	G/G	T/T	PD	0.39	0.39	1.00
A/G	C/G	T/T	C/C	PD	1.21	0.88	1.38
A/G	C/G	T/T	C/T	PD	1.71	1.49	1.15
A/G	C/G	T/T	T/T	PD	0.61	0.39	1.57
A/G	G/G	G/T	C/C	PD	1.54	1.16	1.33
A/G	G/G	G/G	C/C	PD	0.61	0.33	1.83
A/G	G/G	G/G	T/T	PD	0.28	0.17	1.67
A/G	G/G	T/T	C/C	PD	0.83	0.39	2.14
A/G	G/G	T/T	C/T	PD	0.94	0.55	1.70
A/G	G/G	T/T	T/T	PD	0.72	0.17	4.33
A/G	C/C	G/T	C/T	PD	2.04	1.21	1.68
A/G	C/C	G/T	T/T	PD	0.39	0.11	3.50
A/G	C/C	G/G	C/C	PD	0.44	0.22	2.00
A/G	C/C	G/G	C/T	PD	0.61	0.55	1.10
G/G	C/G	G/T	C/C	PD	0.83	0.50	1.67
G/G	C/G	G/T	C/T	PD	0.66	0.50	1.33
G/G	C/G	G/T	T/T	PD	0.22	0.11	2.00
G/G	C/G	G/G	C/C	PD	0.50	0.06	9.00
G/G	C/G	G/G	T/T	PD	0.11	0.11	1.00
G/G	C/G	T/T	C/C	PD	0.44	0.00	∞
G/G	C/G	T/T	T/T	PD	0.11	0.00	∞
G/G	G/G	G/T	C/T	PD	0.44	0.39	1.14
G/G	G/G	G/T	T/T	PD	0.11	0.06	2.00
G/G	G/G	G/G	C/C	PD	0.11	0.06	2.00
G/G	G/G	G/G	C/T	PD	0.28	0.22	1.25
G/G	G/G	T/T	C/T	PD	0.22	0.06	4.00
G/G	G/G	T/T	T/T	PD	0.28	0.00	∞
G/G	C/C	G/T	C/C	PD	0.44	0.11	4.00
G/G	C/C	G/T	T/T	PD	0.22	0.17	1.33
G/G	C/C	G/G	C/C	PD	0.06	0.06	1.00
G/G	C/C	G/G	C/T	PD	0.44	0.06	8.00
G/G	C/C	G/G	T/T	PD	0.17	0.06	3.00

G/G	C/C	T/T	C/C	PD	0.11	0.11	1.00
G/G	C/C	T/T	C/T	PD	0.33	0.28	1.20
G/G	C/C	T/T	T/T	PD	0.22	0.00	∞
A/A	C/G	G/T	C/T	Ctr	1.93	3.42	0.56
A/A	C/G	G/G	C/T	Ctr	0.83	1.21	0.68
A/A	C/G	G/G	T/T	Ctr	0.28	0.33	0.83
A/A	C/G	T/T	C/C	Ctr	0.33	1.16	0.29
A/A	C/G	T/T	T/T	Ctr	0.39	0.44	0.88
A/A	G/G	G/T	C/C	Ctr	0.50	0.66	0.75
A/A	G/G	G/T	C/T	Ctr	0.83	1.93	0.43
A/A	G/G	G/G	C/T	Ctr	0.11	0.50	0.22
A/A	G/G	G/G	T/T	Ctr	0.00	0.22	0.00
A/A	G/G	T/T	C/C	Ctr	0.28	0.44	0.63
A/A	G/G	T/T	C/T	Ctr	0.17	0.77	0.21
A/A	G/G	T/T	T/T	Ctr	0.17	0.22	0.75
A/A	C/C	G/T	C/C	Ctr	0.66	0.88	0.75
A/A	C/C	G/T	T/T	Ctr	0.28	0.50	0.56
A/A	C/C	G/G	C/T	Ctr	0.28	0.77	0.36
A/A	C/C	G/G	T/T	Ctr	0.00	0.06	0.00
A/A	C/C	T/T	T/T	Ctr	0.17	0.28	0.60
A/G	C/G	G/T	C/T	Ctr	3.64	5.18	0.70
A/G	C/G	G/G	C/C	Ctr	0.44	1.05	0.42
A/G	C/G	G/G	C/T	Ctr	0.88	1.43	0.62
A/G	G/G	G/T	C/T	Ctr	1.54	1.71	0.90
A/G	G/G	G/T	T/T	Ctr	0.39	0.44	0.88
A/G	G/G	G/G	C/T	Ctr	0.22	0.61	0.36
A/G	C/C	G/T	C/C	Ctr	1.05	1.49	0.70
A/G	C/C	G/G	T/T	Ctr	0.17	0.33	0.50
A/G	C/C	T/T	C/C	Ctr	0.33	0.50	0.67
A/G	C/C	T/T	C/T	Ctr	0.61	0.88	0.69
A/G	C/C	T/T	T/T	Ctr	0.22	0.66	0.33
G/G	C/G	G/G	C/T	Ctr	0.33	0.61	0.55
G/G	C/G	T/T	C/T	Ctr	0.44	0.50	0.89
G/G	G/G	G/T	C/C	Ctr	0.28	0.55	0.50
G/G	G/G	G/G	T/T	Ctr	0.06	0.17	0.33
G/G	G/G	T/T	C/C	Ctr	0.11	0.22	0.50
G/G	C/C	G/T	C/T	Ctr	0.28	0.33	0.83
Total genotype combinations that predict PD status:				PD	31.24	20.22	1.54
				Ctr	18.13	30.41	0.60

Table A3. Distribution of genotypes in the interaction of rs356219 in *SNCA*, rs8111699 in *STK11*, rs456998 in *FCHSD1* and rs1732170 in *GSK3B* with PD risk. Freq.=frequency; PD=Parkinson's disease group; Ctr=Control group

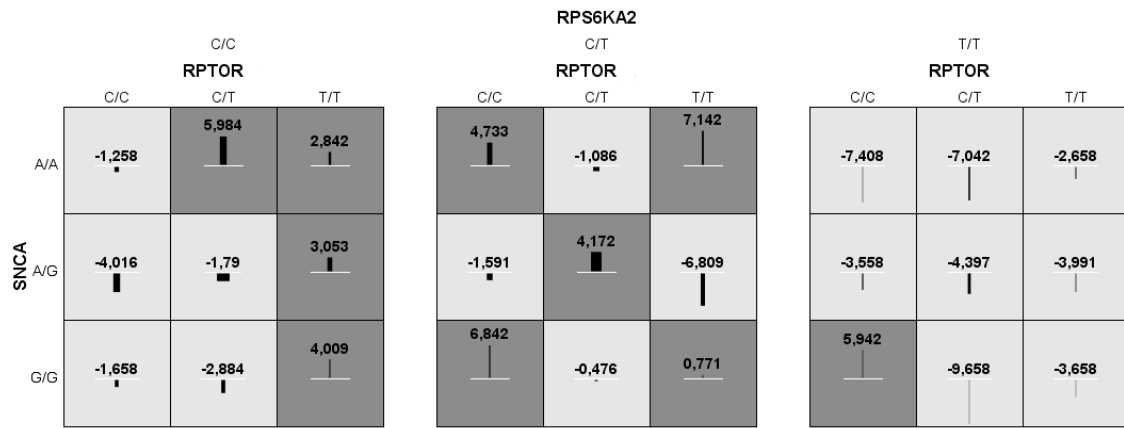


Figure A2. Distribution of high-risk, early PD onset, and low-risk, late PD onset, genotypes in the interaction of rs11868112 in *RPTOR*, rs356219 in *SNCA* and rs6456121 in *RPS6KA2* with PD AAO. Light gray boxes present combinations for early PD onset and dark gray boxes present the combinations for late PD onset. In each cell is shown the average of PD age at onset (56,66 years) in a horizontal line and in vertical the difference in years of each combination from the global mean.

Genotype			Predicted 'PD AAO'	PD onset Average (years)	diff. from global avg. (56,66 years)	Frequency (%)
<i>SNCA</i> rs356219	<i>RPTOR</i> rs11868112	<i>RPS6KA2</i> rs6456121				
G/G	C/T	C/T	Early	56.18	-0.48	2.95
G/G	C/T	C/C	Early	53.77	-2.88	4.16
G/G	C/T	T/T	Early	47.00	-9.66	0.40
A/A	C/T	C/T	Early	55.57	-1.09	6.58
A/A	C/T	T/T	Early	49.62	-7.04	1.74
A/G	C/T	C/C	Early	54.87	-1.79	13.15
A/G	C/T	T/T	Early	52.26	-4.40	3.09
G/G	C/C	C/C	Early	55.00	-1.66	3.89
A/A	C/C	C/C	Early	55.40	-1.26	4.70
A/A	C/C	T/T	Early	49.25	-7.41	0.54
A/G	C/C	C/T	Early	55.07	-1.59	6.04
A/G	C/C	C/C	Early	52.64	-4.02	7.11
A/G	C/C	T/T	Early	53.10	-3.56	1.34
G/G	T/T	T/T	Early	53.00	-3.66	0.40
A/A	T/T	T/T	Early	54.00	-2.66	1.07
A/G	T/T	C/T	Early	49.85	-6.81	4.43
A/G	T/T	T/T	Early	52.67	-3.99	0.81
A/A	C/T	C/C	Late	62.64	5.98	7.11
A/G	C/T	C/T	Late	60.83	4.17	11.01
G/G	C/C	C/T	Late	63.50	6.84	1.34
G/G	C/C	T/T	Late	62.60	5.94	0.67
A/A	C/C	C/T	Late	61.39	4.73	5.50
G/G	T/T	C/T	Late	57.43	0.77	0.94
G/G	T/T	C/C	Late	60.67	4.01	1.21
A/A	T/T	C/T	Late	63.80	7.14	2.01
A/A	T/T	C/C	Late	59.50	2.84	2.68
A/G	T/T	C/C	Late	59.71	3.05	5.10
Total frequency (%) of genotype combinations that predict PD age at onset:					EARLY	62.42
					LATE	37.58

Table A4. Distribution of genotypes in the interaction of rs11868112 in *RPTOR*, rs356219 in *SNCA* and rs6456121 in *RPS6KA2* with PD AAO.

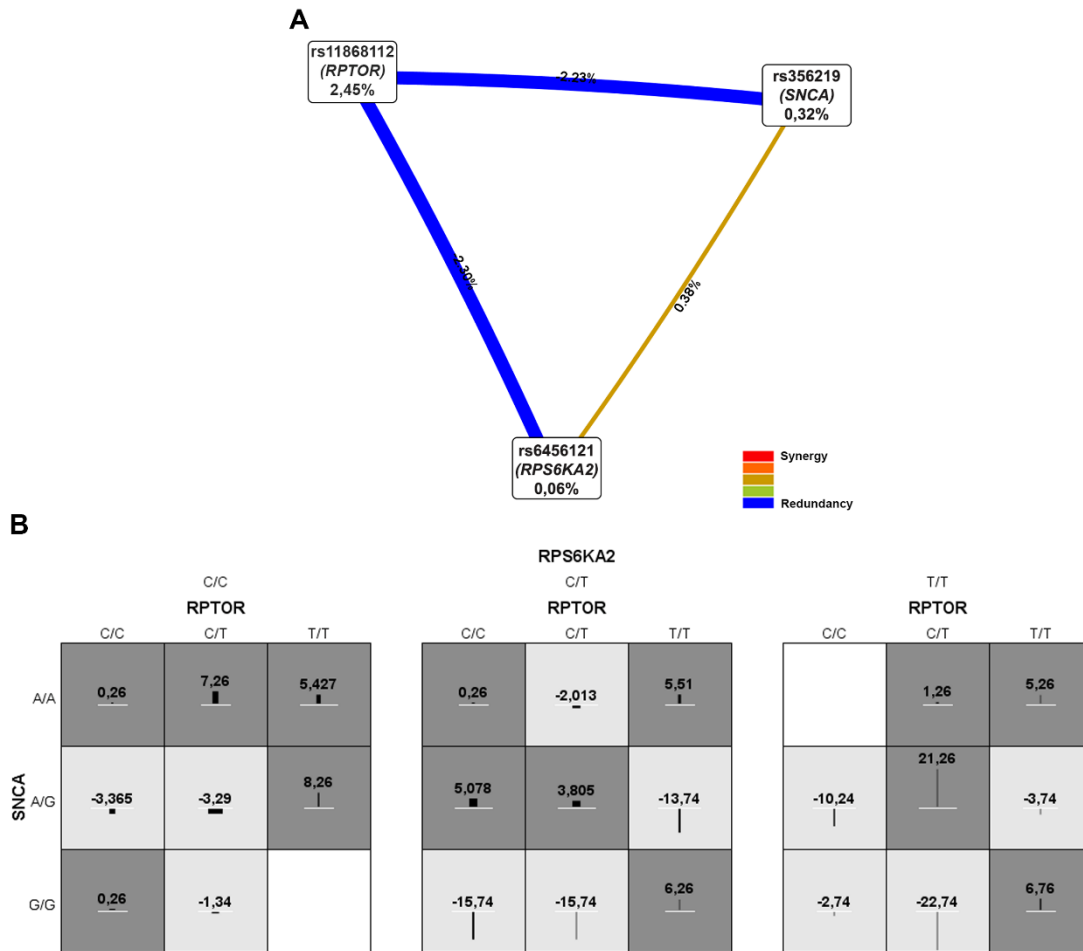


Figure A3. Association of the SNPs rs356219 in *SNCA*, rs11868112 in *RPTOR* and rs6456121 in *RPS6KA2* genes with PD age at onset (AAO) in LRKK2 PD patients. (A) SNP interaction map with PD AAO. The nodes were obtained in the epistatic analyses with the MDR software and represent the polymorphisms, including the gene that contain the SNP, while the numeric values inside represent the main information gain. The links show the interaction between SNPs. The color of the lines indicates the type of interaction explaining synergy or redundancy (blue=correlation and orange=synergistic relationship). **(B)** Distribution of high-risk, early PD onset, and low-risk genotypes, late PD onset. Light gray boxes present combinations for early PD onset and dark gray boxes present the combinations for late PD onset. In each cell is shown the average of PD age at onset (56,74 years) in a horizontal line and in vertical the difference in years of each combination from the global mean.

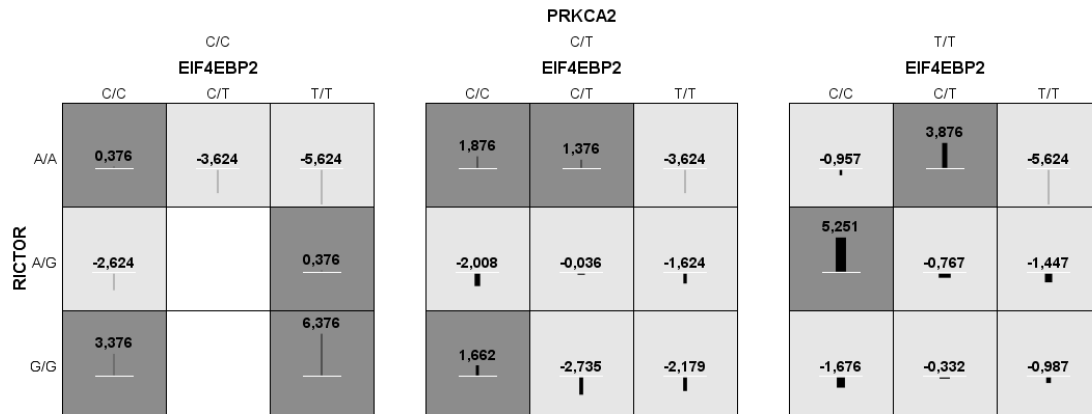
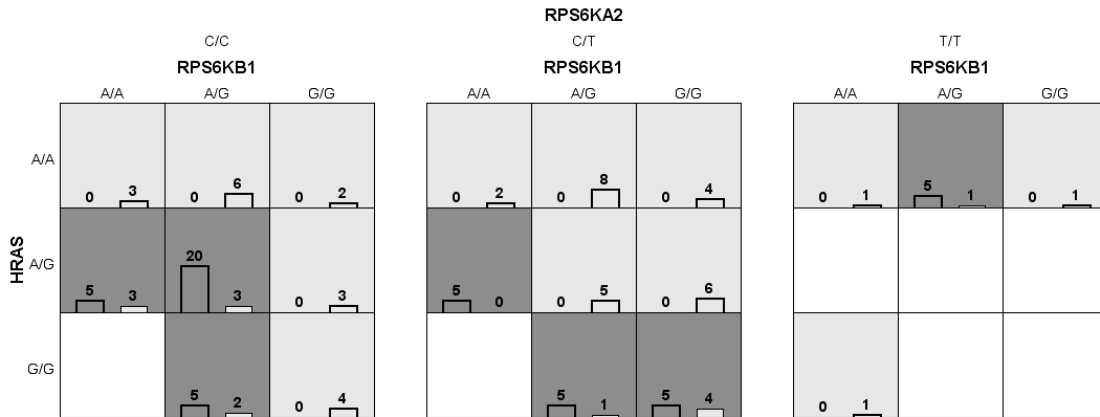


Figure A4. Distribution of high-risk, early LID onset, and low-risk, late LID onset, genotypes in the interaction of rs1043098 in *EIF4EBP2*, rs2043112 in *RICTOR* and rs4790904 in *PRKCA2* with LID onset. Light gray boxes present combinations for early LID onset and dark gray boxes present the combinations for late LID onset. In each cell is shown the TTD average (7,6239 years) in a horizontal line and in vertical the difference in years of each combination from the global mean.

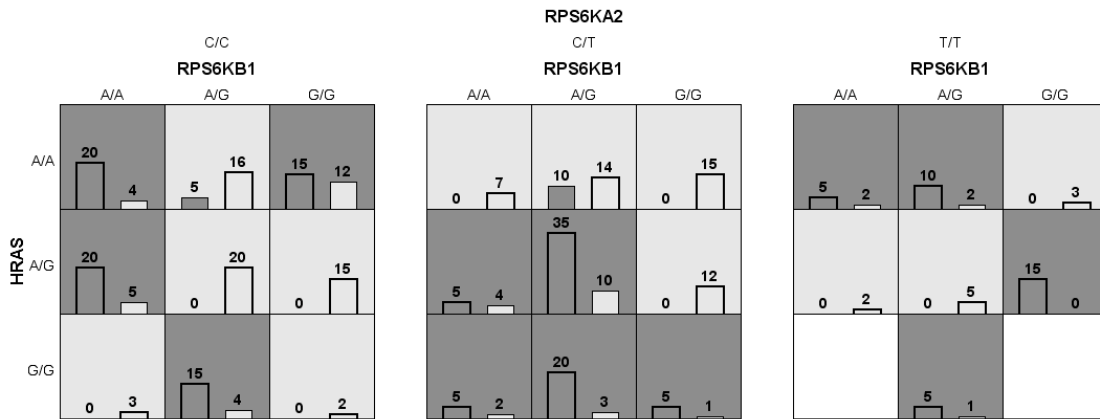
Genotype			Predicted 'LID onset'	LID onset Average (years)	diff. from global avg. (7,62 years)	Frequency (%)
<i>EIF4EBP2</i> rs1043098	<i>RICTOR</i> rs2043112	<i>PRKCA</i> rs4790904				
T/T	G/G	C/T	Early	5.44	-2.18	4.13
T/T	G/G	T/T	Early	6.64	-0.99	5.05
T/T	A/G	C/T	Early	6.00	-1.62	3.67
T/T	A/G	T/T	Early	6.18	-1.45	7.80
T/T	A/A	C/T	Early	4.00	-3.62	0.46
T/T	A/A	T/T	Early	2.00	-5.62	0.46
T/T	A/A	C/C	Early	2.00	-5.62	0.46
C/C	G/G	T/T	Early	5.95	-1.68	8.72
C/C	A/G	C/T	Early	5.62	-2.01	5.96
C/C	A/G	C/C	Early	5.00	-2.62	0.46
C/C	A/A	T/T	Early	6.67	-0.96	2.75
C/T	G/G	C/T	Early	4.89	-2.74	4.13
C/T	G/G	T/T	Early	7.29	-0.33	11.01
C/T	A/G	C/T	Early	7.59	-0.04	7.80
C/T	A/G	T/T	Early	6.86	-0.77	12.84
C/T	A/A	C/C	Early	4.00	-3.62	0.46
T/T	G/G	C/C	Late	14.00	6.38	0.92
T/T	A/G	C/C	Late	8.00	0.38	0.46
C/C	G/G	C/T	Late	9.29	1.66	3.21
C/C	G/G	C/C	Late	11.00	3.38	0.46
C/C	A/G	T/T	Late	12.88	5.25	11.01
C/C	A/A	C/T	Late	9.50	1.88	0.92
C/C	A/A	C/C	Late	8.00	0.38	0.46
C/T	A/A	C/T	Late	9.00	1.38	0.92
C/T	A/A	T/T	Late	11.50	3.88	5.50
Total frequency (%) of genotype combinations that predict					EARLY	76.16
LID onset:					LATE	23.86

Table A5. Distribution of genotypes in the interaction of rs1043098 in *EIF4EBP2*, rs2043112 in *RICTOR* and rs4790904 in *PRKCA* with LID onset.

FCHSD1 = G/G



FCHSD1 = G/T



FCHSD1 = T/T

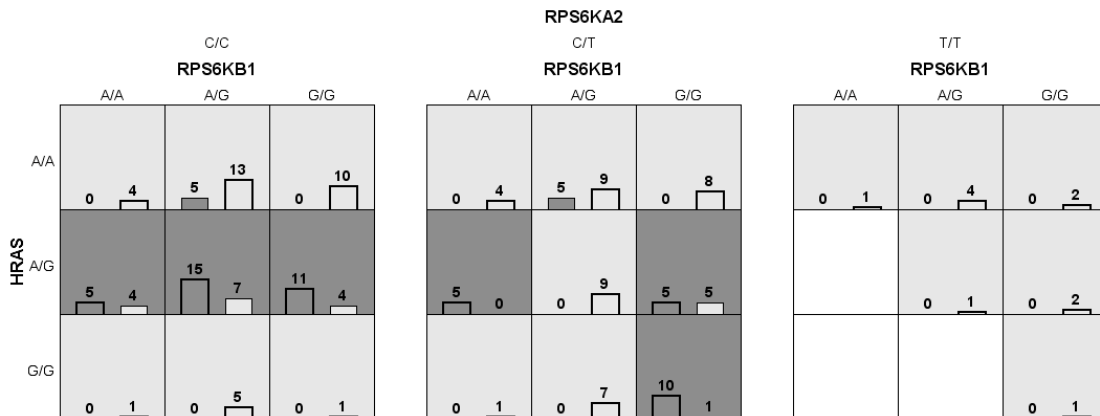


Figure A5. Distribution of high-risk, moderate/severe LID, and low-risk, no/mild LID, genotypes in the interaction of rs1292034 in *RPS6KB1*, rs12628 in *HRAS*, rs6456121 in *RPS6KA2* and rs456998 in *FCHSD1* with LID severity. Dark gray boxes present the high-risk factor combinations (moderate/severe LID severity) and light gray boxes present the low-risk factor combinations (no/mild LID severity). Each cell shows the number of PD patients with moderate/severe LID with that specific genotype on the left bar and control group with no/mild LID on the right bar.

ANNEX I

Genotype				Predicted LID severity	Freq. moderate-severe (%)	Freq. no-mild (%)	Ratio moderate-severe/no-mild
<i>RPS6KB1</i> rs1292034	<i>HRAS</i> rs12628	<i>RPS6KA2</i> rs6456121	<i>FCHSD1</i> rs456998				
A/G	A/A	C/T	G/T	No/very mild/mild	1.58	2.22	0.71
A/G	A/A	C/T	T/T	No/very mild/mild	0.79	1.43	0.56
A/G	A/A	C/T	G/G	No/ very mild/mild	0.00	1.27	0.00
A/G	A/A	C/C	G/T	No very mild//mild	0.79	2.54	0.31
A/G	A/A	C/C	T/T	No/ very mild/mild	0.79	2.07	0.38
A/G	A/A	C/C	G/G	No/ very mild/mild	0.00	0.95	0.00
A/G	A/A	T/T	T/T	No/ very mild/mild	0.00	0.64	0.00
A/G	A/G	C/T	T/T	No/ very mild/mild	0.00	1.43	0.00
A/G	A/G	C/T	G/G	No/ very mild/mild	0.00	0.79	0.00
A/G	A/G	C/C	G/T	No/ very mild/mild	0.00	3.18	0.00
A/G	A/G	T/T	G/T	No/ very mild/mild	0.00	0.79	0.00
A/G	A/G	T/T	T/T	No/ very mild/mild	0.00	0.16	0.00
A/G	G/G	C/T	T/T	No/ very mild/mild	0.00	1.11	0.00
A/G	G/G	C/C	T/T	No/ very mild/mild	0.00	0.79	0.00
A/A	A/A	C/T	G/T	No/ very mild/mild	0.00	1.11	0.00
A/A	A/A	C/T	T/T	No/ very mild/mild	0.00	0.64	0.00
A/A	A/A	C/T	G/G	No/ very mild/mild	0.00	0.31	0.00
A/A	A/A	C/C	T/T	No/ very mild/mild	0.00	0.64	0.00
A/A	A/A	C/C	G/G	No/ very mild/mild	0.00	0.48	0.00
A/A	A/A	T/T	T/T	No/ very mild/mild	0.00	0.16	0.00
A/A	A/A	T/T	G/G	No/ very mild/mild	0.00	0.16	0.00
A/A	A/G	T/T	G/T	No/ very mild/mild	0.00	0.32	0.00
A/A	G/G	C/T	T/T	No/ very mild/mild	0.00	0.16	0.00
A/A	G/G	C/C	G/T	No/ very mild/mild	0.00	0.48	0.00
A/A	G/G	C/C	T/T	No/ very mild/mild	0.00	0.16	0.00
A/A	G/G	T/T	G/G	No/ very mild/mild	0.00	0.16	0.00
G/G	A/A	C/T	G/T	No/ very mild/mild	0.00	2.38	0.00
G/G	A/A	C/T	T/T	No/ very mild/mild	0.00	1.27	0.00
G/G	A/A	C/T	G/G	No/ very mild/mild	0.00	0.64	0.00
G/G	A/A	C/C	T/T	No/ very mild/mild	0.00	1.59	0.00
G/G	A/A	C/C	G/G	No/ very mild/mild	0.00	0.32	0.00
G/G	A/A	T/T	G/T	No/ very mild/mild	0.00	0.48	0.00
G/G	A/A	T/T	T/T	No/ very mild/mild	0.00	0.31	0.00
G/G	A/A	T/T	G/G	No/ very mild/mild	0.00	0.16	0.00
G/G	A/G	C/T	G/T	No/ very mild/mild	0.00	1.91	0.00
G/G	A/G	C/T	G/G	No/ very mild/mild	0.00	0.95	0.00
G/G	A/G	C/C	G/T	No/ very mild/mild	0.00	2.38	0.00
G/G	A/G	C/C	G/G	No/ very mild/mild	0.00	0.48	0.00
G/G	A/G	T/T	T/T	No/ very mild/mild	0.00	0.32	0.00
G/G	G/G	C/C	G/T	No/ very mild/mild	0.00	0.32	0.00
G/G	G/G	C/C	T/T	No/ very mild/mild	0.00	0.16	0.00
G/G	G/G	C/C	G/G	No/ very mild/mild	0.00	0.64	0.00
G/G	G/G	T/T	T/T	No/ very mild/mild	0.00	0.16	0.00
A/G	A/A	T/T	G/T	Moderate/severe	1.58	0.32	4.94
A/G	A/A	T/T	G/G	Moderate/severe	0.79	0.16	4.94

A/G	A/G	C/T	G/T	Moderate/severe	5.56	1.59	3.50
A/G	A/G	C/C	T/T	Moderate/severe	2.38	1.11	2.14
A/G	A/G	C/C	G/G	Moderate/severe	3.18	0.48	6.67
A/G	G/G	C/T	G/T	Moderate/severe	3.18	0.48	6.67
A/G	G/G	C/T	G/G	Moderate/severe	0.79	0.16	4.94
A/G	G/G	C/C	G/T	Moderate/severe	2.38	0.64	3.75
A/G	G/G	C/C	G/G	Moderate/severe	0.79	0.32	2.50
A/G	G/G	T/T	G/T	Moderate/severe	0.79	0.16	4.94
A/A	A/A	C/C	G/T	Moderate/severe	3.18	0.64	4.97
A/A	A/A	T/T	G/T	Moderate/severe	0.79	0.32	2.50
A/A	A/G	C/T	G/T	Moderate/severe	0.79	0.64	1.25
A/A	A/G	C/T	T/T	Moderate/severe	0.79	0.00	∞
A/A	A/G	C/T	G/G	Moderate/severe	0.79	0.00	∞
A/A	A/G	C/C	G/T	Moderate/severe	3.18	0.79	4.02
A/A	A/G	C/C	T/T	Moderate/severe	0.79	0.64	1.25
A/A	A/G	C/C	G/G	Moderate/severe	0.79	0.48	1.67
A/A	G/G	C/T	G/T	Moderate/severe	0.79	0.32	2.50
G/G	A/A	C/C	G/T	Moderate/severe	2.38	1.91	1.25
G/G	A/G	C/T	T/T	Moderate/severe	0.79	0.79	1.00
G/G	A/G	C/C	T/T	Moderate/severe	1.75	0.64	2.75
G/G	A/G	T/T	G/T	Moderate/severe	2.38	0.00	∞
G/G	G/G	C/T	G/T	Moderate/severe	0.79	0.16	4.94
G/G	G/G	C/T	T/T	Moderate/severe	1.59	0.16	9.94
G/G	G/G	C/T	G/G	Moderate/severe	0.79	0.64	1.25
Total genotype combinations that predict LID severity:				NO/VERY MILD/MILD	3,95	38,62	0,10
				MODERATE/SEVERE	43,78	13,55	3,23

Table A6. Distribution of genotypes in the interaction of rs1292034 in *RPS6KB1*, rs12628 in *HRAS*, rs6456121 in *RPS6KA2* and rs456998 in *FCHSD1* with LID severity. Freq.=frequency.

ANNEX II

PUBLICATIONS DERIVED FROM THIS THESIS:

Martín-Flores N, Romaní-Aumedes J, Rué L, Canal M, Sander P, Straccia M, Allen N, Alberch J, Canals JM, Pérez-Navarro E, Malagelada C. (2015) RTP801 is involved in mutant huntingtin-induced cell death. *Mol Neurobiol* ⁶⁶⁶

Martín-Flores N*, Fernández-Santiago R*, Anatonelli F, Cerquera C, Moreno V, Matí MJ, Ezquerro M, Malagelada C. (2018) MTOR pathway-based discovery of genetic susceptibility to L-DOPA-induced dyskinesia in Parkinson's disease patients. *Mol Neurobiol*. *Both authors contributed equally to this work.⁶⁶⁷

Martín-Flores N*, Fernández-Santiago R*, Anatonelli F, Cerquera C, Moreno V, Tolosa E Matí MJ, Ezquerro M, Malagelada C. SNCA and mTOR genetic variations interact to modulate risk and age at onset of Parkinson's disease. *Both authors contributed equally to this work. Manuscript under revision.

Martín-Flores N, Pérez-Sisqués L, Llobet-Rosell A, Malagelada C. Stress-induced RTP801/Redd1 neutralizes the protective effect of exosomes in cellular models. Manuscript under revision.

Martín-Flores N, Pérez-Sisqués L, Creus-Muncunill J, Alberch J, Pérez-Navarro E, Malagelada C. RTP801 modulates motor plasticity impairment in Huntington's disease. Manuscript under preparation.

RTP801 Is Involved in Mutant Huntingtin-Induced Cell Death

Núria Martín-Flores¹ · Joan Romaní-Aumedes¹ · Laura Rué^{2,3,4} · Mercè Canal¹ · Phil Sanders^{2,3,4} · Marco Straccia^{2,3,4} · Nicholas D. Allen⁵ · Jordi Alberch^{2,3,4} · Josep M. Canals^{2,3,4} · Esther Pérez-Navarro^{2,3,4} · Cristina Malagelada¹

Received: 16 January 2015 / Accepted: 30 March 2015 / Published online: 16 April 2015
© Springer Science+Business Media New York 2015

Abstract RTP801 expression is induced by cellular stress and has a pro-apoptotic function in non-proliferating differentiated cells such as neurons. In several neurodegenerative disorders, including Parkinson's disease and Alzheimer's disease, elevated levels of RTP801 have been observed, which suggests a role for RTP801 in neuronal death. Neuronal death is also a pathological hallmark in Huntington's disease (HD), an inherited neurodegenerative disorder caused by a CAG repeat expansion in the huntingtin gene. Currently, the exact mechanisms underlying mutant huntingtin (mhtt)-induced toxicity are still unclear. Here, we investigated whether RTP801 is involved in (mhtt)-induced cell death. Ectopic exon-1 mhtt elevated RTP801 mRNA and protein levels in nerve growth factor (NGF)-differentiated PC12 cells and in

rat primary cortical neurons. In neuronal PC12 cells, mhtt also contributed to RTP801 protein elevation by reducing its proteasomal degradation rate, in addition to promoting RTP801 gene expression. Interestingly, silencing RTP801 expression with short hairpin RNAs (shRNAs) blocked mhtt-induced cell death in NGF-differentiated PC12 cells. However, RTP801 protein levels were not altered in the striatum of Hdh^{Q7/Q111} and R6/1 mice, two HD models that display motor deficits but not neuronal death. Importantly, RTP801 protein levels were elevated in both neural telencephalic progenitors differentiated from HD patient-derived induced pluripotent stem cells and in the putamen and cerebellum of human HD postmortem brains. Taken together, our results suggest that RTP801 is a novel downstream effector of mhtt-induced toxicity and that it may be relevant to the human disease.

Keywords RTP801 · Exon-1 mutant huntingtin · Hdh^{Q7/Q111} mice · Putamen · R6/1 mice · Striatum · PC12 cells · Neuron death

✉ Esther Pérez-Navarro
estherperez@ub.edu

✉ Cristina Malagelada
crismalagelada@gmail.com

¹ Department of Pathological Anatomy, Pharmacology and Microbiology, Faculty of Medicine, University of Barcelona, Casanova 143, 08036 Barcelona, Catalonia, Spain

² Department of Cell Biology, Immunology and Neurosciences, Faculty of Medicine, University of Barcelona, Casanova 143, 08036 Barcelona, Catalonia, Spain

³ Institut d'Investigacions Biomèdiques August Pi i Sunyer (IDIBAPS), 08036 Barcelona, Catalonia, Spain

⁴ Centro de Investigación Biomédica en Red sobre Enfermedades Neurodegenerativas (CIBERNED), Madrid, Spain

⁵ Divisions of Pathophysiology & Repair and Neuroscience, School of Biosciences, Cardiff University, Cardiff CF10 3AX, UK

Introduction

RTP801/REDD1 protein, encoded by the DDIT4 gene, was first identified on the basis of its induction by hypoxia [1] and DNA damage [2]. Other stressors induced its expression such as dexamethasone, thapsigargin, tunicamycin, heat shock in murine T cell lymphoma cells [3], or cigarette smoke in lung cells [4].

In the central nervous system, RTP801 expression is increased in response to ischemia, β -amyloid peptide [5, 6], 6-hydroxydopamine (6-OHDA) [7, 8], and 1-methyl-4-phenyl-1, 2,3,6-tetrahydropyridine [8]. Importantly, RTP801 not only accumulates in cellular and animal toxic models but also in

samples from patients suffering from neurodegenerative diseases. RTP801 protein levels are elevated in dopaminergic neurons from the substantia nigra in sporadic and mutant parkin Parkinson's disease (PD) patients [8, 9] and in lymphocytes from Alzheimer's disease (AD) patients [10].

RTP801 is sufficient to induce cell death in nerve growth factor (NGF)-differentiated PC12 cells [1, 8] and sympathetic neurons [8]. RTP801 inactivates sequentially mechanistic target of rapamycin (mTOR) and Akt survival kinases via Tuberosus Sclerosis Complex proteins 1 and 2 [8, 11]. As a consequence, the neuronal survival kinase Akt, which is also a substrate of mTOR, cannot be phosphorylated at residue Ser473, and so, it is unable to enhance pro-survival signals thereby triggering neuronal death [12].

The activity of mTOR has been studied in cellular and mouse models of neurodegenerative diseases, as its regulation also controls autophagy and, as a consequence, the clearance of unfolded proteins and protein aggregates [13, 14]. Huntington's disease (HD) is one of the neurodegenerative diseases in which inhibition of mTOR with rapamycin or rapalogs has been suggested to be beneficial [15, 16]. HD is caused by a dominantly inherited expansion of a CAG repeat (≥ 37 repeats) in the huntingtin (htt) gene that generates an aberrant protein [17]. In spite of the ubiquitous expression pattern of htt, the most vulnerable brain regions are the striatum [18] and the motor cortex [19]. However, mutant htt (mhtt) toxicity also extends to other brain structures such as the hippocampus [20] and the cerebellum where atrophy and cell death have been shown recently [21]. Neural dysfunction in these brain areas leads to motor, cognitive, and psychiatric symptoms [22].

Here, we investigated whether RTP801 mediates mhtt-induced toxicity. Ectopic exon-1 mhtt upregulated RTP801 protein levels, both in NGF-differentiated PC12 cells and in primary cortical neurons, by increasing RTP801 gene expression and by decreasing its degradation. RTP801 accumulation was also observed in brain samples and HD-induced pluripotent stem cells (iPSC)-derived telencephalic progenitors. Interestingly, RTP801 knockdown prevents mhtt-induced cell death. Therefore, blockade of RTP801 emerges as a new possible therapeutic target to counteract cell death in HD.

Materials and Methods

Antibodies, Plasmids, and Materials Rabbit polyclonal anti-RTP801 antibody was purchased from Proteintech Group Inc., Chicago, IL, USA. We used different lot numbers of this antibody with one of them detecting an unspecific band below RTP801 band in the Western blots. Whenever this band appears, the RTP801-specific band is always indicated with an arrow in the figures. The mouse monoclonal antibody against green fluorescent protein (GFP) was obtained from Santa

Cruz Biotechnology. Anti-glyceraldehyde 3-phosphate dehydrogenase (GAPDH) was purchased from Merck Millipore. Anti- α -actin antibody was purchased from MP Biomedicals. Goat anti-mouse and anti-rabbit secondary antibodies conjugated to horseradish peroxidase were obtained from Pierce Thermo Scientific. Goat anti-mouse and anti-rabbit secondary antibodies conjugated with Alexa 488 or Alexa 568 were purchased from Life Technologies.

The shRTP801 1 and 4 and scrambled shCT constructs were generated as previously described [8, 23]. The specificity and the effectiveness of shRTP801 1 and 4 were previously proved in cellular models [8, 9, 12] and in vivo, in utero rat brain electroporations [23]. The constructs Q25, Q72, and Q103 were a kind gift of Dr. G.M. Lawless (Cure HD Initiative, Reagent Resource Bank of the Hereditary Disease Foundation, New York, NY). All constructs were verified by DNA sequencing. Actinomycin D was purchased from Gibco, cycloheximide was purchased from Merck Millipore, D-2-Amino-5-phosphonovaleric acid (APV) was obtained from Sigma-Aldrich, and CNQX and NGF were from Alomone Labs.

Cell Culture and Transfection PC12 cells were cultured and differentiated with NGF as described previously [24]. For NGF treatment, cells were grown in RPMI 1640 medium (Thermo Fisher Scientific, Waltham, MA, USA) and supplemented with 1 % heat-inactivated horse serum (Sigma-Aldrich, St. Louis, MO, USA), penicillin/streptomycin (Gibco Life Technologies, Grand Island, NY, USA), and 50 ng/ml recombinant human β -NGF (Alomone Labs, Jerusalem, Israel) for 7–8 days, in a 7.5 % CO₂ atmosphere at 37 °C. Medium was changed every other day and before transfection. Neuronal PC12 cells were transfected at day 5 of NGF exposure, with Lipofectamine 2000 (Invitrogen Life Technologies, Carlsbad, CA, USA) according to the manufacturer's instructions. Media were replaced 4 h later with serum-supplemented RPMI media.

Rat primary cortical cultures were prepared as previously described [25]. Briefly, neurons from embryonic (E18) Sprague–Dawley rat cortex were dissociated in 0.05 % trypsin and plated at a density of 250 cells/mm² on poly-L-lysine-coated coverslips and maintained in neurobasal medium with B27 and 2 mM GlutaMAX (all from Gibco). After 19 days in vitro (DIV 19), cultured neurons in coverslips were transfected with Lipofectamine 2000 in neurobasal medium supplemented with B27, 2 mM GlutaMAX, 50 μ M APV (Sigma-Aldrich) and 10 μ M CNQX (Alomone Labs). Sixty minutes later, the coverslips were transferred back into the original neurobasal medium for further 2 days.

HD Mouse Models For this study, we used male R6/1 transgenic mice (B6CBA background) expressing exon-1 of mhtt containing 145 repeats [26, 27] and their corresponding WT

littermates and heterozygous mutant $Hdh^{Q7/Q111}$ and wild-type $Hdh^{Q7/Q7}$ knock-in mice (C57BL/6 background) [28]. Mouse genotype and CAG repeat length were determined as described elsewhere [28, 29]. Mice were housed together in numerical birth order in groups of mixed genotypes, and data were recorded for analysis by microchip mouse number. The animals were housed with access to food and water ad libitum in a colony room kept at 19–22 °C and 40–60 % humidity, under a 12:12-h light/dark cycle. Experiments were carried out according to European regulation (2010/63/UE) for the care and use of laboratory animals.

Ventral Telencephalic Differentiation of Human-Induced Pluripotent Stem Cells Two non-integrating human iPSC lines CS83iCTR33n1 and CS21iHD60n5 obtained from iPSCs-Core from CEDARS-Sinai (Los Angeles, CA, USA) were differentiated until 12 DIV. hiPSCs were cultured on Matrigel-coated plates (BD Biosciences) in mTeSR1 medium following the manufacturers' protocols (Stem Cell Technologies). For neural induction, hPSCs grown to 70 % confluency were washed three times with phosphate-buffered saline (PBS) and cultured in SLI neural induction medium (advanced DMEM/F12, 2 mM L-glutamine, 1 % penicillin/streptomycin (Life Technologies), 10 μ M SB431542 (Abcam), 1 μ M LDN 193189 (Stemgent), 1.5 μ M IWR1 (Tocris), 2 % NeuroBrew-21 without RA (Miltenyi Biotec)). On day 4, confluent cultures were treated with 10 μ M Y-27632 (Abcam) for 1 h prior to passaging with Accutase (Life Technologies) onto fresh Matrigel-coated plates, with a split ratio of 1:2. On day 8, cultures were passaged 1:2 and cultured in LI medium (SLI without SB431542). At day 12, human iPSC-derived telencephalic progenitors' total protein was extracted from the cultures using TRI Reagent (Sigma-Aldrich) as described elsewhere.

Post-Mortem Brain Tissue Samples of putamen, motor cortex, hippocampus, and cerebellum from control subjects and HD patients were obtained from the Neurological Tissue Bank of the Biobanc-Hospital Clinic-IDIBAPS, following the guidelines of the local ethics committees (for details, see Table 1). Post-mortem tissue was homogenized as described previously [30].

Immunocytochemistry Cells were fixed in 4 % paraformaldehyde for 15 min at room temperature. After washing with PBS, cells were incubated for 1 h at room temperature with the blocking solution Superblock-PBS (Life Technologies, Carlsbad, CA, USA) plus 0.3 % Triton X-100 and then incubated overnight with the primary antibody diluted in PBS. The following primary antibodies were used: rabbit polyclonal anti-RTP801 antibody (1:80) and mouse monoclonal anti-GFP (1:1,000; Santa Cruz Biotechnology, Dallas, TX, USA). The cells were then washed with PBS

and incubated for 2 h with the corresponding secondary antibody (1:500 for goat anti-rabbit conjugated with Alexa 568 and 1:1,000 for goat anti-mouse conjugated with Alexa 488; Life Technologies), diluted in PBS, and co-stained with Hoechst 33342 (1:5,000; Invitrogen Life Technologies) for nuclear staining. After washing in PBS, cells were mounted with mounting medium Prolong Gold Antifade Mountant (Invitrogen Life Technologies). In survival assays, eGFP-positive viable cells were scored by strip-counting, as described previously [8]. Highly stained cells for RTP801 were scored with the help of ImageJ software by setting a common color threshold in each image. Only the brightest cells that overcame this threshold were counted as positive.

Western Blot Whole cell extracts were collected and processed as described previously [8]. Animals were anesthetized and killed by decapitation at different ages. Brains were removed quickly, and the striata were dissected out and homogenized in lysis buffer. Protein extraction and Western blot analyses were performed as described elsewhere [8, 31]. The following primary antibodies were used: anti-RTP801 (1:1,000, Proteintech Group Inc.) and rabbit polyclonal anti-living colors (1:1,000; Clontech Laboratories Inc., Mountain View, CA, USA). Loading control was obtained by incubation with anti- α -actin (1:20,000; MP Biomedicals, Santa Ana, CA, USA) or anti-GAPDH (1:10,000; Merck Millipore; Darmstadt, Germany) antibodies. Goat anti-mouse or anti-rabbit secondary antibodies conjugated to horseradish peroxidase were obtained from Pierce Thermo Fisher Scientific (Rockford, IL, USA). Chemiluminescent images were acquired using a LAS-3000 imager (Fuji) and quantified by computer-assisted densitometric analysis (ImageJ).

Quantitative Reverse Transcription-PCR Total RNA was isolated from NGF-differentiated PC12 cells using the High Pure RNA Isolation Kit (Roche Diagnostics Corporation, Indianapolis, IN, USA). Transcriptor First Strand cDNA Synthesis Kit (Roche Diagnostics Corporation) was used to reverse transcribe cDNA from total RNA. Specific primers for quantitative PCR in amplification were used as follows: RTP801 forward primer, 5'-GCTCTGGACCCAGTCTA GT-3'; RTP801 reverse primer, 5'-GGGACAGTCCTTCA GTCCTT-3'; α -actin forward primer, 5'-GGGTATGGGTCA GAAGGACT-3'; and α -actin reverse primer, 5'-GAGGCATA CAGGGACAACAC-3'. Total RNA extraction from 12-week-old wild-type and R6/1 mice striatal samples and cDNA synthesis were performed as described elsewhere [31]. Specific mouse RTP801 primers were used as follows: forward primer, 5'-ACCTGTGTGCCAACCTGAT-3'; reverse primer, 5'-TAACAGCCCCTGGATCTTG-3'. Quantitative PCR was performed with a 7500 Real-Time PCR System (Applied Biosystems, Foster City, CA, USA) using equal

amounts of cDNA template, normalized by α -actin. The RT-PCR data were analyzed and quantified using the comparative quantification.

RTP801 Protein Half-Life Neuronal PC12 cells were transfected with eGFP, Q25, Q72, or Q103 constructs. Twenty-four hours later, cell cultures were treated with 1 μ M of cycloheximide (Calbiochem Merck Millipore, Darmstadt, Germany) for 10 or 60 min. Subsequently, cells were harvested and subjected to Western blot. Membranes were probed for RTP801 or eGFP and re-probed for α -actin as a loading control. The half-life of RTP801 was calculated by fitting the curve to a one-phase decay type exponential equation (GraphPad Prism).

RTP801 mRNA Half-Life NGF-differentiated PC12 cells were transfected with eGFP, Q25, Q72, or Q103 constructs. Twenty-four hours later, cell cultures were treated with 3 μ g/ μ l of actinomycin D (Gibco) for 10 or 60 min. Subsequently, total RNA was isolated and reverse transcribed to cDNA, and quantitative PCR was performed as described above. The half-life of the mRNA was calculated by fitting the curve to a one-phase decay type exponential equation (GraphPad Prism).

Statistics All experiments were performed at least in triplicate, and results are reported as the mean \pm SEM. Statistical analyses were performed by using the unpaired Student's *t* test (95 % confidence) or one-way ANOVA with Dunnett's multiple comparison test as a post hoc for the comparison of multiple groups, as appropriate and indicated in the figure legends. Values of $P < 0.05$ were considered as statistically significant.

Results

Ectopic mhtt Increases RTP801 Protein Levels in Neural Cells and Induces Cell Death RTP801 is upregulated in neural cells as a response to different types of toxic stimuli [5, 6, 8, 32]. Thus, we asked whether mhtt could also upregulate RTP801 levels. To this end, NGF-differentiated PC12 cells were transfected with eGFP alone (empty vector) or with exon-1-encoded N-terminal htt with 25 (Q25, non-toxic form), 72, or 103 (Q72 and Q103, toxic forms) CAG repeats fused to eGFP. Twenty-four hours after transfection, RTP801 and ectopic htt protein levels were analyzed by Western blot (WB). We detected the protein product of all three forms of htt by WB and, as expected, Q72 and Q103 were found in both the soluble and insoluble fractions. We also observed insoluble Q72 and Q103 retained in the stacking gel (Fig. 1a). We observed that RTP801 protein levels were increased by about 70 % in cells overexpressing Q72 or Q103 in comparison to those cells transfected with the control eGFP- or Q25-

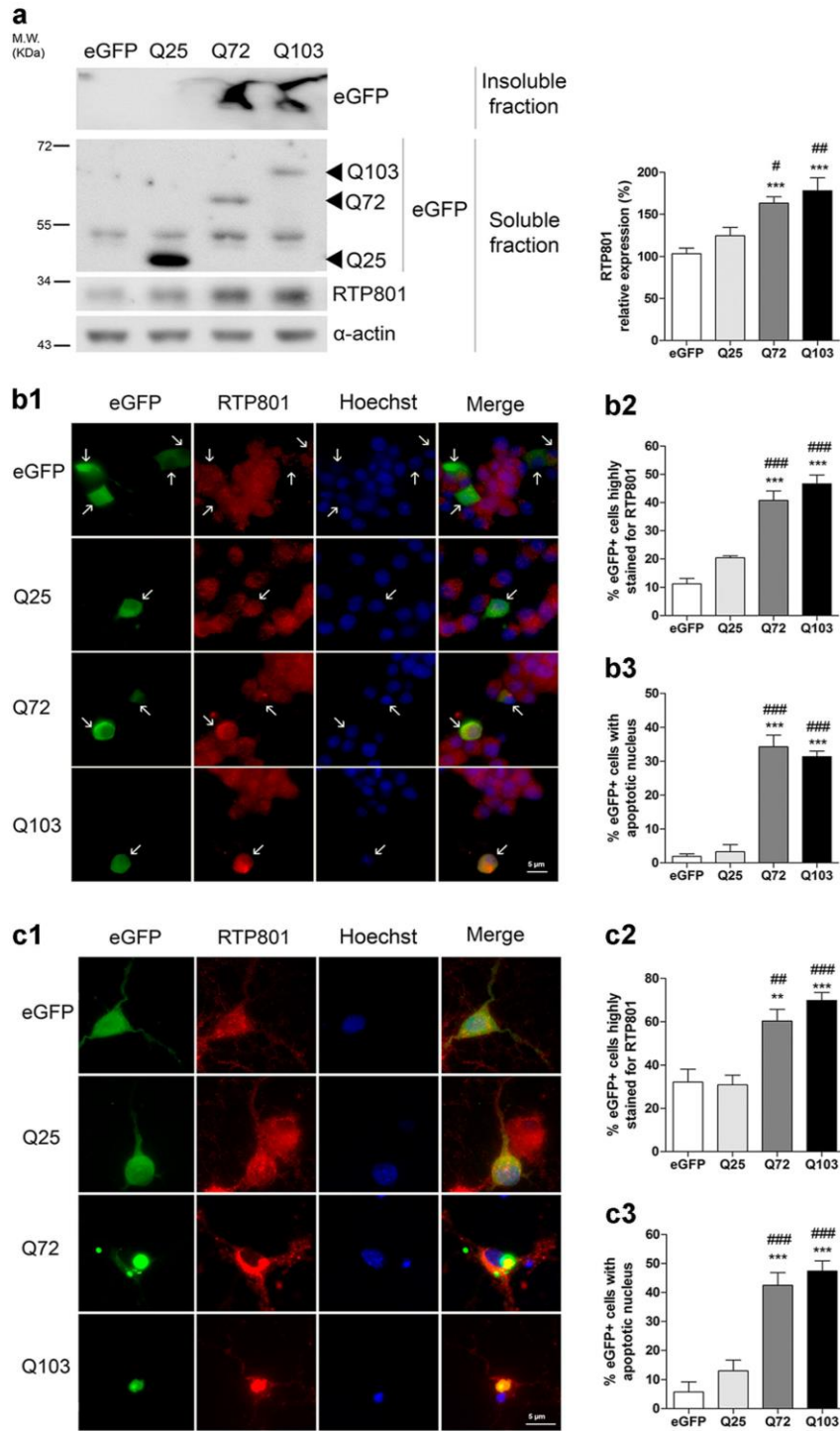
Fig. 1 RTP801 protein levels are increased in cells overexpressing mhtt. **(a)** Extracts from transfected neuronal PC12 cells with eGFP, Q25, Q72, or Q103 constructs for 24 h were subjected to Western immunoblotting. Membranes of the soluble and insoluble fractions were probed with antibodies against eGFP and RTP801 and then re-probed with an anti- α -actin antibody as a loading control. Representative immunoblots are shown along with densitometry analysis for RTP801 signals from at least three independent experiments. Immunostaining of neuronal PC12 cells (transfected cells, marked with *white arrows*) (*b1*) or cortical neurons (*c1*) reveals that RTP801 (*in red*) is increased in cells transfected with Q72 or Q103 fused to eGFP (*in green*). Nuclei were stained with Hoechst 33342 (*in blue*). *Scale bar*, 5 μ m. Proportions of transfected neuronal PC12 cells (eGFP+) (*b2*) or cortical neurons (eGFP+) (*c2*) highly stained for RTP801 were scored under fluorescence microscopy for each condition. (*b3* and *c3*) Proportions of transfected cells (eGFP+) highly positive for RTP801 and with pyknotic nuclei were also scored for each condition. Values represent mean \pm SEM for at least three independent experiments performed in triplicate. Data was analyzed by one-way ANOVA with Dunnett's multiple comparison test (** $P < 0.01$ and *** $P < 0.001$ vs eGFP; # $P < 0.05$, ## $P < 0.01$, and ### $P < 0.001$ vs Q25)

expressing plasmids (Fig. 1a). By immunofluorescence, we confirmed that Q72- and Q103-overexpressing cells showed higher levels of RTP801 (Fig. 1b1, b2), and that in many of these cells, RTP801 formed aggregates that often co-localized with mhtt aggregates (Fig. 1b1). Interestingly, around 35 % of mhtt-transfected cells that were highly stained for RTP801 also displayed pyknotic nuclei (Fig. 1b3). Similar results were obtained in rat primary cortical neurons that were transfected with mhtt (Fig. 1c1–c3).

Both RTP801 mRNA Levels and Protein Degradation Are Altered in Cells Overexpressing mhtt Next, we explored the mechanisms by which mhtt induces RTP801 protein accumulation. We first analyzed RTP801 mRNA levels in NGF-differentiated PC12 cells transfected with eGFP, Q25, Q72, or Q103 mhtt constructs to assess whether mhtt induces RTP801 expression at the transcriptional level. Pathogenic Q72- or Q103-overexpressing cells displayed a threefold increase in RTP801 mRNA levels compared to cells transfected with eGFP- or Q25-expressing plasmids (Fig. 2a).

To investigate whether the increase in RTP801 mRNA levels could result from an upregulation of gene expression or a reduction of the mRNA degradation rate, we analyzed the mRNA half-life in NGF-differentiated PC12 cells transfected with eGFP, Q25, Q72, or Q103 constructs. Twenty-four hours after transfection, actinomycin D, an inhibitor of RNA synthesis, was added to the culture medium for 10 or 60 min. The cells were subsequently harvested and the RNA was isolated. RTP801 transcripts were analyzed by reverse transcriptase-qPCR. As shown in Fig. 2b, mhtt did not alter the half-life of RTP801 mRNA.

RTP801 degradation mostly depends on the proteasome, as shown by its short half-life of 5–7 min [33, 34]. Thus, we next assessed whether mhtt, apart from inducing RTP801 gene expression, could impair RTP801 protein degradation. To this



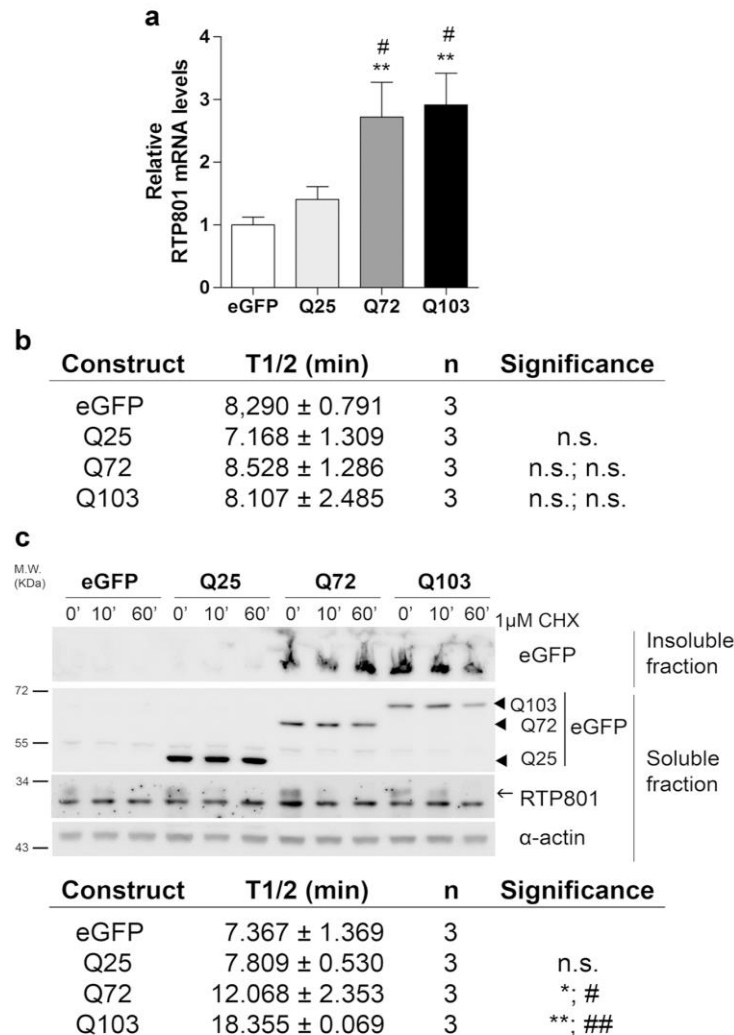


Fig. 2 mhtt alters both RTP801 mRNA levels and protein degradation rate. **a** mhtt regulates RTP801 transcriptionally. NGF-differentiated PC12 cells were transfected with eGFP, Q25, Q72, or Q103 constructs. RNA was extracted 24 h post-transfection, and samples were analyzed by reverse transcription-qPCR to quantify RTP801 mRNA under the indicated conditions. Values represent mean±SEM of at least three independent experiments. **b** mhtt does not alter RTP801 mRNA half-life. NGF-differentiated PC12 cells were transfected with eGFP, Q25, Q72, or Q103 constructs. Actinomycin D was added to the media 24 h post-transfection for 10 or 60 min. RNA was extracted, and reverse transcription-qPCR was performed to quantify RTP801 mRNA under the indicated conditions. RTP801 mRNA half-life (min) was calculated and expressed as the mean±SEM of three independent experiments

performed in triplicate (*n.s.*, not significant). **c** mhtt alters RTP801 protein half-life. NGF-differentiated PC12 cells transfected with eGFP, Q25, Q72, or Q103 constructs for 24 h were treated with cycloheximide (CHX) for 10 or 60 min. Cell extracts were harvested, and insoluble and soluble protein fractions were subjected to Western blot. Membranes were probed with antibodies against eGFP and RTP801 and with anti- α -actin antibody as a loading control. Representative immunoblots are shown. Note that the RTP801 specific band in the WB is denoted with an arrow. RTP801 half-life (min) was calculated and expressed as the mean±SEM of three independent experiments performed in triplicate. Data (**a**, **b**, and **c**) were analyzed by one-way ANOVA with Dunnett's multiple comparison test (* P <0.05, ** P <0.01 vs eGFP; # P <0.05, ## P <0.01 vs Q25)

end, NGF-differentiated PC12 cells were transfected with eGFP-, Q25-, Q72-, or Q103-expressing plasmids. Twenty-four hours later, cultures were treated with cycloheximide, a protein synthesis inhibitor, for 10 or 60 min. Relative RTP801

protein levels were assessed by WB, and the data were used to calculate the protein degradation rate. We observed that ectopic mhtt (Q72 or Q103) increased the RTP801 protein half-life by 4 and 10 min, respectively (Fig. 2c). Taken together, our

results show that mhtt elevates RTP801 protein levels by increasing RTP801 mRNA levels and impairing RTP801 proteasomal degradation.

RTP801 Upregulation Mediates Death in Neuronal PC12 Cells Overexpressing mhtt RTP801 is sufficient and necessary to cause cell death in cellular models of PD [1, 8]. Hence, we next explored whether RTP801 is involved in mhtt-induced cell death. To explore whether RTP801 elevation mediated mhtt-induced toxicity, we co-transfected NGF-differentiated PC12 cells with control Q25 htt or pathogenic mhtt Q72 and shRNAs to knock down RTP801 expression. We tested two different nucleotide sequences (shRTP801 1 and shRTP801 4) to discard off-target effects. Forty-eight hours after transfection, we analyzed RTP801 protein levels by Western blot. RTP801 knock down was about 20–30 % in cells transfected with RTP801 shRNAs compared to those transfected with the scrambled shRNA (a 3A). Interestingly, when mhtt-induced RTP801 accumulation was abrogated with the shRNAs, mhtt-induced cell death was significantly prevented (Fig. 3b). These results thus highlight an important contribution of RTP801 to mhtt-induced toxicity.

RTP801 Protein Levels Are Not Altered in the Striatum of HD Mouse Models Next, we analyzed whether RTP801 levels were altered in the striatum of two different HD mouse models: the R6/1 mouse that overexpresses human exon-1 mhtt and the knock-in model $Hdh^{Q7/Q111}$ that expresses wild-type and full-length mhtt. We observed that RTP801 mRNA levels did not vary in 12-week-old R6/1 mice in comparison to their wild-type littermates ($WT=1.000\pm 0.0977$, $n=7$; $R6/1=1.002\pm 0.1619$, $n=7$; $P=0.9917$, Student's *t* test). RTP801 protein levels were analyzed by WB at different stages of the disease. Interestingly, we did not detect changes in RTP801 protein levels in the striatum of either R6/1 or $Hdh^{Q7/Q111}$ mice at any stage when compared with the corresponding wild-type littermates (Fig. 4a, b).

RTP801 Accumulates in Differentiated HD-iPSCs and in Human Post-Mortem HD Brains We next examined whether RTP801 protein levels were also increased in human HD-iPSCs and brain tissue. To achieve this, we analyzed RTP801 levels by WB in iPSCs derived from a non-affected individual (expressing htt containing 33 CAG repeats, referred as control; Ctr33) and from an HD patient (expressing mhtt containing 60 CAG repeats, referred as HD60) that were differentiated according to a neuronal differentiation protocol that generates striatal medium-sized spiny neurons. Cells were harvested 12 days after starting the differentiation process, when they display a medial telencephalic identity. As shown in Fig. 5a, mhtt-expressing cells displayed a 37 % increase in RTP801 protein levels compared to control cells.

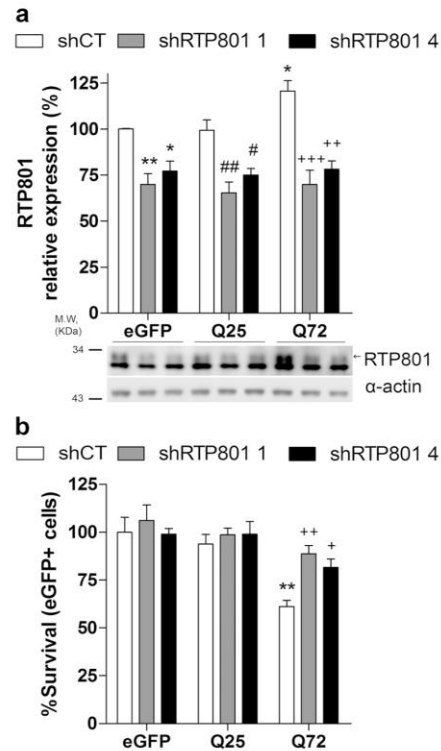


Fig. 3 RTP801 mediates mhtt-induced toxicity. **a** Specific shRNAs against RTP801 abrogated mhtt-induced RTP801 expression. NGF-differentiated PC12 cells were co-transfected with eGFP, Q25, or Q72 and either pCMS eGFP-shG (scrambled shRNA as a control), pCMS eGFP-shRTP801_1, or pCMS eGFP-shRTP801_4. Two days later, RTP801 protein levels were analyzed by Western blot. Representative immunoblots for RTP801 and α -actin (loading control) are shown in the lower panel. The upper panel shows a graph with the values of densitometry analysis as the mean \pm SEM of three independent experiments. Note that the RTP801-specific band in the WB is denoted with an arrow. **b** Under the same transfection conditions, cell survival (eGFP+ cells) was scored using fluorescence microscopy. The graph shows the number of surviving cells in each condition. Values represent the mean \pm SEM of three independent experiments. Data were analyzed using one-way ANOVA with Dunnett's multiple comparison test (* $P<0.05$, ** $P<0.01$ vs eGFP-shG; # $P<0.05$, ## $P<0.01$ vs Q25 shG; + $P<0.05$, ++ $P<0.01$, and +++ $P<0.001$ vs Q72 shG)

Our previous studies showed that RTP801 protein is highly expressed in degenerating nigral neurons from PD patients [8, 9, 12]. Thus, we examined whether this protein was also increased in the brain tissue of HD patients. We analyzed RTP801 protein levels by WB in protein extracts obtained from the putamen, frontal cortex, hippocampus, and cerebellum of seven control and six HD donors (Table 1). We observed increased levels of RTP801 in the putamen and cerebellum (Fig. 5b, c), whereas no changes were detected in frontal cortex and hippocampus (Fig. 5d, e) when compared with controls. Thus, our results show for the first time

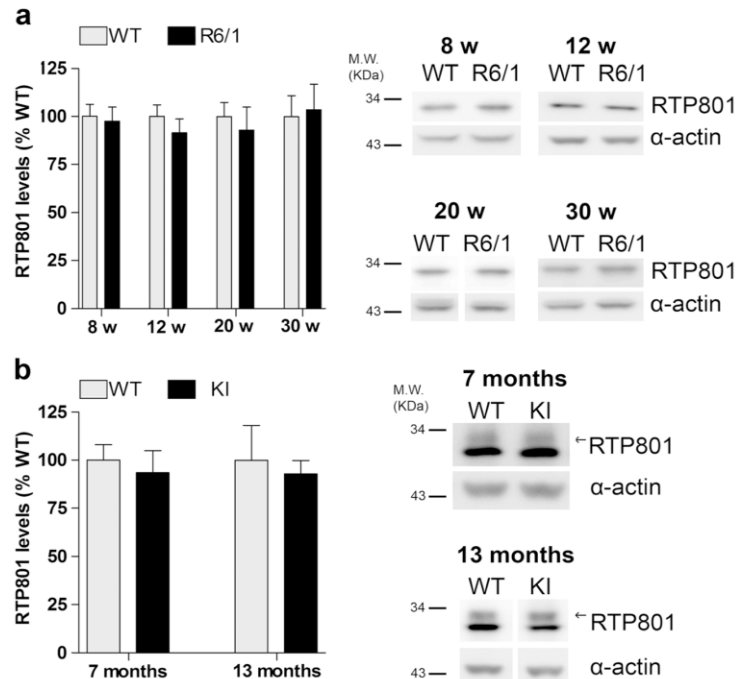


Fig. 4 RTP801 does not accumulate in the striatum of HD mouse models. **a** Striata from WT and R6/1 mice at different stages of disease progression (from 8 to 30 weeks (w) of age) were subjected to SDS-PAGE and Western blot. Membranes were probed with antibodies against RTP801 and α -actin as a loading control. The *left panel* shows densitometric analysis with the values represented as the mean \pm SEM of six animals per condition. **b** Striata from 7- and 13-month-old Hdh^{Q7/Q7}

(WT) and Hdh^{Q7/Q111} knock-in mice were subjected to SDS-PAGE and Western blot. Membranes were probed with antibodies against RTP801 and α -actin as a loading control. The *left panel* shows densitometric analysis with the values represented as the mean \pm SEM of five animals per condition. The specific RTP801 band is denoted with an *arrow*. Data were analyzed using Student's *t* test

that RTP801 protein levels are increased in telencephalic progenitors derived from human HD-induced pluripotent stem cells (iPSCs) and in the striatum and cerebellum of HD patients.

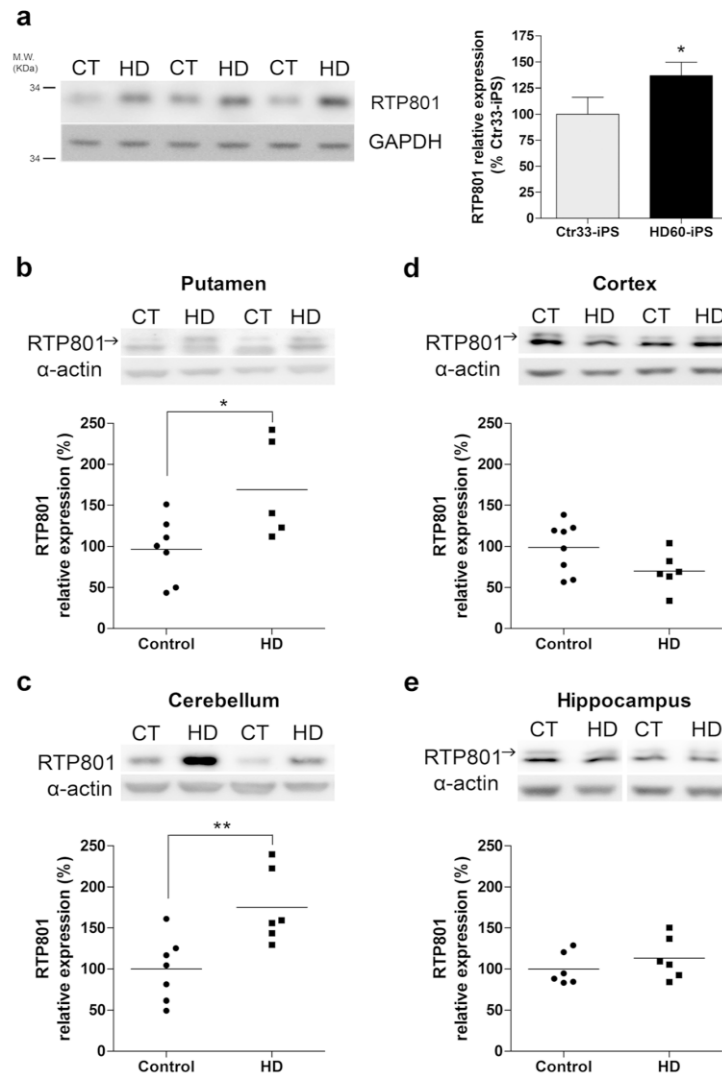
Discussion

This study shows that mhtt regulates the expression of RTP801 in several cellular models of HD. The mechanism by which mhtt elevates RTP801 levels involves increasing gene expression as well as lengthening the half-life of RTP801 protein. Moreover, RTP801 acts as a downstream effector of mhtt toxicity since silencing of RTP801 expression prevents mutant htt-induced cell death. In accordance with these results, we observed increased levels of RTP801 in the striatum and cerebellum of human HD postmortem samples and also in differentiated HD-iPSC cells. However, no alterations of RTP801 protein levels or neuronal death were detected in the striatum of HD mouse models.

Here we show that mhtt induces an increase in RTP801 mRNA and protein levels in cultured cells as has been shown previously to occur in neuronal cells in response to other stressors [5, 6, 8, 32]. This effect was similar in different cell types such as rat NGF-differentiated PC12 cells and rat primary cortical neurons overexpressing exon-1 mhtt with 72 or 103 CAG repeats. Moreover, our results indicate that changes in RTP801 protein and mRNA levels in cellular HD models seem independent of the number of CAG repeats, as similar results were obtained by overexpression of exon-1 mhtt with 72 or 103 CAG repeats.

Many transcription factors regulate RTP801 mRNA levels depending on the stimulus. For example, RTP801 expression is induced by ATF4 via eIF2 in response to endoplasmic reticulum stress, by p53 in response to DNA damage [2], and by HIF-1 and Sp1 in response to hypoxia [35]. Interestingly, activation of endoplasmic reticulum stress [36, 37] and increased p53 and Sp1 protein levels [38–42] have been shown in cellular models of HD and thus could explain the induction of RTP801 mRNA that we have observed. In addition to alterations in gene expression, our results also

Fig. 5 RTP801 is increased human HD models. **a** iPSCs expressing control (Ctr33) or mutant (HD60) htt were subjected to Western blot after 12 days of differentiation towards medium spiny neurons. Membranes were probed with antibodies against RTP801 and GAPDH, as a loading control. The *graph* displays values obtained by densitometric analysis, shown as the mean \pm SEM of three independent iPSC differentiations. Student's *t* test ($*P<0.05$ vs Ctr33). **b–e** RTP801 protein levels were analyzed by Western blot in protein extracts obtained from **b** putamen, **c** cerebellum, **d** cortex, and **e** hippocampus of control individuals and HD patients. The *graphs* display values obtained by densitometric analysis of Western blot data. Note that the specific RTP801 band is indicated with an *arrow*. Results are shown as the mean \pm SEM. Student's *t* test. $*P<0.05$ and $**P<0.01$ vs control



show that mhtt elevates RTP801 protein levels by impairing its proteasomal degradation in NGF-differentiated PC12 cells, which is in accordance with the impairment of the UPS system detected in HD cellular models [43].

Our results show that overexpression of exon-1 mhtt in NGF-differentiated PC12 cells and rat cortical neurons results in htt aggregate formation and induces cell death, in accordance with previous reports [44–49]. One unexpected observation was that mhtt also induced the appearance of RTP801 aggregates in both neuronal PC12 cells and cortical neurons. Interestingly, RTP801 aggregates did not always co-localize with mhtt aggregates. This mhtt effect could also interfere

with RTP801 degradation thereby contributing to RTP801 elevation.

Several mechanisms have been proposed to mediate mhtt-induced cell death including mitochondrial dysfunction, excitotoxicity, and lack of trophic support [50, 51]. Here, we identified RTP801 protein as a new player in mediating mhtt toxicity as demonstrated by the prevention of mhtt-induced cell death by silencing RTP801 expression. Similarly, knock-down of RTP801 expression confers neuroprotection in cellular models of AD [5] or PD [8], and its inhibition protects the brain from ischemic injury [32]. Upregulation of RTP801 also occurs in non-neuronal cells where it has been shown to be an

Table 1 Human post-mortem putamen samples. The table shows the characteristics of human (control and HD) individuals analyzed in the present study

Patient	Pathological diagnosis	Gender	Age (years)	CAG repeats
1	Normal	Female	60	–
2	Normal	Female	68	–
3	Normal	Female	71	–
4	Normal	Female	81	–
5	Normal	Male	39	–
6	Normal	Male	56	–
7	Normal	Male	64	–
8	HD, Vonsattel grade 4	Female	28	62
9	HD, Vonsattel grade 3	Female	72	42
10	HD, Vonsattel grade 3	Male	53	45
11	HD, Vonsattel grades 3–4	Male	55	n.d.
12	HD, Vonsattel grade 4	Male	59	44
13	HD, Vonsattel grade 4	Male	60	43

n.d. non-determined

essential mediator of cigarette smoke-induced pulmonary injury and emphysema [4] and to participate in several ocular disorders [52–54]. Interestingly, the administration of a siRNA targeting RTP801 is being used for the treatment of diabetic macular edema with promising results [55]. In addition, RTP801 has been identified recently as a novel negative regulator of Schwann cell myelination [56]. Taken together, these results identify RTP801 as an important mediator of cellular damage.

Importantly, increased levels of RTP801 are not only detected in cellular models of neurodegenerative diseases but also in cell types such as lymphocytes from AD patients [10] and dopaminergic neurons from the substantia nigra of PD patients [8, 9], thus suggesting a role in the pathophysiology of these diseases. Here, we extended this observation to telencephalic progenitors differentiated from HD-iPSCs, which display many of the biological properties found in the human HD brain, although the lack of the brain architecture and interaction with other non-neuronal cells limit the model. However, since these cells are still proliferative, RTP801 does not induce cell death as it occurs in non-dividing mature neurons [1, 8].

We also studied brain regions affected in HD, and we detected elevated levels of RTP801 in the putamen and cerebellum of HD patients. Consistent with a role of RTP801 in mhtt-induced cell death, massive cell death occurs in the putamen of HD patients [19]. Furthermore, the cerebellum displays considerable atrophy, as well as a consistent loss of Purkinje cells and nerve cells of cerebellar nuclei [21]. Degeneration seen in putamen is much higher than in the cerebellum. This could be explained by differential sensitivity to mhtt observed in each brain region that is still not well understood.

Interestingly, we did not detect changes in RTP801 protein levels in the striatum of two mouse models of HD, the R6/1 and the Hdh^{Q7/Q111} mice, at any of the ages analyzed. These results are in accordance with a role of RTP801 as a mediator of mhtt-induced cell death since these mice have almost no neuronal death in the striatum [57–62]. Supporting this observation, R6/1 and R6/2 mice displayed less neuronal damage following intrastriatal injection of 6-OHDA [63], a parkinsonian toxin that induces RTP801 and neuronal death [1, 7, 8]. These results suggest that striatal neurons from these models would activate mechanisms to counteract oxidative stress involving the blockade of stress-induced RTP801 protein elevation. In accordance with our results, RTP801/DDIT4 mRNA expression has been shown to be increased in the striatum of HD patients, not altered in R6/1 mice, and decreased in other HD murine models [64]. Therefore, RTP801 protein levels in HD striatum could be the product of both gene regulation and altered degradation.

In summary, mhtt elevates RTP801 by inducing its gene expression and impairing its proteasomal degradation in cellular models of HD. Blockade of RTP801 expression prevents mhtt-induced cell death in cellular models of HD. In addition, vulnerable brain regions that degenerate in HD pathogenesis present increased levels of RTP801. Hence, RTP801 is a novel downstream effector of mhtt that is involved in mediating its toxicity.

Acknowledgments The authors thank Dr. M. MacDonald (Massachusetts General Hospital, Boston, Massachusetts, USA) for the Hdh^{Q7/Q111} mice, Neurological Tissue Bank of the Biobanc-Hospital Clinic-IDIBAPS (Barcelona, Spain), and Institute of Neuropathology (Hospital de Bellvitge, L'Hospitalet de Llobregat, Barcelona, Spain) for human tissue samples, Dr. G.M. Lawless (Cure HD Initiative, Reagent Resource Bank of the Hereditary Disease Foundation, New York, NY) for exon-1-mhtt-expressing plasmids and Dr. C. Svendsen (Regenerative Medicine Institute, Cedars-Sinai Medical Center, Los Angeles, CA, USA) for the iPSC cells. iPSCs were obtained and characterized in the context of the HD-iPSC Consortium supported by the NINDS and CHDI Foundation, USA. M. MacDonald, C.S., PS, MS, NA, and JMC are members of the HD iPSC consortium. We also thank Ana López, Maria Teresa Muñoz, and Georgina Bombau for technical assistance and Dr. Teresa Rodrigo and the staff of the animal care facility (Facultat de Psicologia, Universitat de Barcelona) for their help. We thank Dr. Silvia Ginés for helpful discussion. Financial support was obtained from the Ministerio de Economía y Competitividad (grants SAF2010-21058 and SAF2013-45888R to C.M., SAF2012-37417 to J.M.C., and SAF2011-29507 to J.A.), projects integrated in the *Plan Nacional de I + D + I y cofinanciado por el ISCIII-Subdirección General de Evaluación y el Fondo Europeo de Desarrollo Regional (FEDER)*; grants P113/01250 to E.P.-N. and RETICS RD12/0019/0002 to J.M.C.), the European Commission with a Marie Curie International Reintegration Grant (PIRG08-GA-2010-276957), Spain, CHDI Foundation, USA (grants A-4528 to N.A. and A-7332 to J.M.C.), and funds obtained via the crowdfunding platform Goteo.org, sponsored by “Momentum: early detection of neurological disorders” and Portal d’Avall SL. to C.M.

Conflict of Interest The authors declare no competing financial interests.


References

- Shoshani T, Faerman A, Mett I, Zelin E, Tenne T, Gorodin S, Moshel Y, Elbaz S (2002) Identification of a novel hypoxia-inducible factor 1-responsive gene, RTP801, involved in apoptosis. *Mol Cell Biol* 22:2283–2293
- Ellisen LW, Ramsayer KD, Johannessen CM, Yang A, Beppu H, Minda K, Oliner JD, McKeon F et al (2002) REDD1, a developmentally regulated transcriptional target of p63 and p53, links p63 to regulation of reactive oxygen species. *Mol Cell* 10:995–1005
- Wang Z, Malone MH, Thomenius MJ, Zhong F, Xu F, Distelhorst CW (2003) Dexamethasone-induced gene 2 (dig2) is a novel pro-survival stress gene induced rapidly by diverse apoptotic signals. *J Biol Chem* 278:27053–27058
- Yoshida T, Mett I, Bhunia AK, Bowman J, Perez M, Zhang L, Gandjeva A, Zhen L et al (2010) Rtp801, a suppressor of mTOR signaling, is an essential mediator of cigarette smoke-induced pulmonary injury and emphysema. *Nat Med* 16:767–773
- Kim JR, Lee SR, Chung HJ, Kim S, Baek SH, Kim JH, Kim YS (2003) Identification of amyloid beta-peptide responsive genes by cDNA microarray technology: involvement of RTP801 in amyloid beta-peptide toxicity. *Exp Mol Med* 35:403–411
- Morel M, Couturier J, Pontcharrard R, Gil R, Fauconneau B, Paccalin M, Page G (2009) Evidence of molecular links between PKR and mTOR signalling pathways in A β neurotoxicity: role of p53, Redd1 and TSC2. *Neurobiol Dis* 36:151–161
- Ryu EJ, Angelastro JM, Greene LA (2005) Analysis of gene expression changes in a cellular model of Parkinson disease. *Neurobiol Dis* 18:54–74
- Malagelada C, Ryu EJ, Biswas SC, Jackson-Lewis V, Greene LA (2006) RTP801 is elevated in Parkinson brain substantia nigral neurons and mediates death in cellular models of Parkinson's disease by a mechanism involving mammalian target of rapamycin inactivation. *J Neurosci* 26:9996–10005
- Romani-Aumedes J, Canal M, Martin-Flores N, Sun X, Perez-Fernandez V, Wewering S, Fernandez-Santiago R, Ezquerro M et al (2014) Parkin loss of function contributes to RTP801 elevation and neurodegeneration in Parkinson's disease. *Cell Death Dis* 5, e1364
- Damjanac M, Page G, Ragot S, Laborie G, Gil R, Hugon J, Paccalin M (2009) PKR, a cognitive decline biomarker, can regulate translation via two consecutive molecular targets p53 and Redd1 in lymphocytes of AD patients. *J Cell Mol Med* 13:1823–1832
- Brugarolas J, Lei K, Hurley RL, Manning BD, Reiling JH, Hafen E, Witters LA, Ellisen LW et al (2004) Regulation of mTOR function in response to hypoxia by REDD1 and the TSC1/TSC2 tumor suppressor complex. *Genes Dev* 18:2893–2904
- Malagelada C, Jin ZH, Greene LA (2008) RTP801 is induced in Parkinson's disease and mediates neuron death by inhibiting Akt phosphorylation/activation. *J Neurosci* 28:14363–14371
- Sarkar S (2013) Regulation of autophagy by mTOR-dependent and mTOR-independent pathways: autophagy dysfunction in neurodegenerative diseases and therapeutic application of autophagy enhancers. *Biochem Soc Trans* 41:1103–1130
- Maiese K, Chong ZZ, Shang YC, Wang S (2013) mTOR: on target for novel therapeutic strategies in the nervous system. *Trends Mol Med* 19:51–60
- Ravikumar B, Rubinsztein DC (2006) Role of autophagy in the clearance of mutant huntingtin: a step towards therapy? *Mol Aspects Med* 27:520–527
- Sarkar S, Ravikumar B, Floto RA, Rubinsztein DC (2009) Rapamycin and mTOR-independent autophagy inducers ameliorate toxicity of polyglutamine-expanded huntingtin and related proteinopathies. *Cell Death Differ* 16:46–56
- The Huntington's Disease Collaborative Research Group (1993) A novel gene containing a trinucleotide repeat that is expanded and unstable on Huntington's disease chromosomes. *Cell* 72:971–983
- Vonsattel JP, Myers RH, Stevens TJ, Ferrante RJ, Bird ED, Richardson EP Jr (1985) Neuropathological classification of Huntington's disease. *J Neuropathol Exp Neurol* 44:559–577
- Mann DM, Oliver R, Snowden JS (1993) The topographic distribution of brain atrophy in Huntington's disease and progressive supranuclear palsy. *Acta Neuropathol* 85:553–559
- Rosas HD, Koroshetz WJ, Chen YI, Skeuse C, Vangel M, Cudkovicz ME, Caplan K, Marek K et al (2003) Evidence for more widespread cerebral pathology in early HD: an MRI-based morphometric analysis. *Neurology* 60:1615–1620
- Rub U, Hoche F, Brunt ER, Heinsen H, Seidel K, Del Turco D, Paulson HL, Bohl J et al (2013) Degeneration of the cerebellum in Huntington's disease (HD): possible relevance for the clinical picture and potential gateway to pathological mechanisms of the disease process. *Brain Pathol* 23:165–177
- Martin JB, Gusella JF (1986) Huntington's disease. Pathogenesis and management. *N Engl J Med* 315:1267–1276
- Malagelada C, Lopez-Toledano MA, Willett RT, Jin ZH, Shelanski ML, Greene LA (2011) RTP801/REDD1 regulates the timing of cortical neurogenesis and neuron migration. *J Neurosci* 31:3186–3196
- Greene LA, Tischler AS (1976) Establishment of a noradrenergic clonal line of rat adrenal pheochromocytoma cells which respond to nerve growth factor. *Proc Natl Acad Sci U S A* 73:2424–2428
- Leal-Ortiz S, Waites CL, Terry-Lorenzo R, Zamorano P, Gundelfinger ED, Garner CC (2008) Piccolo modulation of Synapsin1a dynamics regulates synaptic vesicle exocytosis. *J Cell Biol* 181:831–846
- Giralt A, Rodrigo T, Martin ED, Gonzalez JR, Mila M, Cena V, Dierssen M, Canals JM et al (2009) Brain-derived neurotrophic factor modulates the severity of cognitive alterations induced by mutant huntingtin: involvement of phospholipase C γ activity and glutamate receptor expression. *Neuroscience* 158:1234–1250
- Rue L, Alcalá-Vida R, Lopez-Sooop G, Creus-Muncunill J, Alberch J, Perez-Navarro E (2014) Early down-regulation of PKC δ as a pro-survival mechanism in Huntington's disease. *Neuromol Med* 16:25–37
- Wheeler VC, Auerbach W, White JK, Srinidhi J, Auerbach A, Ryan A, Duyao MP, Vrbancac V et al (1999) Length-dependent gametic CAG repeat instability in the Huntington's disease knock-in mouse. *Hum Mol Genet* 8:115–122
- Giralt A, Saavedra A, Carreton O, Xifro X, Alberch J, Perez-Navarro E (2011) Increased PKA signaling disrupts recognition memory and spatial memory: role in Huntington's disease. *Hum Mol Genet* 20:4232–4247
- Saavedra A, Giralt A, Arumi H, Alberch J, Perez-Navarro E (2013) Regulation of hippocampal cGMP levels as a candidate to treat cognitive deficits in Huntington's disease. *PLoS One* 8, e73664
- Saavedra A, Garcia-Martinez JM, Xifro X, Giralt A, Torres-Peraza JF, Canals JM, Diaz-Hernandez M, Lucas JJ et al (2010) PH domain leucine-rich repeat protein phosphatase 1 contributes to maintain the activation of the PI3K/Akt pro-survival pathway in Huntington's disease striatum. *Cell Death Differ* 17:324–335
- Wu XM, Qian ZM, Zhu L, Du F, Yung WH, Gong Q, Ke Y (2011) Neuroprotective effect of ligustilide against ischaemia-reperfusion injury via up-regulation of erythropoietin and down-regulation of RTP801. *Br J Pharmacol* 164:332–343
- Kimball SR, Do AN, Kutzler L, Cavener DR, Jefferson LS (2008) Rapid turnover of the mTOR complex 1 (mTORC1) repressor REDD1 and activation of mTORC1 signaling following inhibition of protein synthesis. *J Biol Chem* 283:3465–3475

34. Malagelada C, Jin ZH, Jackson-Lewis V, Przedborski S, Greene LA (2010) Rapamycin protects against neuron death in vitro and in vivo models of Parkinson's disease. *J Neurosci* 30:1166–1175
35. Jin HO, An S, Lee HC, Woo SH, Seo SK, Choe TB, Yoo DH, Lee SB et al (2007) Hypoxic condition- and high cell density-induced expression of Redd1 is regulated by activation of hypoxia-inducible factor-1 α and Sp1 through the phosphatidylinositol 3-kinase/Akt signaling pathway. *Cell Signal* 19:1393–1403
36. Duennwald ML, Lindquist S (2008) Impaired ERAD and ER stress are early and specific events in polyglutamine toxicity. *Genes Dev* 22:3308–3319
37. Reijonen S, Putkonen N, Norremolle A, Lindholm D, Korhonen L (2008) Inhibition of endoplasmic reticulum stress counteracts neuronal cell death and protein aggregation caused by N-terminal mutant huntingtin proteins. *Exp Cell Res* 314:950–960
38. Trettel F, Rigamonti D, Hilditch-Maguire P, Wheeler VC, Sharp AH, Persichetti F, Cattaneo E, MacDonald ME (2000) Dominant phenotypes produced by the HD mutation in STHdh(Q111) striatal cells. *Hum Mol Genet* 9:2799–2809
39. Qiu Z, Norflus F, Singh B, Swindell MK, Buzescu R, Bejarano M, Chopra R, Zucker B et al (2006) Sp1 is up-regulated in cellular and transgenic models of Huntington disease, and its reduction is neuroprotective. *J Biol Chem* 281:16672–16680
40. Illuzzi J, Yerkes S, Parekh-Olmedo H, Kmiec EB (2009) DNA breakage and induction of DNA damage response proteins precede the appearance of visible mutant huntingtin aggregates. *J Neurosci Res* 87:733–747
41. Chae JI, Kim DW, Lee N, Jeon YJ, Jeon I, Kwon J, Kim J, Soh Y et al (2012) Quantitative proteomic analysis of induced pluripotent stem cells derived from a human Huntington's disease patient. *Biochem J* 446:359–371
42. HD iPSC Consortium. (2012) Induced pluripotent stem cells from patients with Huntington's disease show CAG-repeat-expansion-associated phenotypes. *Cell Stem Cell* 11:264–278
43. Li XJ, Li S (2011) Proteasomal dysfunction in aging and Huntington disease. *Neurobiol Dis* 43:4–8
44. Igarashi S, Morita H, Bennett KM, Tanaka Y, Engelender S, Peters MF, Cooper JK, Wood JD et al (2003) Inducible PC12 cell model of Huntington's disease shows toxicity and decreased histone acetylation. *Neuroreport* 14:565–568
45. Poirier MA, Jiang H, Ross CA (2005) A structure-based analysis of huntingtin mutant polyglutamine aggregation and toxicity: evidence for a compact beta-sheet structure. *Hum Mol Genet* 14:765–774
46. Tagawa K, Marubuchi S, Qi ML, Enokido Y, Tamura T, Inagaki R, Murata M, Kanazawa I et al (2007) The induction levels of heat shock protein 70 differentiate the vulnerabilities to mutant huntingtin among neuronal subtypes. *J Neurosci* 27:868–880
47. Bertoni A, Giuliano P, Galgani M, Rotoli D, Ulianich L, Adornetto A, Santillo MR, Porcellini A et al (2011) Early and late events induced by polyQ-expanded proteins: identification of a common pathogenic property of polyQ-expanded proteins. *J Biol Chem* 286:4727–4741
48. Scotter EL, Goodfellow CE, Graham ES, Draganow M, Glass M (2010) Neuroprotective potential of CB1 receptor agonists in an in vitro model of Huntington's disease. *Br J Pharmacol* 160:747–761
49. Sontag EM, Lotz GP, Agrawal N, Tran A, Aron R, Yang G, Necula M, Lau A et al (2012) Methylene blue modulates huntingtin aggregation intermediates and is protective in Huntington's disease models. *J Neurosci* 32:11109–11119
50. Perez-Navarro E, Canals JM, Gines S, Alberch J (2006) Cellular and molecular mechanisms involved in the selective vulnerability of striatal projection neurons in Huntington's disease. *Histol Histopathol* 21:1217–1232
51. Cisbani G, Cicchetti F (2012) An in vitro perspective on the molecular mechanisms underlying mutant huntingtin protein toxicity. *Cell Death Dis* 3, e382
52. Brafman A, Mett I, Shafir M, Gottlieb H, Damari G, Gozlan-Kelner S, Vishnevskia-Dai V, Skalter R et al (2004) Inhibition of oxygen-induced retinopathy in RTP801-deficient mice. *Invest Ophthalmol Vis Sci* 45:3796–3805
53. del Olmo-Aguado S, Nunez-Alvarez C, Ji D, Manso AG, Osborne NN (2013) RTP801 immunoreactivity in retinal ganglion cells and its down-regulation in cultured cells protect them from light and cobalt chloride. *Brain Res Bull* 98:132–144
54. Rittenhouse KD, Johnson TR, Vicini P, Hirakawa B, Kalabat D, Yang AH, Huang W, Basile AS (2014) RTP801 gene expression is differentially upregulated in retinopathy and is silenced by PF-04523655, a 19-Mer siRNA directed against RTP801. *Invest Ophthalmol Vis Sci* 55:1232–1240
55. Nguyen QD, Schachar RA, Nduaka CI, Sperling M, Basile AS, Klammer KJ, Chi-Burris K, Yan E et al (2012) Dose-ranging evaluation of intravitreal siRNA PF-04523655 for diabetic macular edema (the DEGAS study). *Invest Ophthalmol Vis Sci* 53:7666–7674
56. Nosedà R, Belin S, Piguat F, Vaccari I, Scarlino S, Brambilla P, Martinelli Boneschi F, Feltri ML et al (2013) DDIT4/REDD1/RTP801 is a novel negative regulator of Schwann cell myelination. *J Neurosci* 33:15295–15305
57. Mangiarini L, Sathasivam K, Seller M, Cozens B, Harper A, Hetherington C, Lawton M, Trotter Y et al (1996) Exon 1 of the HD gene with an expanded CAG repeat is sufficient to cause a progressive neurological phenotype in transgenic mice. *Cell* 87:493–506
58. Martin-Aparicio E, Yamamoto A, Hernandez F, Hen R, Avila J, Lucas JJ (2001) Proteasomal-dependent aggregate reversal and absence of cell death in a conditional mouse model of Huntington's disease. *J Neurosci* 21:8772–8781
59. Wheeler VC, Gutekunst CA, Vrbancic V, Lebel LA, Schilling G, Hersch S, Friedlander RM, Gusella JF et al (2002) Early phenotypes that presage late-onset neurodegenerative disease allow testing of modifiers in Hdh CAG knock-in mice. *Hum Mol Genet* 11:633–640
60. Canals JM, Pineda JR, Torres-Peraza JF, Bosch M, Martin-Ibanez R, Munoz MT, Mengod G, Erfors P et al (2004) Brain-derived neurotrophic factor regulates the onset and severity of motor dysfunction associated with enkephalinergic neuronal degeneration in Huntington's disease. *J Neurosci* 24:7727–7739
61. Diaz-Hernandez M, Torres-Peraza J, Salvatori-Abarca A, Moran MA, Gomez-Ramos P, Alberch J, Lucas JJ (2005) Full motor recovery despite striatal neuron loss and formation of irreversible amyloid-like inclusions in a conditional mouse model of Huntington's disease. *J Neurosci* 25:9773–9781
62. Garcia-Martinez JM, Perez-Navarro E, Xifro X, Canals JM, Diaz-Hernandez M, Triouillet Y, Brouillet E, Lucas JJ et al (2007) BH3-only proteins Bid and Bim(EL) are differentially involved in neuronal dysfunction in mouse models of Huntington's disease. *J Neurosci Res* 85:2756–2769
63. Petersen A, Hansson O, Puschban Z, Sapp E, Romero N, Castilho RF, Sulzer D, Rice M et al (2001) Mice transgenic for exon 1 of the Huntington's disease gene display reduced striatal sensitivity to neurotoxicity induced by dopamine and 6-hydroxydopamine. *Eur J Neurosci* 14:1425–1435
64. Kuhn A, Goldstein DR, Hodges A, Strand AD, Sengstag T, Kooperberg C, Becanovic K, Pouladi MA et al (2007) Mutant huntingtin's effects on striatal gene expression in mice recapitulate changes observed in human Huntington's disease brain and do not differ with mutant huntingtin length or wild-type huntingtin dosage. *Hum Mol Genet* 16:1845–1861



MTOR Pathway-Based Discovery of Genetic Susceptibility to L-DOPA-Induced Dyskinesia in Parkinson's Disease Patients

Núria Martín-Flores^{1,2} · Rubén Fernández-Santiago^{3,4,5} · Francesa Antonelli⁴ · Catalina Cerquera^{4,6} · Verónica Moreno⁴ · Maria Josep Martí^{3,4,5} · Mario Ezquerro^{3,4,5} · Cristina Malagelada^{1,2} 

Received: 23 February 2018 / Accepted: 29 June 2018
© Springer Science+Business Media, LLC, part of Springer Nature 2018

Abstract

Dyskinesia induced by L-DOPA administration (LID) is one of the most invalidating adverse effects of the gold standard treatment restoring dopamine transmission in Parkinson's disease (PD). However, LID manifestation in parkinsonian patients is variable and heterogeneous. Here, we performed a candidate genetic pathway analysis of the mTOR signaling cascade to elucidate a potential genetic contribution to LID susceptibility, since mTOR inhibition ameliorates LID in PD animal models. We screened 64 single nucleotide polymorphisms (SNPs) mapping to 57 genes of the mTOR pathway in a retrospective cohort of 401 PD cases treated with L-DOPA (70 PD with moderate/severe LID and 331 with no/mild LID). We performed classic allelic, genotypic, and epistatic analyses to evaluate the association of individual or combinations of SNPs with LID onset and with LID severity after initiation of L-DOPA treatment. As for the time to LID onset, we found significant associations with SNP rs1043098 in the *EIF4EBP2* gene and also with an epistatic interaction involving *EIF4EBP2* rs1043098, *RICTOR* rs2043112, and *PRKCA* rs4790904. For LID severity, we found significant association with *HRAS* rs12628 and *PRKN* rs1801582 and also with a four-loci epistatic combination involving *RPS6KB1* rs1292034, *HRAS* rs12628, *RPS6KA2* rs6456121, and *FCHSD1* rs456998. These findings indicate that the mTOR pathway contributes genetically to LID susceptibility. Our study could help to identify the most susceptible PD patients to L-DOPA in order to prevent the appearance of early and/or severe LID in a future. This information could also be used to stratify PD patients in clinical trials in a more accurate way.

Keywords mTOR · L-DOPA · Dyskinesia · Single nucleotide polymorphism · Parkinson's disease · Epistasia

Abbreviations

6-OHDA 6-Hydroxydopamine
DA Dopamine

LID L-DOPA-induced dyskinesia
mAF Minor allele frequency
MDR Multifactorial dimensionality reduction

N.M-F & R.F-S. contributed equally to this work.

M.J.M., M.E. & C.M are joint senior authors.

Electronic supplementary material The online version of this article (<https://doi.org/10.1007/s12035-018-1219-1>) contains supplementary material, which is available to authorized users.

✉ Cristina Malagelada
cristina.malagelada@ub.edu

⁴ Neurology Service, Hospital Clínic de Barcelona, Barcelona, Catalonia, Spain

¹ Department of Biomedicine, Unit of Biochemistry, Faculty of Medicine, Universitat de Barcelona, 08036 Barcelona, Catalonia, Spain

⁵ Centro de Investigación Biomédica en Red sobre Enfermedades Neurodegenerativas (CIBERNED), Madrid, Spain

² Institut de Neurociències, Universitat de Barcelona, 08036 Barcelona, Catalonia, Spain

⁶ Present address: Neurology Unit, Medical School, Hospital Universitario San Ignacio, Pontificia Universidad Javeriana, Bogotá, Colombia

³ IDIBAPS-Institut d'Investigacions Biomèdiques August Pi i Sunyer, 08036 Barcelona, Catalonia, Spain

Published online: 10 July 2018



mTORC	Mechanistic target of rapamycin complex
PD	Parkinson's disease
SNPs	Single nucleotide polymorphisms
TTD	Time to dyskinesia
TTL	Time to L-DOPA
TLP	Time to LID Peak
LED	L-DOPA equivalent dose

Introduction

Parkinson's disease (PD) is characterized by the degeneration of midbrain dopaminergic neurons located in the substantia nigra pars compacta (SNpc) leading to a deficit of dopamine (DA) release in the striatum and impaired DA synaptic transmission. Progressively to this neural loss, the classical motor symptoms including tremor, rigidity, and bradykinesia, become evident [1, 2].

DA replacement therapy by oral administration of L-DOPA (or levodopa) is still the gold standard treatment used to counteract and improve the motor symptoms of PD [3]. L-DOPA is the immediate precursor of DA and its administration enhances striatal DA production, restoring the balance between the direct and the indirect basal ganglia pathways. However, chronic treatment with L-DOPA often triggers motor complications such as L-DOPA-induced dyskinesia (LID) which can be as much disabling for the patient as the initial motor symptoms themselves. It is estimated that about 80% of L-DOPA-treated PD patients develop LID within 5–10 years after initiation of the DA replacement therapy (reviewed in [4]). Imbalances in L-DOPA metabolism induce LID in a dose-dependent manner [5]. Thus, known risk factors for LID appearance include early PD onset, severe nigrostriatal denervation due to DA neural loss, prolonged L-DOPA treatment, or excessive L-DOPA doses [6]. Still, there is a largely unexplained clinical heterogeneity regarding LID onset and LID severity that suggest the existence of additional factors modulating LID susceptibility [7]. Recent studies using single-gene candidate approaches have reported association of specific single nucleotide polymorphisms (SNPs) with LID susceptibility (reviewed in [4]). These studies suggest that common genetic variability could play a role in the development of LID in L-DOPA-treated PD patients.

In this scenario here, we have performed a candidate genetic pathway analysis by screening 64 SNPs located at genes from the mTOR pathway in a retrospective cohort of 401 PD patients treated with L-DOPA. The mTOR pathway has been consistently related to the pathogenesis of PD [8–10]. mTOR is a serine/threonine kinase that is the central component of mTORC1 and mTORC2 multiprotein complexes. When the complex contains mTOR and Raptor, among others, is called mTORC1 and controls protein translation and autophagy [11]. Alternatively, when the mTOR complex binds to Rictor is

called mTORC2 and regulates actin polymerization and survival via Akt signaling [12]. In the brain, mTOR plays a key role in development, neuron survival, synaptic plasticity, and memory formation (reviewed in [13, 14]). Furthermore, deregulation of mTOR signaling appears to be a common hallmark of human neurological disorders including PD [15]. More specifically, the inhibition of mTOR with rapamycin or analog molecules called rapalogs has been shown to prevent both DA neuron cell death [10, 16] and also LID in PD animal models [17, 18]. However, the exact mechanism by which mTOR mediates LID is not yet understood.

Little is known whether genetic variations in the mTOR pathway could be related to the differential sensitivity to L-DOPA in PD patients. For this reason, here we have explored potential associations of SNPs in the mTOR pathway, or high order epistatic interactions involving SNPs of this pathway, with the susceptibility to LID in L-DOPA-treated PD patients. More specifically, we have assessed the potential modulatory effect of SNPs from the mTOR candidate pathway on LID onset and LID severity. To this end, we have performed classic allelic and genotypic association analyses of individual markers with these clinical parameters. In addition, we have also carried out a multifactor dimensionality reduction (MDR) analysis as to identify unnoticed epistatic effects of SNPs at the mTOR pathway. These high order SNP interactions are commonly ignored in classic association studies but have yet been suggested to contribute to the missing heritability in complex disorders such as PD. Our study identifies genetic variants from the mTOR candidate pathway related with a differential susceptibility to develop LID after initiation of L-DOPA treatment.

Materials and Methods

Cohort of Study and Data Collection

Our cohort consisted mostly in individuals diagnosed with PD from European origin from the northeastern region of Iberian Peninsula. Patients had a clinical diagnosis of definite PD according to UKPDS criteria [19] except that family history was not used as exclusion criterion, or a neuropathological diagnosis of definitive PD according to proposed criteria [20]. A total of 401 PD cases had complete recorded data of L-DOPA treatment and LID in their clinical histories. Of these, 70 PD cases had moderate/severe LID whereas 331 had no or mild LID. All subjects were recruited at the Movement Disorders Unit from the Hospital Clínic Provincial de Barcelona. Written informed consent and whole blood samples were obtained from each subject. The clinical histories were mostly available in paper format from the hospital archives and reviewed by expert neurologists. The study was approved by the Ethics Committee of the Hospital Clínic de Barcelona.

The total PD population was divided in groups depending on the appearance of LID and degrees of severity. In our cohort and for the analysis, LID onset after starting the DA replacement treatment was considered as a continuous variable with an average of 7.6 years ($n = 218$).

We also compared the population based on LID severity, which was graded following the unified Parkinson's disease rating scale section IV (UPDRS-IV) that assesses disability due to LID [21]. Accordingly, LID severity was categorized as "0" (no LID), "1" (very mild LID), "2" (mild LID), "3" (moderate LID), and "4" (severe LID) and samples were stratified to compare two groups: no / very mild / mild LID (0–2) ($n = 331$) vs. moderate / severe LID (3–4) ($n = 70$).

Selection Criteria of SNPs

We selected 64 SNPs from 57 genes in the mTOR pathway and also from genes involved in PD (*SNCA*, *MAPT*, *LRRK2*, or *PRKN*). We selected the SNPs based on the following criteria: (i) a minor allele frequency (MAF) > 0.1 according to data from the HapMap project and (ii) an already published (Pubmed) association of the SNP with a neurological disorder, a psychiatric disorder, or other diseases (Online Resource Table 1 and Online Resource Fig. 1).

Genotyping

Genomic DNA was isolated from peripheral blood lymphocytes as previously described [22] and stored at -80°C until use. All the samples were genotyped in the Genomics Core facility (Universitat Pompeu Fabra, Parc de Recerca Biomèdica de Barcelona, Barcelona, Catalonia, Spain) using TaqMan® OpenArray® Genotyping Plates, Custom Format 64 QuantStudio TM 12 K Flex. We genotyped all 64 SNPs in our entire sample of $n = 401$ subjects and filtered out SNPs

which did not surpass our stringent genotyping quality threshold of unambiguous genotypes in above 90% of all studied samples. This quality control reduced the list to 54 SNPs which were further included in the association analyses of single SNPs or their combination.

Statistical Analyses

In the different analyses of independent markers, we computed allelic associations using the UNPHASED 3.0.6 software. Allelic associations of the 54 SNPs were performed using the quantitative trait model considering as main variables the time-to-dyskinesia (TTD)—defined as the time period in years from initiation of L-DOPA treatment until the appearance of LID—and the time-to-LID-peak (TLP)—defined as the time period in years from initiation of L-DOPA treatment until the appearance of the peak of most severe LID symptoms. We adjusted the analyses by potential covariates including sex, age, time-to-L-DOPA (TTL)—defined as the time period in years from PD diagnosis until time to initiation of L-DOPA treatment, and L-DOPA equivalent dosage (LED). We also adjusted all P values by false discovery rate (FDR) multiple testing correction ($n = 54$ tests). Statistically significant SNPs detected in the allelic analysis were further analyzed at the genotypic level using the SNPStats software, and also considering the covariates mentioned above (<http://bioinfo.iconcologia.net/SNPstats>) [23].

In the epistatic analysis, we evaluated high-order SNP interactions using the multifactor dimensionality reduction (MDR) software (<http://www.multifactor dimensionality reduction.org>) [24]. The MDR software provides a data mining strategy for detecting and characterizing nonlinear interactions among discrete attributes such as SNPs, or their multiple combinations, that are predictive of a discrete outcome such

Table 1 Allelic association of SNPs with LID peak (TLP) and with LID onset (TTD)

LID peak					LID onset				
Gene	SNP	<i>P</i> value	FDR <i>P</i> value	Addval	Gene	SNP	<i>P</i> value	FDR <i>P</i> value	Addval
<i>EIF4EBP2</i>	rs1043098	<i>0.0003</i>	<i>0.0179</i>	0.2204	<i>EIF4EBP2</i>	rs1043098	<i>0.0152</i>	0.5481	0.1572
<i>CDK5</i>	rs2069442	<i>0.0043</i>	0.3520	0.2167	<i>PIK3CB</i>	rs361072	<i>0.0238</i>	0.5481	0.1407
<i>RPS6KB1</i>	rs1292034	<i>0.0236</i>	0.3520	0.1347	<i>HRAS</i>	rs12628	<i>0.0486</i>	0.5481	0.1207
<i>SIRT2</i>	rs10410544	<i>0.0367</i>	0.3520	0.1239					
<i>TBC1D7</i>	rs2496143	<i>0.0380</i>	0.3870	0.1412					
<i>NEDD4L2</i>	rs4149601	<i>0.0391</i>	0.1150	0.1417					

Allelic test calculated in Unphased 6.0 software using the quantitative trait model. Sex was used as a cofounder and L-DOPA dosage and time from PD onset to L-DOPA onset as modifiers. P values were adjusted for 54 multiple testing by using FDR correction. Addval: for quantitative traits. Unphased shows the estimated additive genetic value between different alleles. ($N = 216$ for LID Peak and $N = 230$ for LID Onset). Statistically significant P values are highlighted in italics

as case-control status [24]. MDR reduces multidimensional data into only one dimension and therefore it improves the ability to detect combined epistatic effects of specific allelic combinations from different SNPs associated with disease risk. The MDR software combines attribute selection, attribute construction, and classification with cross-validation providing a powerful approach to model interactions. MDR analyses were performed using tenfold cross-validation; therefore, the training set comprises 90% of the data, whereas the testing set comprises the remaining 10% to test the predictive power of the interaction. The cross-validation consistency is the measure of the number of times a particular SNP interaction is identified in each possible 90% of the subjects [25]. *P* values were obtained by permutation analysis; *P* values of explicit test of interaction were obtained by permutation test for just the interaction component. All the analyses and permutations were performed using the MDR v.3.0.4. All *P* values were two-sided and considered statistically significant with less than 0.05.

Results

Association of SNPs with LID Onset and LID Peak

We first performed the allelic association analysis of individual SNPs with TTD, i.e., the time period from initiation of L-DOPA treatment to development of LID, and with TLP, i.e., the corresponding time to highest LID, or LID peak. We found a statistically significant allelic association of the SNP rs1043098 in *EIF4EBP2* with TLP (FDR-adjusted *P* value = 0.0179). In addition, we found a trend of association of this SNP with TTD (*P* value = 0.015) which did not reach statistical significance after multiple testing correction (Table 1). However, both associations were statistically significant at the genotypic level (Table 2). More specifically, CC homozygous for *EIF4EBP2* had 2.84 years delay of LID onset and 3.84 years of delay in the appearance of LID peak than TT carriers (*P* value = 0.0004 for LID onset and *P* value < 0.001 for peak LID). Both *P* values passed the Bonferroni correction. A level of significance of 0.0009 is equivalent to the significance level of 0.05 when a Bonferroni correction is used to adjust for comparisons at the 54 SNPs.

Association of Epistatic Combinations of SNPs with LID Onset and LID Peak To investigate whether combinations of SNPs could be associated with TTD, we performed an epistatic association analysis using the data mining MDR software assuming TTD trait as a quantitative and continuous variable. We found a borderline association of SNPs *EIF4EBP2* rs1043098 and *RICTOR* rs2043112 (*P* value = 0.05) with LID onset (TTD), which was confirmed using the classical interaction analysis of SNPstats (*P* value = 0.014). Importantly, the combined association of these two loci with LID onset was statistically significant in combination with a third SNP rs4790904 located in the *PRKCA* gene, which yielded the maximum cross-validation consistency score of 10/10 (*P* value < 0.001) (Table 3 and Online Resource Fig. 2). Among all distributions, highlighted two protective combinations of *EIF4EBP2* rs1043098/*RICTOR* rs2043112/*PRKCA* rs4790904 with high frequency and high impact on the LID onset. The combination CC/AG/TT with a frequency of 11.01% in the total PD population that delayed the appearance of LID in 5.25 years, and the combination CT/AA/TT with a frequency of 5.50% that delayed the appearance of LID in 3.878 years (Online Resource Fig. 3 and Online Resource Table 2). Collectively, these results indicate that the SNP rs1043098 in *EIF4EBP2* alone or in combination with other SNPs from the mTOR pathway is associated with the time to develop LID after initiation of L-DOPA treatment in PD patients.

Association of SNPs with LID Severity We next studied whether SNPs in the mTOR pathway were associated with LID severity. We stratified the samples in two groups including no/mild LID vs. moderate/severe LID. We first performed a crude association analysis of mTOR SNPs with LID severity adjusting by gender, age, LED, and TTD. We found that the SNPs rs12628 in *HRAS* and rs1801582 in *PRKN* were individually associated with LID severity (FDR-adjusted *P* values = 0.0108, respectively) (Table 4).

Association of Epistatic Combinations of SNPs with LID Severity

We next performed the epistatic association analysis of SNPs with LID severity using the MDR software. One of the main premises of MDR software is that the subjects in the groups to

Table 2 Association of rs1043098 genotypes in *EIF4EBP2* gene with LID Peak (TLP) and LID Onset (TTD)

LID peak				LID onset					
	<i>n</i>	Years (mean ± SE)	Difference (95% CI)	<i>P</i> value		<i>n</i>	Years (mean ± SE)	Difference (95% CI)	<i>P</i> value
CC	61	10.52 ± 0.65	0	< 0.0001	CC	61	8.34 ± 0.62	0	0.0004
CT	68	9.28 ± 0.54	- 1.54 (- 3.06 -- -0.01)		CT	74	7.89 ± 0.49	- 0.96 (- 2.26 -- -0.35)	
TT	41	7.2 ± 0.67	- 3.89 (- 5.63 -- -2.15)		TT	42	6.05 ± 0.56	- 2.84 (- 4.35 -- -1.33)	

P value under the Log additive model are calculated by SNPstat software, and adjusted for gender, L-DOPA dosage and time from PD onset to L-DOPA treatment as implemented in SNPstat software

Table 3 MDR analysis of SNP-SNP interaction with LID onset

Gene	SNP	T-statistic CV Training	T-statistic CV Testing	CVC	Odds-ratio (95% CI)	<i>P</i> value *	<i>P</i> value [#]
<i>PRKCA</i>	rs4790904	2.7069	-9.1020	4/10	1.98 (1.11–3.50)	0.934–0.935	0.973–0.974
<i>EIF4EBP2</i>	rs1043098	3.9678	2.9091	7/10	2.48 (1.42–4.31)	<i>0.049–0.05</i>	0.091–0.092
<i>RICTOR</i>	rs2043112						
<i>EIF4EBP2</i>	rs1043098	6.1882	4.7244	10/10	6.85 (3.57–13.16)	<i>< 0.001</i>	<i>< 0.001</i>
<i>RICTOR</i>	rs2043112						
<i>PRKCA</i>	rs4790904						

Interaction of SNPs with time to L-DOPA initiation to LID onset. *N* = 218; Random seed = 10; CVC = cross-validation count = 10; *Normal *P* value and #*P* value of Explicit test of interaction obtained with 1000 permutations. Statistically significant *P* values are highlighted in italics. Odds-ratio was obtained generating a dichotomous dataset comparing early LID population (before 7 years) and late LID population (after 8 years) based on the average LID onset found with the MDR (7.64 years)

compare must be balanced in number. To balance the no/mild LID group (*n* = 331) with the moderate/ severe LID group (*n* = 70), different datasets were created randomly to under-sample the no/ mild severity group or, on the other way around, to over-sample the mild/ moderate severity group, as specified by the MDR developers. Each data set from one group was compared to the others independently. Using this dual approach, we detected a significant interaction of four-loci including rs1292034 *RPS6KB1*, rs12628 *HRAS*, rs6456121 *RPS6KA2*, and rs456998 *FCHSD1* which was associated with LID severity (10/10 of cross-validation score. *P* value < 0.001) (Table 5 and Online Resource Fig. 4). Importantly, we confirmed this 4-loci interaction by comparing only the no LID group versus the moderate/severe LID group (Online Resource Table 3). Online Resource Fig. 5 and Online Resource Table 4 summarize the distribution of high-risk (develop moderate/severe LID) and low-risk (develop no/mild LID) genotypes for this interaction. From this analysis raised many different genotype combinations to predict the status of LID severity with similar frequencies in the PD population (Online Resource Table 4). As an illustrative example for *RPS6KB1* rs1292034, *HRAS* rs12628, *RPS6KA2* rs6456121, and *FCHSD1* rs456998 interaction, we found that the combination AG/AG/CT/GT was present in a frequency of 5.56% of the total population in the group of moderate/severe LID and 1.59% in the control group of no/mild LID. The

resultant ratio (3.5) indicated that this specific genotype combinations would predict moderate/severe LID. All ratios above 1 were considered as risk combinations to develop moderate/ severe LID status. The four-loci interaction was confirmed in silico using the forced analysis MDR option, which allows to evaluate only this particular combination for all generated datasets (Online Resource Table 5). Importantly, the average of the sensitivity and the precision of the method, as measures to correctly predict and discriminate LID severity was 83 and 86% respectively (Online Resource Table 5).

In summary, we found associations of individual SNPs or also combinations of SNPs in the mTOR pathway associated with both LID onset and LID severity, suggesting a role of this genetic pathway in the development of LID.

Discussion

Using a candidate pathway genetic association approach our study explores for the first time the influence of individual SNPs or epistatic combinations of SNPs in genes from the mTOR pathway on the susceptibility to LID in L-DOPA treated PD patients. Regarding LID development, we found a significant association of SNP rs1043098 in the *EIF4EBP2* gene with the time from the initiation of L-DOPA treatment until the

Table 4 Association of SNPs in *HRAS* and *PRKN* with LID severity, adjusted by LED, TTD, gender, age, and multiple testing

Gene	SNP	Alleles (M/m)	mAF LID severity 3–4	mAF LID severity 0–2	<i>P</i> value	FDR <i>P</i> value
<i>HRAS</i>	rs12628	A/G	0.49	0.33	<i>0.0006</i>	<i>0.0180</i>
<i>PRKN</i>	rs1801582	C/G	0.1	0.21	<i>0.0007</i>	<i>0.0180</i>
<i>RPTOR2</i>	rs7211818	A/G	0.16	0.24	<i>0.0007</i>	0.0590
<i>RPS6KB1</i>	rs1292034	G/A	0.51	0.4	<i>0.0293</i>	0.3961
<i>RPTOR</i>	rs11868112	C/T	0.54	0.41	<i>0.0452</i>	0.4087
<i>STK11</i>	rs8111699	C/G	0.59	0.48	<i>0.0454</i>	0.4087

Allelic test calculated in Unphased 6.0 software using the dichotomous analysis. Age, sex, LED, and TTD were used as cofounders. *P* values were adjusted for 54 multiple testing by using FDR correction. *N* = 401 PD cases; 70 severe LID, 331 with no/mild LID. M = major allele; m = minor allele; mAF = minor allele frequency. Statistically significant *P* values are highlighted in italics

Table 5 MDR analysis of SNP-SNP interaction with LID severity

Gene	SNP	Bal. Acc. CV training	Bal. Acc. CV testing	CVC	Odds-ratio (95% CI)	<i>P</i> value *	<i>P</i> value [#]
<i>HRAS</i>	rs12628	0.6082	0.5924	9/10	2.56 (1.65–3.33)	0.0310–0.0300	> 0.5
<i>HRAS</i>	rs12628	0.6603	0.6382	9/10	3.79 (2.66–5.35)	0.0020–0.0030	> 0.5
<i>RPTOR</i>	rs7211818						
<i>ULK1</i>	rs12303764	0.7226	0.6206	4/10	7.01 (4.37–9.09)	0.0050–0.0060	> 0.5
<i>PPARG</i>	rs2959272						
<i>EIF4EBP2</i>	rs1043098						
<i>RPS6KB1</i>	rs1292034	0.8297	0.8173	10/10	31.56 (19.57–50.91)	< 0.001	< 0.001
<i>HRAS</i>	rs12628						
<i>RPS6KA2</i>	rs6456121						
<i>FCHSD1</i>	rs456998						

Interaction of SNPs with LID severity. $N = 328$ with no to mild LID (1–2 in LID severity scale); $N = 301$ with moderate to severe LID (3–4 in LID severity scale) in an oversampling dataset. Random seed = 10; CVC = cross-validation count = 10; *Normal *P* value and #*P* value of Explicit test of interaction obtained with 1000 permutations. Statistically significant *P* values are highlighted in italics

highest peak of LID. At the multi-locus level, we also identified that *EIF4EBP2* rs1043098 was part of a high order epistatic combination also involving the SNPs *RICTOR* rs2043112 and *PRKCA* rs4790904. We also found independent significant association of the polymorphisms rs12628 in the *HRAS* gene and rs1801582 in the *PRKN* gene, with the severity of LID. At the multi-locus level, we identified a high order epistatic interaction of *HRAS* rs12628 in combination with rs5456121 in *RPS6KA2*, rs1292034 in *RPS6KB1* and rs456998 in *FCHSD1* which was associated with LID severity. Collectively, these results indicate that common genetic variability in the mTOR pathway is associated with differential time to develop LID after initiation of L-DOPA treatment and differential severity of LID in PD patients treated with L-DOPA.

Classic genetic association studies for disease risk, in complex disorders, have contributed to explain what has been called the missing heritability of these diseases, yet explaining only a limited portion of the population attributable risk. Only recently, other studies have started deciphering the complex effects of high order genetic interactions among several SNPs on disease risk [26]. This approach has already contributed to the identification of several gene-gene interactions associated with higher risk of different neurological disorders [27] including PD [28] but also with differential response of patients to neurological treatments [29]. More specifically, the majority of studies investigating genetic susceptibility to LID in L-DOPA treated PD patients have focused in genes coding for DA receptors or transporters [30, 31], genes involved in synthesis and metabolism of DA [32–34], or neurotrophin genes such as BDNF [32]. Let alone that reproducibility of some studies has been limited, epistatic effects of risk SNPs in these studies have been largely not previously explored.

Biochemically, the mTOR pathway controls processes such as cell survival, proliferation, growth and differentiation [15] and in neurons is crucial for survival and neural plasticity [35]. Related to PD, the degeneration of DA neurons and the

consequent nigrostriatal denervation leading to plasticity impairment have been linked to LID phenotypes [4, 36]. More importantly, the pharmacological inactivation of mTOR with rapamycin or rapalogs abrogate both DArgic neuron cell death [10, 16] and LID [17, 18] in animal models of PD suggesting a role of the mTOR pathway in the modulation of LID which we further underpinned in the present study. Our findings regarding SNPs' association support the idea that, apart from dopamine receptors and metabolism genes, indeed variations in the mTOR pathway condition the response to L-DOPA and could be concomitant to the pathogenesis.

At the single locus level, we found that the *EIF4EBP2* rs1043098 variant, more specifically the TT risk genotype, was significantly associated with nearly 4 years earlier time to dyskinesia and also with nearly 3 years earlier peak LID. In addition, the risk genotype was relatively common in our sample with a population frequency of 24% (44% for the risk T allele). Interestingly, *EIF4EBP2* has been previously associated with PD risk [37] but not to LID until the present study. As a protein, EIF4EBP2 is a translational repressor involved in synaptic plasticity [38] which shows an aberrant expression in the corticostriatal pathway after L-DOPA treatment prior to the appearance of LID [39]. In addition, gene expression levels of *EIF4EBP2* are upregulated in PD post-mortem brain [37] and peripheral blood [40] and diminished at the striatum of 6-OHDA-lesioned mice after acute administration of L-DOPA [41]. Altogether, these evidences suggest that genetic variations in the *EIF4EBP2* gene could influence differential susceptibility to L-DOPA and LID development, potentially by impairing protein synthesis and therefore affecting synaptic plasticity.

At the multi-locus level, we found an epistatic interaction involving *EIF4EBP2* rs1043098 together with *RICTOR* rs2043112 and *PRKCA* rs4790904 which was associated with differential time to LID onset in L-DOPA-treated PD patients. Among others, we identified a protective genotypic combination of these SNPs, more specifically CC/AG/TT, which was

associated with 5 years later time of LID development after first administration of L-DOPA. This finding may have clinical interest since 80% of L-DOPA-treated PD patients develop LID within 5–10 years after initiation of the DA replacement therapy [4]. In addition, the epistatic combination mentioned above was relatively common in our sample affecting to 11% of the patients. Both *RICTOR* and *PRKCA* genes encode for proteins, Rictor and PKC α , respectively, controlling survival and actin polymerization [42–44]. Interestingly, actin polymerization is an essential process for synaptic plasticity in neurons and is mostly regulated by PKC α [42–44]. Therefore, this multiple association could suggest that a deregulation in mTORC2 activities could be related to the timing of LID onset. Hence, these findings again suggest that epistatic interactions in the mTOR pathway may influence differential susceptibility to LID in L-DOPA-treated patients potentially by impacting synaptic plasticity.

Regarding LID severity, we found that the SNPs rs12628 in *HRAS* and rs1801582 in *PRKN* were independently associated with LID severity. Thus, we found that the G risk allele *HRAS* rs12628 was associated with a more severe LID manifestation. This allele was present in 49% in L-DOPA treated patients with more severe LID vs. 33% in those with no or mild LID. *HRAS* is a GTPase protein, which activates PI3K and results in the activation of Akt and mTOR pathway [45, 46]. Accordingly, deregulation in this gene could lead to Akt and mTOR signaling impairment.

We also found the protective G allele in *PRKN* rs1801582 was associated with no/mild LID. We observed that the frequency of this allele was double in patients with no/mild LID (21%) vs. those with severe LID (10%). *PRKN* encodes for parkin protein, an E3 ubiquitin ligase that when mutated cause autosomal recessive juvenile PD [47]. In physiological conditions parkin targets specific substrates to proteasomal degradation [48], is involved in neuroplasticity by controlling neurotransmitter trafficking at the presynaptic terminal [49] and is neuroprotective in front of alpha-synuclein toxicity [48]. Therefore, *PRKN* expression and/or activity levels may influence the severity of LID presentation in L-DOPA-treated patients.

At the multi-locus level, we found that rs12628 SNP in *HRAS* along with rs5456121 in *RPS6KA2*, rs1292034 in *RPS6KB1* and rs456998 in *FCHSD1* were associated with LID severity. Among other multiple combinations, the risk AG/AG/CT/GT epistatic combination was associated with more severe LID. This risk combination was present in 6% patients with more severe LID vs. 2% in those with no/mild LID. In all the datasets assessed by multifactor dimensionality reduction analysis, the precision and the sensitivity to correctly predict and discriminate LID severity was above 80%. The proteins encoded by these four genes are related with processes which are impaired in PD such as survival and neural plasticity. For instance, *HRAS* modulates Akt

and mTOR whereas *RPS6KA2* and *RPS6KB1* are downstream effectors of ERK and mTORC1 respectively [50, 51]. Such pathways modulate a crucial process in plasticity including protein synthesis initiation via the phosphorylation of the eukaryotic translation initiation factor B (eIF4B) [52]. In addition, the striatal expression of *FCHSD1* is sensitive to L-DOPA administration in 6-OHDA-lesioned mice [41]. *FCHSD1* encodes for a protein that regulates actin polymerization in hair stereocilia and cuticular plate in vitro [53] and its orthologue in *Drosophila* controls F-actin assembly and regulates synaptic growth [54]. Under a cisplatin treatment, rs456998 in the *FCHSD1* gene is significantly associated with the expression of *DDIT4*, which encodes for a protein called RTP801 [55], that negatively regulates mTOR and Akt. Moreover, RTP801 is up regulated in PD models and in PD human brain [8]. These data suggest the interaction between the genetic variability of the *FCHSD1* gene and the regulation of the mTOR pathway.

Altogether, our study identifies previously unnoticed high-order epistatic interactions in the mTOR pathway which may influence the severity of LID in L-DOPA-treated patients.

Our study has several limitations. First, the sample size of our PD cohort although relatively large ($N=401$) might still be limited to detect subtle associations incurring in type II error or false negative. Second, although we performed adjustment of P values for multiple testing to prevent type I errors of false positive, further validation of findings in another independent cohorts are needed. Third, LID clinical data was collected in a retrospective manner but in light of our findings, future prospective studies are warranted. Finally, we screened a limited number of common SNPs ($N=64$) from the mTOR pathway-based functional significance of the selected variants according to the literature but given the large number of SNPs in this pathway other functional variants not studied here could also be analyzed.

In conclusion, taking into account that about 80% of the L-DOPA-treated PD patients develop LID within 5–10 years after initiation of the DA replacement therapy, our findings may have relevant implications for the clinical practice in PD. They may help to identify subjects who are more susceptible to develop earlier LID, with up to 5 years differences, and those who are more susceptible to develop severe LID, with the ultimate goal to redesign the therapeutic approach, accordingly. These findings may also help to stratify PD patients in clinical trials for disease-modifying drugs or possible anti-dyskinetics, when available.

Acknowledgements We thank Dr. Jason H. Moore and Dr. Peter Andrews for their kind assessment with the MDR software use and helpful discussion. We also thank Dr. Roger Anglada from the Genomics Core Facility from the Universitat Pompeu Fabra (Barcelona) for his work and helpful assessment with sample analysis. We acknowledge the CERCA Program from the Generalitat de Catalunya and the FEDER Program from the European Union to IDIBAPS.

Compliance of Ethical Standards

All subjects were recruited at the Movement Disorders Unit from the Hospital Clínic Provincial de Barcelona. Written informed consent and whole blood samples were obtained from each subject. The study was approved by the Ethics Committee of the Hospital Clínic de Barcelona.

Conflict of Interest This work has been granted by the Michael J. Fox Foundation, Dyskinesia Challenge 2014. The technology derived from this work has been filed for a European patent application (File number: EP17382248), to develop a diagnostics method of personalized medicine for PD patients.

References

- Fahn S (1998) Medical treatment of Parkinson's disease. *J Neuro* 245:P15–P24
- Fahn S (2008) Clinical aspects of Parkinson disease. In: *Parkinson's disease*, 1st edn. Academic Press, New York, p 1–8
- Cotzias GC, Papavasiliou PS, Gellene R (1969) Modification of parkinsonism—chronic treatment with L-Dopa. *N Engl J Med* 280:337–345. <https://doi.org/10.1056/NEJM196902132800701>
- Bastide MF, Meissner WG, Picconi B, Fasano S, Fernagut PO, Feyder M, Francardo V, Alcaccer C et al (2015) Pathophysiology of L-dopa-induced motor and non-motor complications in Parkinson's disease. *Prog Neurobiol* 132:96–168
- Chondrogiorgi M, Tatsioni A, Reichmann H, Konitsiotis S (2014) Dopamine agonist monotherapy in Parkinson's disease and potential risk factors for dyskinesia: a meta-analysis of levodopa-controlled trials. *Eur J Neuro* 21:433–440. <https://doi.org/10.1111/ene.12318>
- Jankovic J (2005) Motor fluctuations and dyskinesias in Parkinson's disease: clinical manifestations. *Mov Disord* 20:S11–S16. <https://doi.org/10.1002/mds.20458>
- Nadjar A, Gerfen CR, Bezdar E (2009) Priming for l-dopa-induced dyskinesia in Parkinson's disease: a feature inherent to the treatment or the disease? *Prog Neurobiol* 87:1–9. <https://doi.org/10.1016/j.pneurobio.2008.09.013>
- Malagelada C, Ryu EJ, Biswas SC, Jackson-Lewis V, Greene LA (2006) RTP801 is elevated in Parkinson brain substantia nigral neurons and mediates death in cellular models of Parkinson's disease by a mechanism involving mammalian target of rapamycin inactivation. *J Neurosci* 26:9996–10005. <https://doi.org/10.1523/JNEUROSCI.3292-06.2006>
- Sarkar S, Ravikumar B, Floto RA, Rubinsztein DC (2009) Rapamycin and mTOR-independent autophagy inducers ameliorate toxicity of polyglutamine-expanded huntingtin and related proteinopathies. *Cell Death Differ* 16:46–56. <https://doi.org/10.1038/cdd.2008.110>
- Tain LS, Mortiboys H, Tao RN et al (2009) Rapamycin activation of 4E-BP prevents parkinsonian dopaminergic neuron loss. *Nat Neurosci* 12:1129–1135. <https://doi.org/10.1038/nn.2372>
- Kim DH, Sarbassov DD, Ali SM, King JE, Latek RR, Erdjument-Bromage H, Tempst P, Sabatini DM (2002) mTOR interacts with raptor to form a nutrient-sensitive complex that signals to the cell growth machinery. *Cell* 110:163–175
- Sarbassov DD, Guertin DA, Ali SM, Sabatini DM (2005) Phosphorylation and regulation of Akt/PKB by the rictor-mTOR complex. *Science* (80-) 307:1098–1101. <https://doi.org/10.1126/Science1106148>
- Calabresi P, Galletti F, Saggese E, Ghiglieri V, Picconi B (2007) Neuronal networks and synaptic plasticity in Parkinson's disease: beyond motor deficits. *Parkinsonism Relat Disord* 13(Suppl 3): S259–S262. [https://doi.org/10.1016/S1353-8020\(08\)70013-0](https://doi.org/10.1016/S1353-8020(08)70013-0)
- Bockaert J, Marin P (2015) mTOR in brain physiology and pathologies. *Physiol Rev* 95:1157–1187
- Laplante M, Sabatini DM (2012) mTOR signaling in growth control and disease. *Cell* 149:274–293. <https://doi.org/10.1016/j.cell.2012.03.017>
- Malagelada C, Jin ZH, Jackson-Lewis V, Przedborski S, Greene LA (2010) Rapamycin protects against neuron death in vitro and in vivo models of Parkinson's disease. *J Neurosci* 30:1166–1175. <https://doi.org/10.1523/JNEUROSCI.3944-09.2010>
- Santini E, Heiman M, Greengard P, Valjent E, Fisone G (2009) Inhibition of mTOR signaling in Parkinson's disease prevents L-DOPA-induced dyskinesia. *Sci Signal* 2:ra36. <https://doi.org/10.1126/scisignal.2000308>
- Decressac M, Bjorklund A (2013) mTOR inhibition alleviates L-DOPA-induced dyskinesia in parkinsonian rats. *J Parkinsons Dis* 3: 13–17. <https://doi.org/10.3233/JPD-120155>
- Hughes AJ, Daniel SE, Blankson S, Lees AJ (1993) A clinicopathologic study of 100 cases of Parkinson's disease. *Arch Neurol* 50: 140–148
- Dickson DW, Braak H, Duda JE, Duyckaerts C, Gasser T, Halliday GM, Hardy J, Leverenz JB et al (2009) Neuropathological assessment of Parkinson's disease: Refining the diagnostic criteria. *Lancet Neurol* 8:1150–1157
- Fahn S, Elton R (1987) Unified Parkinson's disease rating scale. In: *Recent developments in Parkinson's disease*, 2nd edn. Macmillan Healthcare Information, Florham Park, p 153–163
- Fernández-Santiago R, Irazo A, Gaig C, Serradell M, Fernández M, Tolosa E, Santamaría J, Ezquerro M (2016) Absence of *LRRK2* mutations in a cohort of patients with idiopathic REM sleep behavior disorder. *Neurology* 86:1072–1073. <https://doi.org/10.1212/WNL.0000000000002304>
- Sole X, Guino E, Valls J, Iniesta R, Moreno V (2006) SNPStats: a web tool for the analysis of association studies. *Bioinformatics* 22: 1928–1929. <https://doi.org/10.1093/bioinformatics/bti268>
- Ritchie M, Hahn L, Roodi N et al (2001) Multifactor-dimensionality reduction reveals high-order interactions among estrogen-metabolism genes in sporadic breast cancer. *Am J Hum Genet* 69:138–147. <https://doi.org/10.1086/321276>
- Motsinger AA, Ritchie MD (2006) The effect of reduction in cross-validation intervals on the performance of multifactor dimensionality reduction. *Genet Epidemiol* 30:546–555. <https://doi.org/10.1002/gepi.20166>
- Reijmerink NE, Bottema RWB, Kerkhof M, Gerritsen J, Stelma FF, Thijs C, van Schayck CP, Smit HA et al (2010) TLR-related pathway analysis: novel gene-gene interactions in the development of asthma and atopy. *Allergy* 65:199–207. <https://doi.org/10.1111/j.1398-9995.2009.02111.x>
- Shen Y, Xun G, Guo H, He Y, Ou J, Dong H, Xia K, Zhao J (2016) Association and gene-gene interactions study of reelin signaling pathway related genes with autism in the Han Chinese population. *Autism Res* 9:436–442. <https://doi.org/10.1002/aur.1540>
- Holmans P, Moskvina V, Jones L, Sharma M, The International Parkinson's Disease Genomics Consortium (IPDGC), Vedernikov A, Buchel F, Sadd M et al (2013) A pathway-based analysis provides additional support for an immune-related genetic susceptibility to Parkinson's disease. *Hum Mol Genet* 22:1039–1049. <https://doi.org/10.1093/hmg/dd5492>
- Mas S, Gassó P, Ritter MA, Malagelada C, Bernardo M, Lafuente A (2015) Pharmacogenetic predictor of extrapyramidal symptoms induced by antipsychotics: Multilocus interaction in the mTOR pathway. *Eur Neuropsychopharmacol* 25:51–59. <https://doi.org/10.1016/j.euroneuro.2014.11.011>
- Zai CC, Tiwari AK, Mazzoco M, de Luca V, Müller DJ, Shaikh SA, Lohoff FW, Freeman N et al (2013) Association study of the vesicular monoamine transporter gene SLC18A2 with tardive

- dyskinesia. *J Psychiatr Res* 47:1760–1765. <https://doi.org/10.1016/j.jpsychires.2013.07.025>
31. Comi C, Ferrari M, Marino F, Magistrelli L, Cantello R, Riboldazzi G, Bianchi M, Bono G et al (2017) Polymorphisms of dopamine receptor genes and risk of L-Dopa-induced dyskinesia in Parkinson's disease. *Int J Mol Sci* 18:242. <https://doi.org/10.3390/ijms18020242>
 32. Cheshire P, Bertram K, Ling H, O'Sullivan SS, Halliday G, McLean C, Bras J, Foltynie T et al (2014) Influence of single nucleotide polymorphisms in COMT, MAO-A and BDNF genes on dyskinesias and levodopa use in Parkinson's disease. *Neurodegener Dis* 13:24–28. <https://doi.org/10.1159/000351097>
 33. Devos D, Lejeune S, Cormier-Dequaire F, Tahiri K, Charbonnier-Beaupel F, Rouaix N, Duhamel A, Sablonnière B et al (2014) Dopadecarboxylase gene polymorphisms affect the motor response to l-dopa in Parkinson's disease. *Parkinsonism Relat Disord* 20:170–175. <https://doi.org/10.1016/j.parkrelidis.2013.10.017>
 34. Kaplan N, Vituri A, Korczyn AD, Cohen OS, Inzelberg R, Yahalom G, Kozlova E, Milgrom R et al (2014) Sequence variants in SLC6A3, DRD2, and BDNF genes and time to levodopa-induced dyskinesias in Parkinson's disease. *J Mol Neurosci* 53:183–188. <https://doi.org/10.1007/s12031-014-0276-9>
 35. Polakiewicz RD, Schieferl SM, Gingras AC, Sonenberg N, Comb MJ (1998) μ -opioid receptor activates signaling pathways implicated in cell survival and translational control. *J Biol Chem* 273:23534–23541. <https://doi.org/10.1074/jbc.273.36.23534>
 36. Picconi B, Centonze D, Håkansson K, Bernardi G, Greengard P, Fisone G, Cenci MA, Calabresi P (2003) Loss of bidirectional striatal synaptic plasticity in L-DOPA-induced dyskinesia. *Nat Neurosci* 6:501–506. <https://doi.org/10.1038/nm1040>
 37. Grünblatt E, Mandel S, Jacob-Hirsch J et al (2004) Gene expression profiling of parkinsonian substantia nigra pars compacta; alterations in ubiquitin-proteasome, heat shock protein, iron and oxidative stress regulated proteins, cell adhesion/cellular matrix and vesicle trafficking genes. *J Neural Transm* 111:1543–1573. <https://doi.org/10.1007/s00702-004-0212-1>
 38. Banko JL (2005) The translation repressor 4E-BP2 is critical for eIF4F complex formation, synaptic plasticity, and memory in the hippocampus. *J Neurosci* 25:9581–9590. <https://doi.org/10.1523/JNEUROSCI.2423-05.2005>
 39. Zhang Y, Meredith GE, Mendoza-Elias N, Rademacher DJ, Tseng KY, Steece-Collier K (2013) Aberrant restoration of spines and their synapses in L-DOPA-induced dyskinesia: involvement of corticostriatal but not thalamostriatal synapses. *J Neurosci* 33:11655–11667. <https://doi.org/10.1523/JNEUROSCI.0288-13.2013>
 40. Mandel SA, Youdim MBH, Riederer P, et al (2013) Peripheral blood gene markers for early diagnosis of Parkinson's disease. (Patent reference number: US20130217028A1) Google Patents web. <https://patents.google.com/patent/US20130217028>. Accessed 26 October 2010
 41. Charbonnier-Beaupel F, Malerbi M, Alcacer C, Tahiri K, Carpentier W, Wang C, Doring M, Xu D et al (2015) Gene expression analyses identify Narp contribution in the development of L-DOPA-induced dyskinesia. *J Neurosci* 35:96–111. <https://doi.org/10.1523/JNEUROSCI.5231-13.2015>
 42. Anglikier N, Rüegg MA (2013) In vivo evidence for mTORC2-mediated actin cytoskeleton rearrangement in neurons. *Bioarchitecture* 3:113–118. <https://doi.org/10.4161/bioa.26497>
 43. Jacinto E, Loewith R, Schmidt A et al (2004) Mammalian TOR complex 2 controls the actin cytoskeleton and is rapamycin insensitive. *Nat Cell Biol* 6:1122–1128. <https://doi.org/10.1038/ncb1183>
 44. Sarbassov DD, Ali SM, Kim DH et al (2004) Rictor, a novel binding partner of mTOR, defines a rapamycin-insensitive and raptor-independent pathway that regulates the cytoskeleton. *Curr Biol* 14:1296–1302. <https://doi.org/10.1016/j.cub.2004.06.054>
 45. Rodriguez-Viciana P, Warne PH, Dhand R, Vanhaesebroeck B, Gout I, Fry MJ, Waterfield MD, Downward J (1994) Phosphatidylinositol-3-OH kinase direct target of Ras. *Nature* 370:527–532. <https://doi.org/10.1038/370527a0>
 46. Pacold ME, Suire S, Perisic O, Lara-Gonzalez S, Davis CT, Walker EH, Hawkins PT, Stephens L et al (2000) Crystal structure and functional analysis of Ras binding to its effector phosphoinositide 3-kinase gamma. *Cell* 103:931–943
 47. Kitada T, Asakawa S, Hattori N, Matsumine H, Yamamura Y, Minoshima S, Yokochi M, Mizuno Y et al (1998) Mutations in the parkin gene cause autosomal recessive juvenile parkinsonism. *Nature* 392:605–608. <https://doi.org/10.1038/33416>
 48. Petrucelli L, O'Farrell C, Lockhart PJ et al (2002) Parkin protects against the toxicity associated with mutant alpha-synuclein: proteasome dysfunction selectively affects catecholaminergic neurons. *Neuron* 36:1007–1019
 49. Helton TD, Otsuka T, Lee MC et al (2008) Pruning and loss of excitatory synapses by the parkin ubiquitin ligase. *Proc Natl Acad Sci U S A* 105:19492–19497. <https://doi.org/10.1073/pnas.0802280105>
 50. Wang L, Gout I, Proud CG (2001) Cross-talk between the ERK and p70 S6 kinase (S6K) signaling pathways: MEK-dependent activation of S6K2 in cardiomyocytes. *J Biol Chem* 276:32670–32677. <https://doi.org/10.1074/jbc.M102776200>
 51. Pardo OE, Seckl MJ (2013) S6K2: The neglected S6 kinase family member. *Front Oncol* 3:191. <https://doi.org/10.3389/fonc.2013.00191>
 52. Shahbazian D, Roux PP, Mieulet V, Cohen MS, Raught B, Taunton J, Hershey JWB, Blenis J et al (2006) The mTOR/PI3K and MAPK pathways converge on eIF4B to control its phosphorylation and activity. *EMBO J* 25:2781–2791. <https://doi.org/10.1038/sj.emboj.7601166>
 53. Cao H, Yin X, Cao Y, Jin Y, Wang S, Kong Y, Chen Y, Gao J et al (2013) FCHSD1 and FCHSD2 are expressed in hair cell stereocilia and cuticular plate and regulate actin polymerization in vitro. *PLoS One* 8:e56516. <https://doi.org/10.1371/journal.pone.0056516>
 54. Coyle IP, Koh YH, Lee WCM, Slind J, Fergestad T, Littleton JT, Ganetzky B (2004) Nervous wreck, an SH3 adaptor protein that interacts with Wsp, regulates synaptic growth in Drosophila. *Neuron* 41:521–534. [https://doi.org/10.1016/S0896-6273\(04\)00016-9](https://doi.org/10.1016/S0896-6273(04)00016-9)
 55. Huang RS, Duan S, Shukla SJ, Kistner EO, Clark TA, Chen TX, Schweitzer AC, Blume JE et al (2007) Identification of genetic variants contributing to cisplatin-induced cytotoxicity by use of a genome-wide approach. *Am J Hum Genet* 81:427–437. <https://doi.org/10.1086/519850>

